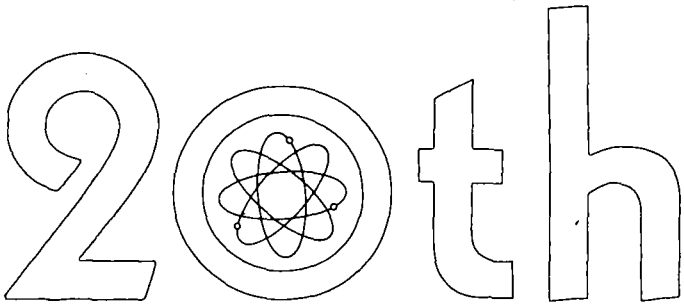

Annual Conference on Mass Spectrometry and Allied Topics

June 4-9, 1972

Dallas, Texas

Next Meeting: San Francisco May 20-25, 1973

Twentieth Annual Conference on Mass Spectrometry and Allied Topics

June 4-9, 1972
Dallas, Texas

Arranged by the
American Society for Mass Spectrometry
in cooperation with ASTM Committee E-14

Table of Contents

Introduction

This volume is a collection of papers presented at the Twentieth Annual Conference on Mass Spectrometry and Allied Topics, held in Dallas, Texas, June 4-9, 1972. It is intended that this volume be distributed only to members of ASMS, and registrants of the Conference, and therefore should not be considered as a publication.

It is suggested that any future reference to individual reports be cited in the form: author(s), presented at the Twentieth Annual Conference on Mass Spectrometry and Allied Topics, Dallas, Texas, June 4-9, 1972.

F. H. Field, Program Chairman

Arranged by the American Society for Mass Spectrometry (ASMS), in cooperation with ASTM Committee E-14.

ASMS

President: R. E. HONIG, RCA Laboratories, Princeton, New Jersey 08540

Vice-President (Program): F. H. FIELD, Rockefeller University, New York, New York 10021

Vice-President (Arrangements): G. L. KEARNS, AEI Scientific Apparatus, Inc., 500 Executive Blvd., Cross Westchester Executive Park, Elmsford, New York 10523

Vice-President (Data & Standards): H. R. HARLESS, Union Carbide Technical Center, S. Charleston, West Virginia 25303

Secretary: F. E. SAALFELD, Naval Research Laboratories, Washington, D. C. 20390

Treasurer: H. D. COOK, Westinghouse Bettis Atomic Power Laboratories, Box 79, West Mifflin, Pennsylvania 15122

Past President: J. L. FRANKLIN, Department of Chemistry, Rice University, Houston, Texas 77001

Directors-at-Large:

A. G. SHARKEY, Jr., U. S. Bureau of Mines, 4800 Forbes Avenue, Pittsburgh, Pennsylvania, 15213

A. L. WAHRHAFTIG, Department of Chemistry, University of Utah, Salt Lake City, Utah 84112

ASTM COMMITTEE E-14

Chairman: H. R. HARLESS, Union Carbide Technical Center, South Charleston, West Virginia 25303

Vice-Chairman: H. E. LUMPKIN, Esso Research & Engineering Co., P. O. Box 4255, Baytown, Texas 77520

Secretary-Treasurer: W. F. KUHN, Philip Morris, Inc., Richmond, Virginia 23206

ACKNOWLEDGMENTS

We thank the following companies for their support and the sponsorship of this meeting:

AEI Scientific Apparatus
Applied Research Laboratories
AVCO Electronics Division
Cameca Instruments, Inc.
Digital Equipment Corporation
Laboratory Data Products Group
DuPont Company
Instrument Products Division
Extranuclear Laboratories, Inc.
Finnigan Corporation
Hewlett-Packard
JOEL (U.S.A.), Inc.
LKB Instruments, Inc.
Nuclide Corporation
Perkin-Elmer Corporation
Process Analyzers, Inc.
Subsidiary of Electronic Associates, Inc.
Scientific Research Instruments Corporation
S. S. R. Instrument Co.
3M Company
UTHE Technology International
Varian MAT
Xerox Corporation

*Plenary Lecture
**Invited Paper

Decomposition of 1,3,5-Trinitrobenzene Under Electron Impact

SEYMOUR MEYERSON and ROY W. VANDER HAAR

Standard Oil Company (Indiana)
Naperville, Ill. 60540

and

ELLIS K. FIELDS

Amoco Chemical Corporation
Naperville, Ill. 60540

Metastable scanning of fragment ions in the mass spectrum of 1,3,5-trinitrobenzene yielded 96 metastable peaks. Coupled with precise-mass measurement on selected peaks, this approach defines the underlying chemistry in considerable detail. Primary loss of NO_2 seems to play a central role in the network of competing and consecutive reactions, and may well be the rate-controlling step for a large part of it, releasing vibrational energy to drive further decomposition steps.

Electron Impact Studies of Methylmercaptobenzothiazoles and Their Oxygen Analogs. THEODORE L. FOLK* and S. M. PATEL, The Goodyear Tire & Rubber Company, Akron, Ohio 44316

The mass spectra of S-methyl- and N-methyl-2-mercaptobenzothiazole are very nearly identical. Mass measurements, metastable peaks, and investigation of the methyl-(d_3) derivatives assisted in establishing fragmentation routes which demonstrated their differences. The subsequent mass spectral investigations of the methyl derivatives of 2-mercaptobenzoxazole, 2-hydroxybenzothiazole, and 2-hydroxybenzoxazole were also discussed. The complete paper will be submitted to Organic Mass Spectrometry for possible publication.

FRAGMENTATION OF SOME BICYCLIC KETONES ON ELECTRON IMPACT

J. D. Henion
Department of Chemistry
State University of New York at Albany
Albany, New York 12203

D. G. I. Kingston*
Department of Chemistry
Virginia Polytechnic Institute and State University
Blacksburg, Virginia 24061

Studies of the McLafferty rearrangement[1] have shown clearly that rearrangement is subject to pronounced steric effects. Thus rearrangement will not occur if the γ-hydrogen atom and the carbonyl oxygen atom cannot approach closer than 1.8 A°. The effect on the rearrangement of the angle τ between the plane of the carbonyl group and the γ-hydrogen atom has been discussed in a theoretical paper,[2] but no experimental information has been available on this point.

We have prepared a series of bicyclic ketones in which the value of τ varies from around 50° to 80°. Two of these are shown below, with their

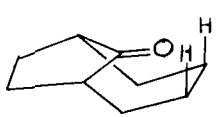

1 $\tau = 80°$

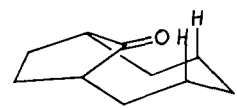

2 $\tau = 50°$

respective τ values (measured from Dreiding models) indicated. The occurrence of McLafferty rearrangement in each compound was followed by the observation of an ion (at m/e 84 for (1) and (2)) due to the double McLafferty rearrangement. Compound 1 gave no peak at m/e 84, indicating that McLafferty rearrangement is precluded in this compound by the high τ value, even though the critical O-H distance is within the 1.8 A° limit. Compound 2 did yield a substantial ion at m/e 84 (40% of base peak), suggesting that McLafferty rearrangement is occurring in this compound in spite of the high value of τ. Examination of specifically deuterated 2 indicated that the rearrangement to yield m/e 84 involves transfer of both γ-hydrogen atoms to the extent of about 60%, suggesting either hydrogen scrambling prior to rearrangement or the operation of multiple pathways. A detailed analysis of the spectra of the deuterated analogs of 2 showed

that the ion at m/e 84 was most readily explained as being formed largely by a double McLafferty rearrangement.

A full account of this work will be published elsewhere.

1. H. Budzikiewicz, C. Djerassi, and D.H. Williams, "Mass Spectrometry of Organic Compounds", Holden-Day, Inc., San Francisco, 1967, p. 155.

2. F.P. Boer, T.W. Shannon, and F.W. McLafferty, J. Amer. Chem. Soc., 90, 7239 (1968).

*Author to whom enquiries should be addressed.

EFFECT OF THE STERIC HINDRANCE INTRODUCED BY AN AROMATIC RING ON THE FRAGMENTATIONS OF BIFUNCTIONAL LONG-CHAIN MOLECULES.

R.E.Wolff, M.Greff and G.Teller
Laboratoire associé au C.N.R.S.n°31, Institut de Chimie,
Université Louis Pasteur,Strasbourg,France.

Long-chain bifunctional aliphatic compounds often undergo major fragmentations which result from the interaction of remote functional groups(1). Following a study of these interactions in long-chain hydroxy- and ketoesters (2,3,4) in which it was found that hydrogens and alcoxyl groups were transferred from the vicinity of one functional group to the vicinity of the other, the fragmentations of p-hydroxyalkyl- (I) and p-ketoalkyl- (II) benzoic acid methylesters have been investigated.

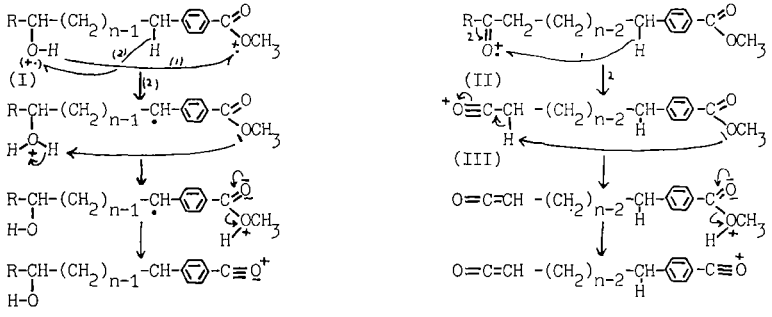

The study of the hydroxyesters (I, n=7 to n=3) shows that, when n is large, the major fragmentation paths are the same as in aliphatic hydroxyesters(2) and follow a specific transfer of the hydroxyl hydrogen to the carbomethoxyl group (arrow 1). In addition, loss of CH_3OH by the molecular ion is observed, and has been shown to involve specifically a benzylic hydrogen which is transferred first to the hydroxyl group (arrow 2), then to the carbomethoxyl group (sequence); in the case of the benzylic d-2 analogs, the benzylic deuterium thus transferred suffers a 1:1 isotopic dilution at the intermediate step. Such a loss of CH_3OH by the molecular ion is found neither in aliphatic hydroxyesters (2,5) nor in methyl p-alkylbenzoates, but it is observed with methyl ω-phenylalkanoates (6).

Our results show that, when n decreases, the transfer of hydrogen across the aromatic ring becomes increasingly difficult and the abundance of the ions then formed decreases correspondingly; the transfer does not take place any more when the transition state has less than nine to ten members, plus the aromatic ring (n < 4-5); in that case, the fragments then observed are derived from $(M-H_2O)^{+\cdot}$, the formation of which still involves the transfer of a benzylic hydrogen to the hydroxyl group. It is interesting to note that the synthesis of p-phenylene alkanones by para condensation of ω-phenyl alkanoic acid chlorides under Friedel-Crafts conditions (7) has the same transition state size requirements.

The study of the ketoesters (II) has shown that the loss of CH_3OH by the molecular ion is very important (base peak for n=7 to n=5) and that a benzylic hydrogen is transferred to the carbomethoxyl group by a mechanism (arrow 1) similar to the one found for hydroxyesters; the transfer of a hydrogen α to the carbonyl group competes to some

extent when n is small (n=5 and 4), and the transfer is again completely inhibited when $n < 4$. As in long-chain ketoesters (3), loss of CH_3OH by the α-cleavage ion (III), involving a hydrogen in position α to the carbonyl group is also found here (sequence); the transfer of this hydrogen to the carbomethoxyl group is again limited in the same manner as above by the size of the transition state (limit: $n \geq 6$). Some hydrogen scrambling occurs here and renders the study more difficult; besides, metastable defocussing and exact mass measurements have shown that an ion of same mass and elemental composition is also derived from $(M-CH_3OH)^{+\cdot}$; its formation has then the same transition state size limitations as the one of its parent ion ($n \geq 4$).

Detailed account of this work will be submitted to Organic Mass Spectrometry.

References.

1. J.R.Dias and C.Djerassi, Org.Mass Spectrom. 1972,6,385; for leading references, see therein ref. 2,3,4,9,15,16,19a.
2. R.E.Wolff, M.Greff and J.A.McCloskey, Adv. in Mass Spectrom. vol.4, Elsevier Publ.Co New York, 1968, p.193.
3. G.Wolff, R.E.Wolff, and J.A.McCloskey, Tetr.Letters 1966, 4335.
4. A.Caspar, G.H.Draffan, M.Greff, G.Teller, J.A.McCloskey and R.E.Wolff ,in preparation.
5. R.Ryhage and E.Stenhagen, Arkiv för Kemi, 1960,15,545.
6. S.Meyerson and L.C.Leitch, J.Am.Chem.Soc. 1966,88,56; 1971,93 2244.
7. R.Huisgen,W.Rapp,I.Ugi,H.Walz,I.Blogger, Annalen, 1954,586,52. R.Huisgen and V.Vossius Monatsh. 2957,88,517.

FRAGMENTATION VIA INTRAMOLECULAR HYDROGEN BONDING?

Phillip T. Funke and Allen I. Cohen

The Squibb Institute for Medical Research
New Brunswick, New Jersey 08903

In a recent review article[1], Bentley and Johnstone suggested that the intramolecular hydrogen-bond (H-bond) may be implicated in some fragmentation processes. In a paper[2] presented at the last ASMS meeting, we suggested that intramolecular H-bonding could contribute to the major fragmentation

$$M^+ \longrightarrow (M-C_2H_6O)^+$$

in the mass spectrum of [(1-ethyl-3-methyl-5-pyrazolyl)amino]methylene malonic acid; such bonding had been shown to occur[3]. Williams and his coworkers[4] studied the mass spectrum of an analogous compound, 3-amino-but-2-enoate, where the major fragment ion is due to the loss of C_2H_6O from the M^+. The amino proton was found not to be involved, to any great extent, in the proton abstraction, as demonstrated by the mass spectrum of the N-deutero derivative, which lost only C_2H_6O. It was then demonstrated by deuterium-labeling on the phenyl ring that the proton ortho or para to the amine function was lost during the fragmentation. The cis-trans configuration of the compound was not established, however, and, as a consequence, the possibility of intramolecular H-bonding could not be established. Intramolecular H-bonding was shown by IR to be present in 1-ethyl-3-methyl-4-hydroxy-1H-pyrazolo[3,4-b]-pyridine-5-carboxylic acid, ethyl ester. Deuterium-labeling demonstrated that the hydroxy proton was lost from the M^+ almost exclusively as C_2H_5DO. In contrast, the 4-amino analog which had been shown by IR to be not intramolecularly H-bonded, yielded an insignificant peak for the loss of C_2H_6O from the M^+.

Thus, the mass spectra of various alkyl-substituted amines (Figure 1) were studied to ascertain the effect of the alkyl function on the retention of the remaining amino proton. The rate of reaction for bond cleavage of the alkyl group (in this case, beta-bond cleavage) is, of course, much greater than that for rearrangement. Thus, we observe the fragmentation of the alkyl side chain followed by the elimination of the elements of ethanol, as shown by the presence of metastable ions in the mass spectrum. All compositions were established by high-resolution mass spectrometry. A summary of the pertinent data is given in Table 1. Deuteration of the alkyl amine by repeated dissolution in CH_3OD yielded products with ~ 90% deuterium on the amine nitrogen. Paralleling the previous observations from the unlabeled derivative, the major fragmentation involves the beta-bond cleavage, followed by elimination of predominately C_2H_5DO, the base peak. Since the unlabeled compound shows only a very small peak (<1% relative to the base peak) for the elimination of C_2H_5O after the beta-cleavage, the intensities could be corrected for residual unlabeled sample and for the P+1 ion of the base peak in the spectrum of the labeled sample. A summary of the percentage proton transfer vs deuterium transfer at 70 eV and 10 eV in the labeled compound, after correction, is shown in Table 2. Assuming that the percent proton transfer depends upon the number of protons, the t-butyl group with six remaining protons in the alkyl side chain after elimination of one of its methyl groups shows the largest proton transfer relative to deuterium. Likewise, the sec-butyl and isopropyl groups having four remaining protons after elimination of ethyl and methyl groups, respectively, yield a lower percent proton transfer. Correspondingly, the iso- and n-butyl and n-propyl compounds yield the least proton transfer, since only two protons are available. The low-voltage spectra also support these conclusions and, furthermore, indicate an overall increase in

proton transfer. The deuterium transfer remains much larger than the proton transfer for all energies between 10 and 70 eV, and the deuterium must have a much larger rate of transfer than do protons. Participation of the proton ortho to the ester has not been ruled out.

Beynon et al.[5] showed that the D_5-ethyl ester of benzoic acid-O^{18}, labeled on the carboxyl group, loses C_2D_4, with the subsequent loss of OH and OD arising from the scrambling of the ortho protons with deuterium due to free rotation of the carboxyl group on the metastable time scale. On the other hand, Benezra and Bursey[6] found that the scrambling for a freely rotating carboxyl group was not observed in the case of deuterium-labeled (hydroxyl group) salicylic acid. They attributed this result to intramolecular H-bonding.

The n-butyl, n-propyl and isobutyl amines show a very large metastable peak (not corrected for ^{13}C isotope contribution) for the loss of C_2H_5OD after removal of the alkyl group. The transfer of deuterium in these three compounds occurs more readily than does the transfer of hydrogen, because of the stabilizing influence of a nitrogen-carbon double bond formed by the fragmentation. The remaining three compounds, the t-butyl, sec-butyl and isopropyl derivatives, have an additional carbon atom that allows two factors to influence the intensities of the metastable ion(s). First, the number of hydrogens can influence the overall ratio. Second, there is competition between the formation of a carbon-carbon double bond and of a carbon-nitrogen double bond. A combination of both effects could produce the much larger proton transfer metastable ion, suggesting that carbon-carbon bond formation may be more favored than carbon-nitrogen double bond formation on the metastable ion time scale. Thus, other processes may be operating, but H-bonding may not be ruled out.

The isobutyl amine derivatives shows a more substantial difference in deuterium-proton transfer than does either the n-butyl or the n-propyl compound, even though the beta-cleavage should yield the same fragment structure in all three compounds. Since deuterium is transferred more readily at high energies than at low energies, the fragment coming from the isobutyl compound by loss of isopropyl from the M^+ may have more excitation energy than the corresponding fragments arising from the other two compounds. This difference could come about if the average amount of energy per molecule and the energy removed by the alkyl radical is the same for all three compounds, but the bond energy of the isopropyl CH_2 is lower than that of the n-propyl CH_2 and ethyl CH_2. Excess energy would then be present in the fragment ion coming from the isobutylamine compound, in comparison with those from the n-butyl and n-propyl compounds. Although alternate fragmentation pathways are possible and might, by chance, contribute to the loss of deuterium in the isobutylamine, the observation of the phenomenon at ~10 eV seems to rule out this possibility.

In conclusion, then, we can see that a number of factors can play a part in the fragmentations studied here and, in particular, H-bonding may play a dominant role.

REFERENCES

1. T. W. Bentley and R. A. W. Johnstone, Adv. Phys. Org. Chem., 8, pg. 151, V. Gold, Ed., Academic Press, London, 1970.
2. P. T. Funke and A. I. Cohen, Nineteenth Ann. Conf. on Mass Spectrometry and Allied Topics. Atlanta, Ga. (1971).
3. M. S. Puar, B. T. Keeler and A. I. Cohen, J. Org. Chem., 36, 219 (1971)
4. H. J. Jakobsen, S.-O. Lawesson, J. T. B. Marshall, G. Schroll and D. H. Williams, J. Chem. Soc. (B) 940 (1966).
5. R. H. Shapiro, K. B. Tomer, R. M. Caprioli and J. H. Beynon, Org.

Mass Spectrom., 3, 1333 (1970).
6. S. A. Benezra and M. M. Bursey, Org. Mass Spectrom., 6, 463 (1972).

FIGURE 1

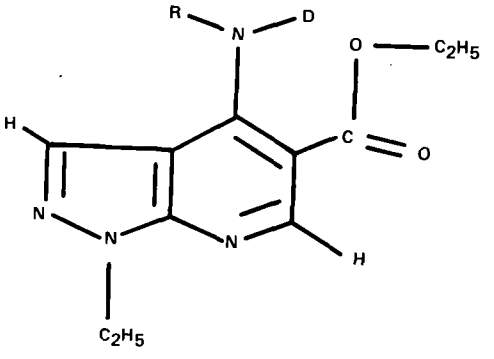

R

$-C(CH_3)_3$
$-CH(CH_3)CH_2CH_3$
$-CH_2CH(CH_3)_2$
$-CH_2CH_2CH_2CH_3$
$-CH(CH_3)_2$
$-CH_2CH_2CH_3$

TABLE 1

Summary of Intensities
in Percent of Total Ionization Σ

R	R^1	M^+	M^+-1	M^+-R^1	M^+-46	M^+-47	M^+-R^1-46
$-C(CH_3)_3$	CH_3	9.0	.1	3.3	.1	.4	20.5
$-CH(CH_3)CH_2CH_3$	C_2H_5	9.2	.2	6.6	.4	2.2	36.8
$-CH_2CH(CH_3)_2$	$CH(CH_3)_2$	12.4	.3	6.0	.3	.8	43.4
$-CH_2CH_2CH_2CH_3$	$CH_2CH_2CH_3$	22.0	.4	3.0	.7	3.2	37.6
$-CH(CH_3)_2$	CH_3	19.5	.3	2.0	1.2	8.2	30.6
$-CH_2CH_2CH_3$	C_2H_5	20.5	.4	2.1	.5	2.9	37.6

TABLE 2

Relative Percentages of M^+-R^1-47 and $^*M^+-R^1-46$
From Deuterated Compounds After Corrections

	70 ev		ca. 10 ev	
R^1	M^+-R^1-47	$^*M^+-R^1-46$	M^+-R^1-47	$^*M^+-R^1-46$
CH_3	67	33	61	39
C_2H_5	81	19	71	29
$CH(CH_3)_2$	94	6	83	17
$CH_2CH_2CH_3$	87	13	71	29
CH_3	80	20	73	27
C_2H_5	86	14	67	33

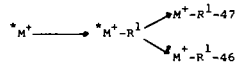

$$\% = \frac{(M^+-R^1-47)}{(M^+-R^1-47) + (M^+-R^1-47)} \times 100$$

TABLE 3

Relative Metastable Intensities

R	$^*M^+-R^1-46$	M^+-R^1-47
$-C(CH_3)_3$	77	23
$-CH(CH_3)CH_2CH_3$	67	33
$-CH_2CH(CH_3)_2$	9	91
$-CH_2CH_2CH_2CH_3$	23	77
$-CH(CH_3)_2$	71	29
$-CH_2CH_2CH_3$	23	77

MASS SPECTROMETRY OF METHYLCYCLOSILOXANES

W. J. A. VandenHeuvel, J. L. Smith, R. A. Firestone and J. L. Beck

Merck Sharp & Dohme Research Laboratories
Rahway, New Jersey 07065

McCloskey et al.[1,2] have observed that the trimethylsilyl (TMSi) derivatives of di-substituted long chain compounds yield intense doubly-charged M-30 ions, resulting from the loss of two methyl radicals plus two electrons. Our work with the TMSi derivatives of several groups of 4,4'-di-substituted diphenyls disclosed that these compounds also exhibit this behavior.[3,4] In addition, the TMSi derivatives of m- and p-aminophenols as well as 2,6- and 2,7-disubstituted naphthalenes,[5] and a variety of heterocycles,[6,7] including 2,4- and 4,6-pyrimidines and 2,4-pteridines, produce the intense $[M-30]^{++}$. With the di-TMSi derivatives of ortho- and peri-substituted aromatics, however, M-103 ions (loss of a methyl radical plus the elements of tetramethylsilane via a cyclic mechanism) are intense, and the doubly-charged M-30 ions are absent.[5,7]

We have recently identified hexamethylcyclotrisiloxane, octamethylcyclotetrasiloxane, decamethylcyclopentasiloxane, and dodecamethylcyclohexasiloxane (I - IV, respectively) as among those compounds responsible for the gas-liquid chromatographic peaks which are occasionally observed to elute unexpectedly during temperature programed analysis.[8] The compounds causing these peaks are generally held to arise from dimethylpolysiloxane stationary phases and/or especially silicone rubber septa.[9,10] The mass spectra of I and II contain intense doubly-charged M-30 and weak singly-charged M-103 ions, whereas III and IV yield intense M-103 and m/e 73 ions and weak $[M-30]^{++}$ (see Table I). This inverse relationship is analogous to that observed earlier for the same ions with the aromatic TMSi compounds. The presence of these ions in the spectra of methylcyclosiloxanes has been reported by Orlov, et al.;[11] three pathways for the production of the M-103 ion were presented but no mechanism was proposed.

Transannular reactions are common in 8-membered and larger rings in carbocyclic chemistry.[12] The onset of transannular reactions with methylcyclosiloxanes would be expected to be shifted toward rings of greater size because of the larger bond angles in these compounds.[13] A transannular mechanism is presented below to account for the loss of tetramethylsilane from, and the formation of $[Si(CH_3)_3]^+$ by, the methylcyclosiloxanes of larger ring size.

Formation of the cyclized M-CH_3 ion A is a key step in the mechanism. White, et al.[14] have invoked the formation of a similiar cyclic ion in the fragmentation of long-chain α,ω-bis-TMSi ethers. Ion B is a branch point for the formation of both $[M-103]^+$ and $[Si(CH_3)_3]^+$, and the intensity ratios for these ions are similiar with each of the four methylcyclosiloxanes. This mechanism is precluded by sterochemical factors with the cyclic compounds of smaller ring size, allowing the alternative pathway - formation of $[M-30]^{++}$ - to dominate.

TABLE I

Compound	$[M-30]^{++}$	$[M-103]^+$	m/e 73
Hexamethylcyclotrisiloxane	16	<1	<1
Octamethylcyclotetrasiloxane	14	3	11
Decamethylcyclopentasiloxane	<1	37	100
Dodecamethylcyclohexasiloxane	<1	50	100

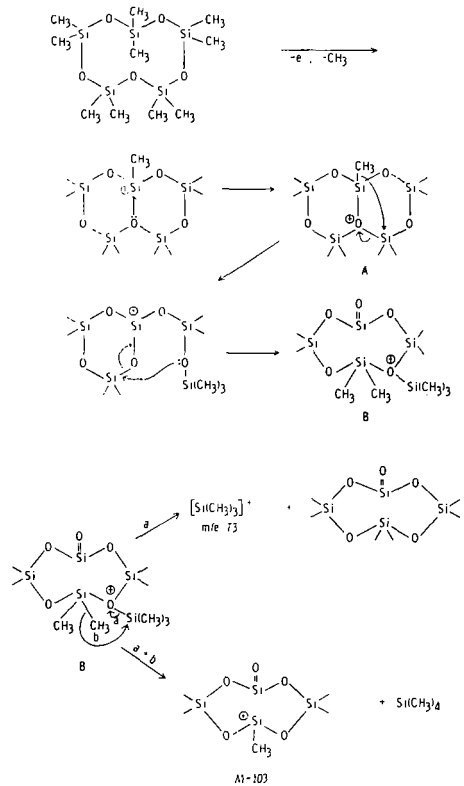

W. J. A. VandenHeuvel, J. L. Smith, R. A. Firestone and J. L. Beck

REFERENCES

1. J. A. McCloskey, R. N. Stillwell, and A. M. Lawson, Anal. Chem., 40, 233 (1968).

2. G. H. Draffan, R. N. Stillwell, and J. A. McCloskey, Org. Mass Spectrom., 1, 669 (1968).

3. J. L. Beck, W. J. A. VandenHeuvel, and J. L. Smith, Org. Mass Spectrom., 4, 237 (1970).

4. W. J. A. VandenHeuvel, J. L. Smith, and J. L. Beck, Org. Mass Spectrom., 4, 563 (1970).

5. J. L. Smith, J. L. Beck, and W. J. A. VandenHeuvel, Org. Mass Spectrom., 5, 473 (1971).

6. E. White, V, P. M. Krueger, and J. A. McCloskey, J. Org. Chem., 37, 430 (1972).

7. W. J. A. VandenHeuvel, J. L. Smith, P. Haug, and J. L. Beck, J. Heterocycl. Chem., 9, 451 (1972).

8. W. J. A. VandenHeuvel, J. L. Smith, R. A. Firestone, and J. L. Beck, Anal. Letters, in press.

9. E. D. Smith and K. E. Sorrells, J. Chromatog. Sci., 9, 15 (1971).

10. W. J. A. VandenHeuvel, J. L. Smith, G. Albers-Schonberg, B. Plazonnet, and P. Belanger, in "Modern Methods of Steroid Analysis", E. Heftmann, Ed., Academic Press, New York, in press.

11. V. Yu. Orlov, N. S. Nametkin, L. E. Gusel'nikov, and T. H. Islamov, Org. Mass Spectrom., 4, 195 (1970).

12. E. L. Eliel, N. L. Allinger, S. J. Angyal, and G. A. Morrison, "Conformational Analysis", Interscience, New York, 1966, p. 223.

13. H. Steinfink, B. Post, and I. Fankuchen, Acta Cryst., 8, 420 (1955).

14. E. White, V, S. Tsuboyama, and J. A. McCloskey, J. Am. Chem. Soc., 93, 6340 (1971).

FRAGMENTATION MECHANISMS LEADING TO CHARACTERISTIC IONS IN THE MASS SPECTRA OF STEROID TRIMETHYLSILYL ETHERS

Paul Vouros and D. J. Harvey

Institute for Lipid Research
Baylor College of Medicine
Houston, Texas 77025

The presence of the trimethyl substituent in hydroxy steroids has been known to direct the fragmentation of these compounds, and often results in the formation of diagnostically useful fragment ions. The main fragment ions occurring in the high mass region of the spectrum are usually due to the stepwise elimination of trimethylsilanol (90 amu). Factors influencing the specificity of this process have been investigated by means of ^{18}O-labeling. Characteristic trimethylsilyl-containing ions in the mass spectra of some 16- and 11-hydroxy steroids have been observed in high abundance. The mechanisms leading to their formation have been investigated by means of deuterium, ^{18}O and selective $\underline{d}_9$-TMS labeling.

For more details see:

1. P. Vouros and D. J. Harvey, Org. Mass Spectrom., (in press).

2. P. Vouros and D. J. Harvey, J. Chem. Soc (D), (in press).

MASS SPECTROMETRIC FRAGMENTATIONS EXHIBITED BY THE TRIMETHYLSILYL ESTERS OF VARIOUS DERIVATIVES OF AMINOALKYLPHOSPHONATES

A8

D.J. Harvey and M.G. Horning
Institute for Lipid Research, Baylor College of Medicine, Houston, Texas 77025

The mass spectrometric fragmentations of the trimethylsilyl (TMS) derivatives of a series of alkyl- and aminoalkyl- phosphonates have been investigated with the aid of deuterium labelling and high resolution mass measurements. Ions characteristic of the trimethylsilylphosphonate group were observed at m/e 195, 211, and in the range of m/e 225-227. The abundance of the ions in the m/e 225-227 range reflected the mobility of hydrogen atoms in the molecular ion. The ion at m/e 225, $OP[Si(CH_3)_3]_2$ was produced by simple cleavage of the trimethylsilyl-phosphonate group, whereas the ions at m/e 226 and 227 were produced by cleavage of the same group accompanied by migration of one or two hydrogen atoms respectively to the phosphonate moiety. Fragmentation of the ions at m/e 226, 227 and $[M-15]^+$ gave rise to m/e 211. This ion, in turn, lost methane to produce m/e 195. The spectra of the aminoalkylphosphonates which contained an N-TMS group exhibited a prominant ion at m/e 298, $P[OSi(CH_3)_3]_3$ produced by migration of a TMS group to the phosphonate moiety. This migration was apparently in competition with the transfer of a hydrogen atom to yield m/e 226.

The mass spectra of these derivatives generally exhibited molecular ions of very low relative abundance. In addition, the derivatives containing an N-TMS group gave poor gas chromatographic properties and consequently these derivatives are not ideal for characterisation purposes. In order to overcome this disadvantage, the amino group was converted into its N-acetyl, Acetone Schiff base or isothiocyanate derivative; TMS ester formation was retained for the phosphonate moiety. These derivatives, especially the isothiocyanates, gave good gas chromatographic properties and the N-acetyl and isothiocyanate derivatives exhibited structurally informative mass spectra. The molecular ions and ions characteristic of the phosphonate moiety were present in high abundance.

A number of rearrangement ions were also prominent in these spectra. The formation of many of these was initiated by the reactive siliconium center of the

$[M-15]^+$ ions (loss of a methyl radical from a TMS group). Examples of such rearrangements are the loss of CH_3CN from $[M-15]^+$ in the spectra of the N-acetyl/TMS derivatives, and the formation of m/e 268 (a) in the fragmentation of the isothiocyanates.

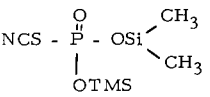

(a)

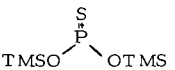

(b)

Ion (b), observed in the spectra of the latter compounds at m/e 241 was a fragment of the molecular ion.

The presence of abundant rearrangement ions, produced by interaction of the derivatised functional groups is of considerable mechanistic interest. Their presence in the spectra of unknown phosphonates of biological origin could be misleading. For example, the presence of m/e 241 (b) and its structural similarity to m/e 225 could be misinterpreted as indicating the presence of a thiophosphonate group. Consequently, their presence must be taken into account when interpreting the spectra of unknown compounds.

This work was supported by grant GM-16216 from the National Institute for General Medical Sciences.

Mass Spectrometric Characterization of Anhydronucleosides and their Derivatives.
DENIS LIN, J.B.WESTMORE and K.K.OGILVIE, Department of Chemistry, University of Manitoba, Winnipeg, Canada.

Anhydronuclesides are important analogues of natural nucleosides and can be used as intermediates in the synthesis of specific nucleotides and oligonucleotides. For example, in the case of 2,2'-anhydrouridine, I, the anhydro-ring effectively acts as a protecting group for the 2'-position. By utilizing the greater reactivity of the 5'-OH than the 3'-OH group to trityl chloride, base-labile groups can be placed on either the 3'- or 5'- oxygen atoms, as illustrated by the scheme:

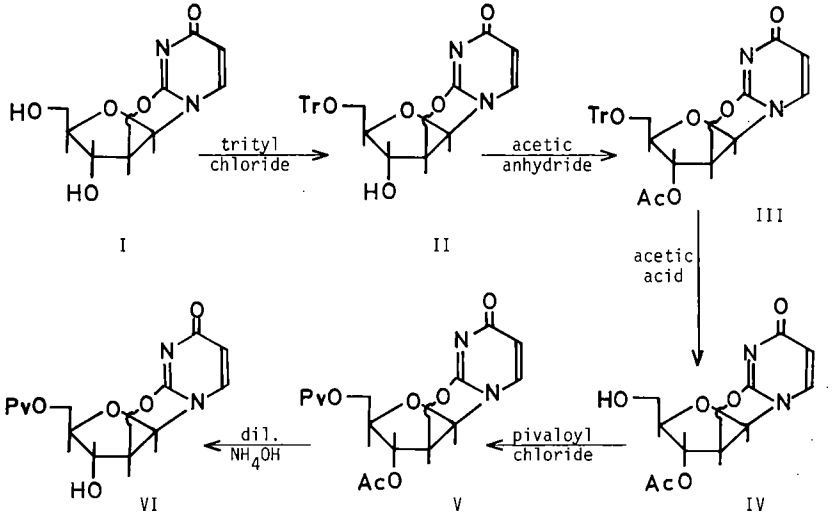

Phosphorylation of II, IV and VI can be readily achieved and the nucleotides may then be used in oligonucleotide synthesis. The protecting groups may then be removed under mild conditions. Finally, if desired, hydrolysis or displacement of the anhydro-linkage under specific conditions may then yield either the arabino- or ribo- form of the nucleosidic entity. To allow for the maximum flexibility in the synthesis of oligonucleotides it is essential to have available acid- and base- labile protecting groups for the 3'- and 5'- positions, and to be able to readily distinguish between isomeric pairs.

The anhydronucleosides studied were of the types:

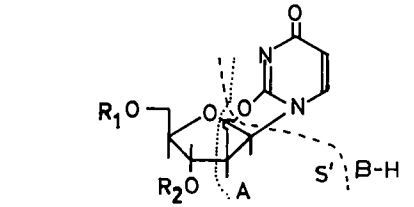

R_1 and/or R_2 = H,D,CH_3CO,CD_3CO, CF_3CO, Me_3CCO,Ph_3CCO, $Si(CH_3)_3$, $Si(CD_3)_3$

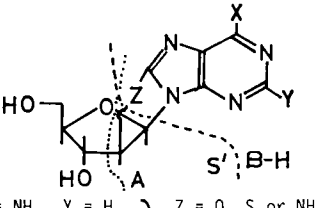

X = NH_2, Y = H
X = OH, Y = H
X = OH, Y = NH_2
X = OH, Y = OH

Z = O, S or NH.

Spectra were obtained as trimethylsilyl derivatives.

Some of the basic ion types observed in the mass spectra can be formulated as M^+, B^+, $(B+H)^+$, $(B+2H)^+$, $(S'-H)^+$, $(A+H)^+$, $(A+TMS)^+$, $(A+31)^+$ and $(A+30+TMS)^+$. Ions which carry structural information are the $(A+H)^+$, $(A+TMS)^+$, $(A+31)^+$ and $(A+30+TMS)^+$ ions. Their formation may be rationalized as follows:

$(A+H)^+$ and $(A+TMS)^+$

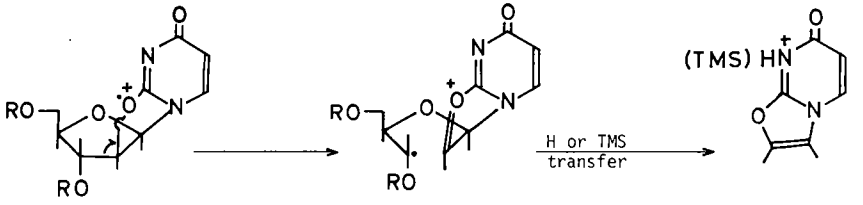

$(A+31)^+$ and $(A+30+TMS)^+$

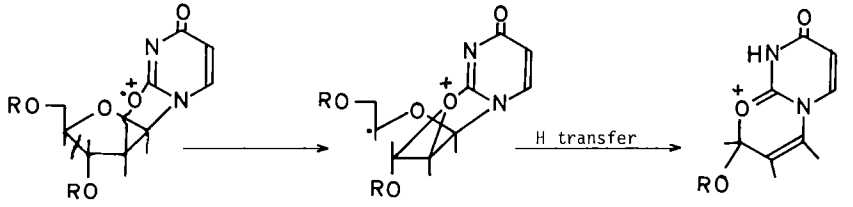

These ion types are also observed in the mass spectra of the purine analogues. In the case of the $(A+H)^+$ ions, hydrogen transfer occurs from OH, OAc or OPv groups, when present. When CF_3CO groups are present then hydrogen transfer occurs from the ribose skeleton. When TMS groups are present then hydrogen transfer can occur from TMS groups or ribose skeleton depending upon, in the case of the purine analogues, the base and upon the heteroatom of the anhydro-linkage.

The mass spectra of 2,2'-anhydrouridines substituted with different groups in the 3' and 5' positions were also studied. For monoacyl compounds the mass spectra are not suitable for distinguishing between isomers owing to thermal transacylation reactions in the sample probe of the mass spectrometer. However, these difficulties could be resolved by additional derivatization. When the substituents were acetyl, acetyl-d_3, trifluoroacetyl, pivaloyl or trimethylsilyl it was found that specific fragmentations occurred which could identify the position of the substituent. These fragmentations often resolve earlier ambiguities in the interpretation of mass spectra of 2,2'-anhydropyrimidine derivatives. In a similar way it may be possible to extend the method to characterizing derivatives of natural nucleosides.

Detailed reports of this work have been submitted to ORGANIC MASS SPECTROMETRY for publication.

Dissociative Electron Attachment to Maleic and Succinic Anhydride[†] [‡]

C. D. Cooper
University of Georgia, Athens, Georgia 30601
and
R. N. Compton, H. C. Schweinler, and V. E. Anderson
Health Physics Division, Oak Ridge National Laboratory
Oak Ridge, Tennessee 37830

Long-lived metastable ions, $C_4H_2O_3^{-*}$ (252), $C_3H_2O_2^{-*}$ (41), $C_3H_2O^{-*}$ (62), $C_2O_3^{-*}$ (130), and CO_2^{-*} (60),[1] were produced by dissociative electron attachment to maleic anhydride. Correspondingly, $C_3H_4O_2^{-*}$ (150) and CO_2^{-*} (26)[1] were observed from succinic anhydride. The number in parentheses is the lifetime for each ion in microseconds at the peak in the cross section. Lifetimes of $C_4H_2O_3^{-*}$, $C_3H_4O_2^{-*}$, and $C_2O_3^{-*}$ decrease with increasing energy of the incident electrons. Broad time-of-arrival distributions of the neutral beams in a TOF mass spectrometer indicate that $C_3H_4O_2^{-*}$, $C_3H_2O_2^{-*}$, $C_3H_2O^{-*}$, and $C_2O_3^{-*}$ dissociate following autodetachment. Theoretical analyses of the shape of the neutral peak for $C_3H_4O_2^{-*}$ indicate a dissociation energy of ~ 0.3 eV, assuming that the dissociation products are C_2H_4 and CO_2. Appearance potentials of the above ions and of several other weak ions which were observed are included in Tables 1 and 2 along with cross section data. Cross section values were determined by comparison with the O^-/O_2 cross section at 6.4 eV (1.5×10^{-18} cm^2), utilizing ion gauge readings for the pressure measurements.

Table 1
Negative Ions from Maleic Anhydride
$C_4H_2O_3$

Negative Ion	Energy at Maximum Intensity (eV)	σ (cm^2) $\times 10^{18}$	Lifetime (μsec)
$C_4H_2O_3^-$	0	33	250*
$C_2H_2CO_2^-$	2.3	0.6	40 b
$C_2H_2CO^-$	2.8	0.2	58 b
$C_2O_3^-$	1.2	0.02	117* b
	0	0.004	
C_3OH^-	2.8	0.01	
C_3O^-	6.4	0.02	
C_2OH^-	4.0	0.01	
	8.0	0.03	
CO_2^-	3.1	3.5	60
$C_2H_2^-$	4.1	0.01	
C_2H^-	7.6	0.45	
O^-	7.6		
CO^- or $C_2H_4^-$	0	0.004	

*Energy dependent. b-Neutral peak is broader than ion peak.

[†]Research sponsored by the U. S. Atomic Energy Commission under contract with Union Carbide Corporation. [‡]To be published in J. Chem. Phys.

[1]C. D. Cooper and R. N. Compton, Chem. Phys. Letters 14, 29 (1972).

Table 2
Negative Ions from Succinic Anhydride
$C_4H_4O_3$

Negative Ion	Energy at Maximum Intensity (eV)	$\sigma(cm^2) \times 10^{18}$	Lifetime (μsec)
$C_4H_2O_3^-$	0	0.05	
$C_4H_3O_3^-$	0	0.007	
	1.8	0.08	
$C_2H_4CO_2^-$	1.1	29	145* b
$C_2H_4\dot{C}O^-$	1.0	0.002	
$C_2OH_2^-$	7.2	0.001	
CO_2H^-	1.1	0.003	
CO_2^-	1.7	0.4	26
$C_2H_3^-$	1.1	0.006	
	6.5	0.05	
	8.7	0.02	
$C_2H_2^-$	1.8	0.03	
CH_2^-	9.0	0.003	
OH^-	9.0	0.005	
O^-	8.2	0.03	

*Energy dependent. b-Neutral peak is broader than ion peak.

Anions Produced by Cesium Collisions with Succinic and Maleic Anhydride[†] [‡]

R. N. Compton and P. W. Reinhardt
Health Physics Division, Oak Ridge National Laboratory
Oak Ridge, Tennessee 37830

and

C. D. Cooper
Department of Physics, University of Georgia
Athens, Georgia 30601

A neutral cesium beam was produced by allowing charge exchange between a Cs^+ beam and neutral cesium vapor. Collisions of the neutral cesium with maleic anhydride produced $C_4H_2O_3^-$, $C_3H_2O_2^-$, $C_3H_2O^-$, and CO_2^{-*}. Correspondingly, $C_3H_4O_2^-$ and CO_2^{-*} were observed from succinic anhydride. The cross sections at threshold for negative ion production appear to be a step-function for some but not all ions. In general, the thresholds are close to those observed for dissociative electron attachment. Parent negative ions of maleic anhydride were observed to be stable, and a preliminary measurement of its threshold gives the electron affinity of maleic anhydride to be ~ 1.3 eV. The mean lifetime of CO_2^{-*} was measured to be the same (60 ± 10 μsec) when produced by cesium collision with either maleic or succinic anhydride or by electron collision with maleic anhydride.

[†]Research sponsored by the U.S. Atomic Energy Commission under contract with Union Carbide Corporation.

[‡]To be published in J. Chem. Phys.

NEGATIVE ION FORMATION IN FLUOROCARBON COMPOUNDS*

J.M. Madson and J.H. Mullen
McDonnell Douglas Research Laboratories
McDonnell Douglas Corporation, St. Louis, Mo. 63166

This paper presents measurements of negative ion formation resulting from the interaction of various fluorocarbon compounds with an argon plasma at a gas temperature of 2100 K. These measurements are part of a program to determine the effectiveness of various chemicals in removing electrons by electron attachment from a high temperature (1500 to 3000 K) flowing plasma. High temperature electron attachment information is important for the modification of shock-ionized flow fields which interfere with communication and navigation systems of vehicles during planetary entry. The deleterious effects of these shock-ionized flows can be reduced by the injection of electrophilic molecules into the flow field where these molecules act as electron scavengers.

The experimental laboratory apparatus used for these investigations shown schematically in Fig. 1 has been described elsewhere[1]. An argon induction plasma is expanded isentropically into a reaction channel where it interacts with supersonically injected electrophilic molecules (target molecules) for approximately 10 μsec. The flowing plasma undergoes a free jet expansion into a low pressure chamber where the centerline core flow is sampled with a conical extractor nozzle. The sampled species are then mass analyzed with a quadrupole mass spectrometer.

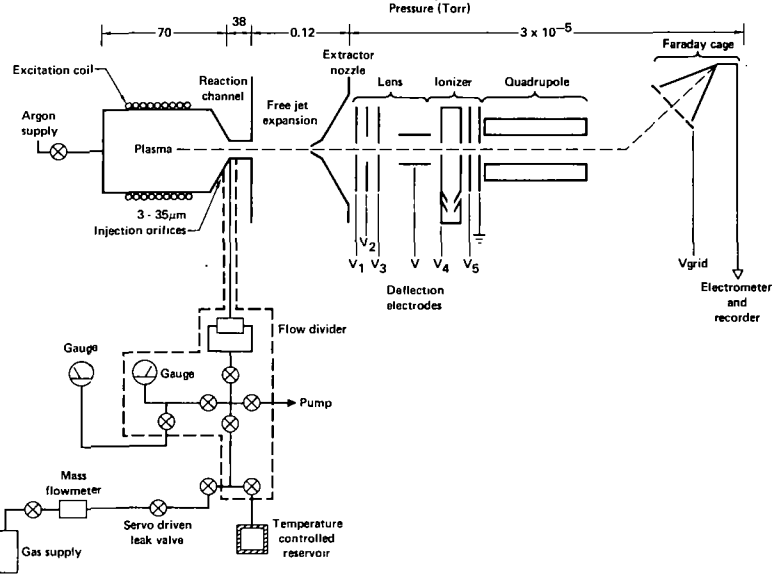

Fig. 1 Schematic representation of experimental apparatus

Target molecules are injected through three 35 μm injection orifices located 120 deg apart around the circumference of the reaction channel. The three identical injection arms are connected to a cylindrical flow divider chamber which provides equal backpressure to each of the orifices. Injection of gaseous target molecules is metered and controlled by a mass flowmeter - servo leak valve system. For injection of compounds normally liquid at room temperature, the temperature controlled reservoir and valve system shown within the dashed lines of Fig. 1 are used. The injection mass flow rate is controlled by the backpressure on the orifices which is determined by the vapor pressure of the compound at the reservoir temperature.

High temperature electron attachment measurements with N_2O and SF_6 using this system have been previously reported[2]. The present measurements of negative ion formation in three fluorocarbons at 2100 K are compared with those in N_2O and SF_6. The compounds investigated are (1) dibromotetrafluoroethane $CBrF_2$ - $CBrF_2$ (Freon 114B2), (2) perfuorodimethylcyclobutane C_6F_{12} (Freon C-51-12), and (3) hexafluoroethane - nitrous oxide C_2F_6/N_2O (Freon 116/N_2O) mixture in 90/10 ratio by weight. The first two fluorocarbons are room temperature liquids and the third is a gas.

*Research supported by Air Force Cambridge Research Laboratories under Contract F-19628-71-C-0024.

Figures 2 and 3 show the normalized negative ion currents resulting from argon plasma - SF_6, C_6F_{12}, $CBrF_2$-$CBrF_2$, C_2F_6/N_2O and pure N_2O reactions. In both these figures the negative ion currents have been normalized to the maximum negative ion current collected for the particular compound. For example, in Fig. 2 for 0.05 mole % of $CBrF_2$-$CBrF_2$ in argon the Br^- ion is approximately 10% of the F^- ion. The initial slope of the ion current curves in these two figures is an indication of the negative ion formation rate in each compound. Thus the curves in Fig. 3 indicate that the O^- formation rate from N_2O is much slower than that for F^- from C_2F_6/N_2O mixture. Effects of non-uniform injection were observed for both $CBrF_2$-$CBrF_2$ and C_6F_{12} at about 0.06 mole % injection. At this injection rate the reservoir pressure and temperature correspond to the boiling point of the compounds.

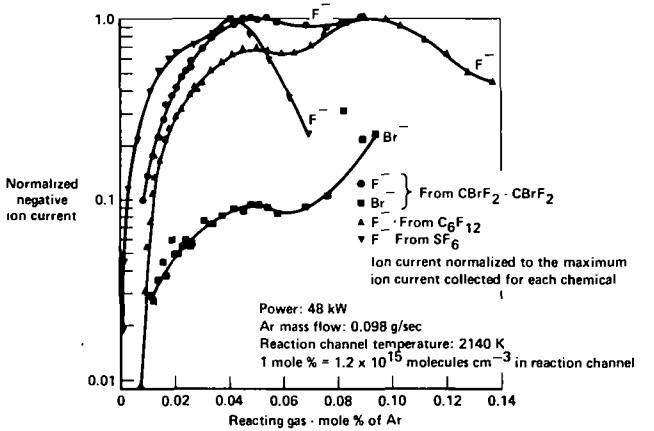

Fig. 2 Normalized negative ion current resulting from argon plasma - SF_6, C_6F_{12} and $CBrF_2$ - $CBrF_2$ reactions

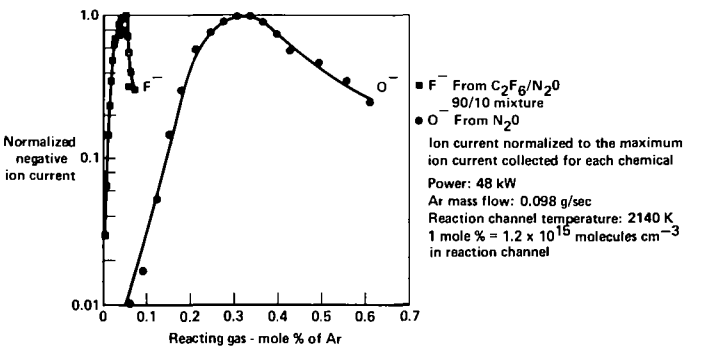

Fig. 3 Normalized negative ion current resulting from argon plasma - N_2O and C_2F_6/N_2O mixture reactions

In Fig. 4 the electron scavenging effectiveness, as indicated by negative ion formation for each compound is compared with that for SF_6. The comparison is made over a range of target gas concentrations which include the initial slopes of the ion current curves. Under the conditions of these measurements SF_6 is the most effective electron scavenger of the compounds/mixture listed, especially when injected in small concentrations. C_2F_6 approaches SF_6 in effectiveness at somewhat higher concentrations (~ 0.03 mole %).

Measurements of negative ion formation in these as well as other fluorocarbons is continuing. Furthermore, positive ion formation as well as the effects of dissociation and fragmentation of the molecules in this high temperature environment are being investigated.

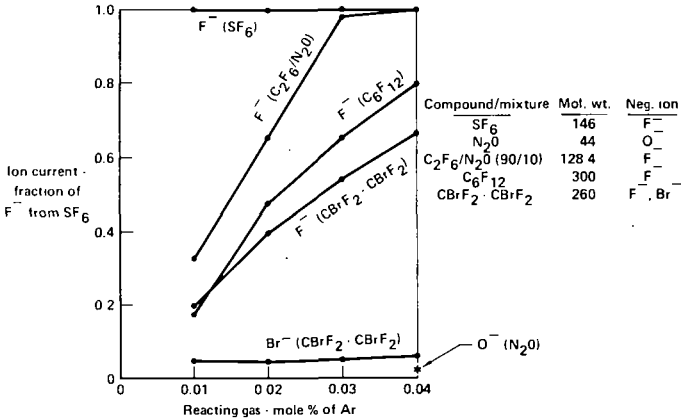

Fig. 4 Negative ion formation compared with F^- formation from SF_6

References

1. *J.H. Mullen, J.M. Madson, L.N. Medgyesi-Mitschang, T.C. Peng, and P.M. Doane, Rev. Sci. Instr. 41, 1746 (1970).*

2. *J.H. Mullen, J.M. Madson, and L.N Medgyesi-Mitschang, Proc. IEEE, 59, 605 (1971).*

NEGATIVE ION FORMATION AND NEGATIVE ION-MOLECULE REACTIONS IN CYCLOPENTADIENE

P. W. Harland, A. Di Domenico and J. L. Franklin

Department of Chemistry

Rice University

Houston, Texas 77001

The low pressure source of a Bendix time-of-flight mass spectrometer has been employed for a study of positive and negative ion formation in cyclopentadiene (C_5H_6). Six negative ions in the mass spectrum of C_5H_6 have been investigated and particular attention has been paid to the cyclopentadienyl negative ion ($C_5H_5^-$). The appearance potential data for $C_5H_5^+$ and $C_5H_5^-$ ion formation were used to estimate the following previously unknown thermochemical parameters: $\Delta H_f(C_5H_5^-) = 19 \pm 2$ kcal mole^{-1}, $\Delta H_f(C_5H_5) \leq 70 \pm 5$ kcal mole^{-1}, $\Delta H_f(C_5H_5^+) \leq 273 \pm 4$ kcal mole^{-1}, $EA(C_5H_5) \leq 2.2 \pm 0.3$ eV and $D(C_5H_5\text{-}H) \leq 3.9 \pm 0.2$ eV. A high pressure source was employed to carry out negative ion-molecule proton transfer and proton plus hydrogen transfer reactions between C_5H_6 and a variety of reactant ions. An evaluation of the energetics for these processes provided a second approach for the estimation of a value for $\Delta H_f(C_5H_5^-)$ and also gave an upper limit of 57 kcal mole^{-1} for $\Delta H_f(C_5H_4^-)$.

Published: J. Chem. Phys. 56 5299 (1972)

Dissociative Attachment in H_2S, C_2H_2, H_2CO and their Deuterated Homologues

Florence FIQUET-FAYARD, Michel TRONC and Roger AZRIA
Laboratoire de Collisions Electroniques,
Université Paris-Sud, Centre d'Orsay, 91405 ORSAY (France)

In C_2H_2, four negative ions peaks are observed as a function of energy for dissociative attachment of electrons, with a total ionization chamber. The first peak is $C_2H^-(C_2D^-)$, the second contains $H^-(D^-)$, C_2^- and $C_2H^-(C_2D^-)$ and the two last peaks are C_2^-.

We have measured the absolute cross section and determined the ionization efficiency curves : the onset of the ionization curve for C_2H^- is 2.3 ± 0.1 eV ; this curve exhibit the shape characteristic of a vertical onset process and the cross section at the maximum is $(2.2 \pm 0.3) \times 10^{-20}$ cm^2. The theoretical dissociation limit is significantly lower (1.2 eV), and the discrepancy is attributed to a bump in the potential surface. This bump is due to a conical (Teller) intersection. A large isotope effect is observed for the peak $C_2H^-(C_2D^-)$ and a small one for the peaks C_2^-. The possible states of the fragments have been determined by kinetic energy considerations.

A full account of these results, and other results in H_2CO, will be published in Journal de Physique.

In H_2S and its deuterated homologue, we have studied the formation of H^- and D^- by dissociative attachment at 5.35 eV. These experimental results show a competition between the breaking of either $HS-D^-$ or $DS-H^-$ bond. This effect is well explained in a theoretical model based on the Franck-Condon principle. In this model the ground state is represented by a gaussian wave-packet ; the time evolution of this wave-packet, as given by time-dependent quantum mechanics, as been studied ; the packet enters preferably the H^- + SD valley but a substantial density is found in the D^- + SH valley, because of the rapid spreading of the packet. Full results will be published in the Journal of Chemical Physics.

NEGATIVE ION PROCESSES IN NITROUS OXIDE AND CARBON DIOXIDE

R.P. CLOW and T.O. TIERNAN
Aerospace Research Laboratories, Chemistry Research Laboratory
Wright-Patterson Air Force Base, Ohio 45433

Recently reported theoretical[1,2] and experimental[3] studies dealing with the negative molecular ions of nitrous oxide and carbon dioxide have prompted a systematic study of the negative ion processes in these systems in our laboratory. In addition, it was of interest to determine whether negative-ion electron transfer reactions to N_2O and CO_2 could be employed to estimate the electron affinities of these species, in the manner which we have recently applied to other molecules[4-6]. Ferguson and coworkers have suggested that formation of N_2O^- and CO_2^- from the corresponding neutral molecules may involve an activation energy as large as 1eV[1,2]. This might be expected because both N_2O and CO_2 are linear (16 valence electron systems), while theory predicts that the 17 electron systems of N_2O^- and CO_2^- should be bent[7]. In any case, the electron affinities are not well established.

The ARL double mass spectrometer which has been described previously[8,9] was employed for these experiments. Reactant ions were produced by electron impact or in some cases by ion-molecule processes in the first stage ion source. The energy resolution of the incident ion beam in these experiments is on the order of $\pm$ 0.3eV (lab).

Cross sections for the negative ion processes in N_2O and CO_2 and their dependences on ion translational energy were determined. Representative values of these cross sections and measured reaction thresholds (in cases where thresholds were observed), are listed in Tables I and II for N_2O and CO_2 respectively. All cross section values reported were determined relative to the cross section for the O^-/NO_2 charge transfer reaction, for which a value of $63X10^{-16}cm^2$ has been reported at 0.3eV O^- energy[10].

It is apparent from Tables I and II that a large number of negative ion processes, both endothermic and exothermic were observed with N_2O and CO_2. Owing to space limitations, only the O^-/CO_2 interaction will be discussed in detail here. In Figure 1, relative cross sections for the several reaction channels from the O^-/CO_2 collision are plotted as a function of translational energy. At energies below 2eV, only the exothermic (or thermoneutral) isotope switching reaction (producing O^-) is observed. At higher energies, both CO_2^- and O_2^- appear, having energy thresholds of 2.6 and 4.6eV respectively. The fine structure observed in the cross section dependences for the latter two products was quite reproducible and appears to be real. While the origin of this structure for O_2^- is not clear, the CO_2^- structure apparently arises because of competition among the several reaction channels. Experiments with isotopically labelled reactants show that the maximum in the CO_2^- plot at 55eV is due to a resonant charge transfer process. The dip in the CO_2^- relative cross section at approximately 7eV is likely due to the opening of the O_2^- reaction channel, which onsets at 4.6eV. A close examination shows that the CO_2^- curve deviates from linearity exactly at the O_2^- threshold.

Other isotopic experiments in which $^{16}O^-$ is impacted on $C^{18}O^{18}O$, indicate that the reactant O^- species is always retained in the O_2^- product. The CO_2^- product behaves differently, however. At energies above about 9eV, only $C^{18}O^{18}O^-$ is observed as a charge transfer product, while at lower energies isotope mixing occurs to an increasing degree, and $C^{16}O^{18}O^-$ is also detected. At about 4.0eV, the theoretically expected ratio of $C^{16}O^{18}O^-/C^{18}O^{18}O^- = 2/1$, (assuming a CO_3^{-*} intermediate), was observed. It should be noted that CO_3^- is an observed product from the reaction of O_2^- with CO_2.

Some qualitative conclusions concerning the electron affinity of N_2O can be drawn from the cross section values and the thermochemical data of Table I. Since both reactions I-3 and I-10 are apparently exothermic, the E.A.(N_2O) must be comparable to E.A.(NO) ~ 0.09eV. Observance of the exothermic reaction I-9 suggests that EA(N_2O) is less than EA(O_2) = 0.43eV. If it is assumed that the reactant and product ions are formed without internal excitation energy and that the product species are formed with zero translational energy at threshold, then the measured threshold values can be used to obtain a quantitative electron affinity value for nitrous oxide.

For the generalized endothermic reaction having a threshold, E_{CM},

$$A^- + B + E_{CM} \rightarrow B^- + A \qquad H_R \qquad (1)$$

one may write,

$$H_R = Hf(B^-) + Hf(A) - Hf(A^-) - Hf(B) - E_{CM}$$

$$= Hf(B) - EA(B) + Hf(A) - Hf(A) + EA(A) - Hf(B) - E_{CM} \qquad (2)$$

At the threshold, $H_R = 0$, and one obtains:

$$EA(B) = EA(A) - E_{CM} \qquad (3)$$

Using this method, a value $E.A.(N_2O) = 0.50eV$, was obtained from the I-2 threshold value. A value of 0.25 was obtained from a similar treatment of the thresholds for I-2 and I-5, while a value of 0.38 was obtained from the I-2 threshold and the average value of 0.40eV for the energy of the dissociative electron capture process,

$$e + N_2O \rightarrow O^- + N_2$$

which is derived by averaging the results of Chantry and Wentworth et. al.[12]. From these three results, an average value $E.A.(N_2O) = 0.35 \pm 0.15eV$ was determined. This is in fair agreement with literature values of $0 \pm 0.3eV$ reported by Compton et. al.[13] and a theoretical value of $0.3 \pm 0.2eV$ given by Wentworth, et. al.[12], considering the experimental constraints discussed earlier.

The electron affinity for CO_2 is not as well established by the present studies. Only one value of $EA(CO_2) = 0.5eV$ has been measured from reaction II-7. Instrumental modifications are presently underway to enable measurement of $EA(CO_2)$ from other reactions, and to investigate more fully the role symmetry plays in the formation of the negative molecular ions of N_2O and CO_2. A more detailed description of these studies will be submitted for publication in the Journal of Chemical Physics.

REFERENCES

1. E.E. Ferguson, Advan. Electronic and Electron Phys. 24, 23 (1968).
2. E.E. Ferguson, F.C. Fehsenfeld, and A.L. Schmeltekopf, J. Chem. Phys. 47, 3085 (1967).
3. J.F. Paulson, J. Chem. Phys. 52, 959 (1972), ibid., 52, 963 (1972).
4. C. Lifshitz, B.M. Hughes and T.O. Tiernan, Chem. Phys. Letters 7, 469 (1970).
5. T.O. Tiernan, C. Lifshitz and B.M. Hughes, J. Chem. Phys. 55, 5692 (1971).
6. T.O. Tiernan, B.M. Hughes and C. Lifshitz, Twenty-seventh Symposium on Molecular Structure and Spectroscopy, The Ohio State University, June 13, 1972, Paper K 6.
7. G. Herzberg, "Electronic Spectra of Polyatomic Molecules", (D. Van Nostrand, Princeton, N.J., 1966), p. 319.
8. J.H. Futrell and C.D. Miller, Rev. Sci. Instr. 37, 1521 (1966).
9. B.M. Hughes and T.O. Tiernan, J. Chem. Phys. 55, 3419 (1971).
10. J.L. Paulson, Advan. Chem. Ser. 58, 28 (1966).
11. P.J. Chantry, J. Chem. Phys. 51, 3369 (1969).
12. W.E. Wentworth, E. Chen and R. Freeman, J. Chem. Phys. 55, 2075 (1971).
13. S.J. Nalley, R.N. Compton, H.C. Schweinler, and P.W. Reinhardt, ORNL Report TM 2620 (1971).
14. J.A. Stockdale, R.N. Compton, and P.W. Reinhardt, Bull. Am. Phys. Soc. 14, 260 (1969).
15. P.J. Chantry, J. Chem. Phys. 51, 3380 (1969).

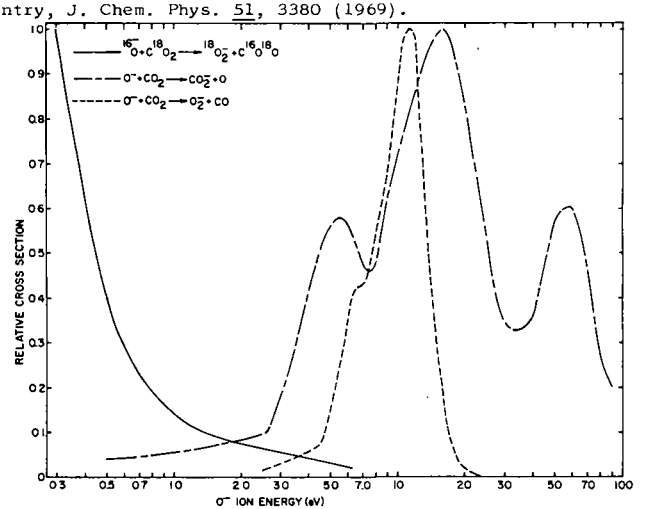

Figure 1. Relative cross sections for the various reactions of O^- with CO_2 as a function of ion energy.

TABLE I. NITROUS OXIDE

	Reaction	Experimental Cross Section cm^2X10^{16}	Energy (eV CM)	Threshold Energy (eV CM)	Previously Reported Cross Section Values (cm^2X10^{16})
1.	$^{16}O^- + N_2{}^{18}O \rightarrow {}^{18}O^- + N_2{}^{16}O$	5.38	0.2	--	
2.	$O^- + N_2O \rightarrow NO^- + NO$	6.01	0.2	--	1.4[a], 30[b], 1.5[c], 3[d]
3.	$NO^- + N_2O \rightarrow N_2O^- + NO$	1.36	0.2	--	0.5[a], 1[d]
4.	$NO^- + N_2O \rightarrow O^- + N_2 + NO$	3.02	3.8	1.0	
5.	$O_2^- + N_2O \rightarrow O^- + O_2 + N_2$	3.39	13.7	1.0	
6.	$S^- + N_2O \rightarrow NS^- + NO$	3.15	2.2	1.0	
7.	$S^- + N_2O \rightarrow SO^- + N_2$	1.34	4.0	3.2	
8.	$S^- + N_2O \rightarrow O^- + S + N_2$	1.23	4.9	1.5	
9.	$N_2O^- + O_2 \rightarrow O_2^- + N_2O$	35.0	0.1	--	
10.	$N_2O^- + NO \rightarrow NO^- + N_2O$	6.77	0.1	--	
11.	$N_2O^- + Ar \rightarrow O^- + N_2 + Ar$	22.6	2.9	0.78	
12.	$Cl^- + N_2O \rightarrow O^- + N_2 + Cl$	0.62	18.4	5.4	
13.	$Br^- + N_2O \rightarrow O^- + N_2 + Br$	1.99	25.0	6.0	
14.	$I^- + N_2O \rightarrow O^- + N_2 + I$	2.35	29.6	5.6	

a. Ref. 2

b. Ref. 6

c. Ref. 14

d. Ref. 15

TABLE II. CARBON DIOXIDE

	Reaction	cm^2X10^{16}	Energy (eV CM)	Threshold Energy (eV CM)	Previously Reported Cross Section Values[a] (cm^2X10^{16})
1.	$^{16}O^- + C^{18}O_2 \rightarrow {}^{18}O^- + C^{16}O^{18}O$	53	0.2	--	
2.	$O^- + CO_2 \rightarrow CO_2^- + O$	0.26	11.0	2.0	0.35
3.	$O^- + CO_2 \rightarrow O_2^- + CO$	0.25	7.0	3.2	0.20
4.	$NO^- + CO_2 \rightarrow CO_2^- + NO$	0.60	8.9	3.6	0.80
5.	$NO^- + CO_2 \rightarrow O^- + CO + NO$	1.46	13.7	5.8	
6.	$O_2^- + CO_2 \rightarrow CO_3^- + O$	0.20	4.0	2.5	0.12
7.	$O_2^- + CO_2 \rightarrow CO_2^- + 2O$	0.30	9.8	5.0	0.26
8.	$O_2^- + CO_2 \rightarrow O^- + CO_2 + O$ $\rightarrow O^- + CO + O_2$	3.85	8.8	4.5	
9.	$Cl^- + CO_2 \rightarrow O^- + CO + Cl$	0.12	18.0	10.3	
10.	$Br^- + CO_2 \rightarrow O^- + CO + Br$	2.45	25.7	12.2	
11.	$I^- + CO_2 \rightarrow O^- + CO + I$	2.81	24.5	10.9	

a. Ref. 2

LOW ENERGY ELECTRON ATTACHMENT TO GASEOUS GROUP 6B OXIDES

J. Ling-Fai Wang, F. Petty, J. L. Margrave and J. L. Franklin

Department of Chemistry

Rice University

Houston, Texas 77001

ABSTRACT

Solid CrO_3, MoO_3 and WO_3 were vaporized from a Knudsen cell into the source of a time-of-flight mass spectrometer in order to study their negative ions in the gas phase. Species observed include CrO_3^-, $(CrO_3)_2^-$, $(CrO_3)_3^-$, MoO_3^-, $(MoO_3)_2^-$, $(MoO_3)_3^-$, WO_3^- and $(WO_3)_2^-$. Dissociative resonance electron attachment processes of the gas phase species were studied and measurements were made of the appearance potentials of the negative ions produced. From the energetics of the fragmentation we reaffirmed the finding of previous positive ion mass spectrometry studies that trimer, tetramer and pentamer were the most abundant neutral species in the vapor. All the negative ions observed were formed through dissociative attachment from the higher polymer neutrals. The appearance potentials obtained were used to estimate the previous unknown thermochemical data.

Mass Spectra of Juglone Derivatives. Hydroxy, Acetyl and Ethyl Substituents. THEODORE L. FOLK*, HARJIT SINGH** and PAUL J. SCHEUER, Dept. of Chemistry, Univ. of Hawaii, Honolulu, HI 96822

Nowhere is the utility of mass spectrometry better illustrated than in natural product structure elucidation problems. In 1966, Moore et al. reported the isolation of thirty different pigments from the sea urchins Echinothrix diadema Linn. and E. calamaris Pallis.[1] Of these thirty compounds, several 5-hydroxy-1,4-naphthoquinone (juglone) derivatives were later synthesized as a final proof of structure.[2] As the amounts of these compounds ranged as low as a few milligrams, mass spectrometry proved to be the answer for both conservation of material and providing valuable information as to the structures. Discussion of the fragmentation routes will include references to some acetylnaphthoquinone decomposition mode generalizations proposed by Becher et al.[3]

The complete paper will be submitted to Organic Mass Spectrometry for possible publication.

*Presently with The Goodyear T. & R. Company, Akron, OH.
**Present address: Panjab Agricultural University, Ludhiana, India.

[1]R. E. Moore, H. Singh and P. J. Scheuer, J. Org. Chem., 31, 3645 (1966).

[2]H. Singh, T. L. Folk and P. J. Scheuer, Tetrahedron, 25 5301 (1969).

[3]D. Becher, C. Djerassi, R. E. Moore, H. Singh and P. J. Scheuer, J. Org. Chem., 31, 3650 (1966).

MASS SPECTRA OF ORGANIC COMPOUND IV

Electron Impact and Chemical Ionization Spectra of C-glucosyl-compounds of Aromatic Aglycones and their Derivatives

H. G. Boettger

For a number of years we have studied the behavior of organic pigments such as carotenoids and porphyrins under electron impact conditions. More recently we became interested in flavonoid pigments. One of the reasons was our involvement in the elucidation of the mechanisms, which make certain polyhydroxy compounds expel an oxygen atom under electron impact while others will not. We will report about this subject elsewhere. Another, perhaps less mundane, but certainly more practical reason was a request to look at two samples of a certain flavonoid derivative. These samples had been attained by methylating Lucenin at the phenolic hydroxyl-groups and subsequently peracetylating the remaining hydroxyl-groups.

Fig. 1 shows the formula of the compound which should have been obtained, namely 3',4',5,7,-Tetramethoxy-peracetyl-lucenin. The spectrum of the first sample (Fig.2) shows an acceptable molecular ion at m/e=1002 and ions corresponding to the expected fragmentation reactions. The spectrum of the second sample (Fig. 3) was very similar except that the masses of the molecular ion and of certain of the fragments had been shifted by 14 mass units. Careful study of the spectra, which were obtained with a temperature programmed probe, showed that the sample consisted of a series of compounds most of which contained at least one ethoxy-group in place of one of the phenolic methoxy groups. Furthermore, there were indications that there were very small amounts of compounds having additional methoxy-groups replaced by ethoxy-groups. The conclusion was that the methyliodide, which was used in the preparation, had been contaminated with ethyl iodide. After this rather successful demonstration of the effectiveness of mass spectrometry, we were induced to become involved in a more detailed investigation of the mass spectra of flavonoid pigments as a tool in the structural analysis of these compounds.

A review of the literature (1) and the investigation of some model compounds revealed the following primary fragmentations:

(1) The pyranose rings undergo successive cleavages as shown in Fig. 1. These reactions have been confirmed by mass measurement and metastable ions.

(2) The cleavage in the heterocyclic ring resulted in the loss of a phenyl-acetylene fragment followed by the loss of C≡O. It was this reaction which showed that in the major portion of the Tetramethyl-peracetyl-lucenin-2 the ethoxy-group was lost with the phenyl ring.

(3) The third major fragmentation pathway consists of the loss of C=O followed by the loss of the phenyl-acetylene group and/or $C_4H_5O_4R_4$, where R depends upon the substituent on the glucosidic OH-groups.

In the larger, more complex molecules, which require derivatization to enhance their volatity, these structurally significant fragmentations are more or less extensively masked by multiple losses of derivative groups which by themselves do not provide much structural information. These usually consist of the loss of ketene and/or acetyl groups, etc. from actylated compounds and methoxy- and methyl-groups from methylated compounds. An example of this is shown in Fig. 3.

In order to find a way to simplify the analysis, we investigated the spectra of the methyl and/or acetyl derivatives of a wide variety of flavonoids as well as the underivatized compounds under EI and CI conditions. The results of this investigation can be summarized as follows:

(1) CI helps us little, if anything, in this case. The spectra of the simple aglycones and other underivatized low molecular weight glucosides are simplified as expected. But as is shown in Fig. 4, the EI spectra are already quite simple and are dominated by the structurally important fragments.

In case of the derivatized larger molecules, CI presented a problem which we had not expected to the extent to which it occurred. The undesirable losses of acetic acid and/or methanol were enhanced to such a degree where the structurally significant processes were almost totally suppressed. Therefore, in this phase of our work, we made no more use of CI.

(2) The EI spectra increase in simplicity as we proceed from peracetyl to permethyl derivatives.

(a) Peracetyl derivatives yield even in the case of small flavonoid molecules at best unreproducible spectra due to side reactions leading to undesirable artifacts.

(b) Underivatized compounds show extensive fragmentation and weak molecular ions in those cases where spectra can be obtained without thermal decomposition.

(c) Methylated-Phenolic-Hydroxyl/peracetylated-glycosyl-hydroxyl derivatives show a good molecular ion and a limited amount of structurally significant fragments.

(d) Permethylated derivatives always produce good molecular ions and

structurally significant fragments.

These results are demonstrated in Fig's. 5, 6, and 7. Unfortunately, time does not permit us to go into the details of these spectra. The work will, however, be published in full detail later on.

I wish to thank Dr. Horowitz from USDA for the samples, Dr. Yinon for his help with the CI spectra, Miss Holwick for her efforts in preparing some of the derivatives.

This paper presents the results of one phase of research carried out at the Jet Propulsion Laboratory, California Institute of Technology, under Contract No. NAS 7-100, sponsored by the National Aeronautics and Space Administration.

(1) 'Massenspectrometrische Untersuchung Einiger Naturlicher C-Glukosyl-Verbindungen', A Prox Tetrahedron, 24, 3697-3715 (1968).

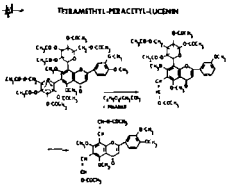

Figure 1

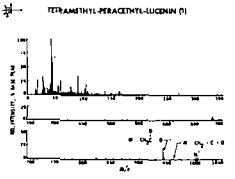

Figure 2

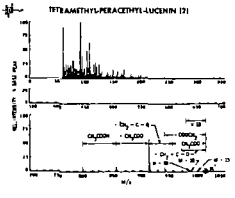

Figure 3

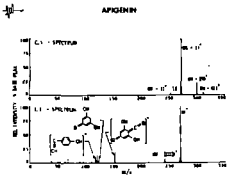

Figure 4

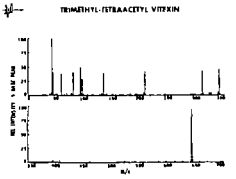

Figure 5

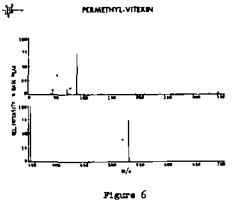

Figure 6

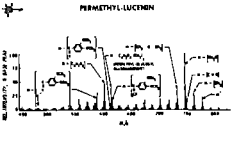

Figure 7

^{18}O-Labeled Sugars: Identification of Specific Oxygen Atoms

William E. Seifert, Jr. and Richard M. Caprioli
Department of Chemistry, Purdue University
West Lafayette, Indiana 47906

In the course of studies of carbohydrate metabolism of cells grown on various nutrients labeled with ^{18}O, it became necessary to investigate the fragmentation pattern of glucose on electron impact in the mass spectrometer. The purpose of this work was to identify the individual oxygen atoms of glucose in the various fragment ions permitting the measurement of the ^{18}O abundance incorporated into any position of glucose. The pentaacetyl derivative was used because of the low volatility of glucose. Several glucoses labeled with ^{18}O in specific positions were prepared and were used as standards.

EXPERIMENTAL

(1-^{18}O)Glucose[1] containing an enrichment of approximately 54 atom % excess in position 1, (2-^{18}O)glucose[2] containing approximately 34 atom % excess in position 2, and (6-^{18}O)glucose[4] containing approximately 48 atom % excess ^{18}O in position 6, were prepared as previously described. (3-^{18}O)Glucose was prepared by the oxidation of 1,2:5,6-diisopropylideneglucofuranose to 1,2:5,6-diisopropylidenehexofuranose-3-ulose followed by hydration with $H_2{}^{18}O$[3]. The hydrate was reduced with $NaBH_4$ to give a mixture of (3-^{18}O)diisopropylideneglucose and (3-^{18}O)diisopropylideneallose. These compounds were separated by gas chromatography and subsequently hydrolyzed to give (3-^{18}O)glucose and (3-^{18}O)allose. The allose was the major product, containing a considerably greater ^{18}O abundance (approximately 26 atom % excess in position 3). Since the mass spectra of glucose and allose are virtually identical, (3-^{18}O)allose was used for these studies.

All mass spectra were obtained from a CEC 21-110B double-focusing mass spectrometer at an ionizing voltage of 70 eV. Metastable ions were recorded to verify some of the transitions involved using the IKES or H.V. scanning technique with a modified Hitachi-Perkin Elmer RMH-2 double-focusing mass spectrometer[4].

Peracetylation was accomplished on treatment of the hexose with an acetic anhydride-HCl mixture (100:1) for 5 hr. at 80° followed by removal of the excess reagents under vacuum.

RESULTS AND DISCUSSION

The isotopic abundance of some of the major ions obtained from the mass spectra of the variously labeled peracetylated hexoses is given below.

m/e	(1-^{18}O) glucose	(2-^{18}O) glucose	(3-^{18}O) allose	(6-^{18}O) glucose
347	100	100	100	100
331	9	100	100	100
317	94	94	100	10
288	91	100	-	100
245	85	56	77	13
242	0	100	0	100
211	0	0	85	44
200	0	82	0	94
169	0	65	46	94
157	0	94	0	0
131	95	0	4	80
115	0	91	0	0

It can be seen from these results that selected ions can be used to measure ^{18}O incorporation in certain positions. However, since positions 4 and 5 of glucose were not specifically labeled, it was necessary to investigate the fragmentation pattern on pentaacetylglucose in order to identify fragments containing these oxygen atoms. The following considerations are based on data obtained in this study together with work previously published by Biemann et. al.[5] and Heyns and Müller[6]. The molecular ion is not observed in the mass spectra of pentaacetylhexoses. Considering only those ions of interest, m/e 347 is formed through loss of one of the acetyl groups; m/e 331 mainly

from loss of the C-1 acetate group; and m/e 317 primarily from loss of the C-6 (CH_2-O-$\overset{O}{\overset{\|}{C}}$-$CH_3$) group. Another series of fragmentations involves as the first step loss of the acetate group at position 3 together with the acetyl group at position 1, giving an ion at m/e 288. This ion can fragment to give m/e 131, 157, and 242. Ions 242 and 157 can further fragment to give m/e 200 and 115, respectively. From these fragmentations, the distribution of the oxygen atoms in the fragment ions can be determined and is given below.

m/e	Position of Oxygen Atoms in the Original Hexose					
347	1	2	3	4	5	6
331	-	2	3	4	5	6
317	1	2	3	4	5	-
288	1	2	-	4	5	6
242	-	2	-	4	-	6
200	-	2	-	4	-	6
157	-	2	-	4	-	-
131	1	-	-	-	5	6
115	-	2	-	4	-	-

It can be seen that ^{18}O incorporation into positions 1 and 6 of the glucose molecule can be measured directly from the ions at m/e 331 and 317, respectively, by comparing them with m/e 347. Similarly, the ^{18}O incorporation into position 3 can be measured from m/e 288. Since isotopic incorporation into positions 1 and 6 can be measured, the abundance of label in oxygen 5 can be determined from m/e 131 by subtraction. The sum of the 2- and 4-oxygens can be found from m/e 157. However, the data do not permit the differentiation of the 2- and 4-oxygen atoms.

This work proved immediately useful in the verification of the position of ^{18}O in (4-^{18}O)glucose which was enzymatically prepared in our laboratory. Fructose-1,6-diphosphate was hydrolyzed by the enzyme aldolase in the presence of $H_2{}^{18}O$. Under these conditions, this reaction produces (2-^{18}O)dihydroxyacetone phosphate and (1-^{18}O)glyceraldehyde-3-phosphate through isotopic exchange of the carbonyl oxygens of the trioses with the labeled water. The reaction is reversible with the equilibrium favoring fructose-1,6-diphosphate. (2,4-^{18}O)Fructose-1,6-diphosphate was then removed from the enzymatic reaction mixture, the ^{18}O was exchanged out of the 2-position, and the product enzymatically converted to (4-^{18}O)glucose. This compound had an isotopic enrichment of approximately 75 atom % excess, assuming the label to be in the 4-position. However, the problem which may arise in this synthesis involves the presence of small amounts of the enzyme triosephosphate isomerase (TPI) in the aldolase preparation. TPI catalyzes the interconversion of the triose phosphates obtained from the aldolase reaction and has an extremely high specific activity. Thus, if TPI was present, one would expect to see some ^{18}O appearing in positions 3 and 5 as well as 2 and 4. From an analysis of the mass spectrum as given above, this was determined not to be the case, i.e., ^{18}O was found only to be present in positions 2 and/or 4. Of course, from the particular method of preparation of this compound, ^{18}O could only be present in position 4. Thus, TPI was not present in sufficient concentration to interfere with the synthesis. In addition, it was found that the mass spectrum of (4-^{18}O)glucose was identical to that of (2-^{18}O)glucose, confirming the fact that only the sum of positions 2 and 4 can be measured easily in the pentaacetyl derivative.

This work demonstrates that the position of oxygen-18 incorporation into glucose either by enzymatic reactions in the living cell or by synthetic means can be distinguished in the mass spectrum of the pentaacetyl derivative. Work is now in progress to examine polysaccharides and other glucose containing compounds obtained from cells grown on various ^{18}O-labeled nutrients.

REFERENCES

1. D. Rittenberg, Laura Ponticorvo, and Ernest Borek, J. Biol. Chem., 236, 1769 (1961).

2. R. M. Caprioli and D. Rittenberg, Biochemistry, 8, 3375 (1969).

3. H. Follmann and H.P.C. Hogenkamp, J. Amer. Chem. Soc., 92, 671 (1970).

4. J. H. Beynon, R. M. Caprioli, W. E. Baitinger, and J. W. Amy, Org. Mass Spectrom., 3, 313 (1969).

5. K. Biemann, D. C. DeJough, and H. K. Schnoes, J. Amer. Chem. Soc., 85, 1763 (1963).

6. K. Heyns and D. Müller, Tetrahed. Lett., 48, 6061 (1966).

THE ENOLIC ION R-C(OH)=$CH_2^{+\cdot}$; STRUCTURE AND REACTIVITY.

R. G. COOKS, R. M. CAPRIOLI, E. G. JONES AND J. H. BEYNON

Department of Chemistry, Purdue University

Lafayette, Indiana 47907

Abstract

The structures of reactive and non-reactive ions formed by McLafferty rearrangement in a variety of ketones are studied using metastable ion abundances and the kinetic energy released in metastable ion fragmentations. The loss of methyl radicals is studied in $C_5H_{10}O^{+\cdot}$ ions and the mechanism delineated for ions formed in an initial configuration corresponding both to ketonic and enolic forms; the major mechanism in both cases appears to involve a common intermediate. Partial scrambling of hydrogen atoms on the C-1 and C-5 carbons and on the oxygen precedes methyl elimination. Loss of neutral ethylene from $C_5H_{10}O^{+\cdot}$ ions is also studied and again the major mechanism occurs via a common species, intermediate in structure between a ketone and an enol; scrambling of hydrogen is much faster for ions that lose ethylene than for those which lose a methyl radical. Keto-ions of formula $C_3H_6O^{+\cdot}$ show no unimolecular loss of methyl. The stable $C_3H_6O^{+\cdot}$ ions generated in the keto and enol forms are shown to preserve their initial structures, confirming the results of ion cyclotron resonance experiments. Reactive $C_3H_6O^{+\cdot}$ ions formed from 2-pentanone molecular ions by McLafferty rearrangement are shown to have the same structures as reactive ions originally generated as enolic structures from 1-methylcyclobutanol.

The paper highlights the relationship between hydrogen scrambling and keto-enol isomerization reactions in aliphatic ketones.

Submitted to Org. Mass Spectrom. for publication.

ELECTRON IMPACT INDUCED FRAGMENTATION OF 5-SUBSTITUTED 3-PHENYL-1,2,4-OXADIAZOLES

L.F.Zerilli, B.Cavalleri and G.G.Gallo
Laboratori Ricerche Lepetit S.p.A., 20158 Milano

A.Selva
Istituto di Chimica del Politecnico, 20133 Milano

The recent interest for the chemotherapeutic properties of some 1,2,4-oxadiazoles prompted us to investigate the electronic impact behavior of a number of 5-aryl-3-phenyl-1,2,4-oxadiazoles. Our previous data[1], namely exact mass measurements and metastable transition determinations by means of the defocussing technique, led us to the conclusion that the main fragmentation process of 3,5-diphenyl-1,2,4-oxadiazole (I) brings about the cleavage of the heterocycle at the bonds 1-5 and 3-4, yielding the fragment $C_7H_5NO^{\ddagger}$, m/e119. This process was confirmed by labelling experiments, namely by the spectrum of 3-phenyl-5-(4-d_1-phenyl)-1,2,4-oxadiazole (II)[2] in which the fragment $C_7H_4DNO^{\ddagger}$ m/e120 is completely absent. Thus, the phenyl of the fragment of mass 119 derives exclusively from the phenyl in position 3 and the alternative heterocycle cleavage at the bonds 1-2 and 3-4[3] is conclusively ruled out. The structure of the major fragment ion $C_7H_5NO^{\ddagger}$ has been interpreted as represented by the isomeric benzonitrile oxide and phenylisocyanate structures, the latter isomerizing irreversibly from the former. The benzonitrile oxide structure is consistent with the $C_7H_5NO^{\ddagger}$ formation by cleavage of the 1-5 and 3-4 bonds.

The study of the spectrum of the deuterated compound allowed us to evidentiate two other primary fragments, less abundant than the one previously discussed. They are the monodeuterated benzonitrile ion, m/e104, and the deuterated benzoyl ion m/e106.

We found it interesting to study the effect of the substituents at the phenyl ring in position 5 on the three primary fragmentation processes indicated in the scheme, taking into account the fact that the benzonitrile oxide ion incorporates only the phenyl ring at position 3, while both benzonitrile and benzoyl ions incorporate the phenyl ring at position 5. The substitutent effect reported in table I can be qualitatively interpreted as inducing the cleavage of given bonds of the heterocycle. In the first column some substituents of various electronic effect are reported, starting from the more electron-withdrawing ones. In the other columns the ratios of the relative abundance of each of the three fragments under examination over the total abundance of the three fragments are reported. It can be observed that going from a strong withdrawing group such as nitro towards a strong electron donor group such as amino, the effect of the substituent dramatically materializes by diminishing the relative intensity of the benzonitrile oxide fragment and by increasing the relative intensity of both the benzonitrile and the benzoyl ions. We have in program the study of quantitative correlations between electronic parameters of the substituents and fragmentation by low energy measurements.

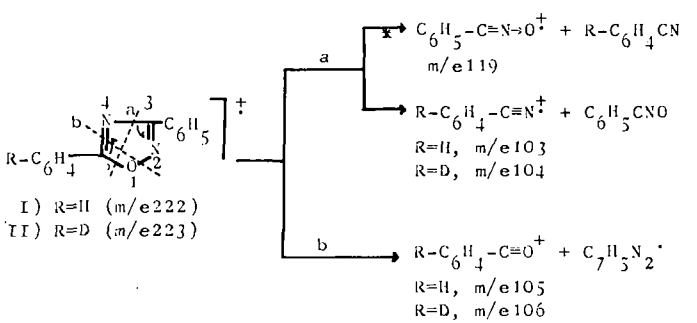

Table I

X		[A]	[B]	[C]
meta	para	[A]+[B]+[C]	[A]+[B]+[C]	[A]+[B]+[C]
	NO_2	1.00	0.00	0.00
NO_2		0.96	0.00	0.04
Cl		0.92	0.03	0.05
	Cl	0.88	0.05	0.08
H	H	0.86	0.05	0.09
	CH_3	0.85	0.06	0.09
CH_3		0.82	0.09	0.09
OCH_3		0.37	0.34	0.29
	OCH_3	0.13	0.57	0.29
NH_2		0.1	0.26	0.64
	NH_2	0.04	0.35	0.63

[A] = relative intensity of $C_6H_5\text{-}CNO^+$

[B] = " " " $R\text{-}C_6H_4\text{-}CN^+$

[C] = " " " $R\text{-}C_6H_4\text{-}CO^+$

References

1) A.Selva, L.F.Zerilli, B.Cavalleri and G.G.Gallo, EUR report 4765 f.i.e., 365 (1971).
2) A.Selva, L.Zerilli, B.Cavalleri and G.G.Gallo, Org.Mass.Spectrom., in press.
3) J.L.Cotter, J.Chem.Soc., 5491 (1964).

To be submitted to Organic Mass Spectrometry for publication.

QUASI-EQUILIBRIUM THEORY OF IONIC FRAGMENTATIONS: FURTHER CONSIDERATIONS*

Cornelius E. Klots
Health Physics Division, Oak Ridge National Laboratory
Oak Ridge, Tennessee 37830

At last year's meeting of this society a reformulation of the quasi-equilibrium theory of unimolecular decompositions was described which by-passes the conceptual difficulties of the transition-state formalism. Among its more interesting consequences were the clarification of the role of angular momentum and the implication of one for tunneling in unimolecular reactions. These findings have prompted a further examination of the formalism.

When Langevin cross-sections for the reverse bimolecular reaction are assumed, very simple expressions are obtained for unimolecular rate constants. The manner in which these formulas depend upon the rotational degrees of freedom of the final products and on details of the potential energy surface has been exposed and the pertinent parameters tabulated.[1] Simple expressions have also been obtained for the kinetic and rotational temperatures of the products.

The recent measurements by Andlauer and Ottinger[2] of unimolecular decay constants of ions at selected energies pose a challenge to the quasi-equilibrium model. We find that two important considerations must be heeded in order to establish a correspondence between theory and experiment. Firstly, heats of formation of many of the pertinent ionic species are not well-known. Tabulations of these quantities have often failed to allow for the kinetic shift in assessing appearance potentials. Hence the endothermicities of ionic fragmentations are largely unknown and must be treated accordingly. Secondly, O. K. Rice noted several years ago[3] that anharmonicities should play an important role in reactions involving loose transition states. Since loose transition states and the use of Langevin cross-sections are equivalent, it is then logically imperative to introduce anharmonicities into the present calculations.

Figure 1 illustrates the totality-of-states for a 4-12 oscillator as a function of energy, measured from the potential minimum. The great excess of states near the dissociation asymptote is evident. We now assume that when an excited ion is in one of these "anharmonic" levels, the remaining degrees of freedom correspond to those of the separated fragments. The totality of states available to the parent ion is then assessed. With these considerations, then, and upon treating the endothermicities as an adjustable parameter, satisfactory agreement between theory and the experiments of Ottinger is achieved.

*Research sponsored by the U. S. Atomic Energy Commission under contract with Union Carbide Corporation.

1. C. E. Klots, Z. für Naturforschung 27a, 553 (1972).
2. B. Andlauer and Ch. Ottinger, J. Chem. Phys. 55, 1471 (1971); Z. für Naturforschung 27a, 293 (1972).
3. O. K. Rice, J. Phys. Chem. 65, 1588 (1961).

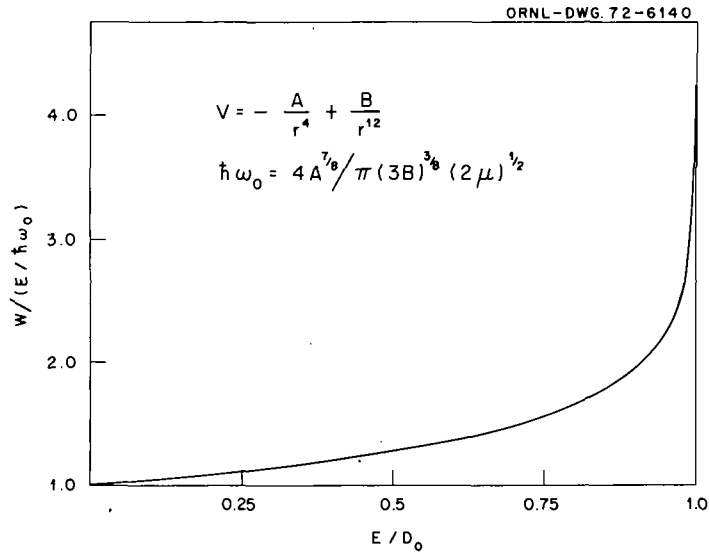

Figure 1. Number of states with energy ≤ E of a 4-12 oscillator, normalized to that of an equivalent harmonic oscillator, as a function of energy.

Interpretation of Fragment Ion Thresholds in Photoionization of Large Molecules

John T. Larkins, James A. Walker, and Henry M. Rosenstock
National Bureau of Standards
Washington, D. C. 20234

It is well known that in ion fragmentation, quasiequilibrium theory predicts large kinetic shifts. Further, internal thermal energy, the slow variation of decomposition rate with ion energy, and the possibility of autoionization and non-ideal threshold law behavior produce a situation such that even in photoionization the meaning of a "threshold" is vague. Model calculations have been carried out for parent ion fragmentation processes in benzene, using known ion heats of reaction wherever possible. It is concluded that the fragmentation processes leading to $C_6H_5^+$ and $C_6H_4^+$ occur from the benzene ion ground state, whereas those leading to $C_4H_4^+$ and $C_3H_3^+$ occur from the first excited state of $C_6H_6^+$ or some isomeric form having a similar heat of formation. It is shown that the activated complex parameters, i.e. entropies of activation, are similar to those of corresponding neutral molecule decomposition processes. It is also shown that quasiequilibrium theory is applicable to each pair of competing processes. The experimental threshold curves indicate large kinetic shifts. These are quantitatively accounted for by the model.

REEVALUATION OF CARBON VAPOR PRESSURES AND THIRD LAW HEATS OF SUBLIMATION*

R. T. Meyer and A. W. Lynch
Sandia Laboratories
Albuquerque, New Mexico 87115

The mass spectrometer has been employed for the determination of partial pressures and heats of sublimation for the carbon vapor species.(1-3) The reported data may be in error, however, due to the omission or incorrect use of conversion factors in transforming the measured ion intensities to partial pressures. Equation [1] provides the conversion to absolute pressures if the absolute pressure for one species, e.g. $P(C_1)$ is known.

$$\frac{P(C_n)}{P(C_1)} = \frac{I^+(C_n)}{I^+(C_1)} \cdot \frac{\sigma(C_1)}{\sigma(C_n)} \cdot \frac{\Delta E(C_1)}{\Delta E(C_n)} \cdot \frac{\gamma(C_1)}{\gamma(C_n)} \cdot \frac{\beta(C_1)}{\beta(C_n)} \qquad [1]$$

The ratio $I^+(C_n)/I^+(C_1)$ is for the measured ion intensities at the same temperature. The conversion factors include ratios of maximum ionization cross sections σ, ionization probabilities at the effective energy of the ionizing electrons ΔE, secondary electron yields of the electron multiplier γ, and spectrometer transmission coefficients β.

Palmer and Shelef empirically derived a modified ionization cross section formula, $\sigma(C_n)/\sigma(C_1) = (1.5)^{n/2}$ for $n > 1$, from experimental data for dimers and monomers. (4) The expanded version of this paper will present compilations of data for molecules having atom ratios of 3/2, 3/1, and 4/1, which show cross sections ratios which agree with values calculated from the modified formula within about 10%. The experimental cross section ratios are generally lower than the values calculated from the additivity rule, $\sigma(C_n)/\sigma(C_1) = n$, using Mann's theoretical values for atomic cross sections. (5)

A mass dependence of the electron multiplier yield has been reported by many investigators. Studies using rare gas ions, alkali metal ions, and isotopes showed that the secondary electron yield generally decreases with increasing mass of the incident ion. Inghram and Hayden, Farber, Ploch, and Ackerman demonstrated that the multiplier yield is inversely proportional to the square root of the ionic mass. (6-9) A theoretical treatment by Parilis and Kishinevskii also predicted this behavior. (10)

Less information exists on the effect of molecularity on secondary electron yield. Data by Inghram and Hayden (6) and by Stanton et al. (11) indicate a weak dependence, whereas results by Petrov (12) for N_2^+ and N^+ and a formula proposed by Lau (13) indicate that no molecularity effect should exist for ions of carbon vapor species at the same acceleration energy.

Computation of the relative ionization probabilities from $\Delta E = EE - AP$, where EE is the energy of the ionizing electrons and AP is the appearance potential of the ion, is believed to be valid based upon the finding by Williams that the shapes of the ionization efficiency curves for the carbon species are nearly the same in the low energy regions. (13)

The transmission coefficient is an instrument factor which probably varies over broad ranges of mass. For the present purposes, ratios of unity are assumed.

The total conversion factors, $CF = [I^+(C_n)/I^+(C_1)]/[P(C_n)/P(C_1)]$, recommended for the conversion of ion intensities to partial pressures are 1.00, 0.93, 0.82, 0.87, and 0.98 for the species C_1, C_2, C_3, C_4, and C_5, respectively. These values are to be compared with Drowart's (2) values of 1.00, 2.30, 3.66, 4.96, and 6.30 and with the JANAF (14) values of 1.00, 3.18, 2.65, 7.13, and 7.44; the latter values were derived from a comparison of the JANAF partial pressures with Drowart's ion intensities.

The recommended value for the total conversion factor for C_3 was applied to the ion intensity and partial pressure data reported by Drowart et al., JANAF, Palmer and Shelef, and Zavitsanos in order to obtain revised values of the absolute vapor pressures. The free energy functions of Stauss and Thiele (15) were used for the reevaluation of

*This work was supported by the U. S. Atomic Energy Commission.

the Second and Third Law heats of sublimation. The values of ΔH_0°, calculated from the data of Drowart et al., JANAF, and Palmer and Shelef, were assigned a weighting factor of one-third each relative to the reevaluated data of Zavitsanos and the recent results of Wachi and Gilmartin (16), which are not subject to a reevaluation using our conversion factors. The averaged values for the Second and Third Laws ΔH_0°'s were 193.5 and 195.1 kcal/mole, respectively. In view of the closeness of these two values, the recommended ΔH_0° for C_3 vaporization is 194.3 kcal/mole. This value is preferred in conjunction with the free energy functions of Strauss and Thiele for the calculation of the absolute vapor pressure of C_3 as a function of temperature. At 3000K, the newly evaluated vapor pressure of C_3 is approximately 2.5 times higher than the value tabulated by JANAF.

REFERENCES

1. W. A. Chupka and M. G. Inghram, J. Phys. Chem., 59, 100 (1955).
2. J. Drowart, R. P. Burns, G. DeMaria, and M. G. Inghram, J. Chem. Phys., 31, 1131 (1959).
3. P. D. Zavitsanos, to be published.
4. H. B. Palmer and M. Shelef, in Chemistry and Physics of Carbon, (P. L. Walker, Jr., Ed.) (Marcel Dekker, Inc., New York, 1968), Vol. 4, pp. 85-136.
5. J. B. Mann, in Recent Advances in Mass Spectroscopy, (K. Ogata and T. Hayakawa, Eds.), University Park Press, Baltimore, Md., 1970, p. 814.
6. M. G. Inghram and R. J. Hayden, A Handbook on Mass Spectroscopy, Nuclear Science Series Report No. 14, National Research Council Publication No. 311 (1954).
7. M. Farber, R. D. Srivastava, and O. M. Uy, J. Chem. Soc. Faraday Trans., January 1972.
8. W. Ploch, Z. Physik 130, 174 (1951).
9. M. Ackerman, F. E. Stafford, and J. Drowart, J. Chem. Phys., 33, 1784 (1960).
10. E. S. Parilis and L. M. Kishinevskii, Soviet Phys.-Solid State, 3, 885 (1960).
11. H. E. Stanton, W. A. Chupka, and M. G. Inghram, Rev. Sci. Inst., 27, 109 (1956).
12. C. La Lau, in Topics in Inorganic Mass Spectrometry, (A. L. Burlingime, Ed.), Wiley-Interscience, New York, 1970, p. 93.
13. C. H. Williams, Paper presented at 18th Annual Conference on Mass Spectrometry and Allied Topics, San Francisco, California, June 1970.
14. JANAF Thermochemical Tables, Second edition, (D. R. Stull and H. Prophet, Eds.), Nat. Stand. Ref. Data Ser., Nat. Bur. Stand., (U.S.), 37, June 1971.
15. H. L. Strauss and E. Thiele, J. Chem. Phys. 46, 2473 (1967).
16. F. M. Wachi and D. E. Gilmartin, Paper presented at 20th Annual Conference on Mass Spectrometry and Allied Topics, Dallas, Texas, June 1972.

RELATIVE PARTIAL PRESSURES OF CARBON VAPOR SPECIES FROM LASER HEATED GRAPHITE*

D3

R. T. Meyer, J. M. Freese, and A. W. Lynch
Sandia Laboratories
Albuquerque, New Mexico 87115

The vapor composition of graphite under pulsed laser or pulsed electron beam heating has been explored previously by Howe (1), Berkowitz and Chupka (2), Zavitsanos (3), Lincoln (4), and Steele (5). A principal purpose has been to extend knowledge of the temperature dependence of the partial pressures of the C_n species to considerably higher temperatures than can be achieved using conventional heat sources. Other goals have included identification and measurement of higher molecular weight, polymeric carbon species for comparison with theoretical treatments of the carbon vapor system. Along with these objectives, the present work has attempted to probe the mode of vaporization associated with laser heating--that is, whether it is free evaporation or equilibrium vaporization in nature--and to assess effective values of laser vaporization coefficients. While our studies have identified C_n species from C_1 to C_{11}, the data to be reported will include only the species C_1 to C_5.

Time resolved mass spectrometry (6,7) was used in conjunction with a Korad K1Q neodymium laser for the vapor composition studies. A Pyroid graphite sample, with its c-face perpendicular to the laser beam, was located within the ion source of a Bendix model 14-107 time-of-flight mass spectrometer approximately 5 cm below the ionizing electron beam (18.6 ev). The laser beam (Q-switched, 25 nsec duration) was focused with telescope optics to an incident energy density of about 50 joules/cm^2. Peak ion intensities of the carbon vapor species were measured immediately after the laser pulse and averaged for several experiments. Measurements of mass loss and total vaporization at higher laser energy densities (1000 to 1500 joules/cm^2) were obtained using a gas phase oxygen titration technique (8). These experiments were conducted with the graphite sample located in a spherical one liter reaction vessel. The gaseous products were quantitatively analyzed with a Bendix model 3015 mass spectrometer.

The relative ion intensities measured for C_1, C_2, C_3, C_4, and C_5 were 1.0, 0.9, 5.1, $\sim$ 0.25, and $\sim$ 0.5, respectively. The ion intensities for C_1, C_2, and C_3 were converted to relative partial pressures for comparison with the equilibrium data reported by JANAF (9) and by Palmer and Shelef (10). The best agreement was obtained at an effective temperature of 4500K assuming that free evaporation occurred; the Langmuir vaporization coefficients reported by Zavitsanos were used ($\alpha(C_1) = 0.24$, $\alpha(C_2) = 0.50$, $\alpha(C_3) = 0.023$)(11).

As the laser energy was varied over an order of magnitude, large changes in the absolute ion intensities of C_1, C_2, and C_3 occurred but with little change in the relative ion intensities. This result implied that the effect of varying the laser energy was to change the amount of material vaporized but not to change the temperature of the condensed phase.

Extension of the pulsed laser heating to incident energy densities of 1000 to 1500 joules/cm^2, using the gas phase titration techniques, yielded mass losses from the graphite sample and amounts of CO + CO_2 produced that were equivalent and also approximately proportional to the laser energy (12). Since the rate of vaporization is proportional to exp ($-\Delta H_s/T$), it was expected that the mass loss would be exponentially related to the laser energy if the sample temperature were increased. However, it was concluded that the increased laser energy mainly increased the amount of material heated to the same high temperature. Calculations of the amount of laser energy possibly absorbed by the graphite showed that vaporization of all C_n species could occur and that a surface temperature of at least 4500K could be achieved.

Comparison of the relative ion intensities for C_1 to C_5 with the laser vaporization data reported by Berkowitz and Chupka (2), Zavitsanos (3), and Lincoln (4) revealed that all of the results were approximately the same within experimental error. The vaporization temperatures estimated by these workers all fell within the range of 4000 to 4500K, which is in agreement with the temperature estimated by Howe (1) from velocity measurements on the expanding vapor. Hence, the relative partial pressures and vaporization temperatures were found to be independent of the operational mode of the laser (normal mode vs. Q-switched) and independent of the laser energy density (50 to 8000 joules/cm^2). The conclusion drawn from all these studies is that the temperature of

*This work was supported by the U. S. Atomic Energy Commission.

laser vaporization was a maximum and that the maximum was in the vicinity of the reported triple point of carbon (4100 to 4600K)(10).

Insight into this phenomenon comes from the calculation of effective Langmuir coefficients for the laser vaporization. Drowart et al.(13) reported relative ion intensities for equilibrium vaporization extrapolated to 4100K of 1.0, 6.4, 16., 1.7, and 3.2 for C_1, C_2, C_3, C_4, and C_5. The averaged values of the ion intensities from this work and from the other laser studies are 1.0, 2.0, 6.0, 0.34, and 0.80. Hence, the laser vaporization coefficients, calculated relative to C_1, are 1.0, 0.31, 0.36, 0.20, and 0.25. This result implies that the vaporization was limited by the kinetics of the dissociation and release of molecules at the surface of the condensed phase. It is concluded from these laser experiments that a temperature near the triple point was achieved and that the specific rate of the phase transformations became constant and kinetically limited. A model for the vaporization and the vapor expansion will be presented in the expanded version of this paper (to be published).

REFERENCES

1. J. A. Howe, J. Chem. Phys. 39, 1362 (1963).
2. J. Berkowitz and W.A. Chupka, J. Chem. Phys. 40, 2735 (1964).
3. P. D. Zavitsanos, "General Electric Space Sciences Laboratory Report No. R67SC11," March 1967.
4. K. A. Lincoln, in High Temperature Technology (Butterworths and Co., London, 1969) pp. 323-332.
5. W. Steele, Private communication.
6. R. T. Meyer, J. Sci. Inst. 44, 422 (1967).
7. R. T. Meyer, in Time-of-Flight Mass Spectrometry, (D. Price and J. E. Williams, Ed.) (Pergamon Press, Oxford, 1969), pp. 61-87.
8. R. T. Meyer, A. W. Lynch, and J. M. Freese, Paper presented at 19th Annual Conference on Mass Spectrometry and Allied Topics, Atlanta, Georgia, May 1971; to be published.
9. JANAF Thermochemical Tables, Second Edition (D. R. Stull and H. Prophet, Eds), Nat. Stand. Ref. Data Ser., Nat. Bur. Stand., (U.S.), 37, June 1971.
10. H. B. Palmer and M. Shelef, in Chemistry and Physics of Carbon,(P. L. Walker, Jr., Ed.)(Marcel Dekker, Inc., New York, 1968), Vol. 4, pp. 85-136.
11. P. D. Zavitsanos, General Electric Company Report No. R66SC31, May 1966; also in Dynamic Mass Spectrometry (Heyden & Son, Ltd., 1970) p. 1.
12. R. T. Meyer and A. W. Lynch, High Temp. Sci., Vol. 4, No. 4, (1972).
13. J. Drowart, R. P. Burns, G. DeMaria, and M. G. Inghram, J. Chem. Phys., 31, 1131 (1959).

HEAT OF FORMATION AND ENTROPY OF C_3 MOLECULE*

F. M. Wachi and D. E. Gilmartin

The Aerospace Corporation

El Segundo, California 90045

ABSTRACT

Partial pressures of $C_{3(g)}$ have been measured with a high resolution mass spectrometer using a Knudsen effusion cell in the temperature range from 2300 to 2800°K. The derived third-law heat of formation, using the thermodynamic functions of Strauss and Thiele[1], is $\Delta H_0^\circ(C_3) = 199.2 \pm 0.4$ kcal mole^{-1}. The second-law value is 200.1 ± 4 kcal mole^{-1}. The entropies for $C_{3(g)}$ at 2400 and 2600°K are 81.47 eu and 82.91 eu, respectively. These experimental values are in excellent agreement with $S^\circ_{2400} = 81.41$ eu and $S^\circ_{2600} = 82.46$ eu computed by Strauss and Thiele from spectroscopic data.

*Submitted for publication in High Temp. Sci.

[1]H. L. Strauss and E. Thiele, J. Chem. Phys. 46,

VAPOR PRESSURE AND HEAT OF VAPORIZATION OF COBALT*‡

F. M. Wachi and D. E. Gilmartin

The Aerospace Corporation

El Segundo, California 90045

ABSTRACT

New vapor pressure data for cobalt have been obtained in the temperature range from 1519° to 1926°K from Knudsen effusion experiments. The derived Third-Law heat of vaporization for cobalt is $\Delta H^{o}_{298} = 101.0 \pm 0.6$ kcal/mole. Plausible explanations are presented that account for the widely differing vapor pressure data and heats of sublimation published in the literature. It is shown that the evaporation coefficient for cobalt is unity rather than 3×10^{-4} and that the electron impact ionization cross section for cobalt is $\sigma(Co) = 4.4 \pm 1 \times 10^{-16}$ cm^2 for 50-eV ionizing electrons.

---

*This work is supported by the U. S. Air Force under Contract FO4701-71-C-0172

‡Accepted for publication in J. Chem. Phys.

DISSOCIATION ENERGIES OF SOME HIGH TEMPERATURE MOLECULES CONTAINING ALUMINUM*

Carl A. Stearns and Fred J. Kohl
NASA Lewis Research Center
Cleveland, Ohio 44135

ABSTRACT

The Knudsen cell mass spectrometric method has been used to investigate the gaseous molecules Al_2, AlSi, AlSiO, AlC_2, Al_2C_2, and $AlAuC_2$. Parent molecular species were established on the basis of measured appearance potentials. Special attention was given to the experimental considerations and techniques needed to identify and measure ion intensities for very low abundance molecular species. Second- and third-law procedures were used to obtain reaction enthalpies for pressure calibration independent and isomolecular exchange reactions. Dissociation or atomization energies for the molecules were derived from the measured ion intensities, free-energy functions obtained from estimated molecular parameters, and auxiliary thermodynamic data:

Reaction	Third-law ΔH_0° (kJ mol^{-1})	D_0°, atoms (kJ mol^{-1})
$AlAu(g)+Al(g)=Al_2(g)+Au(g)$	171.5±18	Al_2, 149.8±20
$2AlAu(g)=Al_2(g)+Au_2(g)$	273.7±18	
$Al(g)+Si_2C(g)+C(s)=AlSi(g)+SiC_2(g)$	296.1±19	AlSi, 225.5±30
$Al_2O(g)+Si(g)=AlSiO(g)+Al(g)$	47.2±16	AlSiO, 996.3±20
$Al(g)+2C(s)=AlC_2(g)$	315.1±21	AlC_2, 1104±21
$Al_2(g)+2C(s)=Al_2C_2(g)$	61.4±20	Al_2C_2, 1507±29
$AlAu(g)+2C(s)=AlAuC_2(g)$	323.4±20	$AlAuC_2$, 1418±21

*A complete account of this work will be published as an NASA Technical Note.

Study of Ionization Processes by the Angular Distribution Technique. ROBERT T. GRIMLEY AND LAWRENCE C. WAGNER, Dept. of Chemistry, Purdue University, Lafayette, Indiana 47907.

A major difficulty in the application of the mass spectrometer to high temperature vapor systems is the task of identifying the neutral vapor species from the observed mass spectrum. A new technique has been developed which is particularly useful in the case of polymeric vapor systems. For such systems it has been observed that different molecules flowing through long orifices exhibit distinguishable angular number distributions. In the specific case of AgCl, the vapor system consists of five polymeric vapor species, and the mass spectrum is comprised of thirteen ions. The application of the angular distribution technique and its advantages compared to the standard methods will be considered in the case of the AgCl vapor system.

Details of this work are to be published in the Journal of Physical Chemistry.

IDENTIFICATION OF REACTIVE SPECIES IN VARIOUS GAS PHASE REACTIONS WITH A T.O.F. MASS SPECTROMETER*

J.J. DeCorpo, M.V. McDowell and F.E. Saalfeld
Naval Research Laboratory
Washington, D.C. 20390

Techniques developed to permit the identification of very reactive gas phase species with a Bendix T.O.F. mass spectrometer have been reported. The presentation pointed out the required instrumental modifications needed to allow near adiabatic sampling of low temperature flames. A horizontal quartz reactor has been incorporated in the ion source housing of the mass spectrometer. The reactor has a simple and unique sampling port which consists of a cone-shaped hole "drilled" through the vessel's wall. The narrow section of the cone comes in contact with the reacting gases and has a diameter of 25 microns. By controlling the temperature of the reactor one can initiate and sustain the reactions and provide an environment conducive to the study of flames. This temperature control is accomplished by passing an electrical current through a resistive coating on the reactor tube. The resistance of the coating is varied to effect the desired temperature gradients along the reactor. The flame is generated within the reactor, it may be separated, stabilized or positioned in any part of the reactor by varying the gas flow and the heat applied to the reactor. The section of the flame directly over the sampling port and in contact with the heated wall is sampled and analyzed. The medium being studied is introduced into the mass spectrometer approximately 1 mm from the ionizing electron beam. Surface effects are minimized as a result of the homogeneity of the flame around and in contact with the heated walls of the reactor.

*This paper will be submitted in detail for formal publication at a latter date.

MEASUREMENT OF HEATS OF VAPORIZATION OF ORGANIC COMPOUNDS BY MICROMOLECULAR DISTILLATION IN A MASS SPECTROMETER

Ronald D. Grigsby

Department of Biochemistry and Biophysics
Texas A&M University
College Station, Texas 77843

The technique of "micromolecular distillation" was first presented before the ASMS at the San Francisco meeting in 1970[1,2]. At that time it was shown that a simple mixture could be distilled from a probe inlet system at constantly increasing temperature to give data analogous to those obtained from macro-scale molecular distillation. During the run multiple spectra are taken under fast-scan conditions at recorded temperatures. Plots are then made of peak intensities for given masses vs. temperature to give elimination curves similar to those obtained for ordinary molecular distillation[3,4]. Mathematical analysis of the spectra provides the relative intensities of peaks for the individual components together with the amounts of the components present in the mixture. The method is related to mass spectrometric thermal analysis[5], to the integrated ion-current method of quantitative analysis[6,7], and to a quantitative method of molecular distillation in the ion source at constant temperature[8].

During the Atlanta meeting of the ASMS in 1971, it was shown that micro-molecular distillation can be applied to mixtures containing derivatives of amino acids and oligopeptides[9]. The method thus provides a rapid means of obtaining protein sequence information without extensive separation of the oligopeptides that result from chemical and enzymatic degradation of proteins[10-14].

The data obtained from micromolecular distillation are analyzed by a least-squares fit to the empirical equation

$$I = A \frac{e^{-B/T}}{1 + e^{C(T-D)}} \qquad (1)$$

where I is the intensity of a mass peak, T is absolute temperature, and A,B,C, and D are parameters evaluated for the points[15]. The parameters A and B determine the exponential increase of the curve during the initial phase of the distillation, while C and D force the curve back to zero as the component is distilled away.

The purpose of the present discussion is to explain theoretically the shapes of the curves and to show how heats of vaporization can be obtained from the data.

In 1913, Irving Langmuir showed that the rate of distillation from a surface into a vacuum is given by

$$\frac{dn}{dt} = \sqrt{\frac{M}{2\pi RT}} \cdot pa \qquad (2)$$

where M is the molecular weight of the component, R is the ideal gas constant, T is absolute temperature, p is the vapor pressure of the component, and $\underline{a}$ is its surface area[16]. For distillation in a mass spectrometer the intensity of a mass peak is given by

$$I = \alpha \frac{dn}{dt}$$

Thus by substitution into the above equation,

$$I = \alpha \sqrt{\frac{M}{2\pi RT}} \cdot pa \qquad (3)$$

or by combining the constants,

$$I = \beta \frac{pa}{\sqrt{T}} \tag{4}$$

Using the integrated form of the Clausius-Clapeyron equation to substitute for the vapor pressure, the equation

$$I = \gamma \frac{e^{-\Delta H°/RT}}{\sqrt{T}} \cdot a \tag{5}$$

is obtained.

The only problem remaining in the derivation is the provision of an analytical expression for the surface area. If it is assumed that the molecules are distilling from a uniform surface, then the area should remain fairly constant until the substance is almost distilled away, at which time it should drop sharply to zero. Using this model, the surface area can be represented by an empirical expression

$$a = \delta \frac{1}{1 + e^{C(T-D)}} \tag{6}$$

the denominator of which is the same as in equation 1. Substitution for a from equation 6 into equation 5 gives

$$I = \varepsilon \cdot \frac{e^{-\Delta H°/RT}}{\sqrt{T}(1 + e^{C[T-D]})} \tag{7}$$

which allows I to be calculated as a function of T.

It should be noted that if $D >> T$, the factor in the denominator remains approximately equal to one, corresponding to conditions where the surface area remains practically constant during the distillation. This will be the case when the sample size is large enough (e.g. 1-2 mg) to prevent an appreciable loss during the initial part of the run. For distillation under these conditions, equation 7 becomes

$$I = \varepsilon \cdot \frac{e^{-\Delta H°/RT}}{\sqrt{T}} \tag{8}$$

Or

$$\ln(I \cdot T^{\frac{1}{2}}) = \ln \varepsilon - \Delta H°/RT \tag{9}$$

Thus a plot of $\ln(I \cdot T^{\frac{1}{2}})$ *vs.* $1/T$ *gives a slope equal to* $-\Delta H°/R$, *from which* $\Delta H°$ can be evaluated.

Although equation 9 was derived under conditions representing molecular distillation, the same equation is obtained from a model for molecular effusion[17]. True molecular distillation conditions are probably not attained in a mass spectrometer probe, i.e., the real conditions are probably intermediate between molecular distillation and molecular effusion. However, the value of $\Delta H°$ obtained from equation 9 should be practically independent of the true conditions.

Using equation 9, the heat of vaporization (or sublimation, depending on compound and conditions) was obtained for stearic acid, benzoic acid, and 1-naphthol. A plot of equation 9 for the molecular ion of stearic acid (m/e 284) over a temperature range of 70 to 110°C is shown in Figure 1. A value of 24.6 Kcal/mole was obtained for the heat of vaporization, $\Delta H_V°$. The average value of $\Delta H_V°$ taken over several sets of data was 24.2±1.2 Kcal/mole, which lies within a range of values from 22.0 to 29.0 Kcal/mole located in the literature[18-21].

For benzoic acid, the measured value of the heat of sublimation, $\Delta H_S°$, over a temperature range of 0 to 30°C was 16.4±1.2 Kcal/mole. Values in the literature range from 15.3 to 21.9 Kcal/mole[21-23]. The 1-naphthol data gave a value of 21.5±1.4 Kcal/mole for $\Delta H_S°$ over a temperature range of 0 to 40°C.

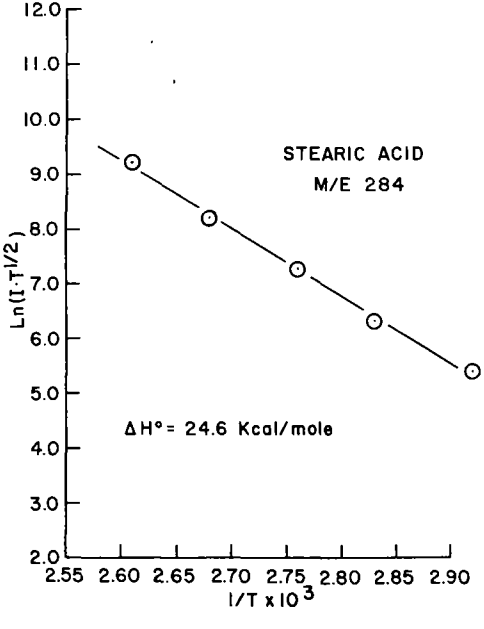

Figure I. Evaluation of heat of vaporization for stearic acid

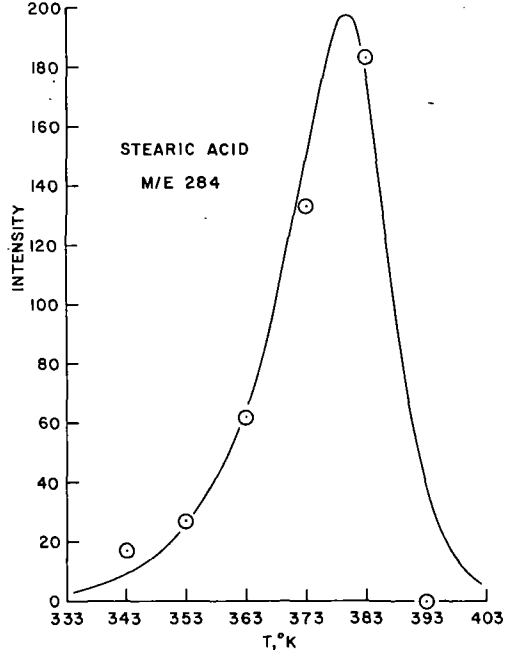

Figure 2. Elimination curve for stearic acid

Only one literature reference could be located. This gave a value of 21.87± 0.90 Kcal/mole for the heat of sublimation as calculated from the heats of fusion and vaporization[24-26].

Using the experimental value of 24.2 Kcal/mole for the heat of vaporization and empirical values of ε, C, and D in equation 7, the original data for stearic acid can be fitted with reasonable accuracy, as shown in Figure 2. The points at 383 and 393°K are the most difficult to fit because the surface area is rapidly diminishing toward zero, i.e., the sample is almost distilled away in this region. A better fit might be obtained by using an improved expression for the area.

The use of micromolecular distillation to measure heats of vaporization and sublimation for organic compounds leads to the possibility of correlating measured values obtained from this technique with those predicted from structural considerations. This would provide an additional piece of structural information to be considered when deducing the structure of a compound from the mass spectrum itself. A number of methods for predicting heats of vaporization for simple organic compounds are available[27], but accuracy diminishes as the structure of the compound becomes more complex. Heats of sublimation are even more difficult to predict and only a few attempts have been made[27].

A more detailed study of the measurement of heats of vaporization and sublimation by micromolecular distillation is underway, and the results of the investigation will be submitted for publication in a journal yet to be selected.

Appreciation is expressed to Mr. G. M. Gable for valuable assistance in obtaining the data.

REFERENCES

1. R. D. Grigsby, R. H. Cole, W. G. Fox, and G. M. Gable, Southwest Regional Meeting of the American Chemical Society, Tulsa, Oklahoma, December, 1969.
2. R. D. Grigsby, R. H. Cole, W. G. Fox, and G. M. Gable, Eighteenth Annual Conference on Mass Spectrometry and Allied Topics, San Francisco, California, June, 1970, paper no. K8.
3. N. D. Embree, Ind. Eng. Chem., 29, 968 (1937).
4. G. Burrows, "Molecular Distillation," Oxford University Press, London (1960).
5. H. G. Langer, R. S. Gohlke, and D. H. Smith, Anal. Chem., 37, 433 (1965).
6. M. G. Allcock, R. Belcher, J. R. Majer, and R. Perry, ibid., 42, 776 (1970).
7. B. R. Kowalski, T. L. Isenhour, and R. E. Sievers, ibid., 41, 998 (1969).
8. R. A. Hites, ibid., 42, 1736 (1970).
9. R. D. Grigsby, J. S. Bird, and K. E. Bird, Nineteenth Annual Conference on Mass Spectrometry and Allied Topics, Atlanta, Georgia, May, 1971, paper no. H4.
10. F. W. McLafferty, R. Venkataraghavan, and P. Irving, Biochem. Biophys. Res. Commun., 39, 274 (1970).
11. P. Roepstorff, R. K. Spear, and K. Brunfeldt, FEBS Letters, 15, 237 (1971).
12. F. Franek, B. Keil, D. W. Thomas, and E. Lederer, ibid., 2, 309 (1969).
13. H. R. Morris, D. H. Williams, and R. P. Ambler, Biochem. J., 125, 189 (1971).
14. P. Roepstorff and K. Brunfeldt, FEBS Letters, 21, 320 (1972).
15. R. D. Grigsby, C. O. Hansen, D. G. Mannering, W. G. Fox, and R. H. Cole, Anal. Chem., 43, 1135 (1971).
16. I. Langmuir, Phys. Rev., 2, 329 (1913).
17. J. D. Cox and G. Pilcher, "Thermochemistry of Organic and Organometallic Compounds," Academic Press, New York (1970), p. 117, 118.
18. ibid., p. 247.
19. R. R. Mod, E. L. Skau, and R. W. Planck, J. Am. Oil Chemists' Soc., 30, 368 (1953).
20. Landolt-Börnstein, "Zahlenwerte und Funktionen aus Physik, Chemie, Astronomie, Geophysik, und Technik," 6th ed., Vol. 2, Part a, Springer-Verlag, Berlin (1960) p. 155.
21. D. R. Stull, Ind. Eng. Chem., 39, 517 (1947).
22. "International Critical Tables," Vol. 3, McGraw-Hill Book Company, Inc., New York (1928) p. 208.
23. M. Davies and J. I. Jones, Trans. Faraday Soc., 50, 1042 (1954).
24. D. H. Andrews, G. Lynn, and J. Johnson, J. Am. Chem. Soc., 48, 1274 (1926).
25. O. E. May, J. F. T. Berliner, and D. F. J. Lynch, J. Am. Chem. Soc., 49, 1012 (1927).
26. J. D. Cox and G. Pilcher, loc. cit., p. 217.
27. ibid., p. 121ff.

The Mass Spectra of N,O-Peralkyl Derivatives of Nucleosides

David L. von Minden and James A. McCloskey
Baylor College of Medicine, Houston, Texas 77025

A detailed study of the derivatization reaction, structures of products formed, and mass spectrometric fragmentation reactions of N,O-peralkyl (CH_3, CD_3, C_2H_5, C_2D_5) nucleosides has been carried out.[1] Derivatization was based on a modification[2] of the permethylation procedure introduced by Das, et. al.,[3] involving alkyl iodide and methylsulfinylmethide carbanion catalyst. Characterization of products was based on similarity of mass spectra of the reaction product and that from a peralkylated model which was originally substituted at known positions in the base. For example the spectrum of pentamethylated adenosine (I) was identical to that derived from authentic N^6, N^6-dimethyladenosine, thus excluding formation of a 1,N^6-dimethyl moiety in I.

Permethyl and perethyl derivatives of nucleosides are in general sufficiently volatile for introduction to the mass spectrometer by gas chromatograph. Their mass spectra include a number of basic ion types common to nucleoside derivatives in general[4], as reported in an earlier survey[5]: b(base) + H, b + 2H, b + CH_2O, s(sugar), s-H, s-ROH (R = alkyl). In nearly all cases the percents of sigma of the structurally diagnostic base - containing ions are higher than in the case of the corresponding trimethylsilyl[6] or trifluoroacetyl[7] derivatives. These characteristics, along with high chemical stability and relatively low molecular masses, indicate peralkylation to be an excellent alternative to other forms of derivatization.

Applications of this technique have recently been demonstrated in the structure determination of N^4-acetylcytidine, a modified nucleoside isolated from the first position of the anticodon of *E. coli* $tRNA^{Met}$ [8]

References

1. D. L. von Minden and J. A. McCloskey, to be published.
2. P. A. Leclercq and D. M. Desiderio, Jr., Anal. Lett., 4, 305 (1971).
3. B. C. Das, S. D. Gero and E. Lederer, Biochem. Biophys. Res. Commun., 29, 211 (1967).
4. J. A. McCloskey, in Basic Principles in Nucleic Acid Chemistry, Vol. I, P.O.P. Ts'o, Ed., Academic Press, New York, in press.
5. J. J. Dolhun and J. L. Wiebers, Org. Mass Spectrom., 3, 669 (1970).
6. J. A. McCloskey, A. M. Lawson, K. Tsuboyama, P. M. Krueger and R. N. Stillwell, J. Amer. Chem. Soc., 90, 4182 (1968).
7. W. A. Koenig, L. C. Smith, P. F. Crain and J. A. McCloskey, Biochemistry, 10, 3968 (1971).
8. Z. Ohashi, K. Murao, T. Yahagi, D. L. von Minden, J. A. McCloskey and S. Nishimura, Biochim. Biophys. Acta, 262, 209 (1972).

GAS PHASE ANALYSIS OF PHOSPHOLIPIDS

Noel Einolf and Catherine Fenselau
Department of Pharmacology and Experimental Therapeutics
The Johns Hopkins School of Medicine, Baltimore, Maryland 21205

The analysis of phospholipids accumulating in pulmonary alveolar proteinosis has relied entirely on one dimensional thin layer chromatography (tlc) for separation and identification of the phosphorous-positive spots. We have analyzed the phospholipids from two patients with this lung disease by a gas phase procedure which employs gas chromatography-mass spectrometry (gc-ms) to separate and identify the phospholipid backbones.[1] The phospholipids were extracted from the saline lung wash and deacylated with a methonolic sodium hydroxide solution. The acid form was generated by ion exchange and the trimethylsilyl derivative prepared.

A mixture was prepared from commercially available phospholipids to demonstrate the success of the technique: phosphatidyl serine, phosphatidyl inositol, glyceryl-phosphate, and phosphatidyl glycerol were separated and identified as the deacylated trimethylsilyl derivatives.

The α and β isomers of several phospholipids were distinguished by their resolution on the gc column and subsequent mass spectrum. For the three TMS derivatives of glycerylphosphatides studied, glycerylphosphate, glycerylphosphatidyl glycerol, and glycerylphosphatidyl inositol, the ratio of m/e 243 to m/e 357, or I_{243}/I_{357}, is always smaller for the α than for the β isomer. The gc peak for the β isomer preceeds the peak for the α isomer in each of these cases.

The gas phase analysis of two samples from patients with pulmonary alveolar proteinosis produced gc peaks identified from their mass spectra as the trimethylsilyl (TMS) derivatives of glycerylphosphatidyl glycerol, glyceryl phosphate, and glyceryl-phosphatidyl inositol. Glycerylphosphatidyl glycerol has not been previously identified in extracellular pulmonary fluid and its significance in our patients is being evaluated.

Lung lipids from one patient were also analyzed by two dimensional tlc. Eight phosphorous-positive spots were detected using a molybdenum spray reagent. Three of these were identified as phosphatidyl choline, lysophosphatidyl choline, and sphingomyelin, none of which is amenable to the gas phase analysis. Of the other five, phosphatidyl inositol, phosphatidyl glycerol, and phosphatidyl ethanolamine were identified. Two unknown components are being studied.

A detailed report of this study will be published elsewhere.

1. J. H. Duncan, W. J. Lennarz, C. C. Fenselau, Biochem. 10, 927 (1971).

Structurally Significant Fragmentation of Urinary Glucuronides. STEPHEN BILLETS, PAUL S. LIETMAN and CATHERINE FENSELAU, Johns Hopkins University School of Medicine, Baltimore, Maryland 21205 E3

Elucidation of the metabolic path of a drug or pesticide presupposes that the metabolic products can be structurally identified. The formation and excretion of acidic urinary conjugates plays an important role in drug metabolism. Yet the structure of these conjugates is usually assigned on the basis of analysis of their hydrolysis products, or of ambiguous comparison of chromatographic retention times with tediously synthesized reference conjugates.

In order to evaluate the information obtainable by mass spectrometry we have analyzed the mass spectra of eight hydroxyl-linked glucuronides. The fragmentation pattern was analyzed with the aid of high resolution mass measurements and deuterium labeling studies. Some general principles are presented by which metabolites may be identified as glucuronides, and by which structures, or partial structures may be deduced from their mass spectra without the necessity of synthesizing reference compounds.

The glucuronides were prepared for GC-MS analysis by esterification with diazomethane and subsequent conversion to trimethyl silyl ethers. Spectra were obtained both from direct probe and GC inlet systems. Molecular ions were not always observed using the gas chromatographic inlet system, perhaps reflecting some thermal excitation.

If molecular ions are not present, the molecular weight of these compounds can be determined from the molecular ion set formed by fragmentation of the TMS ether groups. In all compounds studied the abundance of M-15 ions was equal to or greater than the molecular ion. Other silyl fragmentation at M-73, M-90 and M-105 occur to varying extents in all spectra.

Cleavage of the acetal link between drug and glucuronic acid with charge retention in the derivatized glucuronic acid portion of the molecule leads to abundant ions of masses 407, 406, 317, 275, 217 and 204. The base peak in these spectra usually occurs at m/e 317, while the 217 and 204 ions occur with varying intensity dependent on the operating conditions of the instrument. They probably represent pyrolysis as well as fragmentation products.

Cleavage of the acetal bond also occurs with charge retention in the drug portion of the molecule. Two different pathways of fragmentation were observed depending on whether an aliphatic or aromatic ether link is formed in the conjugation. An M-334 ion is formed by a fragmentation-rearrangement process from aromatic ethers, while a simple cleavage reaction leading to an M-423 ion is observed with aliphatic ether linked glucuronides.

The mass spectrum allows the site of glucuronic acid attachment to be distinguished in the chloramphenicol molecule which has multiple sites available for conjugation.

Our studies also indicate that fragmentation in the aglycon can be used to locate structural changes in a drug due to metabolism.

This investigation will be described in detail elsewhere.

Mass Spectrometry of Daunomycin.

John Roboz, Dov Kruman, and Ferenc Hutterer,

The Mount Sinai Hospital, New York, N.Y. 10029.

Daunomycin, an antitumor antibiotic widely employed in protocolls of chemotherapy for various forms of leukemia, consists of a pigmented aglycone (daunomycinone) in glycoside linkage with an amino sugar (daunosamine). In the course of developing analytical techniques for the simultaneous analysis of daunomycin and other antileukemia drugs, such as cytosine arabinoside, vincristine, and asparaginase in various body fluids and tissues, the mass spectra of daunomycin and its trimethylsilyl derivatives were ivestigated. Experimental conditions are described for obtaining both low and high resolution spectra using a combined gas chromatograph-mass spectrometer-computer system. Technique for the determination of daunomycin in crude extracts, *via* direct probe introduction, is also described. Fragmentation patterns of pure daunomycin and its trimethylsilyl derivatives are discussed.

Comparison of Mass Spectra of Epimeric Bile Acids. By William H. Elliott and Paul M. Hyde, Department of Biochemistry, St. Louis University School of Medicine, St. Louis, Missouri 63104. E5

Fragmentation patterns of the methyl esters and TMS ethers of hydroxy bile acids epimeric at C-5 have been studied via direct probe or gas chromatography with an LKB 9000. Of the four isomeric C-3 monohydroxy bile acids, only lithocholate (3α-hydroxy-5β-cholanate) did not provide a significant molecular ion. Base peak for the 3,7-diols epimeric at C-3 and C-5 appeared at m/e 388 (M-18) in all cases except for chenodeoxycholate (3α,7α-dihydroxy-5β-cholanate) at 70 or 20 ev and various temperatures of the ion source and direct probe. ^{18}O was incorporated into the C-3 or C-7 positions and the spectra recorded. In the 5α-series the 7α-ol was lost consistently before the C-3-ol. Significant differences appear in the spectra of the TMS ethers of the methyl esters of the trihydroxy acids. The spectra of the TMS ethers of methyl esters of epimeric 3α,6,7-trihydroxy-5β and 5α-cholanates offer assistance for identification. (Supported by NIH Grant HE-07878.)

MASS SPECTROMETRY IN THE DETERMINATION OF THE STRUCTURE OF HYPOTHALAMIC HORMONES.

R.M.G.Nair, A.J.Kastin and A.V.Schally

Tulane University School of Medicine, Department of Medicine and Endocrine and Polypeptide Laboratories, Veterans Administration Hospital, New Orleans, Louisiana 70112.

Introduction. Hypothalamus situated in the mid-brain exercises control over the anterior pituitary hormones such as luteinizing hormone (LH), follicle stimulating hormone (FSH), growth hormone (GH), thyrotropin (TSH), and melanocyte-stimulating hormone (MSH). This control is mediated by neurohumoral substances designated LH/FSH-releasing hormone (LH/FSH-RH), GH-releasing hormone (GH-RH), TSH-releasing hormone (TRH), MSH-release-inhibiting hormone (MRIH) and others(1). We have isolated these valuable releasing or inhibiting factors or hormones from porcine and bovine hypothalami, in microquantities. Our preliminary investigations on the chemical nature of the hypothalamic hormones indicated that they are polypeptides. Since the availability of these hormonal peptides for structural studies, by the conventional chemical degradation methods, was very limited, we attempted high and low resolution mass spectrometry for the elucidation of the structure, utilizing microgram amounts of the peptides before and after derivatization.

Derivatization and mass spectrometry. The peptides(20-50 µg) were subjected to acetylation and permethylation before and after methanolyses, according to the methods described previously (2-4). The methods lead to acetylation of $-NH_2$ groups ($-NH_2 \rightarrow -NHCOCH_3$), methylation of amide nitrogen [$-CONH_2 \rightarrow -CON(CH_3)_2$, $-CONH- \rightarrow -CON(CH_3)-$] and hydroxyl and carboxylic acid functions ($-OH \rightarrow -OCH_3$, $-COOH \rightarrow -COOCH_3$). Modification of the arginine moiety was effected by mild hydrazinolysis(5,6). Nanomole quantities of the arginine containing peptides were treated with 20% aqueous hydrazine in partially evacuated sealed tubes at 80 to 90°, for one hour, and the excess reagent removed in vacuum. After checking the purity by thin-layer chromatography, the resultant peptide materials were relyophilized and subjected to further derivatization reactions, using ^{14}C-acetic anhydride for acetylation and ^{14}C-methyl iodide for permethylation. The completion of derivatization was confirmed by measurement of the resultant radioactivity.

High and low resolution mass spectra were recorded in an AEI MS 902 mass spectrometer (MS) equipped with a PDP-8 computer and MSDS II MS data system. Low resolution spectra were recorded on a Hitachi-Perkin Elmer model RMU-4 instrument as well. The direct inlet probe was used for the peptides and their derivatives. Probe samples were prepared by placing 5-10 µg portions of a concentrated solution of the corresponding peptide or its derivative in aqueous methanol at the quartz tip of the direct insertion probe and removal of the solvent under slight vacuum in a desiccator, taking care to avoid splattering during evacuation. Spectra were recorded at ion source temperatures 225-300°, 70 ev ionizing energy, and resolving power 15 to 20,000 for high resolution and 1500-3000 for low resolution studies. An initial background scan was performed before each set of experiments, the probe was then introduced into the ion source of the MS by using the standard vacuum-lock system. The temperature of the ion source was gradually increased from 200 to 300° and at each 15° interval (215, 230, 245, 260, 275 and 300°) the probe tip was moved into the ion source, the spectrum monitored on the oscilloscope, and the relevant spectra recorded.

Results and Discussion. Mass spectral fragmentation of TRH after permethylation or permethylation subsequent to methanolysis, yielded not only the sequence (pyro)Glu-His-Pro, but also the parent molecular ions of the fully permethylated amide (432 m/e, Me-(pyro)Glu-Me_2-His-Pro-NMe_2) and the prolyl ester (419 m/e, Me-(pyro)Glu-Me_2-His-Pro-OMe). Thus the Structure of TRH was found to be (pyro)Glu-His-Pro-NH_2, which was confirmed by conventional chemical methods (7).

Fig.1,Sequence spectra of Ch_1 after derivatization.

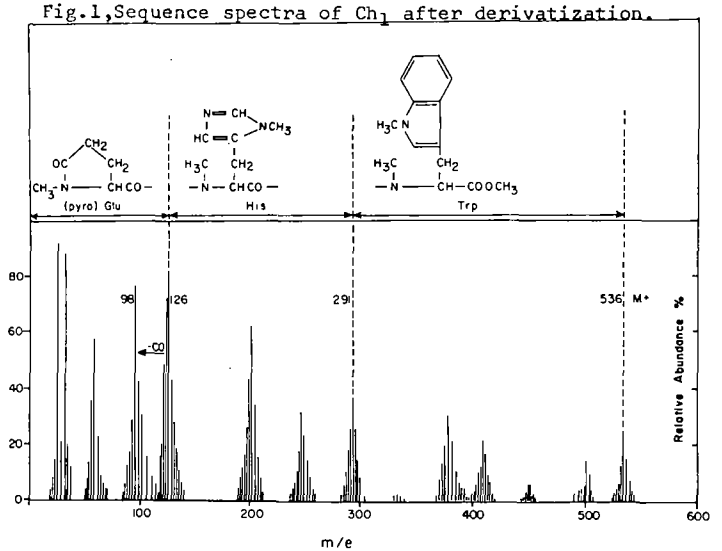

Fig.2, Mass spectra of Ch_2 after derivatization.

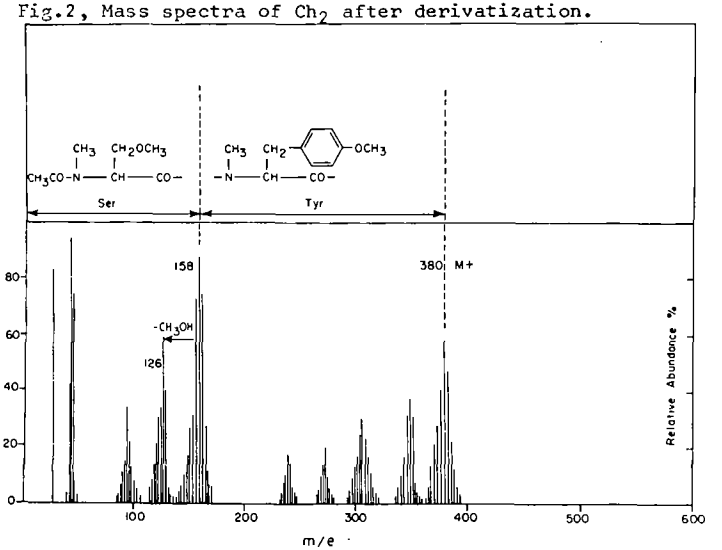

Fig.3, Sequence spectra of Ch_3 after derivatization

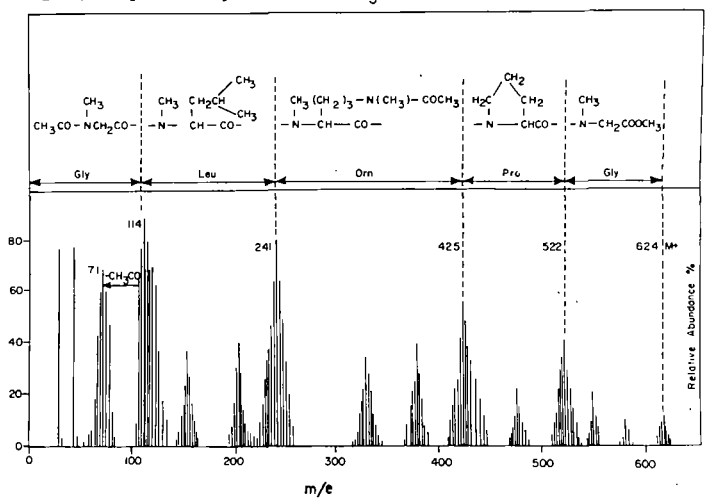

Fig.4,Sequence spectra of LH-RH after derivatization.

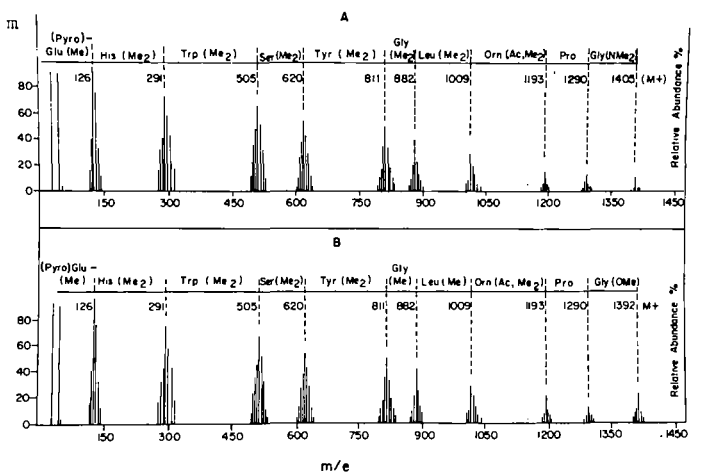

Two peptides with MSH-release-inhibiting activity were isolated from bovine hypothalami. After derivatization and mass spectrometry one was found to be a tripeptide possessing the structure Pro-Leu-Gly-NH_2 or Pro-Ileu-Gly-NH_2. Syntheses of these two isomers and comparison of the biological activities proved that the structure is Pro-Leu-Gly-NH_2, (8). The other MRIH-active peptide consisted of five amino acids. Derivatization and mass spectrometry yielded the structure Pro-His-Phe-Arg-Gly-NH_2, which was confirmed by conventional chemical sequencing and also syntheses (9).

LH/FSH-RH was isolated from porcine hypothalami(10). Amino acid analysis showed it to be a decapeptide and Edman-dansyl degradation was a failure due to a blocked N-terminus. Mass spectral fragmentation of the underivatized hormone suggested that the N-terminus is occupied by a (pyro)-glutamyl moiety. This was confirmed by the fact that pyrrolidone carboxylyl peptidase inactivated the hormone. Chymotryptic cleavage, separation of the three major fragments, derivatization, and mass spectrometry of LH/FSH-RH, showed the sequence (pyro)Glu-His-Trp for fragment Ch_1 (Fig.1), Ser-Tyr for Ch_2 (Fig.2), and Gly-Leu-Arg-Pro-Gly-NH_2 for Ch_3 (Fig.3, Leu or Ileu in the II position).

Mass spectra of the intact hormone(LH/FSH-RH) after modification of arginine and N-,O-permethylation gave a sequential fragmentation pattern, yielding also the parent molecular ion (M^+ =1405m/e) for the derivative ending with the dimethyl glycylamide, and also the molecular ion(M^+=1392 m/e) for the derivative ending with methyl glycylester,(Fig.4 A&B). The molecular ions were of very low intensity and are shown 50-fold in the figure. Secondary decomposition peaks due to aromatic moieties or escape of MeOH from serine and the like are not depicted in the sequence spectra. The sequences obtained from the derivatized decapeptide and from the three major chymotryptic fragments coincided. Hence the structure was proved to be (pyro)Glu-His-Trp-Ser-Tyr-Gly-Leu-Arg-Pro-Gly-NH_2. This was confirmed by conventional chemical sequencing on a micro scale and also by syntheses,(11).

GH-RH isolated from porcine hypothalami, was found to be a decapeptide After cleavage of this peptide with trypsin, separation of the two fragments T_1 and T_2, their derivatization, and mass spectrometry, as in the previous cases, yielded the structure: Val-His-Leu-Ser-Ala-Glu-Glu-Lys-Glu-Ala-OH. This was confirmed by conventional chemical sequencing and also synthesis(12).

References

1. Schally,A.V.,Arimura,A.,Baba,Y.,Nair,R.M.G.,Matsuo,H.,Redding,T.W. and Debeljuk,L. Biochem.Biophys.Res.Commun. 43: 393, 1971
2. Thomas,D.W.,Das,B.C.,Gero,S.D.,and Lederer,E. Biochem.Biophys.Res. Commun.32: 199, 1968.
3. Thomas,D.W.,Das,B.C.,Gero,S.D.,and Lederer, E. Biochem.Biophys.Res. Commun. 32: 519, 1968.
4. Agarwal,K.L.,Kenner,G.W., and Sheppard,R.C. J.Am.Chem.Soc. 91: 3096, 1969.
5. Shemyakin,M.M.,Ovchinnikov,Yu.A.,Vinogradova,E.I.,Feigina,M.Yu., Kiryushkin,A.A.,Aldanova,N.A.,Alakhov, Yu.B.,Lipkin,V.M. and Rosinov,,B.V. Experientia 23: 428, 1967.
6. Morris,H.R.,Williams,D.H., and Ambler,R.P. Biochem.J. 125: 189, 1971.
7. Nair,R.M.G.,Barrett,J.F.,Bowers,C.Y.,and Schally,A.V. Biochemistry 9: 1103, 1970.
8. Nair,R.M.G.,Kastin,A.J.,and Schally,A.V. Biochem.Biophys.Res.Commun.43: 1376, 1971.
9. Nair,R.M.G.,Kastin,A.J.,and Schally,A.V. Biochem.Biophys.Res.Commun.47: (June 1972),in press.
10. Schally,A.V.,Nair,R.M.G.,Redding,T.W.,and Arimura,A. J.Biol.Chem.246: 7230, 1971.
11. Nair,R.M.G.,and Schally,A.V. In preparation.
12. Schally,A.V.,Baba,Y.,Nair,R.M.G.,and Bennet,C.D. J.Biol.Chem. 246: 6647, 1971.

Mass Spectral Fragmentation of Prostaglandins

Lubomir Baczynskyj, Ernest W. Yankee and Richard J. Wnuk; The Upjohn Company, Kalamazoo, Michigan 49001.

The mass spectra of $PGF_2\alpha$ (Ia) and PGE_2 (IIa) and their methyl esters (Ib and IIb) show intense peaks at M^+-90 and M^+-89, respectively.

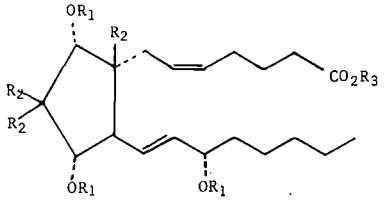

I. a. R_1, R_2, R_3 = H
b. R_1, R_2 = H; R_3 = CH_3
c. R_1 = D, R_2 = H, R_3 = CH_3
d. R_1 = H, R_2 = D, R_3 = CH_3
e. R_1 = TMS, R_2 = H, R_3 = CH_3

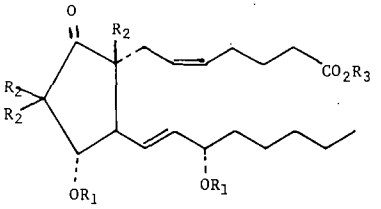

II. a. R_1, R_2, R_3 = H
b. R_1, R_2 = H; R_3 = CH_3
c. R_1 = D, R_2 = H, R_3 = CH_3
d. R_1 = H, R_2 = D, R_3 = CH_3
e. R_1 = TMS, R_2 = H, R_3 = CH_3

Proposed mechanisms for these losses have been postulated (1) as follows:

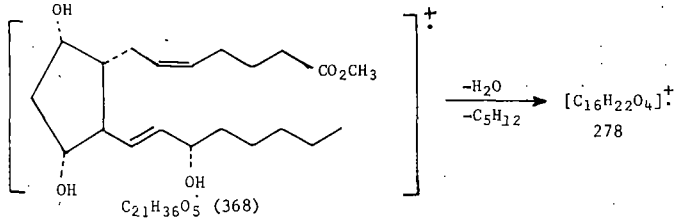

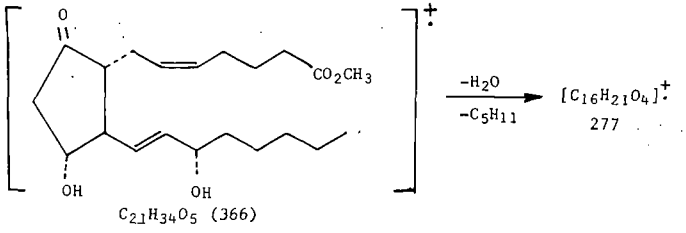

High resolution measurements of the M^+-90 peak of Ia and Ib indicated that the elements lost from the molecular ion are those of water and malonaldehyde and not those of water and pentane. The M^+-89 peak in the case of IIb was a doublet corresponding to the loss of (H_2O + $C_3H_3O_2$) and the loss of (H_2O+C_5H_{11}). The relative intensities of the resulting ions were in a ratio of 3:2, respectively.

A revised mechanism to explain these results follows:

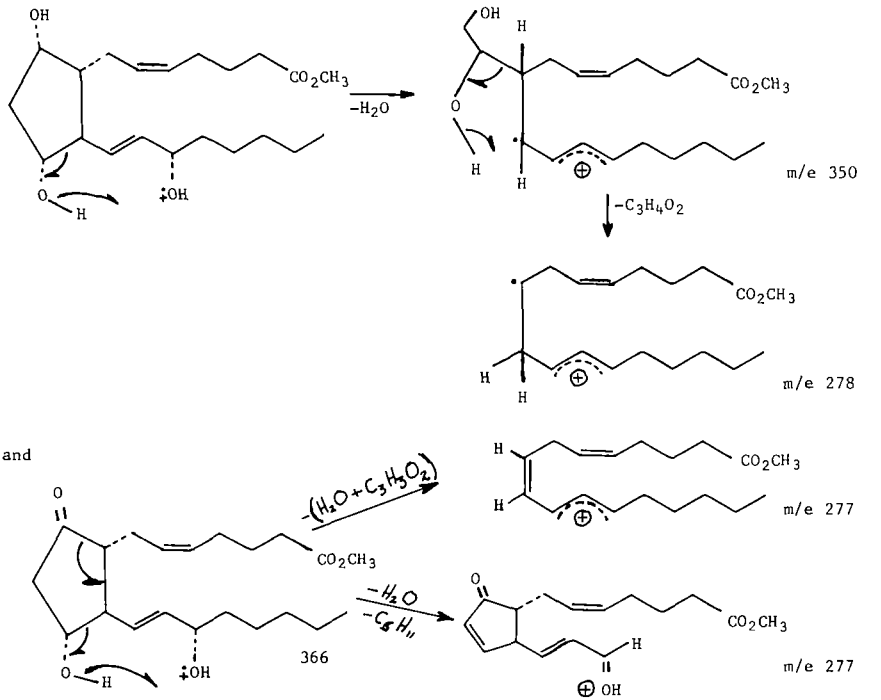

To verify the proposed mechanisms, deuterated analogs Ic, Id, IIc and IId were prepared. Appropriate mass displacements were observed in accord with the proposed mechanism.

The mass spectrum of Ie shows an intense peak at m/e 217 indicating the fragmentation of the cyclopentane ring with charge retention on the smaller fragment represented by:

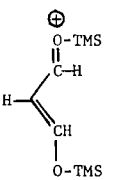

m/e 217

Whereas IIe shows the loss of C_5H_{11} and fragmentation of the cyclopentane ring giving rise to an ion of the type.

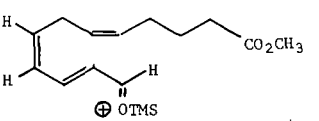

m/e 295

A full account of this work will be published at a later date.

References

(1) P. W. Ramwell, *et al.*, Progress in the Chemistry of Fats and Lipids, Vol. IX, Part 2, Pergamon Press, New York (1968).

Prostaglandin Analysis with a GC-MS-Computer System

J. Throck Watson, Donald Pelster, B.J. Sweetman and J.C. Frolich
Department of Pharmacology, Vanderbilt University
Nashville, Tennessee 37232

Development of reliable analytical methodology for specific prostaglandins is essential to research involving the physiological role of these potent hormones. With our interest in vapor phase analysis we have found the methyl ester (ME), trimethylsilyl (TMS) ether of prostaglandin PGA or PGB to be the derivatives of choice (1). These derivatives have good thermal stability, low polarity, and simple mass spectra which facilitate their detection into the picogram range (1) without a deuterium labelled carrier as is necessary with the more polar ME, methoxime, TMS derivative of PGE which requires a 250-fold to 1000-fold excess of carrier for successful detection into the low nanogram range (2).

Concomitantly with studying the integrity of PGE conversion to A or B (1) and derivatization of the latter at the low nanogram level both in the presence and absence of a realistic biological matrix, we have been concerned with acquisition and reduction of multiple ion detection (MID) data. Recording of MID data with a conventional oscillograph produces a complex data record of transient sweeps since the recording medium cannot be interrupted as the accelerating voltage is switched (3) between preset values for the ions of interest. Such an oscillographic record can be confusing, especially in analysis of a biological sample, when 3 ions are being monitored.

We have developed an interface and software for a PDP-12 computer to control the MID (AVA) unit on an LKB-9000 GLC-MS and acquire and reduce the data on-line (4). The reduced data are displayed on an oscilloscope to facilitate recognition of the various ion profiles and interpretation by the investigator. Consider the comparison of oscillographic and oscilloscopic (computer) presentation in Figure 1 of the MID data resulting from the co-injection of PGB_2-ME-TMS (ions at m/e 321 and 349) and d-4-PGB_2-ME-TMS (ion at m/e 325). The oscillographic record is shown at the upper left of Figure 1 in which 3 profiles, at the end points of the transient sweeps, can be discerned. The same data acquired in parallel by the computer are shown in the upper right panel which is actually a photograph of the computer oscilloscope. Although the 3 m/e values are displayed on the screen, the question remains, "Which profile is which?" The investigator may identify the individual profiles by manipulating switches on the computer console which remove a given profile and its corresponding m/e value from the display. In the sequence going to the lower left of Figure 1, then to the lower right panel, the operator has switched off the display of m/e 325 and finally that of m/e 349.

In addition to the easy and unequivocal identification of the various ion profiles, the computer facilitates the calculation of peak areas. The calculation option displays the selected m/e profile and 3 adjustable cursors (which resemble 3 sides of a rectangle) on the computer oscilloscope. The investigator adjusts the position of each of the 3 cursors to the peak baseline, leading and trailing edges of the peak prior to depressing the "C" key on the teletype which prints the value of the peak area within the designated limits. Small peaks may be magnified on the computer screen to facilitate judgment on the positioning of the area-limiting cursors.

Figure 3 shows a composite of computer displays of MID data resulting from the addition of 900 picograms of PGB_2-ME-TMS and 9.0 ngm d-4-PGB_2-ME-TMS to an aliquot (1/20th) of extract from 5 ml blood-bank plasma. A trace amount of radioactive PGE_2 was added to the 5 ml plasma. After solvent extraction and silicic acid column chromatography with gradient elution, the appropriate fractions (radioactive) were consolidated and treated with methanolic KOH to form PGB_2 (1,5). After treatment with diazomethane and a silanizing reagent an aliquot was injected on to a 2 m x 2.5 mm ID 1.5% OV-17 column (GLC-MS) at 265° for MID analysis. The result (upper left of Figure 3) shows that no prostaglandins were detected at the expected retention time (4.85 min) although there is a small peak on the m/e 323 profile (confirmed by display of this profile only as in the bottom left panel) which could be PGB_1-ME-TMS. Another aliquot of this plasma blank was "spiked" with 900 picograms of PGB_2-ME-TMS and 9.0 ngm d-4-PGB_2-ME TMS; the MID results of this run are shown in the bottom right panel of Figure 3. The MID trace resulting from an aliquot of the prostaglandin standard only (900 pgm PGB_2-ME-TMS and 9.0 ngm d-4-PGB_2-ME-TMS) was used to establish the retention time (upper right of Figure 3) for these derivatives. The time-cursor is also displayed with the composite data (lower right) to help identify the PGB_2-ME-TMS peaks in the biological background.

Acquisition, reduction, and display of the MID data by a small computer (8K) greatly facilitate data interpretation, especially in the detection of trace materials in biological samples.

Acknowledgement

Mrs. Betty Fox routinely operated the GLC-MS-computer system. This work was supported by a Center Grant for Clinical Pharmacology and Drug toxicology NIH-GM-15431; J.C.F. by Deutsche Forschungsgemeinschaft.

References

1. B.J. Sweetman, J.C. Frolich and J.T. Watson, submitted for publication.

2. B. Samuelsson, M. Hamberg, C.C. Sweeley, Anal. Biochem. 38:301, 1970.

3. C. C. Sweeley, W.H. Elliott, I. Fries, and R. Ryhage, Anal. Chem. 38:1549, 1966.

4. D.R. Pelster and J.T. Watson, unpublished results although presented in preliminary form at the Fifth Great Lakes Regional ACS Meeting, Peoria, Ill., June, 1971.

5. G.H. Jouvenaz, D.H. Nugteren, R.K. Beerthuis, and D.A. Van Dorp, Biochim. Biophys. Acta 202:231-234, 1970.

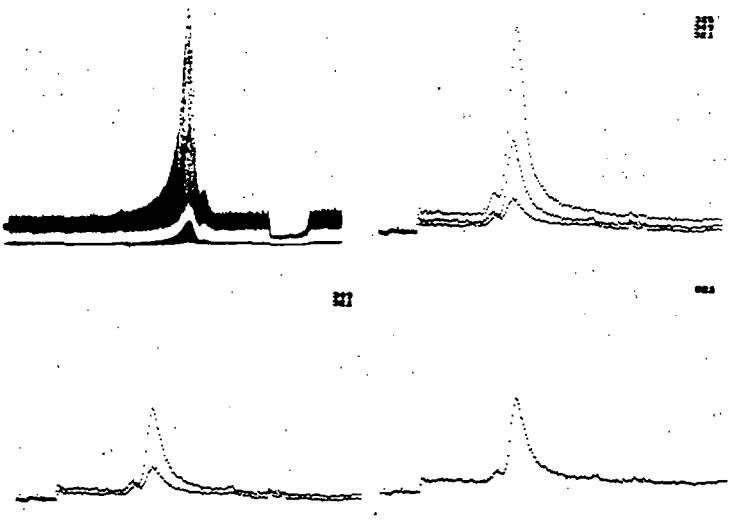

Figure 1: Comparison of oscillographic (upper left) and oscilloscopic presentation (from PDP-12 computer) of MID data of m/e 321,325,349. The upper panels are parallel recordings of the composite group of ion profiles; the lower panels illustrate a sequence in which the ion profile of m/e 325 and then that of m/e 349 are removed from the oscilloscope screen.

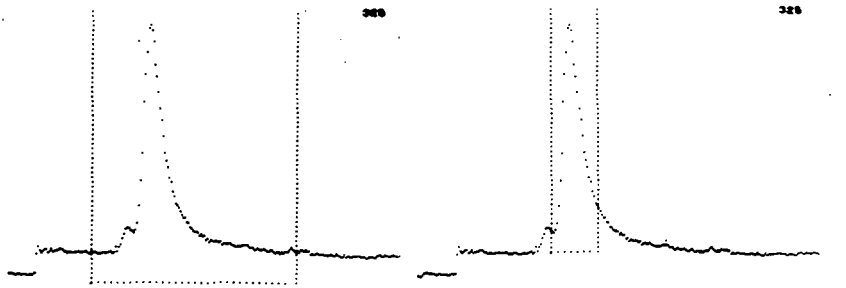

Figure 2: Photographs of oscilloscopic screen on PDP-12 computer showing selected ion current profile and presentation of area cursors before (left) and after (right) the operator has positioned the cursors prior to peak area calculation.

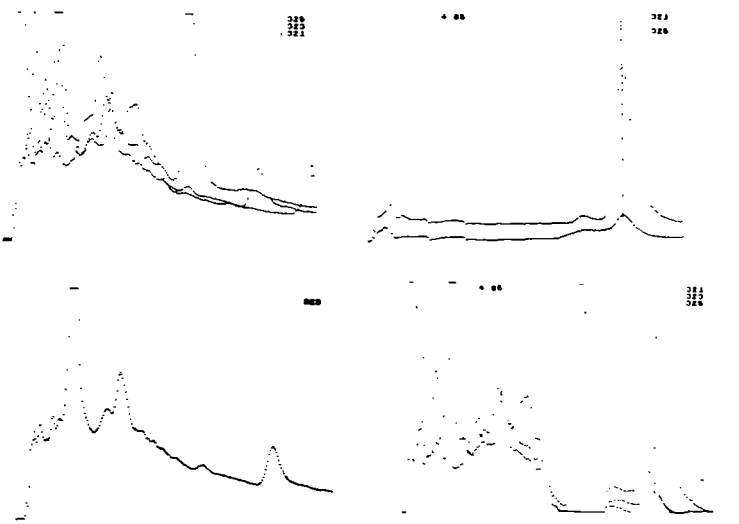

Figure 3: Photographs of oscilloscope showing MID results of plasma blank extract only (upper and lower left). The upper right panel represents the MID results from 900 picogram H4 and 9.0 ngm D4-PCB_2-ME-TMS as standard solution only while the lower right results from the same amount of standard plus the plasma blank extract. A time cursor was also displayed in the right panels to facilitate location of the PG peaks (retention time = 4.85 min).

F1

Use of Photoelectron Spectra in Predicting Mass Spectra.* J. BERKOWITZ and J. L. DEHMER, Argonne National Laboratory, Argonne, Illinois 60439

Theories of mass spectra in recent years have emphasized the quasi-equilibrium theory and its application to the prediction of the fragmentation patterns of large molecules. By contrast, for small (diatomic and triatomic) molecules, only a few attempts[1,2] have been made. In the rather specific approach to be described, the wealth of recent photoelectron spectroscopic data on such simple systems is used together with correlation rules and electron-impact theory; and on this basis the fragmentation patterns are deduced for various classes of molecules—from the purely covalent (e.g., H_2, O_2, diatomic halogens) to the strongly ionic (alkali halides) and involving such intermediate bonding cases as hydrogen halides and other metal halides. The photoelectron spectra of several metal halides that have recently been obtained in this laboratory graphically illustrate the very different bonding in these systems and help to explain the various contributions to the fragmentation pattern in more detail than is possible with ionic models.

*Work performed under the auspices of the U.S. Atomic Energy Commission

[1]J. C. Lorquet, J. Chim. Phys. 57, 1078 (1960).
[2]E. N. Nikolaev, Khim, Vys. Ener. 3, 491 (1969).

ENERGY DEPOSITION FUNCTIONS IN MASS SPECTROMETRY: PREDICTION OF PHOTOIONIZATION MASS SPECTRA†

G. G. Meisels and R. H. Emmel
Department of Chemistry
University of Houston
Houston, Texas 77004

ABSTRACT

The application of the optical approximation to the calculation of energy-deposition functions resulting from electron impact suffers conceptually from uncertainties in the applicability of the Bethe-Born theory and from the neglect of multiple ionization and autoionization. Moreover, paucity and possibly unreliability of input data required for evaluation limit usefulness. The contribution of some of the difficulties introduced by experimental parameters can be assessed by calculating theoretical photoionization mass spectra from 21.21 photoelectrons spectra and breakdown graphs. Comparison with experimental photoionized mass spectra shows that previous discrepancies in predicted and experimental mass spectra for electron impact are not necessarily an indication of the inapplicability of the primary concepts.

INTRODUCTION

The statistical or quasi-equilibrium of mass spectra[1] assumes that ions are formed with a range of excitation energies on initial electron impact and that this energy is rapidly degraded into vibrational energy of the ground electronic state of the ion. The subsequent fragmentation is then described in terms of first order rate theory. Primary emphasis in the development of this model since its original introduction has been on the correct description of first order rate constants, and good approximations to actual state density counting are now available.[2-13] This aspect of the theory is therefore well able to calculate breakdown curves[14,15] and shows good agreement with such data obtained by charge exchange or photoionization.[11-13] The second major factor affecting the calculation of mass spectra produced by 70 eV electrons, the internal energy distribution function, has received considerably less attention. A variety of approximations have been employed to estimate this quantity since the direct evaluation is extremely difficult and time consuming.[16] Unfortunately, the assumptions underlying the use of the indirect methods may well be invalid.[12] Experimental determinations can give directly at best the energy transferred to the species an electron impact, that is, the energy transferred to the ion in excess of the adiabatic ionization potential, which is the energy-deposition function.

Our model for evaluating this energy-deposition function is based on the optical approximation.[17-19] One method of obtaining the optical approximation utilizes the Born theory of atomic collisions and the relationship set forth by Bethe between the optical properties of an atom or molecule and its cross section for inelastic electron collisions. The resulting Bethe-Born theory of collisions[17] is, in essence, a quantum mechanical impact parameter treatment.

A similar relationship can be derived by correlating the collision process with radiation theory.[20,21] This approach, the Weizsaecker-Williams method of virtual quanta, analyzes the time-dependent perturbing field of the impinging electron or other charged particle using classical mechanics.

The optical approximation can be readily converted to equation I:

$$P(E_n) = (\sigma_n/E_n)/\left(\int_{IP}^{E_{max}} (\sigma_n/E_n)dE_n\right) \qquad (I)$$

This equation is a probability function $P(E_n)$ that on passage of highly energetic electrons an ion pair is created by an energy loss (E_n). $P(E_n)$ may also be regarded as a quasi-photon interaction (absorption) spectrum.

When ionization results, the energy E_n of the quasi-photon cannot be associated uniquely with a given excited state, but will be divided between the kinetic energy of the ejected electron(s) and the ionization energy. It is possible to estimate the energy partitioning from photoelectron spectra taken with incident photon energy $E_n = h\nu$; this will not give correct results for systems where multiple ionization is important because in such processes the energy difference between E_n and the energy remaining with the multiply charged ion may be divided between two or more electrons. Moreover, since photoelectra spectra are usually available only at one or two energies, further approximation was made by merely truncating the 21.21 eV photoelectron spectrum at E_n-IP and

renormalization. This is essentially equivalent to assuming stepfunction threshold behavior and, we repeat, is a requirement of practice not an inherent weakness of the approach.

The validity, limitations, and applications of the optical approximation for calculating energy-deposition functions in mass spectrometry have been discussed in detail.[22] This is the most questionable concept.

There are however also several practical problems in the evaluation of this approach. Although total photoionization cross sections are available up to ca. 25 eV from the work of Schoen[23] and that of Metzger and Cook[24] the data are not in very good agreement with each other. Breakdown graphs may differ as a function of the method by which they were obtained, and are not known with great accuracy or reliability. Photoelectron spectra discriminate against ions resulting from autoionizing states and their intensity amplitudes are not consistent between various investigators. Mass spectra obtained with various instruments differ substantially from each other. Among the reasons for this discrepancy are instrumental mass discrimination and ion source temperature.

The contributions of some of the difficulties introduced by uncertainties in the experimental data can be assessed in part by calculating photoionization mass spectra from photoelectron spectra and breakdown graphs and comparing the results with experimental spectra, thereby eliminating the optical approximation. Multiple ionization should not be an important factor if low photon energies are employed. Autoionization should not be an important complication since only one photon energy is relevant. Photoionization cross sections do not enter into the calculations. The result, therefore, is an evaluation of possible experimental problems arising from photoelectron spectra and breakdown graphs.

EXPERIMENTAL

The experimental photoionization mass spectra, breakdown graphs obtained by photoionization and the first derivative of the total ionization efficiency curves with respect to energy produced by photoionization (illustrated as I.E.D.F. in the Figures) were taken from the data of Chupka and Berkowitz.[25] The breakdown graphs produced by charge exchange were obtained as follows: ethane from von Koch,[26] n-propane from Pettersson and Lindholm,[27] and n-butane from Chupka and Lindholm.[28] Photoelectron spectra produced by a He I or He II resonance lamp were corrected for possible instrumental discrimination by applying an energy analyzer bandpass correction of the type suggested by Berkowitz and Guyon.[29]

RESULTS

The experimental mass spectrum obtained by photoionization (P.I.) appears at the extreme left hand side of each Figure for comparison. Figure 1 illustrates that the experimental mass spectrum of ethane can be completely resynthesized by numerically folding the first derivative of the total ionization efficiency curve, with respect to energy, obtained by photoionization into a breakdown graph also obtained by photoionization. The regenerated mass spectra of n-propane and n-butane, obtained by this procedure are also in excellent agreement with their respective experimental mass spectra as illustrated in Figures 2 and 3. Since the data of Chupka and Berkowitz[25] extend only to 14 eV, photoelectron spectra were truncated at that energy and comparison is made with photoionization mass spectra also at 14 eV.

When convoluting the first derivative of the total photoionization efficiency curve with a breakdown graph obtained by means of charge exchange (Figures 1 - 3) the contribution of ions associated with higher energy processes is suppressed while ions associated with lower energy processes are enhanced. When threshold photoelectron spectra are folded into breakdown graphs obtained by photoionization, agreement with experimental mass spectra results. When threshold photoelectron spectra are combined with breakdown graphs obtained by charge exchange, the resulting ion fractions are in poor agreement with those obtained directly by photoionization (shown in Figures 2 and 4).

He I or He II photoelectron spectra (bandpass corrected) convoluted with breakdown graphs produced by photoionization again illustrate that the ion fractions associated with low energy processes are enhanced while high energy processes appear to be suppressed. When photoelectron spectra are folded into breakdown graphs obtained by charge exchange, the results are in total disagreement with the experimental mass spectra (illustrated in Figures 2, 5, and 6).

In our previous investigation[22] we used He I photoelectron spectra and breakdown

graphs obtained by charge exchange, in conjunction with the optical approximation, to predict the mass spectrum of ethane; the result was in relatively poor agreement with the experimental 70 eV electron impact mass spectrum (Figure 6). The same kind of disagreement is obtained in the calculation of photoionization mass spectra where the optical approximation is not used; the discrepancy is therefore probably best ascribed to uncertainties in the breakdown graphs and questionable quantitative reliability of photoelectron spectra. Both of these factors appear to reduce the apparent contribution of high energy processes while emphasizing those having a lower threshold. The use of threshold photoelectron spectra and breakdown graphs obtained from photoionization gives best agreement for photoionization mass spectra; the use of threshold photoelectron spectra, where bandpass correction are not necessary, also gives an improvement to the prediction of 75 eV mass spectra.[22] Unfortunately, only few data of this type are available.

We conclude that discrepancies between experimental 75 eV mass spectra and spectra calculated on the basis of the optical approximation do not indicate failure of the optical approximation but are primarily an indication of insufficient reliability of the data used for the evaluation.

ACKNOWLEDGEMENTS

This investigation was supported in part by the United States Atomic Energy Commission under contract AT-(40-1)-3606 and in part by the Robert A. Welch Foundation of Houston, Texas. The computer facilities employed in this research were those of the University of Houston Computer Center. We are sincerely grateful for this assistance.

LITERATURE CITED

† A more detailed account of this work will be submitted for publication in the International Journal of Mass Spectrometry and Ion Physics.

1. H. M. Rosenstock, M. B. Wallenstein, A. L. Wahrhaftig and H. Eyring, Proc. National Acad. Sciences U. S. 38, 667 (1952).
2. M. Vestal, A. L. Wahrhaftig and W. H. Johnston, J. Chem. Phys. 37, 1276 (1962).
3. E. W. Schlag and R. A. Sondmark, J. Chem. Phys. 37, 168 (1962).
4. S. H. Lin and H. Eyring, J. Chem. Phys. 39, 1577 (1963).
5. P. C. Haarhoff, Mol. Phys. 7, 337 (1963).
6. E. Thiele, J. Chem. Phys. 39, 3258 (1963).
7. G. Z. Whitten and B. S. Rabinovitch, J. Chem. Phys. 38, 2466 (1963).
8. K. A. Wilde, J. Chem. Phys. 41, 448 (1964).
9. W. Forst, Z. Prasil, and P. St. Laurent, J. Chem. Phys. 47, 3736 (1967).
10. J. C. Tou, J. Phys. Chem. 71, 2721 (1967).
11. H. M. Rosenstock, Adv. in Mass Spectrom. IV, 523 (1968).
12. M. Vestal, in "Fundamental Processes in Radiation Chemistry," P. Ausloos, Ed., J. Wiley - Interscience, New York (1968), Chapter 2.
13. H. M. Rosenstock and M. Krauss, in "Advances in Mass Spectrometry", 2, 251 (1962).
14. E. Pettersson and E. Lindholm, Arkiv för Fysik 24, 49 (1963).
15. H. von Koch, Arkiv Fysik 28, 559 (1965).
16. H. Ehrhardt, F. Linder, and T. Tekaat, "Advances in Mass Spectrometry," London, Pergamon Press, 4, 705 (1968); Ibid., 5, (in press).
17. H. V. Bethe, Ann. Physik 5, 325 (1930).
18. W. F. Miller and R. L. Platzman, Proc. Phys. Soc. (London) A70, 299 (1957).
19. R. L. Platzman, The Vortex 23, 372 (1962).
20. E. J. Williams, Rev. Mod. Phys. 17, 217 (1945).
21. J. D. Jackson, "Classical Electrodynamics," J. Wiley and Sons, New York (1963).
22. G. G. Meisels, C. T. Chen, B. G. Giessner, and R. H. Emmel, J. Chem. Phys. 56, 793 (1972).
23. R. I. Schoen, J. Chem. Phys. 37, 2032 (1962).
24. P. H. Metzger and G. R. Cook, J. Chem. Phys. 41, 462 (1964).
25. W. A. Chupka and J. Berkowtiz, J. Chem. Phys. 47, 2921 (1967).
26. H. von Koch, Arkiv Fysik 28, 559 (1965).
27. E. Pettersson and E. Lindholm, Arkiv Fysik 24, 49 (1963).
28. W. A. Chupka and E. Lindholm, Arkiv Fysik 25, 349 (1963).
29. J. Berkowitz and P. M. Guyon, Int. J. Mass Spectrom. Ion Phys. 6, 302 (1971).

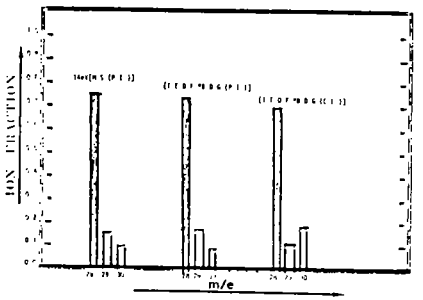

FIGURE 1. Ethane; experimental photoionization mass spectrum (14 eV MS PI), spectrum regenerated from photoionization data (IEDF*BDG(PI)), and differential of total ionization (IEDF) folded into charge exchange breakdown graph (BDG(CE)).

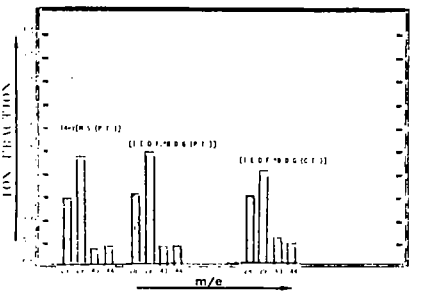

FIGURE 2. Propane; experimental photoionization mass spectrum (14 eV MS PI), spectrum regenerated from photoionization data (IEDF*BDG(PI)), and differential of total ionization (IEDF) folded into charge exchange breakdown graph (BDG(CE)).

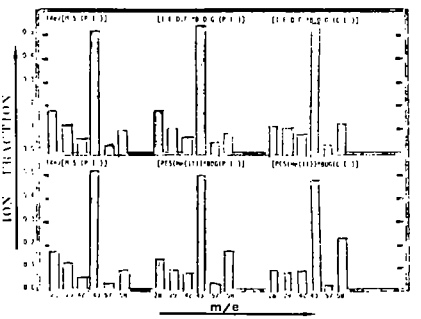

FIGURE 3. n-Butane; experimental photoionization mass spectrum (14 eV MS PI), spectra produced by folding bandpass-corrected He-II photoelectron spectrum (PES(He-II)) into breakdown graph obtained from photoionization (BDG(PI)) and by folding PES(He-II) into BDG(CE).

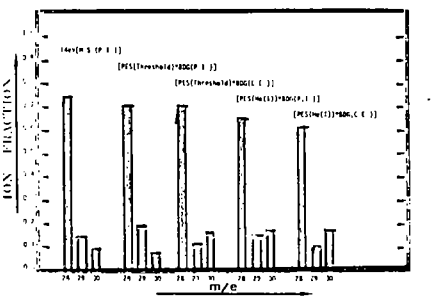

FIGURE 4. Ethane; 14 eV MS PI, Threshold photoelectron spectrum (TPES) folded into BDG(PI), TPES folded into BDG(CE), PES (He-I) folded into BDG(PI) and into BDG(CE).

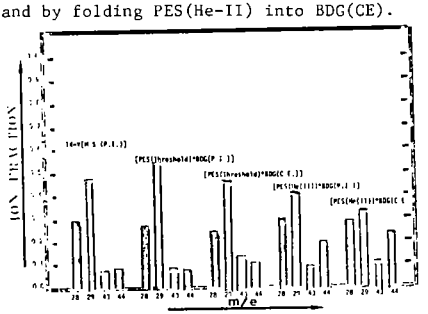

FIGURE 5. Propane; 14 eV MS PI, Threshold photoelectron spectrum (TPES) folded into BDG(PI), TPES folded into BDG(CE), PES (He-I) folded into BDG(PI) and into BDG(CE).

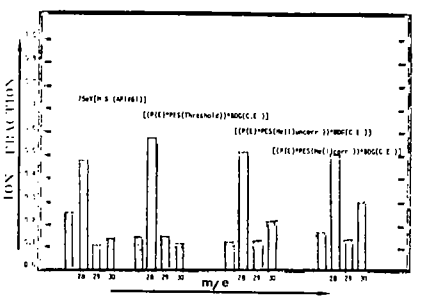

FIGURE 6. Ethane; mass spectrum produced by impact of 75 eV electrons and those obtained by optical approximation using: TPES and BDG(CE), PES(He-I, uncorrected) and BDG(CE), and PES(He-I, bandpass-corrected) and BDG(CE).

Photoionization of Carbon Dioxide*

Kenneth E. McCulloh

National Bureau of Standards

Washington, D. C. 20234

The mass-analyzed photoionization of CO_2 has been reinvestigated with optical resolution of 0.25 Å, revealing a number of features not observed in an earlier study[1] at lower resolution. The photon energy region from the CO_2^+ threshold at 13.77 eV up to 14.2 eV (900-875 Å) exhibits more than twenty autoionization peaks. This structure will provide information relevant to processes occurring in the atmosphere of Mars -- possible competition between photoionization and photodissociative excitation of CO fluorescence, and the related radiative recombination of CO_2^+ with electrons. The yield of O^+ by dissociative ionization is very low from the thermochemical threshold at 19.07 eV up to 19.39 eV, where a sharp increase occurs. Because this energy coincides with the onset of the $C^2\Sigma_g^+$ state of CO_2^+, it is suggested that predissociation plays an important role in this dissociative ionization process.

* Work supported in part by NASA.

1 V. H. Dibeler and J. A. Walker, J. Opt. Soc. Am. 57, 1007 (1967).

A STUDY OF THE EXCITED IONIC STATES OF CO_2^+, H_2S^+, AND $n\text{-}C_5H_{12}^+$ BY OPTICALLY MODIFIED MASS SPECTROMETRY

R. E. Ellefson and A. B. Denison
Department of Physics, University of Wyoming, Laramie, Wyoming 82070

and

J. H. Weber
U.S. Department of the Interior, Bureau of Mines
Laramie Energy Research Center, Laramie, Wyoming 82070

A technique has been developed for studying the excited states of ions. The technique relies on reducing or increasing the intensity of the ions recorded in a mass spectrum by changing the populations of excited states of the ions that lead to fragmentation. The populations of the excited ionic states are changed by induced emission or absorption of photons. We call the effect produced an optically modified mass spectrum.

The photo-induced transitions are accomplished by irradiating the ionized sample in the source of a time-of-flight mass spectrometer with a 1,000 W-Hg high pressure arc lamp. Small sample concentrations (partial pressure $<10^{-9}$ Torr) are used to observe the effect. Wavelength dependences are determined using band pass and long pass filters.

An increase in the parent ion abundance of n-pentane (m/e 72) is observed with light on. Complimentary decreases in abundance of the fragments m/e 43 and m/e 42 are observed, and wavelength studies indicate a fragmentation route of m/e 72 → m/e 43 → m/e 42 proceeds when $C_5H_{12}^+$ has 4.0 eV of excitation energy. Other fragmentation routes involving m/e's 72, 57, 43, and 42 are revealed through complimentary increases and decreases in fractional abundances and through wavelength studies.

The parent ion H_2S^+ and its fragment HS^+ are both observed to decrease in the presence of the light. This is attributed to induced emission competing with autoionization and autoionization-dissociation. This hypothesis is substantiated by the disappearance of autoionization features in the probability for ionization curves when the light is on. The probability for ionization and fragmentation curves are obtained using a modified energy distribution difference technique (see paper F 7 on "Resolution of Fine Structure..." in these proceedings).

The intensity of CO_2^+ is observed to increase by a factor of 3 when irradiated. The large amount of electron impact excitation of CO_2 provides a source for this increase in CO_2^+ by photo-assisted ionization of $[CO_2]^*$ using photons with energy <6 eV. A lowering of the measured ionization potential of CO_2 from 13.8 eV with light off to 12.2 eV with light on supports the model of photo-assisted ionization.

The ability to photo-induce changes in the populations of certain excited states of a parent ion and observe complimentary behavior in the intensity of a fragment ion provides evidence for proposing fragmentation routes. With H_2S it is demonstrated that induced emission of photons from $[H_2S]^*$ can compete with autoionization processes. The large amount of electron impact excitation of CO_2 provides the conditions for photo-assisted ionization to occur. Details of these processes are presented in an article submitted to the Journal of Chemical Physics.

EVALUATING METHODS FOR DETERMINING APPEARANCE POTENTIALS. PART 2: COMPETITIVE AND CONSECUTIVE REACTIONS AND A NEW LOOK AT THE CRITICAL SLOPE METHOD.

J. L. Occolowitz and B. J. Cerimele
Lilly Research Laboratories, Indianapolis, Ind. 46206

The calculations presented at the previous meeting were extended to include competitive and consecutive reactions. For consecutive reactions, statistical partitioning of energy between the ionic and neutral species of the first fragmentation was included in the calculations. Evidence was presented to show that the ranking of the methods for determining appearance potentials is independent of the exact nature of the threshold law and the rate constant vs. internal energy relationship.

The following conclusions were derived from the theoretical study:

1. A modified critical slope method, using critical slopes of 1/2kT and 2/3kT for the calibration and fragment ionization efficiency curves, respectively, yields appearance potentials more accurate than those obtained by the Warren, semi-log, energy compensation, linear extrapolation, or second derivative method.

2. For metastable ions, all methods are about equally accurate.

3. The appearance potential of a fragment ion obtained by the critical slope method is equal to or a little less (~0.1 eV) than the appearance potential of the corresponding metastable ion.

4. The appearance potential of a fragment ion determined by the modified critical slope method is about 0.5 eV lower than that obtained using the energy compensation, Warren, or semi-log method.

5. The difference in fragment and metastable ion appearance potentials determined by the semi-log method is 0.4 eV.

6. For higher energy competitive reactions which compete only at higher ionizing energies, the modified critical slope method gives an appearance potential more than 0.5 eV lower than obtained using the Warren, energy compensation, or semi-log method.

Data obtained from an Atlas CH4 single-focusing mass spectrometer and a Varian-MAT SM1B double-focusing mass spectrometer were used to test the above conclusions. A value of kT = 0.25 eV was used for both instruments. In summary, the following experimental observations were made:

1. For nineteen ionic reactions, the mean difference between the appearance potential of a fragment ion and the corresponding metastable ion, both determined by the semi-log method, was 0.45 eV, with a standard deviation of 0.17 eV.

2. For seven ionic reactions studied, the mean difference between the appearance potential of a metastable ion and the corresponding fragment ion, determined by the modified critical slope method, was 0.04 eV.

3. For twenty-one ionic reactions, the difference between the appearance potential of a fragment ion determined by the semi-log and modified critical slope methods was 0.45 eV, with a standard deviation of 0.17 eV.

4. Four higher energy competitive reactions were studied where the appearance potential of the higher energy reaction, as determined by the semi-log method, was at least 1.2 eV higher than that of the lower energy reaction. For each higher energy reaction, the appearance potential determined by the modified critical slope method was 0.9-1.0 eV lower than that determined by the semi-log method.

The experimental data support the inferences derived from theory. On this basis, it is concluded that the appearance potentials of fragment ions determined by the modified critical slope method are, in fact, more accurate.

ION SOURCE CHEMISTRY OF LOW MOLECULAR WEIGHT ALKANES

F6

G. D. Flesch and H. J. Svec

Ames Laboratory-USAEC and Department of Chemistry

Iowa State University, Ames, Iowa 50010

The chemistry occurring in the ion source of the mass spectrometer has been of interest since the beginnings of mass spectrometry. However, nearly all the studies of chemical reactions occurring in ion sources are made with 50 volt electrons or at energies near the onset potential of fragment ions. The information contained in the intermediate energy range is largely ignored.

Two years ago at this meeting we described efforts to draw information from this intermediate energy region for the ions of chromyl chloride and chromyl fluoride. [1] Since that time, we have similarly studied ferrocene, nickelocene and ruthenocene, [2] as well as the hexacarbonyls of chromium, molybdenum and tungsten, [3] all of which have a central metal atom. Today we describe attempts to broaden the application of these techniques to compounds which do not have a central metal atom and whose ionization involve valence electrons. We chose the low molecular weight alkanes because of their volatility and their small number of significant fragment ions. For each alkane we examined those ions which account for one or more percent of the total ions observed for 29 volt electrons.

In the case of ethane, three of the five ionization efficiency (IE) curves were deconvoluted into two or more product ion components. The ion source reactions associated with the product ion components are listed in Table 1, along with the calculated and observed enthalpies of the reactions and their relative abundances. Since the reactions are so simple there is little chance for error in the choices of the reactions. The agreement between the calculated and observed enthalpies is excellent. We assume that the disparity in the case of the higher energy reaction producing $C_2H_3^+$ is the result of our neglecting excess energy in the reaction products. These results give us confidence in the validity of the deconvolution methods which allowed us to extract information about nine reactions rather than the five previously reported.

We also studied propane, normal and isobutane, and normal and neopentane and found many multi-component IE curves for these alkanes. These results are summarized in a general way in Table 2. The ion source reactions were assigned solely on the basis of the energetics. It is encouraging that in every case the charge was indicated to have remained on the product with the lowest ionization potential, in agreement with the findings of Harrison and co-workers. [5]

We were also able to arrange product and reactant components in pairs with reasonably good success to obtain fragmentation schemes for these alkanes. Ionization efficiency curves were convoluted according to these schemes. On the average, the relative RMS error between the calculated and observed IE curves was 1.5 percent over the upper 95 percent of each curve.

The results presented today strengthen out belief that deconvolution-convolution techniques are useful and do provide valuable insights into the chemistry occurring in the mass spectrometer. We intend to submit a detailed description of these experiments to J. Chem. Soc.

References

1. G. D. Flesch and H. J. Svec, J. Chem. Phys. 54. 2681 (1971).
2. G. D. Flesch, G. A. Junk and H. J. Svec, J. Chem. Soc. ****(1972).
3. G. D. Flesch and H. J. Svec, J. Chem. Phys. 55. 4310 (1971).
4. "Ionization Potentials, Appearance Potentials and Heats of Formation of Gaseous Positive Ions" J. L. Franklin, J. C. Dillard, H. M. Rosenstock, J. T. Herron, K. Draxl, and F. Field, NSRD-NBS 26, Washington, D.C., 1969.
5. A. G. Harrison, C. D. Finney and J. A. Sherk, Org. Mass Spectrom. 5, 1313 (1971).

Table 1. Fragmentation Reactions of Ethane

reaction	ΔH(eV) calc[a]	ΔH(eV) obs[b]	rel abund[c]
$C_2H_6^+ \rightarrow C_2H_5^+ + H$	1.1	0.8	132
$\rightarrow C_2H_4^+ + H_2$	0.3	0.5	653
$\rightarrow C_2H_3^+ + H_2 + H$	3.3	3.2	95
$\rightarrow C_2H_3^+ + 3H$	7.8	9.0	26
$\rightarrow C_2H_2^+ + 2H_2$	3.1	3.0	34
$\rightarrow C_2H_2^+ + H_2 + 2H$	7.7	8.2	6
$\rightarrow C_2H_2^+ + 4H$	12.2	12.2	5
$\rightarrow CH_3^+ + CH_3$	2.1	2.2	10
$\rightarrow CH_3^+ + CH_2 + H$	7.0	6.8	1

[a]Calculated from heats of formation in NSRDS-NBS 26. [4]

[b]Determined from the difference in onset potentials of the molecular and fragment ions.

[c]In terms of a total ion abundance of 1000 at 29 eV.

Table 2. Numbers of Ions Studied and the Product Ion Components Found for Each Alkane.

alkane	number of ions studied	product ion components found
ethane	5	9
propane	8	16
n-butane	8	16
iso-butane	8	15
n-pentane	11	24
neo-pentane	9	21

RESOLUTION OF THE FINE STRUCTURE IN THE IONIZATION EFFICIENCY CURVES FOR H_2S^+, $C_2H_2^+$, $C_6H_6^+$, AND $C_6D_6^+$

F7

J. H. Weber
U.S. Department of the Interior, Bureau of Mines
Laramie Energy Research Center, Laramie, Wyoming 82070

and

R. E. Ellefson and A. B. Denison
Department of Physics, University of Wyoming, Laramie, Wyoming 82070

In electron impact ionization efficiency curves, the fine structure (ionization potential and appearance potentials for excited states of the ion) is obscured by the effects of the thermal energy distribution of the ionizing electrons. We have used a modification of the energy distribution difference of Winters, et al.[1] to resolve the appearance potentials of H_2S^+, $C_2H_2^+$, $C_6H_6^+$, and $C_6D_6^+$ and to obtain *relative probabilities for ionization*.

Our modified energy distribution difference (MEDD) method identifies the operating conditions of a mass spectrometer necessary to obtain reliable appearance potentials and relative probabilities for ionization by the EDD method. The method demands a constant filament temperature in an attempt to maintain a constant electron energy distribution as the electron accelerating voltage, V, is changed. The resulting variation in electron beam current, J(V), is measured as a function of V and is used to *normalize measured ion currents to unit electron beam current. The modified difference equation is*

$$\Delta\left[\frac{I(V)}{J(V)}\right] = \frac{I(V)}{J(V)} - b\,\frac{I(V-\Delta V)}{J(V-\Delta V)}. \qquad (1)$$

By specifying instrument conditions and measuring J(V), the quantity $\Delta[I(V)/J(V)]$ in Eq. 1 better reflects the molecule's probability for ionization.

The reliability of the MEDD method was verified by obtaining appearance potentials and relative probabilities for ionization for vibrational excitation in $C_2H_2^+$ in agreement with photoionization and monoenergetic electron impact results. Using the MEDD method on the parent molecular ions of C_6H_6 and C_6D_6, several interesting features were observed: (1) There are no differences in the energetics for the two parent ions (this implies that C-H vibrational excitation does not occur with vertical ionization), (2) all appearance potentials previously reported from photoelectron spectroscopy (using multiple excitation sources) are observed by electron impact, and (3) a population inversion occurs in the excited states of these ions at energies only 2 eV above the ionization potential. With H_2S, the MEDD method revealed not only direct ionization processes but, in addition, five autoionization processes.

Additional details of the MEDD method will appear in a paper to be submitted to the Journal of Chemical Physics.

[1] Winters, R. E., J. H. Collins, and W. L. Courchene, J. Chem. Phys. 45, 1931 (1966).

DISSOCIATION OF ETHYLENE BY ELECTRON IMPACT

S.M. Gordon, G.J. Krige and J.F. Brown

Chemistry Division, Atomic Energy Board, Pelindaba, South Africa.

Recent studies of isotope effects in the metastable spectra of deuterated ethylenes[1] have been supplemented by electron impact studies of the corresponding effects in the normal mass spectra. Quantitative measurements of the relative losses of molecular hydrogen from C_2D_3H and trans- $C_2H_2D_2$ were carried out as a function of electron energy, and the appearance potentials of the major ions were determined using the retarding potential difference technique. The isotope effects on metastable transitions are very large in comparison with the values which we obtain from the normal mass spectra. The role of H/D scrambling in the molecular ion is considered and the observed relative abundances and isotope effects are discussed in terms of calculations based on the quasi-equilibrium theory of mass spectra.

[1] I. Baumel, R. Hagemann and R. Botter, presented at the Nineteenth Annual Conference on Mass Spectrometry and Allied Topics, Atlanta, Georgia, May 2-7, 1971.

General Problems in the Identification of Drugs and Drug Metabolites by Mass Spectrometry

G1

G. W. A. Milne
National Heart and Lung Institute
National Institutes of Health, Bethesda, Maryland

W. J. A. Vandenheuvel
Merck and Co., Inc.
Rahway, N. J.

This paper constitutes a review of the applications of mass spectrometry to the problems defined in the title. There are various reasons for attempting the identification of drugs in body fluids. Prominent amongst these is the value of such information in emergency treatment of patients suffering from overdoses of drugs. In instances of mild intoxication (coma levels 1-3) supportive therapy is usually adequate and drug identification is not necessary. If the patient is in coma level 4, however, hemodialysis may be necessary, and this can only be undertaken if the identity of the drug is known because many toxic drugs cannot be satisfactorily removed by standard hemodialysis. Another area where identification of drugs has proved to be of value is in the street drug identification is essential to the successful enforcement of the various laws controlling or prescribing drugs. There are many methods of identifying drugs and the success or failure of each of these can only be evaluated in the context of the problem. Thus checking for morphine in urine at the rate of 4,000 samples per day can be done effectively and cheaply by TLC and GLC but this has so far not been possible by mass spectrometry. On the other hand, identification of drugs consumed in overdose quantities has been accomplished for the last two years in our laboratories by combined GC-MS with some success and is now a routine procedure. Once the EI mass spectrum of the various components of a mixture derived from a biological fluid have been obtained, the compounds involved can be identified by comparison of these spectra with those in a file of standard mass spectra. A system has been devised at NIH whereby the data can be the results of the search are converted into a voice message by the computer and returned to the same telephone which thus supplants the computer terminal. The use of GC in this approach can be obviated if chemical ionization mass spectrometry is used. Here, the mass spectra are so simple that the components of a mixture can readily be identified from the CI mass spectrum of the mixture, run from a direct insertion probe.

Identification of metabolites is a much more difficult problem. This is an area however, in which mass spectrometry has had a significant impact, primarily because of its high sensitivity. A major problem in this area is to prove that an isolate is indeed a metabolite of the drug under study. This can be conveniently accomplished by tagging the drug with a radioisotope. The various compounds eluted from a gas chromatograph of an extract of, say, urine can be simultaneously examined by the mass spectrometer and by a radioactive monitoring device. Eluted peaks which are radioactive can be identified from their mass spectra. Trimethylsilylation is often of great value in this connection and if this is carried out with BSA and with BSA-D18, the number of trimethylsilyl groups that has been added to the molecule is immediately apparent and the molecular weight of the material follows. This, in conjunction with the molecular weight of the starting drug limits greatly the number of possibilities for the metabolite.

A variation on this technique, used in studying the metabolism of the anthelmintic cambendazole, involves separation of the components of urine by TLC. The chromatogram is then scanned for UV absorption and radioactivity. Spots with both of these properties are eluted and can be examined mass spectrometrically, with or without trimethylsilylation and gas chromatography.

The metabolism of the anthelmintic rafoxanide produces two isomeric dihydroxy iodophenyl derivatives. These can be distinguished mass spectrometrically because the BIS-TMS derivatives of O-dihydroxy compounds lose consecutively, -OTMS (89) and $SiMe_4$ (88) upon electron impact. The second of these losses is not observed with the M- or P- isomers. Cyclic boranate formation (possible only with O-dihydroxy compounds) can be used as confirmation of the assignment.

Finally, two examples of the use of stable isotope labelling in this area are given. The stable isotope may be incorporated into the drug before administration. Thus the N-methyl group in nortriptyline is replaced by 50% trideuteromethyl. The result is a compound with a 1:1 doublet (M/E 359, 362) in the mass spectrum. This doublet should be seen (at a different M/E value of course) in any metabolite - provided the label is not removed during metabolism - and, like a radiolabel, can be used to identify a metabolite as such. Conversely, the label may be incorporated biologically into the drug. Thus the conversion by hepatic microsomes of naphthalene to 1,2-dihydro-1,2-dihydroxy naphthalene has been shown to proceed with the incorporation of 1 atom of oxygen from atmospheric oxygen and one from water. This was done by allowing the metabolism to proceed in an atmosphere of O-16 oxygen (50%) and O-18 oxygen (50%) and demonstrating by mass spectrometry that the resulting diol contains either zero or one (but not two) atoms of oxygen-18.

MASS SPECTROMETRIC DETECTION OF VERY SMALL QUANTITIES OF BIOLOGICALLY IMPORTANT AMINES

by

Alan A. Boulton, David A. Durden and Stephen Philips

Psychiatric Research Unit, University Hospital

Saskatoon, Saskatchewan, Canada.

INTRODUCTION

The relatively simple non-catecholic amines p-tyramine, tryptamine and β-phenylethylamine have been shown to be excreted in abnormal amounts in the urine of patients suffering with depression (1,2), schizophrenia (3) and Parkinsons disease (4,5,6). Using the mass spectrometric Integrated Ion Current (I.I.C.) technique first introduced by Major (7) p-tyramine in a urine extract has been identified and quantitated (8). The values obtained were in close agreement with those obtained by a chromatographic procedure based on assessment of the 1-nitroso-2-naphthol fluorophore. p-Tyramine has also been identified and quantitated in rat brain (9,10). Again the data obtained with the I.I.C. procedure was in close agreement with a thin layer chromatographic procedure in which amines as their fluorescent dansyl derivatives were assessed. In the case of cerebral p-tyramine it has proved possible to demonstrate that only the para isomer is significantly present (11) and that 3,4-dihydroxyphenylethylamine (dopamine) as well as tyrosine is a precursor (12,13).

Using a recently installed AEI MS-902S we have been able to show that β-phenylethylamine, as its dansyl derivative, is present in various tissues of the rat and is amenable to quantitative analysis by the I.I.C. procedure.

MATERIALS AND METHODS

Crystalline dansyl β-phenylethylamine was kindly donated by Dr. Nikolaus Seiler (Max-Planck Institut für Hirnforschung, Frankfurt). The dansyl reagent (1-dimethylaminonaphthalene-5-sulfonyl chloride) was purchased from CALBIOCHEM, Los Angeles, California.

Rats were stunned and the brain, liver, lung, heart and kidneys removed,

chilled on solid CO_2, weighed and homogenized in 20ml ice cold 0.4N $HClO_4$. TRITON X-100 (CANADIAN LABORATORIES, Toronto, Ontario), to a final concentration of 0.5% (w/v) and on occasions β-phenylethylamine-^{14}C (in order to assess recovery) were added. After centrifugation at 12,000xg for 10 minutes the supernatant was neutralized, percolated through a Dowex 50 (H^+) resin column and after washing with water sodium acetate and water (12,13) eluted with 10ml methanol:HCl, 73:27 (v/v). After drying, this eluate was dissolved in 1ml sodium carbonate (10% w/v) mixed with 1.5ml dansyl reagent (1mg/ml in acetone) and allowed to stand at 37°C for 2 hours. After precipitation of the sodium carbonate with excess acetone (9ml) the resultant solution after drying was triturated in benzene:acetic acid (99:1 v/v, 2x100µl) and transferred to the origin of a thin layer of silica gel (Mondray Ltd., Montreal) and developed with chloroform;butyl acetate, 5:2 (v/v). After separation the plate while still damp, was sprayed with isopropanol:triethanolamine, 4:1 (v/v) to stabilize the fluorescence and the DNS-phenylethylamine zone eluted [benzene:acetic acid, 99:1 (v/v)] and separated in two further solvent systems (14). In the case of the quantitative assessment of the amount of fluorescence the final separated stabilized DNS phenylethylamine zone was measured in a fluorimeter (excitation 335nm, fluorescence 486nm). Further details of the fluorescent chromatographic procedure will be published elsewhere. For I.I.C. analyses the final non stabilized DNS-phenylethylamine zone was eluted while the plate was still damp, dried and redissolved in 500µl ethanol. Aliquots (5µl) of this final solution were placed within the tip (pyrex glass) of the direct insertion probe and the solvent was pumped off in the insertion lock of the mass spectrometer. Heptacosafluoro-tri-n-butylamine was used as standard and the decade resistance set to the ratio between the standard ($^m/_e$ 337.9839) and the molecule ion ($^m/_e$ 354.1402) of DNS-phenylethylamine. Using the peak switching system of the mass spectrometer the recorder trace records both the reference ion and DNS-phenylethylamine ion signal as the derivative evaporates from the probe tip in the ion source at 295°C. See references (8-10) for further details.

RESULTS

A typical calibration curve obtained using aliquots of a suitably diluted, in both ethanol and methanol, standard solution of crystalline DNS phenylethylamine is shown in the upper curve of figure 1. It can be seen that a linear relationship obtains between the area enclosed by the I.I.C. envelope and concentration in the range 10^{-12} to 10^{-7}g. The lower curve in figure 1 (placed as shown simply for

convenience) indicates that linearity is similarly maintained over the range

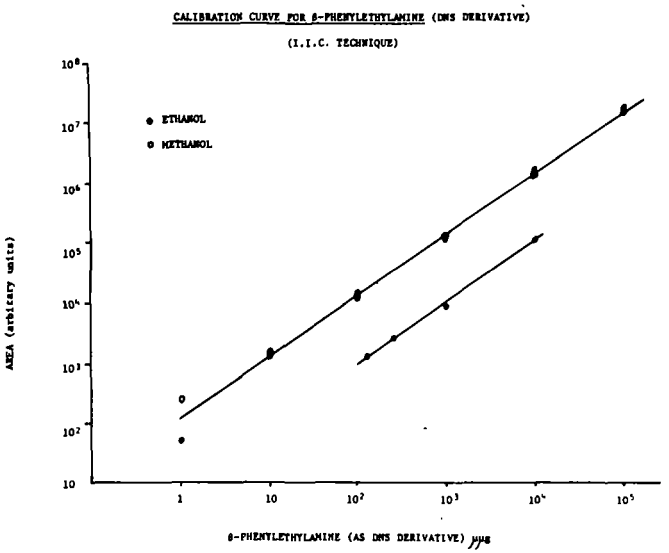

10^{-10} to 10^{-8}g when β-phenylethylamine is subjected to the procedure used to dansylate and separate this amine in tissue extracts. The mass spectrum and precise mass (354.1402) of the molecule ion of the isolated DNS-phenylethylamine zone from β-phenylethylamine, tissue extracts and tissue extracts supplemented with β-phenylethylamine were identical to those obtained with crystalline DNS-phenylethylamine. The overall recovery of β-phenylethylamine through the entire procedure was 50%.

A comparison of the tissue concentration of β-phenylethylamine in the rat as determined by quantitative fluorimetry (n=8) and the I.I.C. procedure (n=1) is shown in figure 2. It can be seen that the agreement between the two procedures is extremely good in all cases except one.

COMPARISON OF CHROMATOGRAPHICALLY SEPARATED

DNS-β-PHENYLETHYLAMINE ISOLATED FROM SOME TISSUES OF A RAT

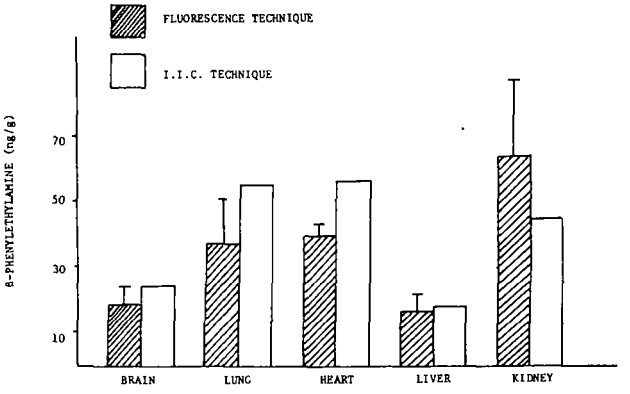

DISCUSSION

The isolation procedure described in this paper was deliberately involved and time consuming for two reasons. First a precise comparison between the two analytical methods with confirmation of the unambiguity of the chromatographic procedure was possible and secondly a procedure with such extensive separation of the amine to be analyzed prevented any possible increase in the value of the molecule ion current due to identical fragment ions from large molecules which might have occurred for such a simple amine had unpurified non-derivatized biological extracts been used. For the future it will probably be permissible simply to separate the formed DNS derivatives in a single chromatographic system. The use of derivatives seems warranted on the grounds that the increased molecular weight allows an analysis in a relatively clean part of the spectrum with perhaps an increase in sensitivity. The other advantage is that the same methodological procedures can be used for both analytical and metabolic experiments. Applications and extensions of the I.I.C. technique to an analysis of a variety of interesting biogenic substances in regions of the brain, in subcellular fractions of the cell and in investigating the effect of several drugs on these distributions is underway.

ACKNOWLEDGEMENTS

We thank the Psychiatric Services Branch of the Saskatchewan Department of Public Health and the Medical Research Council of Canada for continuing financial support.

REFERENCES

1. Fischer, E. Arzneim. Forsch. 18 (1968) 1486
2. Boulton, A.A. and Milward, L. J. Chromatog. 57 (1971) 287
3. Boulton, A.A. Nature 231 (1971) 22
4. Boulton, A.A., Pollitt, R.J. and Majer, J.R. Nature 215 (1967) 132
5. Smith, I. and Kellow, A.H. Nature 221 (1969) 1261
6. Boulton, A.A. and Marjerrison, G.L. Nature 236 (1972) 76
7. Majer, J.R. and Jenkins, A.G. Talanta 14 (1967) 777
8. Boulton, A.A. and Majer, J.R. J. Chromatog. 48 (1970) 322
9. Majer, J.R. and Boulton, A.A. Nature 225 (1970) 658
10. Boulton, A.A. and Majer, J.R. Res. Meth. Neurochem. 1 (1972) 341 Ed. R. Rodnight and N. Marks, Plenum Publishing, New York
11. Boulton, A.A. and Majer, J.R. Can. J. Biochem. 49 (1971) 993
12. Boulton, A.A. and Quan, L. Can. J. Biochem. 48 (1970) 287
13. Boulton, A.A. and Wu, P.H. Can. J. Biochem. 50 (1972) 261
14. Philips, S. and Boulton, A.A. Communication #467 Can. Fed. Biol. Soc. Meeting, Quebec, June 1972

IDENTIFICATION OF DRUGS IN BODY FLUIDS, PARTICULARLY IN EMERGENCY CASES OF ACUTE POISONING

C.E. Costello, T. Sakai and K. Biemann

Department of Chemistry
Massachusetts Institute of Technology
Cambridge, Massachusetts 02139

For about a year, the NIH Mass Spectrometry Facility of the Chemistry Department at MIT has been providing an emergency service for hospitals in the Boston area and the Boston Poison Information Center. Its main purpose is the rapid identification of drugs present in the body fluids of comatose patients in those cases where the hospital's own laboratory or local commercial firms are unable to make a correct or unambiguous identification. There are about 1-3 such cases per day and the patients are located at some fifteen local hospitals, with the majority being admitted to five of these. Results are reported by telephone within 1-2 hours after receipt of the sample at the laboratory.

The specimens received include gastric contents, blood or urine. After filtration or centrifugation (and neutralization if necessary), the body fluid is extracted twice with a fivefold volume of methylene chloride. This treatment is adequate to retrieve all drugs thus far encountered, with the exception of quarternary salts and morphine. (Morphine can be extracted into 9:1 chloroform-isopropyl alcohol after the addition of solid sodium bicarbonate. Quarternary salts are not detectable by this approach, without prior degradation.) The extract is evaporated to a small volume before analysis.

The instrumentation used in this project consists of a Perkin Elmer 990 Gas Chromatograph interfaced through a low volume splitter linked to a porous fritted glass tube pressure reduction unit[1] by a heated stainless steel capillary and microvalve. The exit of the pressure reduction unit is connected to a glass line leading into the ionization chamber of a Hitachi RMU-6L Mass Spectrometer, which is operated on-line to an IBM 1800 data acquisition and control system.[2,3] The computer has 32,768 words of core memory, three IBM 2315 magnetic disks and two IBM 2401 magnetic tape drives. All this equipment is already available as part of the NIH Mass Spectrometry Facility at MIT; its use is pre-empted when an emergency sample arrives.

A single run consists of up to 400 mass spectra taken continuously at 4-second intervals. Both gas chromatographic effluents (5'3%OV-17 column, programmed from 80° to 270° at 12°/min) and direct insertion samples may be introduced into the mass spectrometer and their spectra recorded. Immediately after a run, the time-to-mass conversions are made by the computer with calibration against a perfluoro-alkane reference. The spectra are displayed as bar plots during processing on a Tektronix 611 oscilloscope and are microfilmed with a Bolex Cine Camera.[4] Mass chromatograms[5] are also generated for each m/e value and are similarly filmed. Processing with a Kodak Prostar developer in the laboratory makes the films available immediately for ready use of the data. The microfilm is loaded into cartridges for examination in a Kodak Microstar reader.

Because rapid identification is of utmost importance in this particular application, selected spectra or the entire run are at the same time compared to a reference collection of relevant mass spectra, currently consisting of spectra of about 225 drugs, metabolites and other materials frequently encountered in body fluids. Output of the library search may be either a listing of the ten closest matching spectra together with their similarity indexes or a listing of the closest fit for each spectrum printed adding the contours of the total ion plot (Fig. 1a), together with a summary of the major components identified during the run, which is printed at the end (Fig. 1b).[6] If any spectra remain unassigned, they can also be compared to the general library of about 8000 spectra. For locating minor but significant components which elute at the same time as other components present in much larger concentrations, mass chromatograms are often useful (Fig. 1c). If new drugs are encountered and identified on the basis of their spectra, authentic samples are then obtained and the spectra are added to the library. For example, the drug phencyclidine, an anesthetic used in veterinary medicine, appearing in Fig.1 was first encountered as a substance confiscated from illegal sources, but it has since figured in several poisonings and in each instance was correctly identified by library searching of the data from a urine extract. The 1-phenyl cyclohexene is a common contaminant in illegally manufactured samples of this drug and its spectrum too has been added to the collection for easy recognition. Similar additions are made wherever appropriate.

The utility of the rapid, repetitive scanning feature of the system is illustrated in Fig. 2. In this case, the extract of urine from an infant 24 hours after birth presented an extremely complex mixture of drugs, metabolites and artifacts. In the scans shown, which are separated by only 4 seconds, two entirely different spectra were ob-

tained. Scan 161 (taken on the side of the GC-peak) is that of a contaminant, tri-2-butoxyethyl phosphate originating from the stopper of the "B.D. Vacutainer" used as a container for the sample. The very next scan (number 162) clearly corresponds to that of promazine, a drug which had been administered to the mother.

Especially when the body fluid received is urine, metabolites rather than the original drug may be present in the extract. As an example, in a case involving the drug Mellaril and two of its metabolites (Fig. 3), the search was successful in deducing the type of drug (phenothiazine) represented by metabolite A, scan number 202. The drug itself, structure B, was correctly identified from scan number 275. The spectrum of the second metabolite C, in scan number 280, retained enough of the characteristics of the initial drug to produce a "best fit" for the Mellaril, although the similarity index was much lower than that found for scan 275, because the mass spectrum of the metabolite retains only part of the characteristics of the original drug. It is this aspect of the complex but structure-related character of electron impact spectra which is much to be preferred over the one-peak approach of chemical ionization if one wishes to cover cases where previously unknown or unexpected substances are to be identified on the basis of the still detectable metabolites.

Our experience has been that the wide variety of drugs ingested in toxic quantities and the complexity of the mixtures often present in body fluids justify, indeed necessitate, the approach which we are taking for those cases where the patient's condition is very serious, the available information scanty or the capability of other analytical methods inadequate. Rapid identification of the toxic material leads to prompt and proper treatment of the individual and to more judicious use of the limited supply of medical equipment and personnel. A negative finding is also useful because it directs the doctors' attention to other probable causes of the coma.

Our data indicate that the most susceptible age groups are 2-year-olds whose natural curiosity leads them to sample indiscriminately and about 14-year-olds whose relatively narrow experience with illegal sources of drug supply often causes them to ingest misrepresented materials in harmful doses or applications.

The success of a program such as the one described depends to a large extent on the adequacy of communications channels with the medical community. In the Boston area, this is being assisted by a listing compiled by the Poison Bureau, which summarizes all the facilities available for analytical services and their capabilities. Use of this information sheet assures that our laboratory receives only those samples with which it should be concerned and that these will be rapidly dispatched. Continuing contact between our laboratory and the patient's doctor results in further studies of the cases of special interest.

The response to this service has demonstrated that it is fulfilling a need which exists in our community. Similar needs probably exist in other urban areas and one could expect that even wider applications of this approach will develop as physicians and mass spectrometrists come into closer contact through this type of activity.

References

1. Watson, J.T., and Biemann, K., Anal. Chem., 36, 1135 (1964).

2. Hites, R.A., and Biemann, K., Anal. Chem., 40, 1217 (1968).

3. Biller, J.E., Ph.D. Thesis, Massachusetts Institute of Technology, June 1972.

4. Biller, J.E., Hertz, H.S. and Biemann, K., Proceedings of the 19th Annual Conference on Mass Spectrometry and Allied Topics, Atlanta, Georgia, 1971, p. 85.

5. Hites, R.A., and Biemann, K., Anal. Chem., 42, 855 (1970).

6. Hertz, H.S., Hites, R.A., and Biemann, K., Anal. Chem., 43, 681 (1971).

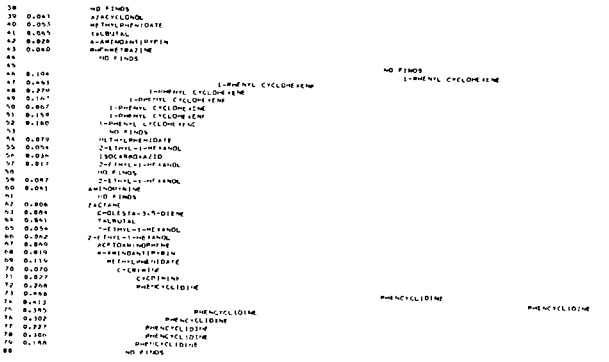

MOST PROBABLE COMPOUNDS

0.2936E 07	OLEIC ACID
0.2581E 07	PALMITIC ACID
0.2241E 07	PHENCYCLIDINE
0.2136E 07	DIBUTYL PHTHALATE
0.1669E 07	CHOLESTEROL
0.1176E 07	DIOCTYL ADIPATE
0.1059E 07	1-PHENYL CYCLOHEXENE
0.8655E 06	DIOCTYL PHTHALATE
0.7373E 06	CHOLESTA-3,5-DIENE
0.6222E 06	PHENYRAMIDOL

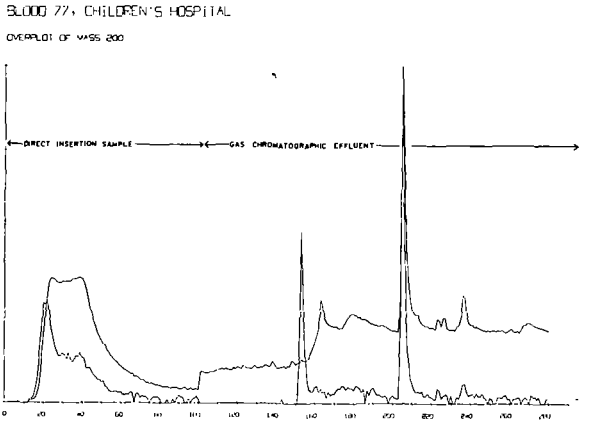

Fig.1 (a) Section of printout of library search results along the contours of the total ion plot for gc/ms run on extract of urine from a teenage patient who had ingested phencyclidine.
(b) Listing of the ten most probable compounds in the urine and serum extracts for this patient.
(c) Overplot of the total ionization plot and mass chromatogram of m/e 200 for probe (spectrum index nos. 1 to 100) and gc/ms run (nos. 101-280) for extract of blood serum of a child who had ingested phencyclidine.

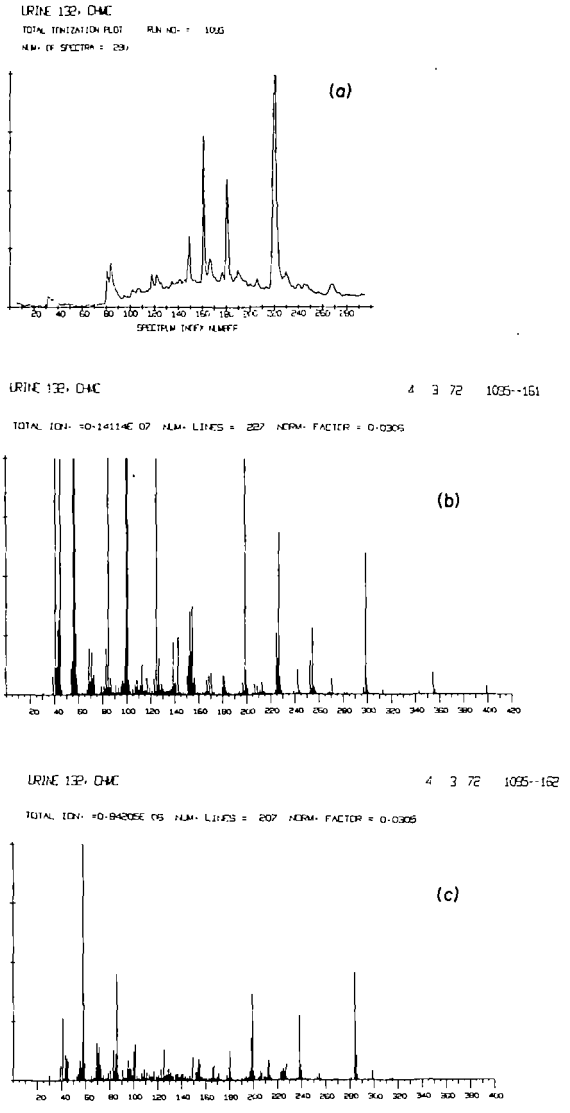

Fig. 2 (a) Total ionization plot for gc/ms run on extract of urine from an infant 24 hours after birth, who had shown signs of drug withdrawal.
(b) and (c) Mass spectra obtained during scans 161 and 162 of this run.

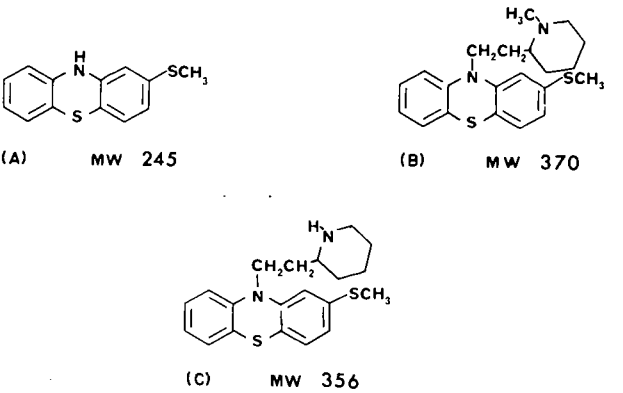

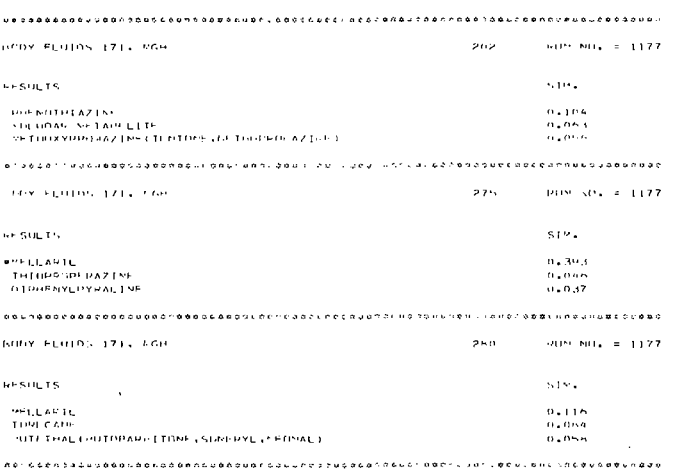

Fig. 3 Structures of the drug Mellaril (B) and two of its metabolites (A) and (C) which were found in the urine of an overdose victim and part of the output of the drug library search for the spectra obtained during the elution of these compounds from the gas chromatograph.

G5 The Use of Mass Spectrometry in the Study of Urinary Metabolites. M.G. Horning, D.J. Harvey and E.C. Horning, Institute for Lipid Research, Baylor College of Medicine, Houston, Texas 77025.

In the study of urinary drug metabolites, the mass spectrometer has been used mainly for identification. However, the combined GC-MS can also be used to study clinical problems. For example drug toxicity in the newborn caused by placental transfer of drugs given to the mother during labor is under study in our laboratory. In studies of drug metabolism, the isolation of a suitable analytical sample that can be converted to derivatives for quantification and identification by GC-MS is usually the most difficult step. Since multiple drug therapy is common, the problem becomes that of identifying multiple drugs and metabolites of differing structure. When separation of all metabolites is impractical, methods of identification based on single or multiple ion detection (chemical ionization) are employed. A computer search of mass spectra, obtained by repetitive scan, can also be used to identify metabolites. (Supported by NIH Grant NIGMS-16216.)

INTERNAL ENERGY DISTRIBUTIONS IN GASEOUS ORGANIC IONS. MECHANISM OF ELECTRON IMPACT INDUCED DECOMPOSITION OF 4-METHYLBENZIL. H1

S. E. Scheppele, R. K. Mitchum, and K. F. Kinneberg
Department of Chemistry, Oklahoma State University
Stillwater, Oklahoma, 74074

G. G. Meisels and R. H. Emmel
Department of Chemistry, University of Houston
Houston, Texas, 77002

Cleavage of the C-1--C-2 bond in the molecular ion of 4-methylbenzil, m/e 224, (1-phenyl-2-(4-methylphenyl)ethan-1,2-dione) produces either the benzoyl ion, m/e 105, or the 4-methylbenzoyl ion, m/e 119. These ions then fragment with loss of CO forming m/e 77 and 91, respectively. Loss of C_2H_2 from m/e 77 and 91 are high energy processes and thus not investigated.

The fragmentation mechanism has been investigated by determining internal energy distribution functions. The appearance potentials are consistent with the formation of the benzoyl and p-methylbenzoyl radicals accompanying production of the 119 and 105 ions respectively. Some of the evidence suggests that fragmentation may occur from more than one electronic state of the molecular ion. However, the variation in the ratio of rate constants for formation of m/e 105 and m/e 119 suggests that energy randomization is essentially complete in the molecular ion prior to its decomposition up to an internal energy of about 5 ev. One plausible interpretation of the relative rate constant plot and the breakdown graph at higher internal energies is that the molecular ion rearranges prior to decomposition.

The agreement between the experimenal 70 ev ion intensities and those calculated from the energy distribution functions is excellent for the 224, 119, 105, and 91 ions but poor for the 77 ion.

The paper is being submitted for publication to J. Amer. Chem. Soc.

Mass Spectrometric Study of Molecular Species in the C-S-F System

D. L. Hildenbrand

McDonnell Douglas Astronautics Company
Huntington Beach, California 92647

The reaction of SF_6 with carbon at elevated temperatures was studied by Knudsen-cell mass spectrometry in order to obtain thermochemical data for the lower sulfur fluorides and for other molecular species which may be of importance in the C-S-F system. Gaseous SF_6 was admitted to the base of a graphite effusion cell, the lower half of which was packed with graphite cloth, and the upper half of which contained platinum baffling to promote gaseous equilibrium. With the cell at about 1500°K, a rich spectrum of molecular species was observed, as determined from the mass and threshold appearance potential measurements cited in Table I. The molecular ion thresholds were determined by the extrapolated voltage difference method with xenon or argon as standard, using an automatic recording technique, and they are generally in good agreement with literature values where accurate comparisons with photoelectron or photoionization data are possible. With the cell at room temperature, the fragment ion appearance potential $AP(SF_4^+/SF_6)$ was found to be 18.44 eV, and this was combined with $IP(SF_4)$ to give ΔH_0° = 146.7 kcal for the process $SF_6 \rightarrow SF_4 + 2F$.

Parent-ion abundances measured at 2 eV above threshold were then used to evaluate the equilibrium constants of four isomolecular reactions over the range 1400° to 1600°K, and these were coupled with known or estimated spectroscopic constants to calculate the heats of reaction given in Table II. The derived equilibrium constants for the tabulated reactions were found to be essentially independent of the SF_6 flow rate and of the varying partial pressures of the molecular species, verifying that equilibrium was attained. On the other hand, data for similar reactions involving SF_4 and SF_6 varied widely with the SF_6 flow, indicating that equilibration of these species could not be achieved under the experimental conditions. In fact, it seems unlikely that equilibration of these larger polyatomic molecules can be achieved under Knudsen flow conditions.

On combining the derived enthalpy changes with available thermochemical data, one can evaluate the standard heats of formation of SF, SF_2, CS and SCF_2. Likewise, the electron-impact data described above and a literature photoionization value for $AP(CF_2^+/C_2F_4)$ can be combined to yield heat of formation values for SF_4 and CF_2. The results are summarized and compared with literature values in Table III. It is possible to go one step further and utilize available dissociative electron attachment and charge exchange data to derive thermochemical values for molecular SF_3 and SF_5, unobserved in the present experiments. With this information in hand, one can now evaluate each of the six bond dissociation energies in the SF_6 molecule. It is worth emphasizing that mass spectrometry provides an almost unique capability for thermochemical studies of radicals and other molecular fragments of the type encountered here.

Table I

THRESHOLD APPEARANCE POTENTIALS OF SPECIES RESULTING FROM SF_6 + C REACTION AT ~ 1500°K

ION	AP	NEUTRAL	LITERATURE
S^+	10.5 ± 0.3	S	10.36 (S)
S_2^+	9.42 ± 0.10	S_2	9.36 (PI)
SF^+	10.09	SF	10.0 (TC)
SF_2^+	10.29	SF_2	———
SF_3^+	12.63*	SF_4	12.70 (RPD)
SF_4^+	12.08*	SF_4	12.28 (RPD)
SF_5^+	15.50*	SF_6	15.29 (PI)
CF_2^+	11.54	CF_2	11.7, 11.86 (EI)
CS^+	11.39	CS	11.33 (PE)
CS_2^+	10.07	CS_2	10.06 (PI, PE)
SCF_2^+	10.53	SCF_2	———

*Also Measured on Room Temperature Gases

Table II

THERMOCHEMICAL DATA DERIVED FROM EQUILIBRIUM MEASUREMENTS

GASEOUS REACTION	ΔH_{298}, kcal	
	THIRD LAW	SECOND LAW
$CS_2 + S = CS + S_2$	6.5 ± 2	5.1 ± 4.1
$CS + SF_2 = CF_2 + S_2$	-11.3	-10.6 ± 3.1
$CS_2 + 2SF = CF_2 + 2S_2$	-16.1	-13.9 ± 5.9
$S + SCF_2 = CF_2 + S_2$	- 4.0	- 4.9 ± 5.3

Table III

DERIVED HEATS OF FORMATION

	ΔHf^o_{298}, kcal/mole	
	THIS WORK	LITERATURE
SF	3.2 ± 1.2	(3), (-1), (-13)
SF_2	-71.4 ± 2.5	(-61), (-68)
SF_4	-180.0 ± 3.2	-186.6, (-162)
CS	70.0 ± 2	55.0, 65.4, 72.8
CF_2	-42.6 ± 2.3	- 43.5
SCF_2	-75.0 ± 2.5	———

*Values in Parentheses are Estimates

ENERGY PARTITIONING DATA AS AN ION STRUCTURE PROBE.

M. Bertrand, J. H. Beynon and R. G. Cooks

Department of Chemistry, Purdue University
Lafayette, Indiana 47907

The use of energy partitioning data in determining ionic reaction mechanisms and ion structures is introduced. Metastable peak profiles indicate that ionized anisoles lose formaldehyde upon electron impact by two competitive reaction channels. Energy partitioning studies support the view that these two processes involve 4- and 5- centered hydrogen transfers, respectively, so accounting for the existence of evidence in the literature supporting each of these mechanisms. For the four-centered hydrogen transfer approximately 16% of the reverse activation energy appears as kinetic energy in the reaction of the p-substituted anisoles and some 10% for the meta-compounds. These values are independent of the nature of the substituent. The variation in relative abundance of the two H_2CO elimination processes with substituent provides evidence that hydrogen transfer occurs to a radical site in the formaldehyde elimination reactions. It is suggested that energy partitioning in reactions involving rearrangements to radical sites may in general be nearly independent of the nature of the substituent. Methyl radical loss from the molecular ion of p-substituted anisoles generally occurs by a single reaction channel with a small reverse activation energy (simple cleavage), but methylanisole reacts by two mechanisms, the energy release data indicating that ring expansion can precede expulsion of $CH_3^{\cdot}$ possibly with formation of protonated tropone as the ionic product.

Similar results are also obtained in the metastable loss of $NO^{\cdot}$ from substituted nitrobenzenes. These compounds also show composite metastable peaks and loss of $NO^{\cdot}$ is believed to occur through a three and a four membered cyclic intermediate. The energy partitioning parameter T/ϵ_{excess} for the three membered transition state averages 63% for the para substituted nitrobenzenes.

The results obtained for several systems indicate that one of the factors that governs the partitioning of the potential energy of the activated complex into translational and internal energy of the products is the "tightness" of the activated complex.

This work has been submitted for publication in J. Amer. Chem. Soc.

MECHANISTIC STUDIES IN ORGANIC MASS SPECTROMETRY AT 10^{-12} TO 10^{-5} SEC USING FIELD IONIZATION

P. J. Derrick, A. M. Falick and A. L. Burlingame

Space Sciences Laboratory
University of California, Berkeley, California 94720

That field ionization permits the measurement of ionic lifetimes at times as short as 10^{-12} sec was pointed out by Beckey over ten years ago (1). The kinetics of an ionic fragmentation can be determined over the extremely wide time range of 10^{-12} to 10^{-5} sec. Moreover the reactions induced by field ionization at times of 10^{-11} sec and longer are not peculiar to field ionization, but typically appear to be essentially the same reactions as induced by low energy electron impact (2-4). Thus, whereas electron impact yields an integrated view of reaction – integrated over the lengthy and arbitrary time of a few microseconds, field ionization provides a time-resolved view of reaction. It might be said that field ionization introduces another dimension, namely time, into mass spectrometry.

Field ionization therefore possesses unique capabilities. Yet field ionization has had only slight impact on mechanistic and energetic studies within organic mass spectrometry. We hope in this short paper to be able to demonstrate that field ionization, when properly applied, does in fact possess a tremendous potential for such studies, and that field ionization can yield a deeper insight into the processes induced by ionization than is possible from electron impact measurement alone.

We shall not dwell on either the theory or the technique of the field ionization kinetic measurements. Both are described in the literature (2,4-6). We shall merely present refined kinetic data. All measurements reported here were made on a double-focussing mass spectrometer. It is worth noting they could not have been made on a single-focussing instrument (4). An important feature of the measurements is that they all concern isotopically labelled molecules. We consider the use of isotopic labelling techniques to be almost essential if the full potential of field ionization for mechanistic studies is to be realized. The reasons for this will, hopefully, be apparent from the results.

In the brief space available we will only touch upon three molecules, and it will not be possible to discuss the results in any detail. Instead we hope to reveal some more general features of mechanistic studies with field ionization. The first molecule is hexanal, and Figure 1 shows the formation of fragment ions from hexanal-3,3-d_2 as functions of time from 10^{-11} to 10^{-9} sec (a complete paper on hexanal is in preparation for the Journal of the American Chemical Society). The ion currents on the y-axes are related to rates of formation. It can be seen that the structure in these curves occurs at 10^{-11} to 10^{-10} sec. This is true for most of the molecules which we have examined. The fragments m/e 82, 83, and 84 represent loss of water; m/e 72 and 74 both represent loss of ethylene; m/e 44 is the McLafferty rearrangement with charge retention on the oxygenated moiety and m/e 58 is the McLafferty rearrangement with charge retention on the alkyl group; m/e 45 is the so-called "McLafferty + 1" and m/e 60 is the so-called "McLafferty + 14". We will not attempt to discuss specific curves, but there is one general point we wish to make. This is that the time-resolution of field ionization allows fragmentation processes to be clearly distinguished from isotopic randomization or scrambling. In the case of hexanal-3,3-d_2, it is possible to confidently conclude that the formation of these fragment ions at 10^{-11} to 10^{-9} sec is not affected by hydrogen-deuterium randomization. This knowledge is a great asset in the deduction of mechanisms. So, for example, the observation of the three ions m/e 82, 83, and 84 at 10^{-11} to 10^{-9} sec firmly establishes that at least three distinct processes are operative in the elimination of water from hexanal. The loss of water therefore involves nonspecific transfer, and not specific transfer preceded by partial randomization.

In electron impact studies of course, isotopic randomization can be a severe problem in the interpretation of results. We contend that these problems can very often be avoided with field ionization.

The second molecule we wish to discuss is hexanol, n-hexyl alcohol. We have studied the elimination of water from hexanol-3,3-d_2 and hexanol-4,4-d_2 (a complete paper has been submitted to the Journal of the American Chemical Society) and we hope to show the considerable benefits to be derived from measuring by field ionization and comparing the kinetics of competing reactions. Figure 2 shows phenomenological rate constants for the loss of HDO over the time range 10^{-11} to 10^{-5} sec. The loss of

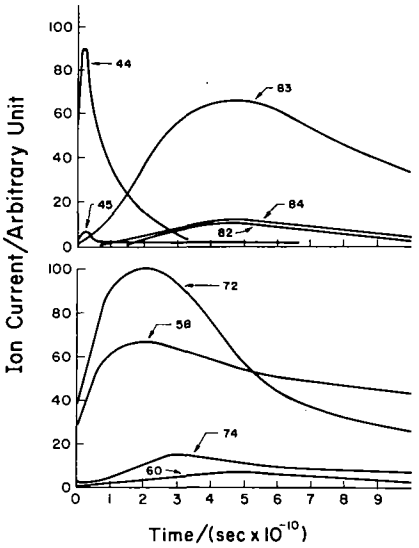

Figure 1. The dependence on time for the formation of the various fragment ions from hexanal-3,3-d_2.

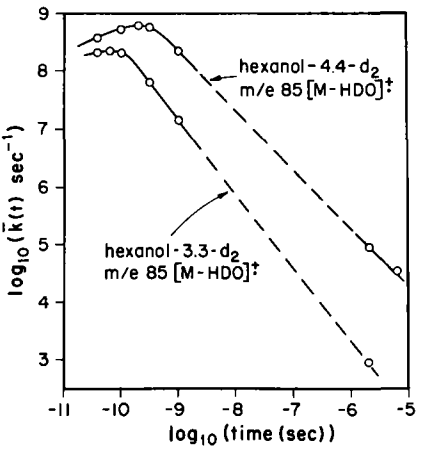

Figure 2. The dependence on time of the phenomenological rate constants for the formation of m/e 85 $[M - HDO]^+$ from hexanol-3,3-d_2 and from hexanol-4,4-d_2.

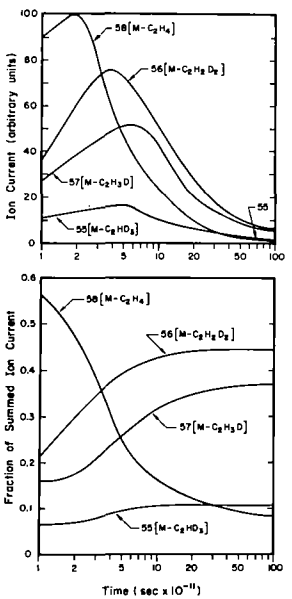

Figure 3. The loss of ethylene from cyclohexene-3,3,6,6-d_4 following ionization.

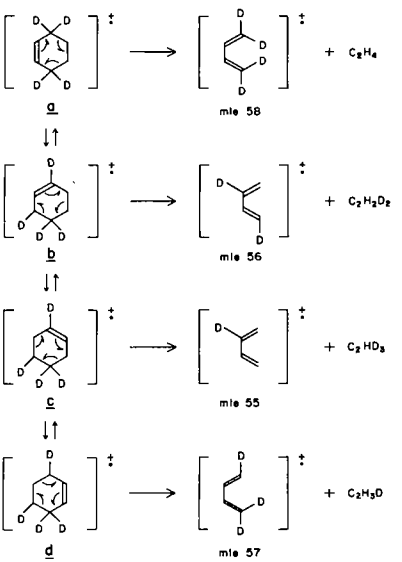

Figure 4. Allylic rearrangements in cyclohexene-3,3,6,6-d_4 following ionization.

HDO from hexanol-3,3-d_2 is assumed to involve deuterium transfer via a five-membered cyclic transition state and loss from hexanol-4,4-d_2 transfer via a six-membered transition state. The initial energy available for reaction is the same for both processes; the products of the two processes are probably very similar. It is therefore reasonable to conclude that the differences between the kinetic curves reflect the influence of transition state size. The most energetic reactant ions will decompose at the shortest times, and the less energetic at longer times. Thus in the most energetic reactant ions the two processes occur at almost equal rates, however as the energy of the reactant ions decreases so the process via the six-membered transition state is increasingly preferred. Without entering into details, this seems to imply that the six-membered transition state is energetically stabler than the five-membered, but that the frequency factors associated with the two transition states may be of comparable magnitudes.

The third molecule we will discuss is cyclohexene (2). We hope with this molecule to demonstrate the power of field ionization for studying isotopic randomization. Figure 3 shows ion currents as functions of time for four fragments representing elimination of ethylene from cyclohexene-3,3,6,6-d_4. The actual ion currents are plotted in the upper figure. In the lower figure the ion current of each fragment at any particular time is expressed as a fraction of the total ion current at that time due to all four fragments. The observation of four fragment ions all representing loss of ethylene indicates that rapid hydrogen-deuterium rearrangements occur prior to fragmentation. Careful consideration of the variation with time of the relative intensities of the four fragments suggests that the reaction scheme shown in Figure 4 is set up. It is proposed that the molecular ion can undergo 1,3 allylic rearrangements thus effecting isotopic randomization. The fragmentation is proposed to be a retro Diels-Alder reaction. The electron impact mass spectrum of cyclohexene-3,3,6-6-d_4 reveals that hydrogen-deuterium rearrangements occur prior to fragmentation but gives little direct information as to the nature of the rearrangements.

We will briefly reiterate the main points of the paper. First, reactions induced by field ionization at times longer than a few x 10^{-11} sec typically appear to be essentially the same reactions as are induced by low energy electron impact. The full potential of field ionization for mechanistic studies is only realized using defocussing techniques on a double-focussing instrument in conjunction with the use of isotopically labelled molecules. The high time-resolution of field ionization allows fragmentation processes to be distinguished from isomerization reactions effecting isotopic randomization. Finally, it is important to measure and compare the kinetics of competing fragmentation processes.

We would like to conclude the paper with a suggestion. This is that measurements of the rates of unimolecular gas-phase reactions induced by field ionization at times from 10^{-12} to 10^{-5} sec be referred to as "field ionization kinetics (FIK) measurements".

References

1. H. D. Beckey, Z. Naturforsch. 16a, 505 (1961).
2. P. J. Derrick, A. M. Falick, and A. L. Burlingame, J. Amer. Chem. Soc., in press.
3. K. Levsen and H. D. Beckey, Int. J. Mass Spectrom. Ion Phys. 7, 341 (1971).
4. A. M. Falick, P. J. Derrick, and A. L. Burlingame, to be published.
5. H. D. Beckey, "Field Ionization Mass Spectrometry," Pergamon Press, New York, N.Y., 1971, pp. 143-180.
6. P. J. Derrick and A. J. B. Robertson, Proc. Roy. Soc. Ser. A. 324, 491 (1971).

MASS SPECTRAL INVESTIGATION OF PRODUCTS FROM GASIFICATION OF COAL

By

A. G. Sharkey, Jr., J. L. Shultz, T. Kessler,
C. E. Schmidt and R. A. Friedel

Pittsburgh Energy Research Center, Bureau of Mines
U. S. Department of the Interior, Pittsburgh, Pa. 15213

As part of a program at the U. S. Bureau of Mines to produce an environmentally acceptable, synthetic natural gas, the Synthane Process has been developed for the gasification of coals.[1,2] The purpose of this report is to describe the analytical techniques used to determine the composition of various streams from the process and, in particular, the determination of possible trace pollutants.

The analytical schemes for the major products from the fluid-bed gasification of coal are shown in table 1. The gas and tar were analyzed for major components as well as the trace sulfur compounds. The condensate water was investigated by extracting the organic material with methylene chloride prior to spectrometric analysis.

Major components in the gas from the gasification of coal are shown in table 2. In large scale operation, the nitrogen would be less than one percent rather than the 49 percent shown as the present stream includes a constant "bleed" of nitrogen. The trace components of particular interest are shown in table 3. Hydrogen sulphide, the major sulfur contaminant is usually present in a concentration of several tenths of a percent. In addition to COS the other sulfur gases detected included

Table 1.--Fluid Bed Gasification of Coal

Product	Analysis
Gas	- Trace sulfur components
Tar	- Major components and trace sulfur compounds
Condensate water	- Organics extracted with CH_2Cl_2; phenols primarily

Table 2.--Major Components in Gas from Gasification of Coal

Component	Percentage
H_2	15
N_2	49
CH_4	9
CO	9
C_2H_6	1
CO_2	16

Table 3.--Trace Components in Gas from Coal Gasification

Compound	Concentration (ppm)
H_2S	6,500
COS	107
Benzene	480
Toluene	66
C_8 Aromatic	34
Thiophene	43
C_1-thiophene	24
C_2-thiophene	5
Methylmercaptan	80

thiophenes and methylmercaptan. In addition, benzene and toluene are present in low concentrations. The above trace components were determined by fractionation using liquid nitrogen, dry ice and ice water on three liter, batch samples of the gas. Fractionation was carried out directly on the inlet system of the mass spectrometer.

Analysis of the gasifier tar was carried out by combined gas chromatography-mass spectrometry (GC-MS) and by high-resolution mass spectrometry (HRMS).[3,4] While identification of the structural types containing sulfur was of prime importance, survey data for other structural types was also of interest. The light-ends of the tar were examined using a OV-101 column programmed over the temperature range 150-160° C. A major portion of the tar was analyzed using a polyphenyl ether column programmed from approximately 100° C to 300° at 8° per minute. The high-resolution mass spectrum was obtained with a resolving power of approximately 1 in 15,000.

The most abundant sulfur compounds detected in the tar from the process were those containing the thiophene nucleus including thiophene, benzothiophene, dibenzothiophene and their alkyl derivatives. Identifications based on the combined GC-MS data were confirmed by high-resolution data as shown in table 4.

Table 4.--Organic Sulfur Compounds in Tar from Coal Gasification

m/e	Formula	Example of structural type
84	C_4H_4S	Thiophene
98	C_5H_6S	C_1[a]-thiophene
112	C_6H_8S	C_2-thiophene
134	C_8H_6S	Benzothiophene
148	C_9H_8S	C_1-benzothiophene
184	$C_{12}H_8S$	Dibenzothiophene
198	$C_{13}H_{10}S$	C_1-dibenzothiophene
212	$C_{14}H_{12}S$	C_2-dibenzothiophene

a/ Indicates number of carbon atoms in alkyl group(s).

Table 5.--Analysis of Condensate Water from Gasifier

Mass Range	Structural types[a]	Percent of condensate
94-164	Phenols	0.32
110-166	Dihydricphenols	.02
120-204	Acetophenones/indanols[b]	.06

a/ Includes alkyl derivatives.
b/ Tentatively identified.

Material extracted from the condensate water by methylene chloride indicated primarily phenols and dihydricphenols and their alkyl derivatives, as shown in table 5. Acetophenones and/or indanols have been tentatively identified. Alkyl derivatives containing up to six carbon atoms were observed for the phenols as shown by the mass range indicated in table 5. The identifications have been confirmed by high-resolution mass spectrometry.

Analysis of these streams has given an insight into the purification required to make gas from Synthane Process an acceptable fuel supplement.

REFERENCES

1. Forney, Albert J., Stanley J. Gasior, William P. Haynes and Sidney Katell. A Process to Make High Btu gas from Coal. BuMines TPR-24, April 1970, 66 pp.

2. Forney, A. J., W. P. Haynes, and R. C.Corey. Present Status of the Synthane Coal-to-Gas Process. Preprint 46th Annual Fall Meeting, Society of Petroleum Engineers of AIMI, New Orleans, La., Oct. 3-6, 1971.

3. Sharkey, A. G., Jr., J. L. Shultz, T. Kessler, and R. A. Friedel. Mass Spectral Investigation of Organic Contaminants in Airborne Particulates. Proc. Second International Clean Air Congress, Arthur Stern Ed., 1972.

4. Shultz, J. L., R. A. Friedel and A. G. Sharkey, Jr. High-Resolution Mass Spectrometric Study of Organic Components in Atmospheric Dusts. Tenth National Society for Applied Spectroscopy Meeting, St. Louis, Mo. Oct. 18-22, 1971.

HIGH RESOLUTION MASS SPECTROGRAPHIC ANALYSIS OF PETROLEUM PRODUCTS

A. W. Peters and J. G. Bendoraitis, Mobil Research and Development Corporation, Paulsboro, New Jersey 08066.

A high resolution (15,000 to 25,000) mass spectrographic method for petroleum analysis has been developed. The high resolution spectra are recorded on Ilford Q2 photoplates with a duPont-CEC 21-110B high resolution mass spectrometer. A Grant-Datex comparator-densitometer is used to collect data from the photoplate. The data are then reduced using a modified version of a program (Part I of Hi Res I) written by Tunnicliff and Wadsworth[1] and other original programs developed in this laboratory.

The relative ion intensity I is obtained using the relation $I = M^q \exp(-\alpha(100-d)$ discussed by Hayes[2] where M is the mass of the ion, d is the maximum plate darkening and $q \approx 0.5$. Mass measurements are obtained in the usual way and are sufficiently accurate ($\pm$ 1 mmu) to distinguish sulfur containing from hydrocarbon ions which differ by only 3.4 mmu.

The analysis is performed by identifying from exact mass measurements all peaks associated with various possible hydrocarbon and heteroatomic chemical formulae. The intensities of all identified peaks for which $m/e > 100$ are then summed by heteroatomic or hydrocarbon type, where a type is specified by both heteroatom content and the number of rings plus double bonds. For each type both M^+ and $(M-1)^+$ ions are included in the summations, where M^+ is a molecular ion peak. The result is a set of intensity percentages without corrections for either sensitivities or possible interferences.

The analysis appears to give qualitively reasonable results for a wide variety of samples. For aromatic petroleum fractions the method is consistent with the low resolution method developed by Robinson and Cook.[3] The method has been successfully applied to the analysis of hydrotreated and untreated shale oils boiling up to 800°F. The amount of nitrogen

containing aromatics detected by the method varied from 10% to 27% of the total and were distributed over six different types. Also the method has been successfully applied to crude oil polar fractions obtained by liquid chromatographic methods. For example, an analysis of the polar fraction (1% by weight) of a Lybian crude distillate (650° - 800°F) gave measurements on 1800 peaks at an effective resolution of $\geq$ 20,000. The intensity percentages were distributed over 40 different heteroatomic compound types.

In summary, in spite of some anticipated difficulties in the accuracy of intensity measurements and in the high cost of data processing, the use of photoplate detection for high resolution mass spectral analysis of petroleum products provides a means of obtaining detailed and reasonably reliable composition information. The major advantage in the use of photoplate detection in petroleum analysis lies in the ability to obtain measurements for a large number of peaks (1000-2000) at reasonably high resolution ($\sim$ 20,000).

References

1. D. D. Tunnicliff and P. A. Wadsworth, Anal. Chem. 40, 1826 (1968).
2. J. M. Hayes, Anal. Chem. 41, 1966 (1969).
3. C. J. Robinson and A. C. Cook, Anal. Chem. 41, 1548 (1969); 43, 1425 (1971).

Submission to Analytical Chemistry is planned.

THRESHOLD RESPONSE OF A THERMOGRAVIMETRIC ANALYZER (TGA)-MASS SPECTROMETRIC (MS) SYSTEM TO SELECTED DEGRADATION PRODUCTS OF POLYMERIC MATERIALS

David L. Geiger and Gerd A. Kleineberg

Aerospace Medical Research Laboratory
Toxic Hazards Division
Wright-Patterson Air Force Base, Ohio 45433

INTRODUCTION

New synthetic nonmetallic materials are constantly being developed. These materials along with many of the well known "established" polymeric compounds are being utilized to an ever-increasing extent in the construction of aircraft interiors. The improved materials used for such construction, however, are often synthesized from toxic chemicals and because of their specific application are sometimes subject to thermal degradation. Since the habitable interiors of passenger and cargo aircraft represent a confined space, a potential hazard may exist due to accumulation of toxic compounds by outgassing of construction materials under normal use and especially by the thermal degrading of such materials under catastrophic conditions such as fire.

The Chemical Hazards Branch of the Aerospace Medical Research Laboratory initiated a program utilizing simultaneous mass spectrometric thermal analysis for the identification of potentially toxic thermal breakdown products providing the essential information for subsequent toxicological evaluation of these materials.

INSTRUMENTATION

The Mass Spectrometric-Thermal Analysis instrumentation comprises a multi-component arrangement which is outlined in the block diagram of Fig. 1. The two main components of the system are a Cahn Electrobalance Model RH (j) and a Bendix Time-of-Flight Mass Spectrometer Model 12-107 (l) equipped with four analog scanners and a variable total output integrator. The interfacing of the electrobalance and the mass spectrometer is accomplished by means of a stainless steel capillary (a), 900 mm in length with an inner diameter of 0.25 millimeter. The capillary is heated by resistance employing a D. C. power supply (i) in order to prevent higher boiling material from condensing on its inner walls during analysis. A nonobstructing bellows valve (g) serves to isolate the mass spectrometer.

A restricting orifice is formed on the tip of the capillary. The quantity of gas which passes through the orifice is defined by the equation,

$$Q = C\,(p_1 - p_2)$$

where: Q = quantity of gas in l torr/sec

C = conductance through the orifice in l/sec

$(p_1 - p_2)$ = pressure drop in torr

Since the sample is analyzed under ambient pressure, C approximates Q closely enough that we can state as a working equation, $C = Q$. Q was measured in our laboratory and a value of 1.2×10^{-6} l/sec at 760 torr was obtained.

The effective diameter of the orifice can be calculated from the equation,

$$C = 3.3 \times 10^{-5} D^4 p/\eta L$$

where: C = conductance through the orifice in l/sec

D = diameter of the restricting orifice (effective)

p = pressure in microns

η = Viscosity in poises

L = length of the orifice

Using the previously stated value for C, i. e., 1.2×10^{-6} l/sec, a value for D of 9.5×10^{-3} mm was obtained. The ratio of the diameter of the orifice to the inner diameter of the capillary is 1:26. The mean free path (10^{-5} cm) of the sample molecules entering the restricted orifice at the tip of the capillary is therefore still much smaller than the diameter of the restriction. Viscous flow exists under these conditions and no mass discrimination occurs.

A sample ranging from 10 to 30 mg taken from the material to be investigated is placed in a platinum stirrup pan which is freely suspended from a wire inside a quartz hangdown tube (k) of the balance. The sample is positioned about 5 mm from both the tip of the capillary, which is bent slightly upward, and the fused tip of a chromel-alumel thermocouple used to record the sample temperature. The sample is heated with a Lindberg Hevi-Duty clam shell furnace (d), and the heating rate is controlled employing a Fisher linear temperature programmer, Model 360 (e). The sample weight is accurately determined by adjusting the balance controller (f). Changes in sample weight and temperature are recorded on a dual pen strip chart recorder.

A variety of environmental conditions for the sample can be achieved utilizing the gas mixing system (c) and employing any of the different temperature profiles possible. The sample can be analyzed under either an isothermal or a programmed temperature mode of operation. Condition changes from those of normal use of the sample under investigation to a situation as it exists during a fire can be simulated.

Immediately prior to analysis before sample heating is initiated, a background mass spectrum is recorded which is subtracted from all subsequent spectra obtained with the mass spectrometer during analysis. After the heating of the sample is initiated and as soon as a weight change is indicated by the weight trace on the recorder a complete mass spectrum is recorded with the mass spectrometer. A complete history of the evolved products from the sample at distinct points of weight loss and temperature is thus obtained. In addition to identifying gas-off or degradation products by interpretation of the spectra, the three analog-scanners of the mass spectrometer can be used to monitor ions of specific m/e values known to arise from such products and thus provide kinetic data.

EXPERIMENTAL

As a typical example, analytical data obtained for a polyvinyl chloride (PVC) sample are represented in Fig. 2. This polymer (9.5 mg) was analyzed to determine the thermal degradation products formed under static room air. The temperature was programmed to increase 10°/minute. The large broken line represents the TGA trace with the % weight loss plotted against temperature.

Moderate weight change occurs up to about 250°C with a loss of about 5% at this point. A rapid first decomposition step follows immediately until a temperature of 325° is reached. Subsequent thermal degradation between 325° and 625° is much slower with a discernible second maximum at about 525°. Constant weight is reached at about 625° with 14% weight remaining as residue.

During the entire decomposition process, a constant sample stream of the evolved gaseous degradation products was introduced into the mass spectrometer. Three analog scanners of the mass spectrometer were locked onto three different preselected m/e ratios for constant and simultaneous monitoring. The solid line represents the ion current for m/e 94 arising from the ion species $[C_6H_5O+H]^+$, indicative of a phenylphosphate derivative that was used as a plasticizer. As soon as an appreciable weight loss is observed, this ion current raises rapidly and reaches its maximum at about 255°.

The small dashed line represents the ion current derived from evolved hydrogen chloride for m/e 36. This ion species was selected for monitoring because it best characterizes the thermal decomposition of the polymer structure itself which reaches its maximum at about 300°. The dotted-dashed line represents the ion current for m/e 44 for CO_2. Three distinct maxima of the evolving rate of this combustion product are observed, indicating multiple steps of the overall thermal decomposition process.

In addition to the information that is presented in Fig. 2, other mass spectral scans were recorded. Each subsequent scan was initiated as soon as the preceding one was completed. Typical instrument parameters for the mass spectrometer during analysis were:

Ion Source Pressure: 1×10^{-4} to 5×10^{-5} torr

Ion Source Temperature: 120°C

Electron Energy: 70 e V (variable)

Ionizing Current: 0.5×10^{-6} amp

Scan Speed: 20 to 134 sec for amu 20 to 200.

The data presented in Fig. 2 indicate that several combustion products are evolving from the sample at the same time and are introduced simultaneously into the mass spectrometer. This renders the recorded mass spectral data very complex and extremely difficult to quantitate without additional knowledge of the quantitative mass spectrometer response.

In order to provide a quantitative estimation for the different identified thermal degradation products, and also to investigate whether these compounds can be identified with our mass spectrometer down to concentrations of about 100 ppm. It became necessary to investigate the threshold response of our instrumentation for these degradation products.

Cylinders of analyzed gas containing 10, 50 and 100 ppm CO and CH_4 in H_2 were connected to a flow-through flask into which the tip of the capillary was tightly fitted. After complete purging, mass spectral scans were obtained and the detection levels were calculated. Bag samples of 100, 200 and 400 ppm of NO, SO_2, N_2O, CH_4, and CO_2 were prepared by mixing 4.5, 9.0, and 18.0 ml, respectively, of the various gases with 45 liters of air in Saran® bags. After mixing, the capillary tip was inserted into the bag and a mass spectrum was recorded of the contents. The calculated threshold values for the materials investigated are summarized in Table I. The minimum detection level was calculated for a m/e peak height equal to two times the noise level.

TABLE I

THRESHOLD VALUES

Compound		PPM
NO		100
SO_2		125*
N_2O		90
CO_2		25
CH_4	(in air)	100
	(in H_2)	20
CO	(in H_2)	3

*Capillary was passivated with SO_2 prior to analysis.

SUMMARY

Nonmetallic materials considered for application in enclosed habitable spaces are analyzed to identify thermal decomposition and gas-off products for the assessment of potential toxic hazards. A thermogravimetric analyzer-mass spectrometer system capable of establishing environments for the sample that simulate either normal usage or catastrophic situations is used for these investigations. Chemical analytical data indicative of material behavior under these conditions are essential for complete toxicological evaluation of candidate materials. In many situations, the toxicologist is concerned with short term exposure limits of toxic materials, many of which are in the 100 to 200 ppm region for a 15 min exposure. The threshold values obtained indicate that the instrumentation described is capable of providing extremely useful data which are essential for subsequent toxicological evaluations.

FIGURE I

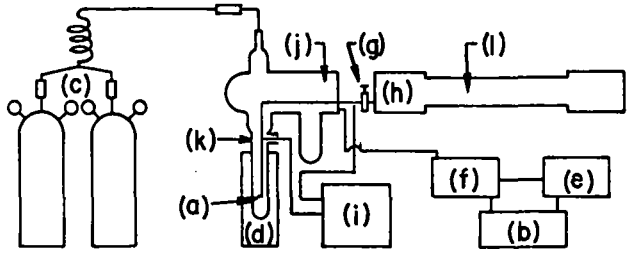

(a)CAPILLARY
(b)RECORDER
(c)GAS MIXING SYSTEM
(d)FURNACE
(e)PROGRAMMER
(f)BALANCE CONTROLLER
(g)VALVE
(h)IONISATION SOURCE
(i)DC POWER SUPPLY
(j)CAHN RH ELECTRO-BALANCE
(k)HANGDOWN TUBE
(l)MASS SPECTROMETER

FIGURE II

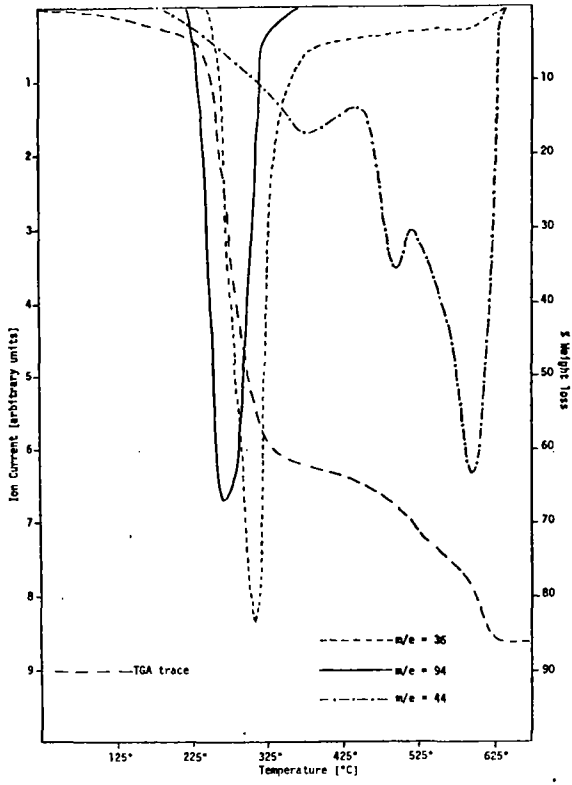
Ion Current (arbitrary units)
% weight loss
1
2
3
4
5
6
7
8
9
10
20
30
40
50
60
70
80
90
125°
225°
325°
425°
525°
625°
Temperature [°C]
TGA trace
m/e = 36
m/e = 94
m/e = 44

The Application of a GC-MS-Computer Combination to the Analysis of the PAH Content of Airborne Pollutants

R.C. Lao, R.S. Thomas, H. Oja and J.L. Monkman
Chemistry Division, Air Pollution Control Directorate
Department of Environment, Ottawa, Canada

R.F. Pottie
Chemistry Division, National Research Council
Ottawa, Canada

Introduction

In recent years, the combination of GC-MS has been widely used as a powerful analytical tool. It results in the removal of any doubt in the qualitative and quantitative determination of organic mixtures. Though the GC analysis of polycyclic aromatic hydrocarbons (PAH) in urban airborne particulates has been described by a number of workers (1), chromatographic methods alone are not able to provide a complete analysis of the complex mixture of PAH encountered in pollution studies. Despite the importance of the PAH containing five or more rings as air pollutants, little attention has been given to the mass spectra of individual compounds. A study is in progress to obtain standard mass spectra for these PAH (2) and to evaluate the GC-MS technique as applied to the analysis of PAH in air.

Experimental

The GC-MS-computer system used in our work consists of the hardware shown in Fig. 1. A Perkin-Elmer 900 gas chromatograph (with data processor unit PEP 1) is used as the sample introduction system to a Hitachi RMU-6L mass spectrometer. The chromatograph has a twelve foot column of 3% SE 30 ultraphase on Chromosorb W (HP), and it is programmed from 165 °C to 295 °C at a rate of 4 °C/min. The initial temperature is maintained for 2 min., the final temperature is retained until the sample elution is complete. Helium is used as the carrier gas with a flow rate of 40 ml/min. A He flow of 25 ml/min. is fed to the flame ionization detector in the GC. The remainder of carrier gas plus sample is passed through a heated stainless steel capillary tubing to the Markey effusion type separator (3) placed directly on the inlet pipe to the ion source of the mass spectrometer. The critical leak on the source side of the separator has been adjusted to maintain 4.0×10^{-6} Torr ion source pressure with 15 ml/min He flow at the separator exit. Temperatures throughout the interface are maintained at 325^{0}C. The mass spectrometer is scanned at 15 amu/sec using an accelerating voltage of 3500 volts and electron energy of 70 eV.

Synthetic mixtures of PAH of known compositions were prepared to check the GC-MS operation, and for the standardization of the data processing. Airborne particulate samples collected using a commercial high volume sampler were tested. Methylene chloride was the solvent for all GC runs.

For each GC effluent peak, mass spectra were obtained for identification. More than forty major PAH were identified and measured from the aromatic fraction of a particulate sample. The results are shown in Figure 2 and Figure 3.

Data Processing

There are, in effect, two data processing systems. One is a dedicated GC data system (PEP1) which identifies and calculates GC effluent peaks by using either normalization, internal standard or external standard techniques. The MS data system utilizes a Digital Equipment Corporation PDP-8/L computer with 8K words of core memory. Peripherals include a 32K disk, high speed reader and two dectape units. Data, at present, is stored only on the disk during run time. However, software modifications will build files to be transferred to dectape between runs to conserve high speed random access storage capacity.

The data acquisition interface includes a 10 bit 16 channel A/D converter. The amplified EM output signals and Hall probe converted output are gathered during scans and digitized. Interface timing is provided by a programmable interval real time clock. Provisions exist for the batch inlet micromanometer readings of the ion source during the GC runs.

Various programs have been developed for on-line digital computer systems (4,5,6). Modifications are being made to adapt portions of these systems to our unit. The data from each scan is stored on the disk and it may be submitted to a variety of analyses at the conclusion of the GC run. Included in the analyses contents are systems to tabulate and plot the mass spectra, subtract background, quantitative analyis of gaseous samples and a growing library search routine for unknown identification. The various routines are accessible to the analyst by simple word dialogues with the computer.

Conclusion

The initial work on the feasibility of measuring quantitatively submicrogram quantities of PAH found in polluted air has been very succesful. Studies are actively underway to use different GC columns for the complete separation of isomeric PAH. The application of a GC-MS technique to trace air contamination analysis will provide a definitive approach to complete PAH analysis which to date has been impossible.

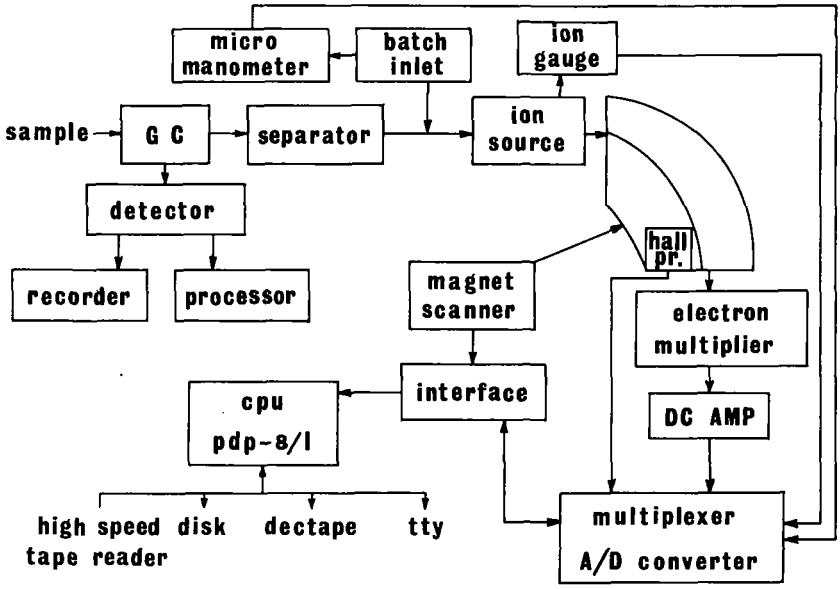

Fig. 1 GC-MS-Computer System

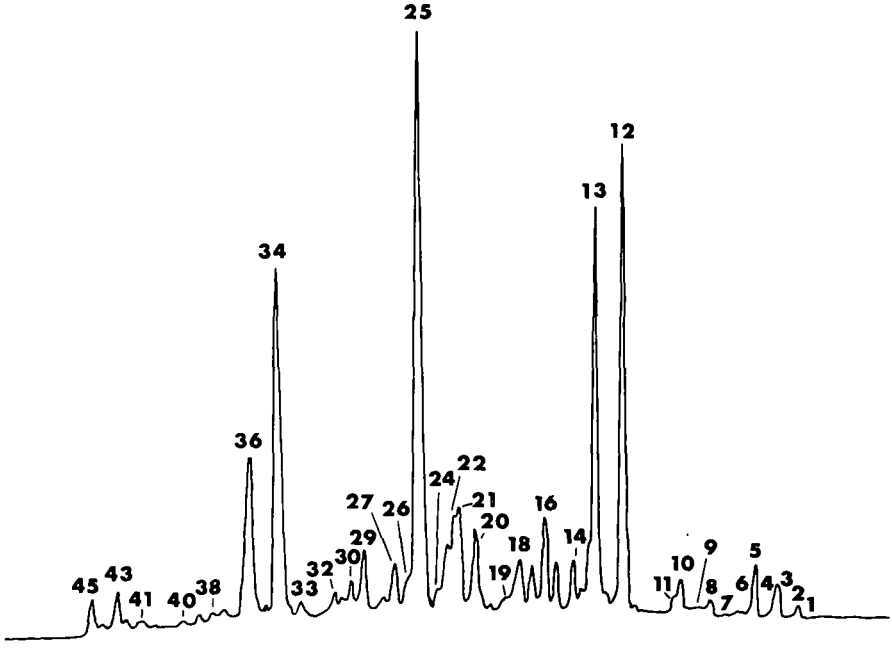

Fig. 2 Gas Chromatogram of Aromatic Fraction of Air Sample Particulates

Fig. 3 Relative Concentration of Air Sample on SE-30

Peak No.	Compound	Relative Concentration (%)
1	Fluorene	2.52
2	Methylfluorene	1.72
3	Phenanthrene	5.88
4	Hydro-phenanthrene	1.72
5	Anthracene	9.24
6	Hydro-anthracene	1.87
7	3-Methylphenanthrene	1.12
8	1-Methylphenanthrene	2.52
9	9-Methylanthracene	0.50
10	Ethylphenanthrene	5.04
11	Ethylanthracene	2.94
12	Fluoranthrene	77.31
13	Pyrene	68.06
14	Benzo[a]fluorene " [b] " " [c] "	6.72 7.56
15		
16	Methylpyrene	14.28
17	Methylfluoranthrene	5.88
18	Methylbenzofluorene	6.72
19	Methylbenzofluorene	1.22
20	Terphenyl	12.60
21	Benzo[ghi]fluoranthene	15.96
22	Hydro-benzo[ghi]fluoranthene	15.12
23	Dihydro-benzo[ghi]fluoranthrene	10.08
24	Dimethyl-benzo[ghi]fluoranthrene	2.34
25	Chrysene Benzo[a]anthracene	100.00
26	Dihydrochrysene	3.24
27	Triphenylene	7.56
28	Methylbenzanthracene	1.68
29	Methylchrysene	10.08
30	Methylchrysene	3.78
31	Methylchrysene	0.84
32	Methylchrysene	2.52
33	Binaphthyl	2.13
34	Benzo[b]fluoranthene Benzo[k]fluoranthene	59.66
35	Benzo[e]pyrene	1.68
36	Benzo[a]pyrene	26.89
37	Perylene	1.26
38	Methylcholanthrene	1.26
39	Indeno(1,2,3-c.d.)fluoranthene	1.68
40	Indeno(1,2,3-c.d.)pyrene	2.52
41	Benzo[c]tetraphene	1.26
42	Dibenz[a,b]anthracene	0.64
43		5.46
44	Picene	0.84
45	Benzo[ghi]perylene	5.84

References

(1) Hoffman, D. and Wynder, E. L. in "Air Pollution" Vol. II, Chapter 20, pp 187-247 Ed. Stern,A.C. Academic Press (1968).

(2) Lao, R. C., Thomas, R. T., Monkman, J. L. and Pottie, R. S. Proceedings 19th Annual Conference ASMS Atlanta, Georgia, May 2-7 (1971).

(3) Markey, S. P. Analytical Chemistry 42, 306 (1970).

(4) Sweeley, C. C., Ray, B. D., Wood, W. I., Holland, J. F. and Krichevsky, M.I. Analytical Chemistry, 42, 1505 (1970).

(5) Hites, R. A. and Biemann, K. Analytical Chemistry, 39, 965 (1967).

(6) Plattner, J. R. M. S. Thesis. University of Colorado (1971).

Computerized Interpretation of Spark Source Mass Spectra for Water Analysis

by

CHARLES E. TAYLOR and JOHN M. McGUIRE
National Water Contaminants Characterization Research Program
Environmental Protection Agency
National Environmental Research Center, Corvallis
Southeast Water Laboratory
Athens, Georgia 30601

and

WILLIAM H. McDANIEL
Surveillance and Analysis Division Chemical Services Branch
Environmental Protection Agency
Southeast Water Laboratory
Athens, Georgia 30601

Spark source mass spectrometry shows significant potential for sensitive identification and measurement of essentially all elements in environmental samples without extensive preconcentration. A major obstacle in applying spark source mass spectrometry to multi-element samples is the time required for manual data computation. Computerized interpretation of spark source mass spectra overcomes this obstacle. At the Southeast Water Laboratory, the AEI-DS-40 data reduction system has been applied to samples of water and of sludge from a sewage treatment plant.

Our AEI MS 702 spark source mass spectrometer is equipped with both photographic and electrical detection systems, including auto spark, log-ratio amplifier, a ten-channel peak switching unit, and a scanning unit. The AEI-DS-40 data reduction system was added recently for use with samples that do not require high-resolution photoplate detection. This system includes the mass spectrometer-computer interface, a reference clock, a DEC PDP8/e 4K computer, a 12 bit A/D converter, a 32K disc memory, a teletype, and a high-speed reader/punch.

Spectra are recorded by two methods. The log-ratio signal appears directly on a Honeywell 2106 Visicorder, and the analog signal is taken by the interface. To discount most of the noise, a signal threshold can be selected initially or adjusted while scanning. After the signal is digitized, the centroid and absolute intensity of each peak are calculated. In a print-out of these data (Figure 1 shows a typical sample of a portion of this output), the first column lists the appearance sequence starting with the highest mass peak; the other three columns show the number of points sampled, raw data intensity, and centroid time for each peak. This information can be processed immediately or stored on the disc while more data are being collected. If disc space is needed, the data can be transferred to paper tape and the disc cleared of any or all runs.

To make computer interpretation possible, the analyst must identify from three to ten reference peaks from the log recorder. After receiving these reference details (Figure 2), the computer calculates accurate mass data using time-to-mass calculations, normalizes all intensities to the most intense line, and marks reference peaks with (R) (Figure 3). In most cases, unique isotopes are used for identification and semi-quantitative analysis[1]. The computer lists some of the interfering ions contributed by "overlap" and complex ions.

---

[1] R. Brown, P. Powers, and W. Wolstenholme, "Computerized Recording and Interpretation of Spark Source Mass Spectra," Anal. Chem., 43, 1079-1085 (1971).

Although the polyatomic carbon lines can provide useful reference inputs, they also produce interfering mass lines and false identifications. We modified the computer program to minimize these interferences. When a polycarbon line coincided with the isotope line used by the computer in the original program for identification and quantification, a different isotope (free of interference) of the same element was selected for the modified program.

Figure 4 shows the machine computation of elemental composition before program changes were made. When the same raw data were processed after program changes, erroneous identifications, due to carbon, of tantalum, thulium, neodymium, cesium, molybdenum, rubidinum, germanium, and magnesium were eliminated (Figure 5). The quantitative information is now expressed in ppm by weight compared with ppm atomic in the original interpretation. The standard has also been changed due to the nature of the weight conversion calculation in the present program.

Figure 6 shows the analysis of a solution prepared from primary standards for 22 elements. For 10 determinations (5 aliquots scanned in duplicate) of this solution the coefficients of variation for different elements ranged from 14% to 50%. Values are expressed as ppm in water, without relative sensitivity (RS) corrections. All values are within a factor of three of the known values.

Water samples are prepared for spark source analysis by evaporating a 100-ml sample onto 100 mg of graphite, from which electrodes are pressed in polyethylene plugs. Relatively homogeneous electrodes are easily prepared with graphite, whose matrix effect on the sample is reproducible.

A 100-ml water sample containing contaminants in the low µg/l range will provide signal-to-noise ratios compatible with computer analysis. Spectra are recorded at 30% power, 300 pulses/second, 200 µseconds pulse length, and X1 or X3 amplifier gain settings.

Figure 7 shows the computer interpretation of a spectrum from municipal sewage sludge. The sample was ashed, homogenized with graphite, and sparked at the above conditions. This scan provides quantitative information for all elements listed except zinc, iron, chromium, manganese, calcium, potassium, and sulfur, which are at concentrations that saturate the amplifier. A second scan at lower multiplier gain can quantitate these elements.

Manual interpretation of a multi-element sample requires numerous calculations as outlined in Figure 8. The computer reduces computation time from 3 hours to 1/2 hour for typical samples and simultaneously eliminates errors arising from manual calculations.

Use of trade names does not imply endorsement by the Environmental Protection Agency or the Southeast Water Laboratory.

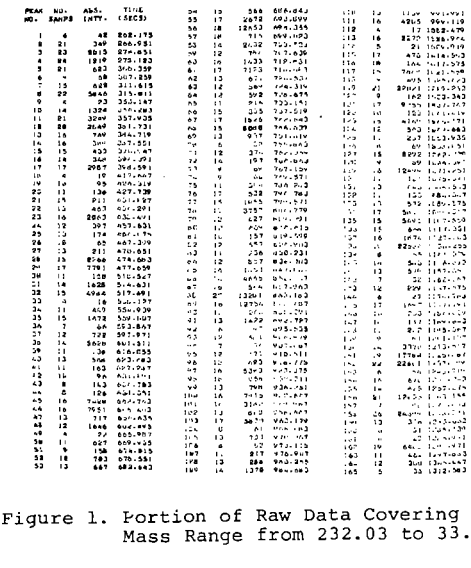

Figure 1. Portion of Raw Data Covering Mass Range from 232.03 to 33.50

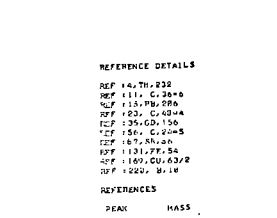

Figure 2. Reference Details

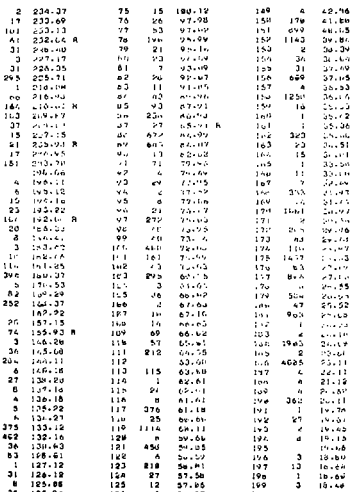

Figure 3. Accurate Mass Data

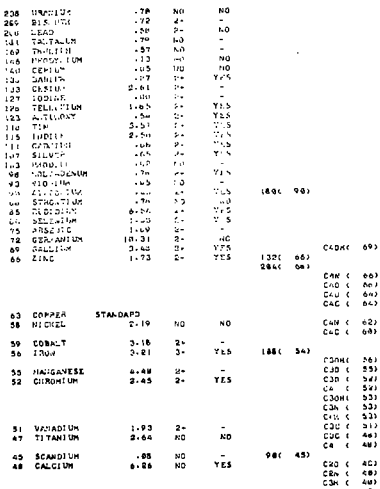

Figure 4. Original Interpretation

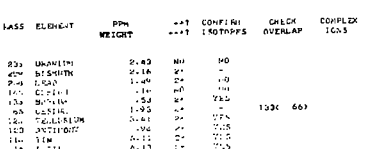

Figure 5. Present Interpretation

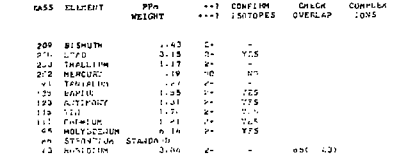

Figure 6. Computer Calculation of Standard Solution of Elements

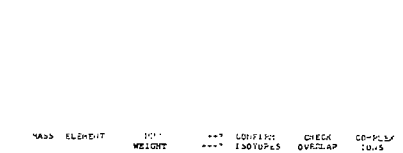

Figure 7. Computer Calculation of Elements in a Sludge Sample

An intensity measurement is made directly from a strip chart for each element. The calculation is then made using this equation:

$$\frac{S_{el}}{S_{std}} \times \frac{I_{std}}{I_{el}} \times \frac{A_{el}}{A_{std}} \times C_{std} \times K = C_{el}$$

S_{el} intensity of isotope used for unknown element

S_{std} intensity of isotope used for internal standard

I_{std} atomic percent for isotope used in calculation

I_{el} atomic percent for isotope used in calculation

A_{el} atomic weight of element of interest

A_{std} atomic weight of internal standard

C_{std} concentration of internal standard

K relative sensitivity factor

C_{el} concentration of element of interest

Figure 8. Manual Interpretation Calculations

The Reduction of a Matrix Effect in Spark Source Mass Spectrometry Using a Solution Doping Technique

R. J. Guidoboni
Ledgemont Laboratory, Kennecott Copper Corporation, Lexington, Massachusetts 02173

C. A. Evans, Jr.*
Materials Research Laboratory, University of Illinois, Urbana, Illinois 61801

ABSTRACT

When performing a spark source mass spectrographic analysis, the analyst must determine a relative sensitivity coefficient if a quantitative analysis is required. This requirement is often quite difficult to fulfill, thus one is often limited to a semiquantitative analysis. This investigation describes a simple solution doping technique which permits a quantitative analysis to be obtained through the use of synthetic standards. The technique has been applied to the analysis of several NBS standards with precision of ±8 - 10% and average deviations from certified values of ±10%.

(A full manuscript will be published in the September issue of Analytical Chemistry.)

*The contributions of this author were supported by the Advanced Research Projects Agency under Contract HC 15-67-C-0221.

TRACE ELEMENT ANALYSIS OF GLASS BY HIGH RESOLUTION SPARK SOURCE MASS SPECTROMETRY

Y. Ikeda and A. Umayahara
Nippon Sheet Glass Co. Ltd., SELFOC Div. Itami, Japan

and

E. Kubota, T. Aoyama and E. Watanabe
JEOL LTD., Akishima, Tokyo Japan

INTRODUCTION

Recently light communication systems, especially laser communication systems using a light waveguide (made of glass fiber) have been studied in many countries throughout the world.

An essential requirement to accomplish the laser communication system, which uses the light waveguide as a transmission line, is to develop a low-loss glass fiber which makes it possible to transmit light with low attenuation in the order of kilometers.

Therefore, to produce low-loss glass, we have to achieve a technique to allow the precise analysis of trace elements. On the basis of this technique, advanced techniques for material refining and glass melting must be established. To further the research and development for low-loss glass production, we have already attempted atomic absorption spectrophotometry and colorimetric method, with some good results.

However, we have met with many difficulties due to the chemical preparation process essential to these chemical methods and due to the presence of disturbance elements.

The spark source mass spectrometry (SSMS) has many advantages over other analysis methods. But its application to the sub-ppm trace element analysis of glass has been considered very difficult due to the interference by many spectral lines of Si, O, complex ions, etc.

We have recently made an analysis of trace elements in glass, ranging from a hundred ppb to several tens of ppb, using spark source mass spectrometry; and as a result, we have found it a excellent routine analysis method.

PREPARATION OF SAMPLE ELECTRODES

When glass is analyzed by the SSMS, it cannot be directly used as a sample electrode because of its insulation characteristics. So, the method of pelletizing with conductive powder, and the gold counter electrode method were examined.

As for the concentrations of the impurities contained in low-loss glass, our target values are as follows: Cr : 0.02, Fe : 0.3, Co : 0.02, Ni : 0.01, Cu : 0.02 ppm/glass. Therefore, high purity materials were selected as supporting materials.

Table 1 shows the analytical results of commercially available conductive powders and gold wire. These results were obtained by the SSMS. And finally pelletizing with graphite powder was adopted as the most suitable method, in consideration of these analytical results, ease of analysis, costs of supporting materials, simultaneous analysis of all elements, and routine analysis of low-loss glass. As graphite powder, grade SP-1 made by Union Carbide Corp was used. The sample/graphite powder mixing ratio was 2:1 (by weight). Mixing was carried out for 30 minutes by the use of a Mixer Mill of SPEX. The mixture was molded into sample electrodes in a hard resin molding device by applying a pressure

of about 10 tons.

EXPERIMENT

(1) When glass is analyzed, it is presumed that a number of multinuclear complex spectral lines arise from oxygen and silicon in glass, and from carbon in graphite and interfere with the spectra from elements. Table 2 shows the isotopes of elements; Fe, Co, Ni and Cu, and the resolutions required to separate these isotopes from complex ions. A resolution of more than 5,000 is required for the analysis of low-loss glass. Moreover, it is necessary to perform routine sub-ppm order analysis under high resolution condition.

In view of these requirements JEOL's JMS-01BM-2 Mass Spectrometer we used is considered to be suited to this kind of experiment because this model features low aberration ion optics and a low energy aberration ion source. In other words, the instrument has the following advantages: i) The second order aberration is restricted by the shim placed at the incidence plane at the magnetic field. ii) As a result of an experiment using a wide and a narrow accelerating slit for the ion source, it is noted that the ion beam current increases in a narrow energy region when the narrow slit is used. iii) Moreover, undesirable space charge effects are eliminated because a canal-shaped slit installed behind the earth slit cuts off useless ion beams.

(2) Experimental Conditions

The instrument used for this experiment was JEOL's JMS-01BM-2 Mass Spectrometer. Beam control was by the synchronous passer, and the repetition rate was fixed at 1,000 Hz. The other conditions were: Pulse width, 20 μsec; accelerating voltage, 30 kV; exposure range, $1 \times 10^{-13} \sim 1 \times 10^{-7}$ or 3×10^{-7} coulomb (corresponding to $0.03 \sim 0.01$ ppm atomic); photoplate Ilford Q_2.

RESULTS AND DISCUSSION

Glass with graphite powder produces many complex ions lines covering a wide range intensities, thus making the identification of trace elements difficult. Thus, ion compositions were identified by precise mass measurement results.

Many spectrum lines for multi-silicon ions, multi-carbon ions and complex ions were observed. Their intensities are shown in Fig. 1.

It requires due care to distinguish between a strong spectrum line of m/e 56 = $^{28}Si_2^+$ and a trace iron line, and between a weak spectrum line of m/e 59 = $^{28,29}Si_2^+$ and a trace cobalt line.

As a result of analysis of various glass materials, optical glasses and low-loss glasses, the reproducibility was found to be about 30 %. Here, results of some samples are described. Also, results of atomic absorption analyses are shown.

Table 3 shows the analytical results of NBS standard reference materials 614 and 616 (Glass Matrix). This spectrum was photographed at a maximum exposure of 1×10^{-7} coulomb, and time required for photography was about 30 minutes. The relative sensitivity factor of Fe, Co, Ni, and Cu were all within 3.

Table 4 shows the analytical results of three kinds of low-loss glass. The maximum exposure was 3×10^{-7} coulomb, and the photographing time was about 50 minutes. The concentrations of Cr, Fe, Co, Ni and Cu were all less than 3 ppm for each sample. Co was not detected from any of the samples. This provies that the concentration of Co is less than 10 ppb.

CONCLUSION

Routine analysis of trace elements in silicate glass, ranging from a hundred ppb to several tens of ppb, was made possible by spark source mass spectrometry.

Since this method can be employed with comparative ease, we believe that we now have an established routine criterion required to develop anti-contamination techniques for glass refining and melting processes. In other words, this method can be thought to be a breakthrough to solve one of the essential and complicated problems in the development of low-loss glass.

Table 1. Analysis of Supporting Materials by Spark Source Mass Spectrometry (JMS-01BM-2)

	Concentration (ppm)		
Element	Graphite Powder	Silver Powder	Gold Wire
Cr	0.03	0.2	0.03
Mn	<0.03	0.4	0.03
Fe	0.2	9.0	2.0
Co	<0.03	<0.1	<0.03
Ni	<0.1	0.3	<0.1
Cu	0.02	0.5	1.5

Table 2. Spectrum Identification Through Mass Measurement (Optical Glass) and Necessary Resolution for Low Loss Glass Analysis.

m/e	Ions	Measured Mass	Exact Mass	Error (mmu)	Required Resolution
54	^{54}Fe	-	.940	reference line	> 1600
	$^{30}SiC_2$	.974	.974	0	
56	^{56}Fe	.935	.935	0	> 3000
	$^{28}Si_2$	.955	.953	2	
57	^{57}Fe	-	.935	reference line	> 3100
	$^{28,29}Si_2$	.954	.953	1	
58	^{58}Fe	.934	.933	1	> 3300
	$^{28,30}Si_2$	.950	.951	1	
59	^{59}Co	.933	.933	0	> 3500
	$^{29,30}Si_2$	.949	.950	1	
60	^{60}Ni	.930	.931	1	> 1700
	$^{28}SiO_2$	-	.967	reference line	
	$^{12}C_5$	.999	.000	1	
61	$^{29}SiO_2$	.970	.966	3	
63	^{63}Cu	.929	.930	1	> 4000
	$^{28}Si^{35}Cl$	.945	.946	1	
64	^{64}Zn	.930	.929	1	
	$^{28}SiC_3$	.977	.977	0	

Fig. 1. Mass Spectrum and Its Intensity of Optical Glass

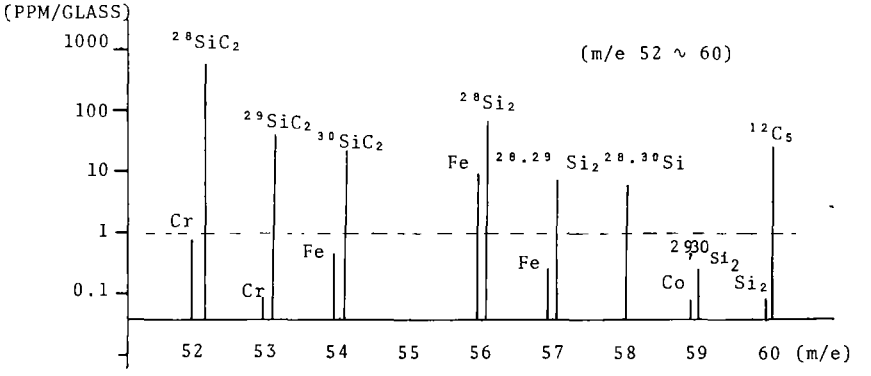

Table 3. Analysis of N.B.S. Glass Standard 614 and 616

Element	NBS-614 (ppm/glass)			NBS-616 (ppm/glass)		
	MS	Certified	R.S.F.	MS	Certified	R.S.F.
Cr	1.5	-	-	0.82	-	-
Mn	2.8	-	-	1.8	-	-
Fe	26	13.3	1.9	17	11	1.5
Co	0.99	0.73	1.3	1.9	0.80	2.3
Ni	1.5	0.95	1.6	-	-	-
Cu	2.6	1.6	1.6	-	-	-

Table 4. Analysis of Low Loss Glass

Element	Concentration (ppm/glass)					
	GLASS-1		GLASS-2		GLASS-3	
	MS	A.A.	MS	A.A.	MS	A.A.
Cr	0.23	impossible	0.039	impossible	0.071	impossible
Fe	2.0	1.8	2.5	3.6	2.2	2.2
Co	<0.0075	0.00	< 0.0075	0.003	<0.0075	0.01
Ni	0.089	0.12	< 0.029	0.07	<0.029	0.06
Cu	0.23	0.17	0.17	0.08	0.15	0.12

MS: Mass Spectrometry
A.A.: Atomic Absorption Method

SPARK SOURCE MASS SPECTROMETRY AND ION SCATTERING SPECTROSCOPY FOR THE DETECTION OF SURFACE CONTAMINATION ON ELECTROPLATES

by

D. L. Malm and M. J. Vasile
Bell Laboratories
Murray Hill, New Jersey 07974

Spark source mass spectrometry has been applied to analyze the impurities present on the surfaces of electroplated gold, platinum, palladium and copper. Of these metals, electroplated gold was consistently most contaminated by organic impurities. The elements sodium, potassium, and calcium appeared in many of the spectra as minor constituents (1 to 3 percent of the total ions detected). Corresponding studies of the surfaces of high purity samples of each metal showed that the levels of contaminants were between a factor of 5 and 10 times lower than electroplated specimens. Ion scattering spectra of electroplated gold surfaces showed an initial surface contamination due to hydrocarbons which was removed at a depth of approximately 30 monolayers.

On-Line Computer Control System For Spark Source Mass Spectrometry

J. R. Roth, B. N. Colby,* and G. H. Morrison
Department of Chemistry, Cornell University
Ithaca, N. Y. 14850

With the increased use of electrical detection in spark source mass spectrometry has come a need for direct acquisition of data using computers. Although large time-sharing computer systems can be used, small dedicated computers offer the advantages of direct data acquisition as well as control of the mass spectrometer in real time where focus can be placed on the experimental needs rather than on computer availability.

The design and operation of a versatile on-line computer controlled electrical detection system in spark source mass spectrometry has been described (1). This system involves computer control of the mass spectrometer in either a scanning or peak switching mode with simultaneous acquisition and reduction of data using a Digital Equipment Corp. PDP-11/20 dedicated computer.

Computing System.

This system is built around the PDP 11/20 central processor using 16-bit word structure and byte addressability. This word length offers adequate number size for most analytical calculations. Currently we have 16K of read-write core memory and a moving head disk cartridge system which permits higher language (FORTRAN) programming. The disk, which has 1.2 million words of storage, also appears to the programmer as virtual memory allowing execution of very large programs. Also included are a real time clock for programmer reference to the real time world, and a hardware loader to facilitate loading of the disk operating system. An extended arithmetic element has been included to speed up the arithmetic calculations. Input-output devices presently include a Teletype which functions as the computer controller, a Versatec high speed line printer, and a Houston Instrument incremental plotter. A high speed paper tape reader-punch is used to provide permanent records of both programs and data. A nine track magnetic tape unit is also used to store large blocks of experimental data for future use. See Figure 1.

Mass Spectrometer System.

The signals from the beam monitor and the electron multiplier of a Nuclide GRAF-2 spark source mass spectrometer are individually amplified, converted to frequency and subsequently ratioed with a Hewlitt-Packard 5245L counter equipped with a preset unit. The counter is interfaced to the computer. The ratio is determined by collecting/integrating the two signals until the beam monitor signal, the denominator of the ratio, has reached a preset value so that the electron multiplier signal for this period of time is directly related to the concentration of the element in the sample.

On-line computer control of the mass spectrometer is accomplished by Nuclide DAC-16 16-bit digital-to-analog converters interfaced to the computer and connnected to the electrostatic analyzer potential regulator and the magnet regulator. See Figure 2.

Operation.

The computer is programmed to acquire and analyze the data from the counter and either wait for another value at the same instrument settings or change the instrumental parameters to permit measurement of ions of a different mass. This system can be operated in either a scanning or peak switching mode by software control of either or both the electrostatic analyzer and magnetic field.

In the scanning mode of operation the system is programmed for either a timed interval scan or intervals of constant total beam collection. The latter permits equal weighing of all points in the spectrum. Both of these methods of operation can be accomplished by scanning the electrostatic analyzer and/or magnetic field. The scan can be programmed as a linear, exponential or any other desired function.

Peak switching is accomplished by computer setting of peaks selected by the spectroscopist. In the selection of peaks for measurement, the digital-to-analog converters offer an almost infinite number of channels for selecting a given mass.

A particular advantage of this system is the ability to use FORTRAN as the primary programming language. This allows faster program development, easier modification of the software, and is more universally employed by spectroscopists. Assembly language subroutines are used only when necessary to couple to FORTRAN programs.

Use of the system for the evaluation of electrical detection measurements of powdered samples has been described (2). An automatic spark gap controller needed for electrical detection measurements has also been described (3).

Acknowledgments.

Financial support was provided by the National Science Foundation under Grant Nos. GP-6471X and GP-30940X and the Advanced Research Projects Agency through the Cornell Materials Science Center.

1. G. H. Morrison, B. N. Colby, and J. R. Roth, Anal. Chem., 44, 1203 (1972).
2. G. H. Morrison and B. N. Colby, Anal. Chem. 44, 1206 (1972).
3. B. N. Colby and G. H. Morrison, Anal. Chem. 44, 1263 (1972).

* Present address, Materials Research Laboratory, University of Illinois, Urbana, Ill.

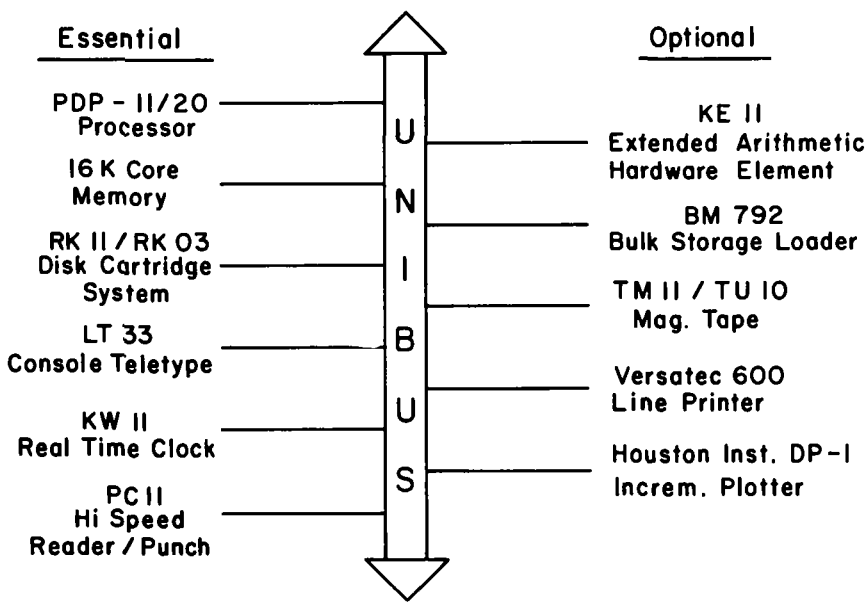

Figure 1. PDP11/20 Computer System.

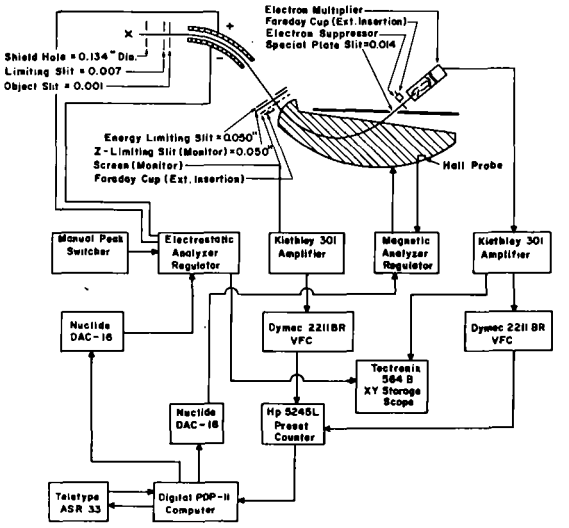

Figure 2. Mass Spectrometer System.

A COMBINED ION PROBE/SPARK SOURCE ANALYSIS SYSTEM

A.E. Banner, R.H. Bateman, J.S. Halliday and E. Willdig,
AEI Scientific Apparatus Limited, Urmston,
Manchester, England.

The layout of the complete ion optical system is shown schematically in Figure 1.

The primary positive or negative ions, of either reactive or inert gases, are formed in the duoplasmatron source, at voltages up to 25kV. This source includes a hollow cathode, which allows 1000 hr working life, and a variable magnetic field, for easy optimisation of the brightness. The extracted ions can be mass analysed in the stigmatic focusing magnetic sector, so that a chosen isotope can be selected for ion bombardment; or alternatively the flanges of this separator have been designed so that it can be omitted from the probe system. Two electrostatic Einzel lenses which focus the ions onto the specimen vary the probe diameter continuously from 800μm down to 2μm. The deflector plates after the final lens provide for the generation of a mass analysed scanning ion micrograph of the specimen. The two beam defining apertures, one before each lens, permit differential pumping of the column. Finally the specimen and the secondary ion extractor electrode system are mounted in the source housing, which is mounted directly in place of the normal spark source housing of the AEI MS7 mass spectrometer.

The specimen surface may be positioned through a bellows and gimbal mounting by three orthogonal micrometers, which allow ± 5 mms movement in any direction within the surface and 5 mms normal to it. An optical microscope enables the user to view the specimen directly while in the position for analysis and an accessory, not shown, will allow seven specimens to be introduced at one loading.

With the duoplasmatron switched on, the normal operating pressure in the specimen chamber is 10^{-8} torr. A cryogenic flange may be fitted in place of the top plate in the specimen chamber to assist the pumping in the vicinity of the specimen surface.

The positive or negative ions sputtered from the surface are extracted and focused onto a variable slit. They then pass into the MS7 mass spectrometer, where they are mass analysed. The consequent spectrum may be recorded either by means of the photoplate, or the electrical detection system. The latter can be used in analogue mode with the magnet scanning facility, or in digital mode with the ion counting and magnet peak switching units.

Spark source analysis can readily be carried out by replacing the probe specimen and extractor lens with electrodes mounted in the normal positions for this method of analysis. The isolation valves present on the MS7 and an additional valve in the probe column enable the specimen chamber to be quickly isolated from the rest of the instrument. Thus specimens can be changed within 10 minutes, or the mode of operation changed from ion probe to spark source or vice versa in under 30 minutes.

The curve in figure 2 is the computed variation of the probe current of positive argon or oxygen ions with focused spot diameter. The four dots indicate the measurements already made and, within the limits of the temporary electronics used so far, the agreement is indeed encouraging. The instrument has been used with a 4μm diameter spot size, which will be improved when the correctly stabilised standard electronics are incorporated.

The following analytical results were obtained using a geological sample of olivine provided by Dr. C.A. Evans of the University of Illinois. Figure 3 is an electrical detection mass spectrum obtained from this synthetic iron magnesium silicate when bombarded with argon ions. The mass resolution was 1500 (10% valley). Besides the major lines of magnesium, silicon and iron, perhaps the most prominent feature is the recurring pattern of lines beginning at mass numbers 64, 80, 96 etc. These are the successive orders of the magnesium and silicon oxide complexes. Figure 4 illustrates mass 25 at a resolution of 5000 (10% valley), and shows the presence of both ^{25}Mg and ^{24}MgH.

Similar mass spectra were recorded on photoplates. Figure 5 shows a small section, from mass 40 to 43 inclusive. The resolved doublet at mass 40 was micro-densitometered, revealing a resolution of 19,000 (50% density), see figure 6. This resolution was sufficient to enable the two peaks to be mass measured and identified as argon and magnesium oxide.

Finally, the specimen was analysed in the spark source mode of operation, and both the spark source and ion probe plates consisted of eight exposures, each successively a factor 3 greater. The plates were examined visually and unity sensitivity was assumed for all elements on both occasions. For the spark source plate the normal sensitivity of 1 ppm per nano-coulomb was assumed, whereas on the ion probe plate the ^{54}Fe and ^{57}Fe lines were used as internal standards taking as concentration values those derived from the spark source analysis. On this basis, a comparison has been drawn up between the spark source and ion probe analyses of the transition elements in the neighbourhood of iron in the periodic table.

The relevant part of the ion probe photoplate is illustrated in figure 7 and the results are shown in Table I.

TABLE 1

COMPARISON OF SPARK SOURCE AND ION PROBE ANALYSES OF TRANSITION METALS IN OLIVINE

Element	Spark Source Analysis	Ion Probe Analysis
	(ppm atomic)	(ppm atomic)
Ti	5	30 (60000)
V	3	<2 (100)
Cr	70	100 (60000)
Mn	1000	600
Co	100	30
Ni	1000	100

Bearing in mind that spark source elemental sensitivities typically may vary by a factor 3:1, the comparative ion probe measurements indicate a gradual decrease in sensitivity from titanium through to nickel, which is in reasonable agreement with the published data on secondary ion coefficients for these elements (1).

However, strong possible interferences were observed from the complex ions Mg_2^+ and $MgSi^+$ for the titanium, the vanadium and all the chromium isotopes. These complex ions were clearly resolved in the present experiments, requiring a mass resolution of greater than 2300. Had they not been resolved then the erroneous data, bracketed in Table 1, would have been recorded.

In conclusion, the instrument has already been used with a primary beam spot size down to 4μm diameter. A demonstrated mass resolution of 19,000 is an indication of the readily obtainable working resolution of 10,000.

(1) H.E. Beske. Z. Naturforsch, 22a, 459-467 (1967)

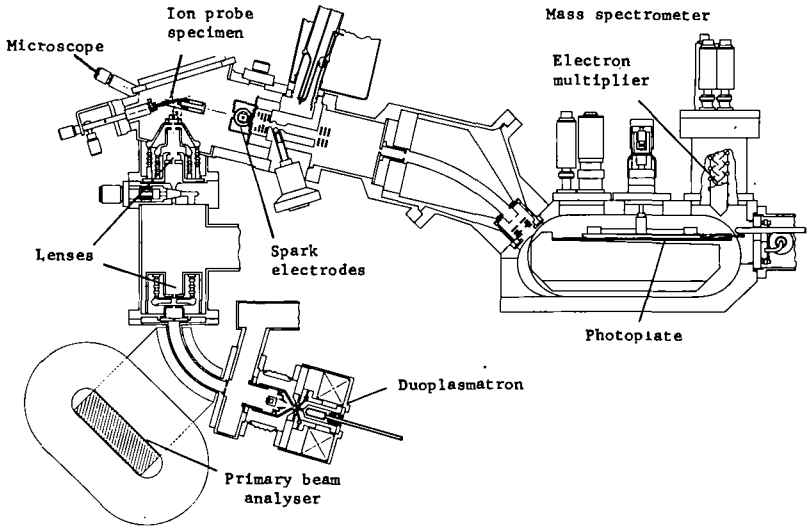

Figure 1 Schematic of ion probe-spark source mass spectrometer

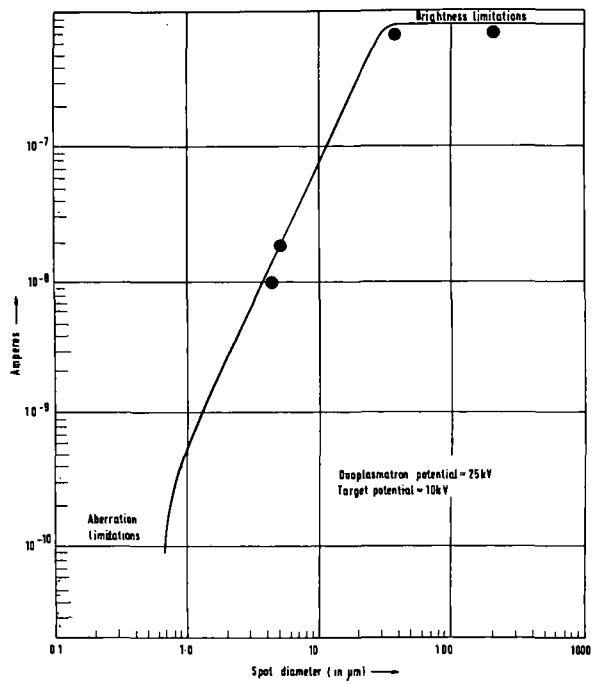

Figure 2 Primary ion current versus spot size

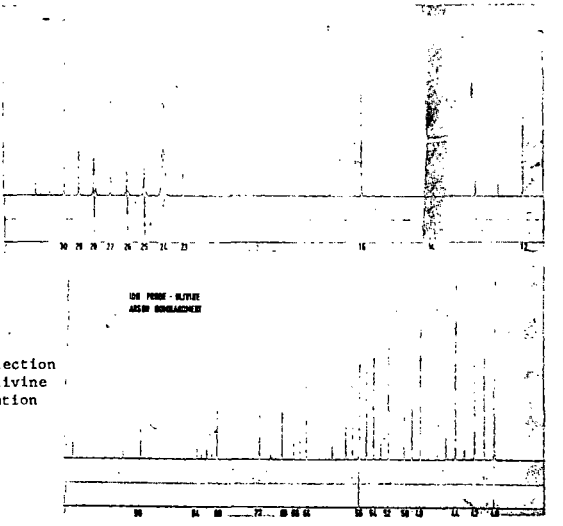

Figure 3
Electrical detection spectrum of olivine at 1500 resolution

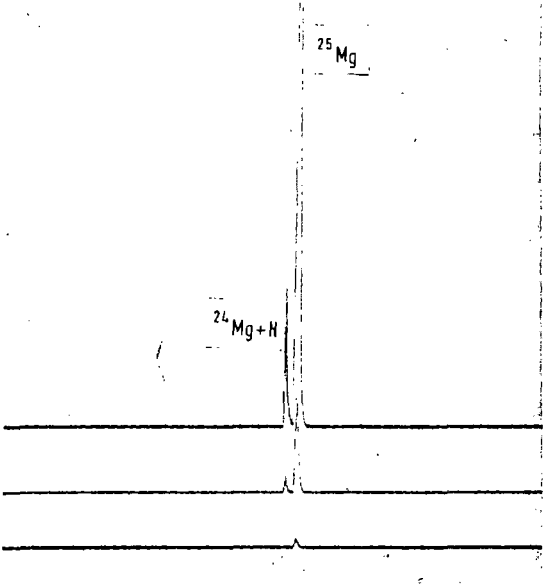

Figure 4 Mass 25 doublet from olivine showing 5000 resolution

Figure 5 Photoplate spectrum of mass 40 region from olivine at 19000 resolution

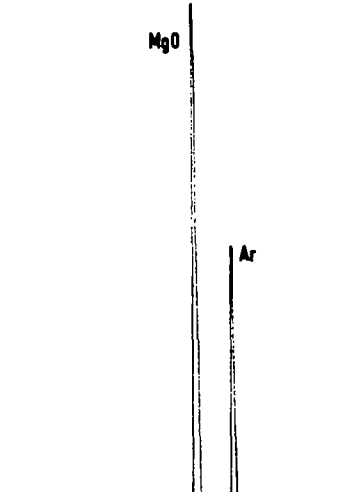

Figure 6 Microdensitometer trace of mass 40 line from olivine showing resolution of 19000

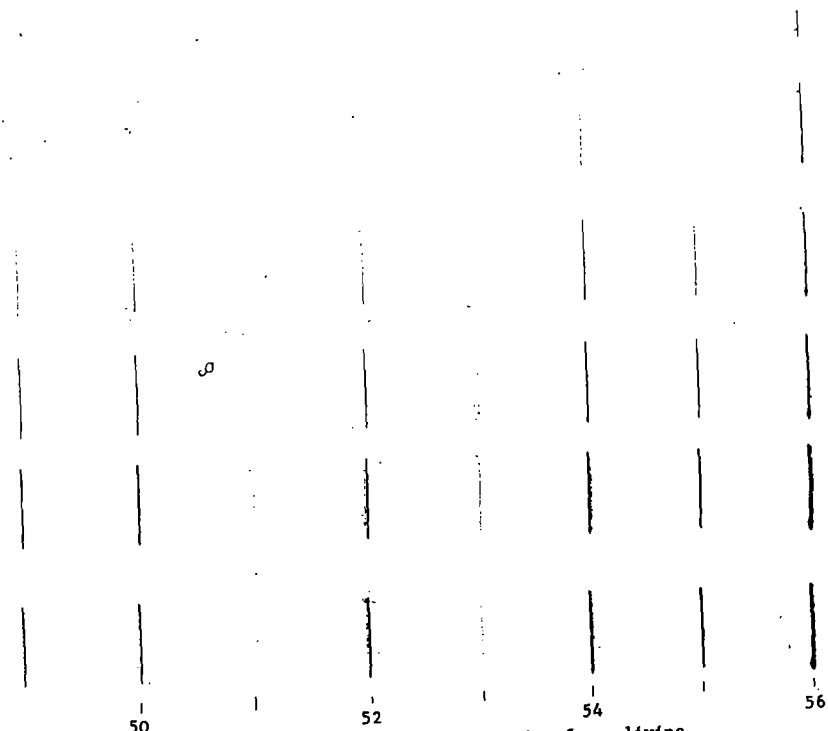

Fig. 7 Photoplate of mass 50 region from olivine

Measurements of Barbiturates and their Metabolites in Small Volumes of Biological Fluids by Quantitative Gas Chromatography-Mass Spectrometry

by
G H Draffan, R A Clare, F M Williams, B Krauer, D S Davies and C T Dollery

The Royal Postgraduate Medical School, London W 12

Techniques for the measurement of amylobarbitone and its principal metabolite, 3'hydroxyamylobarbitone, in 40-100 µl plasma samples are described. An AEI MS 12 mass spectrometer at low resolving power is employed in "single ion monitoring" mode as a gas chromatographic detector. Protectively methylated barbiturates are detectable to 0.02ng as pure samples injected on to the gas chromatograph. The methods have limits for reproducible quantitative estimation after recovery from plasma of 1 ng for amylobarbitone and 5 ng for the metabolite, and were initially developed to permit pharmacodynamic studies in human newborns where conventional measurement is precluded by available sample size. They are in principle extendible to butobarbitone, pentobarbitone, and the metabolites 3'-hydroxybutobarbitone and 3'-hydroxypentobarbitone. It has been shown that metabolite measurement in micro scale liver microsomal enzyme assays can be made permitting enzyme activity measurement at high dilution and low percentage conversion of substrate (barbiturate) to product (hydroxymetabolite).

Mass Spectrometry and Inlet Systems

The gas chromatographic behaviour of barbiturates is significantly enhanced by methylation (1). The mass spectra of N,N'-dimethyl barbiturates with an aliphatic side chain R have in common fragment ions at m/e 169 (2) which carry a substantial fraction of the total ion current.

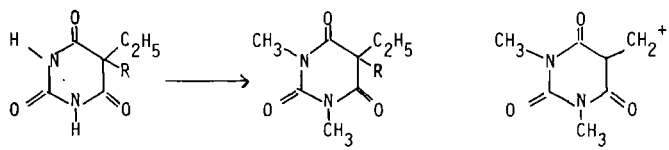

	R	m/e 169(%Σ_{40}23eV)	t_R(min)
Amylobarbitone	$-CH_2.CH_2.CH(CH_3)_2$	33.4	3.6(140°)
Pentobarbitone	$-CH_2.CH(CH_3).CH_2.CH_3$	37.2	3.7(140°)
Butobarbitone	$-CH_2.CH_2.CH_3$	39.5	2.9(140°)
3'-hydroxyamylobarbitone	$-CH_2.CH_2.C(OH)(CH_3)2$	28.5	2.4(170°)
3'-hydroxypentobarbitone	$-CH(CH_3).CH_2.CH(OH).CH_3$	19.2	3.0(170°)
3'-hydroxybutobarbitone	$-CH_2.CH_2.CH(OH).CH_3$	22.0	2.2(170°)

Barbiturate derivatives were assayed on a 6'x⅛" 3% OV-1 column with helium as carrier gas (inlet pressure 50 psi) on a Varian 1400 gas chromatograph coupled to an AEI MS 12 mass spectrometer via either a Watson-Biemann glass frit (3) or a silicone membrane separator (4), both operated at 240°. Mass spectrometer operating conditions were: accelerating voltage 8kV (unless used with accelerating voltage switching), trap current 250 µA, ionising voltage 23eV, electron multiplier voltage (1.8-2.2 kV, source temperature 250°, source slit 0.005 in., collector slit 0.010 in (R.P. ca 800). The magnet current was initially adjusted to the mass selected for quantitation using a perfluorokerosene marker bleed. Subsequently beam centering, ion extraction voltage and magnet current were finely reoptimised during several injections of standard barbiturate derivative. Output from the mass spectrometer head amplifier (modified to incorporate a 1000 megohm grid resistor) via the bandwidth filter at 1 c/s and main signal amplifier was recorded on a potentiometric recorder with variable input for full-scale deflection. Quantitation was made by peak height measurement of sample response relative to internal reference response (cf ref (5)).

N,N'-Dimethylamylobarbitone

Methylation of amylobarbitone was effected on column (injection port

(250°) using 0.1M tetramethylammonium hydroxide (TMAH) (1) in methanol. Monitoring m/e 169, 0.1 ng on column was detectable with a signal to noise ratio of 6/1; the detection limit was 0.02 ng. Response at 0.1 ng was not significantly enhanced in the presence of 10 ng D_6 carrier (6)($(CD_3)_2$ derivative prepared from D_6-dimethylsulphate) implicating no significant loss through column and separator. Butobarbitone was adopted as the internal reference for quantitative assay of amylobarbitone recovered from plasma: to plasma (0.04 to 0.1 ml), butobarbitone (25 ng/10 µl) was added, and the barbiturate recovered by ether (1.0 ml) extraction at pH 5. The ether extract was reconstituted in 10 µl TMAH and 1 µl injected into the gas chromatograph. The calibration curve of peak height ratio of amylobarbitone/butobarbitone derivatives against amylobarbitone concentration in plasma was linear over the range 2 to 100 ng per 0.1 ml plasma (0.2 to 10 ng injected, R=0.995). Reproducibility of measurement of amylobarbitone in plasma at 20 ng per 0.1 ml aliquot was ± 2.2% SD (6 observations) and at 1 ng was ± 20% SD (6 observations). Replicate measurement of a standard containing 2 ng amylobarbitone and 2.5 ng butobarbitone as the dimethylderivatives gave ± 2.1% SD (6 observations over 2 hours) ± 3.8% SD (10 observations over 1 week).

N,N'-Dimethylhydroxyamylobarbitone

Quantitative conversion of hydroxyamylobarbitone to its N,N'-dimethyl-derivative required treatment with ethereal diazomethane/methanol 10/1. Methylation of hydroxyamylobarbitone did not prevent adsorptive losses in the Watson-Biemann glass frit separator (cut off 40 ng) but losses were minimal using the silicone membrane separator. Phenobarbitone was adopted as the internal standard; the ion at m/e 175 in N,N'-dimethyl-phenobarbitone being used for quantitative measurement. After elution of dimethylhydroxyamylobarbitone the accelerating voltage was switched to a lower value, using an AVA in its manual mode, to bring m/e 175 into focus. The calibration curve of peak height ratio of hydroxyamylobarbitone/phenobarbitone derivatives against hydroxyamylobarbitone concentration in plasma was linear over the range 2 to 100 ng per 0.1 ml aliquot (R=0.999). Reproducibility of measurement at 15 ng per 0.1 ml plasma extracted was ± 7% SD (6 determinations) and at 30 ng was ± 4.7% SD (6 determinations). SD on repeat injection of the same sample was ± 3.6%. In microsomal incubation estimations it was necessary to measure hydroxyamylobarbitone (10 to 100 ng) in the presence of 1 mM amylobarbitone (11.3 µg/50 µl). Unchanged barbiturate was therefore removed by preliminary extraction with heptane/1.5% isoamylalcohol and N,N'-dimethylhydroxypentobarbitone (m/e 169) was used as internal standard. A linear calibration was obtained for hydroxyamylobarbitone recovered from incubation in the range 10 to 100 ng per 50 µl. (R=0.998). This represented 0.1 to 0.9% conversion to metabolite in the incubation. Reproducibility of measurement at 10 ng was ± 8.4% SD (6 determinations).

These techniques have been used to follow the plasma levels of amylobarbitone in mothers and their newborns following a dose of amylobarbitone to the mothers prior to birth; the hydroxymetabolite has also been measured. It is also feasible to measure 0.1% conversion of amylobarbitone to its hydroxymetabolite in a microsomal incubation prepared on the micro scale.

REFERENCES

1. G W Stevenson, Anal.Chem. 38, 1948 (1966).

2. J N T Gilbert, B J Millard and J W Powell, J. Pharm.Pharmac. 22,897 (1970).

3. J T Watson and K Biemann, Anal.Chem. 37,844 (1965).

4. J E Hawes, R Mallaby, V P Williams, J Chromatog.Sci. 7,690 (1969).

5. R W Kelly, J.Chromatog. 54,345 (1971).

6. B Samuelsson, M Hamberg and C C Sweeley, Anal.Biochem. 38,301 (1970).

A more detailed account of this work will be submitted for publication.

GAS-LIQUID CHROMATOGRAPHY AND MASS SPECTROMETRY OF BIOGENIC AMINES J3 AND AMPHETAMINES AS THEIR ISOTHIOCYANATE DERIVATIVES

N. Narasimhachari

Thudichum Psychiatric Research Laboratory
Galesburg State Research Hospital
Galesburg, Illinois 61401

Paul Vouros

Institute for Lipid Research
Baylor College of Medicine
Houston, Texas 77025

Primary amines react with carbon disulfide in ethyl acetate solution to form isothiocyanate derivatives. The reaction is fast and quantitative and can be done in a variety of conditions. The isothiocyanate derivatives thus formed have excellent gas chromatographic properties which render the GC/MS method highly suitable for the identification and quantitative determination of biogenic amines and amphetamines.

Methods are described for the GC separation of various phenylethylamines, amphetamines and tryptamines as their isothiocyanate derivatives. A 2.5% OV-225 column is found suitable for the separation of NCS-derivatives of phenylethylamines and amphetamines and 1% OV-101 or SE-30 column for the NCS derivatives of tryptamines. As a representative example the gas chromatographic profile of the NCS-derivatives of a series of amphetamines is shown in Figure 1. On an OV-225 column, the amphetamines had a lower retention time than the corresponding phenylethylamines. Positional isomers, such as o- and p-tyramines, 3 and 4-O-methyl ethers of dopamine, TMA-2 and TMA-6, are distinctly separable by this method. Hydroxy compounds (e.g. p- and o-tyramines, 3 and 4-O-methyldopamines, serotonin etc.) can be readily converted to TMS or TFA derivatives for further characterization.

The mass spectra of the NCS- or mixed NCS-TMS-derivatives of these compounds are generally characterized by the favorable elimination of a $\cdot CH_2$-NCS radical. Figures 2 and 3 show as a representative example the mass spectra of the NCS-TMS derivatives of the two isomeric 3- and 4-O-methyl ethers of dopamine (3-methoxy-tyramine-NCS-TMS and 3-OH, 4-MeO-phenylethylamine-NCS-TMS). The base peak (m/e 209) in the spectra of both compounds corresponds to the loss of $\cdot CH_2$-NCS from the molecular ion whereas the other two major peaks at m/e 179 and m/e 193 may be represented by the ions a and b, whose structures are supported by evidence obtained from the spectra of the d_9-TMS labelled derivatives. It is significant that the pronounced difference inthe ratio of m/e 179:m/e 193 allows for identification and differentation between these two important isomeric compounds (see ref. 1b). The peak at m/e 73 is, of course, due to the ubiquitous $(CH_3)_3$-Si^+ ion.

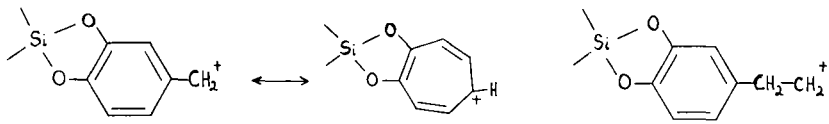

m/e 179 (a) m/e 193 (b)

High volatility, small increase in molecular weight, good GC characteristics, quantitative reproducibility, combined with characteristic mass spectra make this derivatization procedure a highly suitable method for the GC/MS analysis of phenylethylamines, amphetamines and tryptamines.

Some of the results reported here are published in recent reports.[1] Work on biological applications will be communicated shortly.[2]

References

1. (a) N. Narasimhachari and P. Vouros, Anal. Biochem., 45, 154 (1972).
   (b) N. Narasimhachari and P. Vouros, J. Chromatog., (in press).

2. R. L. Lin, et al , (in preparation).

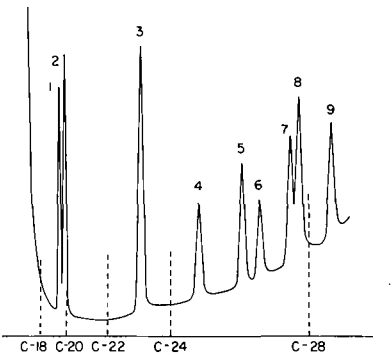

Fig. 1. Gas chromatographic profile of isothiocyanate derivatives of various amphetamines using a 4 ft 2.5% OV-225 column (initial temperature 160°, programmed at 5°/min): (1) D-amphetamine, (2) phenylethylamine, (3) p-methoxyamphetamine, (4) 2, 5-dimethoxyamphetamine, (5) 3, 4-dimethoxyamphetamine, (6) 3, 4-dimethoxyphenylethylamine, (7) 3, 4, 6-trimethoxyamphetamine, (8) 2, 3, 4-trimethoxyamphetamine, (9) 3, 4, 5-trimethoxyphenylethylamine (mescaline).

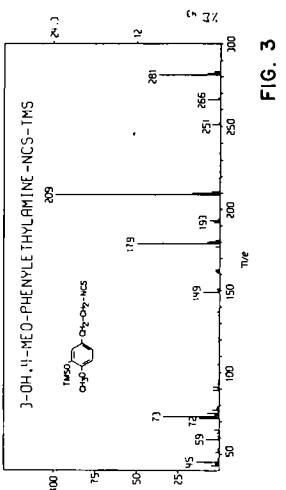

FIG. 3

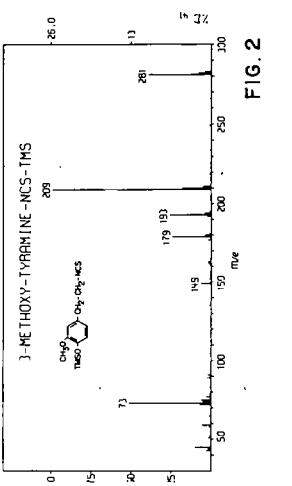

FIG. 2

ULTRATRACE DETERMINATION OF CHROMIUM IN PLASMA AND SERUM USING GS-MS TECHNIQUES

M.L. TAYLOR, B.M. HUGHES, W.R. WOLF, R.E. SIEVERS, and T.O. TIERNAN
Aerospace Research Laboratories, Chemistry Research Laboratory
Wright-Patterson Air Force Base, Ohio 45433

Quantitative determination of metals at the part per billion level (1 ppb = 1 nanogram/gram) is required in investigating the role of minute amounts of metals in both life-sustaining processes and in toxicological processes. Detection of ultratrace amounts (less than 1 nanogram) of metals in complex matrices such as biological and environmental samples requires not only ultrasensitive methods of detection but also methods which permit unequivocal identification of the metals of interest. We summarize here our use of specific ion monitoring gas chromatography-mass spectrometry to determine picogram amounts of chromium in aqueous samples and certain serum and plasma specimens.

A Dupont 21-491 Mass Spectrometer coupled through a Biemann-Watson separator to a Loenco Model 120 Gas Chromatograph was employed with modifications as follows. The standard object slit was increased to 0.012 inches, the slit at the entrance to the electric sector was removed entirely and the slit ahead of the electron multiplier was variable, but typically operated at 0.015 inches. The electron multiplier was operated at maximum gain with the recorder time constant extended to 0.3 Hz. These modifications led to a marked (75%) decrease in resolution (1:300 with 10% valley in the region of m/e 350); however, an increase of 10^3 in sensitivity was realized.

Chromium was analyzed as the trifluoroacetylacetonate, $[Cr(tfa_3)]$. The mass scale of the mass spectrometer was calibrated by introducing the crystalline chelate into the source via the solids probe and tuning to the m/e of interest, usually the base peak at m/e 358. For calibration of the GC-MS, benzene solutions of the chromium chelate (concentrations ranging from 0.5 - 50 nanograms chromium per milliliter) were injected into the chromatograph using a 10 microliter syringe and, after waiting 30-60 seconds for the solvent to be pumped away, the isolation valve was opened and the effluent from the chromatographic column was admitted into the mass spectrometer. The electron multiplier response was recorded using a 1 mv Honeywell-Brown Recorder Equipped with a Disc Integrator. A calibration curve constructed by plotting peak area vs. *picograms chromium injected was linear over the range of* 5 - 1000 *picograms*. The chromium in 0.05 ml of the aqueous or biological sample was simultaneously chelated and extracted using a benzene solution of trifluoroacetylacetone in a sealed tube procedure. Aliquots of the benzene solution were injected into the GC-MS following removal of excess ligand. Preliminary results obtained with this system have been published (1) and the reader is referred to this article for additional details. Chromium in human serum and plasma obtained from randomly selected donors was determined to be present at levels ranging from 0.1 - 10 nanograms chromium/gram of sample. In determining chromium concentrations <2 ppb the sensitivity and specificity of the GC-MS technique was more than adequate. However, blank corrections were objectionably high, on the order of 50% of the total chromium determined. Further experiments utilized low temperature ashing of 200-500 mg of sample in order to magnify the sample/blank ratio.

The GC - MS technique was utilized also in studying certain aspects of the chemistry of chromium trifluoroacetylacetonate. Results of this study indicate that the method of Hansen et. al. (2) for synthesis of $Cr(Tfa)_3$ gives rise to an anomalous chromium chelate which is not readily separated from chromium trifluoroacetylacetonate. Standard solutions prepared from impure chromium trifluoroacetylacetonate led to results which were 10 - 14% higher than the actual value. This has serious implications where low level recovery studies are being performed to evaluate methods for chelating and extracting chromium. A complete manuscript describing this work is being prepared for publication.

(1) W.R. Wolf, M.L. Taylor, B.M. Hughes, T.O. Tiernan, and R.E. Sievers, Anal. Chem. 44 (3), 616 (1972).

(2) L.C. Hansen, W.G. Scribner, T.W. Gilbert, and R.E. Sievers, Anal. Chem. 43, 349 (1971).

Protein Sequencing by the Mass Spectrometric Examination of Peptide Mixtures

J5

by *H.R. Morris*

University of Cambridge Chemical Laboratory, Lensfield Road, Cambridge CB2 1EW, England.

In recent years, considerable effort has been devoted to the study of the application of mass spectrometry to the amino-acid sequence analysis of oligopeptides. The majority of this work has involved the use of large quantities of synthetic peptides or isolated protein-derived peptides of known sequence. Except in particular circumstances, for example peptides with blocked amino groups, mass spectrometry offers no significant advantage, either in terms of time-saving or sensitivity, to the classical Dansyl-Edman approach to sequencing individual peptides.

However, the rate-determining step in protein sequence analysis is not the actual sequencing stage, but rather the laborious peptide isolation and purification stages preceding this.

Recently, a strategy has been proposed[1] to overcome this problem, involving the study of peptide mixtures. In this work, the first demonstration of the mass spectrometric sequencing of an 'unknown' protein-derived peptide mixture was given. This mixture analysis strategy has now been applied to the protein Ribitol Dehydrogenase (m.wt. >30,000; 310 amino-acid residues). The protein was examined without a knowledge of its sequence, a classical study of which is now nearing completion.[2] Using low-resolution mass spectrometry and manual interpretation, over two-thirds of the amino acid residues have been placed in sequence, including some not yet determined by classical methods. The use of different chemical and enzymic digests has created some 'overlap' in sequences (essential to a complete structural determination) but these have been restricted by the problematical amino acids Histidine, Methionine, Cysteine and Arginine. The use of a new derivatisation procedure designed to prevent quaternisation of Histidine-containing peptides[3] has now been applied successfully to peptides containing the other problematical amino acids Methionine, Cysteine as Carboxymethyl-cysteine and Arginine as Ornithine of Pyrimidylornithine and more 'overlaps' are being created.

A detailed account of this work will appear under the authorship of H.R. MORRIS, D.H. WILLIAMS, G. MIDWINTER and B.S. HARTLEY in Biochemical Journal.

1. MORRIS, H.R., WILLIAMS, D.H., and AMBLER, R.P., BIOCHEM. J. 125, 189 (1971).

2. MOORE, C., HARTLEY, B.S., IN PREPARATION.

3. MORRIS, H.R., FEBS LETTERS 22, 257 (1972).

A Protein Sequenator-Mass Spectrometer Interface.

R. E. LOVINS*, J. CRAIG and T. FAIRWELL, Department of Biochemistry, University of Georgia, Athens, Georgia 30601

An interface for directly coupling an automated protein sequenator to a low resolution mass spectrometer has been developed. The system is designed to; 1) transfer a solution composed of the product of the Edman degradation reaction (2-anilino-thiazolinone) in chlorobutane from the reaction vessel of the sequenator to a 5 ml glass reservoir, 2) reduced the sample volume to 0.5 ml under vacuum, 3) flash evaporate the remaining 0.5 ml of solution on a gold gauze matrix which is incorporated as an integral part of the tip of a modified solid probe. After sample isolation, the probe is inserted and the mass spectrum is obtained. The interface in its present configuration is manually operated but is being altered so that it can be made to function completely automatically. The interface was designed for use on a Dupont model 21-490 mass spectrometer and is being used to couple the mass spectrometer to a Bio-Cal ES-300 protein sequenator. The interface has potential for coupling other liquid extraction systems such as liquid chromatographs to mass spectrometers.

*R.E.L. is an N.I.H. Career Development Awardee.
Supported by NSF grant # GB 27555 and NIH grant # RO1 AI 10086

This paper will appear in Analytical Biochemistry

Field Desorption Mass Spectrometry in Peptide Analysis

J8

H.U. Winkler and H.D. Beckey
Institut für Physikalische Chemie der Universität Bonn, 53 Bonn, Germany

The development of the Field Desorption (FD) technique of organic molecules for the structure elucidation of unvolatile organic compounds has been a major field of effort in our laboratory. Generally, derivatization of the molecules is not necessary to obtain interpretable mass spectra because in contrast to EI, CI and normal FI-methods the sample is not evaporated from the heated inlet system. The sample is deposited directly onto the field anode by dipping it into a solution of the compound. The solvent is evaporated in the vacuum system of the mass spectrometer. In a high electric field (about 0.5 V/Å) the sample is desorbed from the field anode surface, the heat of ionic desorption being strongly reduced by the high electric field. In this way the thermal decomposition is also strongly reduced. The high sensitivity (the amount of substance needed for a low resolution mass spectrum is less than 10^{-7} g) and the low fragmentation are good reasons for regarding FD as a good complement to the other ionization methods and further, as an very suitable method for analyzing extremely unstable molecules.

By applying the FD-technique in peptide analysis it could be shown that the mass spectra of free pentapeptides and peptides containing free arginine[1)] display an intense molecular ion peak in contrast to common ionization techniques.
Also the FD-mass spectrum of Glutathion (γ-Glutamyl-cysteinyl-glycine)displays an intense molecular ion peak and several cleavage peaks containing sequence information, so that a complete determination of the amino acids composition is possible. Another important result is the detection of the quasi-molecular ion ($(M+1)^+$) of an amino acids salt: the aspartic acids monopotassium salt (MW = 171). This compound was dissolved in a KOH-H_2O mixture. Besides the quasi-molecular ion peak (100 % rel. intensity) the FD-mass spectrum displays also satellite peaks at m/e 208, 209, 210 and 211. These peaks are due to the binding of a second potassium atom to the salt other peaks of lower intensity (<20 % rel. intensity) correspond to splitting-off of COOH, COOK, H_2O and KOH from the molecular ion.

1) H.U. Winkler and H.D. Beckey, Biochem. Biophys. Res. Comm. 46(2),391(1972)

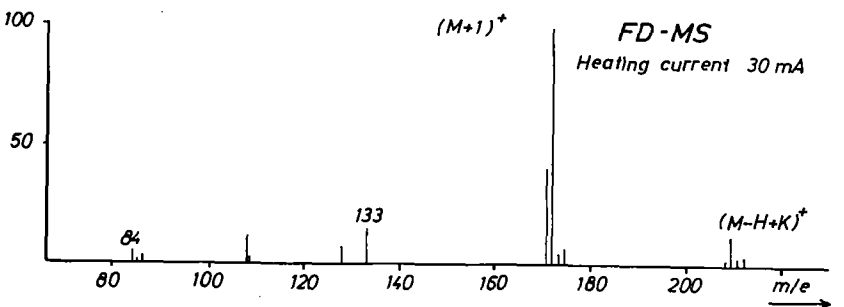

FD-MS:Aspartic acid monopotassium salt

J10

Mass Spectral Study of Surface Effects on the Volatility of Small Samples of Peptide Derivatives.* R. J. BEUHLER, E. FLANIGAN, L. J. GREENE, L. FRIEDMAN, Brookhaven National Laboratory, Upton, N. Y. 11973

Volatility of peptides and peptide derivatives has been a limiting factor in structural mass spectral studies. Significant sample losses are encountered when competitive decomposition and condensation processes occur at temperatures required for evaporation of peptides in an ion source. Basic information on evaporation and competitive decomposition processes can be obtained by study of temperature coefficients of the more abundant ions in a particular spectrum. We have determined proton transfer spectra of Thyrotropin Releasing Hormone (TRH), (PCA-His-Pro-NH_2) and a series of N-acetyl methyl esters of di-, tri-, tetra-, and pentaalanines as a function of sample and collision chamber temperature. Spectra were determined using methyl ammonium ions as ionizing reagent in the tandem mass spectrometer.

Significant enhancement of volatility was observed when samples were dispersed from solution on chemically inert surfaces. Maximum efficiency in studying TRH was achieved using a Teflon coated sample probe and a Teflon collision chamber. Thermochemical data and mass spectra were obtained with samples as small as 0.5 microgram of TRH ($\sim$ 1 nanomole).

*Research performed under the auspices of the U. S. Atomic Energy Commission.

New Techniques in Single and Multiple Ion Monitoring used in Quantitative Steroid Estimation. J.R. Chapman, K.R. Compson, D. Done, T.O. Merren and P.W. Tennant. AEI Scientific Apparatus Limited, Manchester, England.

The techniques of single and multiple ion monitoring are theoretically capable of specifically detecting and estimating chosen compounds with a sensitivity of a few picograms. As such they are ideally suited to the quantitative determination down to very low levels of compounds in body fluids with the minimum of pre-purification. These techniques have been implemented using the AEI MS30 double beam mass spectrometer and a 6-channel peak monitoring system of novel design which is capable of operation at low and high resolving powers. The system is capable of switching at a speed of 0.15 seconds per channel, each channel having an independent output with its own gain and backing off controls. The signal detected at each mass is integrated over the dwell time and the integrated values held during the rest of the switching cycle. The resulting stepped signals are then smoothed to provide continuous traces for each channel.

To illustrate these techniques, we have developed assay methods for testosterone in human plasma. In these methods, the testosterone is assayed as its bromomethyldimethylsilyl (BDMS) ether (I) introduced via the gas chromatograph and characterised by monitoring the two parent ions at m/e 438 and m/e 440. The two parent ions correspond to the presence of the ^{79}Br and ^{81}Br isotopes respectively and are therefore of equal intensity, so that monitoring these two masses provides a built in check for gas chromatographic peak homogeneity.

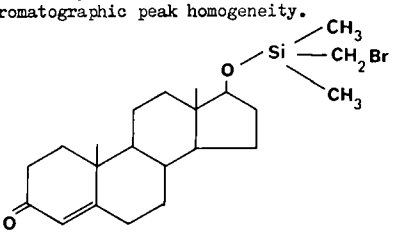

(I)

Initially, standard solutions of testosterone BDMS ether were introduced via an 18", 2% OV 225 column into the mass spectrometer to determine the limits of detection. Figure 1 shows the result obtained with 5 x 10^{-11}g testosterone BDMS ether at a resolution of 1000 (10% valley). Whilst at m/e 438 the signal to noise ratio would certainly allow the detection of 1 x 10^{-11}g on column, the noise at m/e 440 is much higher because of column bleed at this mass. The background level at m/e 440 can be seen to increase as the column temperature is raised and reaches such a level that the detection of less than 5 x 10^{-11}g testosterone BDMS ether on column would be difficult. This illustrates the very common situation in which the detection limit for compounds is determined by the background contribution at the mass or masses concerned rather than by instrumental sensitivity. The limit set by this background arising from the sample or from the gas chromatography column, can be an order of magnitude higher than the instrumental limit.

However, the background levels observed in these experiments are low enough to permit the quantitative determination of testosterone in human plasma by this method. Figure 2 shows the analysis of a sample prepared by direct extraction of male plasma with an organic solvent followed by formation of the BDMS ether. No other pre-purification was attempted. The major peaks at m/e 438 and m/e 440 represent 1-2 x 10^{-9}g of testosterone BDMS ether on the column. Smaller peaks eluting approximately three minutes before the testosterone are due to dehydroepiandrosterone BDMS ether, which has the same molecular weight. As in figure 1 the two pen traces are physically displaced with respect to each other and the peak tops are in fact coincident in time.

A further possible source of interference in addition to column bleed is other materials in the extract. Whilst such interference is relatively infrequent, nevertheless its unpredictable occurrence makes it important, particularly in a routine analytical method. Figure 3 shows the single peak monitoring trace at m/e 438 obtained from the extract of a male plasma prepared by the same simple method in which peaks that interfere to some extent with the measurement of the testosterone peak can be seen.

Because the molecular ion of testosterone BDMS ether contains bromine and silicon it is considerably more mass deficient than other impurities which might be expected to interfere at m/e 438. For example, the exact molecular weight of testosterone BDMS ether is 438.1590 whereas that of a typical saturated hydrocarbon at this mass is approximately 438.4, so that a resolution of 3000 is quite sufficient to separate out such impurities from the parent ion. At 3000 resolution, the overall sensitivity is reduced by only a small factor, but the reduction in background achieved by resolving out the impurity peaks may be far greater. This is illustrated in Fig. 4 which shows a single peak monitoring trace from the same extract, run at a resolution of 3000. For this figure the gain had been increased so that the testosterone peak did not decrease in size.

Resolution of impurities in this manner opens up the possibility of dispensing with the gas chromatographic separation and running such extracts directly on the probe after a preliminary TLC separation of the isomeric dehydroepiandrosterone BDMS ether. As this TLC separation could be carried out on a batch basis, the overall method would still be much more rapid than the gas chromatographic method.

To be submitted to Clin. Chim. Acta.

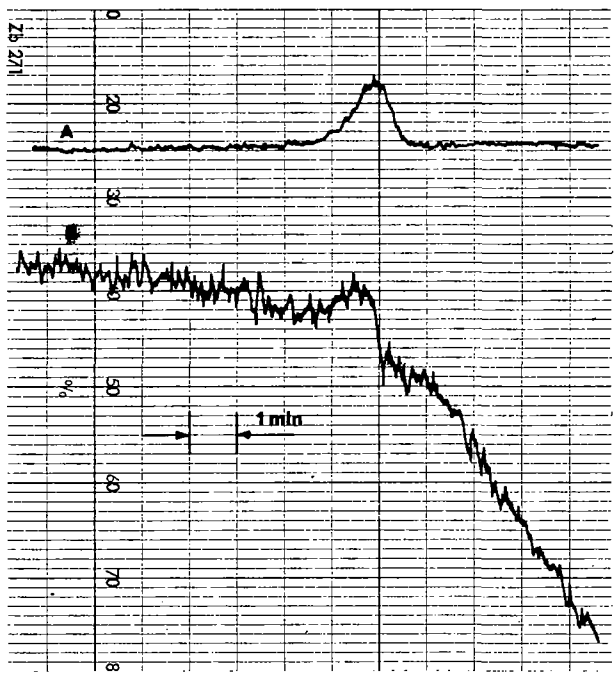

Figure 1: Multiple peak monitoring at m/e 438 (A) and m/e 440 (B) of standard testosterone bromo-dimethylsily ether (5×10^{-11}g on column).

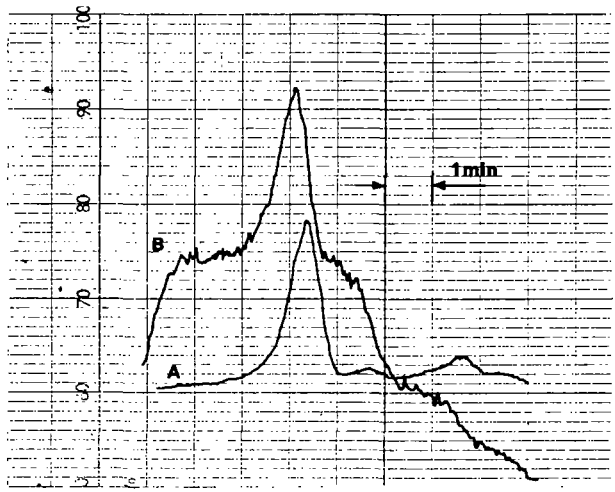

Figure 2: Multiple peak monitoring at m/e 438(A) and m/e 440 (B) of testosterone bromo-dimethylsilyl ether in male plasma extract.

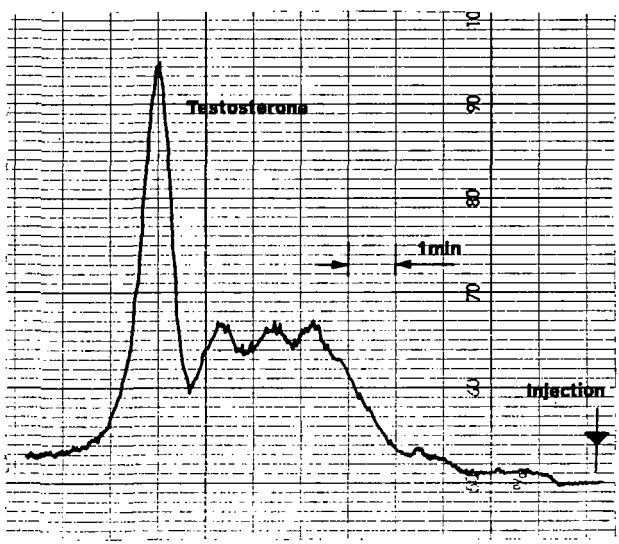

Figure 3: HP1000. Single peak monitoring at m/e 438 to assay testosterone in plasma extract as the bromodimethylsilyl ether.

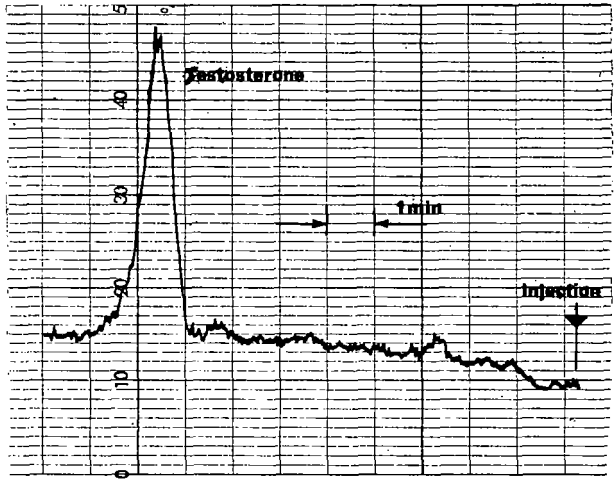

Figure 4: RP 3000.Single peak monitoring with sweep at m/e 438 to assay testosterone in plasma extract as the bromodimethylsilyl ether.

COMPUTERIZED HIGH RESOLUTION ISOTOPE MEASUREMENT

by

William F. Haddon*, Harold C. Lukens*, and Marilyn Crim†

*Western Regional Research Laboratory, Agricultural Research Service, U.S. Department of Agriculture, Berkeley, California 94710

†Department of Nutritional Sciences, University of California, Berkeley, California 94720

Accurate abundance measurement of N^{15}, C^{13} and O^{18} isotopes can be obtained on microgram samples by averaging successive electric sector scans of a high resolution mass spectrometer. Measurements are made at a single mass with resolution sufficient to separate or partially separate the different isotopic contributions at the same integral m/e value. Use of the complete mass spectrum for isotope measurement can provide confirmation of the specific location of an isotopic label in a molecule as illustrated previously[1]. Results on creatinine ($C_4H_7N_3O$) doubly labelled with N^{15} illustrate that the precision and accuracy are better than 0.5% relative standard deviation at label incorporation below 1.0 atom percent excess. The computer is used for data acquisition, real time display of averaged multiple scans, and deconvolution of overlapping components of isotopic multiplets.

[1]G. R. Waller, R. Ryhage and S. Meyerson, Anal. Biochem. 16, 277 (1966).

Full paper submitted to Analytical Chemistry.

Studies on ^{13}C-incorporation in Prodigiosin by Mass Spectrometry

R.J. Sykes, W.J. McMurray, J. Gage, P. Arneson, H.H. Wasserman and S.R. Lipsky

Yale University, New Haven, Connecticut 06510

The isotopic abundances were measured on the AEI-MS-9: IBM-1800 system in our laboratory. To measure the incorporation, the mass range of interest was selected using the SET START control on the MS-9. Short, repetitive sweeps of up to 5% of the selected mass range, controlled by the computer, permitted the amplitudes of a large number peaks to be measured simultaneously. The digital data from each sweep was accumulated with the summed result of the previous scans. Two 16 bit words were used to store the accumulated data. When the sweeps were stopped, the programs then select the peaks, normalize them and determine precent relative to-largest peak. Measurements on reference samples, polyhalogenated compounds, indicated intensity ratios greater than 1800:1 could be measured. The accuracy of intensity measurement were on the order of 0.2% and the precision was generally a factor of two or three better.

The isotope abundances measured for prodigiosin produced from carboxyl labeled ^{13}C acetate were shown not to fit the predicted abundances based on statistical incorporation of ^{13}C using the amount of enrichment determined by ^{13}C N.M.R. The deviations between the observed and predicted were much too large (>x10) to be a function of the measurement. A model was presented to show that the deviations could be accounted for by assuming the isotopic pool is being diluted during the production of the pigment. It was further shown that the dilution could be simulated by an exponential function. When the predicted abundances are calculated utilizing the exponential dilution, the observed values and the predicted values for the isotopic enrichment in prodigiosin agree within experimental error. The complete study on the ^{13}C-incorporation in prodigiosin will be presented in a full paper.

Measurement of Levels of Biologically Significant Molecules by Stable Isotope Techniques

Bruce H. Albrecht, James R. Plattner, Dwain Hagerman, Sanford Markey and Robert C. Murphy

University of Colorado Medical Center, Denver, Colorado 80220

There has been recent interest in employing molecules labelled with stable isotopes (^{13}C, ^{2}H, ^{15}N, and ^{18}O) in clinical research tracer studies due to the possible radiochemical hazard of molecules labelled with ^{14}C or ^{3}H. Several mass spectrometric techniques have been described which allow one to measure the stable isotope content of molecules with sufficient accuracy necessary for tracer studies. These techniques involve rapid accelerating voltage alternation to sequentially focus ions of interest on the electron multiplier and to output the signal to a light beam oscillograph (1) or a multichannel analyzer (2). More recently a high resolution technique was described (3) and a technique using the peak switching device of a high resolution mass spectrometer with subsequent computer data processing (4).

The method for stable isotope measurement we chose to investigate is based on rapid, repetitive accelerating voltage scanning over a limited mass range and computer summation of the signal from the electron multiplier (an ensemble addition technique). This method required a minimum of instrument modification on an existing system. The mass spectrometer (MS-12) available had previously been interfaced to a small, dedicated computer (PDP-8i, 8K core) for GC-MS data acquisition (5), and in addition was equipped with accelerating voltage scan circuitry. The mass spectrometer-computer system is illustrated in Figure 1. The accelerating voltage scan is accomplished by a voltage

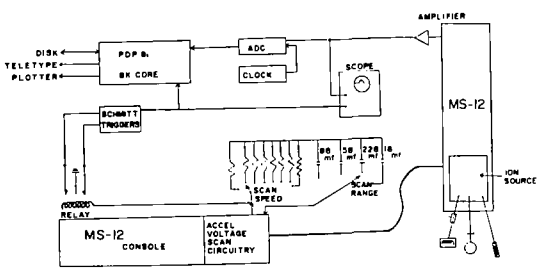

Fig. 1: Diagram of the mass spectrometer computer system.

decay through the RC network shown in Figure 1. The capacitance of the circuit determines the mass range scanned and was increased to 226 mfd in order to decrease the range and thereby increase the number of data points one could obtain across each mass unit. The signal from the electron multiplier is digitized by a 12-bit analog to digital converter (ADC) at a rate controlled by a variable oscillator. A rate of 140 microseconds for each data point was found optimal for the experiments described below. The mass spectrometer scan is synchronized with the data acquisition by a Schmitt trigger which senses the position of relay in the scan circuit.

The oscilloscope illustrated in Figure 1 enables the operator to adjust the magnetic field until the mass values of interest appear on the screen, since the scanning circuit triggers the oscilloscope as well as data acquisition. This feature allows one to witness any fluctuations of the mass position which would indicate instability in either the magnetic field or accelerating voltage. The oscilloscope is used to monitor the voltage level of all masses being accumulated in the computer, because the amplifier must not be saturated with the intensity of any mass to be

measured.

Evaluation of the precision of this system for isotope ratio measurements was carried out initially with xenon, because it contains 9 stable isotopes with abundances ranging from 95% to 0.4% relative to the isotope at m/e 132. Use of xenon allowed adjustment of the many instrument parameters and computer software to maximize precision while minimizing effects due to sample pressure variation by introducing xenon through the gas inlet system.

It became immediately apparent that in order to measure weak ions in the presence of abundant ions a wide dynamic range of data storage is necessary. Therefore, the data from the 12-bit ADC is stored and summed in core in double precision (2 words); this provides a range of 1 to 16 million for each data point in core while still allowing over 3000 such data points to be stored. Figure 2 is a computer plot of the data stored

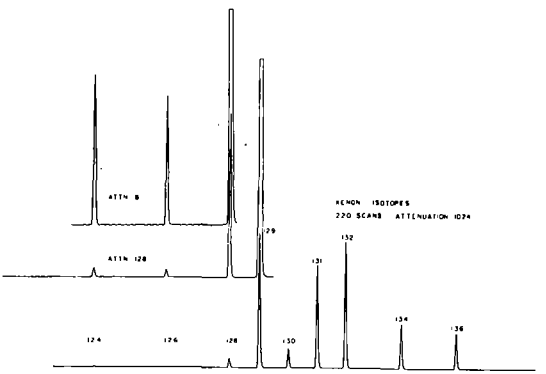

Fig. 2: Plot of the data accumulated in core from 220 scans of the isotopes of xenon.

in core after summation of 220 scans of the xenon multiplet. In this presentation the data had to be attenuated at different values for the maxima of all ions to be observed.

After the data is recorded by the computer, a further program that identifies peaks and establishes peak heights is called. This program first identifies the baseline, then locates a peak by finding a rising slope of 5 consecutive points above baseline. If the data points return to the baseline only after a pre-set minimum number, those data points are defined as a peak. The highest point in this region is called the peak height. The time and height of the peak, as well as the peak width, are printed on the teletype and further calculations can then be performed.

The results of the analysis of the data from the xenon isotopes is given in Table 1. The ion of greatest abundance was found to be m/e 129, and the intensity (peak height) of the other isotopes were compared to this ion. Statistical analysis of ten separate determinations of these isotopes indicated quite good precision, being 0.001 S.E.M. for m/e 126, the least abundant ion, to 0.12 S.E.M. for m/e 132, the most abundant ion.

The accuracy of our measurement appears to be low when the results are compared with the literature values. Probably the main factor involved in this discrepency is that the accelerating voltage scanning changes the kinetic energy of the ions, thus one would expect greater sensitivity for m/e 124, and less for m/e 136, as was observed. As evidence for this the abundance difference between the experimental and literature values plotted aganist the literature abundance for each mass produced a straight line as seen in Fig. 3 except for the point at m/e 124.

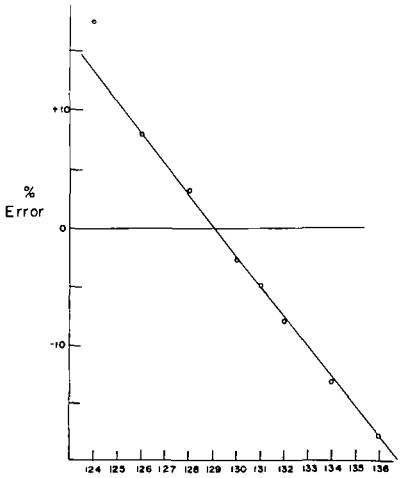

Fig. 3: Plot of the percent error (difference between the experimental and literature abundances divided by the literature abundances x 100) versus the mass of the ion.

This system was used to determine the excretion of dideuterio-estriol which had been injected intravenously into a woman late in pregnancy. These and results of further patient studies will be summarized in other publications.

References

1. C-G Hammar and R. Hessling, Anal. Chem., 43: 298 (1971).
2. P. D. Klein, J. R. Haumann, and W. J. Eisler, Clin. Chem., 17: 735 (1971).
3. W. F. Haddon, H. Lukens, and M. Crim, Paper J12, ASMS 20th Annual Conference, Dallas, 1972.
4. N. M. Frew and T. L. Isenhour, Anal. Chem., 44: 659 (1972).
5. S. P. Markey, Anal. Chem., 42: 306 (1970).
6. Handbook of Chemistry and Physics, 45th Edition, 1964.

Table 1 XENON ISOTOPES

m/e	Percent m/e 129	± S.E.M.	Literature[6]
124	0.427	0.001	0.36
126	0.367	0.001	0.34
128	7.49	0.014	7.26
129	100	-----	100
130	15.02	0.02	15.43
131	76.20	0.07	80.11
132	93.49	0.12	101.70
134	34.25	0.05	39.49
136	27.57	0.05	33.55

CHEMICAL IONIZATION MASS SPECTROMETRY- EARLY AND RECENT DEVELOPMENTS

Burnaby Munson
Department of Chemistry
University of Delaware
Newark, Delaware 19711

Chemical ionization mass spectrometry was the almost accidental outgrowth of several years' work on gaseous ionic reactions at increasingly higher pressures. From the number of papers about or using chemical ionization mass spectrometry which are being presented at this meeting, it appears to have captured the interest of mass spectrometrists and seems to be fulfilling a real need.

In the CI technique, the ions of the compounds of interest are produced by gaseous reactions of a set of reactant ions. The methods of production of these reactant ions are more or less irrelevant to the technique; but because most CI mass spectrometers are modified EI mass spectrometers, the primary ions of the reactant gas are generally produced by electron ionization. For most CI reactant gases, these primary ions produced by electron ionization react in one or more steps to produce other ions which react with the additive to produce the CI mass spectrum. It is not of fundamental significance to the CI technique whether or not the reactant ions change composition on collision with the reactant gas; and I doubt that the requirement of a set of ions stable in the reactant gas is actually necessary. However, it is extremely convenient in the interpretation of CI mass spectra if only a few ions are produced whose reactions need be considered. Similarly, if comparisons are to be made of spectra obtained with different instruments the distribution of the reactant ions which produce the spectra must be relatively insensitive to experimental conditions.

Small amounts of the additive are necessary in this technique, primarily for three reasons. Direct ionization of the additive can occur, particularly in those reactant gases with small ionization cross sections. This direct ionization does not invalidate the CI spectra, but it will complicate the interpretation since $M^{+\cdot}$ ions and fragment ions derived from these molecular ions will be present. Similarly, if the additive concentration is relatively large, ionization by reaction of the primary ions of the reactant gas may occur. The major complication from large sample sizes, however, results from reactions of additive ions with additive molecules to give addition ions or protonated dimer ions. If one knows the compound in question, these ions can be understood quite easily; however, if the compound is unknown, they may well cause complications in the determination of the molecular weight of the unknown. We have found that keeping the additive ionization as 10% or less of the total ionization virtually eliminates these complications.

Many gases are available to produce different sets of reactant ions, and one can compound the confusion by using gaseous mixtures as well. This variation of reactant ion (among gases of the same type) is the analog of changing the electron energy in EI mass spectrometry. Many CI reactions involve proton or hydride transfer to give $(M \pm H)^+$ ions, but transfer of larger groups, like H_3O^+, Cl^-, OH^-, has also been observed and can be used. If one uses a reactant gas which contains no hydrogen, then one can eliminate proton transfer altogether and high pressure charge exchange mass spectrometry is also a very useful technique. Hydrogen, methane, propane, isobutane, water, and ammonia have been used successfully in CI mass spectrometry.[1] Useful high pressure charge exchange spectra have been obtained with nitrogen, carbon monoxide, carbon dioxide, nitric oxide, and oxygen.[2] The spectra obtained using helium as a reactant gas contain reasonable amounts of molecular ions, probably from direct ionization.[3, 4]

The majority of the CI mass spectra have been obtained with methane as the reactant gas, partly from habit since methane was the first reactant gas studied, partly because there are already many methane CI spectra with which to make comparisons, and partly because methane CI

spectra generally show reasonably abundant $(M\pm H)^+$ ions as well as structually useful fragment ions. Methane is probably the best general purpose CI reagent gas. It is easily possible to discuss the effects of some of the experimental parameters on the spectra obtained with methane and to generalize these observations to other gases.

Since CI mass spectra are produced by reactions of a set of ions, any changes in instrumental parameters which do not change the distribution of reactant ions or their reactions should have no effect on the CI mass spectra. CI mass spectra are independent of electron current, electron energy, and acceleration voltage over wide ranges.

It has been known for some time that the distribution of product ions in methane (with very low levels of impurities) is substantially independent of pressure above 0.2 torr in most CI instruments.[5] Consequently, in a well-pumped instrument, one would expect the methane CI mass spectra to be independent of pressure. In our instrument methane CI spectra are substantially independent of pressure from 0.3 to 1.3 torr. Small changes are observed which we attribute to collisional decompositions in the region just outside the source.

If, on the other hand, one uses as a compound for which the ionic distribution changes in the accessible pressure region, then the spectra will be pressure dependent. In the pressure region of 0.2 to 1.5 torr the relative abundances of CO^+ and $(CO)_2^{+\cdot}$ in CO change markedly[6], and the high pressure charge exchange spectra obtained with CO as the reactant gas are, indeed, sensitive to pressure: the relative abundance of the dimer ion increases with increasing pressure, and the relative abundance of $M^{+\cdot}$ ions from benzophenones increases with increasing pressure.[2]

CI spectra are substantially independent of repeller voltage for small repeller voltages, but are significantly affected by larger voltages. Both CI and CE spectra are substantially independent of repeller below about 5 v. For high voltages, 30-50 v., collisionally induced decompositions occur within the source of the instrument.[7] However, in the carbon monoxide system, the changes produced in the spectra by repeller voltages of 5-15 v. are due to changes in the relative abundances of monomer and dimer ions of the reactant gas.

The variation in the abundances of $CO^{+\cdot}$ and the major fragment ions of the benzophenones, $\emptyset CO^+$ and $Y\emptyset CO^+$, with pressure and repeller voltage are the same; therefore, the monomer ion, $CO^{+\cdot}$, reacts predominantly by dissociative charge exchange. The abundances of the dimer ion, $(CO)_2^{+\cdot}$, and the molecular ions of the benzophenones vary in the same manner with pressure and with repeller; therefore, the dimer ion reacts predominantly by simple charge exchange.[2]

It was noted in replicate scans of the spectra of a set of steroidal ketones over a long period of time, that the abundances of certain of the ions, particularly $(M+29)^+$, showed erratic behavior. These ions may be useful in assigning structures since $(M+29)^+$ is 10-15% of the additive ionization for several 3-ketosteroids and approximately 5% for several 17-ketosteroids. It was noted that this variation could be attributed generally to variations in amounts of H_3O^+ in the methane spectrum. For valerophenone the ratio, $(M+29)^+/(M+1)^+$, decreased from about 0.24 to 0.05 as the ratio H_3O^+/CH_5^+ increased from 0.05 to 5.[8] It was also noted in these spectra that the extent of fragmentation decreased as the stronger acids, CH_5^+ and $C_2H_5^+$, were replaced by the weaker acid, H_3O^+.[8]

It has been established for some time that changing the reactant gas drastically changes the CI spectrum of a compound: H_3^+ from hydrogen gives predominantly dissociative proton transfer; CH_5^+ and $C_2H_5^+$ from methane give both $(M+1)^+$ and fragment ions; and $t\text{-}C_4H_9^+$ from isobutane gives predominantly spectra containing one chemical species.[1,4] We cannot yet correlate quantitatively the extent of fragmentation with reaction energetics, but the extent of fragmentation is directly related to the Bronsted and Lewis strengths of the reacting acids. These acid strengths are given by proton and hydride affinities. In order for the proton or hydride transfer reactions of CI mass spectrometry to occur with the necessary rapid rate, the $(M+H)^+$ or $(M-H)^+$ ions of the additive

molecules must be weaker acids than the reacting ions of the reagent gas: the greater the difference in acid strength of the reactant ions and the $(M+H)^+$ or $(M-H)^+$ ions of the additive, the greater the exothermicity of the proton or hydride transfer reaction, and the greater the extent of fragmentation in the CI mass spectrum.

In some of the early work in CI mass spectrometry it was postulated that the $RCO_2H_2^+$ ions formed in the methane CI spectra of aliphatic esters of ethyl or higher alcohols were formed by a reaction involving transfer of a hydrogen from the β-carbon atom through a six-membered transition state, *reminiscent of the McLafferty rearrangement*:[9]

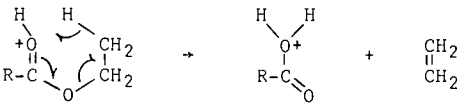

In the methane CI mass spectrum of the α-dideuteroethyl acetate, it was observed that $RCO_2HD^+/RCO_2H_2^+$ was only about 0.10 ± .01; consequently, the reaction does go predominantly through a six-membered ring with transfer of the β- and not the α-hydrogen.

For multifunctional compounds it is a convenient assumption that protonation occurs at each functional group, followed by reaction localized primarily in that region of the molecule. As an illustration of this, one of the major ions in the spectrum of a chloroester is the $(M+H-HCl)^+$ ion which should be formed by process (a) rather than (b):[9]

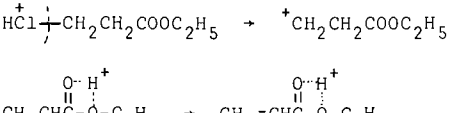

(a)

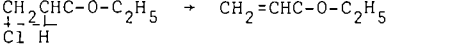

(b)

In the spectrum of β-chloroethyl propionate, the ratio of (M+D-HCl) to $(M+D-DCl)^+$ was about .07; consequently, the reaction proceeds predominantly by the predicted path, (a).

If one takes a rigid steroidal nucleus with two substituents on opposite sides of the molecule, say the 3- and 17-positions, then it is reasonable to consider that these substituents are protonated independently of each other. Since some compounds, like alcohols or chlorides, give essentially no $(M+H)^+$ ions in their spectra but dissociate almost completely after protonation to give $(M+H-H_2O)^+$ or $(M+H-HCl)^+$, it is possible to put both of these substituents on a rigid skeleton and determine the relative amounts of protonation at these two sites from the abundances of these (and similar) fragment ions. From reactions like these it is possible to establish an order of effectiveness of functional groups for directing attack of the protonating reagents, CH_5^+ and $C_2H_5^+$:

$$COO > CH_3O > CO > Br \cong Cl > OH$$

Acknowledgement:

The author is very grateful to Drs. Noel Einolf and John Michnowicz for their very valuable assistance and to the National Science Foundation, Grant GP20231, for support of this research.

References:

1. Burnaby Munson, Anal. Chem. 43, 28A (1971).
2. Noel Einolf and Burnaby Munson, J. Mass Spectr. and Ion Physics 9, 141 (1972).
3. D. M. Schoengold and Burnaby Munson, Anal. Chem. 42, 1811 (1970).
4. R. M. Foltz, 19th Conference on Mass Spectrometry, Atlanta, Georgia, May, 1971.

5. F. H. Field and M. S. B. Munson, J. Am. Chem. Soc. 87, 3289 (1965).
6. S. Chong and J. L. Franklin, J. Chem. Phys. 54, 1487 (1971).
7. John Michnowicz and Burnaby Munson, Org. Mass Spectrometry 4, 481 (1970).
8. John Michnowicz and Burnaby Munson, Org. Mass Spectrometry 6, 283 (1972).
9. M. S. B. Munson and F. H. Field, J. Am. Chem. Soc. 88, 4337 (1966).

Experiences in Chemical Ionization Mass Spectrometry. H. M. Fales, G. W. A. Milne, D. J. Pedder and K. G. Das, National Institutes of Health, Bethesda, Md. and National Chemical Laboratory, Poona, India.

Experiences during the past year have tended to confirm the validity of the specific protonation theory in chemical ionization: at the very least it is a useful construction in predicting fragmentation of a wide variety of more complicated molecules.

Isobutane has been found to be a very useful reagent gas in quantitative analysis: in the case of $C_6H_5C(OH)CH_3$ $COCH_3$ at 25°, six independent checks are available on the location and extent of ^{18}O labeling via the intensities of M + 1, M + 1 - H_2O, 2M + 1, 2M + 1 - H_2O, 3M + 1, 3M + 1 - H_2O ions.

Using this gas it even appears possible to differentiate isomers: in the case of 2-nitro-1,3,4-triphenylcyclohexene, the isomer with all phenyls cis and nitro trans showed less loss of HNO_2&C_6H_6 than the isomer with the 5-phenyl trans to the other groups. This is explained on the basis of steric crowding of the transition state.

Anchimeric effects are also observed in a series of ortho-substituted aromatic compounds: o-nitrocinnamic and o-methoxycinnamic acids both lose water much more easily than their m- or p-isomers. Similarly p-nitrobenzyl bromide, chloride, and iodide lost HX easily, proving that the nitro groups is an effective nucleophile under these conditions. Ring size is relatively unimportant in this reaction since loss of water was seen only in the o-isomers of nitrobenzoic nitrophenylacetic, and nitrocinnamic acids. Flanking a carboxyl group with two nitro groups (2,6-dinitrobenzoic acid) causes the water loss to be so intense that the M + 1 ion is only ~10% of the M + 1 - H_2O ion while 3,5-dinitrobenzoic acid showed trivial water loss.

Our recent experience with a computerized quadrupole-mass spectrometer indicates that chemical ionization has several advantages to offer in quadrupole operation. Chemical ionization often supplies an intense ion at high mass (M + 1, M + 1 - HX, M + R, etc.) whose nature can be predicted and sought for among the multiple scans available from such a system. The intensity of these ions thus compensates for the inherent limitations of present-day quadrupoles at high mass. In the case of the antibiotic sisomycin, the total ion monitor maximum corresponded to a decomposition product of this compound, while a reconstructed ion plot of M + 1 revealed the presence of the compound in a later scan. Output of this scan furnished an entirely satisfactory spectrum.

Experiences with a series of glycerides has revealed that monoglycerides give satisfactory M + 1 ions; diglycerides and triglycerides are satisfactory only when the chain length is extremely short, (tributyrin, tricaprylin, etc), and the longer di- and triglycerides of biological importance show only M + 1 - RCOOH ions. This effect is largely due to the high temperature required to volatilize such compounds and efforts are being made to overcome this problem.

Ion Equilibrium Under Chemical Ionization Conditions

Jean H. Futrell and Marvin L. Vestal
Department of Chemistry, University of Utah
Salt Lake City, Utah 84112

Introduction

The several processes taking place in a high pressure ion source of a high pressure mass spectrometer under the conditions of chemical ionization mass spectrometry as currently practiced may be represented by the following series of chemical reactions.

$$XH^+ + M \rightarrow MH^{+*} + X \quad (1)$$

$$MH^+ + M \rightleftarrows M_2H^{+*} \quad (2)$$

$$M_2H^+ + M \rightleftarrows M_3H^{+*}, \text{ etc.} \quad (3)$$

$$MH^{+*} + B \rightleftarrows MH^+ + B^* \quad (4)$$

$$M_2H^{+*} + B \rightleftarrows M_2H^+ + B^*, \text{ etc.} \quad (5)$$

where XH^+ represents the reagent ion participating in the initial chemical ionization activation reaction. This reaction is written as a proton-transfer reaction, which is a very common mechanism, but is not meant to imply that this is the exclusive mode of reaction to which these remarks apply. Dimerization and trimerization, in reactions (2) and (3) are possible condensation reactions which are similarly archetypical but non-exclusive ion molecule reactions involved in chemical ionization mass spectrometry. Asterisks applied as superscripts to these species are used to indicate that all of these reactions are in general quite exothermic chemical reactions. They are written as equilibrium steps in the cases of reactions (2) and (3) and are certainly reversible processes. In order that equilibrium conditions apply, however, it is necessary that the energy exchange reactions (4) and (5) take place on a time scale which is quite rapid with respect to the relaxation time of equations (2) and (3) in order that the species be characterized by a Maxwell-Boltzmann distribution of energy states which may be characterized by a temperature.

An additional instrumental requirement for studying these reactions in a mass spectrometer is that the entire sequence of reactions be very fast compared to the average residence time of an ion within the ion source, i. e., with respect to the contact time of the chemical reactor. This requirement results from the notion that the forward and reverse chemical reactions and all energy transfer reactions must cycle several times in order that an equilibrium population of ion species be established. Yet another instrumental requirement is that these processes be slow compared to the analysis time of the instrument. This results from the usual assumption that the ions which effuse

from the exit slit of the ion source and are accelerated and mass analyzed constitute a representative distribution of the ions exiting the source at the time of measurement -- that is to say, that ions impinging on the ultimate detector of the mass analyzer are a valid indication of the relative concentrations of species in the ion source.

A paradox results from these opposing requirements. We require that all of these processes take place rapidly in a time which is short compared to the ion source resonance time -- typically of the order of 20 to 50 microseconds in conventional sources at pressures of 1 Torr -- and that these processes be very slow compared to the characteristic time for mass analysis, which is of the order of 10 to 20 microseconds. Obviously, therefore, these requirements are contradictory and cannot be fulfilled over an extended range of experimental parameters.

For this reason we have recently constructed a modified chemical ionization source which somewhat relaxes these experimental requirements. Described in more detail elsewhere (Paper P-10, ASMS Proceedings) it provides an average ion source resonance time of several milliseconds, while the analysis time of the single focusing mass analyzer is a few microseconds. The controlling mechanism for ion loss is diffusion to the walls and out of the ion exit slit of the source. This ion source may also be chilled with liquid nitrogen to a temperature of the order of 100° K and may be heated by means of four integral cartridge heaters to about 800° K. A high degree of differential pumping is provided, along with good thermal isolation of the filament of the electron gun, so that experiments may be carried out over a wide range of experimental parameters. We report in this paper some of the preliminary measurements relating to ion equilibrium which have been carried out with this apparatus.

However, even if a suitable range of experimental parameters -- pressure, concentration, flow rate, accelerating voltage, and the like -- may be found, one does not anticipate that these experiments can be carried out over an extended temperature range. The back reactions of equations (2) and (3) are endothermic and will possess a substantial temperature coefficient. At low temperatures, therefore, the rate of the back reaction will be too slow for a substantial number of cycles during the time that ions are present in the source. If the equilibrium is approached from the left, as will generally be the case, this failure to attain an equilibrium population will be reflected by an apparent equilibrium constant which is too low. Similarly, and curiously, if the temperature is too high the rate of the back reaction will be sufficiently fast that the product ion of equations (2) and (3) will dissociate during mass analysis, and the apparent equilibrium constant will once again be too small (since it is based upon the detected ion current) even though equilibrium may be attained

within the ion source. Thus, we may anticipate that van't Hoff plots which are constructed in order to deduce thermodynamic parameters will have a limited linear range and will deviate below the equilibrium line at both high and low values of $\frac{1}{T}$. Experimental deviations of this sort have been observed in this laboratory and elsewhere, producing an apparent curvature in van't Hoff plots.

Theoretical Formulation of Equilibrium and Rate Expressions

As outlined above, one can anticipate that there will be only a limited range of experimental parameters at most over which one may expect to carry out appropriate measurements relating to thermodynamic equilibrium. In order to sharpen our perspective of the likely ranges over which these parameters may be varied and have deductive significance, we have formulated the rate expressions in terms of current theories of unimolecular and bimolecular reaction kinetics. The rate of the forward reaction is an elementary problem in ion-molecule reactions which requires very little discussion. It is not anticipated that there will be a substantial temperature coefficient for this reaction. Consequently, we may assume that the forward rate constant will be of the order of $1\text{-}3 \times 10^{-9}$ cm^3 mol^{-1} sec^{-1} for typical ion molecule reactions.

In the explicit case of reactions of water vapor we can write the general equilibrium reaction

$$(H_2O)_n H^+ + H_2O \rightleftarrows (H_2O)_{n+1} H^+ \qquad (6)$$

and the experimental equilibrium constant

$$K_p = \frac{I_{(H_2O)_{n+1}H^+}}{I_{(H_2O)_n H^+} P_{H_2O}} \qquad (7)$$

where the subscripted I's represent the ion intensities and P represents the partial pressure of water in the ion source of the spectrometer. The equilibrium constant is related to the forward and reverse rate constants in the usual way

$$K_p = \frac{k_f}{k_b} \qquad (8).$$

In the calculations we have carried out to date we use 1×10^{-9} cc./mol^{-1} sec^{-1} for the rate constant of all of the forward reactions and assume no dependence on temperature. At a water pressure of 1 Torr and standard temperature this corresponds to a pseudo first-order rate constant of 3.5×10^7 sec^{-1}.

The thermal rate constants for the unimolecular dissociation reactions were calculated by averaging the rate constants calculated from the quasi-equilibrium theory of mass spectra (QET) over the Maxwell-Boltzmann energy distribution

$$k_b(T) = \frac{\int_0^\infty \rho(E)\rho^{-E/kT}K(E)\,dE}{\int_0^\infty \rho(e)\rho^{-E/kT}dE} \qquad (9).$$

The equivalence of equation (4) to the usual expression for the thermal rate constant from absolute rate theory was noted many years ago by Marcus.[1] The reasons for using this form for the thermal rate constant are given below in the discussion of ion-equilibrium effects.

The methods used in calculating K(E) from the QET have been described previously.[2] The same Fortran IV subroutines used previously were incorporated into a new main program also written in Fortran IV for calculating the equilibrium constants according to equation (8) and the apparent equilibrium constant according to equation (7). The calculations were carried out on the UNIVAC 1108 Computer at the University of Utah Computing Center

The parameters used to represent the reacting systems are summarized in Table I. The frequencies for the normal OH bond stretching and bending frequencies were taken from experimental values from the water molecule and the moment of inertia for free rotation was taken as that of the water molecule about the symmetry axis. The frequencies corresponding to stretching and bending of H bonds were all taken as 200 cm^{-1}, which is in the range of H-bond frequencies that have been measured.[3]

At low temperatures the equilibrium constant for a reaction such as

$$A_nH^+ + A \underset{\beta_{n+1}}{\overset{k_n}{\rightleftarrows}} A_{n+1}H^+ \qquad (10)$$

may be very large, since at sufficiently low temperatures the thermal rate constant, β, for the back reaction approaches zero. In the limited time available for reaction in the ionization chamber of the mass spectrometer the equilibrium concentration of $A_{n+1}H^+$ may not be attained. As a result the experimentally obtained equilibrium constant, as defined by (7) will be smaller than the true value and will approach assymptotically, as the temperature is lowered, to a constant value. It was shown by Beggs and Field that this type of non-equilibrium effect can account for the curvature in the van't Hoff plot observed for some reactions at low temperatures.[4]

The kinetic equations for a set of reactions such as (10) can be written as

$$\frac{dX_i}{dt} = k'_{i-1}X_{i-1} + \beta_{i+1}X_{i+1} - (\beta_i + k_i)X_i \qquad (11)$$

where X_i is the concentration of A_nH^+, β_i the rate constant for the ith reverse reaction as shown in reaction (10), and $k'_i = k_i[A]$ is the pseudo first order rate constant for the ith forward reaction as

written in (10). For a finite set of such reactions we define $\beta_1 = k_o + k_{n+1} = 0$, where a total of n reactions are considered.

In the present work we have solved the set of equations by numeral integration using the Runge-Kutta method. The integration was carried out using a time increment of 10^{-8} sec. over the range from zero to 10^{-5} seconds. Clusters of up to 10 water molecules were considered in the set of reactions. At high temperatures some of the β_i, may become larger than 10^8 sec^{-1} which for an increment of 10^{-8} in the integration causes the method to break down. Therefore, when this occurred equilibrium was assumed for the reactions for which β was greater than 3×10^7 and the kinetic calculation only considered those reactions for $\beta < 3 \times 10^7$ sec^{-1}.

Results and Discussion

Some typical experimental results are shown in Fig. 1 for the 1-2, 2-3, 3-4, 5-6, and 6-7 equilibria. We show in these figures both experimental points for a variety of experimental data by means of the theoretical considerations which have just been discussed. The straight line to the left in each of the plots represents the true equilibrium constant as defined by eq. (8). The line to the right in each figure represents a calculated curve which takes into account decomposition of the product ions in each of the respective equilibrium reactions during mass analysis. The rate of the back reaction is calculated from the QET using eq. (9). This calculation involves, of course, selecting a value for the minimum energy of the dissociation reaction which is to be identified with ΔH of the equilibrium reaction.

This parameter was arrived at by choosing a reasonable value and carrying out a calculation of the two respective curves which were then compared with the experimental data. Since the experiment involves dissociation of ions after they leave the source, the line representing the calculated correction for this dissociation is to be compared with experimental data rather than the true equilibrium constant line. Iteration with new values of ϵ_0 was carried out until reasonably good fit between the calculated line for the curve including dissociation and the experimental points was obtained.

As may be seen from the figure there is very little dissociation in the 1-2 equilibrium so that the true equilibrium constant line and the one including dissociation essentially coincide. This is consistent with expectations for a highly exothermic forward reaction since negligible dissociation of the product ion occurs over the range of temperatures accessible to experiment. For the higher equilibria which are associated with a lower ΔH there is a broader range of temperature over which dissociation is significant and the correction becomes appreciable.

In Table II we summarize results of these experiments and compare them with results obtained by previous workers. It may be seen that our results for the free energies of reaction at 300° K are intermediate among the results obtained by other workers although they are somewhat closer in numerical value to the results of Kebarle, et. al., than to those of Field, et. al..

We also show in Table III the comparison of ΔH values obtained in this work and those obtained by other researchers. It is noted that disagreement on ΔH is substantially larger than that for ΔG. The main reason for this difference is that we have used a curve fitting technique based upon the QET formulation described above to fit the data. Consequently the true equilibrium line deduced from this procedure may have a substantially different slope from the best straight line which is simply drawn through the experimental points. In effect we have used QET to aid us in estimating an apparatus function which corrects for ion-dissociation during mass analysis.

In continuing this research we will carry out a few more experimental measurements of ion-equilibrium in the H_2O system and will also carry out calculations in which we modify certain of the assumptions made in the model which we have used. We shall also evaluate experimentally as best we can the extent of ion dissociation by measuring intensities of metastable ions in these experiments. In so doing we hope to arrive at a definitive specification of the conditions for carrying equilibrium measurements in the gas phase using high pressure ion sources.

References

1. R. A. Marcus, J. Chem. Phys., 20, 359 (1952).
2. M. L. Vestal, "Ionic Fragmentation Processes", Radiation Chemistry, ed. by P. Ausloos, McGraw-Hill 1968; M. L. Vestal and G. Lerner, Fundamental Studies Relating to the Radiation Chemistry of Small Organic Molecules, Air Force Report ARL 67-0114, January 1967.
3. G. C. Pimentel and A. L. McClellan, The Hydrogen Bond, W. H. Freeman and Company, 1960.
4. D. P. Beggs and F. H. Field, "Reversible Reactions of Gaseous Ions. I. The Methane-Water System," J. Amer. Chem. Soc., 93, 4567 (1971).

Table I. Parameters Used in the Calculations of Rate Constants for Dissociation Reactions

Designation	Frequency (cm^{-1})	Number of Water Molecules 2	3	4	5	6	7	8	9	10
		Number of Degrees of Freedom								
O-H Stretch	3500	4	6	8	10	12	14	16	18	20
O-H Bend	1600	2	3	4	5	6	7	8	9	10
H-Bond	200	8	13	18	24	30	36	41	46	51
Free Rotation	28 (1)	1	2	3	3	3	3	4	5	6

(1) Rotational Energy Constant in cm^{-1}

Table II. $-\Delta G_{300}$ (kcal/mole) for the Reaction

$$H(H_2O)_n^+ + H_2O \rightleftarrows H(H_2O)_{n+1}^+$$

n,n+1	k(1)	B & F(2)	B & F(3)	This Work
1,2	25	7.7	11.2	18
2,3	13.6	9.3	9.7	11
3,4	8.5	8.4	8.6	8
4,5	5.5			4
5,6	3.9			3.5
6,7	2.8			3
7,8	2.2			2.5

Table III. ΔH(kcal/mole) for the Reaction

$$H(H_2O)_n^+ + H_2O \rightleftarrows H(H_2O)_{n+1}^+$$

n,n+1	k(1)	B & F(2)	B & F(3)	This Work
1,2	36	7	16.3	22
2,3	22.3	13	14.8	15
3,4	17	16.8	17.6	12
4,5	15.3			8
5,6	13			7.5
6,7	11.7			7
7,8	10.3			6.5

(1) Kebarle, et.al., JACS 89, 6393 (1967) - Neat Water
(2) Beggs and Field, JACS 93, 4567 (1971) - Methane
(3) Beggs and Field, JACS 93, 1576 (1971) - Propane

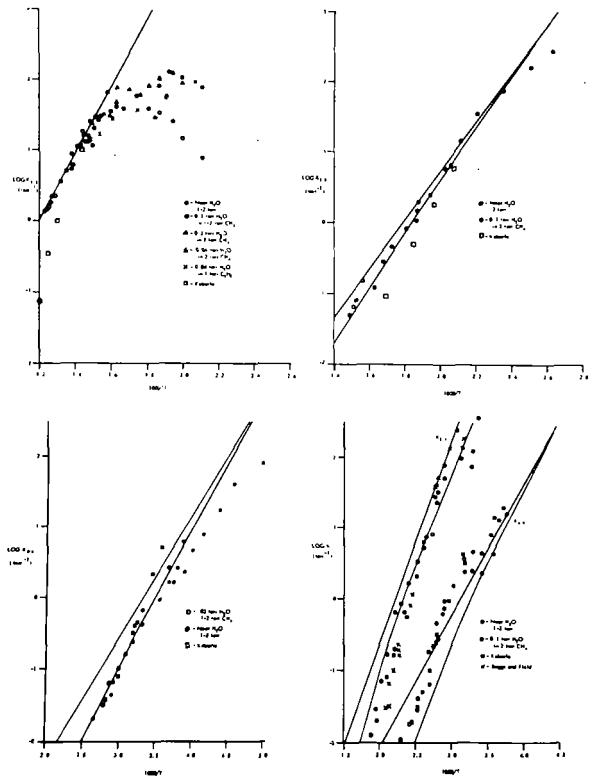

Fig. 1 Van't Hoff plots for the 1-2 (upper left), 2-3 (upper right), 3-4, 4-5 (lower right) and 5-6 (lower left) equilibria according to the reaction $H(H_2O)_n^+ + H_2O \rightleftarrows H(H_2O)_{n+1}^+$

QUANTITATIVE ASPECTS OF CHEMICAL IONIZATION MASS SPECTROMETRY*

G. G. Meisels, C. Chang, and G. J. Sroka
Department of Chemistry
University of Houston
Houston, Texas 77004

ABSTRACT

An evaluation of detection limits in Chemical Ionization and of the application of Chemical Ionization to quantitative analysis of mixtures will be presented. It will be shown that sensitivity is highly dependent on ion source design and on some operating parameters. The use of Chemical Ionization for quantitative analysis requires an evaluation of competition for reactant ions by mixture components, of discrimination resulting from different diffusive properties of the product ions and of preferential interaction of product ions with neutrals. The first of these can be evaluated quantitatively provided that neutral concentration greatly exceeds ion concentration and that the rate constant of primary ion interaction is independent of energy. Under these conditions, a simple correction is possible. The second factor can be obtained empirically if it is assumed to be independent of composition and total sample concentration. The last is minimized when concentrations of unknowns are small.

This investigation was supported in part by the United States Atomic Energy Commission.

* A more detailed account of this work will be submitted for publication in the Journal of the American Chemical Society.

RATE AND EQUILIBRIUM STUDIES AT CHEMICAL IONIZATION CONDITIONS

J. L. Franklin

Department of Chemistry

Rice University

Houston, Texas 77001

ABSTRACT

Studies have been made of a number of ion-molecule reactions at pressures between 0.4 and 1 Torr using the ion source of a Quadrupole mass spectrometer as reactant. The majority of the reactions have involved proton transfer. The technique employed was that of adding small amounts of a secondary reactant to large concentrations of the primary reactant from which a proton was to be transferred. In several studies, especially involving CO_2-methane, CO_2-hydrogen and CO-methane, quite good values for reaction rate constants have been obtained, even when operating at quite high pressures. In several instances where reactions of small exothermicity were involved, proton transfer processes have been shown to attain equilibrium with very consistent values of the equilibrium constant. Since in these reactions the enthropy change would be small, the heat of reaction can be taken as essentially equal to the free energy of the reaction calculated from the equilibrium constant. From such studies the proton affinities of CO_2, water, benzene, toluene, the xylenes, ethane, cyclopropane, furan, phenol and anisole have been determined.

Effects of Chemical Processing on the Thermal Ionization Efficiency of Plutonium

FRANCIS M. ROURKE

and

JACK L. MEWHERTER

Knolls Atomic Power Laboratory

Schenectady, New York 12301

The isotopic analysis of plutonium by surface ionization has generally been performed with microgram or submicrogram amounts of plutonium to limit the activity and toxicity problems associated with the handling of macroamounts of Pu. In recent years many laboratories, particularly those using ion pulse counting, have consistently utilized nanogram amounts of Pu for routine isotopic analysis. Since ^{239}Pu has a specific activity of 140 dpm per nanogram quite often Pu samples of picogram (.14 dpm) quantities have been successfully isotopically analyzed mass spectrometrically in conjunction with the same sample being alpha pulse analyzed. For sample sizes smaller than this it is a still outstanding question whether mass spectrometry or alpha pulse analysis is the better technique to quantitatively detect one tenth of a picogram (10^{-13} gm or .014 dpm) of plutonium.

The first phase of this investigation into the mass spectrometric sensitivity for sub picogram amounts of plutonium consisted in running successively smaller samples of ^{242}Pu, calculating the total number of ^{242}Pu ions which would have been counted while actually measuring the $^{242}Pu/^{241}Pu$ ratio which in our sample was approximately 800. We define the efficiency for a plutonium analysis as the ratio of total Pu ions detected (counted) to total Pu atoms mounted on the filament. The analysis reported in this paper were all made utilizing V-shaped rhenium canoe filaments and were run on the KAPL three-stage mass spectrometer with electron multiplier detectors operated in the ion pulse counting mode.

Table I shows the results of analyzing successively smaller amounts of pure plutonium nitrate aqueously diluted such that at each level of ^{242}Pu approximately 10 microliters of solution were pipetted onto the filament. The efficiency is shown in percent. At the 1 picogram level the isotopic ratio of $^{242}Pu/^{241}Pu$ was still found to be approximately 800 with signal to noise at least 10 to 1.

TABLE 1

1 picogram Pu = 2.5×10^9 atoms

Efficiency of Pu ion Detection For Pure Plutonium Nitrate Solution

Pu sample Size (*picograms*)	Pu Counts/Picogram Pu	Percent Efficiency
1	4×10^6	.16
5	$2.2 \times$ "	.09
10	$.9 \times$ "	.04
100	$1.1 \times$ "	.05
1000	$1.0 \times$ "	.04

Thus it would appear that for total plutonium sample load at the one-picogram level we are successfully measuring the minor isotope three orders of magnitude smaller with another order of magnitude above background. The values shown in the Table are median values of four or five runs at each sample size level, with the range of observed values approximately $\frac{1}{2}$ the values shown to twice the value shown at each level. From these studies we conclude that positive detection and quantitative measurement of 10^{-16} gram of Pu can be obtained with dilute samples of pure plutonium nitrate. We also conclude that for pure plutonium nitrate mounts mass spectrometric sensitivity exceeds that of alpha pulse analysis by two to three orders of magnitude.

Unfortunately there appears to be very little demand for subpicogram analysis of pure plutonium nitrate. In reality we are generally faced with the more practical problem of extracting trace quantities of plutonium, still several picograms, from various matrices and subsequently analyzing the recovered sample for total or isotopic plutonium.

The chemical procedures and reagents utilized to extract and purify trace plutonium from a matrix appear to have a deleterious effect upon the subsequent emission of plutonium ions. In Table II we note the definite decrease in efficiency for merely processing pure plutonium nitrate tracers without even having to recover the plutonium from a massive matrix.

TABLE II

Efficiency of Pu Ion Detection For Processed Plutonium

Sample	Size	Processing	Efficiency (Percent)
^{242}Pu	1.0	None	.10
^{242}Pu	1.0	Hexone-TTA	.001
^{242}Pu	1.0	Hexone-TTA	.007
^{242}Pu	.008	Hexone-TTA	.01
^{242}Pu	.0008	Hexone-TTA	.008
^{242}Pu	1.0	Ether	.007
^{242}Pu	1.0	Stripped Plate	.0008

Obviously any attempt to recover and analyze trace plutonium from a matrix will at least include the above loss of efficiency and quite often even more so. This reduction in efficiency is not in any way related to the chemical yield of recovering the plutonium after processing since alpha pulse analysis performed with ^{236}Pu tracer confirms that the plutonium is indeed in the final solution before mounting either the alpha counting disc or the mass spectrometer filament.

While on occasion 10^{-16} grams of processed plutonium has been barely detected reliable reproducible results at this laboratory generally require 10^{-14} grams of plutonium.

PERFORMANCE OF A SPARK-SOURCE INSTRUMENT WITH IMPROVED CONTROL OF SPARK CONDITIONS AND WITH A DIGITAL RATIO CIRCUIT

L3

T. J. Eskew and A. J. Smith
Nuclide Corporation, State College, Pa. 16801

Since the beginning of spark-source mass spectrometry, it has been known that some form of ratio circuit is essential for electrical detection with the spark; for several years, it has also been known that the spark gap width and position must be closely controlled to obtain reproducible results. As a solution to these problems, we have recently designed a spark gap regulator and a digital integrating ratio circuit. We would like to describe these devices and their performance.

There is a monotonic relationship between the gap width and the peak r-f voltage at the instant of breakdown in each pulse[1]. This voltage can be measured with a capacitive divider and oscilloscope, and can be used as a quantitative index of the gap width. Figure one shows two oscillograms of the voltage during a spark pulse, obtained with such a divider. Note that the voltage builds up to a maximum, and that this maximum is not exceeded at any later instant during the spark.

Colby and Morrison have described a servosystem which regulates the gap width by maintaining a constant peak r-f voltage[2]. We have built a regulator operating on this same principle, but differing from theirs in several details.

Figure two is a block diagram of the regulator. The r-f detector has a short charging time constant, so that its d-c output very quickly reaches a value nearly equal to the peak-to-peak r-f signal from the capacitive divider. The sample-and-hold amplifier is gated by the trigger pulse from the spark generator, so that it "remembers" the d-c voltage during the long interval between pulses. In this way, it is possible to obtain a calibration which is very nearly independent of the pulse repetition frequency.

The d-c output of the sample-and-hold circuit is balanced against a reference voltage set on a ten-turn potentiometer, calibrated in kilovolts. The difference or error signal fluctuates erratically, and is averaged by the integrator which also forms the dominant lag required for a stable feedback loop. The amplified control voltage is applied to a solenoid which is balanced against a spring in such a way that the displacement is roughly linear with respect to the control voltage. The total travel of the solenoid moves one electrode through about one millimeter; this corresponds to a 1/2 mm displacement of the center of the spark, assuming the electrodes burn equally. This is about the largest displacement that can be tolerated without operator intervention.

The sensing electrode is about 12 cm from the anti-corona ring at the r-f end of the coil, and is supported by a type N connector, mounted with an r-f gasket to the inside surface of the amplifier box.

The sensing head is rigidly coupled to the sensing electrode with type N hardware. Thus, the lower end of the capacitive divider is returned to the inside surface of the box through a short, non-inductive path. If an inductive loop should be present in this path, the circuit would respond to the r-f power rather than to the voltage, and its output will not vary monotonicly with the gap width.

A panel meter on the control unit can display either the peak r-f voltage or the output control signal to the solenoid. Both the meter face and the reference-voltage control are directly calibrated in kilovolts, so that direct comparison with other mass spectrometers is possible. A two-position switch selects "set" and "regulate" modes. In the "set" mode, the solenoid position can be adjusted manually, and is normally set near the fully open position. The spark-gap width is set manually at the desired position, and the voltage dial is set to match the meter reading at this position. The switch is then thrown to the "regulate" position, and the circuit will vary the solenoid drive in whatever manner is required to maintain the peak r-f equal to the reference voltage — that is, to maintain a constant spark gap.

A vibration can also be superimposed on the control signal if desired. The vibration is not essential to the operation of the circuit, however.

The use of a voltage-to-frequency converter followed by a counter to measure the time integral of a varying voltage is well known to electrical engineers. This scheme can readily be adapted to measure the ratio of two signals, by using a second converter and counter to determine the time interval during which the first converter and counter perform the integration. Figure three is a block diagram of a ratio circuit built according to this principle. The denominator of the ratio is the integral of the monitor electrometer signal, and is a fixed number of counts from the v-to-f converter: thus, the circuit demands a fixed number of coulombs, just as does the exposure monitor for the photoplate.

The use of a pair of v-to-f converters and counters in this way is not new: it has been described for spark source instruments by Conzemius and Svec[3], by Morrison et al[4], and others, and has often been applied to precision isotope ratio measurements. We believe, however, that this is the first device that has been designed and packaged as a unit especially for spark-source instruments. With modern integrated circuits and v-to-f converter modules, it is a simple matter to fit the entire system behind a 3-1/2" x 19" panel. The converters are linear to better than 0.01%, and their temperature coefficients tend to cancel, since they are mounted alongside each other in an enclosure. The entire power input to the unit is less than 15 watts, most of which is dissipated in the front-panel display and a rear-panel power transistor. No cooling fan is required.

The seven decade counters which tally the numerator are connected to a seven-digit light-emitting diode display. The denominator is selected by a switch, and is 10^7, 10^6, 10^5, or 10^4 counts from the converter. If the monitor electrometer is 10^{-10} ampere full scale and the denominator is 10^5 counts, the denominator will be 10^{-10} ampere-seconds or coulombs. If the meter reading is 1/5 of full scale, the integration will take 5 seconds.

The circuit is designed to operate with a peak stepper and printer. At the end of each integration period, a pulse is produced which serves as the print command and also causes the peak stepper to advance to the next peak. The delay time is set as required to allow the magnet and electrometer to settle on the next peak.

The displayed ratio can be related to the actual ratio of ion currents in a simple way, as illustrated in Figure four.

The signal path to the numerator includes the multiplier of gain G, an electrometer whose feedback resistor is R_1, a range switch calibrated in volts full scale, and an inverter whose gain is precisely -1. For the denominator, the monitor intercepts a fraction X of the beam, and there is a similar electrometer and range switch. In practice, only the factors K_1 and G are changed during an analysis.

The time constants of the electrometers must be nearly equal, so that the error between them is small compared to the integration time. In the experiments described here, R_1 and R_2 were 10^{10} ohm. The time constants were about 10 milliseconds, and the integration times were always 2 seconds or more.

Table one shows the results of repeated readings of the Sn^{120} peak in a Zircalloy sample (NBS reference material #1213) containing 1.76% of Sn. The ratio circuit was set for a 1 full-scale-second denominator; the monitor was $3\ 10^{-10}$ ampere full scale, so that the collected charge was 3×10^{-10} coulomb. The monitor current fluctuated between 1/5 and 1/3 of full scale, so that the actual integration time was 3 to 5 seconds. The gap width is measured in volts, with 16,000 volts being a "typical" gap of about 150 microns. It can be seen that the changes produced by adjusting the gap width and electrode position are large compared with the standard deviations of each set of readings at fixed conditions. The regulator circuit can maintain a constant gap width, but one must depend on the operator's technique to position the electrodes in a reproducible manner. Conzemius and Svec[3] report a standard deviation of .5 to 2% for means of 10 readings at 10 seconds each in a different

sample.

Table two shows the readings for the isotopes of Sn, normalized to 100%. The slits were set for a resolution of about 1000, so that interfering peaks were not resolved.

Each result is the mean of 5 readings, taken with an integrating time of about 4 seconds. The 5 readings were taken "all at once" for each mass, in the order listed. This is clearly the wrong way to measure isotope ratios, but the similarity to the actual ratios of Sn may be taken as an indication of the stability of the instrument. During the measurement of mass 118, it was noted that the solenoid was at the limit of its range; the gap was reset and recentered manually. Note that the readings down to this point are low, and thereafter are high.

Table three shows the isotope ratios of Pb, obtained by cycling through the three major Pb isotopes in sequence with the peak stepper. Five cycles were made for each of these gap settings. The integration time was as before – about 4 seconds – and thus the sample consumption during the analysis is about the same as for the Sn.

Again, the ratios vary widely as the gap is changed, but not in a simple manner. The resolution was about 1000 – not adequate to separate the doublets that can be seen on the photoplate at a resolution above 3000. We do not know the identity of the interfering peaks, but it would appear that they respond in a different way than Pb to changes in the gap width.

To conclude: A precision ratio circuit which incorporates the best features of previously described systems can be built as a single compact unit at modest cost. The spark-gap regulator is essential for precise measurements using electrical detection, but is only part of the answer, since the operator must still intervene to control the centering and position of the spark.

We would like to acknowledge the assistance of Mr. Joseph Mannaerts of the Nuclide instrument testing department who operated the spectrograph while these tests were made.

References

1. T. J. Eskew, Paper presented at the 16th Conf. on M.S., Pittsburgh, Pennsylvania, May 1968.

2. B. N. Colby and G. H. Morrison, Anal. Chem. 44, 1263 (1972).

3. R. J. Conzemius and H. J. Svec, Talanta 16, 365 (1969).

4. G. H. Morrison, B. N. Colby and J. R. Roth, Anal. Chem. 44, 1203 (1972).

Table I. Sn^{120} in Zircalloy (N.B.S.#1213)

Gap Width	Ratiometer Reading	Relative S.D.
9,600 volts	2.958	6.6%
16,000	2.115	4.6%
24,000	1.734	1.5%
Electrodes moved back about two mm, and recentered for maximum beam:		
24,000	1.860	4.65%
Electrodes repositioned to spark fresh surfaces:		
16,000	1.795	3.0%

Table II. Isotopes of Sn in N. B. S. #1213 Zircalloy

Mass	% Of Nat. Sn	measured ± S.D. (means of 5 readings)
112	.96	.88 .027
114	.66	.58 .012
115	.35	.30 .0081
116	14.30	13.29 .143
117	7.61	7.07 .075
118	24.03	23.80 3.14 (gap shifted out of range)
119	8.58	10.04 .23
120	32.85	33.43 .66
122	4.92	4.90 .074
124	5.94	6.22 .014

Table III. Isotopes of Pb in N. B. S. #1213 Zircalloy

Gap	206/208 ± S.D.	207/208 ± S. D.
9,000 volts	.583 ± .047	.448 ± .025
16,000	.452 ± .052	.401 ± .040
24,000	.502 ± .047	.421 ± .030
Ratios for natural Pb:	.451	.432

PUBS 1266-0672

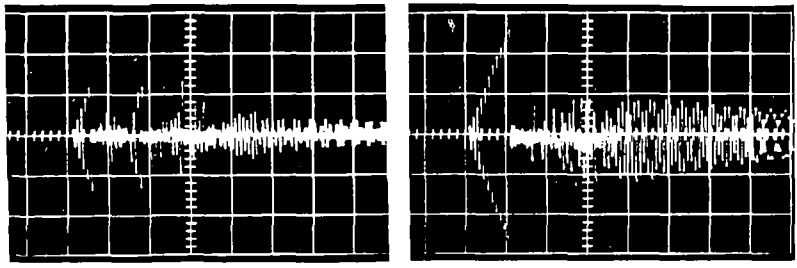

10.8 kV/cm
75 μm gap

10.8 kV/cm
300 μm gap

Fig. 1.

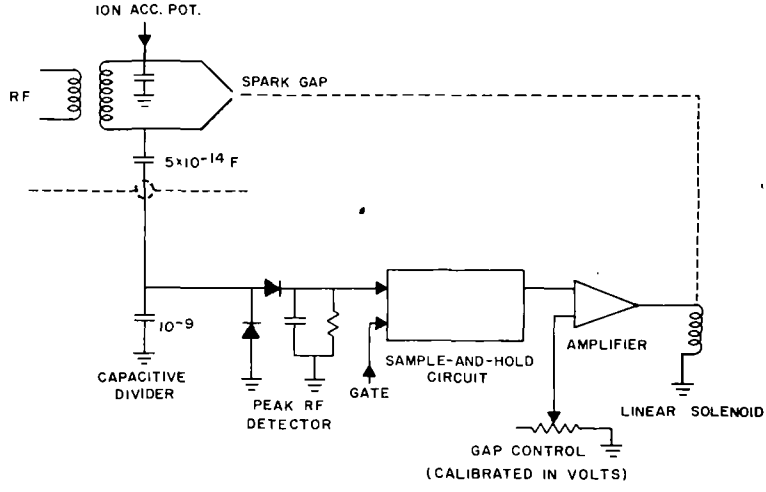

Fig. 2. Spark Gap Regulator

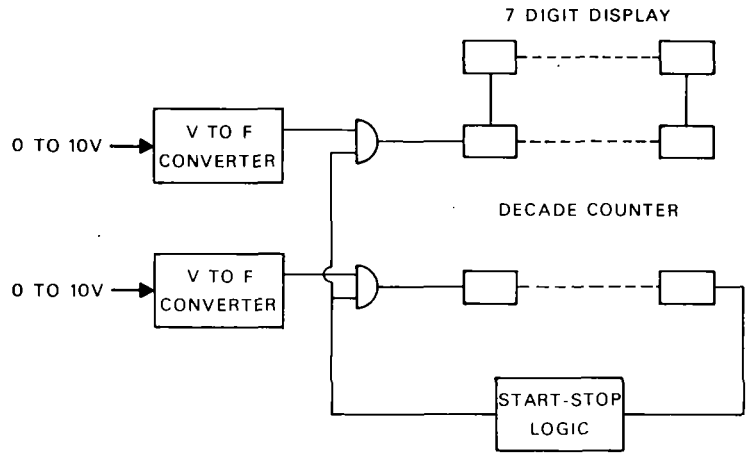

Fig. 3. Integrating Ratiometer

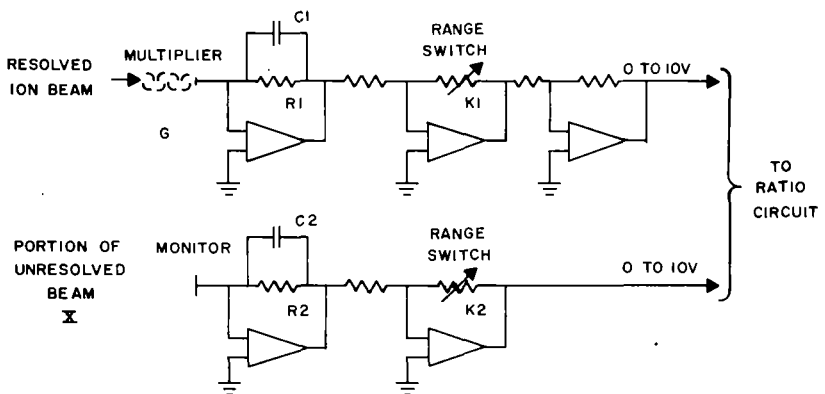

$$\text{ION-CURRENT RATIO} = \frac{X}{G} \times \frac{R_2}{R_1} \times \frac{K_1}{K_2} \times \text{RATIOMETER READING}$$

Fig. 4. Scale Factors

AUTOMATIC CONTROL OF THE ION ILLUMINATION ANGLE IN A SPARK SOURCE MASS SPECTROMETER

L4

R. J. Conzemius and H. J. Svec

Ames Laboratory-USAEC and Department of Chemistry

Iowa State University, Ames, Iowa 50010

At the 1969 ASMS meeting a means of automatically adjusting a spark gap width was described by Bingham, Powers and Wolstenholme. This was a very useful development, especially for relieving the task of maintaining the spark manually. However a disadvantage of relying only upon this means of electrode control is that it is indifferent to the ion optical system. The development described here utilizes feedback from the ion optical system as well as the spark gap voltage for maintaining an optimum spark gap. A complete description will be published in Talanta.

A schematic view of the Z-axis of a double focussing ion optical system was shown. The aperatures in the field-free region located between the magnetic and electrostatic analysers are of particular interest. The first aperature consists of separate upper and lower plates which intercept that portion of the beam due to extreme values of Z-angular divergence. These plates are followed by a total beam monitor, the magnetic field, a slit which further limits the beam in the Z direction, and the electrical ion detector at the image. Z-focusing effects due to the fringe fields of the magnetic field will be ignored for the purpose of this presentation. Consider the upper spark sample electrode to be stationary. Concentrate your attention on two items. First, consider a X-axis movement of the lower spark electrode relative to the opposing upper electrode. What effect would this movement have on the ion currents impinging on the upper and lower Z-limiting plates? Second, what effect will the movement have on the ion current reaching the ion detector at the image?

The answers to these two questions were given by showing two plots. A plot of the ion current ratio of the upper to the lower Z-limit plates as a function of relative movement of the lower spark electrode indicated a monotonic change in the ratio as the lower electrode is moved along the X-axis. Thus the center of density of the beam moves along the Z-axis. This effect was called the ion illumination angle. The ion illumination angle setting was the point chosen where the ratio is maintained. A plot of the ion current reaching the ion detector at the image showed a definite broad maximum with sharp decreases at either extreme of the ion illumination angle settings. Thus electrical signals are available for feedback to an electromechanical system for automatic adjustment of the electrode on the X-axis. The ion illumination angle setting can be held at any preset ratio of ion signals to the upper and lower Z-limiting plates. A schematic of the mechanical system was shown. The spark sample is attached inside the vacuum where movement of one ten thousandth of an inch can be controlled simultaneously along both the X and the Z axes. When this was done, the system was shown to maintain a high and steady ion current at the image of the instrument.

Reproducibility of measurements is a greater concern than simply maintaining a high and constant instrument sensitivity. Reproducibility involves the ratio of the signal at the optical image to that at the total beam monitor. A definite dependence of the ratio upon the angle setting (especially for low settings) was shown.

Data was shown to indicate how well isotopic abundance measurements could be made with simultaneous automatic angle and gap control. The data was obtained with a Dy metal sample with faraday cup collection in the following manner. Each isotope signal was measured as a ratio of image signal to total beam monitor signal for three consecutive readings. Each reading took approximately 10 seconds. After the seven isotopes were all read, each set of three readings were averaged and summed. Each averaged isotopic signal was then divided by the total and an isotopic abundance obtained. This experiment was repeated three times. Thus, three abundance determinations were made. The average of these

three abundance measurements was shown along with the average deviation and the relative average deviation.

Deviations ranged from 0.2 to 1.9 percent. The measured values agreed well with abundances reported in the literature.

Another series of measurements of the relative abundances of the minor isotopes, Dy-156, 158, and 160 were shown. The measurements were based upon 21 readings. Seven sets of three readings each were made in the series 160, 158, and 156 etc. This resulted in six interpolated isotopic ratio measurements. The average, standard deviation, and percent standard deviation of these six determinations were shown along with reported values for natural abundances. An electron multiplier was used for the mass resolved ion current. Operational amplifiers were employed for further amplification. Relative standard deviations of 0.4 and 0.9 percent were observed for the 160/158 and 156/158 isotopic ratios respectively. A brief review was presented. An ion illumination angle as indicated by ion current signals on the extreme Z-divergence plates is a monotonic function of the relative X-axis position of the sparking electrodes. Automatic angle control can be thereby effected simultaneously with automatic spark gap width control. This dual control improves signal stability, long term sensitivity, and reproducibility. The system described does not automatically adjust the Z-axis position of the spark due to erosion of the upper electrode causing the spark to move on the Z-axis although the ion illumination angle is maintained. Maintenance of the upper electrode position in order to keep the spark exactly on one spot of the Z-axis is on our agenda for future development.

Some possible limitations were noted. The use of the concept described may be limited, altered, or impossible in instruments with different focusing parameters, longer object or image distances, with spark samples of very irregular shape, or with very narrow gap widths. However the effect noted here should be present in all spark source instruments. The degree to which the effect contributes to reproducibility should at least be checked and then provisions made for control if warranted.

We would like to acknowledge the help of our technician, Mr. Clarence Ness who operates the spectrograph. It is a happy occasion to be reporting on a contribution which greatly simplifies the task of instrument operation.

A Comparative Study of the Species Produced By the rf Spark and Ion Bombardment

C. A. Evans, B. N. Colby and J. B. Woodhouse
Materials Research Laboratory
University of Illinois, Urbana, Illinois 61801

Secondary ion mass analysis is a rapidly growing technique for the microcharacterization of a wide variety of materials. As the applications of this technique increase, each spark source mass spectroscopist becomes a potential user of secondary ion mass spectrometry. The purpose of this paper is to provide information to these potential users on the ion species produced by ion bombardment, some of the commonly encountered spectral interferences, and the various instrumental operating modes available to the analyst for the reduction of these spectral interferences.

A comparison of the rf spark and ion bombardment produced spectra reveals several obvious features:

a) The rf spark produces many more multiply charged species than ion bombardment. The +1 to +2 ratios are on the order of 3-10 for the rf spark and 100-1000 for ion bombardment. The spark produces multiply charged species up to +6 to +10 while ion bombardment produces very low abundant +3 and negligible amounts of the higher charged states.

b) Ion bombardment produces a high population of polymeric ions while the rf spark produced polymers which are several orders of magnitude less intense.

Thus one can anticipate a higher incidence of high mass interferences due to polymeric species and lower incidence of low mass inferences from the ion bombardment process when compared to rf spark excitation.

Even though there is a high probability of spectral interference in secondary ion mass analysis, there are several instrumental operating modes available which can reduce or remove spectral interferences.

a) Although most of the polymeric ions are due to the matrix or sample components themselves, occassionally the analyst encounters polymer ions which result from reaction of the sample elements and the bombarding gas ion. Thus changing from oxygen to nitrogen primary ions can shift an interference pattern due to the primary ion by two mass units as well as possibly decrease the interfering ion intensity. The use of

argon or other inert gas ions can even remove a potentially harmful interference completely.

b) The yields of both elemental and polymeric ions can change by orders of magnitude when one examines the negative spectrum rather than the commonly used positive spectrum. Thus the analyst can dramatically improve signal-to-interference ratios by judicious choice of the spectral polarity and the chemical nature of the primary ions (this can also dramatically influence ion yields).

c) There are innumerable spectral interferences which will defy the use of the above operating modes. Thus the analyst turns to the classic mass spectroscopic method to reduce interference, higher spectral resolution. Recent investigations employing ion probes on high resolution mass spectrometers have shown that the use of resolutions exceeding $\frac{M}{\Delta M} = 1000$ can be extremely important in many analyses. One can resolve hydrocarbon interferences, simple metal hydride interferences (as encountered when analyzing P in Si, Mn in Fe, As in Ga, etc.) and the more general intra- and interelement polymers from the elemental ions.

A detailed discussion of the above study is in preparation and will be submitted for publication.

This work was supported in part by the Advanced Research Projects Agency under Contract HC 15-67-C-0221 and by the U. S. Atomic Energy Commission under Contract AT(11-1)-1198.

The Use of Scandium Metal Targets for Tuning an Ion Microprobe Mass Analyzer for Thin Film Studies*

J. W. Guthrie and R. S. Blewer

Sandia Laboratories, Albuquerque, New Mexico 87115

For thin film studies where the film depth of interest may be small compared to the diameter of the microprobe primary beam, it may be essential that the sputter crater formed on the sample be uniform in depth so that the sputtered ions in the secondary beam will represent a well defined level in the film. One means of accomplishing this with an Ion Microprobe Mass Analyzer[1,2] is to use a fixed primary beam (normal to the sample surface) and maintain a uniform (non-Gaussian) current density in a circular spot. Deviations will cause an enhanced rate of sputtering where the primary beam is most intense and result in an undesirable crater of uneven depth.

The optical sensitivity (distinct color changes) of scandium thin film targets to 20 keV N_2^+ and O_2^+ ions has been used[3] to observe and record the position, shape, size and current density uniformity of the primary sputtering beam during the beam tuning process (adjustments of beam-optics focus controls). In addition to the range of color shades[4] produced (with N_2^+ for example) at the film surface as a function of beam exposure, color changes also occur in the sputter crater as it proceeds through a scandium oxide layer (several hundred angstroms thick) at the film-substrate interface. For a 20 keV N_2^+ beam the crater (as observed through a microscope during sputtering) changes from a blue color in the scandium to a bright yellow in the scandium oxide and then changes to a gray color at the sapphire substrate. The uniformity of observable color changes is sensitive to the depth uniformity. A typical procedure is to tune the beam using the color changes observed on the surface then allow the beam to sputter through to the substrate for observations near the interface.

The settings of the electrostatic lenses in the primary beam system which produce the best results (uniform craters) have been obtained for a beam whose focal point (cross-over) lies below the sample surface. This condition exists if a slight increase in the objective lens voltage results in a spot of smaller size.

When using the scandium tuning sample and the tuning procedures discussed above, craters with uniform depth profiles[5] have been produced for beam diameters ranging from 50-300 μm, which for beam currents normally used result in convenient sputtering rates for analyzing a variety of thin metal films. For example a 70 μm diameter crater 7500 Å deep (using a 12 Å/sec sputtering rate) in an erbium metal thin film was shown to have a crater bottom flatness uncertainty of less than ± 130 Å.

A scandium target sample is also useful for tuning the beam to small diameters of a few micrometers for use with rastering techniques to produce craters for thin film depth studies.

*This work was supported by the U.S. Atomic Energy Commission.

References

1. Manufactured by Applied Research Laboratories, Sunland, California
2. H. Liebl, J. Mass Spectrom. Ion Phys. 6(1971) 401
3. J. W. Guthrie and R. S. Blewer, Rev. Sci. Intrs. 43 (1972) 654
4. Note: A color version of Figure 2 in Reference 3 is attached to reprints.
5. R. S. Blewer and J. W. Guthrie (to be published in Surface Science)

Ion Probe Mass Spectrometric Analysis of Bubbles in Doped Tungsten Wire

Edgar Berkey and William M. Hickam
Westinghouse Research Laboratories
Pittsburgh, Pennsylvania 15235

1. INTRODUCTION

1.1 Doped Tungsten

The production of tungsten filaments for incandescent lamps is accomplished by a powder metallurgy process involving the doping of WO_3 powder with potassium silicate and aluminum chloride. The blended powders are then hydrogen reduced and sintered at high temperature to form dense ingots from which filament wire is eventually drawn. The chemical reactions occurring during this sequence of events leave the final wire doped with species that impart exceptional high temperature creep resistance to the material. This desirable property is thought to arise from the presence of submicroscopic (<1μm) bubbles in the metal which are formed by the high temperature volatilization of one of the doping species.

1.2 Analysis of Bubbles

The identity of the bubble-forming species has never been experimentally established. This paper summarizes briefly the results obtained from applying both the Cameca and Applied Research Laboratories' ion probe mass spectrometers to determine the chemical composition and physical extent of the condensed material in the bubbles. Since the total amount of such material is only $\sim 10^{-16}$ g in bubbles nominally sized at about 0.1μm diameter, this study not only confirms the high sensitivity of the instruments for certain elements but also establishes their ability to analyze submicron sized inclusions. A more complete presentation of the results from this work will be submitted to Analytical Chemistry.

2. EXPERIMENTAL PROCEDURE

The analyses were performed on the fracture surface of a normally produced tungsten wire that had been previously heated near its melting point to agglomerate bubbles along grain boundaries and thereby simplifying the formation of a mechanically-induced low temperature fracture.

Previous analytical work on the wire had demonstrated the loss of both Si and Al in the final material compared with the initial doped powder. K was observed to be retained, but the final chemical form of this element was in doubt. Either K metal, K_2O, or KOH were possible species having a high enough vapor pressure to be the cause of bubble formation. Consequently, the analytical problem centered around determining the presence or absence of these species in the bubbles.

The analyses with the CAMECA IMS 300 Ion Analyzer were performed with a sputtering rate of approximately 50 Å/sec using both O_2^+ and Ar^+ bombardment. Ion count data were taken on K^+, O^+, O^-, and H^- at the fracture surface and, after substantial sputtering, also within the matrix. A 10μm analytical aperture was employed which restricted the data recording to a circular region of this diameter, thus enabling the analysis of individual bubbles to be performed. Ion images of pertinent species were also recorded.

Work with the ARL Ion Microprobe Mass Analyzer (IMMA) was limited to the generation of successive K^+ ion images as a function of depth over a distance of ~20Å in a single bubble on the fracture surface.

3. RESULTS

With the high sputtering rate employed by the Cameca instrument, the K^+ ion images showed a rapidly changing pattern in real time, indicating that the element was, indeed, segregated into small discrete volumes corresponding to the bubbles. From the sputtering rate and the speed with which

individual K^+ flashes were observed in the 220μm diameter viewing area, the thickness of the K-rich layer on the surface of the bubbles was estimated to be <50Å. Viewing of the O^+ and H^+ images with both O_2^+ and Ar^+ primary beams revealed no correlation with the K^+ images, nor was there a correlation with the O^- image under Ar^+ bombardment. These results, then, represent a direct experimental indication that the K is present in the bubbles in elemental form and not as either an oxide or a hydroxide.

A series of seven K^+ ion images taken using the IMMA within a total sputtered depth of 20Å on a single bubble on the fracture face showed that the thickness of the K layer in the bubbles is in the range of 15-20Å.

Further confirmation of the chemical identity of the K was obtained from the ion count results, and these are summarized in Fig. 1. As indicated by the spikes in the K^+ profiles, use of the 10μm aperture permitted the detection of material from individual bubbles in the 10^{-16} - 10^{-17} g range. The absence of similar spikes in the O^+ profile under Ar^+ bombardment and in the H^+ profile under O_2^+ bombardment are in accord with the presence of K metal in the bubbles.

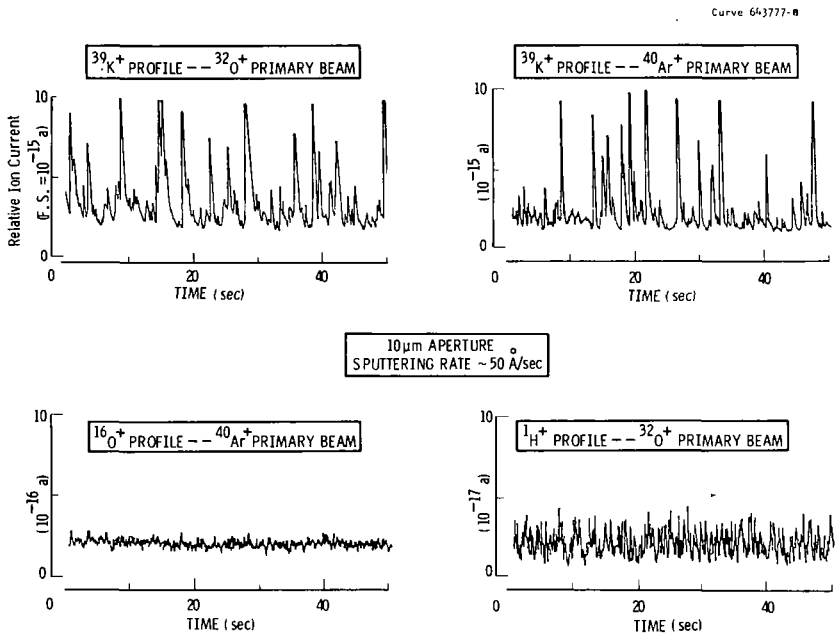

Fig. 1 — K, O, and H profiles from fracture face of doped tungsten wire using the CAMECA ion analyzer

ION SCATTERING SPECTROMETRY OF NON-CONDUCTORS

William L. Harrington and Richard E. Honig
RCA Laboratories
Princeton, New Jersey 08540

We have used Ion Scattering Spectrometry (ISS) to examine several non-metals which include both insulators and semi-conductors. We would like to discuss the application of this technique to depth profiles, to stress, where possible, quantitative relationships, and to point out some problem areas which we have encountered in this relatively new technique.

Figure 1 schematically shows the ion scattering process. A primary beam of rare gas ions is focused on the sample and scattered by surface atoms in elastic, binary collisions. At a scattering angle of 90 degrees the fraction of the primary energy that remains with the scattered rare gas ion is expressed by the following relation,

$$E1/Eo = (M2 - M1)/(M2 + M1)$$

where M1 is the mass of the primary ion and M2 is the mass of the surface atom. By measurement of the scattered ion energy, E1, the mass of the surface atom can be deduced. From this equation, one can also see that only those surface atoms with a mass greater than that of the primary ion can be detected.

In principle, the surface concentration of a given species can be derived from the area under its response peak, provided that its scattering cross section, neutralization factor, and surface geometry are taken into account. The scattering cross section can be computed; it is a function of scattering angle, θ, initial primary energy, Eo, and atomic numbers Z1 and Z2 of the particles involved in the collision. However, since at this time there exists no adequate theory to predict the neutralization factor, and surface geometry may not be known, calibration samples of known composition must be used to obtain absolute concentrations from peak areas or maximum peak heights.

The 3M version of an ion scattering spectrometer is diagrammed in Figure 2. The details of this instrument have been described previously by Goff and Smith (1). Typical operating conditions for the present experiments were 1500 eV primary energy, 10 μA/square cm current density, and a focussed beam about 1 mm in diameter. The sample holder, mounted at 45 degrees to the incoming beam, can contain 6 separate samples each of which can be analyzed at 7-9 reproducible locations, the elliptical spot size on the sample being about 1 x 1.5 mm. The scattered ion energy is measured by a 127 degree sector electrostatic analyzer, and the analyzed ions are detected with a channel electron multiplier operating in a pulse counting mode.

A feature of primary interest for the analysis of non-conductors is a charge neutralization system which controls a tungsten filament located near the bombarded sample. Electrons emitted from this filament prevent positive charge build-up, thus keeping the target surface at a fixed potential near ground. Having experience with sputtering or secondary ion mass analysis, one can appreciate the problems associated with insulators, semi-conductors, and especially layered materials whose conductivity changes with depth. Unless the sample is a good conductor, ion bombardment will change its surface potential and thus affect primary beam density, primary beam energy, sputtering rates, secondary ion yields, and focussing fields which alter instrumental transmission --- all of which greatly affect signal intensities. With the relatively small current densities employed in the ion scattering spectrometer, the charge neutralization filament is effective in keeping the sample surface potential constant, with the result that scattered ion peaks fall at the predicted energies and signal intensity variations truly represent changes in sample composition.

Typical spectra obtained with scattered He ions are illustrated in Figure 3. The sample is an alkali strontium silicate glass which was specially treated to move mobile ions from the surface into the bulk. The intensity axis is expressed as counts per second, and the abscissa shows E1/Eo, the ratio of scattered to initial primary ion energy. The top spectrum shows the glass before treatment with peaks labeled for the major components. In order to more clearly define the response depicted here, the concentration of the glass species in atomic per cent is as follows: O - 60.1, Na - 5.3, Si - 24.5, K - 4.7, Sr - 2.3. The lower spectrum represents the treated glass at about 10 - 20 angstroms below the original surface. Notice that the mobile ions are almost absent, with only Si and O remaining. Depth profiles obtained from a series of such spectra taken at successively sputtered depths are shown in Figure 4. In this particular sample, some mobile ions remain on the surface but in amounts greatly reduced from bulk values. Sr, the largest and least mobile cation, exhibits a sharp interface with a pile-up of ions at about 500 angstroms. This pile-up and gradual decrease is a reproducible effect and is not influenced by surface charging because of the charge neutralization system. At the depth examined the Sr level had not yet returned to its bulk level of about 210 c/s. The small, highly mobile Na ion was shown to move great

distances into the glass and at this depth exhibited only a slow increase back to its bulk level of about 125 c/s. K is an intermediate case with its bulk level being about 250 c/s. Several other features of these profiles are worth mentioning. First, notice the initial low response for all elements including Si and O. Adsorbed species such as hydrogen, carbon monoxide, water, and hydrocarbons must first be sputtered away by the primary beam to expose the true surface. Next, notice the compensation effect exhibited by O and Si during the first 150 angstroms. Because we are looking at a constant sample volume --- i.e., a constant area one monolayer deep --- the sum of the weighted signals (weighted by scattering cross sections and other factors) is a constant. Thus, where oxygen appears in excess, being left uncombined and unshielded by the leaving mobile cations, the Si exhibits a decrease in true surface concentration. Finally, the O/Si intensity ratio in a glass or in other forms of silicon dioxide is a measure of stoichiometry. The observed ratio in Figure 4 and in many similar glasses and also in pure silicon dioxide is certainly not 2:1. If, however, the observed intensities are weighted by their scattering cross sections at 1500 eV energy as determined from extensive data by Bingham(2), the O/Si ratio is 2.0 within experimental error and noise limitations. Data from R. Goff of 3M on aluminum oxide (3), when corrected in the same manner, also yield the correct O/Al ratio. In both of these cases, the two major components apparently show no differences in primary ion neutralization.

Figure 5 illustrates depth profiles for a thin Si film (about 0.2-0.4 μm) vapor deposited on an insulating substrate. Until the film was sputtered away, no charge neutralization was needed; but when charging was noted, use of the electron emitting filament allowed measurements to continue with no apparent effects on signal intensity. Careful observation of such charge-up could even be used to locate conductor-insulator interfaces. The expanded depth axis portion of this figure shows the presence of an oxide layer on the Si film which extends quite some distance into the supposedly pure Si film. Notice also that the presence of a species such as oxygen has no enhancing effect on other elements, as is the case with secondary ion mass analysis.

The question "How quantitative is ion scattering spectrometry?" has no simple answer. We would like to present an example which provides extremely useful information about a surface, but points to problems in quantitation. Figure 6 shows the He ion scattering response for CdSe. It has long been known that such compounds exhibit polar faces in properly oriented single crystals; and Smith, Strehlow, and Goff (1,4) have shown that ISS can distinguish between the faces of such crystals. Thus, the example that is presented in Figure 6 shows extreme sensitivity to surface structure --- useful, but difficult to quantitate where subtle orientation effects may alter response. Notice also the large Cd/Se ratios --- greater than unity even for the Se face. It has been pointed out by Smith that such ratios change with primary beam energy, presumably due to differential neutralization effects. Thus, we have the added complication of neutralization as well as the influence of crystal orientation. Effects of surface structure are certainly no problem when they are expected or even the point of interest, but unexpected orientation effects can greatly complicate quantitation.

Finally, let us continue with CdSe to show an example of primary beam charge transfer. Figure 7 shows the spectrum obtained with 1500 eV Ar ions scattering from CdSe. In addition to the predicted peaks of Se and Cd, there are two other peaks which have shown up in every sample of CdSe examined --- from differently oriented single crystals to randomly oriented deposited films. The peak at E1/Eo = 0.66 falls in the mass location of 190-195, and the fourth peak is located at a point where no atomic species exist. D. Smith has suggested that these peaks are due to doubly-ionized Ar ions striking a surface atom and being scattered as singly-ionized Ar. Such charge transfer peaks fall at exactly twice the energy ratio expected for the singly-ionized, no neutralization event. Although such additions to a spectrum are predictable when doubly-ionized ions are generated in the source, they may mask small concentrations of higher mass elements of interest.

In this brief report we have shown ISS to be a powerful tool for the analysis of true surfaces, especially in-depth studies of non-metals. We have observed that the presence of certain reactive species such as oxygen does not affect the basic sensitivity of other surface atoms. We have also pointed out some problems which hopefully will be solved by future work.

---

(1) R.F. Goff and D.P. Smith, J. Vac. Sci. Technol. 7, 1-5, (1970).
(2) F.W. Bingham, "Tabulation of Atomic Scattering Parameters Calculated from a Screened Coulomb Potential", SC-RR-66-506, TID-4500 Physics, Sandia Corp., August, 1966; see also, J. Chem. Phys. 46, 2003-2004 (1967).
(3) R.F. Goff, J. Vac. Sci. Technol. (to be published).
(4) W.H. Strehlow and D.P. Smith, Appl. Phys. Letters 13, 34-35 (1968).

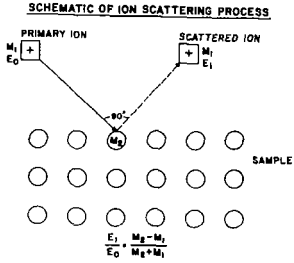

Figure 1. Schematic and equation of ion scattering process at 90°

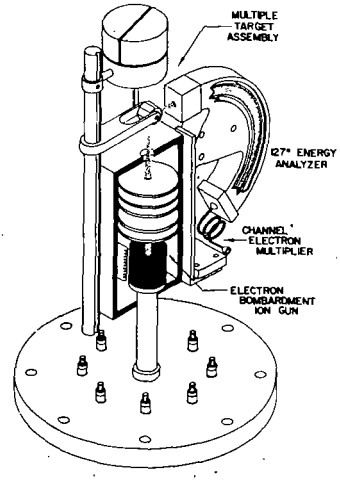

Figure 2. Diagram of 3M ion scattering spectrometer

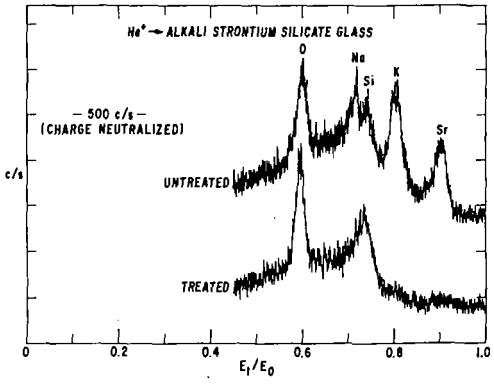

Figure 3. ISS spectra of 1500 eV He^+ ions scattered from alkali strontium silicate glass

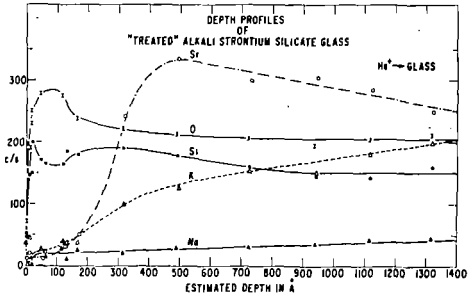

Figure 4. Depth profiles of "treated" alkali strontium silicate glass

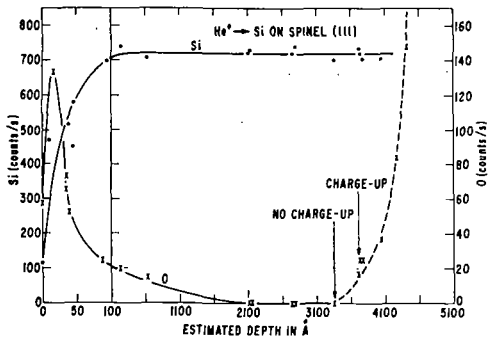

Figure 5. Depth profiles of silicon film on spinel substrate

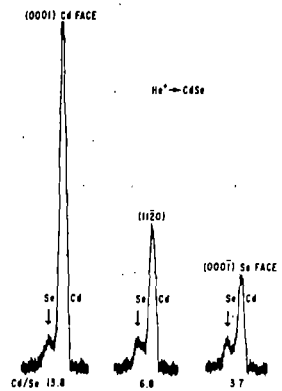

Figure 6. ISS spectra for three orientations of CdSe

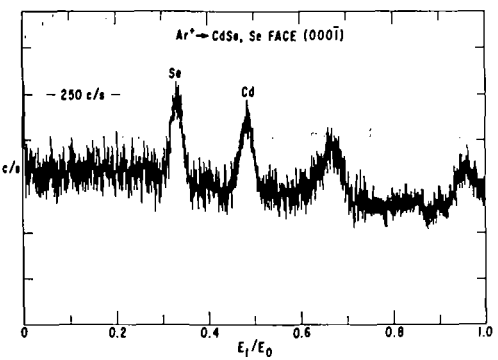

Figure 7. ISS spectrum showing charge transfer peaks of Ar^+ scattered from CdSe

THE GAS CHROMATOGRAPHIC - MASS SPECTROMETRIC IDENTIFICATION OF ORGANIC COMPOUNDS IN METEORITES

J.G. Lawless, C. Boynton, F.C. Tarbox and M. Romiez

Exobiology Division, Ames Research Center

NASA, Moffett Field, Calif. 94035

The initial finding of both protein and nonprotein amino acids with nearly equal abundances of D and L isomers of individual amino acids in the Murchison meteorite extracts has been substantiated by continued investigations of this meteorite. In addition to the 18 amino acids originally identified by GC-MS, there are at least 17 others present. These 17 are tentatively identified only by their mass spectral fragmentation patterns. The tentatively identified compounds appear to consist of a wide variety of polyfunctional, cyclic, and linear amino acids. The concentration of the 35 individual amino acids positively and tentatively identified appears to decrease as the number of carbon atoms in the molecule increases.

In an effort to understand the mode of occurrence of the amino acids, the sample was extracted with D_2O and the N-trifluoracetyl-D-2-butyl esters were prepared. The samples were examined by GC-MS and no deuterium incorporation was noted in any of the amino acids present. This is convincing evidence that the carbon-hydrogen bond is not synthesized during this extraction, nor are the amino acids racemized in this step.

This work has been submitted to Geochim. Cosmochim. Acta for publication.

APPLICATION OF A MOLECULAR BEAM SOURCE MASS SPECTROMETER TO THE STUDY OF REACTIVE FLUORIDES

by

M. J. Vasile, G. R. Jones*, and W. E. Falconer
Bell Laboratories
Murray Hill, New Jersey 07974

ABSTRACT

A molecular beam-mass spectrometer has been designed and constructed to study reactive fluorides and related molecules. This study is concerned with the association in saturated vapors of inorganic pentafluorides. The transmission of the quadrupole mass filter was calibrated to acquire the relative abundances of ions over the wide mass range needed. Contributions to the higher cluster ions from ion-molecule reactions in the ion source or from isentropic expansion at the molecular beam source have been shown to be improbable in the systems studied. The pentafluorides of Nb, Ta, Mo, Re, Os, Ir, Ru, Rh, Pt, Sb, and Bi were all found to be associated in the gas phase. Dimeric and trimeric ions were most readily detected, and tetrameric ions were found for NbF_5, MoF_5, IrF_5, RuF_5, RhF_5, and SbF_5. The extent of association of the neutral species is difficult to ascertain quantitatively because of the fragmentation caused by electron impact ionization. A full report of these studies has been submitted to the International Journal of Mass Spectrometry and Ion Physics.

*Present address: Royal Radar Establishment, Malvern, England.

Flow Programming in Combined GC/MS with Molecular Effusion Type Separators*†

M1

M. A. Grayson, R. L. Levy, and C. J. Wolf

McDonnell Douglas Research Laboratories

McDonnell Douglas Corp., St. Louis, Mo. 63166

Flow programmed gas chromatography (FPGC) has the same overall effect as programmed temperature gas chromatography (PTGC), i.e., it shortens the time required to achieve the separation of a mixture. However, FPGC has several advantages of particular importance in combined GC/MS. For example: a) labile compounds which decompose during a PTGC analysis can be eluted with FPGC; b) less "column bleed" is observed during FPGC; and c) at the end of the analysis the GC column can be rapidly returned to its initial condition. Despite these inherent advantages, apparently FPGC has not been used in combined GC/MS. We have investigated two experimental arrangements for performing FPGC/MS with molecular effusion separators. In one case, the separator is indirectly connected to the column in such a manner that the operating pressure in the separator is independent of the carrier gas flow rate. In the second case, the separator is directly connected to the column so that the operating pressure in the separator increases during FPGC. Both of these arrangements will be discussed in detail.

*This research was conducted under the McDonnell Douglas Independent Research and Development Program.

†To be submitted for publication in Analytical Chemistry.

DESCRIPTION OF A GC/MS QUADRUPOLE INSTRUMENT UTILIZING A CHEMICAL IONIZATION SOURCE AND NO ENRICHING DEVICE

M2

Michael S. Story

Finnigan Corporation, Sunnyvale, California

Through the persistent efforts of the pioneers in chemical ionization, the method is now widely recognized as one of the most useful techniques in mass spectrometry. The many advantages in ease of mass spectral interpretation have been pointed out by many. The combination of chemical ionization with quadrupole GC/MS makes this technique even more useful.

If in conventional gas chromatograph-electron impact mass spectrometry (GC-EIMS) a gas chromatograph is connected directly to a mass spectrometer the much heralded problems of gas flow incompatability are soon encountered. Even though the "art" of enriching devices is a purchasable one there seems to be no "perfect" separator.

It would be desirable to bring the effluent from the gas chromatograph straight into the M.S. without an enriching device. There are severe limitations to employing this technique with GC-EIMS. If the spectrometer has a single pump and a maximum operating pressure of 1×10^{-5} Torr (magnetic deflection) or 1×10^{-4} Torr (quadrupole) in the analyzer region, one needs about 1000 liters/second (magnetic deflection) or 100 liters/second (quadrupole) pumping capability for every atmos-cm^3/min (N_2) of carrier gas. For a GC flow of 20 atmos-cm^3/min a spectrometer would require very large pumps and the result would be very high cost.

Clearly, a differential pumping technique is necessary. If a vacuum baffle is put between the ionizer and analyzer region, these pumping requirements to handle the gas flow can be reduced by a factor of ten or so. However, a typical electron impact ion source with a conductance of 2 liters/sec would have an internal pressure of 0.1 Torr at 20 atmos-cm^3/min. This pressure is clearly too high for electron impact and fragmentation patterns would be seriously altered due to ion molecule reactions.

If, however, the source is intentionally "closed" and a carrier gas for the GC used that is suitable as a reagent gas one has the ideal elements for a gas chromatograph-chemical ionization mass spectrometer (GC-CIMS). It is still necessary to maintain the external vacuum housing of the source at 1.5×10^{-4} Torr which requires at least a 600 liters/sec diffusion pump. In order to be generally useful a gas tight access must be provided for probe samples that will allow the probe and a reagent gas to enter the source coaxially. Such a source and system is shown in Figure I.

A standard Finnigan 1015 GC/MS system is retrofitted with a vacuum baffle, CI elbow and source, 1200 liter/sec diffusion pump and 300 liter/min mechanical forepump. In addition, a controller for source gas and source pressure readout is provided. The interface is a metal 1/8" OD transfer line with a Precision Sampling micro capillary shut off valve to isolate the MS during column change and allows all of the GC effluent to go directly into the mass spectrometer.

Typical pressures and flows for operation with methane are:

Source pressure (T.C. gauge)	1 Torr
Ion source housing	5×10^{-4} Torr
Analyzer housing pressure	4×10^{-5} Torr
Gas flow (calibrated)	18 ml/min

The ion source pressure is measured by a thermocouple type (NRC 801) vacuum gauge. The vacuum chamber pressures were measured with a Bayard-Alpert ionization gauge. All pressure measurements were reported with no correction of the gauge sensitivity for methane. The gas flow was measured by a Matheson Model No.LF100 mass flow meter calibrated for methane.

A system/150 data system was then connected to the GC-CIMS and the resulting system tested with a mixture of parathion, dieldrin and p,p'DDT. A mixture of ten nanograms each was injected on a 5' x .080", 3% OV-1 100/120 mesh Supelcoport glass column and temperature programmed from 170° C at 6°/min. The carrier/reactant gas was methane and the flow was 20 ml/min.

Figure 2 is the resulting reconstructed gas chromatogram (RGC). Figures 3, 4 and 5 are the mass spectra taken at the time of maximum sample concentration in the source.

Figure 3 (Spectra # 84) shows excellent CI behaviour for parathion with the m+1 and the adduct ions as the only peaks in the spectrum. The signal to noise ratio is excellent.

Figure 4 (Spectra # 124) for dieldrin shows much fragmentation and almost limiting signal to noise ratio at the parent ion.

Figure 5 (Spectra # 159) for p,p'DDT has a more intense molecular ion plus one than dieldrin but loses HCl and chlorobenzene. This is quite different than the EI spectrum as reported by Siphon and Damico [1]. The m/e = 85 is the m - 1^+ ion for hexane which was used as the solvent for the mixture. The signal to noise ratio for the molecular ion is somewhat better than that for dieldrin.

The mixture illustrates the variability in ionization and its dependence on the chemistry of the samples and reagent gas.

Acknowledgement

The author would like to acknowledge the able assistance of Robert Squires of Finnigan Corporation in the design and building of the system.

Reference

1. J.A.Siphon, J.N. Damico, Organic Mass Spectrometry 3, 51 (1970)

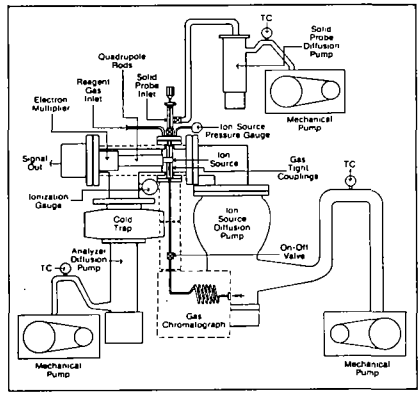
TC
Solid Probe Diffusion Pump
Quadrupole Rods
Reagent Gas Inlet
Solid Probe Inlet
Electron Multiplier
Ion Source Pressure Gauge
Mechanical Pump
Signal Out
Ion Source
Gas Tight Couplings
TC
Ionization Gauge
Cold Trap
Ion Source Diffusion Pump
On-Off Valve
Analyzer Diffusion Pump
TC
Gas Chromatograph
Mechanical Pump
Mechanical Pump

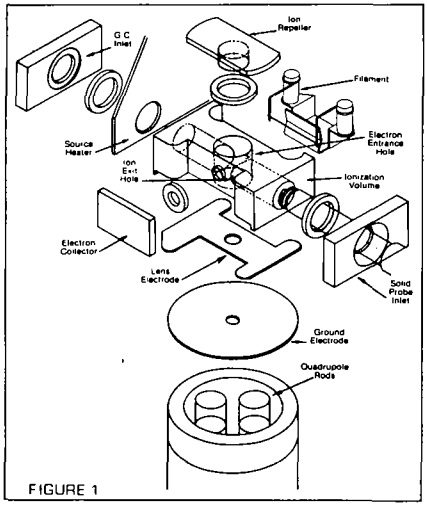
Ion Repeller
G C Inlet
Filament
Source Heater
Electron Entrance Hole
Ion Exit Hole
Ionization Volume
Electron Collector
Lens Electrode
Solid Probe Inlet
Ground Electrode
Quadrupole Rods

FIGURE 1

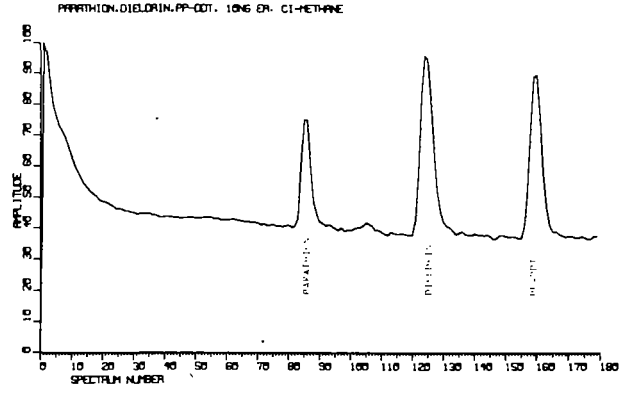

Figure 2. Reconstructed Gas Chromatogram

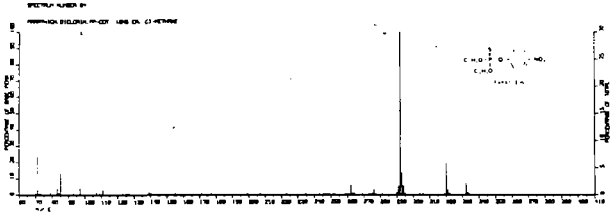

Figure 3. Parathion (Spectra 84)

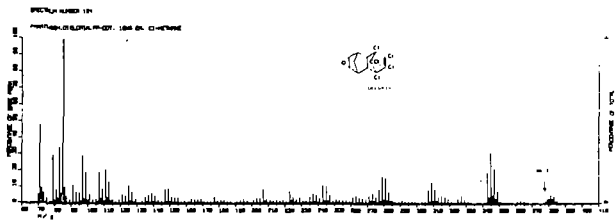

Figure 4. Dieldrin (Spectra 124)

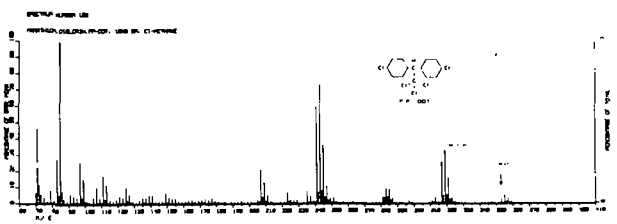

Figure 5. p,p'DDT (Spectra 159)

Some Recent Developments in Quadrupole Mass Spectrometry Instrumentation

J. P. Carrico and R. K. Mueller
Bendix Research Laboratories
Southfield, Michigan 48076

Several factors responsible for limiting the performance of the quadrupole mass spectrometer have been under investigation in this laboratory. These factors include the loss of sensitivity caused by fringing field effects experienced by ions entering and exiting from the field, the adverse effects of geometrical inaccuracies on resolution and sensitivity, and a constraint on the stability property of the oscillating field. This stability constraint may be responsible for peak tailing and for a fundamental limit to the dynamic range of the apparatus. These factors are discussed and efforts to reduce or eliminate their effects on performance described. These efforts include new electrode configurations and new construction techniques and materials.

Several papers describing the details of this work are being prepared for publication.

ION ENTRANCE APERTURE MASKING OF A QUADRUPOLE MASS FILTER

M4

N. IEROKOMOS

PERKIN-ELMER AEROSPACE DIVISION

ABSTRACT

A technique of masking the exit aperture of an ion source used with a quadrupole mass filter is described in this paper. This technique of masking the quadrupole entrance eliminates the penetrating unstable ions which normally appear as tails on either side of a mass peak. Experimental results indicate that by masking, over two decades reduction in tails can be attained.

INTRODUCTION

The requirement for this NASA contract was to develop a flight quadrupole which would operate over the mass range of m/e 1 to 44. It also required the quadrupole to operate with flat topped peaks, and a resolution higher than 1/50. A dynamic range of 10^6 was also required so that low intensity peaks could be monitored.

To achieve the above requirements, the tails found on either side of the mass peaks had to be greatly reduced so that the contribution of adjacent peaks is minimized. To decrease the tails, the number of unstable ions which penetrate the length of the quadrupole must be decreased. Once the geometry of the quadrupole mass filter is fixed, an economical means of decreasing the penetrating unstables was not available prior to the development of the masking technique.

MASKING TECHNIQUE

In order to decrease the penetrating unstable ion component of the signal, considerable theoretical and computer analyses were conducted. The analyses indicated that most penetrating unstable ions are ions which have small initial angles and amplitudes. In the computer programs the amplitude and angle parameters were defined as:

$$\eta = \frac{Y_o}{r_o}$$

and

$$\gamma = \sqrt{\frac{V_I}{V_{ac}}} \sin \alpha$$

where:

Y_o is the initial entry amplitude

$2r_o$ is the quadrupole rod spacing

V_I is the initial ion energy

V_{ac} is the RF potential

α is the initial entry angle to the quadrupole axis.

The computer calculated the trajectories of the unstable ions as they traversed the quadrupole length. A typical plot of the trajectories is shown in Figure 1. In this figure, the ordinant indicates the length of the quadrupole normalized for ions of mass 50, ten volt energy and 1.5 megacycles of frequency. The abscissa is the amplitude normalized to r_o. The angles shown on the graph are the phase of the RF at the time of entrance of a given ion.

From this graph note that the ions which have attained the smallest amplitude at the end of the quadrupole are ions with small values of η and ions with entrance phase of 0 and 180°. Similarly, analysis of transverse energy (γ) indicates that ions with a low γ value are extremely penetrating. From the computer trajectories, plotting the

amplitude of the unstable ions as a function of entry phase was possible. Figure 2 shows the amplitude reached by ions of $\eta = 0.005$ and $\eta = 0.025$ at the end of the quadrupole. This figure is segmented in three regions. Region I is where η value ions, up to and including the maximum detectable, penetrate the quadrupole under any and all initial phases. Region II is a region which allows only some phases to traverse the length of the quadrupole without impacting the rods. Region III defines a region where ions impact the rods and are eliminated. From Figure 2, drawing two rather obvious conclusions is possible. One is that there will always be some ions contributing to the tails. These ions are associated with two phase bandwidths centered around 7 and 176 degrees where the amplitudes cross the Z-Axis. The second conclusion is that if all ions with η values up to the maximum detectable or higher for a given quadrupole were eliminated, the unstable ion intensity can be reduced much faster than the reduction of the stable ion intensity.

Elimination of ions with low η values was accomplished by placing wires (mask) at the ion source exit in both the X and Y-Axis as shown in Figure 3. The thickness of the wires determine the value of η which is masked. Experimentally, a wire thickness of 0.005 inch ($\eta = 0.0125$) was tried with the results shown in Figure 4.

Figure 4 shows the m/e 28 peak without a mask and with the wire cross of 0.005 inch. Note that the tails were reduced dramatically without degradation of the peak top. This figure is a logarithmic scan with normalized peak intensities by increasing the nitrogen pressure in the vacuum system. Having shown that a reduction of tails was possible with the masking technique, the ideal size wires were calculated for both X and Y-Axes. The wire diameter for the Y-Axis was calculated at just over 0.003 inch. That of the X-Axis slightly below 0.003 inch. A three mill cross was thus placed on the ion source exit and logarithmic scans of the required mass range were made. Two typical scans are shown in Figure 5. These scans show a dynamic range of approximately 10^6, better than unit resolution with flat topped peaks. A dynamic range of over 10^6 and a resolution of over 1000 was achieved (separate runs) by this flight quadrupole with six inch rods.

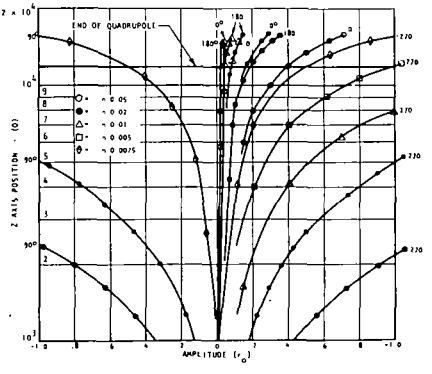

Figure 1. Ion Trajectories for Various η Values

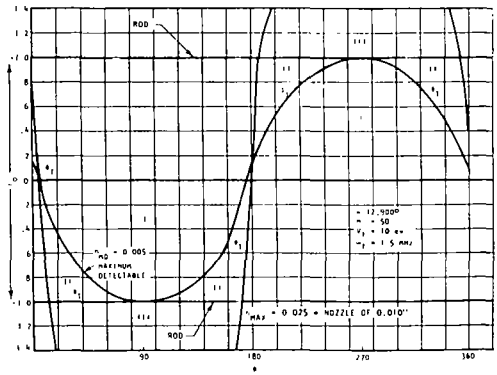

Figure 2. Unstable Ion Transmission, $\Delta q = 20\%$, $\gamma = 0$

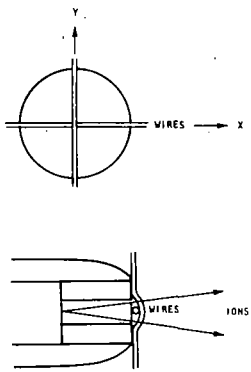

Figure 3. Masking of Source Exit Aperture

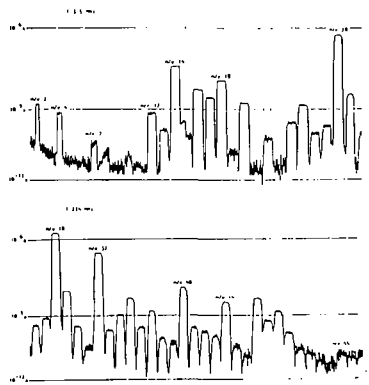

Figure 5. Typical Logarithmic Scan Mass m/e 2 - 55

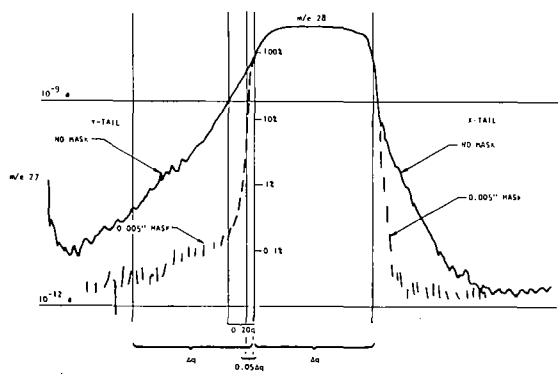

Figure 4. Results of Masking m/e 28

A NEW APPROACH TO THE IMPLEMENTATION OF A DELAYED-DC-RAMP QUADRUPOLE MASS FILTER

W. M. Brubaker
Analog Technology Corporation
Pasadena, California 91107

The "delayed-dc-ramp" mode of operating a quadrupole mass filter permits the passage of ions through the fringe field region at the filter entrance without accompanying momentum impulses which direct them toward the (negative) y-rods. The improvement in the performance of the instrument which results from the use of the delayed dc ramp is well documented.[1],[2]

Previously reported methods of obtaining a delayed-dc-ramp capability use rods with insulated segments at the ion entrance ends. These segments are energized by the same ac potentials as the respective rods, and with zero dc potentials. While this type of construction is quite effective in providing the delayed dc ramp, it is costly to implement. Further, a means must be provided for applying the ac potentials to the insulated rod segments.

The new approach to the implementation of the delayed dc ramp uses conventional, one-piece rods. The delayed-dc-ramp electrodes become tabs which are attached to the ion source. One tab electrode is placed adjacent to each rod, and is energized with a dc potential which has a polarity opposite that of the associated rod. The role of the opposing potential is to neutralize, in the vicinity of the entrance aperture, the influence of the dc potential on the rod. This is accomplished without shielding the region from the ac potentials of the rods.

The use of small tabs on the ion source, spaced symmetrically with the rods and energized by dc potentials only, leads to a structure which is simpler and easier to construct than that of the prior art, which requires insulated segments on the rod ends.

A small quadrupole for breath analysis was assembled. The instrument radius is 0.19 cm, and the length of the hyperbolic rods is 5.08 cm. Tabs attached to the ion source provide the delayed-dc-ramp capability. The influence of the delayed dc ramp on the shape of the mass peaks is shown in the accompanying spectrum of the 15 and 16 peaks of methane. In the conventional mode, the tabs are at ground potential. When they are appropriately energized with dc potentials, the sides of the peaks become much steeper, providing broader tops without changing the width of the peaks near their bottoms. The broad tops are essential for the breath-analyzer use, as the spectrum is skip-scanned to fixed excitation levels.

The xenon spectrum depicts the resolving power of this instrument when operated in the delayed-dc-ramp mode. The peak ac potential applied to a rod pair during the scan of the xenon spectrum was about 500 volts. Thus, the instrument was operating at a low power level.

---

[1] Wilson M. Brubaker, "An Improved Quadrupole Mass Analyzer," Advances in Mass Spectrometry, Volume 4 (1967).

[2] W. Arnold, "The Influence of Segmented Rods and Their Alignment on the Performance of a Quadrupole Mass Filter," 17th Annual Conference on Mass Spectrometry and Allied Topics, May 1969.

4-VOLT IONS

A. CONVENTIONAL B. DELAYED DC RAMP

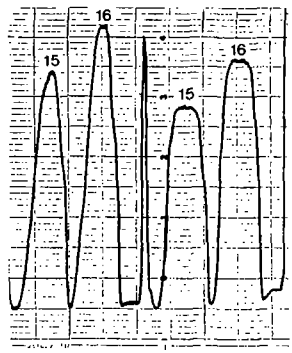

METHANE SPECTRA PRODUCED BY
2-INCH QUADRUPOLE (7-28-71)

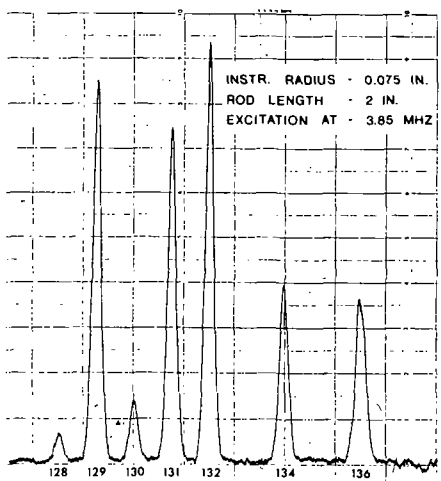

XENON SPECTRA PRODUCED BY
2-INCH QUADRUPOLE (12-29-71)

A MINIATURIZED, AUTOMATED QUADRUPOLE BREATH ANALYZER* FOR USE BY AN ASTRONAUT

M6

W. M. Brubaker and J. H. Marshall
Analog Technology Corporation
Pasadena, California 91107

The quadrupole breath analyzer is designed in miniature, so that the entire vacuum system, including the quadrupole mass filter and the ion pumps, would fit under an astronaut's chin, inside his helmet. Breath gas for mass analysis is admitted from the atmosphere directly into the high-vacuum region through a magnetostrictively-operated needle-valve leak of very small dimensions.

The preliminary work on this project[1] was described at the 18th conference.[2] That work demonstrated the feasibility of such a miniature system, and forms the basis for the present development. Continued work has resulted in a number of refinements, particularly in the development of a magnetostrictively-operated actuator for the needle-valve leak, and in the design and assembly of electronic components of superior stability and performance.

A quadrupole mass filter with rods 5.08-cm long and an instrument radius of 0.190 cm has been assembled for this application. The rods have hyperbolic contours of extreme precision, and they have been meticulously assembled to provide a high-performance mass analyzer. This mass analyzer separates breath-gas ions produced in a miniature ion source connected to the inlet leak. Those ions passing through the quadrupole strike a faraday-cup collector, the current from which provides the output signal. Two miniature diode ion pumps remove the residual gas from the vacuum system.

The electronic system, using mostly digital techniques, skip-scans the rod excitation voltages to those values corresponding to CO_2, N_2, O_2, and H_2O. A low-noise current-to-frequency converter measures the charge produced by the ions from each of these gases and generates both digital and analog outputs yielding directly the relative concentration of each gas. A feedback loop controls the inlet leak to keep the total ion current constant, independently of changes in sensitivity, atmospheric pressure, or properties of the leak. This entire scan cycle, including a period for automatically zeroing the current-to-frequency converter and its electrometer preamplifier, requires about 7.5 ms. This interval is short compared to the 50-ms response time constant of the inlet system. No electron multiplier is necessary.

In order to obtain stable outputs for each breath component, the peaks must have broad tops and the excitation voltages and frequency must not change. Thus, we incorporated the new approach to the implementation of the delayed dc ramp as described in the preceding paper showing "flat-topped" methane peaks.[3] In addition, a quartz crystal determines the excitation frequency with a stability of ±0.005% for temperatures between 0°C and 50°C, and a precision rectification and feedback scheme reduces amplitude drifts to ±0.04% over this same range. As a result, the quadrupole transmission efficiency for each breath gas remains constant for periods of time approaching a year without adjustment.

Early experiments with the ion source with an enclosed pure-rhenium filament revealed a severe attrition of the oxygen peaks. A study of the mass spectra on the admission of air samples indicated that the hot rhenium surface catalyzes the oxidation of hydrogen to form water. A combination of two approaches essentially alleviated this difficulty. First, the filament temperature was substantially reduced by the use of a rhenium filament coated with lanthanum boride.[4] Second, the tight ion-source enclosure was replaced by an open one, and the sensitivity of the source to the incoming breath gas was enhanced relative to the oxygen-deficient residual gas in the vacuum system by introducing the breath gas through a small tube on the axis of the source.

The ion-source sensitivity, the noise levels in this fast-scanning mass spectrometer, and the speed of the miniature ion pumps require a gas flow rate through the inlet leak of 10^{-7} to 10^{-6} torr-ℓ/s. Figure 1 shows that this leak rate is consistent with the properties of the inlet valve.

The power dissipated with 4 V applied to the coil producing the magnetostrictive motion is 0.64 W. This power is comparable to the maximum excitation power of 0.8 W and the filament power, including the losses in the emission regulator, of 1.0 W.

Because the relative flow rate between the various breath gases is most stable and predictable when the leak is molecular, we designed the inlet leak for molecular flow. In order to ascertain whether molecular flow was in fact achieved, we measured the flow of helium through the wide-open leak as a function of the pressure of the helium atmosphere in which the leak was immersed. The results of this experiment, shown in Figure 2, clearly indicate that the leak rate is proportional to pressure within the accuracy (±10%) of the helium leak detector, and thus molecular flow has been achieved.

*This work supported in part by MSC under Contracts NAS9-11307 and NAS9-12765 monitored by Dr. John Rummel.

[1]W. M. Brubaker, Final Report; Contract No. NAS9-8371, Astronaut Breath Analyzer, July, 1969.

[2]W. M. Brubaker, "Miniature Breath Analyzer to be Worn Inside Astronaut's Helmet," 18th Annual Conference on Mass Spectrometry and Allied Topics, June, 1970.

[3]W. M. Brubaker, "A New Approach to the Implementation of a Delayed-DC-Ramp Quadrupole Mass Filter," 20th Annual Conference on Mass Spectrometry and Allied Topics, June, 1972.

[4]Supplied by Dr. David Lichtman, University of Wisconsin, Milwaukee.

Figure 1. Leak Rate as Function of Applied Voltage

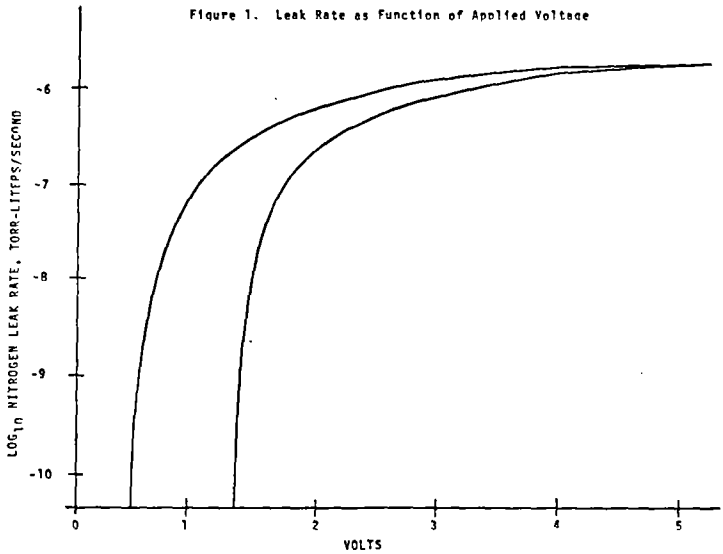

Figure 2. Leak Rate vs Inlet Pressure

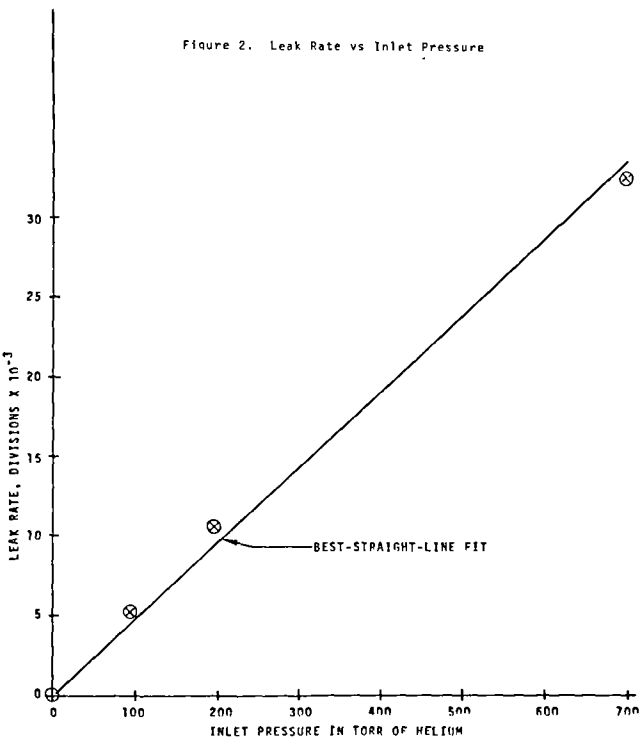

REAL TIME COMPOSITION MONITORING OF A HIGH VELOCITY MOLECULAR BEAM USING A QUADRUPOLE MASS ANALYZER

M7

W. S. Chamberlin,
Martin Marietta Corporation
Denver, Colorado 80201

J. B. French and N. M. Reid
Institute for Aerospace Studies
University of Toronto
Ontario, Canada

The use of a quadrupole mass analyzer for the real time composition and in-flight density monitoring of a high velocity molecular beam was part of the entry simulation testing of a miniature magnetic mass spectrometer for planetary exploration. This work was sponsored under project Viking by the Langley Research Center of the National Aeronautics and Space Administration and was the combined effort of the University of Toronto Institute for Aerospace Studies, The University of Minnesota, and the Martin Marietta Corporation, Denver Division.

To determine the feasibility of measuring the chemical composition of the upper atmosphere of the planet Mars from 10^{-10} to 10^{-4} Mb and with a vehicle velocity of 4.5 kM/sec, a series of entry simulation tests were performed in the high velocity molecular beam facility of the UTIAS. These tests were to determine (1) the effect of entry angle of attack on the instrument's sensitivity to CO_2 and 0, (2) the effect of the ion source cavity surface material on the recombination of 0, and (3) the possibility of dissociation of CO_2 on impact. Professor Nier, of the University of Minnesota who is Chairman of the NASA entry science team, not only collaborated with us in this work but also furnished us with an instrument for these tests which was essentially a prototype of the one to be flown on project Viking.

Nozzle molecular beam techniques were used to generate the high velocity stream of neutral gas molecules. A beam 1 cm in diameter was sufficient to fully illuminate the ion source entrance of the test instrument. All beams used a minimum of 90% helium as the carrier gas to lower the mean molecular weight in the source and hence increase the beam velocities. Velocities were measured by the metastable time of flight method developed at UTIAS.

For all beams, except for atomic oxygen, the source was a zirconium oxide tube with the small orifice in one end heated externally with a spiral molybdenum heater. The atomic oxygen beam was produced from 0_2, H_e and A_r by a 60 watt microwave discharge in a quartz source tube. The $0/0_2$ ratio was optimized by the addition of small quantities of H_20 vapor to the gas mixture.

The in-flight beam composition was measured by allowing the beam to pass axially through an Extranuclear quadrupole mass spectrometer (QMS) fitted with a coaxial high intensity ion source. The standard QMS was modified by the addition of a 5/8" length to the quadrupole rods to which the AC potential only was supplied. This was done so that the instrument could be operated in a "delayed DC ramp mode" which has been shown to give flat-topped peaks and hence improved accuracy by Brubaker[1]. This effect was observed with this instrument and all mass spectra were taken in this mode, however, the main advantage of this mode of operation appeared to be in the reduction of high-mass discrimination which was apparent when the instrument was operated in the normal mode. An off-axis electron multiplier was used to collect the ion signal which was amplified and displayed by conventional means.

During calibration, we found that the cracking pattern of the stagnated (thermalised) beam CO_2 differed from that of the fly-through beam CO_2. To explain this phenomenon consider that in an ideal isentropic expansion process, temperatures of the internal degrees of freedom vary identically with the translational temperature as the energy in all the degrees of freedom is converted into directed motion. If a relaxation time is defined as the time taken to eliminate a temperature difference between any particular degree of freedom and the translational temperature, then isentropic expansion implies that the expansion rate is so slow that the

time required for the gas to pass from one translational temperature to another is much longer than the local relaxation time for any degree of freedom.

However, in the high-pressure-ratio small-scale free jets used in molecular beam work, it is entirely possible to have conditions such that, particularly in the latter stages of the expansion, relaxation times exceed that of the significant translatory temperature change, in which case the rate at which energy flows out of the vibrational or rotational modes decreases and finally ceases as the local relaxation time becomes larger as the gas continues to expand. One speaks of energy 'frozen' in a particular mode, and it is found that the vibrational mode freezes first, then rotation, and finally even translation. From this point on, the gas continues to expand as $1/r^2$ but at a fixed Mach number.

Now, if we consider the process of ionization in a mass spectrometer fly-through ion source, of such a beam where the rotational and vibrational energy has been 'frozen' in relaxed states it can be shown that the 'cracking pattern' of a polyatomic molecule such as CO_2 gives some indication of the extent of vibrational relaxation which has occurred. This is due to the fact that in polyatomic molecules an increase in internal energy results in an increased fraction of the molecules being in configurations which permit excitation to energy levels above dissociation limits of the states of the molecule-ion. This results in a larger fraction of the molecule-ions produced by electron impact dissociation, and thus the parent ion forms a smaller fraction of the total ion current. This behaviour has been reported for other molecules[2].

We would, therefore, expect that the parent-daughter ratios of CO_2 observed in such a beam would be (a) higher than for CO_2 'thermalized' to the normal ion source wall temperature due to the effect of the expansion process, and that (b) these ratios would be independent of beam source temperature and thus beam velocity due to this 'freezing' phenomenon. This is in fact what was observed.

The technique employed to calibrate the QMS for in-flight density of various gases was to use a dynamic leak system in which input and output conductances were known and the input pressure measured on the MKS Barton capacitance manometer. An accurately known mixture of gases was held at a known pressure (measured by the Baratron pressure gauge) behind a thin-walled orifice of known cross-section, and from calculations using gas laws, the ion current response (allowing for multiplier gain) for each molecular species both statically and dynamically was obtained.

In order to calibrate the QMS for beam molecules it was realized that the beam should be reduced in diameter below that of the ion source aperture so that all of the mass flow could be detected by the QMS. A flag was used upstream of the QMS ion source to 'thermalize' the beam molecules so that a static calibration could also be carried out in this mode. It was assumed that all detectable ions were formed only in the ion source region and were produced and extracted homogeneously across this region. However, it was found that ion currents from the QMS were slightly higher for the stagnated (flagged beam) than for the same beam passing through the QMS where the only ions formed were on or near the axis.

One possible explanation is offered in light of some recent work of G. T. Skinner[3]. His work with a Brink ionizer showed that under certain conditions the bulging equipotentials from the focussing electrodes both into the ion source and into the QMS gave preference to ions formed off axis and that those formed on or very near the axis (within the beam) could be forced outside the acceptance cone of the QMS. In conclusion, it has been shown that a modified QMS is a very satisfactory means of monitoring a high velocity molecular beam. We plan to submit an extended version of this paper to the Review of Scientific Instruments.

REFERENCES

1. W.M. Brubaker and W.S. Chamberlin, Recent Developments in Mass Spectroscopy, University Park Press, pp. 98-103 (Invited paper, International Conference on Mass Spectroscopy, Kyoto, 1969).
2. R.E. Fox and J.A. Hipple, J. Chem. Phys., 15, 208, 1947.
3. G.T. Skinner. 'Transient Response of a Mass Spectrometer With a Brink Ionizer'. Final Report Contract No.F44620-71-C-0050, CAL No. RM-362-A-1, April 1972.

A COMPUTER-CONTROLLED ION-COUNTING MASS SPECTROMETER SYSTEM FOR RATIO MEASUREMENTS

M8

D. A. Schoeller, J. M. Hayes, C. A. MacPherson, R. F. Blakely, and W. G. Meinschein

Departments of Chemistry and Geology
Indiana University
Bloomington, Indiana 47401

Carbon-13 isotope abundance measurements have critically aided research in carbon geochemistry (1), and awareness of the danger of carbon-14 tracer studies in humans is now generating interest in the use of carbon-13 tracers in metabolic studies (2). Unfortunately, the same mass spectroscopic instrumentation is not applicable to both problems. While it is easy to obtain 100 micromoles of CO_2 from limestone, the isolation of a large sample is difficult in human metabolic studies. Therefore, there is a need for an isotope ratio measurement technique with substantially reduced sample requirements.

The present instrumentation is derived from the work of McKinney and Nier (3,4), and utilizes dual ion-beam collection and sample switching. This method offers a maximum precision of about 0.05 parts per thousand with 50μmoles of sample (5), and about 1 part per thousand with 1μmole of sample (6).

Because one cause of the large sample requirements in the McKinney-Nier instrument is the Faraday cup collecter system, we have utilized an electron multiplier detector in the ion-counting mode. This single collector requires beam-switching, which is accomplished by computer control of the ion accelerating voltage. The initial series of experiments necessary to characterize all aspects of the system's performance is not yet complete, but progress to date is reported here.

Experimental

A schematic of our system is shown in figure 1. The CO_2 samples are introduced via a standard Nuclide Corp. duel inlet to a modified Varian CH7 mass spectrometer. The CH7 is equipped with a 12 bit digitally controlled 3 kV accelerating voltage, of which the upper 300 V can be scanned. The ion detector is a 21 stage electron multiplier coupled to a low gain amplifier and pulse shaper. The system dead time is less than 10 nsec. The mass spectrometer is used at a resolution of about 700 (10% valley definition).

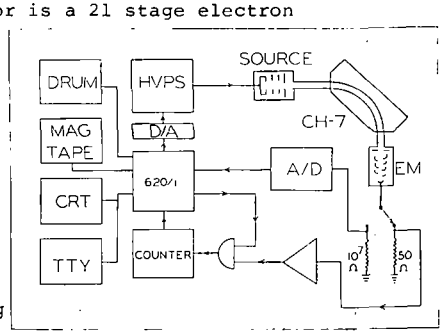

Figure 1. Schematic of Instrumentation

At the start of the operation, the pressures in the CO_2 reservoirs are adjusted so that the count rate at mass 44 ($^{12}CO_2$) is just less than 10^6c/sec. In this way, coincidence losses are kept below 1%, simplifying the count loss correction.

Beam switching under computer control is initiated after positioning the beam between masses 44 and 45. In the first step, the peak sides at half-height of m/e 44 are located and the peak center is defined. Following this, the computer locates and defines m/e 45 with the same accuracy as m/e 44. This entire peak location routine requires less than 15 seconds.

In the second computer-controlled step, data acquisition proceeds in a loop which incorporates a check and correction for beam drift and both up and down scans across the centers of the tops of masses 44 and 45. A ten-times slower rate is used for mass 45 to provide optimum use of counting time for the ratio measurement (7). The peak-switching process is terminated when a predetermined number of ions has been counted, and, at this point, the CO_2 samples are switched. This entire process is repeated until the desired grand total number of counts is accumulated. The sample-reference switching frequency is about 0.01 Hz and the mass switching frequency is about 1 Hz. Since

both of these frequencies lie in relatively clean areas of the noise spectrum, the system has a good noise immunity (8).

Results and Discussion

The results are expressed in per mil units (°/₀₀)(9). The most precise measurement of this relative difference for a fixed analysis time is obtained when an equal number of counts is collected for the $^{12}CO_2$ peaks of both the reference and sample and 1/10 that number is collected for both $^{13}CO_2$ peaks (7). Because the dead time limits the maximum count rate at $10^6 sec^{-1}$, the standard deviation of a measurement can be calculated directly from the total observation time, as shown in Table 1. This precision is the physical limit set by ion-statistics and system dead time.

$\sigma\delta$,°/₀₀	V_δ	V_R	T_{sec}	$N_{^{12}C}$	$N_{^{13}C}$
1×10^{-2}	10^{-4}	5×10^{-15}	2×10^{6}	2×10^{11}	2×10^{10}
3×10^{-2}	10^{-3}	5×10^{-14}	2×10^{5}	2×10^{10}	2×10^{9}
1×10^{-1}	10^{-2}	5×10^{-13}	2×10^{4}	2×10^{9}	2×10^{8}
3×10^{-1}	10^{-1}	5×10^{-12}	2×10^{3}	2×10^{8}	2×10^{7}
1	1	5×10^{-11}	2×10^{2}	2×10^{7}	2×10^{6}

Table 1. Theoretical Precision

We have demonstrated that the accuracy and precision of our counting technique meet the predictions of table 1 for a total counting time of 200 sec. In the present experiments sample consumption was over 100 nanomoles, largely in order to overcome background, a problem which should be remedied in the near future.

Thus, further refinements should lead to a sample requirement of only 10 nanomoles of carbon for relative isotope abundance measurements with a precision of 1 °/₀₀. This instrument system is also applicable to isotope measurements of N_2 and offers interesting possibilities for multiple ion G c/ms.

We would like to thank NSF GB13206 and NIH GM18979-01 for funding.

References

1. E. T. Degens, in G. Eglinton and M. T. J. Murphy (eds.), Organic Geochemistry, Springer, New York, 1969, p. 304.
2. P. D. Klein, J. R. Hauman, and W. T. Eisler, Anal. Chem., 44, 490 (1972).
3. C. R. McKinney, et. al., Rev. Sci. Instru., 21, 724 (1950).
4. A. O. Nier, Rev. Sci. Instru., 18, 398 (1947).
5. Publication 1002, Specifications for 6-60-RMS Mass Spectrometer, Nuclide Corp.
6. I. R. Kaplan, Dept. of Geology, UCLA, personal communication.
7. J. L. Jaech, Anal. Chem., 36, 1164 (1964).
8. J. Coor, J. of Chem. Ed., 45, A533 (1968).
9. H. Craig, Geochim. et Cosmochim. Acta, 3, 53 (1953).

A Fully Automatic Computer-Controlled MS System for UF_6 Isotope Abundance Analyses

by K. Habfast, G. Kappus and G. Heinen

The instrument described below represents our first attempt to fully integrate a computer into a mass spectrometer analysis technique, with the aim to construct an analysis system that supplies highly precise analysis results over days and weeks without an operator being required. We consider this system to be representative for the direction in which mass spectrometry or, generally speaking, analytical techniques, will advance in the years to come. We have started our approach where it can be realized commercially already today: in process automation, and here especially in the automatic control of enrichment process in uranium separation plants.

For years we have been engaged in the development and construction of UF_6 mass spectrometers and data processing systems for mass spectrometers. It was impossible, however, to simply couple an already available mass spectrometer with an already available data system. The problem on hand compelled us to develop a new mass spectrometer with computer compatible sections on the sample inlet, on the ion source and on the ion detection devices, as well as with system-oriented, optimized ion beam positioning.

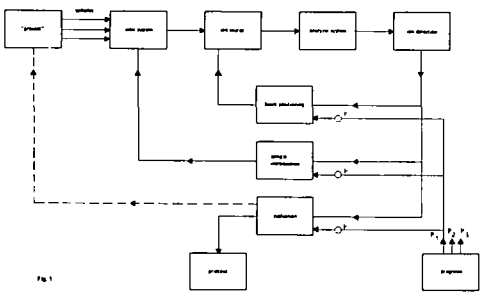

FIG. 1: System setup

The outcome of these endeavors was the analysis system shown in Fig. 1 with several independent control loops. All control loops may be influenced in their characteristics by an arbitrarily selectable program and are tuned and synchronized to each other by the program.

The program control itself can execute as many as three separate programs simultaneously so that three mass spectrometers can be connected at the same time with separate measuring programs.

Some details of the instrument's design are described in the following:

1. The most precise results of isotope abundance measurements are achieved when a double collector is used for the two ion currents in question. The system therefore contains a double collector measuring device. As it cannot be taken for granted that the peak plateaus will always be satisfactorily even, it must be made sure that the ion beams will always impinge on the same spot in the collectors. For this reason an automatic beam position stabilization is included in the system, which is shown in Fig. 2

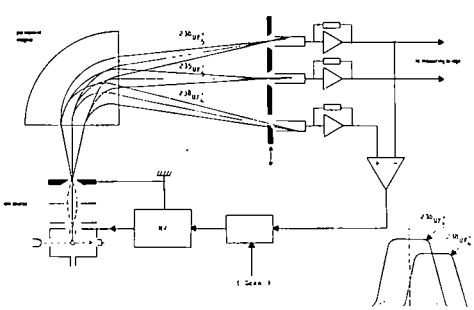

FIG. 2: Beam positioning system

The differential signal of the UF_5^+ and UF_4^+ fragment ions is fed back to the ion accelerating voltage which then always adjusts itself such that the UF_4^+ ion beam impinges on the edge of the collector. For exact geometrical positioning, the slit edge of the UF_4^+ collector can be shifted from outside the vacuum. Since a permanent magnet is used, the position of the ion beams is determined exclusively by the geometrical position of entry and exit slit. This arrangement also ensures that the effective ion energy is adjusted to a constant value. In this way the dependence of the measured isotope ratio on the effective ion energy is avoided. For this reason, this arrangement is better suited to this specific problem than the beam positioning technique by means of an additional coil on the separating magnet reported by Bir et al. two years ago.

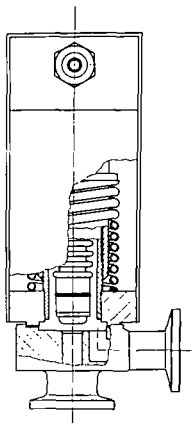

2. The introduction of the samples into the inlet system is effected program-controlled. This required the development of dependable, UF_6 resistant, computer-controllable shut-off valves the design of which is shown in Fig. 3. The actual valve element is a rounded KelF sealing plug which is pressed into a conical steel seat. This design ensures that UF_6 occasionally condensing on the sealing plug is always rubbed off again so that the valve remains vacuum-tight for more than 100 000 actuations in UF_6 operation. The valve guide with lubrication mechanism is located outside the vacuum and the sealing plug is actuated electropneumatically. With the same force acting on the sealing plug, this kind of actuation is much easier on the sealing plug than actuation with a combination of a spring and an electromagnet.

FIG. 3: Pneumatic valve

3. The samples are introduced into the ion source via a molecular beam emitter system with cryo trap already described earlier, in order to extend the ion source life as much as possible (here at least 1.000 hours) and to keep the memory factor as low as possible (here 1.003).

4. The ratio measuring bridge for determining the isotope ratio from the double collector signals works according to the well-known method with two voltage-to-frequency converters (Fig. 4).

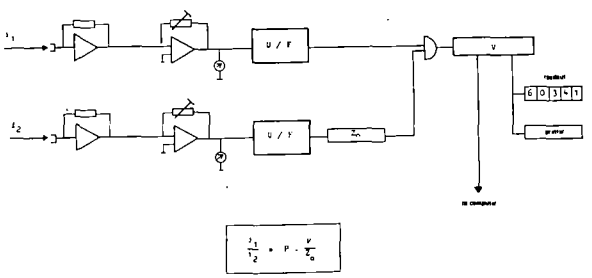

FIG. 4: Digital ratio measuring bridge

The isotope ratio is made available in binary code for further processing in the computer. In addition, it is digitally displayed as a 5-digit number and printed out on a digital printer. All the measuring functions of the measuring bridge can be set either manually or by the computer.

These are, in detail:

a) The selection of measuring technique: single or double collector.

b) The measuring intervals of the current integration for both techniques.

c) The amplification factors of the differential preamplifiers.

Counter overflows and any exceeding of the measuring range are indicated and automatically fed into the computer.

5. Fig. 5 shows again the complete system with the most important program controls of the individual control loops.

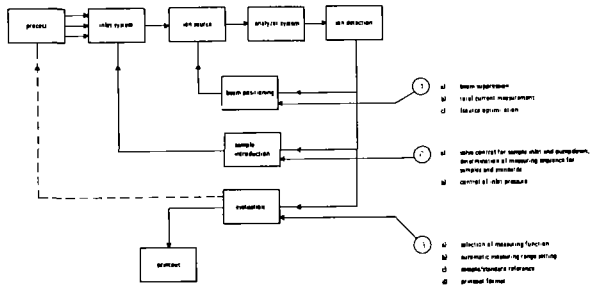

FIG. 5: Control functions of the system

a) The beam position stabilization described above is a closed analog control loop which is interrupted only for checking purposes: either when the ion beam must be suppressed for measuring the amplifier zeros or when the entire system is to be switched over to stand-by condition because a preselected total current has been exceeded.

   Not realized up to now but planned is an automatic, stepping-motor-driven setting of the ion source potentials to the ion current maximum.

b) In the sample introduction loop the valves of the inlet system are controlled in such a way that samples and standards are measured at the required time and that the pressure in the storage reservoir of the inlet system is set to an accuracy of 1 - 2 % before the measurement or decreases below a given minimum value after the measurement by pumping down. The pressure measurement is performed by means of the ion current of the $^{238}UF_5^+$ on the double collector.

c) For evaluation, after selection of the measuring technique, the system determines the optimum measuring range for preamplifier and voltage-to-frequency converter.

   Under these operating conditions one isotope value is then transferred about every second into the memory of the computer. First, it is checked whether the isotope ratio is constant within a given tolerance range. If this is the case, up to 60 single isotope ratios are measured, depending on the given tolerance, averaged and used for the computation of the standard deviation. If more than 30 % of the measured values are outside a preselectable multiple of the standard deviation, the system gives out a warning but continues to measure.

   Before and after the ratio measurement the amplifier zeros are measured and, in case they are not correct, used for the correction of the measured ratio. Then the system continues with the measurement of the next sample.

   Averaged value, standard deviation, time of the measurement and measuring parameters (measuring range etc.) for each measuring channel remain stored in the system. Following specific commands, the system produces the results in the form of a printout. It is able to print out single results, which are not corrected with respect to a standard, as well as results corrected with respect to a standard including error propagation calculation. Moreover, the results can be checked as to whether the limit value has been exceeded and used for direct interaction into the process.

6. The program system itself uses a Varian 620 computer with 8 k core memory. It is subdivided into operating system and application system. The operating system is a rigid time multiplexer with a time slice of 1 ms. The administration overhead is about 100 µs so that each of the mass spectrometers is connected up to the computer for about 900 µs every 3 ms.

The application system is programmed in KOSMIC, a language specially developed by us for analytical application, the syntax of which is shown in Fig. 6

KOSMIC

General:

NAME, P_1, P_2, P_3, ... P_N

Exemple:

```
  5 CLOSE,3,9,27,4
 10 WAIT,5
 51 START,3,8,60,1000,12,17,50,1
100 REP,10,4
```

FIG. 6: Syntax of KOSMIC

Each function that is to be executed by the system is given a name followed by several control parameters. The command

CLOSE,3,9,27,4

for instance, effects the closing of the valves 3,9,27 and 4.

The command

WAIT,5

causes the system to wait 5 s until the execution of the next command.

A complete experiment is programmed by listing the individual function names in appropriate order one after the other with ascending line numbers. If a certain sequence of functions is to be repeated several times one enters, for instance, the command

REP,10,4

which causes the system to repeat the command sequence 4 times starting at line 10.

Fig. 7 shows two program sequences for two mass spectrometers in one system. Two samples (~0.7 % resp. ~1.7 % ^{235}U) have been used for both spectrometer, whereas each sample has been considered also to be its own standard. The measuring sequence is as follows:

Mass spectrometer # 1 resp. #2

channel	#1	Standard	(1.7 %)
"	#2	Sample	(1.7 %)
"	#3	Sample	(0.7 %)
"	#4	Standard	(0.7 %)

Fig. 8 shows a section of the teletype printout from which the obtained experimental precision can also be seen.

Printout format is

##NM: ratio of sample as measured
##NM: ratio of sample, normalized to standard

##NL: ratio of standard as measured

N is the ID-number of the spectrometer
M, L are ID-numbers for measuring channels
16 :: 51 e.g. is the time at which the ratio has been measured

From the printout it can be seen, that channel #3 has been used as a standard for channel #2,as well as a sample, to be normalized by the standard at channel #4.

In continuous operation for several hundred hours precision is better than 0.04 % of the isotope ratio, the statistical confidence limit being 95 %. This is true, as can be seen from the printout, also for such a big difference in isotope ratios, as it has been used for these experiments.

```
READY
EXP,11
1 CLOSE,17,18
2 OPEN,2,7,8
3 START,11,8,150,1400,21,17,50,1
4 MESS,11,2,100,4,15,200,0,170
5 START,12,8,150,1400,21,17,50,1
6 MESS,12,2,100,4,15,200,0,170
7 LIST,12,11,18
8 CLOSE,7
9 PUMP,18,0,0,19,20,60,18,2,8,0,0
10 CLOSE,40,47
11 OPEN,37,38,31
12 START,13,8,150,1240,52,47,50,1
13 MESS,13,1,100,4,15,200,0,170
14 LIST,12,13,18
15 START,14,8,150,1250,52,47,50,1
16 MESS,14,1,100,4,15,200,0,170
17 LIST,13,14,18
18 CLOSE,37
19 PUMP,40,0,0,49,20,60,40,31,38,0,0
20 REP,1,4
21 CLOSE,19,49
22 OPEN,7,8,18,17,37,38,40,47
23 WAIT,60
24 OPEN,19,49
25 WAIT,120
26 CLOSE,7,8,37,38
27 REP
END
```

FIG. 7 a: Program sequence for spectrometer #1

```
READY
EXP,21
1 CLOSE,40,47
2 OPEN,37,38,30
3 START,21,8,150,1400,51,47,50,1
4 MESS,21,2,100,4,15,200,0,170
5 START,22,8,150,1400,51,47,50,1
6 MESS,22,2,100,4,15,200,0,170
7 LIST,22,21,18
8 CLOSE,37
9 PUMP,40,0,0,49,20,60,40,38,31,0,0
10 CLOSE,17,18
11 OPEN,7,8,1
12 START,23,8,150,1250,22,17,50,1
13 MESS,23,1,100,4,15,200,0,170
14 LIST,22,23,18
15 START,24,8,150,1250,22,17,50,1
16 MESS,24,1,100,4,15,200,0,170
17 LIST,23,24,18
18 CLOSE,7
19 PUMP,18,0,0,19,20,60,18,8,2,0,0
20 REP,1,4
21 CLOSE,19,49
22 OPEN,7,8,18,17,37,38,40,47
23 WAIT,60
24 OPEN,19,49
25 WAIT,120
26 CLOSE,7,8,37,38
27 REP
END
```

FIG. 7 b: Program sequence for spectrometer #2

```
READY
RUN,11,1

READY
RUN,21,1
1 M7
2 M7
##12  16::51  .0164681  .0000008
##12  16::51  .0099998  .0000010  ##11  16::47  .0164682  .0000008
2 M7
##22  16::52  .0183945  .0000008
##22  16::52  .0099998  .0000008  ##21  16::49  .0184040  .0000007
2 M7
##12  16::51  .0164681  .0000008
##12  16::51  .0245884  .0000035  **13  16::57  .0066974  .0000006
##22  16::52  .0183945  .0000008
##22  16::52  .0246059  .0000061  **23  16::58  .0074756  .0000015
2 M7
##13  16::57  .0066974  .0000006
##13  16::57  .0099998  .0000022  ##14  17::00  .0066975  .0000009
##23  16::58  .0074756  .0000015
##23  16::58  .0100020  .0000029  ##24  17::01  .0074741  .0000007
##12  17::06  .0164664  .0000010
##12  17::08  .0099996  .0000011  ##11  17::04  .0164670  .0000008
##22  17::09  .0183903  .0000012
##22  17::09  .0099998  .0000020  ##21  17::05  .0183905  .0000024
1 M7
2 M7
##12  17::08  .0164664  .0000010
##12  17::08  .0245929  .0000035  **13  17::12  .0066956  .0000005
##22  17::09  .0183903  .0000012
##22  17::09  .0245976  .0000056  **23  17::13  .0074764  .0000011
2 M7
##13  17::12  .0066956  .0000005
##13  17::12  .0100036  .0000020  ##14  17::16  .0066931  .0000008
##23  17::13  .0074764  .0000011
##23  17::13  .0100002  .0000028  ##24  17::17  .0074762  .0000009
1 M7
2 M7
##12  17::24  .0164556  .0000011
##12  17::24  .0099975  .0000011  ##11  17::20  .0164595  .0000007
##22  17::25  .0183965  .0000016
##22  17::25  .0100001  .0000021  ##21  17::21  .0183962  .0000021
1 M7
2 M7
##12  17::24  .0164556  .0000011
##12  17::24  .0245866  .0000045  **13  17::29  .0066928  .0000007
##22  17::25  .0183965  .0000016
##22  17::25  .0245974  .0000050  **23  17::30  .0074790  .0000008
2 M7
##13  17::29  .0066928  .0000007
##13  17::29  .0100003  .0000022  ##14  17::32  .0066926  .0000007
##23  17::30  .0074790  .0000008
##23  17::30  .0099998  .0000024  ##24  17::33  .0074791  .0000009
##12  17::40  .0164555  .0000009
##12  17::40  .0099999  .0000013  ##11  17::37  .0164555  .0000012
##22  17::41  .0184046  .0000014
##22  17::41  .0100015  .0000014  ##21  17::38  .0184016  .0000012
1 M4
2 M7
```

FIG. 8: Printout of results (for 2 spectrometers)
- x My - are warnings (see § 5 c)
** indicates that sample and standard have been measured with different attenuation factor of the preamplifier

AN AUTOMATED ISOTOPE RATIO DETERMINATION SYSTEM

M10

Gilbert L. Brezler and Stanley R. Gryczuk
Nuclide Corporation, State College, Pa. 16801

I. Introduction

By 1947, A. O. C. Nier had already devised a mass spectrometric system which was capable of measuring differences in isotope ratios in gaseous samples as small as 2 parts in 10,000. Since this system included as essential components not only a double-collector but also matched viscous leaks and a dual gas handling system, it could only be used for elements which have convenient gaseous compounds such as carbon and oxygen (as CO_2), nitrogen, argon, and hydrogen. For elements which had to be ionized using surface-ionization, isotope ratios could only be measured with a reproducibility of about $\pm$ 1%.

This has been a serious limitation in many important study areas. One example is geological age determination.

An uncertainty in geological age dating of say 5% was acceptable in the '50s and '60s when geologists with mass spectrometers were primarily engaged first in proving-out the several age-dating methods such as Rb-Sr, K-Ar, and U-Pb, and establishing the broad outlines of the geological time scale; but there has been an increasingly great need for higher precision as the field has become more sophisticated. Geologists would like to be able to measure parent and daughter element isotope ratios with a reproducibility of $\pm$ 0.1%, or better, $\pm$ 0.01%, as can be done with gases.

The situation has been similar in the nuclear field. Of course one has the possibility of using gaseous (but corrosive) uranium hexafluoride to measure the ratio of the major isotopes of uranium, but there are many cases in which U, Pu and other elements of interest must be analyzed thermionically, especially when minor isotopes must be determined. Again, it is desirable to determine these ratios to $\pm$ 0.01% or better, at least for 1% isotopes.

It has been found that reproducibility can be enhanced somewhat by several improvements, including careful replication of operating conditions; by measuring larger numbers of sets of peaks, and by "stepping" from peak-top to peak-top, eliminating time spent recording valleys; also, by counting ion arrivals rather than measuring currents.

In the present day, minicomputers offer a convenient and versatile means for accomplishing these functions — for controlling and monitoring the mass spectrometer for data-taking, and for processing data automatically and digitally, eliminating the drudgery of measuring peaks on a chart.

Nuclide's model DA/CS-III Data Analysis and Control System is a minicomputer oriented system that is designed to control, acquire, and automatically reduce MS data to achieve the desired results with a minimum amount of operator intervention.

II. An Explanation Of Operations In Utilizing The DA/CS-III System

The operator presses "START" push button, whereupon the DA/CS-III dialogue phase is activated. In the dialogue that follows the operator communicates to the controller the conditions he desires to have followed relating to the analysis. The operator's response is shown to the right of each colon. Each response is terminated with the "RETURN" entry on the teletype keyboard.

1. SAMPLE: EIMER & AMEND STANDARD
2. SAMPLE CODE: SRC03
3. RUN NO.: 1
4. DATE: 5-22-72
5. OPERATOR: GLB
6. INST. CODE: 12-90-SU
7. ENTER MASSES TO BE MEASURED: 88, 87, 86, 85

In response to line 7, the operator enters the masses he wants measured in the sequence of measurement.

8. ENTER REF. MASS: 88

The reference mass must be one of those specified in line 7. The computer will notify the operator that he must re-enter all masses if he inadvertently left out the reference mass in line 7. The reference mass need not be the most abundant peak, but it should be within 10% of the most abundant peak in order for ratios (as printed) to be useful.

9. CALIBRATE (Y OR N): Y

A response of N (No) on this line simply steps the dialogue to the next line of output. A response of Y (Yes) initiates the calibration routine which includes these steps:

A. A coarse magnetic field calculation is performed for each of the masses entered on line 7.
B. The calculated coarse magnetic field for the first approximation is sent to the magnet regulator by way of the coarse Digital-to-Analog Converter (DAC).
C. The operator verifies that he is setting on top of the peak of the first mass. If he is not, he uses the controls on the magnet regulator to fine-tune the magnetic field.
D. Once on the peak, the operator presses the "CONTINUE" button on the operator's control panel. This initiates a searching sequence during which the computer finds and stores the value for the fine DAC which will ensure peak top centering. Searching is done automatically for all remaining masses. Completion of the calibration routine results in the printing of line 10.

10. ENTER NO. OF CYCLES: 5

One "cycle" consists of stepping through a valley-peak-valley sequence for all the masses entered in line 7. The mass order is then reversed and stepping proceeds from the last mass to the first mass selected. This routine provides a mirror-image cycle.

11. ENTER PEAK SAMP. TIME (IN SEC.): 2

The electrometer's output will be sampled for the time specified while focused on the peak top. The effective sampling or measurement rate is 500 samples per second. Any integer time from 1 to 30 seconds may be entered.

12. ENTER BASE SAMP. TIME (IN SEC.): 1

Same as line 11 except that the baseline on the side of the peak will be sampled for the time entered on line 12.

13. SELECT MODE (A,S,M): A

(A = Automatic, S = Semiautomatic, M = Manual)
After the operator selects the mode he wishes to use, the system assumes an idling state and awaits the next command from the operator's control panel.

Under normal operating conditions the operator activates the "CONTROL" push button on the operator's control panel and begins the control phase of the DA/CS-III program. The system time accumulator is zeroed and the mass spectrometer is focused on the top of the first peak in the Automatic mode. The peak amplitude is sampled four times and averaged. If the amplitude is not greater than 40% of full range, the gain of the Digitally Controlled Variable Gain Amplifier (DCVGA) is increased until the amplitude meets this criterion. When the gain is set, the value of the gain is stored and the MS is stepped to the baseline on the low mass side of the first peak. After allowing the system to settle, which is done every time the magnetic field is changed, the output of the DCVGA (amplified

electrometer output) is sampled for the amount of time specified by the operator.

After the accumulated sample is averaged, the MS is stepped to the top of the first peak and the settling, sampling, and averaging sequence is repeated. The MS is then stepped to the baseline on the high mass side of the peak and again settling, sampling, and averaging are repeated. By using the two baseline values just measured, the baseline under the peak center is calculated and subtracted from the value of the peak top. This result along with the gain code for this peak is stored in memory. At this point the DCVGA is reset to a gain of one, the MS is stepped to the top of the second peak and the gain changing and data acquisition procedure is repeated. This operation continues until all specified mass peaks have been measured.

After the last peak has been stored with its corresponding gain code, the base-peak-base sequence is reversed so that the system now steps to last peak baseline on the high mass side, to thelast peak top, and then to the baseline on the low mass side of the last peak, acquiring data at each point. This sequence continues until the measurement of the first mass peak is completed. This results in a mirror-image stepping sequence (one cycle).

After these data are stored, the accumulated time is read. The two times are averaged to give a time corresponding to the sequence reversal. One cycle of the control phase is now complete and the "calculate-print-out" phase begins automatically. In this phase the two values for each mass peak, along with their respective gain codes, are averaged — with a correction for different gain codes if necessary — and stored in memory. Now present in memory are the peak values as they would be at the time of sequence reversal. The ratio calculations are simply the division of the reference mass value into each of the other mass values. After the first cycle is completed, the teletypewriter prints the heading consisting of the run number, time, cycle, ratios to the specified reference mass, and ratios measured. The results for the first cycle are calculated and printed. After first cycle ratios are printed, the system jumps back to the control phase for another cycle of data taking. Results are then printed for the second cycle. This operation continues until the number of cycles specified by the operator are completed. The average ratios and standard deviations are calculated and printed after the last cycle. The operator is then asked if he wants to drop any ratios. An N response directs the system to the idle loop to await operator command via the front panel push buttons. On the other hand, a response of Y permits operator-specified removal of one or more ratios and recalculation of ratio averages and standard deviations. The selected ratio is specified by entering the ratio column number followed by a comma and the cycle number. If more than one ratio is deleted, each change is separated by a semicolon. A "RETURN" entry on the teletype following the last change will initiate recalculation. When the new print-out is completed, the drop ratio question is asked again. If any of the previous entries are re-entered, that ratio would be restored and the recalculation would reflect the restoration. This dropping and restoring of ratios continues until the operator types N on the teletype.

If the operator enters an S on line 13 of the dialogue, the system operates in the Semiautomatic mode during the control phase. The only difference between automatic and semiautomatic operation is that the operator manually changes the gain of the DCVGA by using the thumbwheel switch on the control panel, rather than having the computer make the change. The operator enters the gain code on the teletype so that the computer becomes aware of the new gain selection.

With the availability of these three operating modes, the operator can participate as much or as little as he desires in performing various isotope ratio determinations.

PUBS 1267-0672

A NEW 3" 60° MASS SPECTROMETER SYSTEM FOR ISOTOPE RATIO AND TRACER STUDIES, "STATIC" AND "RESIDUAL" GAS ANALYSIS, GC-MS WORK AND OTHER APPLICATIONS

M11

D. J. Marshall, T. J. Eskew and L. F. Herzog
Nuclide Corporation, State College, Pa. 16801

For many years Nuclide has been building and improving isotope ratio instruments of 6-inch radius, and these have been widely used for CO_2, N_2, SO_2 and HD isotope ratio analyses. In reviewing the uses made of these instruments to date and the growing interest in deuterium/hydrogen analysis for hydrogeologic and other applications, and the new interest in stable isotope tracers, we concluded that less expensive instrumentation would be adequate for much of this work. We were aware that some other manufacturers were offering instruments of 2-inch radius and low ion accelerating voltage for isotope ratio studies, but our analysis indicated that a better approximation to the required performance would be realized with a somewhat more powerful ion analyzer. We selected a 3-inch (7.5 cm) radius, 60 degree sector, magnetic deflection analyzer, since we wished to retain the well-proven geometry, pioneered by Nier in 1940 and used in our 6-60-RMS, and we wished to be able to use the same source and collector configurations used on the 6-inch radius instruments, which now have recorded over 15 years of successful performance in isotope ratio difference determination. The dispersion of a 3-inch magnet is great enough that the dual collector design is straightforward, and yet small enough that even the m/e 2 and 3 collectors can both be contained in one housing without its volume becoming unduly large.

Although gas isotope work was an important consideration in the design of the 3-60, equal attention was given to applications in quantitative partial pressure analysis, thermionic-source isotope ratio measurements, and especially, its use as a small general purpose analytical instrument with GC, DTA, and batch inlets. We call this version the 3-60 Sector®. The geometry of the mass analyzer is shown in Figure 1 for the partial pressure analyzer configuration. The vacuum system is fabricated entirely of stainless steel and Inconel® and uses gold and copper gaskets. Its volume, including the large pumping lead, is 1.5 liters.

The analyzer is compact (only 6-1/4 x 24 x 9 inches) and it weighs 22 pounds. The magnet measures slightly less than 10 x 4 x 7 inches and weighs 49 pounds.

The analyzer is supplied with a rectangular base plate which may be readily attached to other systems. Alternatively, it can be mounted on a small portable cart or attached to a desk-top.

Essentially the same well-regulated electronic circuits used in our isotope ratio and compositional analysis instruments have been repackaged into a single compact panel which contains the 3000-volt ion accelerating voltage supply, trap current regulator, focusing controls, electrometer, and (optionally) the electron multiplier supply.

The electrometer provides nine full-scale output ranges from 10 millivolts to 100 volts, with a relative accuracy of 0.1% between ranges. The feedback or input resistor can have any value from 10^{12} ohms to 10^{8} ohms (or less). The time constant can have any value down to 100 microseconds (with a 10^{8} ohm resistor). The current noise is less than 10^{-15} ampere with a 10^{12} ohm resistor and a 0.5-second time constant. With a 10^{10} ohm resistor and a 0.1-second time constant, the baseline noise is about 200 microvolts which corresponds to 2 ppm of full scale on the 100-volt range. A "buckout" circuit is included to facilitate observing peak tops.

The 3-inch electromagnet has low resistance, high current coils suitable for solid state power supplies, and provides a magnetic field variable up to 8000 gauss at 10 amperes in the 5/16-inch gap. (See Figure 2). The inductance of the magnet is about 0.4 henry.

The regulated magnet supply provides a choice of current or field regulation, and mass scanning may be done using either mode of regulation. The standard unit provides scan rates continuously variable up to 100 mass units/minute for the 1-60 range and up to 1000 amu/minute for the 1-600

mass range. External programming capability is provided, so that scanning can be controlled using an oscilloscope sweep or other suitable source providing a 0-10 volt signal (faster scan rates are possible with external control).

The mass in focus is read directly on a panel meter calibrated in mass (amu). The mass meter and mass scan circuits utilize an analog square root circuit to provide accuracies of 0.5 amu or better over the 1-64 amu range. The same circuit is used to provide a mass scale during magnetic field scanning which is linear with time.

The ion accelerating voltage supply provides 0-3000 volts of acceleration; this control is linear and is also calibrated in mass, which is especially convenient if a permanent magnet is used. The HV control covers a 20:1 mass range.

The nomogram of the mass spectrometer equation for a 3-inch instrument is shown in Figure 3. At the maximum field of 8400 gauss, the mass range is 0-64 with a 3000-volt accelerating potential and 0 to 640 at 300 volts. Very good sensitivity and focusing properties are enjoyed at 3000 volts ion energy and yet the full usual mass range of interest in residual gas and partial pressure studies is covered at this voltage.

At 300 volts ion energy, where sensitivity is still adequate for many studies, the mass range extends to 640 amu.

The first 3-60 Sectorr® was built for quantitative partial pressure analysis and utilized a trap-current regulated EB source and a venetian blind multiplier.

Figure 4, a residual gas spectrum, shows that the Sectorr can produce the flat-topped peaks that are desirable for quantitative analysis in partial pressure and other studies.

Figure 5 is a magnetic-scan spectrum in the xenon mass range ($124<m/e<136$).

A version of the 3-60 has also been designed for use with "organic" ion source with fast pumping which we use in the 12-90-G organic instrument. The model 3-60-G with this source will accept a direct probe and various GC interfaces. This version commonly utilizes source and detector slits of 0.005", and a beam height of 0.050". Under these conditions, the expected resolving power with good sensitivity and analytical reproducibility is about 200. With 0.002-inch source slits, the resolving power capability extends to over 500.

The version of the instrument designed for hydrogen-deuterium analysis, designated 3-60-HD, is equipped with an EB source with external source magnets and two Faraday cup detectors. The system is kept at high vacuum by a 25 liter/second ion pump. The radii of curvature for the mass 2 and mass 3 beams were selected to be 2.7 and 3.3 inches respectively. The focus locations were determined to be as shown in Figure 6 and the two-collector arrangement was built accordingly as shown in Figure 7.

The H/D instrument can use the same dual inlet/capillary leak/sample-switching-valve arrangement that is standard with our 6-60-RMS.

As the description given above indicates, the electrometer on the 3-60 is more than adequate for measuring the mass 2 signal to the desired precision and drift specifications. A second electrometer or a vibrating reed electrometer can be used for the measurement of the (generally much smaller) mass 3 signal. The two amplifiers are used for ratio measurements in conjunction with either a manual isotope beam intensity balancing panel, an automatic dual balance panel, or a digital ratio circuit.

For H/D analysis, the usual slit settings are identical to those used on our 6-inch instrument, i.e., the source contains two 0.036-inch wide slits (1/4-inch spacing) and both collector slits measure 0.055-inch. Other slit settings may, however, be used.

The basic tune-up procedure for H/D work is as follows: The H_2^+ signal is first maximized at the working sample pressure of 5 cm with 200 microamperes of trap current. The maximization is done by adjustment of the external source magnets, the repeller and the ion focusing electrodes. Then the mass 3/2 ratio is then minimized by further adjustment of these parameters, done in such a fashion that one does not lose more than a factor of 2 in the H_2^+ beam intensity.

When the instrument is so tuned, curves of ratio versus sample pressure are typically nearly linear. Figure 8 shows a set of such curves for the 6-inch isotope ratio instrument and Figure 9 shows similar curves for the 3-inch system.

The sensitivity for the 3-60 under these operating conditions may be defined as follows: The H_2^+ signal is 5×10^{-5} ions collected per molecule entering the ionization chamber. Typically, the sample gas flow rate is 10^{15} molecules per second giving a calculated pressure of about 1×10^{-5} torr in the ionization chamber. The actual output ion current is 2×10^{-9} ampere.

With the identical ion source and ion energy, the sensitivity has been found to be usually between 0.8 and 1.6×10^{-5} ions collected/molecule introduced for the 6-60 instrument. Hence the observed sensitivity for hydrogen gas is greater for the 3-inch instrument than for the 6-inch version, even though the beam height used is 1/8-inch in the 3-60 (limited by the inside tube height) while in the 6-60 it is 5/16-inch (limited by thelength of the source slits). One is tempted to attribute the difference to beam divergence in the z direction, occurring over the larger path length in the 6-inch instrument, but this must still be verified by additional research. For heavier-mass species, the 6-inch has higher relative sensitivity.

Of course the important criterion of performance for a H/D instrument is its precision for measuring isotope ratio differences. The final figure shows a typical trace with switching between two samples which differ in ratio by 0.67% or 6.7 parts per mil. By hand calculation of this data, it is found that the sensitivity in this particular run is such that differences of 0.05% are distinguishable. We have also utilized various digital data output systems. When a rather simple digital voltmeter with a 5-second time constant is used for the measurement in place of the recorder, the difference-sensitivity is improved by at least a factor of 3 to 4, to 0.012%. We will report separately the results of tests of a digital ratio circuit providing longer integration times.

The authors would like to acknowledge the extensive assistance provided by Andrew J. Smith and Michael M. Michlik in completing the work described by this paper.

PUBS 1268-0672

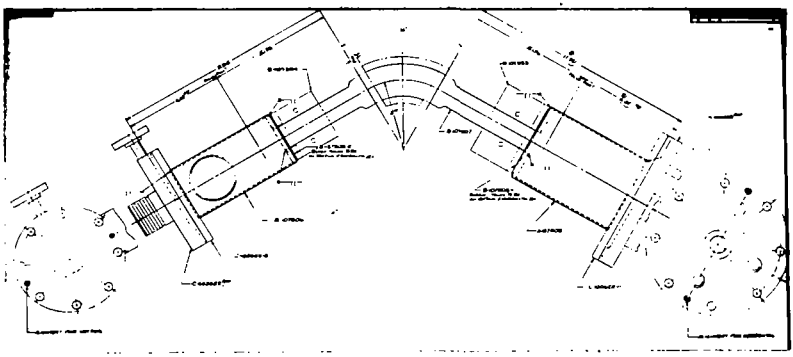

Fig. 1. Plan View of Instrument Showing Source, Collector, Pump, End Flanges, etc.

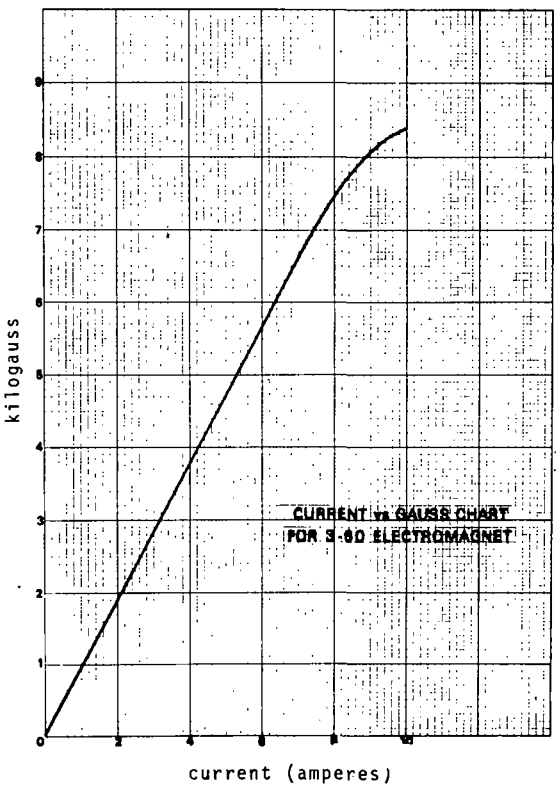

Fig. 2. 3-60-G Magnet Curve, Field vs Current.

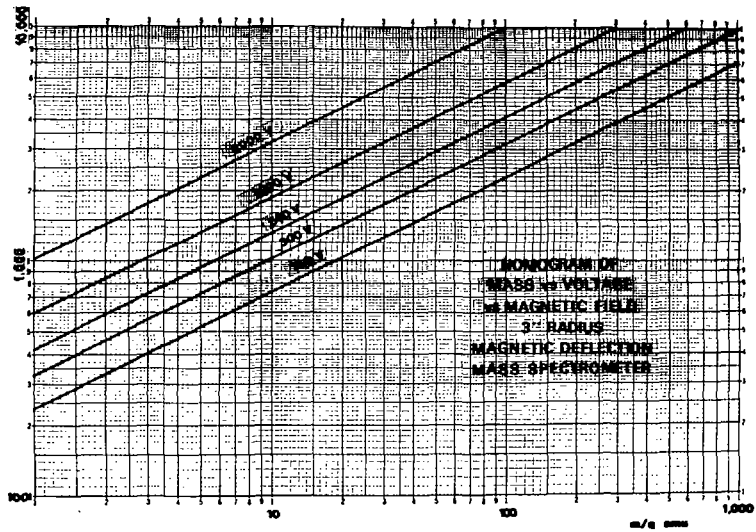

Fig. 3. Nomogram of Mass in Focus A_m = 3".

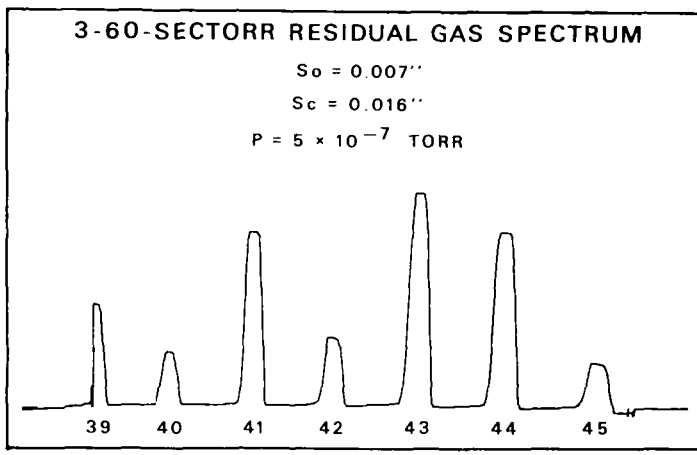

Fig. 4. Residual Gas Spectrum.

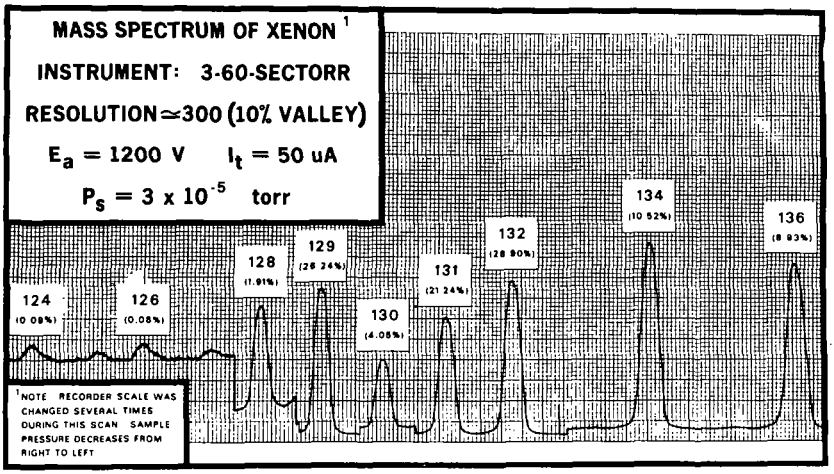

Fig. 5. Xenon Spectrum.

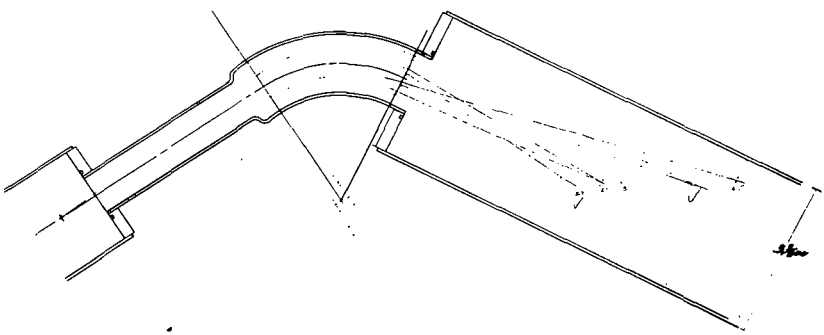

Fig. 6. HD Instrument Geometry.

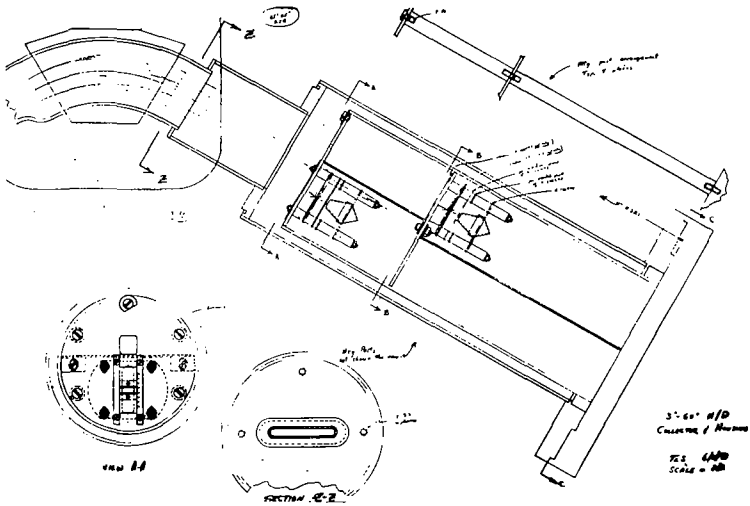

Fig. 7. Dual Collector in H/D Tube.

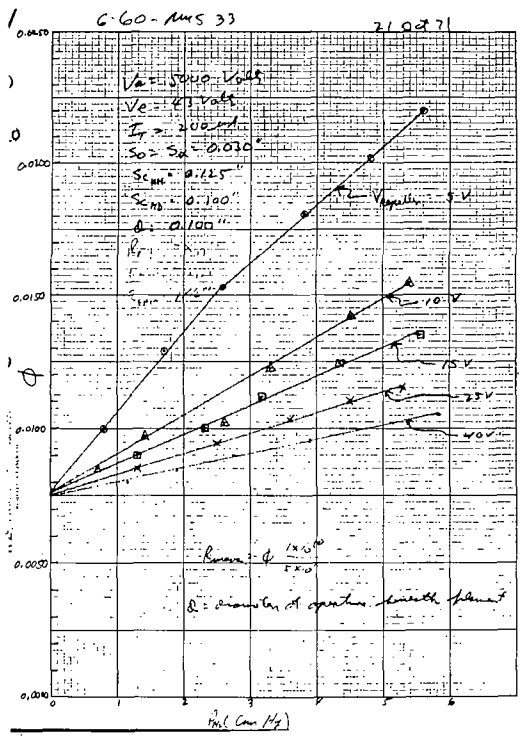

Fig. 8. Ratio vs Pressure for 6" Instrument.

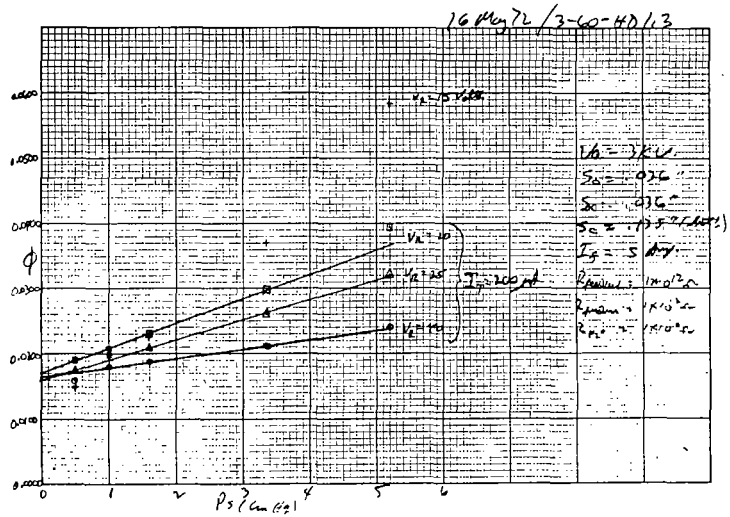

Fig. 9. Ratio vs Pressure for 3" Instrument.

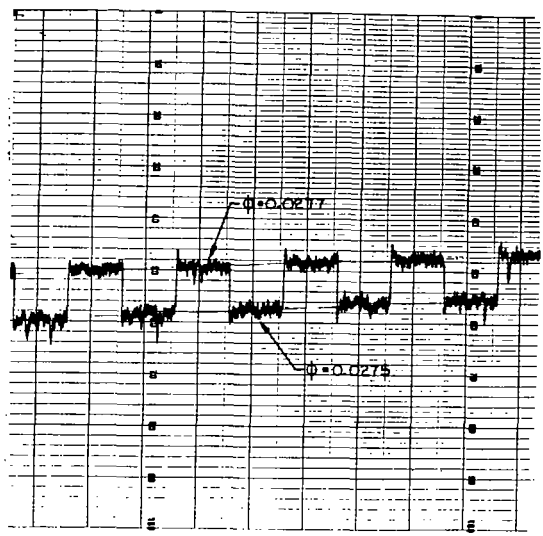

Fig. 10. Isotope Ratio Trace.

Characteristics of a Multipoint Field Ionization Source

W. Aberth, R.R. Sperry and C.A. Spindt
Stanford Research Institute, Menlo Park, CA. 94025

Abstract

A multipoint field ionization source consisting of arrays of points spaced 0.0025 cm apart and covering a circular area of 1.5 mm diameter has been developed at SRI. Details of this source have already been presented[1] and this report will give some recent source structure innovations and related test results.

Figure 1 shows a scanning electron micrograph of a portion of a multipoint array of tips on 0.0025 cm centers. The points are deposited by evaporation on a porous sintered tungsten substrate. Figure 2 is a cross-sectional view of the ion source structure. A 50% transparent, 400 lines/cm grid is placed parallel to the plane of the ionizing points and about 0.0125 cm above them. A point-to-grid potential difference of between 3,000 and 4,000 volts is then applied for normal field ionizing operation.

The field ionizing source shown in Figure 2 was coupled to an Extranuclear Corp. Model 270-9 quadrupole with 1.6 cm dia. × 22 cm long pole pieces. The multipoint source was maintained at +90 V and the extraction grid was kept at -3,600 V. The ions leaving the grid were decelerated and focused by a single aperture lens with a potential of about -400 V. The field produced ions entered the quadrupole analyzer through a 5 mm aperture with a net energy of 90 eV. Using toluene as a test gas, an ionization efficiency of about one in 3,000 and a transmission efficiency of 1 in 330 was measured. Thus for every 10^6 sample molecules of toluene, 1 was ionized, mass analyzed and detected. Under these operating conditions however the quadrupole resolution was only 50 for mass 92. Attempts to improve the resolution beyond 50 resulted in a rapid loss of signal. The poor resolution is attributed to the amplified beam divergence caused by the need to decelerate the source ions from 3,690 eV to the 90 eV required for reasonable quadrupole mass resolution. The resolution could undoubtedly be improved by reducing the quadrupole entrance aperture size from 5 mm to perhaps 1.5 mm but with a proportional loss in transmission.

To circumvent the drawback of deceleration required in quadrupole filters, the multipoint source was adapted to a 22-1/2 degree magnetic deflection mass spectrometer with a theoretical resolution of 160. A working resolution of 100 was obtained with this instrument employing a beam energy of 7,000 eV (see Figure 3). The net efficiency of this instrument was similar to that of the quadrupole or one ion detected per 10^6 sample molecules. It thus appears that until improved focusing can be developed for the multipoint source, instruments that mass analyze at high energies have a distinct advantage over the quadrupole mass filter. Projected improvements in multipoint optics, however, should make the multipoint source more amenable to quadrupole operation.

---

1. 11th Symposium on Electron, Ion, and Laser Beam Technology, Boulder, Colorado p. 631, 1971 (San Francisco Press, Inc.)

Figure 1. Scanning electron micrograph of a portion of a multipoint array of tips deposited on a sintered tungsten substrate and spaced 0.0025 cm apart.

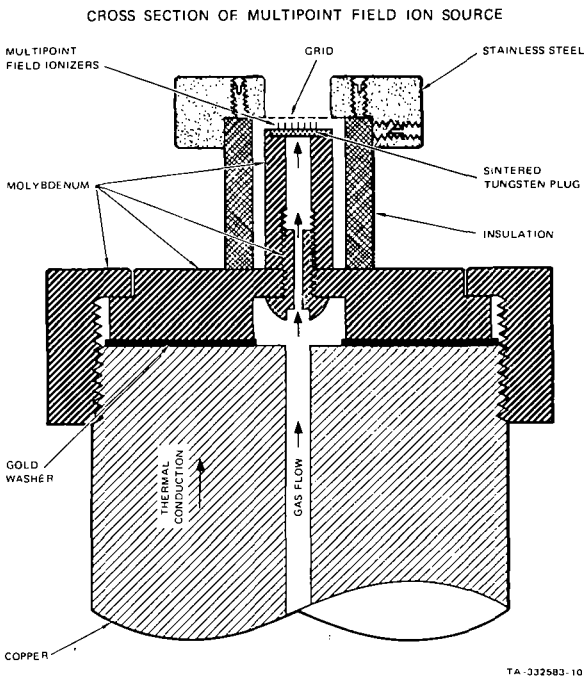

Figure 2. Cross-sectional view of a field ionization source structure. Sample gas molecules enter the multipoint field ionizing region through the porous sintered tungsten plug.

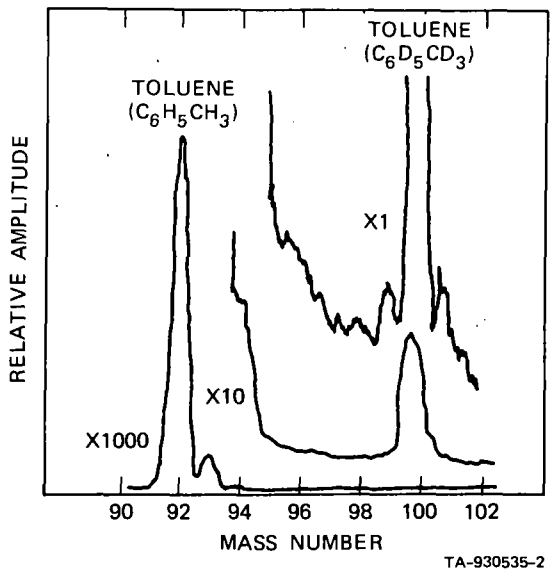

Figure 3. A partial mass scan of a 333/1 mixture of toluene $C_6H_5CH_3$ (mass 92) and toluene $C_6D_5CD_3$ (mass 100). The mass peaks at 93, 94, and 95 represent the natural single, double, and triple ^{13}C isotope contributions to toluene (92).

APPLICATIONS OF CHEMICAL IONIZATION MASS SPECTROMETRY

N1

G.P. Arsenault and J.J. Dolhun

Department of Chemistry
Massachusetts Institute of Technology
Cambridge, Massachusetts 02139

A brief resume of some of our past and current research in chemical ionization mass spectrometry (CIMS) is described in this paper. All of the work was performed on a modified QUAD 300 mass spectrometer. Details of a GC-MS system with a combined electron impact (EI) - chemical ionization (CI) source were reported in 1970 (1,2). The system was later modified by replacing the combined ion source with two ion sources, one EI and one CI (3,4). The modes of operation and advantages of the two-ion-source GC-MS system have been described (3,4).

A single gas was used initially for GC-CIMS (1,2) as illustrated schematically in Figure 1(a); two gases are now being used as shown in Figure 1(b). The methane CI mass spectrum of methyl tuberculostearate in the lower half of Figure 2 is an example of a spectrum obtained using the single-gas concept (Figure 1a). The helium-water CI mass spectrum of the same compound shown in the upper half of Figure 2 is an example of a spectrum obtained using the dual-gas concept (Figure 1b): helium was thus the carrier gas while water vapor was introduced at the outlet of the gas chromatographic column. Advantages of mixtures of charge exchange (CE) and chemical ionization reactant gases for CIMS - and in particular for GC-MS - are the following: (1) there is no limit to the CI reactant gases which may be used; (2) a wide variety of GC detector is possible; (3) alternate or simultaneous CE-CIMS is possible within a single high pressure ion source; (4) analysis of environmental samples which contain air (CE reactant gas) and water (CI reactant gas) is feasible.

Two separate approaches have been used for the analysis of gaseous, environmental samples by CIMS. In the first approach air is sampled continuously by means of an atmospheric probe. To suppress the effect of varying amounts of water in air samples from day to day, a sufficient amount of water is deliberately leaked continuously into the ion source at the same time as the air. This approach leads to the direct analysis of contaminants in air. The second approach is an indirect one in that the gaseous sample is injected into a helium stream which is later mixed with water vapor. A gas chromatographic column need not be used but can be used. An example of the results obtained with this technique for automobile exhaust analysis without a gas chromatograph is shown in Figure 3. The peaks labelled 79, 93, 107, and 121 may be attributed mainly to benzene and alkylated benzenes which are known constituents of automobile exhaust.

Acknowledgement: The authors are indebted to Professor K. Biemann for his continuing and enthusiastic support, and to the National Institutes of Health for financial support (Grant RR 00317 from Biotechnology Resources Branch, Division of Research Resources) and for a traineeship to J.J.D. (Grant No. GM 01523).

REFERENCES

1. G.P. Arsenault and J.J. Dolhun, Eighteenth Annual Conference on Mass Spectrometry, San Francisco, California, June 1970, p. B423.

2. G.P. Arsenault, J.J. Dolhun and K. Biemann, Chem. Communications, 1542 (1970).

3. G.P. Arsenault and J.J. Dolhun, Nineteenth Annual Conference on Mass Spectrometry, Atlanta, Georgia, May 1971, p. 137.

4. G.P. Arsenault, J.J. Dolhun and K. Biemann, Anal. Chem., 43, 1720 (1971).

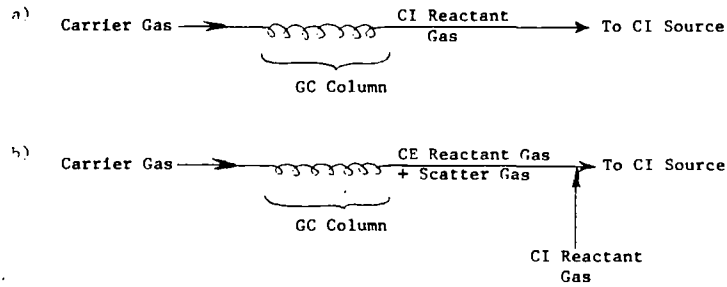

Figure 1. Concepts in GC-CIMS: a) The single-gas concept in which the carrier gas for chromatography is used as the chemical ionization reactant gas in the high pressure ion source; b) the dual-gas concept in which the carrier gas is used as a charge exchange reactant gas as well as a scatter gas in the high pressure ion source and the chemical ionization reactant gas is introduced separately at the outlet of the gas chromatographic column.

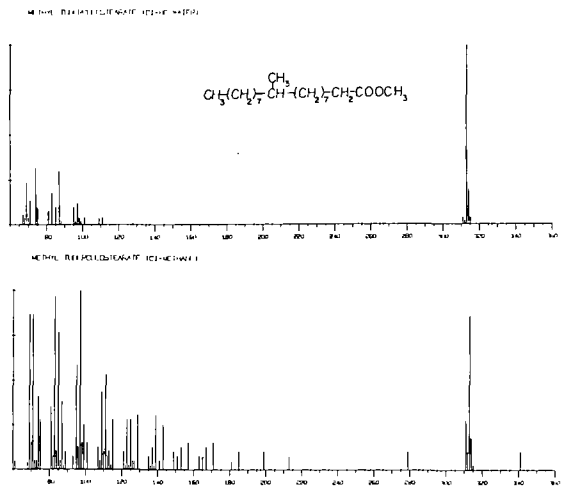

Figure 2. Chemical ionization mass spectra of methyl tuberculostearate; further details are given in the text.

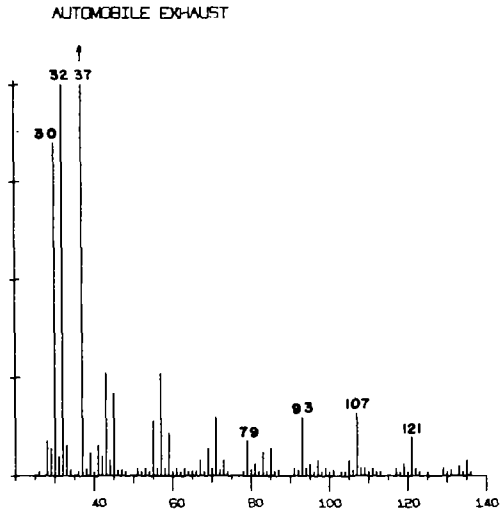

Figure 3. Chemical ionization mass spectrum (helium-water) of automobile exhaust (details are given in the text).

N2 IN Chemical Ionization Mass Spectrometry: A Tool for Structure Elucidation. DONALD F. HUNT, University of Virginia, Charlottesville, Va. N2

In chemical ionization mass spectrometry (CIMS) sample molecules are ionized by chemical reactions in the gas phase rather than by the conventional electron bombardment method. Fundamental to the development of CIMS as an analytical tool for structure elucidation is the finding that the nature of the CI spectrum is dependent on the type of ion-molecule reaction employed to ionize the sample. Different structural information can be obtained with different reagent gases. Primary, secondary, and tertiary alcohols can be differentiated using mixtures of methane-acetaldehyde and methane-acetone as reagent gases.[1] Aldehydes and ketones can be distinguished by using a weak Bronsted acid as the reagent.[1] With deuterated ammonia, primary, secondary, and tertiary amines can be differentiated.[2] Deuterium oxide can be employed to determine the number of active hydrogens present in natural product molecules.[3] CI spectra produced with argon-water mixtures exhibit features characteristic of both EI and CI(CH_4) modes of operation.[4] Many organic functional groups can be identified using nitric oxide as a reagent gas.[5] CI(CH_4) spectra of isomeric vicinal d_2-decanes indicate that the major pathway for formation of alkyl ions from hydrocarbons involves elimination of olefins from the M-1 ion.[6] CI(CH_4) spectra of a number of organometallic compounds have been recorded.[7]

1. D. F. Hunt and J. F. Ryan, III, Tetrahedron Lett., 4535 (1971).

2. D. F. Hunt, C. N. McEwen, and R. A. Upham, ibid., 4539 (1971).

3. D. F. Hunt, C. N. McEwen and R. A. Upham, Anal. Chem., 44, 1292 (1972).

4. D. F. Hunt and J. F. Ryan, III, ibid., 44, 1306 (1972).

5. D. F. Hunt and J. F. Ryan, J. Chem. Soc. (D) 620 (1972).

6. D. F. Hunt and C. N. McEwen, Org. Mass. Spectrom., submitted for publication.

7. D. F. Hunt, J. W. Russell, and R. L. Torian, J. Organometal. Chem., accepted for publication.

CHEMICAL IONIZATION MASS SPECTRA OF MACROLIDE ANTIBIOTICS

Rodger L. Foltz

Battelle-Columbus Laboratories
Columbus, Ohio 43201

Chemical ionization mass spectrometry is being applied to increasingly complex organic molecules. Probably the most significant feature of CI mass spectra is that they are far easier to interpret than EI mass spectra of the corresponding compounds and yet contain extremely useful structural information. The macrolide antibiotics constitute a class of organic compounds whose electron impact mass spectra are very complex and difficult to interpret. We have obtained isobutane chemical ionization mass spectra on a number of 14-membered ring macrolide antibiotics and have found that they effectively illustrate the usefulness of this technique. In addition to abundant protonated molecule ions, the CI mass spectra contain fragment ion peaks that can be correlated with the structure and location of the sugar residues and other oxygenated substituents.

This work will be published in Chemical Communications (in press) and in Lloydia (December, 1972).

NEGATIVE CHEMICAL IONIZATION MASS SPECTRA

N5

Ralph C. Dougherty and J. David Roberts

Department of Chemistry, Florida State University, Tallahassee, Florida 32306

The discovery of the utility of chemical ionization mass spectrometry by Field and Munson[1] paved the way for the utilization of chemical ionization data in an increasingly wide variety of chemical investigations. The development of a commercial chemical ionization source by William Johnston and his co-workers has made it possible for organic chemists to make direct use of chemical ionization data.

We have used negative chemical ionization (NCI) mass spectrometry to study the S_N2 transition state in the gas phase. There is a considerable body of solution data on the S_N2 reaction of simple molecules,[2] and it is reasonable to expect that studying this reaction in the gas phase will give us some insight into the effect of solvation on chemical reactivity. This paper discusses two major topics. These are NCI studies of the S_N2 transition state in the gas phase, and a simplified perturbation molecular orbital (PMO) theoretical approach to solvation. The PMO theory of solvation discusses the coordinate dissection analysis of reactions in solution, and the Born-Oppenheimer approximation for solvation. In summary we will present a classification of solvents based on their ionization potentials and electron affinities.

Negative chemical ionization mass spectra are often dominated by a few distinct ions. Many of these ions are the result of ionic association of dominant ions in the ion source with dominant neutrals. In the self-NCI mass spectra of alkyl halides the dominant ions in the spectrum include the halide anion and the alkyl halide halide anion. It is relatively easy to obtain NCI mass spectra of alkyl halides under conditions such that the halide and the alkyl halide halide anions have nearly equivalent intensities. We have used Field's techniques for studying equilibrium between the ion and molecule and the ion-molecule complex in the S_N2 like anion association reactions. Since the enthalpies for these equilibria are generally in the range of -8 to -20 Kcal/mole, and since we are dealing with dominant species in the ion source, we can be reasonably well assured that we are examining equilibria and not at pseudo-equilibria. We have examined these reactions specifically for pseudo-equilibrium effects by two methods. First, we have run every reaction at two different pressures. If the enthalpy of association that we derive from a van't Hoff plot reflected a pseudo-equilibrium the enthalpy of association would change as the pressure in the source changed, because the relaxation time in the source would change while the relaxation time for the chemical reaction would not. Secondly, we have examined the cycle for exchange of halide on methyl halides. Table I lists the results for the NCI mass spectra of methyl iodide and methyl chloride run, at constant pressures, simultaneously in the source.

Table I

van't Hoff Heats of Reaction For The Methyl Chloride-Methyl Iodide System Under NCI Conditions

Reaction	-ΔHo(Kcal/M)
$CH_3Cl + I^{\ominus} \rightleftarrows CH_3ClI^{\ominus}$	7.6
$CH_3 + Cl^{\ominus} \rightleftarrows CH_3ICl^{\ominus}$	9.8
$CH_3I + Cl^{\ominus} \rightleftarrows CH_3Cl + I^{\ominus}$	measured: -2.0
	calculated from above: -2.2

The measured value of ΔHo for the conversion of methyl iodide plus chloride to methyl chloride plus iodide agrees within experimental error of the value calculated by examining independent equilibria of methyl chloride plus iodide and methyl iodide plus chloride with the methyl chloride iodide ion. If the three reactions were not independently in equilibrium it seems quite unlikely that the enthalpies of reaction would agree. We

have completed similar cycles with methyl bromide and methyl iodide and methyl chloride and methyl bromide with equivalent results regarding the enthalpies in the cycle.

The self NCI mass spectrum of t-butyl bromide shows intense bromide and t-butyl bromide bromide ions. When these two ions are compared in a van't Hoff plot however, the plot shows no linear region. We presume that this is due to thermal activation of disassociative resonance capture of electrons by t-butyl bromide. This will in affect change the bromide ion concentration in the source as the temperature is changed. We counteracted this change by addition of four to one ethylene dibromide to t-butyl bromide and examined again the t-butyl bromide plus bromide to t-butyl bromide equilibrium. This experiment yielded a straight line van't Hoff plot, which gave an enthalpy that was reproducible at two different pressures and in three different experiments.

The establishment of gas phase equilibrium data is difficult, however we feel confident that the data presented below does reflect at least a close approach to gas phase equilibrium and we would be surprised if future measurements changed the relative orders of the heats of reaction. We are aware that our value for the heat of association of chloroform with chloride is roughly 2 Kcal/mole more positive than the value obtained by Professor Kebarle and his students.[4] This quantitative difference may not be significant. The crucial question is the relative order of the enthalpies of association. Future experiments will determine if this order is critically dependent on instrumental parameters.

Table II presents the gas phase heats of association for halide ions with alkyl halides run under conditions of self negative chemical ionization.

Table II

Gas Phase And Solution Data[2a] For S_N2 Transition Structures

$$RX^* + X^{\ominus} \rightleftarrows RX_2^{\ominus} \rightleftarrows RX + X^{*\ominus}$$

R-	X	$-\Delta H^{\circ}_{gas}$ $RX_2^{\ominus}$ (Kcal/m)	$\Delta E^{\ddagger a}$ exchange (Kcal/m)	$\Delta E^{\ddagger a,b}_{solv}$ (Kcal/m)
CH_3-	Cl	8.7	20.2	28.9
CH_2Cl-	Cl	10.9		
$CHCl_3$-	Cl	13.8		
CCl_3-	Cl	9.2		
CH_3-	Br	8.8	15.8	24.6
CH_3-	I	8.6	est.[2] 15.7	24.3
CH_3CH_2-	Br	11.6	17.5	29.1
$CH_3CH_2CH_2$-	Br	11.6	17.5	29.1
$(CH_3)_2$-CH-	Br	12.2	19.7	31.9
$(CH_3)_3$C-	Br	12.4	21.9	34.2
$(CH_3)_2$-CH-CH_2-	Br	12.9	18.9	31.8
$(CH_3)_3$-C-CH_2-	Br	14.5	22.1	36.4

a) Lithium salts in acetone, see ref. 2

b) $\Delta E^{\ddagger}_{solv} = \Delta E^{\ddagger} - \Delta H^{\circ}_{gas}$

Each of the gas phase enthalpies is the average of three experiments for which the enthalpies did not differ than more than 0.5 Kcal/M. At least one of the points in the average was obtained at a pressure which was significantly different from the others. The measured source pressure for these experiments varied from 40 to 130 Pascals. The temperature range over which the reactions were in equilibrium was always greater than 70°, and was normally of the order of 120°. The small range for some systems was due to the high temperature limit that we are willing to

operate our mass spectrometer source, approximately 290°C.

The data for association of chloride with the chloro methanes, methyl chloride through carbon tetrachloride, provides some insight into the structure of the methyl halide halide ions we are observing in the gas phase. The heats of association increase from methyl chloride through chloroform and drop for carbon tetrachloride. This means that the association cannot be purely an ion-dipole phenomenon. We have examined the association of 1-bromoadamantane with bromide in our chemical ionization source. We have run the experiment three different times with pressures of 1-adamantyl bromide in the source of at least 70 Pascals. We have never been able to observe an ion whose m/e corresponded to that of adamantyl bromide bromide. Since 1-bromoadamantane is a bridgehead bromide this result strongly suggests that the ion molecule association complex requires backside association of the halide ion with the alkyl halide molecule. This result directly parallels results from solution,[2] and agrees with the observations for the chloromethanes. Fukui and his students have calculated the structure of the S_N2 association complex for the displacement of chloride on methyl chloride by chloride.[5] These valence-level electron SCF calculations suggest that backside association of chloride with methyl chloride should be favored over frontside association by the order of 40 Kcal/M. The clear indication is that backside association should be exothermic while frontside association should be endothermic.

In contrast to our data, McIver and his students have shown that bromide exchanges with 1-bromoadamantane in an ion cyclotron resonance spectrometer.[6] We have little doubt that the frontside exchange reaction occurs. Our data suggest that the frontside ion-molecule association complex is not very stable, and it would appear that the backside ion-molecule association complex is.

The data in Table I can be used to compare structure and nucleophilicity parameters in S_N2 reactions performed in the gas phase and in solution. The activation energies for the solution reactions are those obtained by Hughes, Ingold and their co-workers for lithium bromide plus alkyl bromide exchange reactions in acetone solution.[2] The desolvation energy of the transition state ($\Delta E^{\ddagger}_{solv}$) maybe approximately obtained as the difference between the solution activation energy and the enthalpy of stabilization of the ion-molecule complex in the gas phase. These desolvation energies are certain to be quantitatively incorrect because the ion-molecule association complex will be pseudo-Jahn-Teller distorted in the gas phase. The magnitude of the distortion will depend upon the alkyl halide structure; however, for a series of related alkyl systems the distortion should be nearly constant and the relative values of the desolvation energy of the transition states should be accurate.

When we consider the data for methyl chloride plus chloride, methyl bromide plus bromide, and methyl iodide plus iodide, in the gas phase and in solution it is clear that the difference in nucleophilicity between chloride and iodide is determined entirely by desolvation of the anion.

The data for the alkyl bromide association experiments are even more remarkable. Neo-pentyl bromide bromide is the most stable of the alkyl halide halides that we have studied thus far. In solution the exchange of bromide on neo-pentyl bromide has the highest activation energy of the series studied by Hughes, Ingold and their co-workers.[2] The difference is due entirely to the desolvation of the transition state in solution. The discrepancy is dramatically illustrated when we plot relative heat of association of bromide with alkyl bromides in the gas phase on the same graph that is used to plot the relative activation energies for bromide exchange in solution. This has been done in Figure 1.

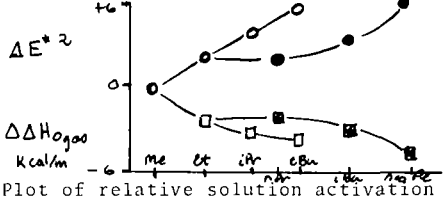

Figure 1. Plot of relative solution activation energies (LiBr, RBr exchange in acetone) and gas phase heats of association ($RBr+Br^{\ominus}$) for a series of alkyl bromides after Hughes, Ingold, et. al.[2]

In an attempt to reconcile these two major pieces of data on alkyl bromide exchange reactions we were prompted to investigate the qualitative theoretical basis for the effect of solvation on chemical reactivity. The material that follows is a summary of some of the results and conclusions of this study. We will be unable in this forum to present a review of the very extensive literature on the theory of solvation and the application of perturbation molecular orbital theory to chemical problems. There are numerous excellent reviews of both of these areas available. A detailed account of our approach to this subject will appear in book form within the year.[7]

The MO interactions between solvent and solute must be of second order or higher perturbations. First order molecular orbital interactions will lead to reaction and not to solvation. The effects of solvation interactions on the energies of the relevant filled and vacant orbitals in solvent, solute, and solvate are illustrated in Figure 2.

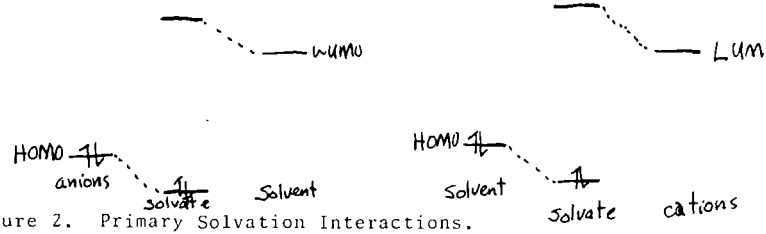

Figure 2. Primary Solvation Interactions.

We have only shown the orbitals for the leading interactions in Figure 2. The remainder of the interactions will quantitatively alter the results, but they should not alter the qualitative orders. In second order perturbation theory the energy of solvation will be given by equation (1), where C_i is a statistical interaction constant for the solvent with the solute. a_{mr} is the orbital coefficient at the interaction site for the

$$\Delta E_{solv} = \sum_{i}^{ions} C_i \cdot 2\left(\sum_{m}^{occ}\sum_{n}^{all} - \sum_{m}^{all}\sum_{n}^{occ}\right)\frac{a_{mr}^2 b_{ns}^2 \beta_{rs}^2}{E_m - F_n} \qquad (1)$$

solute and b_{ns} is an orbital coefficient at the interaction site for the solvent. β_{rs} is the resonance intergral between site r and site s of the solute and solvent, and E_m and F_n are the orbital energies for the solute and solvent respectively.

In equation (1) we can see the effect of changing the charge size of an ion on the solvation of that ion. The charge size is inversely related to the magnitude of the orbital interaction coefficient a_{mr}. As the charge size for an ion or ion-molecule complex increases the solvation interaction for that ion at a given site will decrease. The effect of charge size on solvent effects is particularly important when the charge size changes dramatically between the reagents in the transition state. These factors are illustrated in outline in Table III.

Table III

The Relation of Charge Size in the Transition State to Solvent Effects

charge size (interaction coefficients)		effect of increasing solvent power on reaction rate	examples
reactants	transition state		
small (large)	large (small)	decrease rate	S_N2
large (small)	small (large)	increase rate	S_N1
large (small)	large (small)	little effect	Diels-Alder

Equation (1) may provide an adequate description of solvation interactions for qualitative chemical purposes; however, equation (1) is considerably more complicated than one would like for a laboratory-usable description of solvation interactions. It is possible to substantially simplify equation (1) by using the Mulliken approximation for β, assuming that the orbital interaction coefficients for the anions and the cations are equivalent, and assuming that the only important terms in interaction are those illustrated in Figure 2. When these gross assumptions are made equation (2) can be derived directly. C_1, C_2, C_3 and C_4 all depend on the reaction in question and include terms for the ionization potentials and electron affinities of the reagents throughout the course of the reaction. C_1 can be identified with the susceptibility of the reaction to the ionizing power of the solvent. C_2 can be identified with the susceptibility

$$\Delta E_{solv} = C_1(IP_s + EA_s) + C_2(IP_s) + C_3(EA_s)^2 + C_4 \quad (2)$$

of the reaction to nucleophilicity of the solvent; C_2 should be a negative constant. C_3 could be identified with the susceptibility of the reaction to the electrophilicity of the solvent; C_3 should be a positive constant. The electron affinities in equation (2) will be either the electron affinity of the molecule or its virtual electron affinity. The virtual electron affinity of a protonic solvent is the electron affinity of the radical that is obtained by homolitically cleaving the active hydrogen bond. Unfortunately very few electron affinities are known accurately.

In a very preliminary way we have plotted logs of the rates of methyl tosylate solvolysis as obtained by Schleyer and his co-workers,[8] against the sum of the ionization potentials and the virtual electron affinities of the alcoholic solvents and water in which the reactions were run. This plot gave a remarkably good linear correlation which suggests that equation (2) may be useful in studying solvation interactions. The fact that a straight line was obtained in the correlation of methyl tosylate sovolysis rates with the sum of solvent ionization potential and virtual electron affinity suggests that nucleophilicity and electrophilicity of the solvent are relatively unimportant to this reaction. This result agrees with the early conclusions of Winstein and Grunwald.[9] There are many cases in which the nucleophilicity of the solvent is known to be important to reactivity. These cases may be theoretically examined with the aid of the Bell-Evans-Polanyi (BEP) coordinate disection analysis.[10]

Ionic bond forming-bond breaking reactions in the gas phase which follow the BEP rate-equilibrium relationship must involve only small changed in charge size throughout the course of the reaction. If there were a large change in charge size for a reaction of this type at the transition state it would indicate delocalization between the bond forming and bond breaking parts of the reaction. In the BEP analysis this delocalization is assumed not to occur. Figure 4 illustrates the effect of transferring a BEP ionic reaction from the gas phase to solution. There will be little effect of solvation on the relative energies of the reactant, transition state, and product configurations in the ground state of a BEP reaction. This is because the charge size and the interaction constants for the reaction must be approximately constant throughout the reaction for the BEP relationship to hold. There will be a substantial

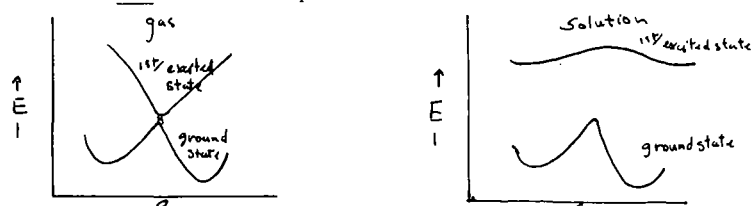

Figure 3. Effect of solvation on BEP reactions; in BEP reactions the ground state charge size does not dramatically change during the reaction.

effect of solvation on the relative energies of the same configurations in the first excited state. In an ionic BEP reaction the charge size in the first excited state increases as you approach the transition state configuration. This means that the reactant and product configurations

will be solvated more heavily than the transition state configuration with a resulting substantial change in the shape of the energy surface. The effects of this change on reactivity in the excited state are obvious.[11]

Figure 4 illustrates the effect of placing an anti-BEP gas phase reaction, like the S_N2 reaction, in solution. The charge size in ionic anti-BEP reactions changes considerably in the reaction coordinate. If there

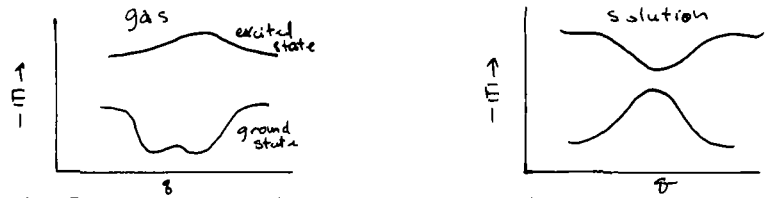

Figure 4. Effects of solvation on anti-BEP reactions; in anti-BEP reactions the ground state charge size changes considerably during the reaction.

is substantial delocalization in the transition state of an ionic reaction the charge size of the transition state will be larger than the charge size of the reactant or the product state, and the ability of the solvent to solvate the transition state will be less than in the case of reactants or products. Placing the reaction in solution will then cause a relative increase in the activation energy for the reaction. Indeed it is possible to reverse the relative stability of the reactant and transition state configurations. In many cases, such as the S_N2 reaction, the charge size in the first excited state will decrease as the transition state configuration is approached. Putting the reaction into a better solvent will then decrease the energy gap between the ground state and the first excited state at the transition state configuration. This is the opposite of the effect of solvation on the ground state-excited state gap in BEP reactions.

When the solvent inverts the shape of the chemical reaction surface as it does in the S_N2 reaction, the solvent is intimately associated with the new reaction surface. The intimate association of solvents with chemical reactions is one of the major sources of confusion in the effects of solvation on chemical reactivity. This confusion is particularly acute for anti-BEP reactions and for reactions that can either follow a Bell-Evans-Polanyi rate equilibrium relationship or be an anti-BEP process depending upon the solvent. One basis for the confusion is our inability to draw a reaction coordinate that specifically involves solvent-substrate interactions. We can do quite well with a bond breaking-bond forming reaction, like an S_N2 process, in a two dimensional diagram. If we insist that the coordinates for solvent association on both sides in the bond forming-bond breaking process be illustrated, we can no longer draw a reaction coordinate on a piece of paper. Intimate solvent association with the reactants will effect both the activation energy for the reaction and the entropy of activation for the reaction. In general as the activation energy increases the entropy of activation will decrease. It is possible however, that the energy of activation and the entropy of activation will change in independent ways and when this happens our conventional views of solvation lead to confusion.

We refer to the conventional view of solvation as the Born-Oppenheimer approximation for solvation. The BO approximation for solvation is distinct from the BO approximation, although both allow us to draw potential surfaces for molecules. The BO approximation allows us to draw potential surfaces for individual molecules by separating electronic and nuclear wave functions. The BO approximation for solvation separates molecular and solvent wave functions. The appearance of the BO approximation for solvation in the conventional solvent-solute picture can be illustrated by employing the classical solvent cage model for solvation.

Reactions that follow the Bell-Evans-Polanyi principle in the gas phase should occur within a solvent cage that is effectively the same size for reactants, transition state, and products. This is because the charge size in the reaction does not significantly change throughout the reaction. The simplest example of reactions of this type are proton transfer reactions, and indeed these reactions were the first reactions used by Bell in

development of the foundations of the BEP principle. Proton transfer reactions in the gas phase occur with frequency factors in the order of 10^{13} per second. When these reactions are carried out in solution most of them occur with frequency factors of the order of 10^{11} per second. This is a diffusion limited rate. Functionally this means that as soon as the reagents diffuse into an appropriate solvent cage the reaction occurs.

The majority of reactions in solution do not occur with diffusion limited rates. Figure 5 illustrates what happens in an anti-BEP reaction

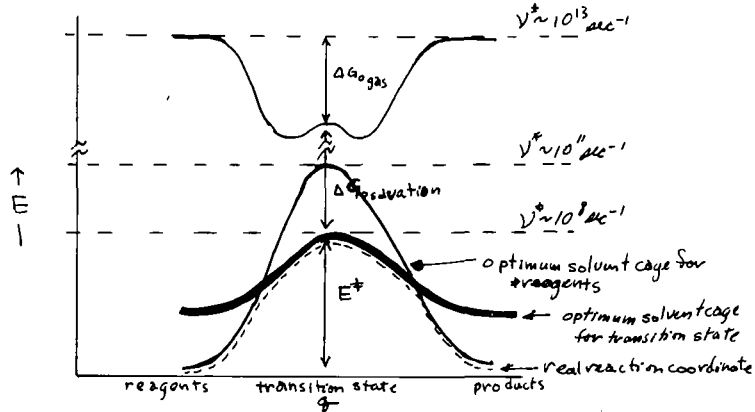

Figure 5. Illustrating the Breakdown in the Born-Oppenheimer Approximation for Solvation.

is placed in a good solvent, and BO approximation for solvation breaks down. Since the charge size for the reagents and the transition state varies considerably, the optimum solvent cage for the reagents and the transition state will be substantially different. If we make the conventional assumption that the solvent cage remains constant throughout the course of the reaction, and plot of the internal energy of the reagents within a specified solvent cage along the reaction coordinate, we will obtain graphs like those in Figure 5. If we conduct the reaction in the optimum solvent cage of the reagents, the transition state, because of its large size, will inevitably by substantially desolvated and the activation energy for the reaction in that solvent cage will be higher than the observed activation energy. If on the other hand we conduct the reaction in the optimum solvent cage of the transition state the reagents will be substantially desolvated, but the activation energy for the process will be substantially lower than the observed activation energy for the reaction. The entropies of activation for these two reaction courses will be related to the activation energies for the individual processes. For the reaction occurring in the solvent cage of the reagents the frequency factor for the reaction will approach diffusion controlled limits, just as in the case of proton transfer reactions. The frequency factor for the reaction occurring in the solvent cage of the transition state will be lower. The actual course taken by the reaction is illustrated by the dotted line in Figure 5. If the reagents have a vibrational energy equivalent to $E^{\ddagger}$ when they are contained in the optimum solvent cage for the reagents they will approach the potential barrier of the solvent cage before they reach the transition state configuration. In a limited number of cases the solvent molecules will be moving with sufficient velocity to punch the reagents through to the optimum solvent cage for the transition state. This will further decrease the frequency factor for the reaction. The net result will be a reaction which occurs with an activation energy intermediate between the activation energy it would have in the optimum solvent cage of the transition state and the activation energy it would have in the solvent cage of the reagents, and a frequency factor that is lower than it would have in either case. In competition between two reactions, both the activation energies and the activation entropies are critically important. If the BO approximation for solvation breaks down to an equivalent extent in a series of reactions it is entirely possible that the reactions will follow a Bell-Evans-Polanyi rate equilibrium relationship in solution. There

are however a number of cases in which changes in solvent cause a breakdown in the Bell-Evans-Polanyi relationship. This breakdown must be due to specific solvent-solute interactions in the different solvents; it must be due to a different extent of breakdown in the BO approximation for solvation in the two solvents.

The PMO treatment of solvent effects provides a basis for enumerating important factors to consider in changing solvents. These factors are outlined in Table IV. In general the solvent should be matched to the reaction. The important solvent parameters are the ionization potential and electron affinity or virtual electron affinity of the solvent and the solvent's reactivity. As the ionization potential of the solvent increases the ionizing power of the solvent increases and the ability of the solvent to solvate cations decreases. As the electron affinity of the solvent or the virtual electron affinity of the solvent increase the ionizing power of the solvent also increases and the solvents ability to solvate anions is substantially increased.

Table IV

Factors to Consider
When Changing Solvents

Solvent

I. Orbital energies - IP, EA
II. Solvent reactivity - protonic, aprotic .....

Reaction

I. Change in the charge size during reaction - BEP, anti-BEP
II. Relative stability of ions along the reaction coordinate.

The important factors to consider in the reaction are the relative changes in the charge size during the reaction and the stabilities of critical intermediates. If the reaction is a gas phase BEP process in which the charge size does not change the reaction will not be impeded but placing it in a good solvent, though side reactions should be considered. If the reaction is a BEP process in which the charge size decreases as one approaches the transition state, e.g. the S_N1 reaction, the reaction should be run in the best solvent possible. If the reaction is an anti-BEP process it should be carried out in the poorest solvent in which the reaction will proceed. If the reaction in question requires a long lived unstable cation the reaction should be run in a poor solvent for cations. The worst solvents for cations that are known are fluosulfonic acid, FSO_3H, and fluosulfonic acid-antimonypentafluoride mixtures. Cationic species as unstable as CH_5^+ can exist, at least for a short time, in fluosulfonic acid-antimonypentafluoride mixtures. In better solvents for cations these species could not exist at all. If the reaction in question requires long lived unstable anionic structures it should be carried out in the poorest solvent for anions in which the reaction will occur. It seems likely that the S_N2 transition state for the Finckelstein halide substitution reaction will be spectroscopically observed in the solvent like hexamethylphosphoramide in the near future. This would be the direct analog of the observation of the S_N1 transition state in fluosulfonic acid antimonyfluoride mixtures. The analog of fluosulfonic acid for anions should be sodium-potassium allow (Na-K). Unfortunately a lot of the literature on the properties of Na-K solutions is not generally available.

The considerations above can be used to produce a classification system for solvents bases on the IP and EA of the solvent. This has been done in Table V.

Table V

Classes of Solvents

Solvent Class	Orbital Energies HOMO	LUMO	virtual LUMO	Solvating Power anions	cations	Example	Favored Reactions
I_P	high		mod	+	++	H_2O	ion-ion exchange; ligand exchange
I_A	high	mod		+	++	$(RO)_3PO$	ion-ion exchange involving strong bases
II_P	low		low	++	$\dot{-}$	HF	ion forming reactions, unstable cations
II_A	low	low		++	$\dot{-}$	SbF_5	ion forming reactions, unstable aprotic cations
III_P	high		high	$\dot{-}$	++	NH_3	ion forming reactions, unstable anions
III_A	high	mod		-	++	$(Me_2N)_3P$	ion forming reactions, strong bases; elimination reactions.
	high	high		--	+++	Na-K	anion forming.
IV_P	low		mod	$\dot{-}$	-	$CHCl_3$	nonionic reactions ion pair processes
IV_A	low	mod		$\dot{-}$	-	ϕNO_2	ion pair processes unstable cation
V	high	high		-	$\dot{-}$	C_6H_6	nonpolar reactions ion pair processes
VI	low	high		--	--	pentane	nonpolar processes radical reactions

Acknowledgement. The National Science Foundation has supported this work.

1. M.S.B. Munson and F.H. Field, J. Amer. Chem. Soc., 88, 2621 (1966); F.H. Field, Accounts Chem. Res., 1, 42 (1968).
2. P.B.D. de LaMare, L. Fowden, E.D. Hughes, C.K. Ingold and J.D.H. Mackie, J. Chem. Soc., 1955, 3200.
3. F.H. Field, J. Amer. Chem. Soc., 91, 2827, 6334 (1969).
4. P. Kebarle, personal communication.
5. K. Fukui, H. Fujimoto and S. Yamabe, J. Phys. Chem., 76, 232 (1972).
6. R.T. McIver, personal communication.
7. M.J.S. Dewar and R.C. Dougherty, "The PMO Theory of Organic Chemistry", Academic Press, New York, 1973.
8. T.W. Bentley, F.L. Schadt and P.v.R. Schleyer, J. Amer. Chem. Soc. 94, 993 (1972).
9. S. Winstein, E. Grunwald and H.W. Jones, J. Amer. Chem. Soc., 73, 2700 (1951).
10. M.J.S. Dewar, "The Molecular Orbital Theory of Organic Chemistry" McGraw-Hill, New York, 1969.
11. R.C. Dougherty, J. Amer. Chem. Soc., 93, 7187 (1971).

A NEW DESIGN FOR A COMBINED ELECTRON-IMPACT/ FIELD-IONIZATION ION SOURCE

A. J. Smith, J. P. Mannaerts, T. J. Eskew,
T. L. Strand and P. M. McCartney
Nuclide Corporation, State College, Pa. 16801

INTRODUCTION

A combination Electron Impact/Field-Ionization ion source was built which incorporates most of the improvements made in this type of source over the past several years.[1,2] It is completely compatible with all normal operating modes of the Nuclide 12-90-G organics mass spectrometer and can be used with all of the usual inlet systems.

Major features of the EI/FI source include:

1. Capability for using both blade and wire-type field emitters.
2. Heating capability for wire as well as blade-type emitters to permit use of the Beckey technique[3] for studying thermally unstable compounds by field desorption.
3. Very short changeover time (usually 30 seconds to one minute) between the electron impact and field ionization modes of operation.
4. A vacuum lock and probe for rapidly inserting emitters into the source.
5. Positioning adjustments which operate from outside vacuum for optimizing emitter-cathode spacing, emitter rotation and lateral displacement of the emitter.

DESCRIPTION

The ion source is shown schematically in Figure 1. Typical operating potentials with respect to ground are shown for both the electron impact and the field ionization modes of operation for an ion accelerating potential of 7000 volts. The focussing and accelerating lens is the same one used in previous 12-90-G ion sources. The source operates in the usual fashion in the electron impact mode so those features will not be described. In the remaining comments the field ionization mode of operation will be emphasized except when the electron impact mode must be referred to for comparison purposes.

In the field ionization mode the emitter is inserted into the ion block from the rear. The ion exit slit is used for the field ion cathode. Sample can be introduced into the source with various inlet systems. Ports in the sides of the ion block direct the sample into the ionization region in both modes of operation.

Since the source electrodes require different potentials for operation in the electron impact and field ionization modes, separate voltage divider strings are provided for each. Both resistor strings are mounted on the same chassis and are connected to the ion source through a two-position high voltage switch so that electrical cables do not have to be interchanged when changing from one mode of operation to the other.

The emitter is retracted about one hundred fifty mils when in the electron impact mode so that it will not intercept the electron beam and interfere with the source operation. It can be reinserted to the correct position in a matter of seconds when switching from the electron impact to the field ionization mode.

Figure 2 shows the region around the emitter in detail. The most important consideration in getting the field ion source to work is the geometry of the cathode slit. A square-edged slit 25 mils wide and 25 mils deep gave the highest beam intensity of the several thicker and thinner ones tried. The slit is identical to the one that worked best in the first Nuclide field ion source built in 1965.

Other workers also report that a thick cathode slit rather than a thin slit provides best beam intensity.[4]

Figures 3 and 4 show the probe and vacuum lock respectively. The emitter spacing and rotation mechanisms are permanently attached to the probe shaft. They couple to the vacuum lock through a quick-disconnect arrangement when the probe is inserted. This design enables the operator to remove the probe from the lock without disturbing the rotation or emitter-cathode spacing adjustment.

Emitter-cathode spacing is adjusted by sliding the probe in the vacuum lock. Precision drive is obtained with a 1-1/2-inch diameter concentrically-mounted micrometer; with this arrangement the emitter can be reproducibly positioned to within 1/2 mil with respect to the cathode slit.

Emitter rotation is achieved by rotating the probe in the lock. Two knurled screws facilitate adjustment. The emitter can be rotated $\pm$ 6° with respect to the cathode slit.

The field emitter can also be moved laterally $\pm$ 50 mils with respect to the cathode slit. This motion requires that the entire vacuum lock and probe assembly be moved with respect to the vacuum flange. A flexible metal bellows maintains the vacuum seal. The lock is held fast to the vacuum flange with a stainless steel and brass slide arrangement which allows for lateral movement. The drive is provided by a pair of knurled screws on opposite sides of the lock.

The probe is hollow back to the handle where the vacuum seal is made. The inside of the probe operates under vacuum. It is pumped through a series of small holes located at the probe tip. High voltage and emitter heating current are brought into the probe through a kovar-to-glass seal. Insulated wires along the probe axis make the connection to the probe tip. A pair of insulated pins are used for fastening the blade and wire-type emitters to the end of the probe.

The blade holder is designed to take a 1/4-inch x 3/8-inch section of any standard double-edged razor blade. The blade can be heated to over 300 °C by a small tungsten heater located inside the blade holder for field desorption work.

The wire emitter is a 10 micron diameter tungsten wire. The wire emitter assembly attaches to the two pins on the probe tip in a fashion similar to the blade holder. The wire is heated directly by passing a current through it when using the Beckey field desorption technique.

Both types of emitters are easily interchanged by slipping the emitter holder from the pins and installing a new holder with a previously mounted emitter in place.

RESULTS

The data for Figures 5, 6 and 7 were obtained in the bell-jar test stand which is somewhat representative of the source behavior observed when the source was used with a double-focussing mass spectrometer. The results were similar for both blades and wires.

Figure 5 shows the variation of ion beam intensity as a function of both ion accelerating potential and field ionization potential. The maximum current obtained for conditioned blades and wires for methyl stearate introduced through an all-glass inlet with molecular leak was about 10^{-12} ampere as measured by the total ion monitor in a double-focussing mass spectrometer. Generally speaking, the ion current obtained was about one hundred times greater for a conditioned blade than for a nonconditioned blade. The current from a conditioned 10 micron diameter tungsten wire was about one thousand times greater than the current from an unconditioned wire. The ion current obtained from conditioned blades was about the same as that obtained from conditioned wires. Much higher currents could have been obtained if the operator were more adept during the emitter conditioning process.

Figure 6 shows the ion beam intensity as a function of field emitter-cathode spacing. Beam intensity falls off slowly with increased spacing. This appears to be the least critical of the three emitter positioning adjustments built into this source.

Figure 7 shows the dependence of beam intensity on emitter rotation. Peak intensity with either blades or wires is obtained when the emitter is parallel to the cathode slit. The data shown was obtained in the bell-jar test stand when the source collimating slits were set at about 100 mils. The peak shown has a half-width of 30 degrees. With the mass spectrometer source collimating slit set at 5 mils, the observed half-width of the peak was approximately one-tenth of that shown. Emitter rotation is by far the most critical of the three emitter positioning adjustments and lateral adjustment is almost as important.

Lateral adjustment was somewhat critical in the mass spectrometer where side to side movements of about $\pm$ 1 mil from the optimum position were sufficient to reduce the beam intensity by more than 50%.

In spite of the apparent critical nature of the rotation and lateral adjustments, little difficulty was encountered in using the field ion source with blade-type emitters. Once the lateral and rotation adjustments were optimized for a blade, the probe could be withdrawn, a new blade installed and an ion beam obtained immediately after the probe was reinserted. More difficulty was experienced with the wire emitter because its holder did not provide the same precise alignment as the blade-holder did.

With the blade or wire emitter position optimized, it was possible to alternately switch between the electron impact and field ionization modes of operation and still return to within about 10% of the initial field ion current- without having to reset either the lateral or rotation adjustments.

Figure 8 shows a recording made on a double-focussing mass spectrometer with a two-pen strip chart recorder. One pen displays the total ion current for methyl stearate while the other displays the parent and P+1 ion peaks as obtained at the output of the electron multiplier. Note that the ion current in both cases is quite stable and that the fluctuations in both cases are only about $\pm$ 1.5%.

Figure 9 is a computer print-out of methyl stearate mass spectra obtained in both the electron impact and field ionization modes of operation. Typically, a 1/2-milligram methyl stearate sample introduced through an all-glass inlet with molecular leak produces a parent ion beam of about 10^{-12} ampere in the electron impact mode and 10^{-13} ampere in the field ionization mode.

When all fragment ions in these spectra are taken into account, one finds that the ion source efficiency is about two orders of magnitude greater in the electron impact mode than in the field ionization mode. Comparable results are also obtained when the total ion monitor currents for each mode are compared. However, sensitivity comparisons of this type are unfair and should not be taken too seriously. Enhancement of the parent ions of certain compounds achieved with field ionization sometimes make it appear that this rather than electron impact ionization is the more sensitive mode of operation. The fact is that field ionization and electron impact ionization are complementary modes of operation and one cannot entirely replace one with the other.

The authors wish to thank W. K. Rohwedder of the U. S. Department of Agriculture in Peoria for his assistance in designing this source.

REFERENCES

1. E. M. Chait, T. W. Shannon, W. O. Perry, G. E. Van Lear and F. W. McLafferty, International Journal of Mass Spectrometry and Ion Physics, 2 (1969), 141-155.

2. P. Schulze, B. R. Simoneit and A. L. Burlingame, International Journal of Mass Spectrometry and Ion Physics, 2 (1969), 181-193.

3. H. D. Beckey, International Journal of Mass Spectrometry and Ion Physics, 2 (1969), 500-503.

4. J. P. Pfeifer, A. M. Falick and A. L. Burlingame, Proceedings of the Nineteenth Annual Conference on Mass Spectrometry and Allied Topics (1971), pp. 52-57.

PUBS 1269-0672

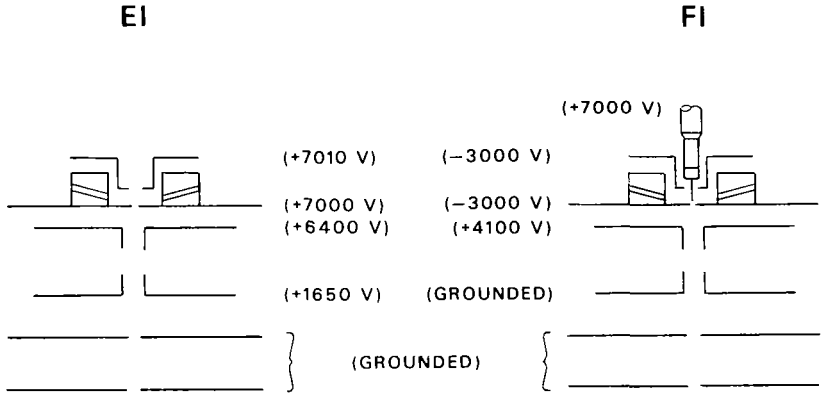

Fig. 1. Schematic Representation of Combined Electron Impact/Field Ionization Ion Source.

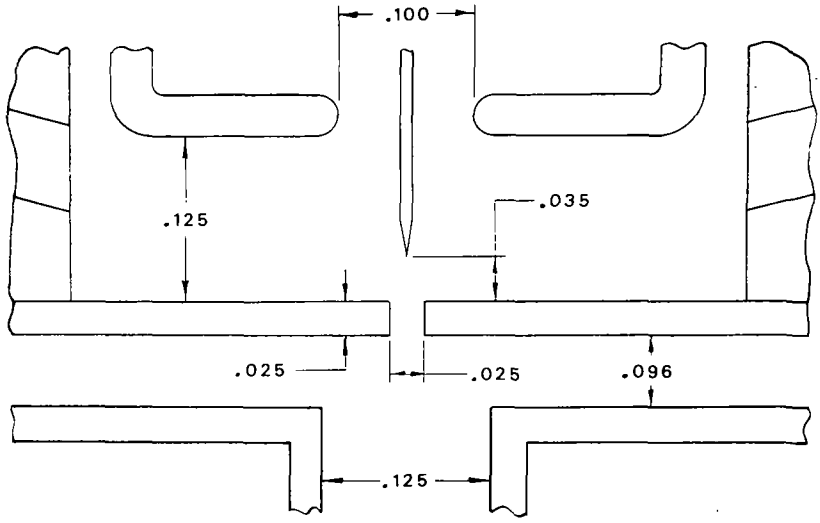

Fig. 2. Field Ion Source Dimensions.

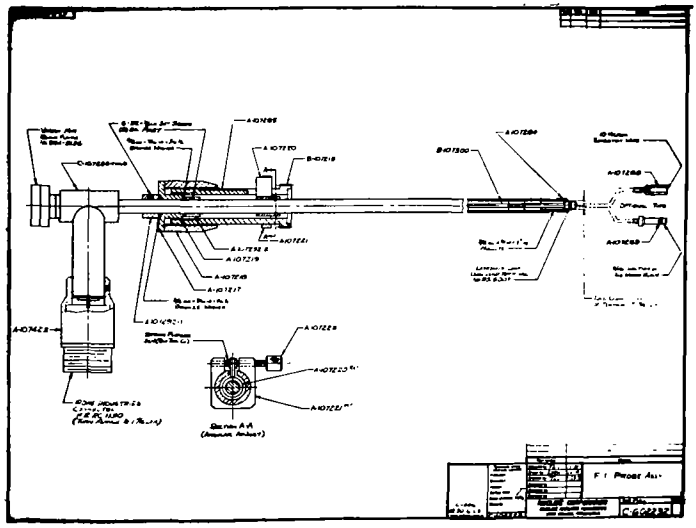

Fig. 3. Field Emitter Insertion Probe.

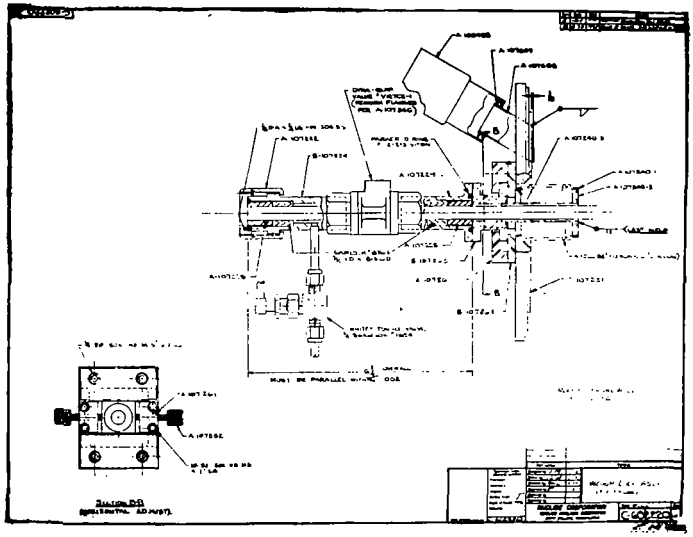

Fig. 4. Vacuum Lock.

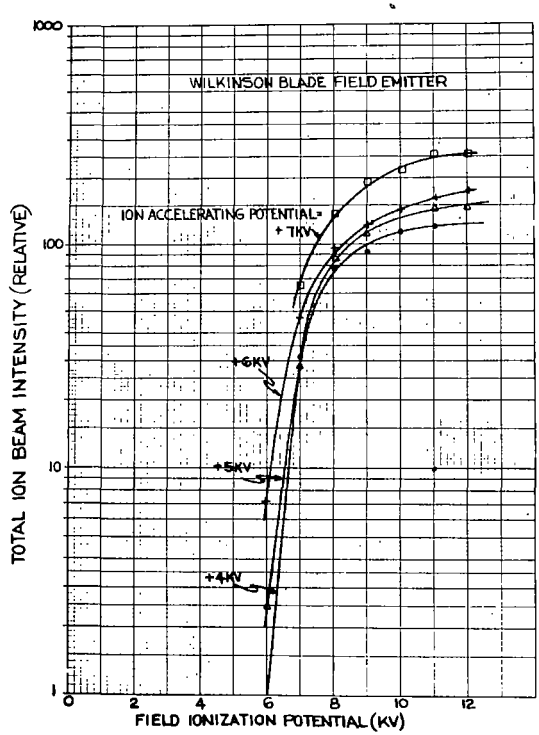

Fig. 5. Effect of Ion Accelerating Potential and Field Ionization Potential on Total Ion Beam Intensity.

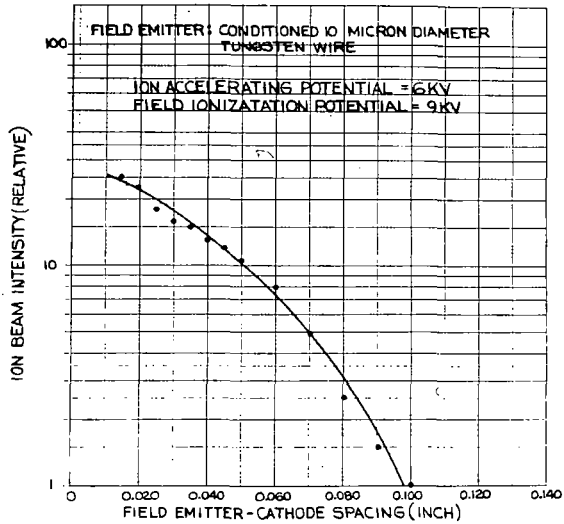

Fig. 6. Effect of Field-Emitter-Cathode Spacing on Total Ion Beam Intensity.

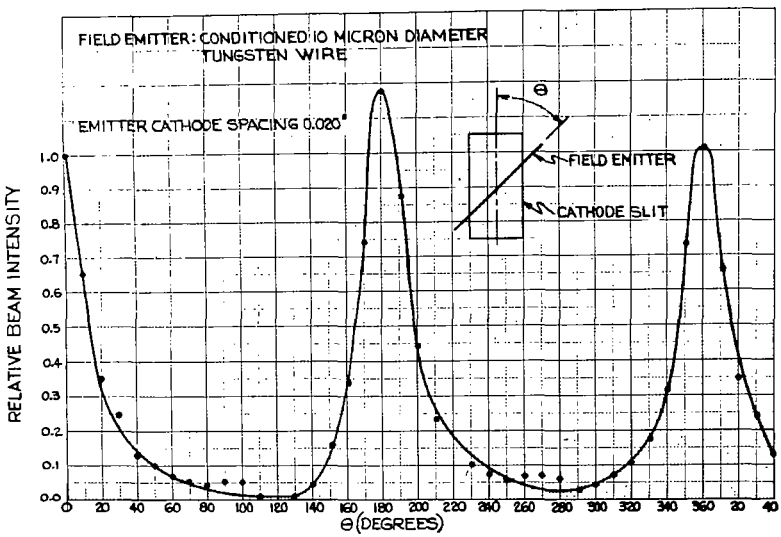

Fig. 7. Effect of Field Emitter Rotation on Total Ion Beam Intensity.

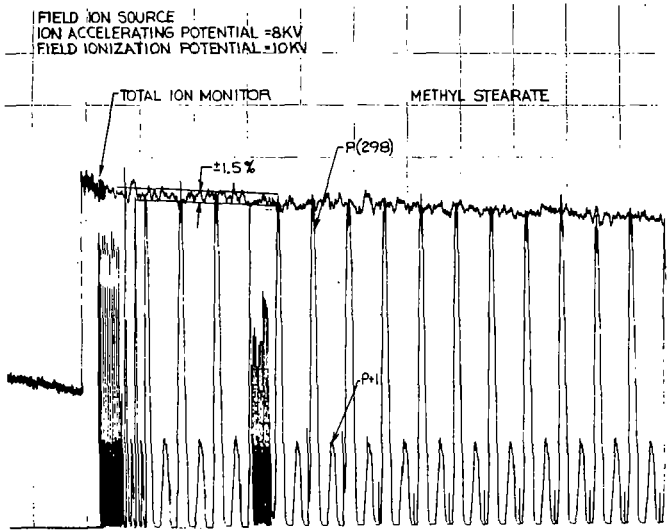

Fig. 8. Ion Beam Stability.

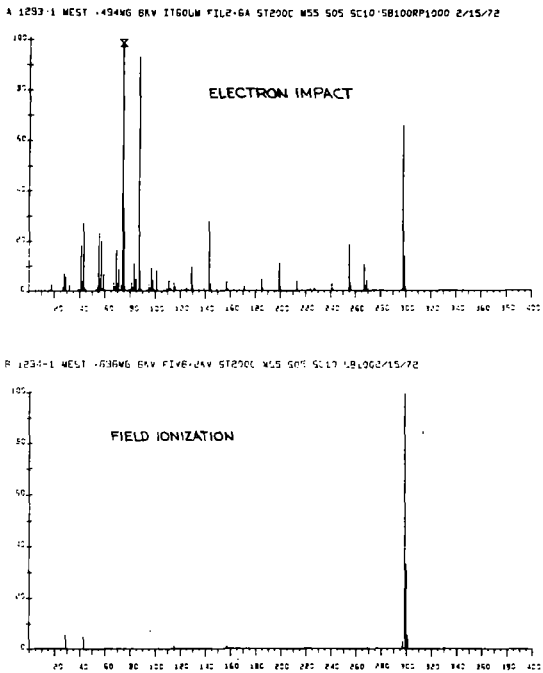

Fig. 9. Computer Print-out of Methyl Stearate Mass Spectra for Electron Impact and Field Ionization Modes of Operation.

APPLICATION OF THE ION-DRIFT SPECTROMETER TO MACROMASS SPECTROSCOPY 02

J. Gieniec, H. L. Cox, Jr., D. Teer and M. Dole
Department of Chemistry, Baylor University, Waco, Texas 76703

The current state of development of producing intact gas phase macromolecules by the electrospray process for use in a macromass spectrometer (MMS) has been reported[1-4] and will only be summarized. In the MMS we produce gaseous suspensions of macroions by a process of electrohydrodynamic atomization (or electrospray) of solutions of macromolecules. The resulting charged droplets containing macromolecules split into smaller droplets due to electrostatic forces as they evaporate in gas at atmospheric pressure. Charged macromolecules remain in gaseous suspension and are injected into a nozzle-beam system for subsequent mass analysis. In this way, we hope to produce mass spectra of polydisperse synthetic polymers and/or monodisperse biopolymers. Low resolution analyses have indicated that intact macroions can be produced and analyzed in this way.

To aid in the interpretation of the data obtained in our researches on the MMS, we have been studying the electrical mobilities of aerosol particles obtained in the electrospraying of solutions. A modified version of the Plasma Chromatograph manufactured by Franklin GNO Corporation is used to measure these mobilities. The stock model of this instrument has been used to measure the mobilities of low and intermediate molecular weight compounds.[5-7]

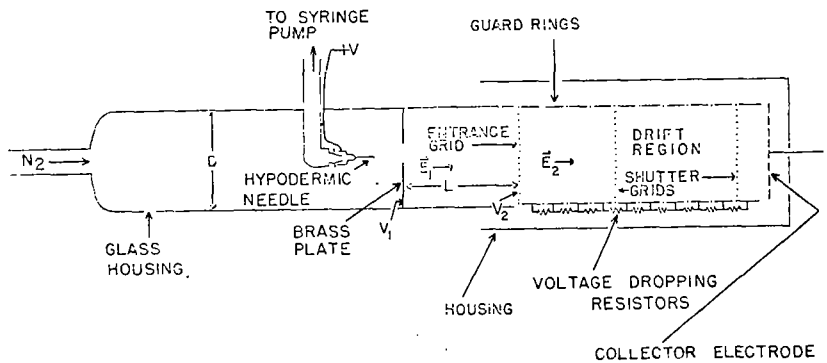

FIGURE 1 - Schematic of Plasma Chromatograph Cell and Spraying Apparatus.

Figure 1 shows a simplified schematic of the ion drift spectrometer portion of the plasma chromatograph and the electrospray system used. The solution is delivered at a constant rate to a 27 gauge hypodermic needle via teflon tubing by a syringe pump. A high voltage relative to the nearby plate is placed on the hypodermic needle creating a strong electric field at the tip. As the solution arrives at the tip, the action of the electric field disperses the liquid into a finely divided aerosol. Dry nitrogen gas is fed into the rear of the spray tube. This gas flow provides a mechanism to sweep the ions downstream and also to supply heat to the droplets as they evaporate and undergo spontaneous fission.

The ions are coupled directly into the drift cell and are moved along the cell at a constant velocity by the electric field established by the guard rings which are kept at proper voltages by the string of resistors. Two Bradbury-Nielson type electrical shutter grids control the flow of ionic current. Opening and closing of the first shutter grid admits discrete ion pulses into the analyzing region where they are separated according to their mobilities.

If the second shutter grid is opened and closed at the proper delayed time, ions of a selected mobility pass through this grid and are collected on the detector electrode, the resulting current amplified by a vibrating reed electrometer and fed into an x-y recorder. By proper

phasing of the opening and closing of the two shutter grids, complete spectra of the mobilities of the ions can be obtained.

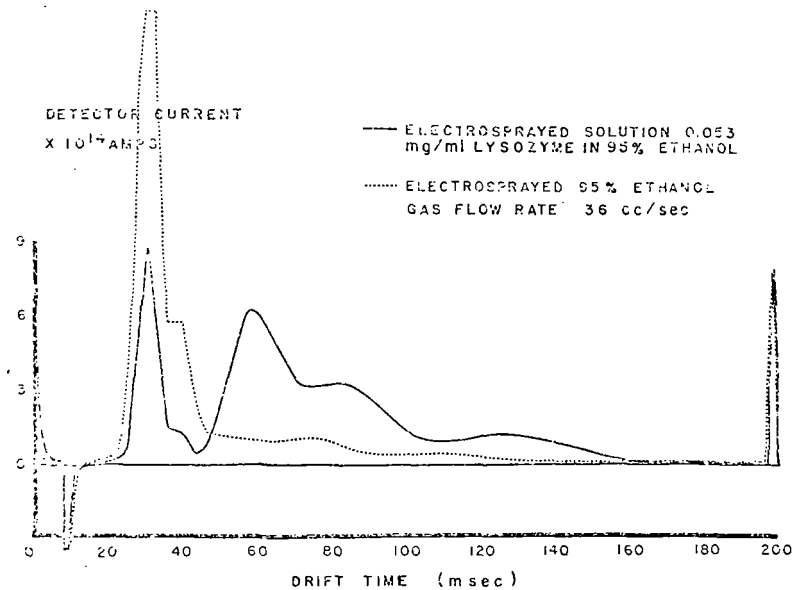

FIGURE 2 - Plasmagram of Electrosprayed Solutions,

Figure 2 shows two scans obtained in this way. Since a trace of water is required to prepare the lysozyme solution (approx. 0.5% V/V) a similar amount of water was added to the ethanol without lysozyme.

Several characteristics are immediately evident. There is a distinct difference between the two spectra. Two peaks from each spectrum appear at approximately the same position on the time scale. The peaks are fairly broad and there is some overlap of peaks in each spectrum.

With regard to the first two peaks, it has been observed that these peaks also occur when no solution is present in the spraying system but with high voltage applied to the hypodermic needle. When the needle to plate voltage is reduced to 3.5 kV, these peaks vanish. The origin of these ions has not yet been determined. However, either the production of these ions is partially quenched by the presence of the lysozyme in the solution or some of the smaller ions combine with the larger ones.

In regard to the width of the peaks, the width of the ion pulses and the time which the second shutter grid remains open is 5 msec. Therefore, all ion peaks observed should have at least 10 msec full width. Diffusion and ion-molecule reactions can also contribute to the broadening. These effects will add to any dispersion in the ion mobility spectrum. A modified design, currently in the planning stage, will reduce these effects.

Note that the peak with the longest drift time is centered at about 125 msec. For the conditions used, this indicates a mobility of 0.26 (cm/sec)/(V/cm). Researchers at Franklin GNO have observed a correlation between mass and drift time in the Plasma Chromatograph. Extrapolation of their data to higher masses which, by the way may not be valid, indicates a mass for this peak between 12 and 16 kamu. Since the mass of the lysozyme molecule is 14 kamu, it is possible that this peak is due to a singly charged lysozyme ion.

The next fastest ion species has a drift time of approximately 85 msec. Similarly, this could indicate a mass between 4 and 6 kamu. However, since drift time is inversely proportional to the charge, it could

also represent an ion with mass between 24 and 36 kamu but with two charges. Such a species could be formed by the combination of two singly charged lysozyme monomers.

The next fastest ion peak has a drift time of approximately 60 msec. Since the drift time is inversely proportional to the charge, it is easy to see that, within the resolution afforded, this could represent a doubly charged lysozyme ion. Since the two peaks of fastest ions occur without a solution, we shall not consider them at this time.

The interpretation of our data up to this point has been speculative. The reason for this is the length of extrapolation from available data. As new data become available at higher masses, the mass estimates should become more precise. As an interim procedure, we plan to collect some of the ions from each of these three peaks on an electron microscope grid. If we are able to observe the molecules directly, we will then be able to make a more positive identification.

In the configuration of the experimental apparatus, the gas from the spraying chamber passes through the drift cell along with the ions. This flow of gas will add to the velocity of the ion and make the drift time shorter. In figure 3, this effect is shown. The solid line was taken from figure 2. The dashed line is a similar scan but with the gas flow trebled. If we ignore losses of gas through the interstices between the guard rings, the flow rates indicated correspond to axial gas velocities of 3 and 9 cm/sec. An ion with a 120 msec drift time would have a velocity of 50 cm/sec. Thus the gas velocity will add substantially to the apparent velocity. In figure 4, we show a scan taken with the gas flow increased to 7 times that of figure 2 and corresponding to a velocity of approximately 21 cm/sec. In this figure, the peaks have been squeezed so closely together that almost all detail is lost.

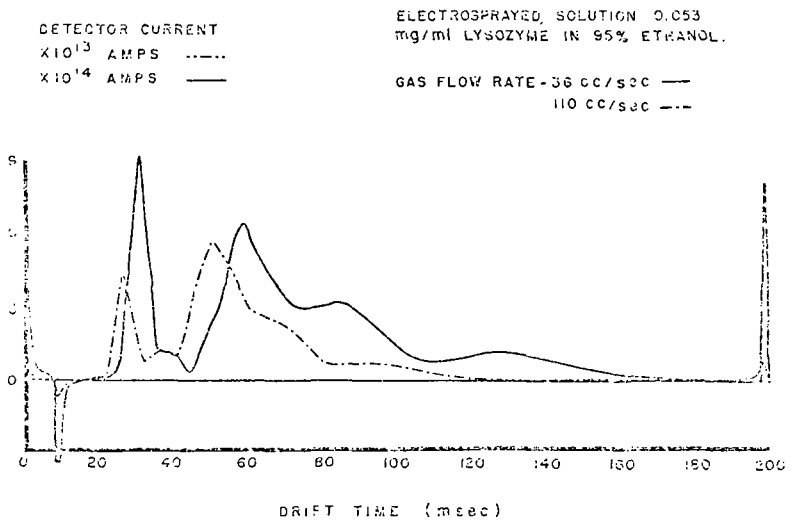

FIGURE 3 - Plasmagram of Electrosprayed Solutions.

If the effect of the flow gas velocity were purely additive, we should be able to plot the apparent velocity of the ions versus the relative gas velocity and obtain a straight line. Figure 5 shows such a plot.

These data were obtained from scans similar to figures 2-4. Although the relations are roughly linear, the slopes are not the same for all species. For comparison purposes, the dashed line represents the idealized slope placed in an arbitrary position on the velocity scale. The slope of this line is somewhat greater than those obtained from the

data. This could be caused by the ions changing their identity slightly or by the increased proportion of nitrogen as compared to solvent vapors. The ions would tend to drift faster in the gas less rich in solvent vapors. We are currently devising techniques to extract the ions from the moving gas and inject them into dry nitrogen gas in the drift cell.

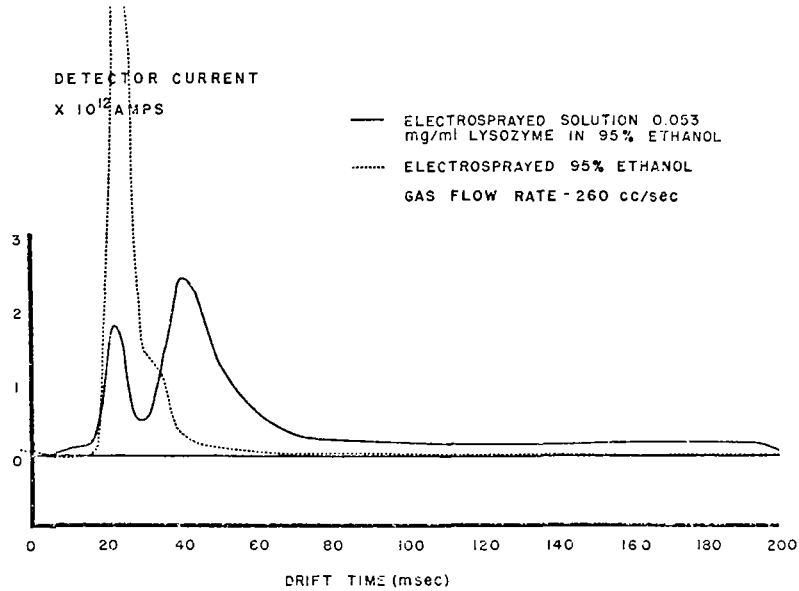

FIGURE 4 - Plasmagram of Electrosprayed Solutions.

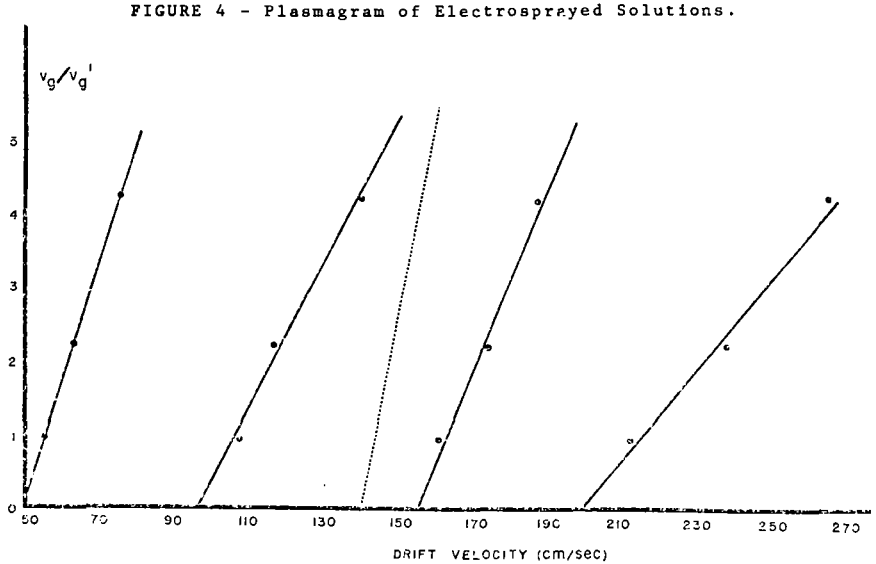

FIGURE 5 - Change in Drift Velocities with Changes in Gas Flow Velocity.

There are many facets of this research, some good, some bad which we have not discussed. However, the net result is that we are optimistic about the future of this research.

In conclusion we would like to extend grateful thanks to Roger Wernlund and Martin Cohen of Franklin GNO whose continued interest,

encouragement and assistance were of incalculable benefit and to the National Science Foundation whose financial support (grant 27-521) made this research possible. We have also benefited from income from the chair in chemistry established at Baylor University by a gift from The Robert A. Welch Foundation.

REFERENCES

1. Dole, M., Hines, R. L., Mack, L. L., Mobley, R. C., Ferguson, L. D., Alice, M. B., J. Chem. Phys. 49, 2240 (1968).

2. Mack, L. L., Kralik, P., Rheude, A., Dole, M., J. Chem. Phys. 52, 4977 (1970).

3. Clegg, G. A., Dole, M., Biopolymers 10, 821 (1971).

4. Gieniec, J., Ph.D. Dissertation, Dept. of Physics, University of Wisconsin, 1971, pp. 38-42.

5. Carroll, D. I. and Mason, E. A., Proceedings of the 18th Annual Conference on Mass Spectrometry and Allied Topics, May 1971, p 315.

6. Kilpatrick, W. D., Proceedings of the 18th Annual Conference on Mass Spectrometry and Allied Topics, May 1971, p 321.

7. Karasek, F. W., Anal. Chem. 43, 1982 (1971).

A NEW DYNAMIC MASS SPECTROMETER FOR THE ANALYSIS OF MACROMOLECULES

R. PAQUIN and M. BARIL
Département de Physique,
Université Laval, Québec, CANADA.

ABSTRACT

A theoretical study has demonstrated the possibility of a new type of dynamic mass spectrometer for the analysis of macromolecules, which presents good resolving power in spite of the chromatic aberration of the macroion source. This aberration is reduced by adding a monochromator which modifies the initial velocity distribution of a pulsed beam in such a way that only ions of a specific mass become monokinetic by increasing the energy of each ion by an amount which depends on the distance travelled after a predetermined time.

INTRODUCTION

In recent years, a new technique of measuring molecular weight and molecular weight distributions of samples of high molecular weight compound by means of a mass spectrometric type technique has been developed. Previous work[1,2,3] has shown that the electrospray technique can produce intact gas phase macromolecules of variable charge. When these ionized intact macromolecules are seeded in a supersonic molecular beam, their velocity becomes equal to the velocity of the beam in a few thousands collisions which take place very rapidly. Therefore all the macromolecules have about the same velocity.

Their kinetic energy is then proportional to their mass and can be easily measured if their state of charge is known. The mass spectrum is obtained from the energy spectrum.

If one employs an energy analyzer as a mass discriminator, the resolving power in terms of mass will be dependent on the resolving power of the energy analyzer and also on the velocity dispersion of the macroions. According to the relation $E = \frac{1}{2} mv^2$, the mass resolution of the spectrometer is determined by

$$\frac{\Delta E}{E} = \frac{\Delta m}{m} + \frac{2\Delta v}{v}$$

where $\Delta E/E$ is the relative energy resolution of the energy analyzer, $\Delta m/m$ is the resolving power in terms of mass and $\Delta v/v$ the relative velocity distribution of macroions.

One way of improving the resolving power is to reduce the velocity distribution, which is accomplished by introducing a velocity monochromator in the system. Fig. 1 shows schematically the action of the monochromator.

OPERATION

The principle and design of our technique of velocity monochromation is based on the following consideration. The macroion possess the same mean velocity and about the same velocity distribution whatever their mass.

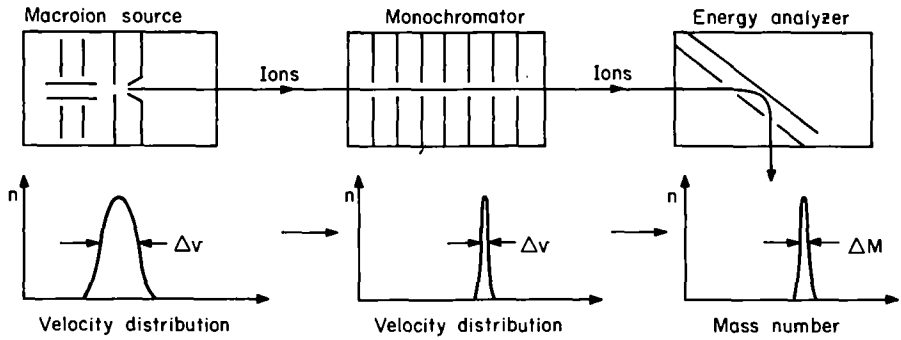

Figure 1 - Schematic illustration of a dynamic macroion mass spectrometer.

The beam of macroions is chopped in narrow pulses which drift into a drift tube of a certain length L. Before entering into the correcting element the macroions are spatially separated (the fastest ones preceding the slowest ones) so that the length of the ion pulses in approximately equal to the dimension of the correcting system. Fig. 2. If v_+ is the velocity of the fastest particule and Δv the velocity distribution, the length of the ion pulses at the end of the drift tube is expressed by:

$$x_m = \left(\frac{\Delta v}{v_+}\right) L$$

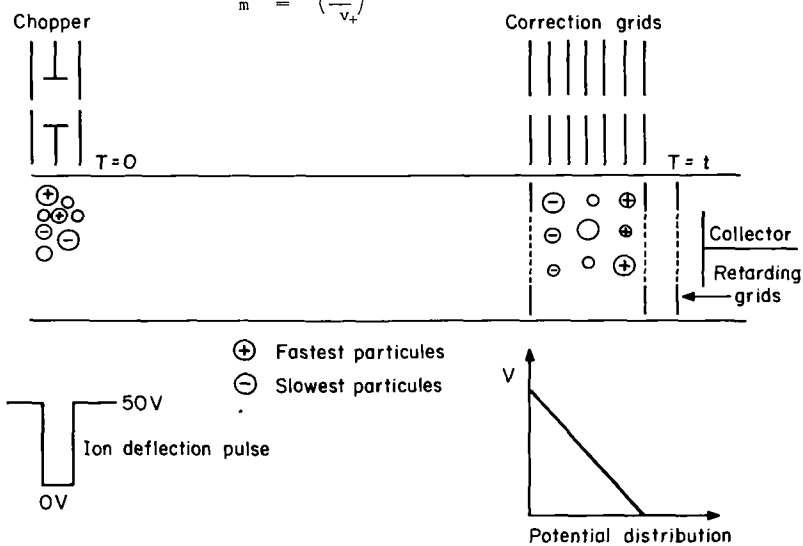

Figure 2 - Dynamic time-of-flight monochromation.

At the time the ion pulses enter into the correcting system, all grids or electrodes are at ground potential. When the pulses of macroions completely fill the correcting element, a potential is instantly applied to the grids and maintained constant until the pulses of macroions have completely passed through the correcting element.

Many kinds of corrections can be used depending on what velocity has been chosen for the beam to possess after it passed the correcting element. The correction we chose for the sake of simplicity in mechanical construction and in the design of the electronic circuit accelerates the macroions so that their velocity is increased up to that of the fastest ones.

To satisfy this condition, the energy increment given to a single charged ion can be written:

$$\Delta E(u) = E_+ - E(u) \qquad 0 \leqslant u \leqslant 1 ,$$

where ΔE is the energy increment, E_+ the energy of the fastest particule, E is the energy of an ion and u is a dimensionless variable which indicates the position of an ion inside the monochromator (u = 0 entrance; u = 1 exit). The potential distribution inside the correcting element, which permits such an energy increment, is held constant as a function of time and can be written:

$$V_{corr}(u) = \frac{\Delta E}{q}(1 - u) + \left(\frac{E_+}{q}\right)\left(\frac{x_m}{L}\right)^2 u(1 - u) \qquad 0 \leqslant u \leqslant 1$$

where $V_{corr}(u)$ is the potential distribution and q the charge of the macroion. If the velocity distribution is small compare to the highest velocity, $\Delta v << v_+$, we can write $x_m << L$ and $(x_m/L)^2 \simeq 0$ and obtain this simple relation fig. 2.

$$V_{corr}(u) = \frac{\Delta E(u)}{q}(1 - u) \qquad 0 \leqslant u \leqslant 1$$

RESULTS

The technique we just described has been analyzed theoretically and verified experimentally using Cesium ions. The drift length is of the order of 1 meter. Fig. 3 shows experimental results for a beam which has a 20 eV energy dispersion over a mean energy of about 150 eV. After the correcting element, using a 45° plane mirror as the energy analyzer, the base width is only five volts. We may conclude that our technique of correction is good and should be applied to the macromass spectrometer.

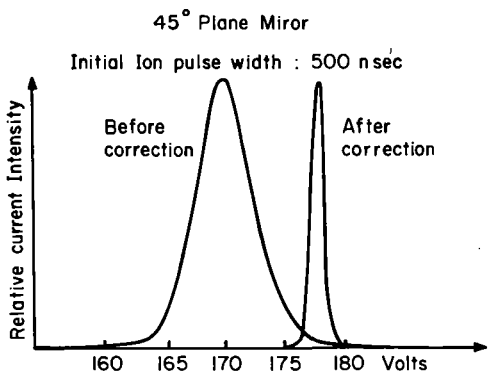

Figure 3 - Energy distribution.

REFERENCES: 1) M. Dole and al., J. Chem. Phys. 49, 2240, 1968. 2) L.L. Mack and al., J. Chem. Phys. 52, 4977, 1970. 3) G.A. Cligg and M. Dole, Biopolymers 10, 821, 1971.

AN ELECTROHYDRODYNAMIC ION SOURCE FOR MASS SPECTROMETRY

04

C. A. Evans, Jr. and B. N. Colby,

Materials Research Laboratory

and

C. D. Hendricks,

Charged Particle Research Laboratory

University of Illinois, Urbana, Illinois 61801

Electrohydrodynamic (EH) ionization of liquid metals producing primarily singly charged monoatomic species has been achieved. A high electric field applied between a needle tip and extractor electrode causes liquid metal at the needle tip to point up and form a cone. Ionization of the liquid occurs at the tip of the cone and is stabilized by a current regulator circuit. The current measured at the needle was up to 30 μamp. Material depletion at the tip was compensated for by a continuous mechanical feed system for the liquid. Spectra of Ga-In eutectic alloy and the same alloy doped with various amounts of Cd, Sn, Hg, Cu and Pb were obtained using the EH ion source on an AEI MS-7 double focusing mass spectrometer. The predominant ions produced were the singly charged, monoatomic species. Some multiply charged and molecular species were also present. Potential uses of the EH ion source are the on-line analysis of liquid metals, a source for ion implantation, a primary ion source for secondary ion mass spectrometry and, most important, a means of ionization for nonvolital organic compounds.

Details of the EH ion sources istrumentation are contained in a paper submitted to the Review of Scientific Instruments and experimental details are to be found in a paper submitted to Analytical Chemistry. This work was partially supported by the Advanced Research Projects Agency under contract HC 15-67-C-0221 and the U.S. Air Force Office of Scientific Research under Grant AFOSR-68-1508.

MASS SPECTROMETRIC AND OPERATIONAL STUDIES OF ELECTROHYDRODYNAMIC IONIZATION

B. N. Colby and C. A. Evans, Jr.,
Materials Research Laboratory
University of Illinois, Urbana, Illinois 61801

Improvements in the electrohydrodynamic (EH) ion source have been made which allow extended operation at up to 200 μamp of needle current. These include easy adjustment of needle position in the extraction electrode operature and a collection cup. The source operating mode may be identified by observation of the collector cup current with an oscilloscope. The extractor electrode was operated at a high voltage (-5 kv) to provide sufficient electric field strength for ionization without exceeding the maximum accelerating voltage (+8 kv) of the MS-902.

Using the improved EH ion source, spectra were taken of a Ga-In-Sn eutectic alloy and Cerrolow 117. The Cerrolow 117 is a commercially available alloy of Bi, Pb, Sn, In, Cd and a minor amount of Hg impurity. It has a melting point of 117°F and consequently it was necessary to operate the ion source at an elevated temperature. The spectra of both these alloys were dominated by the plus one monoatomic species. The weight percent of the elements in Cerrolow 117 was calculated from the peak heights of the singly charged monoatomic species and corrected only for isotopic abundance. These calculated values agreed to within better than a factor of two with the values given by the manufacturer.

A paper containing the details of these experiments will be submitted to the Journal of Applied Physics in the near future. This research was supported by the Advanced Research Projects Agency under Contract HC 15-67-C-0221.

Geometry Reversal of a Commercial Mass Spectrometer for Metastable Data Collection

T. Wachs, P. F. Bente, III, I. Sakai and F. W. McLafferty
Department of Chemistry, Cornell University, Ithaca, N.Y. 14850

Paper in press:

Int. J. Mass Spectrom. Ion Phys., 9 (1972)

INSTRUMENTAL PARAMETERS DETERMINING THE PERFORMANCE OF A HIGH RESOLUTION MASS SPECTROMETRIC SYSTEM

A. L. Burlingame, J. J. Chang and P. T. Holland

Space Sciences Laboratory
University of California, Berkeley, California 94720

Optimization of the mass spectrometer operational parameters implies adjustment of the resolution, gain and scan-rate such that the best possible mass measurements can be made on peaks with a wide range of intensities from a given amount of sample flowing into the source. An understanding of the various factors influencing these settings can aid the day to day running practice as well as allow critical evaluation of the performance of a HRMS system to computer.

In the following discussion it will be assumed that the mass spectrum is obtained by an electrically recorded, exponentially decreasing magnetic scan and covers 1 - 2 decades in mass. The amplifier bandwidth and data acquisition parameters are assumed to be consistent with resolution and scan rate. The mass measurement accuracy is assumed to be without random or systematic error due to ion-beam position instability or method of calculation.

The critical parameter describing the performance of a mass spectrometer is the variation of the intensity of the ion-beam with resolution for a given sample flow rate through the source. If the time to scan a decade in mass is t_{10} and the time per peak is t_p, the number of ions in a peak, N_p, (assuming an approximately triangular peak shape) is given by

$$N_p = \frac{1}{2} \frac{t_p}{t_{10}} \mu S Sr I \qquad (1)$$

where μ is the quantity of sample passing through the source in time t_{10}, and I is the intensity of the peak expressed as a fraction of the total ionization. S is the absolute sensitivity of the source expressed as the number of ions produced for a given sample flow rate and is determined at standard conditions of ionizing current, ionizing energy and source and collector slit settings. Sr is the sensitivity relative to S at some other source and collector slit settings required to give a desired resolution. Convenient standard slit settings for our modified MS-902 would be W_s = 5 mils and W_c set for 100% transmission. Then, at some other source and collector settings, W_s and W_c

$$Sr = \frac{W_s}{S} \quad x\% \text{ transmission of collector}$$

For an exponential scan $$t_p = \frac{t_{10}}{\delta \log_e 10} = \frac{.435\ t_{10}}{\delta} \qquad (2)$$

where $$\delta = \text{resolution} = \frac{M}{\Delta M}$$

so that $$N_p = \frac{.435}{2\delta} \mu S Sr I \qquad (3)$$

The factor governing the mass-measurement accuracy from these peaks is the accuracy of determination of the time of arrival of successive peaks. The weighted mean of the peak area (i.e., the mean) can be shown to be the best measure of peak position [1]. If the frequency distribution of the sample mean approximates to normal then the standard deviation of the mean [2] is

$$\sigma = \frac{a}{\sqrt{6N_p}} \qquad (4)$$

where a is half width and N_p is the number of events contributing, and therefore,

$$\sigma = \frac{10^6}{\delta\sqrt{24N_p}} \quad \text{ppm} \qquad (5)$$

Thus, at a given resolution, determination of the number of ions in the peaks should allow an estimate of their mass-measurement precision.

By combining Eq. (3) and Eq. (5) we can derive

$$\mu = \frac{10^{12}}{5.22\ \sigma^2\ \delta\ Sr\ SI} \tag{6}$$

or

$$\sigma^2 = \frac{10^{12}}{5.22\ \mu\ \delta\ Sr\ SI} \tag{7}$$

Thus, we can compute the sample size required to attain a given mass measurement accuracy at a given resolution. Conversely, we can compute the attainable mass measurement accuracy for a given sample flow rate and resolution.

The use of these equations requires the evaluation of S and Sr for the instrument in question. Sr may be determined by measurement of the relative sensitivity for various resolutions or could be computed from the ion-optical properties of the instrument. The absolute sensitivity can in principle be determined for the instrument and sample under consideration. However, it is instructive to use the equations to compare the behavior expected at one resolution with that of another resolution.

From Eq. (7) it is easy to show that

$$\sigma_2 = \sqrt{\frac{\mu_1\ \delta_1\ Sr_1}{\mu_2\ \delta_2\ Sr_2}}\ \sigma_1 \tag{8}$$

where the subscripts refer to the two different operating conditions.

If the sample flow is assumed constant between the two conditions, i.e., $\mu_1 = \mu_2$, then Eq. (8) can be used to predict the mass measurement accuracy at one resolution from that obtained at a different resolution, if the δSr characteristic is known for the instrument. Table I shows such data which we have obtained for our modified MS-902 spectrometer.

TABLE I

δ	Sr	δSr
2500	0.7	1750
5000	0.35	1750
7500	0.215	1613
10000	0.14	1400
15000	0.058	870
20000	0.03	600
25000	0.014	350
30000	0.007	210

Examination of Table I shows that the δSr product remains approximately constant from a resolution near 2500 to about 10000. Thus, we would predict from Eq. (8) that the mass measurement accuracy should be independent of resolution in this range. However, for resolving powers greater than 10000 the δSr product decreases so that the mass measurement accuracy degrades if μ is constant.

We can, for example, estimate the behavior expected at a resolution of 30000 compared to that at 10000. If we maintain the same sample flow, i.e., μ is constant, we would predict a degradation of mass accuracy at δ = 30000 to 2.58 times that attained at a resolution of 10000. It is then relevant to consider what parameters can be

changed to improve this number. Eq. (8) shows that the important parameters are the sample flow rate and the δSr product.

The sample flow rate may be changed in two ways. One method is to increase the quantity of sample flow. The second method is to increase the scan time, recalling that μ is the sample flow during time t_{10}. If the scan time is doubled, $\mu_2 = 2\mu_1$, and the mass accuracy is improved to $\sigma_2 = 1.83\ \sigma_1$. In our operation this involves changing our scan speed from 16 seconds per decade to 32 seconds per decade. Although further improvement in accuracy is possible by a further increase of scan time, such an increase is undesirable because of operational considerations.

Further improvements are possible only by changing the relative sensitivity which requires modifications to the instrument. Because of fringing magnetic fields which cause image curvature, the height of the ion beam is usually restricted. We have recently installed a hexapole lens accessory for our MS-902 which should correct image curvature and, therefore, permit operation with an increased height of the ion-beam. We expect a sensitivity increase of at least a factor of 2 and hopefully a factor of 4. If the sensitivity increased by a factor of 2, in addition to the increased scan time above, the accuracy at δ = 30000 relative to δ = 10000 should be $\sigma_2 = 1.29\ \sigma_1$.

To test these predictions we have obtained data for perchlorobutadiene with our modified MS-902, both at a resolution of 10000 without hexapoles and at a resolution of 30000 with hexapoles. The scan time for the δ = 30000 data was twice the scan time for δ = 10000. The hexapoles provided slightly better than a factor of two increase in relative sensitivity at δ = 30000. As expected the data obtained at a resolution of 30000 showed slightly worse mass measurement errors than the data at a resolution of 10000. The range of errors was larger for the 30000 resolution data than for the 10000 resolution data.

A more comprehensive account of this work will be submitted to Analytical Chemistry.

References

1. A. E. Sarhan, Ann. Math. Stat. 25, 317 (1954).
2. A. J. Capmbell and J. S. Halliday, ASTM E-14 Committee, 13th Annual Conference on Mass Spectrometry, St. Louis (1965).

A Miniature Mattauch-Herzog Mass Spectrometer

J. P. Carrico
Bendix Research Laboratories
Southfield, Michigan 48076

E. Schaefer and J. Rice
Bendix Aerospace Systems Division
Ann Arbor, Michigan 48107

A miniature double-focusing mass spectrometer based on the Mattauch-Herzog configuration has been developed by Bendix for planetary applications. Instrument design, construction details, and tests results are discussed. The electric field radius is 4.27 cm. Ion detectors were placed in the magnet focal plane at positions corresponding to 0.96 cm and 2.54 cm. The mass range is 1 - 50 AMU. Using a detector slit width of $\sim$0.025 cm we obtained a sensitivity of the order of 4×10^{-5} ion amps/torr for N_2 and were able to resolve the 44, 45, and 46 AMU peaks of CO_2. Instruments of this type have been developed by Nier and co-workers for upper atmosphere research and for the Viking mission to Mars in 1976.[1]

A paper describing the details of this work is being prepared for publication.

[1] See for example, A. O. Nier and J. L. Hayden, International Journal of Mass Spectrometry and Ion Physics 6, 399 (1971).

A MASS SPECTROMETER SYSTEM TO DETERMINE LOW LEVELS OF HELIUM IN SOLIDS

09

Harry Farrar IV

Atomics International Division, North American Rockwell Corporation
Canoga Park, California 91304

ABSTRACT

A small gas mass spectrometer system operating in the static mode is being used to measure helium concentrations as low as 10^{-11} atom fraction in milligram size solid specimens. The helium, which is produced in nuclear reactors by various (n,α) reactions, can adversely affect material properties. The mass spectrometer system has a number of refinements over other similar systems which have led to simplicity of operation and low detection limits. A determination of the helium content is made by weighing a milligram size piece of the material of interest, and melting it in a furnace under vacuum. Just before the ^4He is released, a precisely known quantity of ^3He spike is added. After the mixing of the isotopes, the gas passes over getters directly into the isolated mass spectrometer volume where the $^4He/^3He$ ratio is measured. Numerous determinations of helium in neutron-irradiated pure elements, compounds and alloys, and in α-injected steel specimens have been made routinely. The high sensitivity has made possible the measurement of spectrum integrated (n,α) cross sections after relatively short neutron irradiations.

I. INTRODUCTION

Helium produced by nuclear reactions contributes toward changes in the physical properties that generally occur in neutron irradiated alloys. The neutrons, especially those with higher energies, knock α-particles out of the nuclei of the principal and impurity elements. These α-particles become helium atoms, which accumulate in a year or so to concentrations ranging between 10^{-6} and 10^{-3} atom fraction, depending on alloy, type of reactor, and core location. At these concentration levels, the helium can have both direct and indirect effects on the mechanical properties of the alloys.

At present, the (n,α) cross sections of the principal elemental components of the commonly used alloys are insufficiently well known. Even the importance of some of the trace elements is difficult to assess in the absence of reliable cross section information. To solve this problem, so that helium generation rates may be predicted accurately, and so that alloys can be selected that perhaps minimize or eliminate certain elements, the integrated (n,α) cross sections of essentially all elements of interest are being determined at Atomics International. Irradiations of small specimens of the elements in metallic, crystalline or compound form are being followed by precise high sensitivity mass spectrometric measurement of the helium generated.

Initial efforts to measure helium in steels and beryllium were made with a spark-source double-focusing mass spectrometer.[1] The analyses were, however, hindered by the fact that helium was found to have a very low relative sensitivity (S_R) with respect to iron in a stainless steel matrix, and by an interference at the mass 4 position with the ions $^{12}C^{3+}$ and $^{16}O^{4+}$ at long exposures. As a result, a detection limit of no better than 1 appm for helium in metals whose O and C contents were $\sim$ 4000 appm was obtained, and therefore another system designed specifically for analyses of gases was devised.

II. GAS MASS SPECTROMETER SYSTEM

A. General Description. The mass spectrometer system described here has a number of refinements over other similar systems,[2] which have led to a very low detection limit and simplicity of operation. Hoffman and Nier[3] used a double-focusing mass spectrometer to determine helium from meteorites by allowing the whole gas sample to go into the mass spectrometer source region. This method was modified by others,[4-7] by isolating the whole mass spectrometer tube from the vacuum pumping system in the way first demonstrated by Reynolds,[8] before allowing the helium sample to enter. This "static mode" operation improves the sensitivity by several orders of magnitude over the more conventional "leak" method of introducing a gas sample.

The principal features of the mass spectrometer system are shown in Figure 1. Determination of helium content is made by vaporizing a sample of known weight by resistance heating in one of the various types of crucible located in glass or metal

ovens. Just before the sample is vaporized and the ^4He released, a precisely known amount of ^3He spike is added. After mixing of the isotopes, the helium passes over getters which remove other gases evolved during the heating process. Finally, the mass spectrometer is isolated from its vacuum pumps for "static mode" operation, and a portion of the helium mixture is admitted into the mass spectrometer volume for isotopic analysis. A measurement of the $^4He/^3He$ ratio and a knowledge of the weight of the sample and the number of ^3He atoms added in the spike then gives the helium concentration. The whole system is repeatedly calibrated during each series of runs by analyzing various exactly known mixtures of ^4He and ^3He spikes.

B. Method of Helium Extraction. For the work described in this report, the method most often used to release the helium has been by quick and complete vaporization of each specimen in a resistance-heated 0.01-in. tungsten wire basket. Because the ^3He spike is always added to the "oven" chamber before the heating, complete mixing of the isotopes is assured. Groups of four baskets are supported between five electrical feedthroughs in each of the "ovens" shown in Figure 1. Pyrex glass envelopes with volumes ranging between 100 and 4000 ml can be interchangeably placed over the ovens, using greased vacuum joints. Unwanted gases released by the tungsten coils can easily be adsorbed by the getters, so that prior degassing is unnecessary. The coil and specimen are always observed during the heating cycle.

Many of the materials to be analyzed for helium content, however, have melting points well above 2000°C. These include irradiated specimens of B, Nb, Mo, Ta and compounds containing C and N such as TiC, TiN, HfN, TaN, having melting points as high as 3360°C. Because the tungsten coil baskets, even when enlarged, were unable to release all the helium, other methods of heating, including laser and electron beams were considered. Finally, resistance heating, using a much larger crucible was found to be the most practical solution. A high temperature furnace containing three 0.19-in. diameter cylindrical graphite crucibles was designed and built. The chamber has 0.25-in. thick water-cooled walls and has a Corning 1720 aluminosilicate glass top for viewing.

After degassing the crucibles at $\sim$ 2500°C, the samples are loaded into small holes which are then covered by sliding cylindrical sleeves to restrain the samples from being ejected by escaping gases. At the time of analysis, the current through the graphite is steadily increased over a period of 2 minutes until the crucible decomposes ($\sim$ 350 amps). Milligram size pieces of Ti wire are vaporized along with each sample to adsorb unwanted gases that the crucibles and surroundings persistently release.

C. The Spike System. A network of calibrated volumes which dispenses known quantities of ^3He and ^4He both for calibration and for isotope dilution purposes is attached directly to the mass spectrometer line at valve V_6 (Fig. 1). Glass stopcocks are used throughout the spike system rather than stainless steel valves, mainly because the stopcocks generally provide a more positive and reliable barrier through which helium has little chance of passing unnoticed. Another important advantage over stainless steel valves is the ease with which the stopcock interior volumes could be calibrated. Helium adsorption on vacuum grease appears to be negligible. Although most of the spike system, including all the stopcocks is made of Pyrex glass, the larger volumes which are used for long-term storage of helium, are made either from aluminosilicate glass, which is relatively impervious to helium, or from stainless steel. The amounts of Pyrex on each side of the stopcocks in the latter volumes are minimized.

Before the system was assembled, the volumes of the several sections were measured with an uncertainty of less than 0.02% by filling the space between the stopcocks with mercury or water, and weighing. As it stands, several hundred spikes may be drawn from each storage volume without introducing significant uncertainties to the calculated number of atoms dispensed each time. Four systems at present provide, in a matter of seconds, exactly known spikes of ^3He, ^4He and $^3He+^4He$ in amounts ranging from $\sim 1 \times 10^{13}$ to $\sim 3 \times 10^{15}$ atoms. The ^3He-^4He mixture is used as a "standard" with which to calibrate the relative sensitivity of the mass spectrometer for masses 3 and 4. Other "synthetic" combinations of ^3He and ^4He can be made to verify the relative sensitivity and, more important, to cross check the calibration and linearity of the whole mass spectrometer system.

D. The System of Getters. A system of getters is used to purify the helium gas sample before it is put into the mass spectrometer, and to maintain a high vacuum in the mass spectrometer while it is being operated in the static mode. The two zirconium-titanium alloy getters shown in Fig. 1 are each contained in mullite tubes connected to the stainless steel with an intermediate tube of Pyrex glass. On the outside of each assembly, is another similar mullite-Pyrex envelope; and a vacuum is maintained between the two to eliminate the diffusion of hydrogen and helium into the inner system from

the atmosphere. The getters themselves are specially prepared alloys, the one between valves V_1 and V_2 being 93% Zr-7% Ti, the other being 70% Zr-30% Ti by weight. After periodic baking at 900°-1000°C to remove adsorbed gases, the getters are held at room temperature and ~ 400°C respectively during mass spectrometer operation.

Two activated charcoal traps are cooled with liquid nitrogen (-186°C) during each series of runs. The large charcoal trap directly connected to the mass spectrometer through the 1-in. valve V_c, was installed to cope with the gases released by the high temperature furnace. Not only does it reduce the size of the hydrogen peaks at masses 2 and 3, but also by reducing the level of residual gases bombarding the interior of the mass spectrometer, the rate of helium desorption was reduced from ~ 3×10^8 to ~ 1×10^8 atoms per minute.

E. The Sample Line and Mass Spectrometer. The sample line shown in Fig. 1, with the exception of the double-walled getters, is made entirely of Type 304 stainless steel connected with flanges using gold or copper gaskets. All the line to the left of the cold trap, including the mass spectrometer, may be surrounded by insulation and baked at 300°-350°C. All the metal valves are bellows-sealed with metal seats. The high mobility of helium allowed small orifice valves to be used; the minimum orifice diameter of valves V_1 to V_5 being 0.28-in., and of valves V_6 to V_8 being 0.17-in.

The mass spectrometer is the Veeco model GA-4, which has a 2-in. radius, 60° deflection all-metal tube with an interior volume of approximately 1 litre. The instrument has an electron bombardment gas source, permanent magnet and an electronmultiplier. Output from the electronmultiplier is fed to a vibrating reed electrometer (VRE) and thence to a 1/2-second-response strip chart recorder, or to a digital voltmeter. Digital outputs from the voltmeter, a timer and two BCD encoder switches indicating mass position and VRE scale, are recorded in 12 columns by a high speed printer. Scanning from mass 4 to mass 3 is accomplished by switching the accelerating voltage from approximately 950 to 1270V.

F. The Vacuum System. To minimize the time necessary to pump away gas samples between analyses, a multiple vacuum system consisting of several independent subsystems is used. Rapid pumpout can be best accomplished, especially in the case of helium, when sequential pumping is employed. The first system pumps away most of the helium very rapidly. As soon as the low limit of the system is reached, the pumping speed levels off, and the next system is used to reduce the vacuum to a lower level, and so on. As it stands, the vacuum system consists of 4 two-stage rotary pumps, three ceramic-filled sorption pumps, a turbomolecular pump and three 150 litre/second ion pumps which are designed for noble gas pumping. One of the rotary pumps is used with the turbomolecular pump, the others are used in conjunction with the sorption pumps to make three completely independent but interconnected roughing systems. The three ion pumps are used in sequence. The one attached to the system through valve V_7 (Fig. 1) usually removes the last vestiges of helium from the entire line and mass spectrometer. This leaves the one attached to the mass spectrometer through V_m very little to do except maintain the mass spectrometer in the 10^{-9}-10^{-11} Torr range between analyses.

III. EXPERIMENTAL PROCEDURE AND RESULTS

After the ^4He released from a sample has mixed with the added ^3He spike, it matters little what fraction of the gas is used for the analysis, as long as enough is taken to get an adequate measurement of the isotopic ratio. Consequently, gettering is performed on only a small portion of the total gas sample, as it passes, by successive expansions, from oven to mass spectrometer. As soon as an adequate measurement of the $^4He/^3He$ ratio has been made and the helium in the mass spectrometer is pumped away, the usual procedure calls for a second aliquot of the gas mixture to be introduced for ratio measurement. Any small difference in the ratio between the two aliquots can usually be interpreted in terms of desorption of the helium isotopes from, or diffusion of ^4He through the walls of the oven system. This difference is then used to make a usually small correction to the first measurement by extrapolation.

The reproducibility of the final helium measurements generally[9] has a 1σ standard deviation of less than 2% for concentration levels above 10 atomic parts per billion (10^{-8} atom fraction). The absolute accuracy, determined from uncertainties in sample mass, spike size and isotopic ratio measurement is somewhat less than 3%. Analyses of milligram specimens with helium concentrations of less than 5×10^{-11} atom fraction have been performed routinely with uncertainties of ~ 10%.

A complete description of the experimental procedure and more details of the mass spectrometer system will be given in a paper to be submitted in 1972 to the International Journal of Mass Spectrometry and Ion Physics.

ACKNOWLEDGEMENT

The author acknowledges many interesting discussions with W. B. Clarke (McMaster University) during the early stages of building the mass spectrometer system, and contributions to the development of the system from C. A. Guderjahn and C. H. Knox. This work was supported by the United States Atomic Energy Commission.

REFERENCES

1. H. Farrar IV and C. H. Knox, Proceedings of the 15th Annual Conference on Mass Spectrometry and Allied Topics, Denver, Colorado, pp 221-226, (1967).
2. P. Signer and A. O. Nier, J. Geophys. Res. 65, 2947, (1960).
3. J. H. Hoffman and A. O. Nier, Phys. Rev. 112, 2112, (1958).
4. O. A. Schaeffer and J. Zähringer, Phys. Rev. 113, 674, (1959).
5. I. A. Alimova, B. S. Boltenkov, V. N. Gartmanov, B. A. Mamyrin and B. N. Shustrov, Geokhimiya 9, 1044, (1966).
6. D. D. Bogard, D. S. Burnett and G. J. Wasserburg, Earth Planet. Sci. Letters 5, 273, (1969).
7. G. Kugler and W. B. Clarke, Phys. Rev. C3, 849, (1971).
8. J. H. Reynolds, Rev. Sci. Instr. 27, 928, (1956).
9. W. N. McElroy and H. Farrar IV, "Radiation-Induced Voids in Metals" J. S. Corbett and L. C. Ianiello, Eds., pp 187-229, U. S. Atomic Energy Commission Symposium Series 26, (1972).

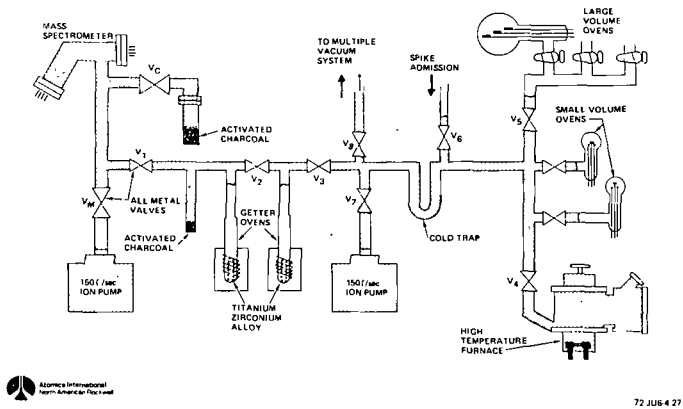

Figure 1: Mass Spectrometer and Sample Line

EXTENDING THE LIMIT OF MEASUREMENT OF SMALL ION CURRENTS AND ISOTOPE RATIO DIFFERENCES BY CHARGING A CAPACITOR

L. F. Herzog
Nuclide Corporation
State College, Pennsylvania 16801

ABSTRACT

As ion "currents" become smaller, statistical variations in intensity become relatively larger - for example, ±10% at 2×10^{-17}A (100 ions/sec) for a one second measurement, and measuring intensity in the conventional way by converting the current into a voltage by passing it through a hi-meg resistor becomes increasingly difficult. Ion counting circuits provide one solution, but a relatively costly one. An alternative method, which has the advantage that often little or no additional equipment is required, is to monitor the rate at which charge accumulates across a calibrated capacitor. Examples will be given of use of this technique to measure ion currents of 10^{-18}A or less with an uncertainty of a few percent or better, and, with larger currents, to measure isotope ratio differences to better than ±0.01% of the ratio.

INTRODUCTION - "Signal", "Noise" and "Statistical Noise"

The standard way to measure the intensity of an ion current is to convert it into a voltage by passing it through a Hi-megresistor, and to display the voltage on a recording device. However, fluctuations in the intensities of ion beams are inherent because both vaporization and ionization are random processes, and such fluctuations, sometimes termed "statistical noise" impose a fundamental limit on measurement accuracy.

The magnitude of these statistical fluctuations is given by the Poisson distribution (which describes all random processes whose probability of occurrence is small and constant) and is numerically equal to the square root of the ion flux. Hence when ion current is large (say 1.6×10^{-9} amp or about 10^{10} ions/second), it the sampling period is of the order of one second, the fluctuations will be relatively small (10^{5} ions or 0.001%) and will not interfere with the accurate measurement of the current. However, as ion "currents" become smaller, statistical variations in intensity become relatively larger - for example, ±10% at 1.6×10^{-17}A (100 ions/sec) for a one second measurement - and measuring intensity in the conventional way becomes increasingly difficult. When average ion currents are this small special problems arise in detecting and measuring them also because of electrical "noise" in the ion detection system, and unwanted ("background") ions.

Today I wish to call attention to a simple and inexpensive technique for detecting and measuring small currents that has been neglected. This is to integrate charge, using a calibrated capacitor to measure the voltages the currents produce.

When one detects an ion beam in this intensity range using a strip-chart recorder in the usual way, it will typically have the appearance of Fig. 1. This shows part of a detection limit/sensitivity test of a 12-90-HT Knudsen-cell mass spectrometer. It shows "shutter tests" made at temperatures between 646°C, and 620°C. At 620°C the vapor pressure of silver-109 is about 2.5×10^{-8} torr. (Ag 109 is a 50% isotope.)

A signal/noise performance criterion we have used in adjusting Knudsen-cell equipped mass spectrometers is to compare the current with the shutter between the K-cell and ionizer open to the current with it closed. With the shutter open, silver atoms effusing from the Knudsen cell can enter the ionization region but when it is closed they cannot. The silver ion current is the "signal" we wish to measure, while the current with the shutter closed is termed "noise". The current observed with the shutter open consists of the sum of "signal" and "noise" so "signal" is the difference between the currents with the shutter open and closed. ("Statistical noise" is in fact not "noise", which the dictionary defines as "an unwanted signal in an electrical system", rather, it is a property of the signal.)

With the shutter open and the silver beam being ionized, the recorder draws a very irregular trace for which the average displacement of the pen from the zero line is, at 646°C, perhaps 3 or 4 chart divisions. With the shutter closed, on the other hand, the recorder trace is only slightly elevated from zero, perhaps by about the width of the line drawn by the pen, except for occasional spikes. If the average flux is 10 ions per unit of time, the standard deviation will be $\sqrt{10}$. 68% of the observations will lie within the band 7-13 but 5% will lie even outside of the band 4-16! To reduce the relative standard deviation to 1%, one must wait long enough to accumulate 10,000 ions; for example, if the time period is one second, for 1000 seconds, when the average flux is 10/sec.

For the traditional output system (consisting of electron multiplier, d.c. amplifier with hi-meg input resistor, and recorder) in use when Fig. 1 was made, the time constant of the output system was about 0.7 second. With such a system, when the number of ions per second is near one, most ions that arrive will produce a single sharp signal pulse, which will usually have had time to decay away nearly completely before the next ion arrives. *In such cases, it is next to impossible to measure the intensity of the* current by the usual method, which is to observe the average displacement of the recorder pen from zero.

However it is quite possible to measure ion arrival rates with good precision merely by counting ion-pulse "spikes" when the average rate of ion arrival is less than the time constant of the output system, e.g.,for this system, for "currents" of about 2×10^{-19} amp or less; but when rates are much higher, this method also fails. One can detect the presence of a current unequivocally, but cannot measure its intensity accurately.

Referring again to Fig. 1, when the shutter is closed the number of pulses is always quite small - there are from 0 to 3 such events at the three temperatures cited. In contrast, with the shutter open, even at 620°C the number of pulses is, clearly, more than three times as great. Counting pulses as recorded on the chart confirms that the instrument is properly adjusted to meet specifications, i.e., the signal/noise ratio is greater than two for a silver-109 vapor pressure of 2.5×10^{-8} torr or 7×10^{-11} atmospheres of silver.

Actually, terming the total current observed with the shutter closed "noise" is a loose usage, because ordinarily the principal contribution to total output current under these conditions is from background gas molecules. The usage is justifiable because operationally it is the ratio of the current with shutter open to the current with shutter closed which determines the smallest vapor pressure one can detect. (Parenthetically, it does little good to devise means to increase ionization efficiency for molecules effusing from the cell if the means of accomplishing this also increases the background-ion current by the same factor or a greater one, since the signal/noise is not thereby increased, but reduced, even though "statistical noise" is thereby reduced.)

"True" noise is actually the output current observed with the ionizer turned off. Then, current reaches the recorder due to the "dark current" of the electron multiplier (10^{-18} amp or less), and also, those electron cascades that pass through the multiplier which result from causes other than ion arrivals - for example, cosmic rays, radioactive decay in materials of construction, and field-emission discharges. In a good multiplier one ion impact causes some 10^4-10^8 electrons to reach the amplifier in a few nano-seconds. In comparison the dark current contributes a completely negligible one electron or so in the same time. Hence, background ions and ion-like pulses are the main limiting factors in measuring small currents. The "spikes" that occur with the shutter closed in this record are, thus, mostly caused by background gas ions, with a few resulting from the other kinds of cascade-producing events just mentioned.

The electron multiplier's current gain was set at 250,000 for this run. Since a single charge is 1.6×10^{-19} coulomb at this gain an ion arriving at the first dynode causes some 4×10^{-14} coulomb of charge to reach the final dynode, and this occurs in a few nanoseconds. The peak intensity of the transitory voltage produced across the input resistor to the electrometer amplifier (typically, 10^9 ohms) by this cascade depends also upon the size of the input capacitor, which was, in this case, 680 picofarads. The

time it takes for the pulse representing a single ion arrival to decay to 65% of its peak intensity, known as the "time constant" of the system (RC) is fixed by this resistance, R, and capacitance C, and as the record confirms was 0.7 sec for this run. Of course, one can change RC by changing the size of the resistor or the capacitor. If the time-constant is reduced, pulses will be better separated and hence easier to count. On the other hand if a longer time constant is used it becomes easier to measure the average displacement of the pen but harder to count pulses.

Merely changing gain or electrometer scale does little good, as Fig. 2 shows. This is a sensitivity test of a different ionizer. The pulses are larger here because the multiplier was set at a considerably higher gain. However, this also caused an increase in electrical noise, making it harder to identify ion pulses. The shutter tests at 626°C and 618°C were recorded on the 250 mV scale, while the 620°C test is on a scale expanded by X10. It is apparent even from visual averaging of the currents with shutter open and closed that the S/N ratio was above 10 in this test, and hence that this source has a detection limit of the order of 5×10^{-9} torr of Ag. But determining average currents from this trace precisely is not possible, because of the "statistical noise".

INTEGRATION OF CHARGE

An excellent method for measuring ion fluxes of up to say 100,000 ions per second is by counting ion arrivals - feeding the output pulses from the EM into an external amplifier followed by a pulse counter and register, using a system with a very fast time constant of the order of 100 nanoseconds or less, and a comparably short "deadtime". But it is not my intent to discuss ion counting today.

Instead, I wish to call attention to a technique which is quite similar but which can be added very inexpensively to most existing mass spectrometers. The technique is by no means new, and actually takes us back to the early days of mass spectroscopy; but its use today is so rare that it might almost be considered a lost art. It is integration of charge. Using it is especially convenient if the amplifier has a switch by which one can switch the input resistor out and observe the rate at which charge reaches the detector by collecting it on a calibrated internal capacitor. The charge flux causes a secular increase in voltage, which can, for example, be observed using a standard strip chart recorder.

THERMIONIC SOURCE MEASUREMENTS

To illustrate how this technique is used, and its power, here are some data obtained using a three-stage mass spectrometer (with two 12", 90° magnets followed by a 14.4" radius electrostatic analyzer), equipped with a thermionic source. The sample was uranium oxide. This instrument has an ion counting system, and also a Model 401 VRE with a switch to cut the input resistor in or out, making it convenient to intercompare charge integration, ion counting and the normal output mode.

This instrument also has externally-removable Faraday cups, which one can use like the shutter in the Knudsen-cell instrument, to intercept the beam.

With the ion-counting register indicating an average uranium-234 ion "current" of about 6 ions/second, the current was first recorded in the standard mode (Fig. 3), first with the Faraday cup "shutter" out then with it in. Then the VRE was switched into the charge accumulation mode. On the 3-volt scale, the trace rose rather regularly by about 55 divisions (1.65 volts) per minute. This record is continued in Fig. 4, on the 10-volt scale. Then a Faraday cup was inserted, blocking the ion flow, to measure the "noise". The rate at which charge increased decreased to about 0.032 volt per minute. From these values one finds that the signal/noise ratio was more than 50/1 under the operating conditions then obtaining. Since the VRE's input capacitor had a value of 20×10^{-12} farad the multiplier output current with the beam on was 6×10^{-13} ampere; since multiplier gain was about 5×10^{5}, the input current was about 10^{-8} amp, or, about 6 ions/second, as the ion counter indicated.

Next, (Fig. 5) the 234U current was reduced by about a factor of three, to simulate the situation of a current with high statistical noise when the signal/"noise" ratio

was about two. As can be seen from this record, when one has a background current corresponding to about 2 ions/second, and a signal that averages about 4 ions/second, one can rather easily determine the magnitude of the signal to within a few percent in a few minutes using the integration of charge technique.

MEASURING ISOTOPE RATIO DIFFERENCES

We find that charge integration can also be used to good effect in measuring small isotope ratio differences with a double-collector. Here, one is dealing with, relatively, very large isotopic ion currents (10^{-11} to 10^{-9}A) but the differences to be measured are below 10^{-16} amp in many cases.

Fig. 6 shows a portion of a measurement of the difference in the HD/HH ratios of two hydrogen gas samples. For the unknown (labeled "2") the decade-resistances that measure ratio were initially set at 0.0129; for the standard ("1") the closest match was given at a setting of 0.0128. The difference-measurement sensitivity of the instrument is shown by the portion of the record in which the decade setting was changed first to 0.0134 and then to 0.0132. A ratio difference of one percent gave a displacement of about 16 chart divisions, compared to a peak-to-peak noise of about 1-1/2 divisions or about 0.07%.

The VRE was then switched into the "charge" mode. (Fig. 7). For the standard ("1"), if the decade was set at 0.0132, the trace moved up-chart at a rate of about 40 divisions/minute, while if the setting was changed to 0.0133, it moved down-scale at about 40 divisions/minute; thus the "sensitivity" for rate-of-charge measurements is about 100 div/min. for a ratio difference of one percent.

We next (Fig. 8) switched back and forth between standard and sample, with the decade always at the same setting. In each case when the switch was made the trace shifted at a rate of 65 to 70 div/min, indicating that the two samples differed in ratio by about 0.6%.

From experiments of this sort we have tentatively concluded that one can determine ratio differences to a given precision more rapidly by perhaps a factor of two by using the rate of charge technique, than by the standard technique.

DETERMINING MICROTRACE CONSTITUENTS IN SPARK-SOURCE ANALYSIS

Another useful application is in locating and measuring microtrace constituents in spark-source mass spectrograph electrical-detection spectra.

Fig. 9 shows a standard-mode trace of uranium-238 in a Zircalloy standard in which the uranium concentration is approx. 800 parts per billion (atomic). The U-238 current is small and the width of the "statistical noise" band, peak to peak, is nearly as large as the average deflection of the trace from its average position when the magnetic field is adjusted so that the collector slit is sampling a peak-free region adjacent to U238. However the 238-U signal can be seen to be of the order of 100 mV (multiplier gain is 2.2×10^5 and Ri is 1×10^{10} ohms). The trace to the right in Fig. 9 shows the same U238 ion current measured in the charge accumulation mode (time flows from right to left; one large chart division is 5 seconds). The trace rises smoothly by 20 volts in 30 seconds; the indicated current is about 7×10^{-17} amp.

Figure 10 (in which time flows right to left) shows the uranium-238 ion signal being recorded normally; then the spark was turned off to observe output system noise in the same mode. Individual pulses are seen indicating a pulse rate of the order of 10^{-19} amp. These ion-like pulses are actually from other causes such as cosmic rays, radioactive materials, and field discharges. In the charge accumulation mode the trace rose by about 20 millivolts in 30 seconds, indicating a noise of about 8×10^{-20} amp. Note that what would be pulse spikes in the normal mode appear in this trace as pulse steps.

After locating the center of the uranium-238 peak, we swept to thorium-232, and noted the magnet current which corresponded to its center. On the basis of the locations of these two peaks we calculated a current value at which U-235 should be in focus and

stepped to it and made measurements. We also measured intensities at two off-peak positions* on each side of the presumed 235. The next figure (11) shows typical measurements, first for the off-peak position 6.1002 amps and then for the assumed 235 position, 6.1112 amps. Several sets of measurements gave "235" signal-plus-"noise" values of (14-18) x 10^{-19} amp compared to off-235 readings of (4-10) x 10^{-19} amp. By subtraction, 235 was 9 $\pm$5 x 10^{-19} amp, giving a 238/235 uranium ratio in reasonable agreement with the known ratio for natural uranium of 140:1.

In this sample U-235 is present only at a level of 5-1/2 parts per billion (atomic); however, not only could its presence be confirmed, but also its relative intensity could be measured to $\pm$10% or so in a few minutes, using the charge accumulation technique.

When the r-f spark is the means of ionization, the reproducibility of the measurements improves considerably if instead of measuring the current to the final detector, one instead measures the ratio of this current to the current to the total ionization monitor, which samples the heterogeneous ion beam before magnetic analysis, using a circuit of the type pioneered by J. A. Hipple in the 1950s. In another talk presented at this conference, T. J. Eskew describes the use of such a circuit, equipped with digital readout.

In conclusion, we have found the charge integration measurement technique to be quite useful for measuring ion currents in the range of 10^{-16} - 10^{-20} amp, and recommend it for its simplicity and ease of application to most existing instruments.

I would like to acknowledge the contributions of T. J. Eskew, A. J. Smith, J. Mannaerts and W. Frye, to obtaining the data presented.

* One of the four off-235 positions consistently gave an intensity reading nearly as great as that of the presumed 238U. Further investigation revealed this was because there was actually a peak at that mass - the tin dimer (117Sn 118Sn); its mass is 234.805 compared to 235.043 for 235U; although the mass difference is 1/1000 the peaks are distinct.

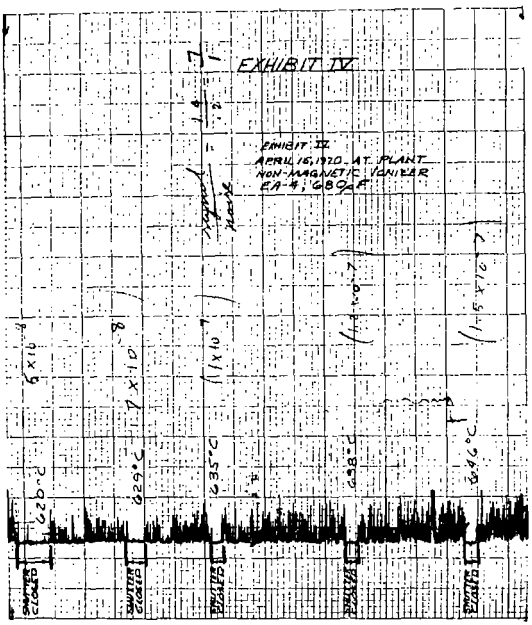

Fig. 1 Shutter tests, 109 Ag^+ from K-cell, normal mode, RC ≃ 0.7 sec.

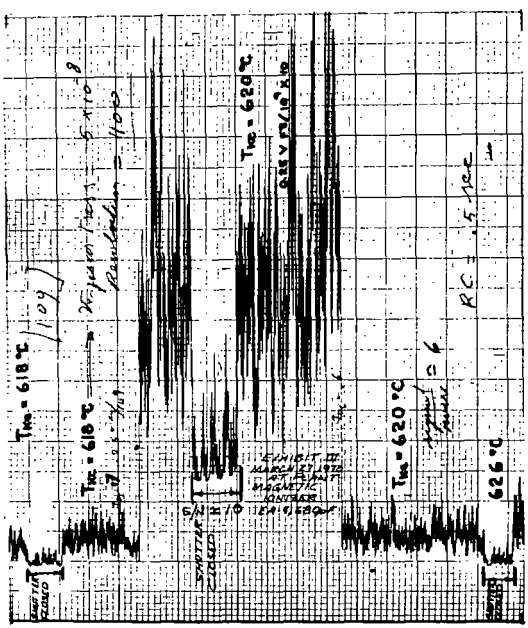

Fig. 2 Shutter tests, 109 Ag^+, at higher gain and lower attenuation than Fig. 1. RC ≃ 0.5

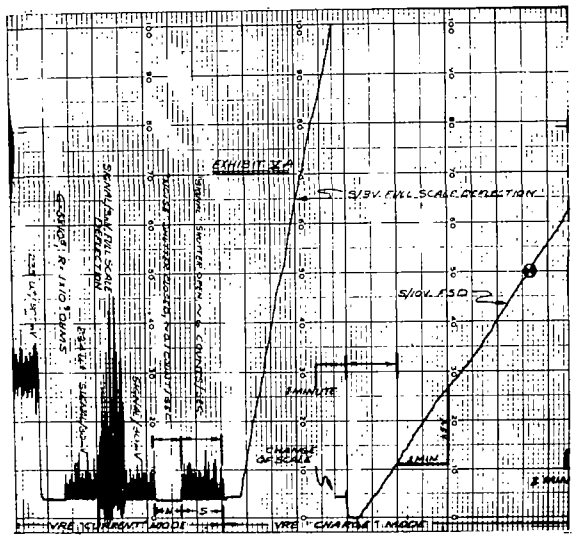

Fig. 3 $234U^{+}$ from thermionic source, 6 ions/sec vs detector noise.

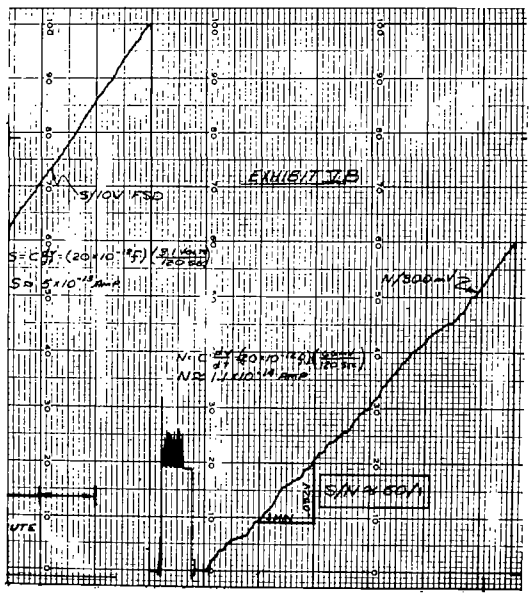

Fig. 4 $234U^{+}$ and noise of Fig. 3 compared by charge integration.

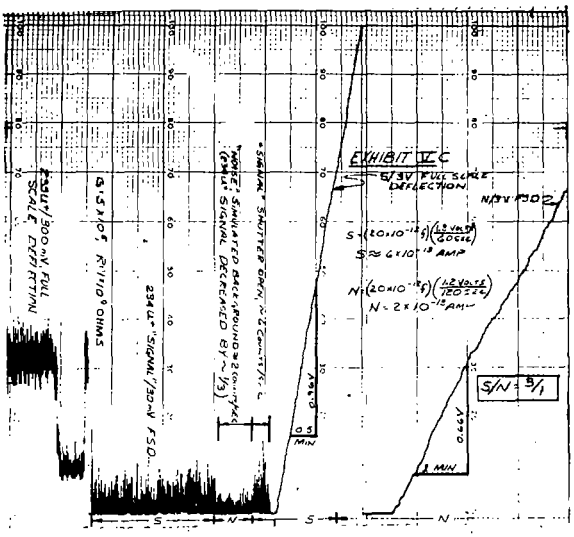

Fig. 5 Normal mode and charge integration compared when signal and background are approx. 4 and 2 ions/sec respectively.

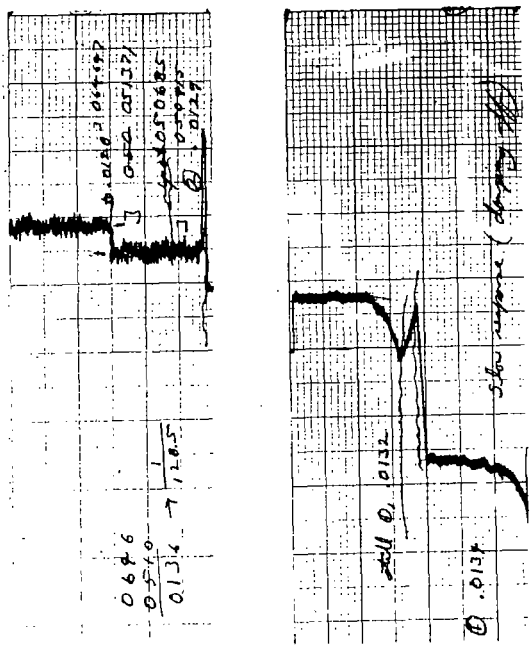

Fig. 6 D/H ratio difference measurement (natural abundance range) normal mode. Sensitivity, 16 div = 1% ratio difference.

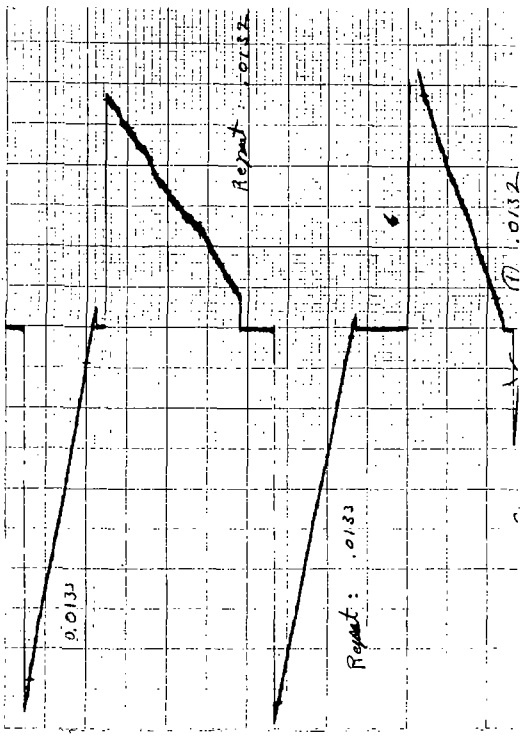

Fig. 7 Sensitivity calibration, D/H ratio difference measurement, charge integration mode.

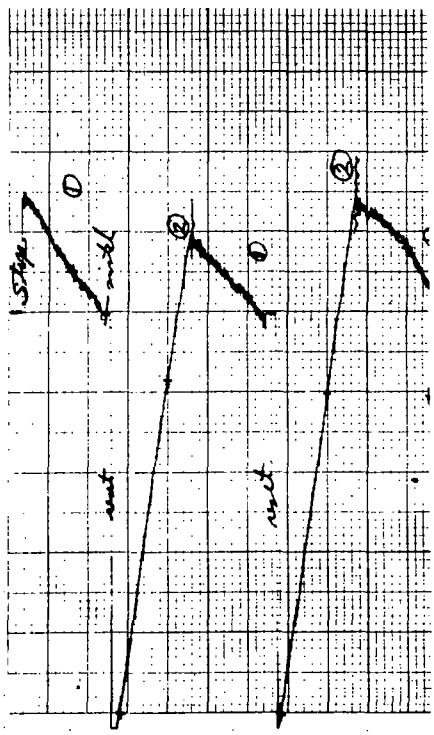

Fig. 8 D/H ratio difference measurement, charge integration mode. Sample and standard differ by about 0.6% in D/H ratio.

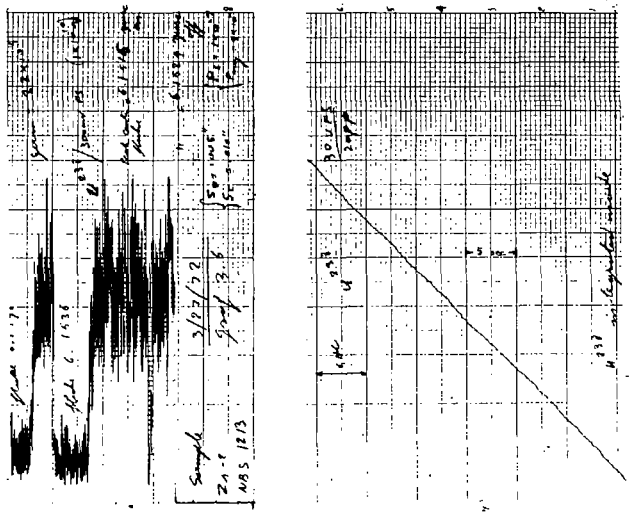

Fig. 9 0.8 ppma U238 in Zircalloy, ionized by spark source, electrically detected, using normal mode and charge integration.

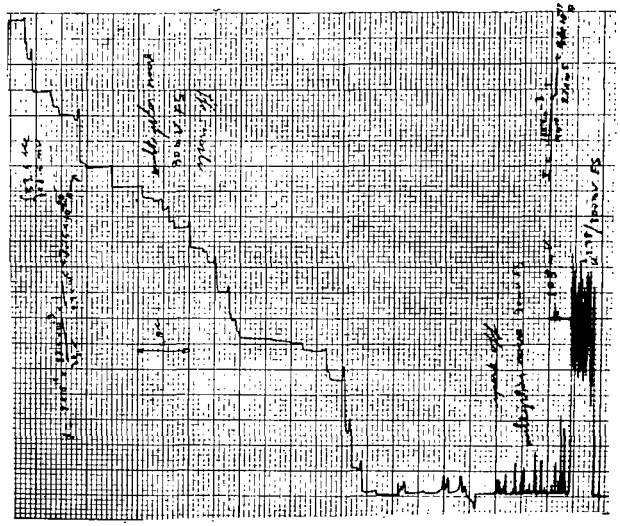

Fig. 10 Electrical output system noise, spark-source spectrograph.

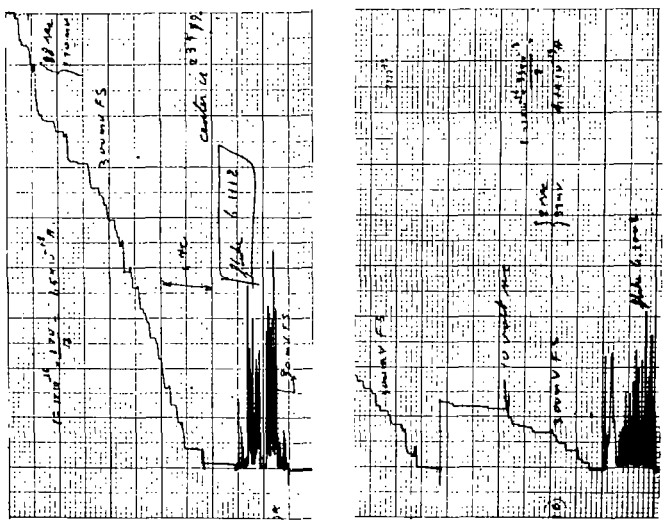

Fig. 11 Determination of intensity of 0.006 ppma 235U peak, Zircalloy sample of Fig. 8, normal and charge integration modes (235U on left, background region on right).

Response of Ion Sensitive Emulsions to Light Ions

B. W. Scott and G. Voorhies

Perkin-Elmer Aerospace Division, Pomona, California 91767

Calibration data is presented for sensitivity of Ilford Q2 and Kodak SC7 to ions simulating the solar wind. The two films were measured with H^+ of 0.500, 0.900 and 1.300 keV, He^{++} of 0.75, 1.65 and 2.5 keV and N^+ of 6, 8 and 10 keV. The sensitivity of the emulsions to light simulating visible solar flux is also presented.

The object of measuring the sensitivity of Ilford Q2 and Kodak SC7 to light ions was to evaluate them as possible detectors for a solar wind mass spectrometer experiment on a manned space flight. Since the time available to perform the measurement was limited, the photoplate capability of integrating the flux from the entire spectrum simultaneously was considered a distinct advantage. The solar wind is composed of ions of various masses with a wide range of charge states all moving at the same velocity, 300 to 500 km per second. This implies energies of approximately 1 keV per M/Q. Because of the highly ionized state, the major species of interest lie in the range M/Q = 1 to 4.5. Most previous published data on sensitivity of ion detecting emulsions is concerned with heavy ions with energies of a few keV. The light ions of the solar wind lie outside the range covered by these calibrations.

The work was performed on a simple 90° magnetic sector analyzer using a large electromagnet. The ion source, source power supply and timing circuit were all mounted on a flange electrically isolated by a large ceramic tube so that voltages of up to 10 kV could be employed. The film and plates were contained in a light tight cassette which could be removed from the instrument. The film moved inside the cassette so that approximately 75 patches could be exposed on each 1 x 4 inch sample. The current was not continuously measured during each exposure, but was measured before and after each set of eight patches exposed at one current density. The exposure time was varied by a factor 2 from one patch to the next in each set of eight. Several different current densities were used at each energy. Typical currents were 5×10^{-14} A over a patch size of 0.008 x 0.080 inch. This is a current density of approximately 25 pA cm^{-2}. Exposure times were in the range of 5 milliseconds to 5 seconds.

Precautions were taken to assure the identity of each ion. H^+ is the only possible ion at M/Q = 1. He^{++} at M/Q = 2 has an interference by H_2^+. These lines are separated by $\Delta M/M = 1/125$ and were easily resolved by our analyzer. The H_2^+ line was most probably due to background water in the source. In order to avoid contamination of N^+ by N_2^{++}, the energy of the ionizing electrons was reduced to 45 eV, below the threshold for production of N_2^{++}.

The films and plates were developed for 3 minutes in Kodak D-19 at 68°F. Good procedures were used, including a preliminary distilled water rinse and the use of solutions in deep tanks, minimizing exposure to air during processing.

The plates and films were scanned with a Jarrell-Ash Mircodensitometer. In some cases, very slight nonuniformities were averaged out by scanning the patch in three areas and taking the average. The patch area was measured with a toolmakers microscope in order to compute the exposure density.

The unit used to describe sensitivity is cm^2 per coulomb for 50% blackening. Since it is generally agreed that sensitivity depends only on mass and energy, and is independent of charge state, the data for He^{++} has been multiplied by X2. This allows a direct correlation between the per coulomb data and sensitivity per ion. Both units are shown in the summary of results (Figure 1).

By making an estimate of the worst possible error that could be present in each of the measurements going into this calibration, it is impossible to account for observed scatter in data. The current, exposure time, densitometer reading, patch dimensions, and developing action were all kept to less than 10% error. In a few cases the ion current uncertainty approached 50% of the extremely low currents. Two reasons speculated for the large scatter in data are nonuniformity of the emulsions and surface charging. The emulsions are prepared with only an extremely thin skin covering

some of the silver halide grains. Slight variations in this skin thickness could cause widely different stopping powers for the ions and, hence, different sensitivities. In addition, the unknown effect of surface charging can contribute certain errors. The films and plates represent a highly insulating target for the ions. Since the charges cannot leak off quickly, the surface assumes a potential nearer to that of the ion source. This causes a defocusing and spreading of the image, as well as changing the effective energy of the ions as they strike the emulsion.

The sensitivity of the two emulsions to simulated solar visible radiation (Figure 2) is approximately the same as for Kodak tri-X. The Ilford Q2 does not achieve very high densities as do the tri-X and SC7.

Acknowledgements

This work was supported under NASA Contract NAS5-11313. A detailed report is being prepared for publication.

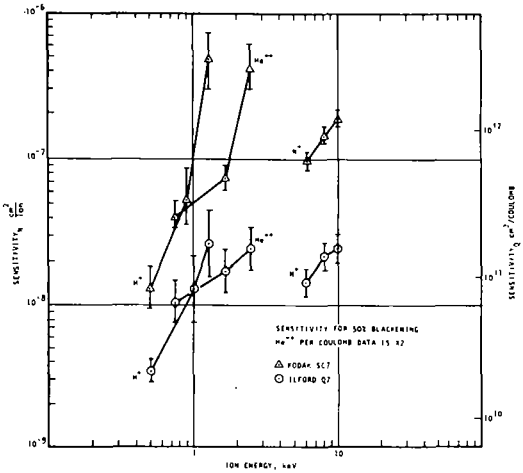

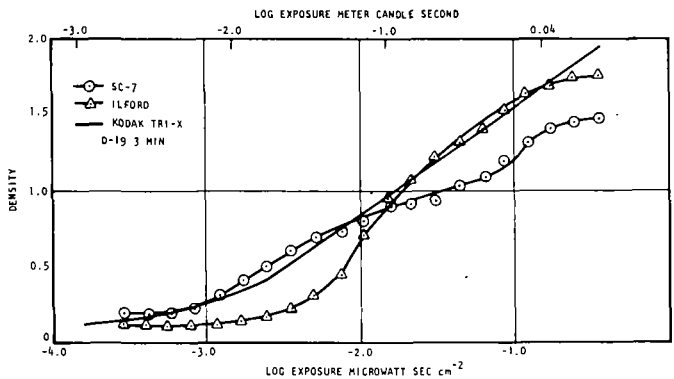

013

Spectrometer for Measuring Secondary-Electron Yields Induced by Ion Impacts on Thin-Film Oxide Surfaces. L. A. Dietz and J. C. Sheffield, GE Co., Knolls Atomic Power Laboratory*, Schenectady, N. Y. 12301

We have developed a spectrometer for studying secondary-electron yield properties of ion-to-electron converter dynodes. It consists of a 5-cm radius, 90° mass spectrometer which is electrically floating, followed by a post-accelerating lens to increase the impact energy of mass-analyzed ions up to 30 keV before they strike an ion converter dynode. Ions are formed by surface ionization. The ion converter dynode is a flat, narrow strip whose surface coincides with the axis of a cylindrical lens. It is rotatable about this axis. Secondary electrons are accelerated to 30 keV in the cylindrical lens and are focused onto a silicon solid state detector and undergo pulse-height analysis in a manner similar to that described by Delaney and Walton.[1] Deconvolution of the resulting energy spectrum leads to precise estimates of secondary-electron yields for monatomic or polyatomic ions of different mass, atomic number, velocity and angle of entry into a given target surface. Typical experimental results will be given.

*Operated for the U. S. Atomic Energy Commission by the General Electric Company, Contract No. W-31-109 Eng. 52.

[1]C. F. G. Delaney and P. W. Walton, IEEE Trans. Nucl. Sci. NS-13, No.1, 742 (1966).

An expanded version of this paper will be presented to The Review of Scientific Instruments for publication.

P1

CHEMICAL IONIZATION MASS SPECTROMETRY OF STEROIDAL AMINOALCOHOLS.* P. Longevialle, G. W. A. Milne and H. M. Fales, Institut de Chimie des Substances Naturelles, 91, Gif-sur-Yvette, Paris, France and National Institutes of Health, Bethesda, Md. 20014 USA

Since the pioneering work of Field and Munson (1), several papers have dealt with the chemical ionization mass spectra (CIMS) of complex molecules such as alkaloids (2, 3,4) and amino acids and peptides (5,6,7). There have been no reports, however, on the effect of stereochemistry on the fragmentation undergone by a molecule during CI.

We have studied the CIMS of a series of β- and γ-aminoalcohols of the steroid family, for which conformational data, derived from IR spectroscopy, are available. The CIMS were measured on a modified MS-9 (AEI Ltd.) (8) using isobutane as a reagent gas with a source pressure of 1 torr and temperature of 200°C. In all cases the spectra have only two ions, the protonated molecular ion at m/e $(M + 1)^+$ and the ion resulting from loss of water from the MH^+ ion, following protonation of the hydroxyl group. When present, hydrogen-bonding between the hydroxyl and amino groups was demonstrated by IR spectroscopy using 0.005 M solutions in carbon tetrachloride in a Unicam SP 100.

We have observed that loss of water is a very important process in CIMS when there is no hydrogen bonding between the hydroxyl and amino groups. On the other hand, when hydrogen bonding is present, loss of water from the protonated molecular ion is almost completely suppressed.

An explanation of this phenomenon may be found in the differing basicity of amino and hydroxyl groups. When the two groups are close together, the proton is captured by the more basic amino group, but in cases where the two groups are separated by some distance, protonation of the hydroxyl group can occur and is followed by rapid dehydration. This observation may be of great value in the determination of the relative configuration of aminoalcohols.

These data, furthermore, suggest that conformation may play a significant role in CIMS. Sicher et al. (9) have shown by IR that 3α-dimethylamino-2β-hydroxy -steroids exist partly (40%) in a hydrogen-bonded ring-a boat conformation. In the case of isomeric 2β-dimethylamino-3α-hydroxyl steroids, the boat form constitutes about 30% of the total.

The CIMS of these two compounds, (in the pregnane series) compared to related compounds in which the hydroxyl group is unbonded, exhibit less dehydration presumably due to the presence of ions derived from the boat forms.

In evaluating the degree of dehydration observed in CIMS as a function of the ratio of boat (bonded) to chair (unbonded) forms it seems logical to suppose that the MH^+ ion represents mainly species protonated on nitrogen in both boat and chair forms. On the other hand, the dehydration ion may only be derived from chair form ions that have been protonated on the hydroxyl groups.

The comparison of the ease of loss of water from these compounds with that from other 1,3-diaxial amino alcohols which have a stable A-chair conformation permits the calculation of the relative amounts of boat and chair forms in the 3α-dimethylamino 2β-hydroxy compound as 35% and in the 2β-dimethylamino-3α-hydroxyl compound as 22.5%. These results compare well with those derived from IR spectroscopy and the similarity of these numbers seems a little too good, in our opinion, to be coincidental. It may seem surprising that a gas phase experiment should lead to numbers comparable to those obtained in solution. It is noteworthy, however, that, in this case, the solvent is CCl_4 which has a minimum of interaction with the compounds.

If our explanation is correct, CI should be useful in corroborating results obtained from IR spectroscopy and other methods, relative to conformational analysis.

(1) - F. H. Field, Accounts of Chem. Res., 1, 42 (1968).

(2) - H. M. Fales, G. W. A. Milne and M. L. Vestal, J. Am. Chem. Soc., 91, 3682 (1969).

(3) - H. M. Fales, H. A. Lloyd and G. W. A. Milne, J. Am. Chem. Soc., 92, 1590 (1970).

(4) - P. Longevialle, P. DeVissaguet, Q. Khuong-Huu and H. M. Fales, C. R. Acad. Sci., Paris, 273 (série C), 1533 (1971).

* - A paper will be submitted to Tetrahedron.

(5) - G. W. A. Milne, T. Axenrod and H. M. Fales, J. Am. Chem. Soc., 92, 5170 (1970).

(6) - A. A. Kiryushkin, H. M. Fales, T. Axenrod, E. J. Gilbert and G. W. A. Milne, Org. Mass Spec., 5, 19 (1971).

(7) - W. R. Gray, L. H. Wojcek and J. H. Futrell, Biochem. and Biophys. Res. Com. 41, 1111 (1970).

(8) - D. Beggs, M. L. Vestal, H. M. Fales and G. W. A. Milne, Rev. Sci. Inst. 42, 1578, 1971.

(9) - M. Svoboda, M. Tichy, J. Fajkos and J. Sicher, Tetrahedron Letters, 717 (1962).

Chemical Ionization Mass Spectrometry of Sugars

A.M. Hogg & T.L. Nagabhushan
Department of Chemistry, University of Alberta, Edmonton, Alberta, Canada

The electron impact spectra of sugars, particularly *O*-methyl and *O*-acetyl derivatives have been studied extensively. However, they are characterized by lack of molecular ions, low intensity of high mass ions and a multiplicity of fragmentation pathways. As a result most carbohydrate chemists, as opposed to mass spectrometrists, do not consider mass spectrometry a very useful tool. In the hope of producing spectra which are more simply interpreted, we have studied the C.I. spectra of a number of sugars and sugar derivatives.

The methane C.I. spectra of glucose and a number of isomeric hexoses exhibit prominent peaks at (MH^+-H_2O), (MH^+-2H_2O) and (MH^+-3H_2O) together with other fragments at m/e 61, 73 & 85. Using D-glucose-2-d, methyl α-D-glucoside, 3-*O*-methyl-D-glucose and methyl 6-deoxy-α-D-glucoside as model compounds and both methane and methane-d_4 reagent gases, the major path for the losses of water in the hexoses was determined to be first from C1, then from C3 and C6. In the case of D-glucose-2-d considerable scrambling of deuterium took place. The ion at m/e 61 apparently has the structure $HOCH_2\overset{+}{C}H{=}\overset{+}{O}H$ where the carbons are C1 & C2, m/e 73 is probably $CH_3COCH{=}\overset{+}{O}H$ involving C1, C2 and C3, while m/e 85 has the structure:

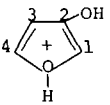

The methane Cl spectrum of glucose pentaacetate is very simple involving losses of four molecules of acetic acid and one of ketene; these peaks accounting for 87% of the total ionization above m/e 50. Labelling with deuterium and ^{13}C atoms and employing suitably *O*-substituted derivatives, the following mechanism was confirmed for the fragmentation of hexose pentaacetates.

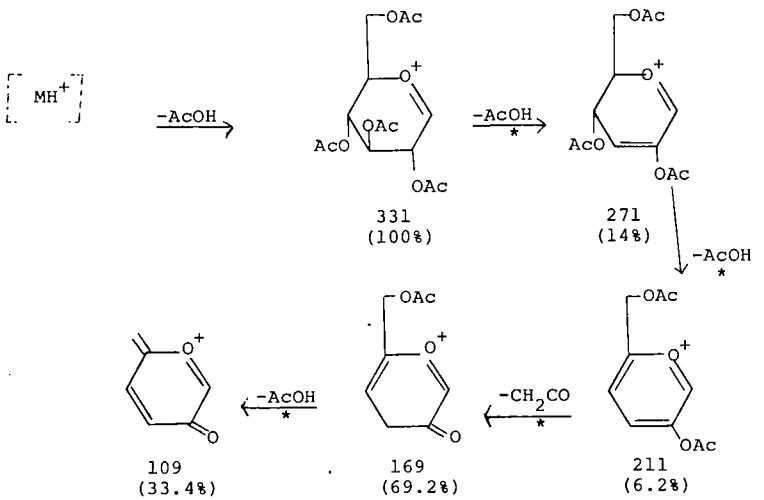

The ion at m/e 271 however appears to rearrange in such a way that the *O*-acetyl groups on C4 and C2 become partially scrambled most probably as illustrated below.

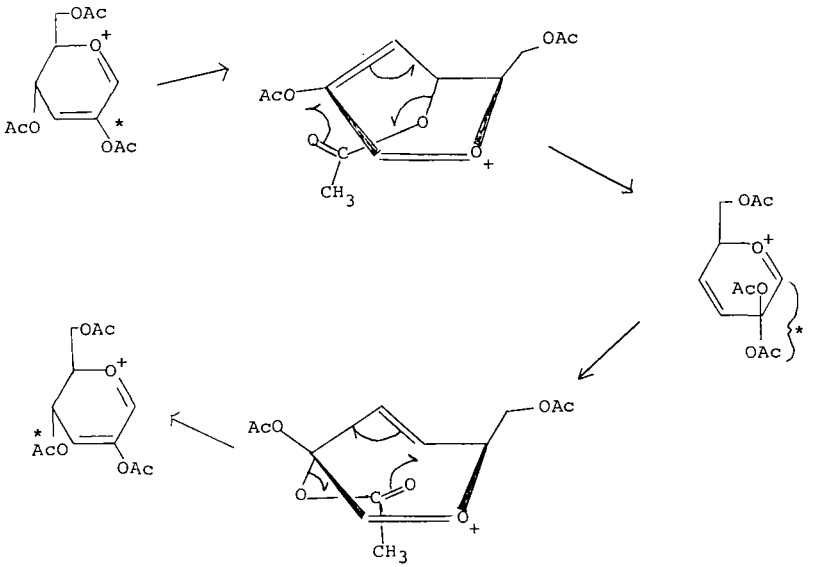

Peracetylated di and trisaccharides give spectra which are readily interpreted on the basis of the mechanism discussed for the monosaccharides.

If ammonia is used as a reagent gas, ions corresponding to $(M+NH_4^+)$ are produced from unsubstituted, methylated and acetylated sugars including di and trisaccharide acetates. This ion gives rise to virtually the only peak in the spectrum in *O*-acetylated sugars. Glucose shows a smaller peak at m/e 180 corresponding to $(M+NH_4^+-H_2O)$ and methyl glucoside a small peak at m/e 180 corresponding to $(M+NH_4^+=CH_3OH)$.

The use of methane as a reagent gas with *O*-acetylated sugars is a useful method for determining positions of substitution on a sugar ring while ammonia reagent gas provides a powerful method for the determination of molecular weights of sugars and substituted sugars on a micro scale.

CHEMICAL IONIZATION STUDIES OF NATURAL COMPOUNDS: PRESSURE AND ENERGY DEPENDENCE

J. Yinon* and H. G. Boettger

Jet Propulsion Laboratory
California Institute of Technology
Pasadena, California 91103

Introduction

The chemical ionization (CI) mass spectra of a series of flavonoid pigments have been studied as a function of the pressure of the reactant gas in the ion source, of the repeller field and of the electron energy. Although several workers had previously found dependence of CI mass spectra on source pressure (1-4) and on repeller voltage (1,2,5), no extensive study into the effects of operating parameters on CI efficiency has been done.

Experimental

We used an AEI MS9 high resolution mass spectrometer which we had modified for CI and electron impact ionization (6). We selected for our study the following three flavonoid compounds (Figure 1): 3-Hydroxyflavone, 4',5,7-Trihydroxyflavone (Apigenin) and 2'-Hydroxychalcone. Methane was used as a reactant gas. We looked at relative intensities of some of the most characteristic ions of the CI mass spectrum: $(M+1)^+$, M^+, $(M-1)^+$ and $(M+29)^+$.

Results and Discussion

Figure 2 shows the pressure dependence of the molecular ion plus one of the three compounds. The mechanistic interpretation of this reaction is "proton capture" leading to a protonated intermediate with a lifetime (10^{-7}-10^{-6} sec) long enough to be stabilized by collision. As the pressure increases there are more collisions and more protonated ions are stabilized. At a certain pressure the number of collisions is so high that the protonated ion dissociates before leaving the ionization chamber. From that point on the number of (M+1) ions decreases with increasing pressure. It seems that the pressure at which this maximum will occur depends on the structure of the compound: the maximum shifts to higher pressure as the number of available oxygens for proton capture decreases. Obviously, more experimental work has to be done to validate this theory. Figure 3 shows the pressure dependence of the peak at

---

* NRC Resident Research Associate. On leave of absence from the Weizmann Institute of Science, Rehovot, Israel.

the mass of the molecular ion of the three compounds. The contribution of this species, which is mostly formed by electron impact, to the intensity decreases with increasing pressure due to the decrease of the mean free path of the ionizing electrons. Contributions to the signal at M^+ may be due to charge exchange, loss of hydrogen from the protonated molecular ion, and to a protonated (M-1) fragment. Figure 4 shows the pressure dependence of the molecular ion minus one. Minima occur at the same pressures at which the maxima of the (M+1) ions occur. The (M-1) ion is essentially a protonated (M-2) fragment formed by dissociative proton capture. This process decreases with increasing pressure to a minimum at which maximum proton capture occurs, then it increases again because of increasing dissociation due to collisions. A part of the signal at $(M-1)^+$ can also be due to hydride transfer from the $C_2H_5^+$ ion. The pressure dependence of the (M+29) ion is essentially similar to that of the (M+1) ion.

The repeller voltage is variable from 0 to 24 volt, which is equivalent to 50 V/cm. Figure 5 shows the repeller dependence of the (M+1) ion. A decrease in protonation with increasing repeller field is observed which is due to higher energy reactant ions as well as shorter residence times of the ions.

In Figure 6 we see an increase in the molecular ion intensity — mostly formed by electron impact — with increase of repeller field, because a higher repeller field enhances ion extraction from the source. The (M-1) ion intensity decreases with increasing repeller field (Figure 7) because there is an increase in the dissociative proton capture due to the increase of the reactant ion energy.

The repeller dependence of the (M+29) ion is again similar to that of the (M+1) ion. Small electron voltage effects, which could be increased by using isobutane as a reactant gas, were also observed. Figure 8 shows the (M+1) ion as function of electron energy. More experimental work has to be done to explain these effects.

An immediate result of the study of these parameters should be greater selectivity in the choice of working conditions when doing chemical ionization. For analysis of unknown compounds, conditions are desirable at which $\frac{I_{M+1}}{\Sigma I}$ is maximum. For structural studies one might prefer conditions giving more fragmentation. This will often eliminate the need of an electron impact mass spectrum.

Acknowledgement

This paper presents the results of one phase of research carried out at the Jet Propulsion Laboratory, California Institute of Technology, under Contract No. NAS 7-100, sponsored by the National Aeronautics and Space Administration.

References

1. J. Michnowicz and B. Munson, Org. Mass Spectr., 4, 481 (1970).
2. J. Michnowicz and B. Munson, Adv. Mass Spectr., 5, 233 (1971).
3. J. J. Solomon and R. F. Porter, JACS, 94, 1443 (1972).
4. L. D. Betowski, J. J. Solomon and R. F. Porter, Inorg. Chem., 11, 424 (1972).
5. Burnaby Munson, Anal. Chem., 43, 28A (1971).
6. J. Yinon and H. G. Boettger, Chem. Instrum., To be published.

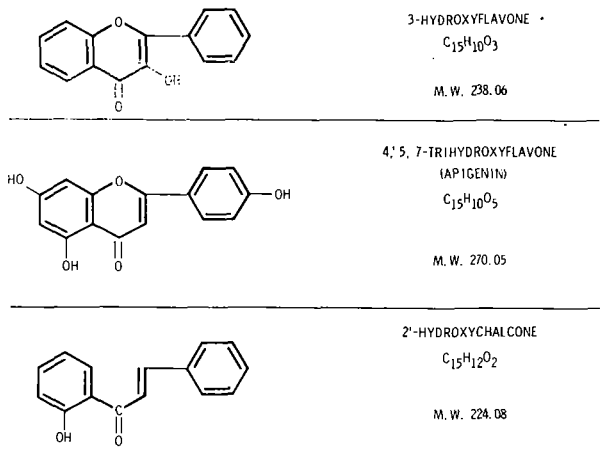

FIGURE 1. STRUCTURE OF INVESTIGATED FLAVONOID COMPOUNDS

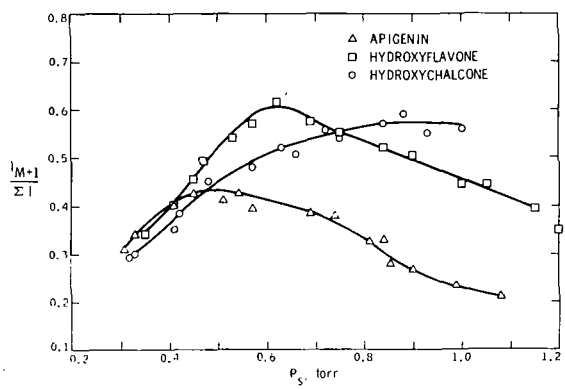

FIGURE 2. $(M+1)^+$ ION AS FUNCTION OF SOURCE PRESSURE

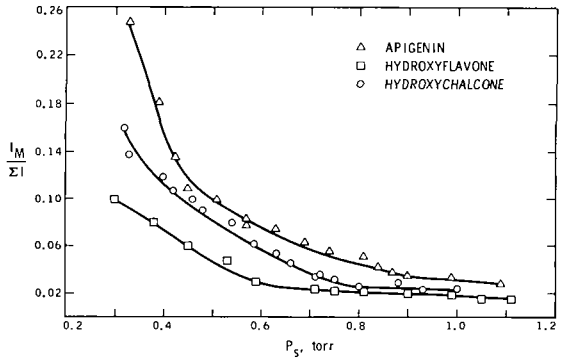

FIGURE 3. M^+ ION AS FUNCTION OF SOURCE PRESSURE

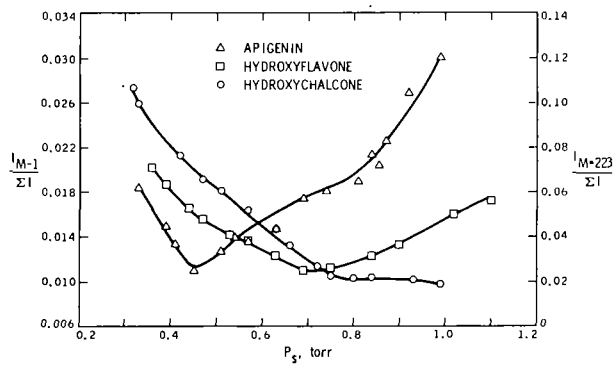

FIGURE 4. $(M-1)^+$ ION AS FUNCTION OF SOURCE PRESSURE

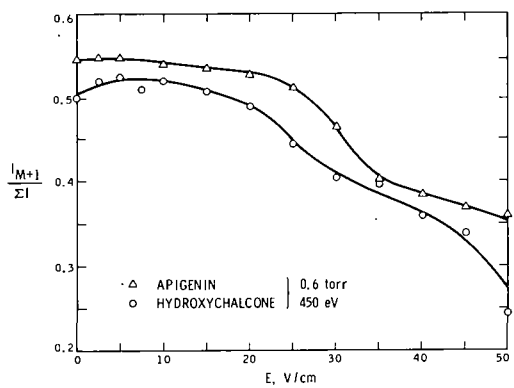

FIGURE 5. $(M+1)^+$ ION AS FUNCTION OF REPELLER FIELD

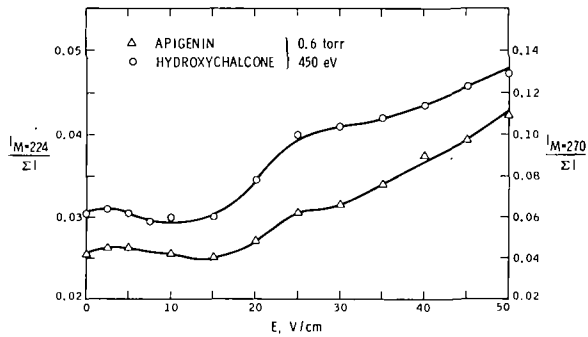

FIGURE 6. M^+ ION AS FUNCTION OF REPELLER FIELD

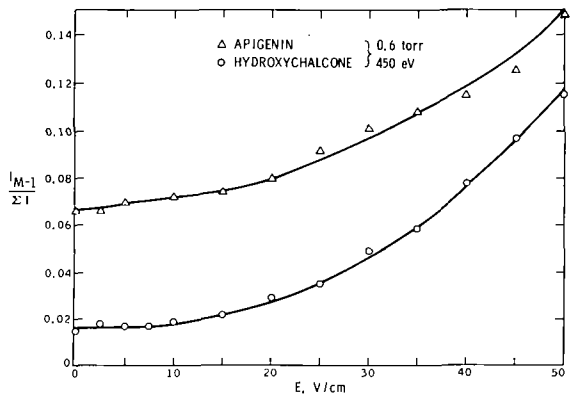

FIGURE 7. $(M-1)^+$ ION AS FUNCTION OF REPELLER FIELD

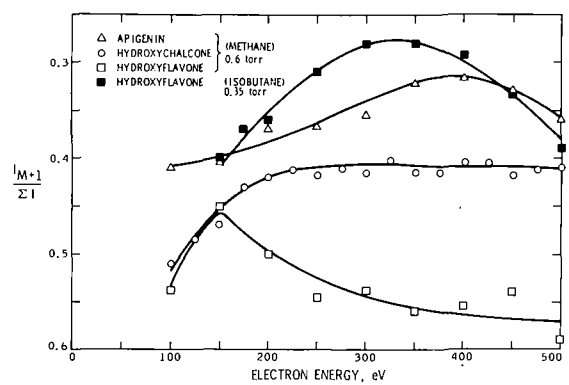

FIGURE 8. $(M+1)^+$ ION AS FUNCTION OF ELECTRON ENERGY

CHEMICAL IONIZATION MASS SPECTROMETRY OF CERAMIDES AND GANGLIOSIDES

S.P. Markey, R.C. Murphy, and D.A. Wenger

Departments of Pediatrics and Pharmacology
University of Colorado Medical Center
Denver, Colorado 80220

Certain commercially available mass spectrometers have a theoretical mass range of 12-8000 using reduced accelerating voltages. In practice, ion stability and sample volatility have imposed a usable mass range of m/e 12-1500. A significant number of compounds of biological interest have molecular weights between 1000-3000. Consequently, studies have been undertaken to yield structurally significant fragment ions and identifiable molecular ions of complex polyfunctional molecules in this molecular weight range. Chemical ionization mass spectrometry was chosen in order to promote rational fragmentation resulting from protonated species ionized with less excess energy than that experienced with electron impact.

An A.E.I. MS-12 mass spectrometer has been modified for C.I. in the following ways:

1) A 1300 l/sec. diffusion pump (Edwards E06) with a butterfly valve and Freon refrigerated baffles was substituted for the standard ion source diffusion pump.

2) A standard type J ion source was made gas tight in order to effect a higher pressure region in the ion source block. An electron beam entrance plate with a 0.35 mm hole and a trap plate with a standard window size were fitted into dovetail grooves (interference fit) on the ion source block in order to provide gas tight seals. The top surface of the ion source block was lapped smooth so that the ion exit slit plate (slit size 3.2 mm x 0.05 mm) would lay flat and seal the ionization chamber. A trap block, plugs for three unused ion source block ports, and a probe guide were machined from a polyimide resin (Vespel SP-1, unmodified resin, Plastics Department, E.I. DuPont, Wilmington, Delaware). Spacers and plugs machined from Vespel were also used to insulate the repeller plate and seal its electrical connector.

3) In earlier efforts, the ionizing gas was introduced through a port other than the probe entrance via a heated quartz inlet or through an inlet under the repeller plate. However, samples introduced on the probe were difficult to analyze because viscous flow conditions forced the vaporized sample away from the region of ionization. Consequently, a combination probe-gas inlet was designed. Gas flows at atmospheric pressure through a stainless tube sealed into a standard probe. A non-conductive leak estimated to be 6 liter-microns/second was made from sintered silicon carbide (Metrosil, AEI) sealed in Pyrex (Figure 1). A Teflon seat provides the seal between the leak and the steel tubing. The leak is compressed into position by a Vespel probe holder, fashioned to provide a sliding seal in the probe guide mounted on the ion source block. The probe is at ground potential, and arc path distances are minimal.

4) Source supply electronics were modified as described by Beggs et al[1] to provide emission regulation of filament current. A standard operating condition of 500 eV electron energy and 0.5 ma emission current has been routinely employed.

5) In an effort to increase the efficiency of ionizing the gaseous medium while decreasing gas leaks, filament assemblies which could operate within the high pressure region were designed. A boron nitride assembly, tested for a month in a standard E.I. source, proved to be unsatisfactory for C.I. due to buildup of a conductive layer on the surface of the supporting block, as well as long outgassing times. A quartz assembly (Figure 2) was then designed and has provided a beam 10-100 times more intense than that observed with the filament mounted outside of the high pressure region. Studies to determine filament lifetime, apparent increased sensitivity, and possible thermal effects are currently in progress.

Using the above modified instrument, C.I. spectra of permethylated and acetylated sphingolipids were obtained. The complete results will be published elsewhere and are summarized here. Preparation of permethylated derivatives is difficult with amounts below 100 μg, and separation of the products significantly decreases yields. Acetylation (pyridine-acetic anhydride) is suitable for micro-scale, and the resulting derivatives were found to produce readily interpretable C.I. spectra using methane as a reagent gas.

Acetylated ceramides, hydroxy fatty acid ceramides, psychosine, ceramide glucose, and a ceramide dihexoside were studied. All produced intense MH^+-AcOH ions, and the lower molecular weight compounds exhibited MH^+ ions. Ions for one or two sugar residues (m/e 331 and 619) were readily distinguishable. In all but the ceramide

dihexoside, cleavage beta to the amide nitrogen yielded intense ions containing the fatty acid amide-sugar residue. In contrast, the EI spectra contained mostly low m/e fragments with little structural information.

Studies of ceramide-trihexosides and gangliosides are in progress, but have been limited by problems of m/e assignment above 1000 due to decreased spectrometer resolution.

1. D.Beggs, M.C. Vestal, H.M. Fales, and G.W.A. Milne. Rev. Sci. Inst., 42, 1578 (1971).

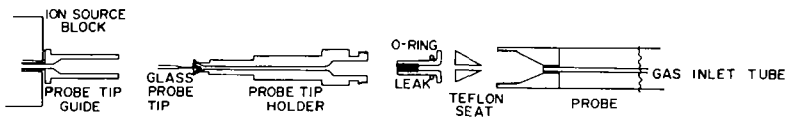

Figure 1. Probe assembly modification used for chemical ionization.

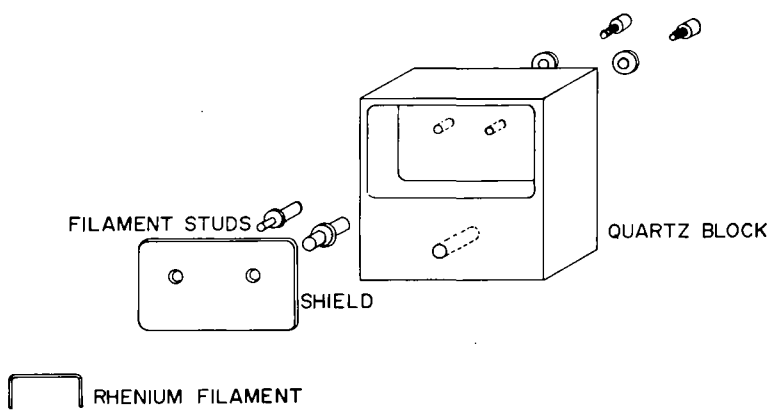

Figure 2. Quartz filament assembly mounted inside high pressure region of ion source block.

P 5 Dual Reagent Mixtures for Chemical Ionization Mass Spectrometry. P5

J. F. RYAN and D. F. HUNT, University of Virginia, Charlottesville, Virginia 22901

In general CI(CH_4) spectra are characterized by the presence of abundant ions in the molecular weight region (M + 1 or M - 1) and relatively few fragment ions at lower mass values. As a consequence, the CI method is ideally suited for molecular weight and elemental composition determinations but often of limited value for structure elucidation of organic compounds. In contrast, EI spectra are frequently devoid of molecular ions, but do contain a large number of abundant fragment ions and are, therefore, comparatively rich in structural information.

Electron bombardment of argon-water mixtures (100/1) at 0.4 Torr affords abundant ions at m/e 19(H_3O^+), 40(Ar^+), and 80(Ar_2^+). The H_3O^+ ion functions as a Brönsted acid in the gas phase and protonates most organic samples. Since the proton affinity of water is quite high (PA_{H_2O} = 164 $\pm$ 4 kcal/mole) the energy transferred to the sample in the protonation reaction is relatively small and the abundant M + 1 ions that result are stable toward fragmentation.

In contrast, electron transfer occurs when sample molecules encounter Ar^+ in the ion source. Since the recombination energy of Ar^+ is 15.8 eV and the ionization potentials of most organic compounds are in the range 9-12 eV, many of the radical cations produced in the above manner undergo extensive fragmentation.

By using a mixture of argon and water as the reagent gas it is possible to obtain low and high resolution CI spectra exhibiting the characteristic features of both CI(CH_4) and conventional EI modes of operation. GC-MS spectra can also be obtained with Ar-H_2O reagent gas mixtures. This is accomplished by using argon as the carrier gas in the GC and adding water to the ion source simultaneously with the GC effluent. No separator is necessary.

This new method should find considerable utility in the analysis of biological samples where the amount of material available for examination is frequently insufficient for more than one experiment. In almost all cases abundant ions are observed in the molecular weight region of the CI(Ar-H_2O) spectrum and the molecular composition of the sample can be easily determined. In addition, abundant fragment ions derived from the molecular ion are produced and afford valuable structural information.

1. D. F. Hunt and J. F. Ryan, Anal. Chem., 44, 1306 (1972).

STUDIES IN CHEMICAL IONIZATION MASS SPECTROMETRY - I. KETONES

by

Arun K. Bhattacharya* and Wilbert R. Powell
Air Force Materials Laboratory, LPA
Wright-Patterson Air Force Base, Ohio 45433

and

Jean H. Futrell**
Department of Chemistry
University of Utah, Salt Lake City, Utah 84112

A DuPont 21-490 analytical mass spectrometer has been modified to operate as a chemical ionization instrument. The basic requirements of a CIMS system and some details of the actual mechanical, electrical and other changes have been described earlier.[1] Some of the salient features will be discussed here.

One of the primary requirements of a chemical ionization mass spectrometer is its capability of operating and maintaining the ion source at elevated gas pressures. In the case of electron impact mass spectrometry, an ionization pressure of $\sim 1 \times 10^{-5}$ Torr is normal; whereas for a chemical ionization source, this must be raised to the region of 1 Torr. The actual physical modifications which this requires can be classified as follows:

1) Improvement of gas tightness of the source block to allow a greater pressure differential between this region and the remainder of the analyzer assembly;

2) Increased pumping capacity to handle the larger gas flow used;

3) Alteration of electric insulation within and around the instrument to protect against possible high voltage discharge or hazard to users; and,

4) Modification of the instrument electronic system to handle the new conditions within the ion source.

The standard ion source of a DuPont 21-490 analytical mass spectrometer contains several orifices which allow gas leakage; these are the inlet slit for the ionizing electron beam, the ion exit slit and the loosely fitted entries for both the sample gas inlet line and the sample probe. In order to reduce gas loss at the electron entrance slit, it has been covered and replaced with an aperture consisting of three small tunnels which simultaneously allow electrons to enter the ionization region and presents a high impedance to gas flow out of the source block.[2] The ion exit slit of the source has been somewhat reduced by spot-welding a tab to the analyzer side of the ion exit slit plate. This tab was made of a disc of stainless steel, 0.010 in. thick with a circular hole of 0.080 in. diameter drilled through the center. The loosely fitted vapor entrance lines have been modified by tapping both parts with screw threads and threading the end of the gas inlet line and the tip of the sample probe. This has necessitated the replacing of the standard ceramic tip with one of stainless steel.

An improved pumping system has been designed to cope with the increased gas flow. The existing source pumps have been replaced by an N.R.C. 4 in. VHS diffusion pump and Welch Model 1376 mechanical pump. A separate roughing pump has been installed to facilitate pumping the excess reagent gas between each run. The standard instrument gauge has been replaced by an N.R.C. ion gauge to measure the pressure which is external to the block. Various thermocouple gauges have been installed to monitor the pressure in the vacuum lines. Provision has been made for the introduction of more than one gas through a new gas inlet system.

The high pressures generated in this way may lead to the possibility of electrical discharge along the gas inlet lines and also cause the probe to operate at accelerator voltage. In order to overcome these problems and to protect the operator from high-voltage hazards, the following changes have been made:

1) The gas inlet line has been redesigned to allow part of it to float at accelerator potential;

2) Various sections have been insulated to prevent conduction to ground;

3) A glass insulator section has been included on the high pressure side of the inlet leak;

*University of Utah, Air Force Contract
**Alfred P. Sloan Fellow, 1968-72

4) All external electrically conducting parts on the low pressure side of the gas inlet line have been insulated; and,

5) The sample probe handle has been sheathed in insulating material.

The electron accelerating voltage power supply has been replaced with an external supply capable of providing up to 500 volts. Experiments have shown, however, that an energy of about 200 eV is optimal in causing ionization under the present conditions. For flexibility of operation, the original 70 volts supply can be restored by means of a switch built in the electronic chassis. Thus, an important feature of this modification is that it allows the normal mode of operation (electron impact) by merely the quick throwing of this switch. The sensitivity of the instrument has been further increased by building a new ion current amplifier circuit. A 100 megaohm resistor has been installed in addition to the usual 10 megaohm resistor and this has resulted in almost a ten-fold increase in the overall sensitivity of the instrument.

A total of eleven (11) different ketones were selected for the purpose of this paper. Chemical ionization spectra were obtained for all of them and the results with propane and methane as reagent gases have been summarized in Figures 1 and 2. The repeller voltages were kept near zero and the temperature was about 185° C. The pressure was estimated to be of the order of 0.5 Torr.

It can be observed that the (M+1) peak is the most abundant peak in all the spectra. It is obvious that propane is a better reagent gas than methane for these ketones. M^+ peaks are obtained in most cases presumably due to the charge transfer process, specially in the case of propane, where $C_3H_8^+$ happens to be a significant peak even at higher pressures. The disolvated proton is also a common product and its mechanism has already been established. (M+29) and (M+41) peaks are observed in the case of methane because of the presence of $C_2H_5^+$ and $C_3H_5^+$ ions in the high pressure mass spectrum of methane. The (M-17) peak corresponds to the loss of water from the protonated molecule. Since this peak is maximum for compound (X), a deuterated analog, namely, 2,6-dideutero-2,6-dimethylcyclohexanone, was prepared. This deuterated compound gave a similar peak due to $[(M+1)-H_2O)]$. This suggests that the loss of water from the protonated molecule is not due to 1,2-elimination. It, therefore, appears that the water loss mechanism under chemical ionization conditions is similar to that which has been established for electron impact dissociation of these molecules. Other fragment ion peaks are due to the loss of some neutral fragments from the (M+1) ion.

The details of these mechanisms and other results with different reagent gases, such as isobutane, hydrogen, nitrogen and argon will be submitted for publication in Organic Mass Spectrometry.

REFERENCES

1. A. K. Bhattacharya, K. A. G. MacNeil and J. H. Futrell, Air Force Materials Laboratory Technical Report, AFML-TR-72-35, Wright-Patterson Air Force Base, Ohio, March 1972

2. Scientific Research Instruments, Inc. of Baltimore, Maryland should be consulted regarding this modification; U. S. Patent applied for

Figure 1. TRENDS OF CIMS OF SOME KETONES (PROPANE AS REAGENT GAS)

Compound	No.	Mol. Wt.	M - 43	M - 42	M - 41	M - 28	M - 17	M - 15	M - 1	M	M + 1	M + 17	M + 43	2M + 1
3-butene-2-one	I	70						0.92		1.34	100			1.34
4-methyl-3-pentene-2-one	II	98					4.05			9.80	100			0.40
2,4-pentanedione	III	100		0.19	0.97	0.97		1.03	0.84	7.09	100		0.39	0.32
3-methyl-2-pentanone	IV	100			2.42		0.38	3.02	0.66	7.19	100			1.34
cycloheptanone	V	112					1.61		0.61	10.58	100			1.11
methylcyclopropylketone	VI	84						4.02		2.15	100			1.57
dicyclopropylketone	VII	110			13.97			0.96	1.47	4.70	100	1.10		0.44
2-methylcyclohexanone	VIII	112				0.46	1.87	1.65	1.25	14.85	100			1.25
3-methylcyclohexanone	IX	112	1.43				1.71	0.55	1.43	14.29	100			4.62
2,6-dimethylcyclohexanone	X	126	0.94			1.37	11.63	0.69	2.37	25.00	100			1.12
2-isopropylcyclohexanone	XI	140	1.45	11.57	1.33	0.36	15.80	2.66	5.92	12.54	100	2.05		0.72

Figure 2. TRENDS OF CIMS OF SOME KETONES (METHANE AS REAGENT GAS)

COMPOUND	No.	Mol. Wt.	M-59	M-43	M-42	M-41	M-17	M-15	M-1	M	M+1	M+29	M+41	2M+1
3-BUTENE-2-ONE	I	70						11.4	0.6	2.4	100	5.0	1.0	75.8
4-METHYL-3-PENTENE-2-ONE	II	98					1.8	5.9		4.8	100	5.9	2.4	8.3
2,4-PENTANEDIONE	III	100				3.1		1.8	1.3	3.1	100	3.1	0.4	4.9
3-METHYL-2-PENTANONE	IV	100		21.7		12.4	6.2	3.1		3.1	100	3.1	2.3	2.3
CYCLOHEPTANONE	V	112			2.1	2.1	23.4		1.4	7.8	100	4.2	4.2	23.4
METHYLCYCLOPROPYLKETONE	VI	84				32.1	1.8	7.9		3.0	100	1.2	4.2	9.1
DICYCLOPROPYLKETONE	VII	110				64.5				5.6	100	4.5	6.0	9.3
2-METHYLCYCLOHEXANONE	VIII	112					23.2			6.1	100	7.3	4.9	3.7
3-METHYLCYCLOHEXANONE	IX	112		20.8			47.6			16.7	100	4.8	8.3	77.9
2,6-DIMETHYLCYCLOHEXANONE	X	126		20.0			98.0		7.0	8.0	100	9.0	9.0	2.0
2-ISOPROPYLCYCLOHEXANONE	XI	140	19.6	5.5	12.8		83.8	10.6	14.5	7.2	100	6.8	4.3	22.1

THERMAL DECOMPOSITION OF $B_5H_{10}^+$ AND $B_4H_9^+$

S. A. Fridmann and R. F. Porter*

Department of Chemistry
Cornell University
Ithaca, New York 14850

Investigation into the thermally induced decomposition of positive molecular ions is an area of research which promises to yield important structural and energetic information. In the present study the decomposition of the ions $B_5H_{10}^+$ and $B_4H_9^+$ by loss of molecular hydrogen has been studied as a function of temperature. The results have yielded activation energies and relative first order rate constants for these processes.

Experimental

The mass spectrometer is a magnetic sector instrument and has been described elsewhere.[1] For these studies it was equipped with a modified chemical ionization source capable of operation at temperatures up to 500°C and pressures up to 1 torr. The source consists of a copper block 1-1/2" x 1-1/2" x 1-1/8" equipped with four cartridge heaters. A central cylindrical cavity 7/16" in diameter and 1" long serves as the ion chamber. A hole in the side of the chamber 1/2" from either end leads to a 1 mm orifice through which electrons generated from a heated rhenium filament are introduced into the source at an energy of 115 eV. The ion exit slit, .002" x 5/16", is located at one end of the cavity, parallel to the electron beam axis. A drawout plate with a slit measuring 1/32" x 3/8" is located about 2 mm beyond the ion exit slit and is kept at a typical operating potential of +2600V, or 400V negative with respect to the copper block.

The source contains no repeller or trap. Sample gas is introduced directly into the end of the cavity opposite the ion exit slit through 1/8" o.d. stainless steel tubing. Pressures are measured on a McLeod gauge attached to the sample inlet system. Temperatures are measured by a chromel-alumel thermocouple inserted into a small hole in the copper block.

Samples consisted of mixtures of about 1% B_5H_9 or B_4H_{10} in CH_4. The sample inlet pressure was maintained constant and the appropriate ion intensities were measured as a function of temperature. The chemical ionization spectra of these boron hydrides in methane at 100°C have been described previously.[2] For B_4H_{10} and

B_5H_9 the major ions are $B_4H_9^+$ and $B_5H_{10}^+$ respectively. As the source temperature is increased, the intensities of these ions decrease relative to those corresponding to loss of H_2, namely $B_4H_7^+$ and $B_5H_8^+$.

Results

Let M_0 be the initial intensity of the major ion of interest before it undergoes decomposition, and M the intensity as observed at the exit slit after decomposition has occurred. If P is the observed intensity of the product ion or ions, then $M_0 = M + P$. The rate law for first order decay will then be $\ln(M_0/M) = kt = (Ae^{-E_a/RT})t$, where t is simply the residence time of the ion in the source. A plot of $\ln[\ln(M_0/M)]$ against 1/T for various temperatures T will yield a straight line whose slope gives E_a.

Mixtures of B_4H_{10} in methane at a source pressure of 0.14 torr were analyzed using the ion intensities at m/e 53 ($B_4H_9^+$) and m/e 51 ($B_4H_7^+$). At temperatures below 450°K, a plot of $\ln[\ln(I_{B_4H_9^+} + I_{B_4H_7^+})/I_{B_4H_9^+}]$ yields a straight line with a slope corresponding to E_a = 4 kcal. Above this temperature positive curvature in the plot occurs, probably as a result of the thermal decomposition of B_4H_{10}.[3]

Mixtures of B_5H_9 in methane at a source pressure of 0.25 torr were studied using the ion intensities at m/e 65 ($B_5H_{10}^+$) and m/e 63 ($B_5H_8^+$). The mass spectrum in the pentaborane region indicated that $B_5H_8^+$ was the only product ion. B_5H_9 itself, unlike B_4H_{10}, does not decompose at low pressures to give significant amounts of volatile products,[4] even above 573°K.[5] The signal at m/e 63 can therefore be attributed to $B_5H_8^+$ from the decomposition of $B_5H_{10}^+$ over the temperature range studied, namely 500° to 630°K. A straight line plot of $\ln[\ln(I_{B_5H_{10}^+} + I_{B_5H_8^+})/I_{B_5H_{10}^+}]$ against 1/T yielded E_a = 6 kcal for the decomposition of $B_5H_{10}^+$ to $B_5H_8^+$.

A comparison of the rates for the two ion decompositions is possible by extrapolation of the results to a common temperature and pressure. At 455°K the ratio $(kt)_{B_4H_9^+}/(kt)_{B_5H_{10}^+}$ is found to be 6.6. However the residence time t varies directly as the pressure in the source.[2] Therefore correcting the residence times for the different source pressures in the two cases gives $k_{B_4H_9^+}/k_{B_5H_{10}^+} = 12$. Although the mobilities of these two ions depends also on their respective masses,[2] this difference amounts to only 2% in the residence times and is neglected here.

Discussion

The heats of formation of $B_4H_9^+$ and $B_4H_7^+$[6] indicate that the reaction by which H_2 is eliminated from $B_4H_9^+$ is endothermic by 7 kcal. This would dictate a

higher activation energy for this process than our value of 4 kcal. The reason for the discrepancy is not obvious, but the results indicate that the activation energy is small and similar to the enthalpy change for the reaction. This in turn suggests that the transition state leading to loss of H_2 is one in which the H—H bond is already well formed.

Similarly, the small activation energy for the decomposition of $B_5H_{10}^+$ indicates that considerable H—H bond formation has occurred in the transition state. However the available heats of formation for the $B_5H_{10}^+$ and $B_5H_8^+$ ions[7] indicate that this is an exothermic reaction. The energy released along the final part of the reaction coordinate may be due to rearrangement of the $B_5H_8^+$ ion to a more stable configuration.

References

1. R. F. Porter and J. J. Solomon, J. Amer. Chem. Soc. 93, 56 (1971).
2. J. J. Solomon and R. F. Porter, ibid. 94, 1443 (1972).
3. A. B. Baylis, G. A. Pressley, Jr., M. E. Gordon and F. E. Stafford, ibid 88, 929 (1966).
4. I. Shapiro and B. Klein, ibid. 77, 2663 (1955).
5. R. E. Hollins and F. E. Stafford, Inorg. Chem. 9, 877 (1970).
6. T. P. Fehlner and W. S. Koski, J. Amer. Chem. Soc. 85, 1905 (1963).
7. "Ionization Potentials, Appearance Potentials, and Heats of Formation of Gaseous Positive Ions", NSRDS-NBS 26, p. 24 (1969).

A New Chemical Ionization Mass Spectrometer

M. L. Vestal, T. A. Elwood, L. H. Wojcik and J. H. Futrell
Department of Chemistry, University of Utah
Salt Lake City, Utah 84112

A new and versatile mass spectrometer system for chemical ionization studies has been devised at the University of Utah. This new design centers around a Varian MAT CH-7 mass analyzer which is capable of mass scans to 3600 a.m.u. at 1 KV accelerating potential. A completely new source was designed specifically for high sensitivity chemical ionization. Source optics were developed to give superior focusing of both the electron and ion beams. The ion chamber, as shown in Figure 1, is designed for gas tight operation at pressures as high as 20 Torr; a 2400 liter/sec diffusion pump is used to evacuate the source housing. The combination of gas-tight operation and a long separation between the electron entrance and the ion exit results in diffusion controlled travel of the ions out of the ion chamber. Pulse mode operation demonstrates that ion residence times under typical operating conditions range from 1-10 msec., consistent with ion diffusion being the dominant ion loss mechanism. Thus, ion source residence times are orders of magnitude longer than earlier CI source designs and orders of magnitude longer than ion analysis times in the CH-7 instrument. The longer residence time also insures that excited-state ions will be collisionally de-activated to ground-state, thermal energies.

A wide degree of latitude is available to the experimentalist. Inlets now available include a gas inlet with a variable leak, a direct insertion probe, a straight-through GC inlet, plus additional sample ports for less traditional designs. The source itself includes a liquid nitrogen chilling loop such that the temperature can be controlled from 200° to 800° K. Source pressures are measured to high accuracy via two pressure transducers (Mks Baratron and Wallace and Tiernan gauge) connected directly into the ion source chamber.

Computerized operation will obviously enhance the utility of this new instrument. Therefore, we have interfaced it to a Digital Equipment Corporation PDP-11/20 computer system. Our unit has 16K of core memory, a 600K work disk and several input/output devices shown in Figure 2. The magnetic field is sampled as its derivative through the use of a bifilar sensing coil. After amplification and analog to digital conversion, the field value is accumulated via a double precision summation. Intensity data, from the multiplier feedback loop, is used to threshold the data storage routine. Field and intensity values are stored alternately until the end of scan whereupon they are curve fitted relative to a standard (perfluorotributylamine). Output of masses versus intensities can be

diverted to the line printer, the CRO, or several other I/O devices. The instrument is currently used for routine biochemical sample analysis as well as basic chemical physics problems.[1]

1. J. H. Futrell and Marvin L. Vestal, 20th Annual Conference on Mass Spectrometry and Allied Topics, Dallas, Texas, June 4-9, 1972, paper K3 IN.

FIGURE I. ION SOURCE

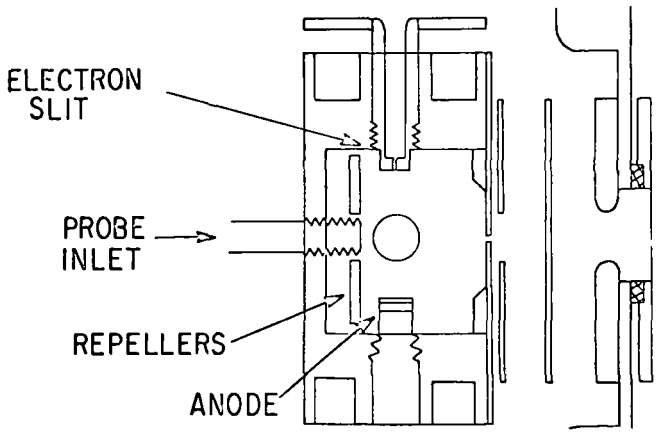

FIGURE II

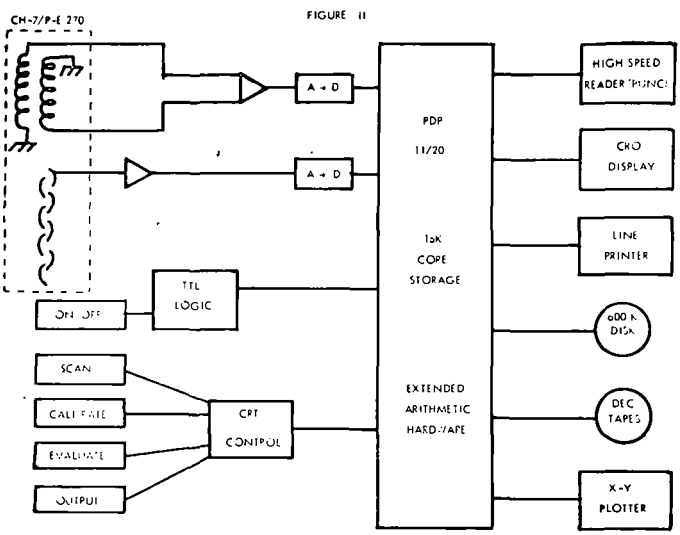

EXPERIMENTAL AND THEORETICAL ION ARRIVAL TIME AND ION ENERGY DISTRIBUTIONS IN CHEMICAL IONIZATION SOURCES*†

G. G. Meisels, C. Chang, J. A. Taylor, and G. J. Sroka
Department of Chemistry
University of Houston
Houston, Texas 77004

ABSTRACT

Arrival time distributions in CI sources differ from those predicted by simple drift theory primarily as a result of (1) electron beam attenuation in the reactant gas which strongly favors ion formation near the electron entrance slit; and (2) the inhomogeneity of electrostatic fields. A complete model is presented which is based on the ion transport equation folded into an exponential distribution of points of origin, each of which is associated with a unique drift length, collection efficiency and field distribution. Insertion of known parameters for methane yields good agreement with experimentally measured arrival time distributions. The calculation of ion energy distributions is possible using the Wannier relationship for ion energies, assuming that longitudinal and transverse random energies differ but are each Maxwellian (elliptical approximation). The ion energy distribution may then differ appreciably from one based on the common assumptions that source temperature is the only determining factor.

INTRODUCTION

Recently the technique of chemical ionization has been employed to derive rate constants for ion-molecule reactions[1-3] and to evaluate equilibrium constants for reversible reactions of gaseous ions.[3,4] There are two essential assumptions in the employment of chemical ionization sources for quantitative kinetic and thermodynamic studies. The first relates to the ability to estimate residence times and their magnitude. For kinetic studies, exact knowledge of ion residence times is required to estimate rate constants accurately, while equilibrium considerations demand that these times be sufficiently long to permit attainment of the equilibrium. The second concerns the ion energies and their distributions. Even though rate constants for exothermic ion-molecule reactions are largely energy independent,[5] endothermic ion-molecule reactions cannot be. Moreover, the equilibrium position from which thermodynamic parameters are derived shifts as a result of ion energy variation.

The calculation of ion residence times from idealized Langevin drift theory[6,7] is known to lead to results often in serious error[7,8] and recent measurements in chemical ionization sources using a pulse technique to measure residence times have confirmed this inadequacy.[3] The identification of ion energies with source temperature is perhaps an even less acceptable approximation, primarily because the drift field brings about an appreciable increase in ion energy and also makes the meaning of temperature uncertain. At somewhat higher applied fields the ion energy distribution loses its Maxwell-Boltzman character which is the only relationship within which temperature can be defined meaningfully in a conventional thermodynamic system.

In this communication, we review ion drift theory and compare it with experimental results, and analyze the conditions under which a reliable estimate of the ion residence times and ion energies and their distributions can be made for chemical ionization sources. This permits us to further investigate the applicability of the technique of chemical ionization in obtaining accurate quantitative results.

ION DRIFT AND DIFFUSION

Low Field. The field is generally assumed to be low when the ratio of field strength to gas pressure (E/P) is 1 volt/cm-torr or less. At this low E/P the ion energy gained by the field is small compared with the thermal energy and the Maxwell-Boltzman distribution of ion velocities is not substantially perturbed due to this field. Under this condition, the ion drift velocity V_d is found to be proportional to the field with the proportionality constant K defined as ion mobility which is also related to the ion diffusion coefficient D by the Einstein relationship. At low field the ion mobility is theoretically accessible from the well-developed Langevin drift equation in the polarization limit.

High Field. At high field (typically E/P > 50 volt/cm-torr) the polarization force between ion-molecule encounter partners becomes unimportant relative to other forces such as hard sphere repulsive and symmetry forces. In this region the ion drift velocity is found to be proportional to the 1/2 power of the electric field.[9] This is character-

ized by an assumption of constant mean free path between two consecutive ion-molecule collisions as opposed to the constant mean free time assumed in the low field.[10] Since mobility now also varies with the electric field it does not remain a useful concept.

Intermediate Field. At intermediate field the ion energy gained by the field is comparable to or greater than the thermal energy and cannot be neglected. This is the field of greatest interest for the present study since many ion-molecule reaction and chemical ionization studies are performed within this region. The dependence of ion drift velocity on the field usually changes gradually from the power of 1 to 1/2 within this region. The range of E/P values where the constant mean free time assumption and predominance of polarization forces are still valid approximations is dependent on the temperature and polarizability of the neutral drift gas. For example, the ion drift velocity is proportional to E/P up to 10 volt/cm-torr for He^+ in He,[9] 20 volt/cm-torr for H^+ in H_2,[11] and as high as 40 volt/cm-torr for CH_5^+ in CH_4.[3] It has been shown[10] that the Langevin drift equation in the polarization limit[5] is exact in spite of the field as long as the assumptions of constant mean free time and of predominance of polarization force are valid. We confine our consideration to the E/P limit where the Langevin drift equation can be applied without significant error. As will be shown in the next section, the mobility K remains constant within this region but the Einstein relation is now no longer valid. Both the transverse (D_T) and the longitudinal (D_L) diffusion coefficients are affected by the field, and this causes broadening of the ion arrival time distribution and a non-Maxwellian energy distribution.

ION ENERGY DISTRIBUTION

The ion energy distribution as a result of the electric field is of particular interest because of its importance in the evaluating of ion-molecule reaction rate constants especially for the case of endothermic reactions or reactions having activation energies. At very low E/P ($\leq$ 1 volt/cm-torr) the change in ion energy induced by the field is negligible. The ion energy distribution simply follows the Maxwell distribution characterized by the gas temperature with its average value equal to 3/2 kT. However, at higher fields this distribution functions is very complex and has not been evaluated reliably either theoretically or experimentally. However, for the case of polarization force and constant mean free time Wannier[5] has achieved considerable success in obtaining the ion energy distribution. Although the calculated distribution is not in closed form, he was able to obtain some exact expressions for the drift velocity and average ion energy as follows:

$$\langle V_x \rangle = \langle V_y \rangle = 0 \quad ; \quad \langle V_z \rangle = V_d \tag{1}$$

$$\langle V_x^2 \rangle = \langle V_y^2 \rangle = eD_T/km \quad ; \quad \langle V_z^2 \rangle = V_d^2 + eD_L/km \tag{2}$$

$$\text{total average ion energy} = \frac{m}{2}\langle V^2 \rangle = \frac{3}{2} kT + \frac{m}{2} V_d^2 + \frac{M}{2} V_d \tag{3}$$

where m and M are masses of ion and neutral molecule and D_T and D_L are diffusion coefficients transverse and longitudinal with respect to the electric field (z axis). These were shown to be

$$D_T = K \frac{kT}{e} + \frac{1}{3} \frac{M(M + m)}{M + 1.908m} \frac{E^2K^3}{e} \tag{4}$$

$$D_L = K \frac{kT}{e} + \frac{1}{3} \frac{M(M + 3.72\ m)}{m + 1.908\ m} \frac{E^2K^3}{e} \tag{5}$$

Here one can consider the Einstein relation to be a special case with E→0. By combining equations (1) to (3) one can easily find that the ion random energies are $eD_T/2K$ in the x or y direction and $eD_L/2K$ in the z axis, with the ratio of total random energy induced by the field to ion drift energy of M/m. Equations (4) and (5) are also used in deriving the ion arrival time distribution as will be discussed later. Representative values of the average CH_5^+ ion energy in CH_4 calculated from equations (3) - (5) are summarized in Table I.

In view of the fact that no explicit form for ion energy distribution is available, we have chosen an approach which is based on the following two assumptions: (a) that thermal equilibrium is achieved in x, y, z axes respectively;[12] one can then define a transverse ion "temperature" T_T and a longitudinal ion "temperature" T_L with their values associated with ion random energy given by equation (2), and (b) that the components of the velocity and energy in the x, y, z axes can be described by one-dimensional Maxwell distributions. The corresponding Maxwell velocity and energy distributions are:

$$f(V_i) = \left(\frac{m}{2\pi kT_T}\right)^{1/2} \exp\left[\frac{-mV_i^2}{2kT_T}\right] \quad ; \quad i = x, y \tag{6}$$

$$f(V_z) = \left(\frac{m}{2\pi kT_L}\right)^{1/2} \exp\left[\frac{-m(V_z - V_d)^2}{2kT_L}\right] \tag{7}$$

$$f(E_{xy}) = \left(\frac{1}{kT_T}\right) \exp\left[-\frac{E_{xy}}{kT_T}\right] \tag{8}$$

$$f(E_z) = \frac{1}{2}\left(\frac{1}{\pi kT_L}\right)^{1/2} E_z^{-1/2} \exp\left[-\frac{E_z - 2\sqrt{E_z E_d} + E_d}{kT_L}\right] \tag{9}$$

where

$$E_d = \frac{1}{2} m V_d^2 \tag{10}$$

$$E_{xy} = E_x + E_y \tag{11}$$

The convolution of equations (6) and (7) should yield the three-dimensional velocity distribution while the convolution of equations (8) and (9) will give the total ion energy distribution.

Figure 1 shows the displaced and elliptical Maxwell velocity distribution contour for $C_2H_5^+$ ion diffusing through CH_4 at a temperature 443°K, pressure 0.567 torr and field strength of 14.3 volt/cm. Figure 2 shows several ion energy distributions at various draw-out potentials. It should be noted that these distributions cannot be matched by a spherical uniform Maxwell energy distribution defined by any single temperature. With an equal ion average energy defined by equation (3) the two types of distributions differ substantially and the elliptically displaced one drops off more rapidly at higher energies as shown in Figure 3.

Perhaps the most critical assumption in arriving at the energy distribution is the second one since its validity in terms of basic principles of momentum transfer remains unjustified. However, the present approach should be a substantial improvement over one based on a spherically uniform velocity distribution.

ION ARRIVAL TIME DISTRIBUTION

Consider a packet of N_o ions released at time zero and point zero, i.e. $(t,x) = (0,0)$. If ions are under an electric field then there will be a drift motion with drift velocity V_d superimposed on an ion diffusive motion. The one-dimensional number density distribution function can be written as

$$n(x,t) = N_o (4\pi D_L t)^{-1/2} \exp\left[-(x - V_d t)^2 / 4D_L t\right] \tag{12}$$

The ion current passing through the exit plane at $x = L$ is then

$$i(t) = -D_L \left(\frac{\partial n(x,t)}{\partial x}\right)_{x=L} + V_d\, n(L,t) = \frac{1}{2}\left(V_d + \frac{L}{t}\right) n(L,t) \tag{13}$$

An idealized ion arrival time distribution was calculated based on equation (13), but it was found that this distribution is narrower with its mean residence time much shorter than the measured arrival time distribution (Figure 4). This can be ascribed to the geometry of our CI source which cannot be considered as an ideal point ion source.

The instrument employed in measuring the ion arrival time distribution has been described previously.[3] Briefly, the gases are introduced into the ion source at a total pressure of 0.5 to 2 torr and a temperature of 170°C. They are then ionized by a 0.1 μsec pulse of electrons having energies varied from 120 to 420 eV. Ions are withdrawn after drift over a minimum of 0.7 cm (electron entrance plane to exit slit distance see Figure 5) using extraction potentials of 2 - 20 volts. They are then mass analyzed and detected individually with an electron multiplier. The delays between the electron pulse and the detected ion pulses are sorted on a pulse height analyzer. The output of this analyzer yields an arrival time distribution of the mass preselected ion.

Figure 5 shows a schematic diagram of the ion source used in the present experiment. The electron beam enters through the electron entrance slit with dimensions as described. Ions formed along this electron beam plane are then drifting downward due to the

potential applied to the extraction plate. Most ions are probably lost to the wall or simply change their identities through chemical reaction. It is only the parts that enter the ion exit slit that are actually detected and analyzed. The first complication arises from electron beam attenuation. Due to the high gas pressure and large ionization cross section, most ions are actually formed in the vicinity of electron beam entrance. As a result, instead of considering the ions formed in the center of the electron beam (directly above the exit slit) alone, one must take into account all ions formed along the electron beam, with main emphasis on the ions formed in the vicinity of electron entrance. The initial ion intensity distribution along the electron beam can be estimated by assuming exponential attenuation of the beam; a total interaction cross section of 10^{-15} cm^2, about 4 times the ionization cross section,[13] appears best.

The second instrumental factor is the inhomogeneous field, particularly near the two edges of the electron beam where the field strength is lower. This causes a substantial decrease of drift velocity. The third factor is that the distance between the ion origin and the exit slit depends on the point of ion origin along the electron beam. This has a similar effect as the inhomogeneous field, i.e. it increases the ion drift time and causes further spreading of the ion arrival time distribution for ions formed in the beginning of the electron beam.

Equation (13) assumes that all ions passing through the plane at L are collected. This is not the case because of the finite size of the exit slit. Therefore a collection efficiency factor must be included to account for ion loss because of transverse diffusion. The value of this factor varies from zero to unity and was found to be a function of both the ion origin and arrival time.

It is possible to take all four factors into account by calculating an arrival time distribution for each point of origin of ions in the electron beam plane and weighting each such distribution by the probability of forming ions at that point. The arrival time distribution of $C_2H_5^+$ in methane so obtained (Figure 4) shows good agreement of the mean residence time with experiment; however, the experimental curve is substantially broader than that calculated. This is the result of several simplifications in calculations. Dominant factors will include the scattering and the physical width of the electron beam, here assumed to be planar, and the effect of space charge on the expansion of the ion packet. Both of these factors will broaden the distribution but should not greatly affect residence times because they are isotropic in character.

CONCLUSIONS

Consideration of ion transport and of the detailed geometries and construction parameters of chemical ionization sources permits the development of quantitative descriptions of mean ion energies, ion energy distributions, and residence time distributions. While the former are not directly amenable to experimental test, mean arrival times are in good agreement with those obtained experimentally.

LITERATURE CITED

* This investigation was supported in part by the National Science Foundation and in part by the United States Atomic Energy Commission.

† A more detailed account of this work will be submitted for publication in the International Journal of Mass Spectrometry and Ion Physics.

1. F. H. Field, J. Am. Chem. Soc. 91, 2827 (1969).
2. S. Vredenberg, L. Wojcik and J. H. Futrell, J. Phys. Chem. 75, 590 (1971).
3. G. Sroka, C. Chang, and G.G. Meisels, J. Am. Chem. Soc. 95, 1052 (1972).
4. D. P. Beggs, and F. H. Field, J. Am. Chem. Soc. 93, 1567 (1971); Ibid., 93, 1576 (1971); Ibid., 93, 1585 (1971).
5. J.H. Futrell and T.O. Tiernan, in "Fundamental Processes in Radiation Chemistry," P. Ausloos, Ed., Wiley-Interscience, New York (1968), Chapter 4.
6. P. Langevin, Ann. Chim. Phys. 5, 245 (1905).
7. E.W. McDaniel, "Collision Phenomena in Ionized Gases," Wiley and Sons, New York (1967), Chapter 9.
8. Y. Kaneko, L.R. Marrill and J.B. Hasted, J. Chem. Phys. 45, 3741 (1966).
9. J.A. Hornbeck, Phys. Rev. 84, 615 (1951).
10. G.H. Wannier, Bell System Tech. J. 32, 170 (1953).
11. L.M. Chanin, Phys. Rev. 123, 526 (1961).
12. S. B. Woo and S. F. Wong, J. Chem. Phys. 55, 3531 (1971).
13. B. Adamezyk, A.J.H. Boerboom, B.L. Schram and J. Kistemaker, J. Chem. Phys. 44, 4640 (1966).

TABLE I. Representative Values of Mean CH_5^+ Ion Energies in CH_4 (0.5 torr, 181°C).

Field Strength (volt/cm)	Ion Energy (eV)
0	0.058
1.0	0.059
2.5	0.065
5.2	0.084
11.8	0.193
21.1	0.483

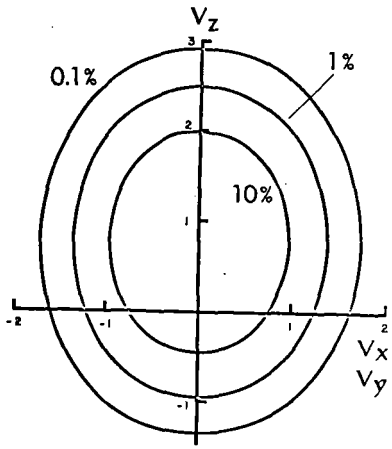

FIGURE 1. Displaced and elliptical Maxwell velocity contour for $C_2H_5^+$ in CH_4 at P = 0.587 torr, T = 443 °K and a drawout potential of 14.3 volt/cm. The center of the contour corresponds to the ion drift velocity (0.75×10^5 cm/sec) Scale: each unit = 10^5 cm/sec.

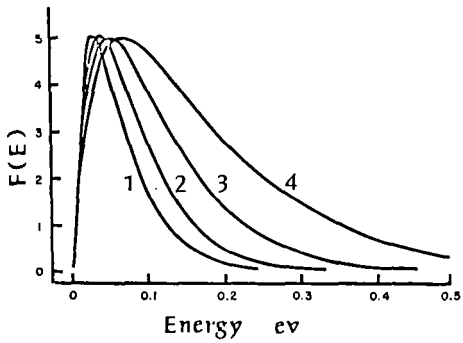

FIGURE 2. $C_2H_5^+$ ion energy distributions at several drawout potentials. P = 0.567 torr, T = 443°K, ion drift length = 0.7 cm.

Line #	Drawout Potential	Average Energy
1	0	0.0579 eV
2	3 volt	0.0744 eV
3	6 volt	0.1083 eV
4	9 volt	0.1533 eV

NOTE: Curve 1 corresponds to thermal ion energy distribution.

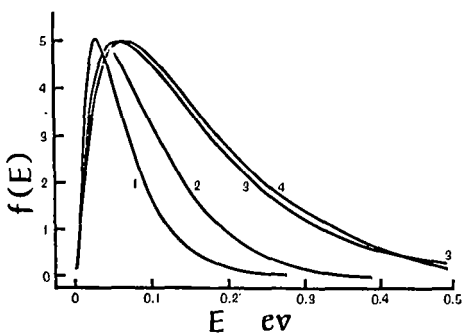

FIGURE 3. Comparison of $C_2H_5^+$ ion energy distribution P = 0.567 torr, T = 443°K, ion drift length = 0.7 cm.
Curve 1: Maxwell-Boltzman distribution at gas temperature 443°K.
Curve 2: Maxwell-Boltzman distribution at $T = (2/3)T_T + (1/3)T_L$=737°K.
Curve 3: Maxwell-Boltzman distribution at T = 1186.6°K which is calculated by 3/2 kT = 0.1533eV
Curve 4: Ion energy distribution at drawout potential 9 volt calculated by the displaced and distorted Maxwellian with average energy 0.1533 eV.

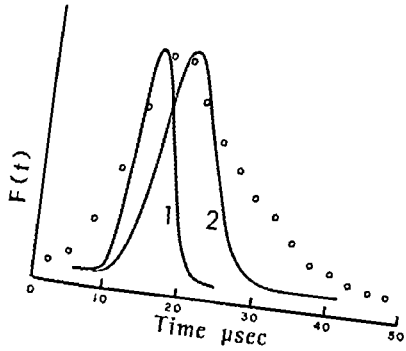

FIGURE 4. Experimental and calculated ion arrival time distribution for $C_2H_5^+$ ion in CH_4. P = 0.567 torr, T = 443°K, drawout potential 6 volt.

Curve	Mean Residence Time	Asaumptions
exp		
1	22.82 sec	
2	15.65 sec	
	19.74 sec	point ion source total ionization cross section = 1.0×10^{-15} cm^2

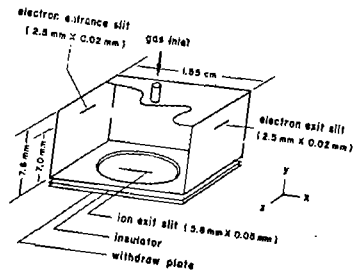

FIGURE 5. Schematic diagram of the ion source.

Abstract

A Motion Picture Summary of Rotational and Vibrational Effects in Ion-Molecule Collisions: Computer Graphics

John V. Dugan, Jr., Raymond W. Palmer, and R. Bruce Canright, Jr.
NASA Lewis Research Center, Cleveland Ohio

Rotational and vibrational effects in ion polar molecule collisions are summarized in a 26-minute, 16-mm., color-sound film. There is particular emphasis on the application of computer graphics to the study of the formation of ion-molecule collision complexes including computer-made motion picture sequences of ion-dipole collisions with rotating and vibrating targets. The variation of capture cross section and collision lifetimes with relative velocity and rotational temperature is reviewed. The behavior of ion-dipole collisions is contrasted with ion-induced dipole (Langevin) collisions.

The film consists of seven separate computer-made collision sequences, five animated sequences, and ten stills, some of which are computer-made time history plots. Each segment of the film is preceded by a brief introduction.

This film supplement C-275 is available on request to:

Chief, Management Services Division (MS 5-5)
National Aeronautics and Space Administration
Lewis Research Center
21000 Brookpark Road
Cleveland, Ohio 44135

The studies summarized in the film are contained in the following publications:

1. J. V. Dugan, Jr., J. H. Rice, and J. L. Magee, "Evidence for Long-Lived Ion-Molecule Collision Complexes from Numerical Studies," Chem. Phys. Lett., Vol. 3, No. 5, May 1969.
2. J. V. Dugan, Jr., R. W. Palmer, and J. L. Magee, "Computer-Made Movies as a Technique for Studying Ion-Polar Molecule Capture Collisions," Chem. Phys. Lett., Vol. 6, No. 3, August 1970.
3. J. V. Dugan, Jr. and J. L. Magee, "Dynamics of Ion-Molecule Collisions," Chemical Dynamics: Papers in Honor of Henry Eyring, John Wiley & Sons, Inc., 1971.
4. J. V. Dugan, Jr. and R. B. Canright, Jr., "A Preliminary Study of Vibrational Effects in Ion-Dipole Collisions: 'Classical Tunneling'," Chem. Phys. Lett., Vol. 8, No. 3, February 1971.
5. J. V. Dugan, Jr. and R. B. Canright, Jr., "Ion Dipole Capture Cross Sections at Low Ion and Rotational Energies; Comparison of Integrated Capture Cross Sections with Reaction Cross Sections for NH_3 and H_2O Parent-Ion Collisions," J. of Chem. Phys., Vol. 56, No. 7, April 1972.

IONIC REACTIONS INVOLVING CH_5^+ AND $C_2H_5^+$

A. G. Harrison and A. S. Blair

University of Toronto

Toronto 181, Canada

Although there have been extensive studies[1] of the products observed when CH_5^+ and $C_2H_5^+$ react with organic molecules there is very little information available concerning the rates of these reactions. The present work reports a study of the rates of reaction of CH_5^+ and $C_2H_5^+$ with a number of polar molecules using the trapped-ion technique developed recently in this laboratory[2].

The experiments were carried out using approximately 10:1 CH_4:additive mixtures at a total ion source concentration of approximately 1×10^{13} molecules cm^{-3}. Under these conditions the primary CH_4^+ and CH_3^+ ions react rapidly yielding primarily CH_5^+ and $C_2H_5^+$ respectively. These products reach a maximum yield at approximately 0.2 msec reaction time and then decrease rapidly due to reaction with the additive. The major product of these reactions in all cases was the protonated molecule, MH^+.

Rate coefficients for reaction of CH_5^+ and $C_2H_5^+$ with five polar molecules are summarized in Table I (Columns 3 and 5). Each value is the average of at least five determinations. Also included in Table I are the rate coefficients calculated from the relationship[3]

$$(1) \quad k(E) = 2\pi e\left(\frac{\alpha}{\mu}\right)^{\frac{1}{2}} + \pi e \mu_D \left(\frac{2}{E\mu}\right)^{\frac{1}{2}}$$

where e is the electronic charge, μ the reduced mass of the colliding pair, α the polarizability of the neutral, μ_D the dipole moment of the neutral and E the relative kinetic energy of the colliding pair taken[2] to be 0.2eV in the centre-of-mass system.

The measured rate coefficients are quite large and in many cases are greater than the values calculated from [1], which assumes complete "locking-in" of the dipole with the incoming positive charge. Ion dipole effects are obviously significant since not only are the rate coefficients large but also they

show a pronounced increase with increasing dipole moment of the neutral reactant.

TABLE I

RATE COEFFICIENTS FOR REACTION OF CH_5^+ AND $C_2H_5^+$[a]

M	Dipole Moment (Debye)	$CH_5^+ + M$ k(expt'l)	$CH_5^+ + M$ k(calc'd)	$C_2H_5^+ + M$ k(expt'l)	$C_2H_5^+ + M$ k(calc'd)
$(CD_3)_2O$	1.30	$2.8_0 \pm 0.2$	2.36	$2.0_0 \pm 0.1$	2.03
C_2D_4O (ethylene Oxide)	1.90	$3.1_1 \pm 0.25$	2.66	1.98 ± 0.2	2.31
CD_3CDO	2.72	$4.2_9 \pm 0.5$	3.27	$3.0_7 \pm 0.2$	2.86
$(CH_3)_2CO$	2.88	$5.1_3 \pm 0.2$	3.51	$3.8_4 \pm 0.1$	3.01
CH_3CN	3.96	$4.9_0 \pm 0.3$	4.23	$3.4_1 \pm 0.2$	3.79

a) all rate coefficients cm^3 $molecule^{-1}$ sec^{-1} x 10^9.

REFERENCES

1. see B. Munson, Anal. Chem. 43, 28A (1971) for a review of chemical ionization mass spectrometry
2. A. A. Herod and A. G. Harrison, Int. J. Mass Spectrom. Ion Phys. 4, 415 (1970)
3. a) S. K. Gupta, E. G. Jones, A. G. Harrison and J. J. Myher, Can. J. Chem. 45, 3107 (1967)
   b) S. E. Butrill, 19th Annual Conference on Mass Spectrometry, Atlanta, May, 1971

Kinetic Energy Effects on the Reaction Rates of Ion-Molecule Interactions in the Region of Thermal and Above Thermal Energies

R. Schnitzer and F.S. Klein

Isotope Department, The Weizmann Institute of Science, Rehovot, Israel

Ion molecule interactions have mostly been studied in two widely differing energy regimes: A. Drift tubes experiments at thermal energies of the reactants, ionic as well as neutral (1), and B. classical experiments performed in an ion source of a mass spectrometer under the accelerating influence of an electric repeller field of a few eV. Starting with the work of Stevenson-Schissler and Field-Franklin this method has seen many refinements (2). But even if some of these studies have reached occasionally ion energies below 1 eV, there still remains an energy gap between a few hundredths eV of thermal to a little below 1 eV ion energy which has not been covered by systematic studies (3). This energy band is of considerable importance to naturally occurring interactions in the atmosphere and stratosphere as well as to reactions observed under various experimental conditions, such as electrical discharges, plasmas etc.

We have undertaken, by a combination of experimental methods, to bridge this energy gap. Studying ion molecule interactions at thermal energies in a pulsed ion source as described by Talrose (4), it is possible by changing the temperature of the ion source to measure the effect of the ion and neutral kinetic energy on the rate constant of the reaction channel. This temperature variations in a conventional ion source covers only a relatively narrow band of energy change.

To cover a wide range of relative energies we added an ion acceleration pulse to the conventional pulse method. Immediately following the electron pulse which forms a swarm of ions by electron impact, a pulse of a variable positive voltage is applied to the exit plate of the ion source (Fig. 1) which accelerates the ions during a short time (~100 nsec) to a constant chosen velocity in the direction of the repeller. The ions are then permitted for a definite but variable time interval τ to coast through the neutral gas and react. A further constant pulse, applied to the repeller, decelerates the ions, reverses their direction of flight, and expels the reactants and products from the source. The ions then pass the mass spectrometer proper for analysis. This process is repeated at a frequency of 100 KHz, operated automatically, the results are recorded on incremental magnetic tape. Allowing for the initial acceleration and further deceleration, one can arrive at the rate constant for the reaction from the change of the ratio of secondary S to primary P ions as a function of time interval τ (Fig. 2). By this ion acceleration method one can, therefore, determine the rate constant as a function of relative reactant ion kinetic energy in the range from thermal up to about 1 eV ion kinetic energy. We also observe that the intercept (Fig. 2) (ion ratio at time interval $\tau = 0$; for ion accelerating pulse = 0 Volt) gives the amount of secondary ion formed during the passage of the reactant ions through the ion source due to the repeller pulse. These exactly are the experimental conditions of the Stevenson-Schissler experiments, namely acceleration of ions from thermal in a constant repeller field. By varying, therefore, the repeller voltage in the pulse experiments and following the magnitude of the intercept as function of the repeller voltage one can obtain the relative rate constant as a function of the reactant ion energy in the range above 1 eV.

We are thus in a position to observe in the same instrument and same experimental set up ion molecule interactions under continuously variable energy conditions, starting with thermal energies, covering the intermediate fractional eV range by the ion acceleration method and reaching the eV range covered by the conventional repeller field acceleration method.

Four reaction systems have been studied over the whole energy range:

1) $N_2^+ + N_2 \longrightarrow N_3^+ + N$ Fig. 3.

2) $O_2^+ + O_2 \longrightarrow O_3^+ + O$ Fig. 4.

3) $CO^+ + CO \longrightarrow CO_2^+ + C$ Fig. 5.
$\qquad\qquad\qquad\qquad\longrightarrow C_2O^+ + O$ Fig. 6.

4) $NO^+ + NO \longrightarrow N_2O^+ + O$ Fig. 7.
$\qquad\qquad\qquad\qquad\longrightarrow NO_2^+ + N$ Fig. 8.

The experimental results are summarized in the Table, which gives the thermal rate constant at 473°K (column 3) for each reaction channel studied (column 1 and 2), the apparent thermal activation energy (column 4), the maximal rate constant ratio (compared to the thermal rate in the intermediate energy range (column 5), and the integral rate constant ratio (compared to the thermal rate) at 5 eV (column 6).

Summarizing our results on these four reactions of the four center type:

$$AB^+ + AB \begin{cases} \nearrow A_2B^+ + B \\ \searrow AB_2^+ + A \end{cases}$$

We observe in the thermal range a tendency, varying in degree, to change from a negative to a positive temperature effect on the rate constant which continues in the intermediate energy range. In the high ion energy range we find generally a decrease in rate constant with increasing energy.

Model calculations on four center systems (5) are in progress. These will attempt to correlate the experimental results with a statistical phase space analysis (6).

Table

reactant	product	$K_{473°K} \times 10^{12}$ $cm^3 molec^{-1} sec^{-1}$	E_{act} thermal cal/mole	$\frac{K_{max}}{K_{473°K}}$ at eV		$\frac{\bar{K}_{5eV}}{K_{473°K}}$
N_2	N_3	1.8_2*	50 ± 25	3.1	.6	1.5
O_2	O_3	4.0_0	170 ± 70	1.2	.5	.45
CO	CO_2	4.2_8	2500 ± 250	4.8	.5	-
	C_2O	1.4_8	670 ± 260	2.6	.5	1.4
NO	N_2O	280.	1065 ± 160	6.2	.4	-
	NO_2	2.2_4	0 ± 100	5.1	.4	-
Ar ; D_2	ArD	1180.**	0 ± 50	$.9_3$	$.4_5$	1.2

** Reference for reaction rate constant (D.P. Stevenson and D.O. Schissler, J. Chem. Phys. 29, 282 (1958). Neutral gas density determination by reverse repeller method.

* M.C. Cress, P.M. Becker and F.W. Lampe, J. Chem. Phys., 44, 2212 (1966) quote: $k_r = 5.7 \cdot 10^{-11}$ cm^3 $molec^{-1}$ sec^{-1} and $k_e/k_i = 9.5 \cdot 10^{-3}$. A related rate constant: $k_{thermal} = k_r \cdot k_e/k_i = .54 \times 10^{-12}$ cm^3 $mole^{-1}$ sec^{-1} can be compared with $k_{473°K}$.

References:

1. L.E. Ferguson, "Thermal Energy Ion-Molecule Reactions" in Adv. in Electronics and Electron Physics, 24, 1 (1968).
2. L. Friedman, Ann. Rev. Phys. Chem., 19, 273 (1968).
   L. Friedman and B.G. Reuben, Adv. Chem. Phys., 19, 33 (1971).
3. R.P. Clow and J.H. Futrell, Int. J. Mass Spectrom. Ion Phys., 4, 165 (1970).
4. a) V.L. Talroze, E.L. Frankevich, Russian J. Phys. Chem., 34, 1275 (1960).
   b) K.R. Ryan and J.H. Futrell, J. Chem. Phys., 43, 3009 (1965).
   c) K. Birkinshaw, A.J. Masson, D. Hyatt, L. Matus, I. Opauszky and M.J. Henchman, Adv. Mass Spectrom., 4, 379 (1968).
   d) A.J. Masson, P.F. Fennelly and M.J. Henchman, Adv. Mass Spectrom., 5, 207 (1971).
5. A. Cohen and F.S. Klein, J. Chem. Phys., 55, 2600 (1971).
6. J.C. Light, Disc. Faraday Soc., 44, 1 (1967).

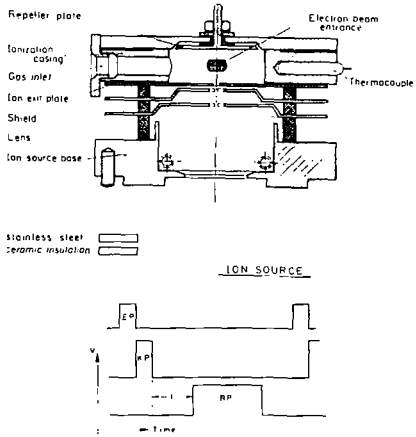

FIG. 1.

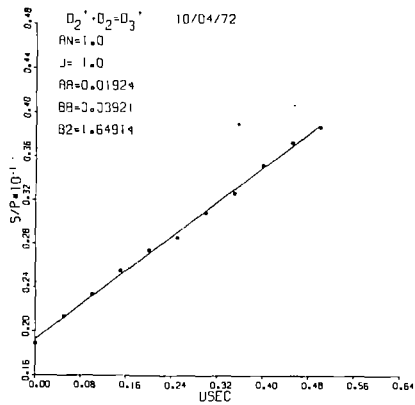

FIG. 2.

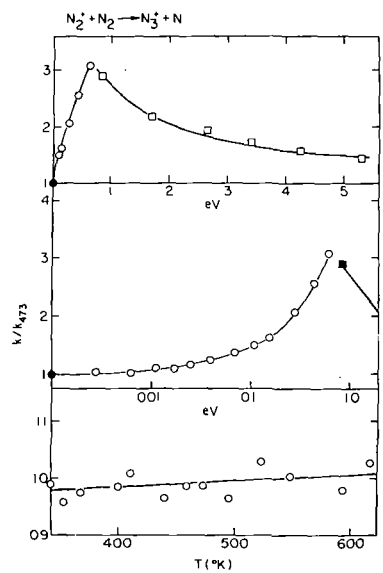

FIG. 3.

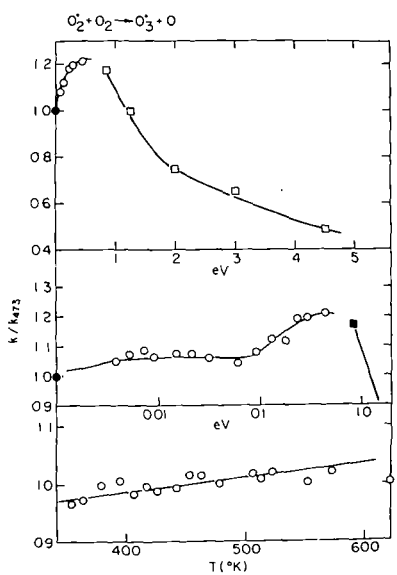

FIG. 4.

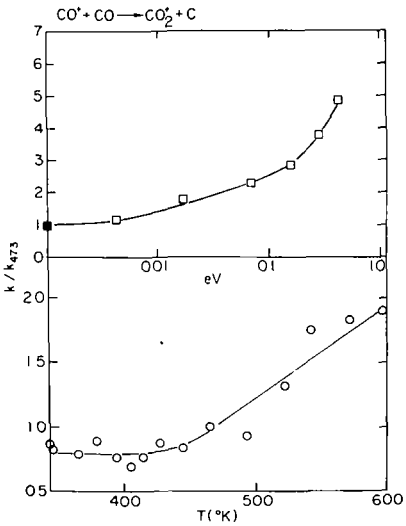

FIG. 5.

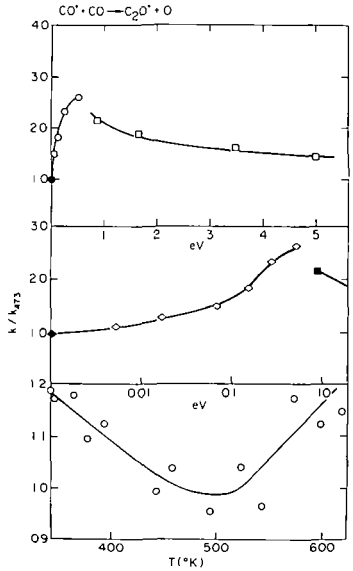

FIG. 6.

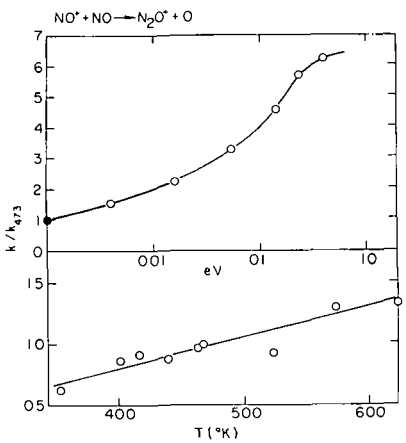

FIG. 7.

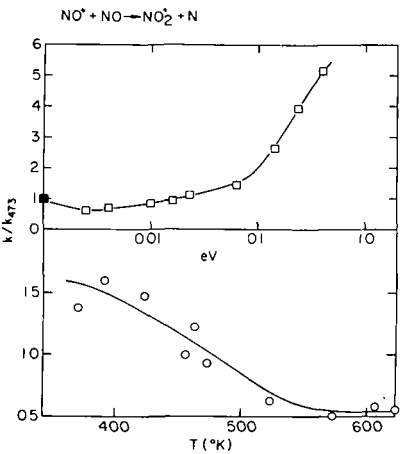

FIG. 8.

Q5

ON THE STRUCTURE OF THE ETHYL CARBONIUM ION

J. H. Vorachek and G. G. Meisels†
Department of Chemistry
University of Houston
Houston, Texas 77004

ABSTRACT

Determination of ground state structure of ions is important in mass spectrometry, as well as in other areas of chemistry. Several experimental techniques are available although some are limited in their usefulness. To assign structure on the basis of appearance potentials, one must know the heat of formation of all possible isomers. Further the heat of formation must be sufficiently different to allow unambiguous assignment of structure. Fragmentation of labelled ions is similarly useful only when the mass spectra of all possible ions are known and are sufficiently dissimilar as to be unambiguous. The results thus obtained are complicated by the possibility of isomerization of excited ions before fragmentation.[1,2] Structure assignment based on ion-molecule reactions and their reaction rates can be utilized only if rate coefficients are known for all possible isomers and if the mixture of ions is very simple.

End product analysis has also been shown to be useful in determination of structure of ions formed in static systems.[3] The requirements are simply that the ion undergo a reaction leading to a stable product and that the ion not change structure during the course of reaction. These conditions have been shown to be met for many hydrocarbon ions. The technique of end product analysis has been applied to a study of structure of $C_4H_8^+$ ions formed by ionization of each of the six C_4H_8 isomers[4] and is used in this work to investigate the structure of the ethyl cation.

Neither experimental evidence nor theoretical conjecture has led to agreement on the structure of the $C_2H_5^+$ ion. A stable ethyl ion ($CH_3CH_2^+$), a stable bridged ion ($CH_2\overset{H}{\frown}CH_2^+$), and a structure capable of complete H atom randomization have been proposed. $CD_3CH_2^+$ has been produced by the direct radiolysis of CD_3CH_2I and the isotopic makeup of the neutral ethanes produced by hydride transfer from isobutane has been determined. The mass spectra of the ethanes are consistent only with those of CD_3CH_3, indicating that less than 5% of the ethanes are CD_2HCDH_2. The symmetrical bridged structure must therefore be either endothermic with respect to the ethyl ion or its attainment must require a substantial activation energy. This investigation was supported in part by the United States Atomic Energy Commission under Contract AT-(40-1)-3606, and in part by the Robert A. Welch Foundation of Houston, Texas.

LITERATURE CITED

† A more detailed account of this work has been submitted for publication in the Journal of the American Chemical Society.

1. F. P. Lossing, Can. J. Chem.; in press.
2. G. G. Meisels, J. Y. Park, and B. G. Giessner, J. Am. Chem. Soc. 91, 1555 (1969).
3. P. Ausloos, in Ion-Molecule Reactions, J. L. Franklin, Ed., (Plenum Press, New York, New York, 1970).
4. S. G. Lias and P. Ausloos, J. Res. NBS. 75A, 591 (1971).

A STUDY OF HALOGENATED COMPOUNDS BY PLASMA CHROMATOGRAPHY

Q7

Francis W. Karasek, Department of Chemistry, University of Waterloo, Waterloo, Ontario

INTRODUCTION

The plasma chromatograph couples an ion-molecule reactor with an ion drift spectrometer and produces both positive and negative plasmagrams of organic compounds present in trace amounts in gases at atmospheric pressure. Reactant ions are formed in a moving carrier gas introduced along with the trace sample into the reactor section. An inert gas flows through the ion-drift spectrometer. These plasmagram patterns give qualitative information about the organic molecules and provide data for fundamental studies of ion-molecule reactions (1). Such halogenated species as CCl_4, $CHCl_3$ and CH_2Cl_2 exhibit distinctive positive and negative plasmagrams. The appearance of the halogen as a negative ion and interpretation of the charged species present can be related to some fragmentation mechanisms established for negative ions in mass spectra and for chemical ionization in positive ion mass spectra.

The data presented here were obtained with the Beta VI Plasma Chromatograph, whose characteristics are described elsewhere (2). The experimental conditions used are indicated in Table I.

PARAMETER	VALUE
Sample temperature	126°C
Reactant gas flow	115 cc N_2/minute
Drift gas flow	500 cc N_2/minute
Electric field	250 V/cm
Injection pulse	0.2 msec
Gating pulse	0.2 msec
Recorded scan	2 minutes

TABLE I. EXPERIMENTAL PARAMETERS FOR PLASMAGRAMS RUN

NEGATIVE PLASMAGRAMS

With N_2 carrier gas the principal reactant producing the negative plasmagrams is thermal electrons. These electrons have energies less than 0.1 eV. From fig. 1 it can be seen that all three chlorinated compounds produce the same plasmagram patterns showing a similar series of charged particles. From previous work (2) with halogenated compounds, the first peak can be identified as the Cl^- ion. When one refers to the negative ion mass spectra produced by bombardment of these compounds with 30 eV electrons, the data summarized in Table II are found (3). The mass spectra of all three compounds contain the same ions and are quite similar in intensity ratios. Since the same is true for the plasmagrams for these compounds, a reasonable assignment of the plasmagram peaks can be made to correspond to those found in the mass spectra. To further confirm these assignments the plot, shown in fig. 2, of mass versus drift time of these peaks follows the relationship expected from previous work.

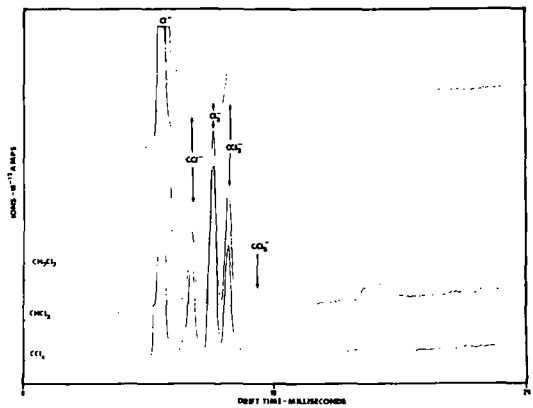

Fig. 1. Negative plasmagrams for CCl_4, $CHCl_3$ and CH_2Cl_2.

NEGATIVE ION MASS SPECTRAL DATA

COMPOUND	RELATIVE INTENSITIES OF FRAGMENTS							
	C^-	CH^-	CH_2^-	Cl^-	CCl^-	Cl_2^-	CCl_2^-	CCl_3^-
CCl_4	2	–	–	1000	22	20	8	2
$CHCl_3$	1	0	–	1000	4	6	1	–
CH_2Cl_2	1	6	2	1000	2	21	–	–
NEGATIVE PLASMAGRAM DRIFT TIMES (milliseconds)	–	–	–	5.43	6.87	7.48	8.86	9.29

TABLE II. COMPARATIVE DATA - NEGATIVE ION MASS SPECTRA WITH NEGATIVE PLASMAGRAM PATTERNS FOR CCl_4, $CHCl_3$ and CH_2Cl_2.

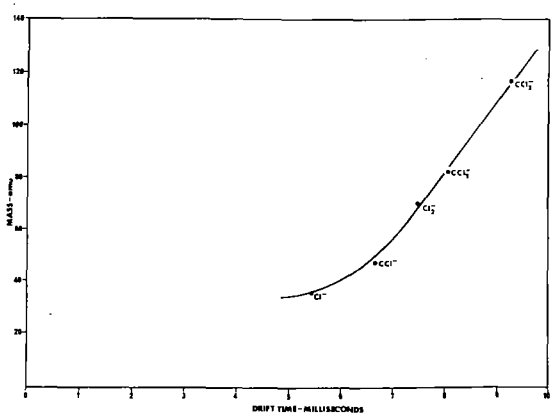

Fig. 2. Correlation of mass versus drift time for the ion peaks in the negative plasmagrams

POSITIVE PLASMAGRAMS

The positive reactant ions from a N_2 carrier gas are a group of $(H_2O)_nH^+$ and $(H_2O)_nNO^+$. The positive plasmagrams (fig. 3) obtained for the chlorinated compounds show peaks that correspond to $(MW)H^+$ and $(MW)_2H^+$. These are the species one usually finds in chemical ionization mass spectrometry, and have been well established as those obtained in the plasma chromatograph.

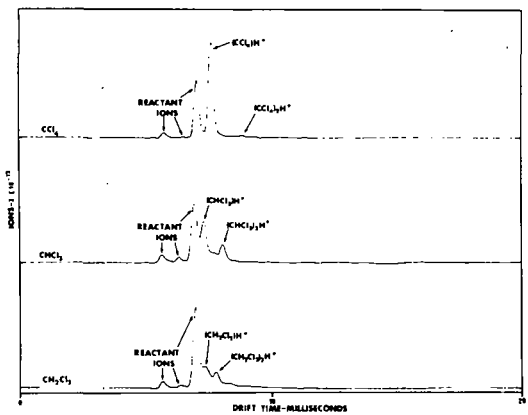

Fig. 3. Positive plasmagrams for CCl_4, $CHCl_3$ and CH_2Cl_2.

CONCLUSIONS

The charged particles observed in the plasma chromatograph must be very stable ion-molecule complexes to have survived the approximately 16 millisecond transit time through the instrument (8 milliseconds reaction time and 8 milliseconds drift spectrometer time) and the several million collisions with nitrogen molecules involved in the separation step in the drift spectrometer. There appears to be a demonstrable similarity of negative plasmagrams to negative ion mass spectra and of positive plasmagrams to chemical ionization mass spectra. Similar results are being obtained in studies with other classes of compounds. It is encouraging to note that a single instrument, operating at atmospheric pressure, can produce results comparable to those from both these techniques and with an unusually high sensitivity.

REFERENCES

1. F. W. Karasek, ANAL. CHEM., 43, 1441 (1971).
2. F. W. Karasek and O. S. Tatone, "Plasma Chromatography of the Mono-Halogenated Benzenes", ANAL. CHEM., IN PRESS.
3. J.C.J. Thynne, K. A. G. MacNeil and K. J. Caldwell, *Negative Ions*, in "Time-of-Flight Mass Spectrometry", D. Price and J. E. Williams (Eds.), Pergamon Press, 1969, p 151 - 155.

A Kinetic Analysis of the Approach to and Attainment of Equilibrium in Selected Proton Transfer Reactions

D. K. BOHME, R. S. HEMSWORTH, H. W. RUNDLE and H. I. SCHIFF

York University, Downsview 463, Ontario, Canada.

In the course of investigations of the forward direction of proton transfer (of the type $XH^+ + Y \rightarrow YH^+ + X$) proceeding at room temperature in a flowing afterglow and far from chemical equilibrium, it became apparent that conditions of concentration and time could be established under which increasing amounts of back reaction were introduced until ultimately the reactants and products existed in chemical equilibrium. Consequently a detailed kinetic analysis of the approach to and attainment of equilibrium was developed by extending analyses to include back reaction. This analysis was then applied to the experimental data obtained for the proton transfer reaction $H_3^+ + N_2 \rightleftarrows N_2H^+ + H_2$ and $CH_5^+ + CO_2 \rightleftarrows CO_2H^+ + CH_4$ proceeding in a large excess of H_2 gas. The latter reaction was investigated independently in both directions. The analysis was applied in order to determine the rate constants for the reverse direction of proton transfer and the thermodynamic equilibrium constants for these two reactions.

Ion Condensation Reactions in Benzene Vapor*†

J. A. D. Stockdale

Health Physics Division, Oak Ridge National Laboratory
Oak Ridge, Tennessee 37830

A pulsed electron source coupled to a time-of-flight mass spectrometer has been used to study thermal energy condensation reactions of $C_6H_6^+$, $C_6H_5^+$, and $C_6H_4^+$ with the benzene molecule. Rate constants for formation of the condensation products $C_{12}H_{12}^+$, $C_{12}H_{11}^+$, and $C_{12}H_{10}^+$ have been measured and an upper limit obtained for the lifetime against dissociation of $C_{12}H_{11}^+$. Rate constants for formation of $C_{12}H_9^+$ and $C_{10}H_9^+$ (dissociation products of $C_{12}H_{11}^+$) were also obtained. The rate constants reported here are substantially in agreement with those obtained by Lifshitz and Reuben[1] who, however, did not observe the formation of $C_{12}H_{12}^+$ from thermal energy $C_6H_6^+$. Table 1 lists the chief results obtained.

---

*Research sponsored by the U.S. Atomic Energy Commission under contract with Union Carbide Corporation.

†To be submitted for publication in J. Chem. Phys.

[1] C. Lifshitz and B. G. Reuben, J. Chem. Phys. 50, 951 (1969).

Table 1. Thermal Energy Ion Condensation Reactions in Benzene Vapor

Reaction	Rate Constant k (molecules^{-1} cm^3 sec^{-1})				
	E_e = 20 eV[a]	E_e = 30 eV	E_e = 50 eV	Lifshitz and Reuben[b]	Field, Hamlet, and Libby[c]
(1) $C_6H_6^+ + C_6H_6 \rightarrow C_{12}H_{12}^+$	7×10^{-12}	1.2×10^{-11}	1.3×10^{-11}	Not observed at thermal energies	7×10^{-12} [d]
(2) $C_6H_5^+ + C_6H_6 \rightarrow C_{12}H_{11}^+$	4.3×10^{-10}	3.0×10^{-10}	3.9×10^{-10}	1.17×10^{-10}	
(3) $C_6H_5^+ + C_6H_6 \rightarrow C_{12}H_{11}^+ \rightarrow C_{12}H_9^+ + H_2$	7.5×10^{-11}	4.7×10^{-11}	7.9×10^{-11}	4.37×10^{-11}	
(4) $C_6H_5^+ + C_6H_6 \rightarrow C_{12}H_{11}^+ \rightarrow C_{10}H_9^+ + C_2H_2$	9.8×10^{-11}	1.6×10^{-10}	2.4×10^{-10}	3.66×10^{-11}	
(5) $C_6H_4^+ + C_6H_6 \rightarrow C_{12}H_{10}^+$		4.7×10^{-10}	3.2×10^{-10}	1.27×10^{-10}	
(6) $C_6H_4^+ + C_6H_6 \rightarrow C_{12}H_{10}^+ \rightarrow C_{12}H_8^+ + H_2$		8.0×10^{-11}	1.3×10^{-10}	1.43×10^{-11}	

(a) E_e = electron beam energy. Half width of electron beam $\approx$ 0.5 eV. Electron beam gate pulse width 1.5 μsec. C_6H_6 pressure 3.4×10^{-4} torr as measured on MKS Baratron capacitance manometer. C_6H_6 temperature 295° K. Rate constants listed for this work are thought to be accurate to within $\pm$ 30%.

(b) E_e not given. C Lifshitz and B. G. Reuben, J. Chem. Phys. 50, 951 (1969).

(c) F. H. Field, P. Hamlet, and W. F. Libby, J. Am. Chem. Soc. 89, 6035 (1967).

(d) Result obtained when $C_6H_6^+$ was produced by chemi-ionization collisions of Xe* with C_6H_6.

REACTIONS OF H_2S^+ WITH H_2S AND H_2O IN A PHOTOIONIZATION MASS SPECTROMETER

J.M. Hopkins and L.T. Bone
Department of Chemistry
East Texas State University
Commerce, Texas 75428

INTRODUCTION

The relative proton affinities of H_2S and H_2O have been in question for some time. Reported values[1] for these quantities do not offer much precision and are otherwise dubious in the light of our observations. We, therefore, considered it worthwhile to study the proton transfer reaction:

$$H_3S^+ + H_2O \rightleftharpoons H_3O^+ + H_2S$$

using a photoionization mass spectrometer capable of producing ground state ions in a field free region.

EXPERIMENTAL

The photoionization mass spectrometer used in these experiments has been described in detail elsewhere.[2] Mixture of H_2S and water were irradiated with a Kr resonance lamp with a LiF window. Under these conditions ground state H_2S^+ is produced but water is not ionized. Source pressure measurements were made with a Granville-Phillips Capacitance Manometer connected to the source. Temperature measurements were made with an iron-constantan thermocouple inside the source.

In these experiments the mixtures were allowed to react at source pressures from zero to 1.5 Torr and spectra were taken at each pressure increment. Graphs of log percent ionization *vs* source pressure were made for each mole fraction at temperatures of 296-, 355-, and 426°K. Mole fractions of water from 0.05 to 0.50 were examined.

RESULTS AND DISCUSSION

The overall reaction scheme is:

1) $H_2S^+ + H_2S \xrightarrow{k_1} H_3S^+ + HS$

1a) $H_2S^+ + H_2O \xrightarrow{k_{1a}} H_3O^+ + HS$

2) $H_3S^+ + H_2O \underset{}{\overset{k_2}{\rightleftharpoons}} H_3O^+ + H_2S$, $K_{eq}=K_1$

3) $H_3O^+ + H_2O + M \xrightarrow{k_3} H(H_2O)_2^+ + M$

4) $H(H_2O)_n^+ + H_2O \longrightarrow H(H_2O)_{n+1}^+$

Graphs of log percent ionization *vs* pressure indicate that reaction 1a) occurs at the higher temperatures. The equilibrium constant K_1 for reaction 2) was found kinetically using steady state approximations for H_3S^+ and H_3O^+ individually. At the H_3S^+ steady state the equation

$$K_1 = \frac{k_1}{k_{-2}} \frac{[H_2S^+]\,[H_2S]}{[H_3S^+]\,[H_2O]} + \frac{[H_3O^+]\,[H_2S]}{[H_3S^+]\,[H_2O]}$$

is a straight line with K_1 as its intercept. At the H_3O^+ steady state the equation

$$K_1 = \frac{k_3 M}{k_{-2}} \frac{[H_3O^+]}{[H_3S^+]} + \frac{[H_3O^+]\,[H_2S]}{[H_3S^+]\,[H_2O]} - \frac{k_{1a}}{k_{-2}} \frac{[H_2S^+]}{[H_3S^+]}$$

yields K, as its intercept. The last term is zero at these pressures since H_2S^+ disappears at lower pressure.

For each mole fraction appropriate terms of the H_3O^+ steady state equation were plotted and extrapolated to the intercept. The extrapolations consistently converged to a single point with little scattering.

Using these techniques thermodynamic values for reaction 2) were found to be:

K_1	$T(^0K)$	
0.15	296	
0.28	355	ΔH^0 = 2.1 kcal/mole
0.47	426	ΔS^0 = 3.1 eu

It is interesting to note that we have never detected ionic species of the type: $H(H_2S)_2^+$, $H(H_2O)(H_2S)^+$, $H(H_2O)_2(H_2S)^+$, etc, while hydrates like $H(H_2O)_2^+$, $H(H_2O)_3^+$, etc, are abundant; perhaps indicating the importance of hydrogen bonding in ion clusters since water can hydroden bond and hydrogen sulfide cannot.

REFERENCES

* Funded by The Robert A. Welsh Foundation, to be submitted for publication to J. Chem. Phys.

1. A fairly complete listing of previous values are reported by M.A. Haney and J.L. Franklin, J. Chem. Phys., 50, 2028, (1969).

2. M.J. McAdams and L.I. Bone, Nineteenth Annual Conference on Mass Spectrometry and Allied Topics, 199-201, Atlanta, Ga., May 1971.

R1

An Interactive Mass Spectral Search System

Stephen R. Heller, Henry M. Fales and G. W. A. Milne
NIH, Bethesda, Md. 20014

An interactive conversational mass spectral retrieval system, available over ordinary telephone lines using a teletype-writer terminal from a central computer in the Division of Computer Research and Technology at the National Institutes of Health (NIH), has been used extensively by many researchers since September, 1971.

The mass spectral search system is based on 8782 uncertified electron impact mass spectra. Compounds whose mass spectra are in the file can be immediately identified and very useful structural inferences can be obtained for compounds that are not represented in the file. The file may be searched in a number of ways. The current options in the system are:

MASS SPECTRAL SEARCH SYSTEM

1. PEAK AND INTENSITY SEARCH
2. MOLECULAR WEIGHT SEARCH
3. MOLECULAR FORMULA SEARCH
   a. Complete
   b. Imbedded
4. MOLECULAR WEIGHT AND PEAK SEARCH
5. MOLECULAR FORMULA AND PEAK SEARCH
6. MOLECULAR WEIGHT AND MOLECULAR FORMULA SEARCH
7. SPECTRUM PRINTOUT

The system uses an "abbreviated spectrum" file consisting of the two most intense peaks in every interval of 14 amu, starting at m/e = 6.[1]

The various files used in the search system have been stored on the computer disk since last September and the search program is available whenever the PDP-10 computer is on. The complete programs now require 14,000 words of 36 bit word computer storage and response time is virtually instantaneous. Normal searches use 2-6 sec. of cpu time and an average user takes 5-15 minutes sitting at a computer terminal to do a search.

At present, the file contains 8782 spectra. As new spectra are added to the file, in addition to the data (masses, intensities, MW and MF), structural information in the form of Chemical Abstracts Registry Numbers (REGN) and, perhaps at a later date, Wiswesser Line Notation (WIN), are being included so that a new and different type of search procedure called "substructure searching" can be incorporated. Substructure searching is a method of finding chemical groups, fragments, or substructures imbedded

in a chemical structure.

Attempts are being made to obtain structural information for the original 8782 compounds, however, the non-systematic nomenclature sometimes used in the file (which was not organized with this use in mind) makes the task difficult. It is hoped that researchers will become more aware of the need for a carefully and well defined data base of mass spectral information and aid in the establishment of a high quality file. One very positive result of having a large centralized data base in constant use by many researchers is that errors in the file are found much more readily, and all benefit immediately from the corrected data base.

Researchers desiring to know how they may obtain access to the system, and a copy of the instruction manual, should address their requests to Dr. Henry M. Fales, Laboratory of Chemistry, National Heart and Lung Institutes, National Institutes of Health, Building 10, Room 7N-316, Bethesda, Maryland 20014.

---

[1] H. S. Hertz, R. A. Hites and K. Biemann, Anal. Chem., 43, 681 (1971).

Diagnostic Functions in Construction of a Mass Spectral Data File

C. Merritt, Jr., D.H. Robertson, R.A. Graham and T.L. Nichols
Pioneering Research Laboratory, U.S. Army Natick Laboratories, Natick, Mass. 01760

Two diagnostic functions, and a binary coding method, have been developed for purposes of providing, in each case, a single-valued representation of the spectrum which can be easily stored in a data file. Once the single-valued function has been calculated for an unknown mass spectrum, its value is compared for match or mismatch against a file of similar functions with the spectra of known compounds.

The first two approaches to the classification of mass spectral data, namely the use of the Khinchine entropy function and the divergence values, are derived from set theory as described in the paper presented last year (1). These, as well as the octal coding method described in a companion paper (2), all reduce the mass spectrum to a single valued number which is diagnostic for the compound.

The Khinchine function, it may be recalled, is expressed as follows:

$$-\eta = \sum_{i=1}^{n} p_i \log p_i$$

The entropy function, η, is calculated by summing the product of the individual ion abundances and their respective logarithms. The mass spectra are converted to their corresponding entropy functions, thus creating a data file consisting of these numbers. In a search of a file of precalculated Khinchine values, a matching index is used to establish the correspondence of the value for an unknown compound with the library value.

In some cases the values for more than one compound may be close enough to prevent unambiguous identification. In practice however the entropy function is uniquely diagnostic in better than 90% of the cases investigated. In the case of the remaining 10% the divergence function serves to differentiate two mass spectra whose entropy functions do not differ by a value sufficient to identify them uniquely.

The divergence function

$$J(1,2) = N_1 \sum_{i}^{n} (p_{1i} - p_i) \log_e \frac{p_{1i}}{p_i} + N_2 \sum_{i}^{n} (p_{2i} - p_i) \log_e \frac{p_{2i}}{p_i}$$

where

$$P_i = \frac{P_{1i} + P_{2i}}{2}$$

is similar in nature to the entropy function, since the calculation is based on the evaluation of the summation of the products of the ion abundances and their logarithms, but in this case the equation is derived to establish a comparison of the values for two compounds, specifically, where P_{1i} and P_{2i} are the ion abundances expressed as percent of total ionization for each of the compounds for which the divergence is calculated. It has been found convenient to refer the calculation of divergence of a given compound in the aliphatic hydrocarbon series to that of the normal alkane of the same carbon number. Thus, in a library file of divergence values, a group of sub sets is established corresponding to the values for the compounds having the same carbon number. This greatly reduces the number of values to be searched and correspondingly the time to execute the search.

The calculations required to encode spectra as entropy, and particularly divergence functions, are somewhat lengthy to perform in a small computer without the aid of a hardware arithmetic unit. Moreover, the variability in the values of relative ion abundances with variations in mass spectrometer design and operation, produces considerable uncertainty in the reliability of diagnostics based on measurement of spectral intensity factors. For these reasons, a codification procedure has been developed for use with low resolution mass spectral data banks which allows compression of the library file through selective binary coding of characteristic peaks and use of variable length logical reocrds. The coding procedure is described in the accompanying paper (2). This paper is concerned mainly with the practical application of octal coding to the processing of analytical data in a laboratory in which use of data processing is constrained by the limitation of the capabilities of the computer system.

A schematic diagram of the equipment available is shown in Figure 1. The mass spectra are acquired by means of the Hewlett-Packard 2116B which is coupled to a gas chromatograph/mass spectometer analysis system. The mass spectrometer is a magnetic deflection type capable of providing 1 second spectrum scans which can be digitized by the computer in real time. The system has only 8K of 16 bit core and its I/O structure includes only paper tape read and punch, and a teletype. It is thus not possible to output in real time or to store large volumes of acquired data for subsequent processing. A LINC-8 computer,

however, which resides in a nearby laboratory, is equipped with a disc storage device. The LINC-8 is an 8K – 12 bit machine having in addition to the disc, a paper tape I/O, a teleprinter and block addressable magnetic tape. By some special output formatting of the H.P. data, the acquired spectral data are transmitted from the H.P. to the LINC-8 for storage on the disc. Subsequent processing is then accomplished in the LINC-8.

A chart of the data flow in the combined H.P.–LINC–8 system is shown in Figure 2. The mass spectrum signal above threshold is digitized, and using centroid computations, is reduced in the H.P. to time and intensity values which are transmitted to the LINC in real time and stored on the disc. At the conclusion of a chromatographic run, the spectra are successively retrieved from the disc, mass and intensity are calculated, converted to octal code and the library searched. An interim printout can be provided if required by the analyst, (e.g., if the spectrum is found not to be in the library and the digitized data is needed for another type of search).

The current system is being used to expedite the interpretation of data obtained from large numbers of samples required to be analyzed by GC/MS in a study of the wholesomeness of irradiated beef. For example, the study in one year may require identification of the components corresponding to 150,000 spectra. Fortunately, the composition of many of the components can be anticipated and thus a limited library file for searching can be established. Some of the expected compounds are listed in the table below:

Compounds In Irradiated Meat Volatiles

C_1-C_{20}	RH	C_2-C_6	RCHO
C_2-C_{20}	$RC=CH_2$	C_3-C_6	R_2CO
C_2-C_{20}	RC≡CH	C_1-C_4	RSH
C_1-C_6	ROH	C_2-C_6	RSR, RSSR

C_4-C_{20} alkadienes

In all, the library contains about 200 compounds. Since the LINC-8 is a 12 bit computer, the computer words for these spectra were reformatted from the H.P. data file to correspond to the smaller word size. Basically, this means an increase in the number of computer words for a given compound. Using subfiles however, the number of compounds to be searched in most cases is usually quite limited. Some examples of subfiles from our limited library are shown on the computer printout reproduced in Figure 3. The top number is the number of computer words needed to encode the spectrum in the LINC-8 and the lower number is the number of compounds in the subfile. The compound names are printed below.

For this practical case, as the number of words increases, the number of components decreases, making actual identification almost trivial, e.g., as seen here the 9 word subfile contains only three components and the 10 word file only one component.

The calculation sequence is as follows:

1. Digitize spectrum – mass and intensity
2. Convert to octal code
3. Search subsets
4. Printout

The printout gives the 5 nearest matches with a code number which reflects the nearness of the match, i.e., the lowest numerical code number indicates the nearest match, but in many cases with the smaller subfiles, this is superfluous.

Figure 4 shows a reproduction of the printout indicating the identification of the component found for mass spectrum No. 10 in a typical chromatographic analysis. The octal code subfile searched was for a compound represented by 9 computer words. Only 3 compounds were found in the file and the best match was given by tridecane.

This method of coding and searching data files for the identification of compounds in GC/MS eluates has greatly expedited the time required to complete analyses and has eliminated the need to utilize the services of a skilled mass spectroscopist for the interpretation of routine analytical data.

1. Robertson, D.H., and R.I. Reed, Proceedings of the 19th Annual Conference on Mass Spectrometry and Allied Topics, American Society for Mass Spectrometry, Atlanta, Ga., 1971, paper no. D5.

2. Robertson, D.H., J.F. Cavagnaro, J.B. Holz, and C. Merritt, Jr., Proceedings of the 20th Annual Conference on Mass Spectrometry, and Allied Topics, American Society for Mass Spectrometry, Dallas, Texas, 1972, paper no. R3.

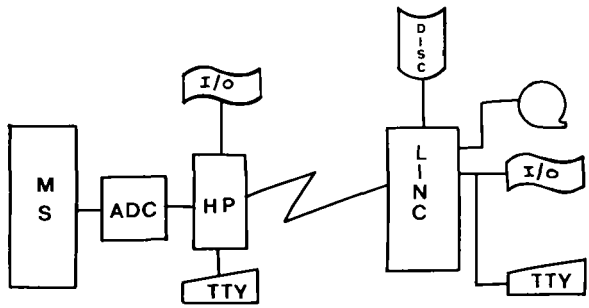

Figure 1. Schematic diagram of computer system

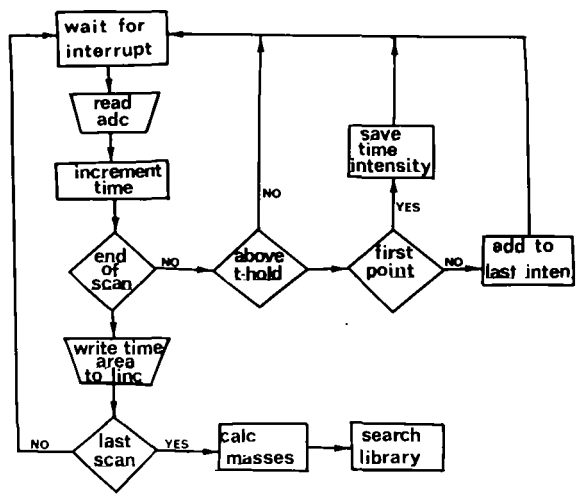

Figure 2. Flow chart for data acquisition and processing

```
      3
      7
2-BUTANONE
2-METHYLBUTANE
N-PENTANE
L-PENTYNE
ACETONE
1-PENTENE
N-PUTANE
      4
      6
N-HEXANE
2-METHYLPENTANE
1-HEXENE
1-HEPTENE
1-HEPTYNE
1-HEXYNE
      5
     10
1-OCTENE
2-METHYLHEPTANE
N-HEPTANE
2-METHYLHEXANE
CIS-1,2-DICHLOROETHYLENE
PHENYL METHYL KETONE
N-OCTANE
1-DECYNE
1-OCTYNE
1-NONYNE

      9
      3
N-TETRADECANE
1-TETRADECENE
TRIDECANE
     10
      1
1-PENTADECENE
```

Figure 3. Computer printout of representative subfiles

```
SCAN NO.:  10        START TIME:  626.  SEC

COMPOUND NAME              MATCHING INDEX

TRIDECANE                          9
N-TETRADECANE                     25
1-TETRADECENE                     43
```

Figure 4. Typical computer printout of identification of GC component

Characteristic Peak Coding For Low Resolution Mass Spectra

D.H. Robertson, J. Cavagnaro, J.B. Holz
and C. Merritt, Jr.
Pioneering Research Laboratory, U.S. Army Natick Laboratories, Natick, Mass. 01760

A basic problem in the processing of spectroscopic data by computer is that of data file management. This involves coding of data for storage in the file and the technique of searching the file for purposes of finding a match among file-data for an unknown spectrum.

The traditional approach has dealt with the basic tables of m/e vs. intensity values that constitute digitized mass spectra. Numerous methods have been proposed for retrieving relevant data from such tables. In general, identification of an unknown mass spectrum involves testing the unknown against a known spectrum to observe their similarity. Some sort of matching index is computed whereby a numerical value is assigned to the similarity or dissimilarity of the two spectra as dictated by the criteria of the test. By comparing the unknown to each known spectrum in the library file, and computing a matching index for each trial, it is possible to achieve identification for the best match of the unknown to a known spectrum in the library file.

Because of the large number of spectra to be searched, the computer configuration required to execute searches of data for unknown component identification is usually quite large, and the time required for retrieval is slow. Moreover, there is a need in many laboratories to be able to perform computer searches on smaller computers that lack adequate peripheral storage facilities for large data files.

In particular, the variability in the values of relative ion abundances with variations in mass spectrometer design and operation produces considerable uncertainity in the reliability of diagnostics based on measurement of spectral intensity factors. For these reasons, this laboratory has recently conceived and tested a codification procedure for use with low resolution mass spectral data banks which allows compression of the library file through selective binary coding of characteristic peaks and use of variable length logical records.

The coding procedure is illustrated in Figure 1. Selective binary coding of characteristic peaks is accomplished by arbitrarily dividing the mass range of interest into multiple groups of seven. The number corresponding to the spectrum peak having the highest intensity is then encoded as a three bit binary number. Thus the fourth peak is encoded in the first grouping, the 7th peak in the second and so on; zero is used to denote the absence of a peak within the grouping, thereby giving a total of 8 possible values, hence the term octal coding.

Representation of an octal number within the computer requires three bits; thus, in a 16 bit machine such as the Hewlett-Packard 2116B used first in setting up this system, five octal characters can be stored in each computer word with one bit left over. Thereby a single computer word is capable of storing information which covers a range of 35 atomic mass units (m/e units). Compounds requiring a greater range of mass units to be encoded require an additional number of computer words. As many are used as are needed to encode the spectrum. The last word is then designated by setting a flag in the 16th bit.

If consideration is given to the m/e values which occur most often in the spectra of organic compounds, a series of octal ranges (as seen in Table 1) beginning with the group of 7 masses, 23-29, serves to provide greater diagnostic character for this method of coding. Subsequent mass ranges would be 30-36, 37-43, etc. The first octade, containing masses 12-14-15-16-17-18-19 was included in the original codification procedure but when it was learned that no additional information was gleaned from using these m/e values, the entire octade was dropped from consideration.

Table 1

Example of Octal Coding

Mass Ranges	23-29	30-36	37-34	44-50
m/e to be Encoded	24	32	43	0
Position of m/e in Octet	2	3	7	0
Binary Code	010	011	111	000
Octal Code	2	3	7	0

The efficiency of a coding procedure is reduced by the need to use "O" for coding, i.e., coding which leads to a large number of zeros. If one codes in octades (or some larger sized grouping) there is more likelihood of a peak appearing and thus, according to the basic principles of information theory, greater entropy, as reflected by more efficient transmission of information. In general, the encoding and retrieval of data from a number system such as this is predicated primarily on the principle of simple manipulation of the numbers. By arranging the mass ranges so that certain ions fall characteristically in particular octets it is also possible to develop qualitative information content that may relate to the functional group structure of the molecule. However, presentation of the details of this aspect must be deferred at this time.

The octal code for a mass spectrum may be readily obtained from digitized mass and intensity data acquired on-line and stored for subsequent processing. A flow chart of the program for encoding the mass spectrum into its corresponding octal code words is shown in Figure 2.

In our laboratory a normal sequence of data processing would involve the following on-line operations.

1. Conversion of the analog mass spectrometer output to digital format, i.e., mass and intensity data.

2. Condensation of the data to octal format to provide a binary equivalent of the "spectrum" for which the data library is searched.

When binary "1" is sensed in the 16th bit, the number of words to encode the "spectrum" is known; thus it is not necessary to search the entire library but only the subset or sub-library collection of spectra which require that number of words for coding. With this coding technique, it is possible to divide the total file into a series of sub files based on the number of computer words necessary to selectively code the spectrum to its highest observed m/e. This particular organizational form appears to be of special utility in fully automated gas chromatographic/mass spectrometric analysis systems, since the highest observed m/e is a quantity readily extracted during the data reduction process. In actual use, such file organization implies pre-filtering of the data tables, since only those subfiles having the same number of words as the unknown must be searched.

As previously indicated, the subfiles, as constructed in this work, use the 16th bit of the word to signify the end of the logical record. The word immediately following the end of the logical record thereby contains an integer pointer to a separate file containing the alphanumeric characters of the compound name. The division into sub files of variable logical record length and creation of a name file were designed to make maximum use of random access mass storage devices. For example: if full binary representation is used to code the spectra of both ethane and tridecane, it is found that sixteen 16-bit words of uniform logical record length are required. However, the use of variable-length logical records for the same pair of compounds requires one and five 16-bit words respectively to identify the reference spectra, i.e., ethane and tridecane. Examples of the subset files are illustrated in Table 2.

Table 2

Subsets of Octally Coded Spectra

One-word	Ethane 147300
Two-word	Benzene 047170, 150374
Three-word	2,3-dimethyl-3-pentanol 052725, 025252, 102000

Since one computer word is capable of representing 35 mass positions, five computer words are needed to encode to a mass of 175. Since the average molecular weight of 6652 compounds contained in the Atlas of Mass Spectral Data is 167, it is seen that five computer words is the average number required for the total collection of data. For each unknown compound being search for in the library, a matching index is calculated; the five best matches, in decreasing order of goodness of match, are printed. This feature is expected to be most useful in future cases when much expanded library files are being searched and the possibility exists for the same matching index to be calculated for more than one compound.

In addition to the utility of construction of subfiles for more efficient retrieval, the octal coding system is found to provide a dampening effect on variations in spectral characteristics due to its relative insensitivity to errors in digitization. For example, errors which may occur in the initial codification of an unknown spectrum, due to a spurious signal or the additive effect of impurities upon peak intensities, have insignificant influence upon correct identification of the compound in question. Likewise, in the case where the spectrum of an unknown compound is incorrectly coded because of variation in relative intensity values due to mass spectrometer instabilities, it is shown that correct identification may result even in cases where a coding error occurs in each word of the spectrum.

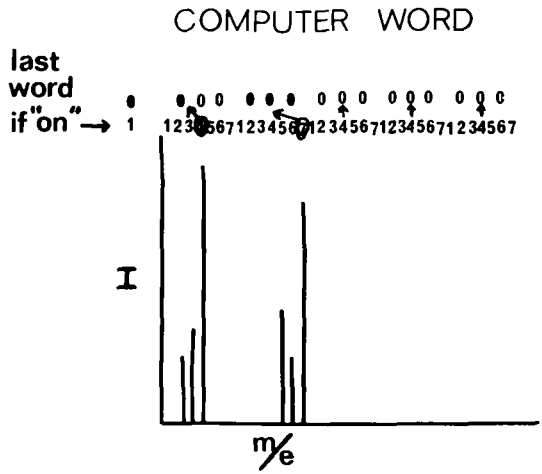

Figure 1.

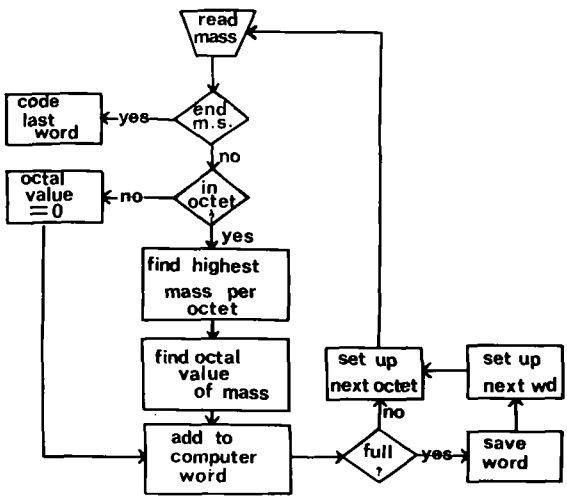

Figure 2. Flow chart, for on line encoding of mass spectra

COMPUTER IDENTIFICATION OF MASS SPECTRA USING HIGHLY COMPRESSED SPECTRAL CODES

Stanley L. Grotch
Jet Propulsion Laboratory
Pasadena, California 91103

Many studies have been reported on the use of computers for the automatic interpretation of chemical spectra. Because of its innate simplicity, generality, and high effectiveness, the file search procedure has received the widest attention,[1] and today is used in most automated identification systems.

In file searching, both the unknown spectrum and a library of known spectra are first encoded. The code of the unknown spectrum is compared with either the entire library file or some subset of the file using a "goodness of fit" criterion. At the conclusion of the search, the N best-fit spectra are displayed.

The two most important attributes of any search scheme are high accuracy of identification and low cost. Low search costs are closely related to the requirements levied on the computer system, particularly in the areas of storage and search times. Both storage requirements and search times can be reduced by compressing spectral data, often without a significant degradation in identification effectiveness.

One technique for compressing spectral information is known as spectral abbreviation.[2,3] Here, a mass spectrum is divided into regions (windows), each of a constant number of amu (commonly, 14 amu is used). Within each window, the M most intense peaks are coded (typically, M=2). For the large libraries now available, encoding 2 peaks/14 amu results in a storage savings of about a factor of five over storing the complete spectra. Additionally, since only 1/5 the number of peaks need be considered, a significant savings in search times is also found.

This concept may be exploited even further by observing that since $14 < 2^4$, the mass position of each peak in any window can be expressed unambiguously using only four bits. If the 4-bit code "0000" is used to denote no peak present in a window (above a lower threshold), each peak position may be encoded using the offset of the given mass from the starting mass in the window, plus one. For example, if the first window begins at mass 6, a code "0000 1000 0111" specifies that the first window (6-19) has no peak, the second window (20-33) has its most intense peak at mass 27, the third window (34-47) has its most intense peak at mass 40, etc. The extension of this coding to higher masses or to more than one peak/14 amu is self-evident. An examination of nearly 7000 spectra in the Aldermaston collection shows that an average of 12 windows is needed for encoding with this method (48 bits/spectrum). This form of coding reduces storage requirements by about a factor of 60 over using the complete spectrum.

Several coding techniques and comparison algorithms were tested using 125 "unknowns" searched against a library of 6880 spectra. These unknowns are organic compounds ranging in molecular weight from 57 to 256 with an average molecular weight of 121.[4] One precondition was imposed on the library compounds searched: the base peak of the library spectrum must be a significant peak (> 75%) in the unknown. At the conclusion of the search, the ten "best fit" compounds are displayed, making it possible to examine the accuracy of any search algorithm.

Using a one peak/14 amu code, with no additional peak height information, it was found that if only the five "best" answers were displayed, the correct answer was among them for 117 of the 125 unknowns. In this case, a matching algorithm is used which weights agreements in matching peaks in terms of the intensities in the unknown. Because of the compactness of this code, it was possible to search the entire library file in less than ten seconds, and a restricted subset of the file in less than one second (IBM 360/44).

Even greater accuracy in the search can be obtained by using an additional two bits for coding the intensity of the most intense peak/14 amu. With this code, storage requirements increase to an average of 72 bits/spectrum, but the efficiency of the search improves markedly. If only the unique "best" answer is displayed from the search, it is correct for 90% of the unknowns. With no intensity information provided, the corresponding figure is 78%. It is interesting to note that for a search using the complete spectrum, the equivalent figure is only 53%. Apparently, the compressed code produces a beneficial filtering effect which aids in the identification process.

This type of coding lends itself very well to most computers manufactured today since almost all have word sizes which are multiples of four bits. Because of their extremely compact nature, these codes should be of great utility in mini-computer applications where storage is often a severe problem.

It is planned to publish a more detailed account of this work in "Analytical Chemistry."

References

1. R.G. Ridley, "Biochemical Applications of Mass Spectrometry", Ed.. G.R. Waller, Chapter 6, Wiley (1972).

2. B.A. Knock.et.al.,"Analytical Chemistry",42, 1516 (1970).

3. H.S. Hertz, R.A. Hites, K. Biemann, "Analytical Chemistry", 43, 681.(1971).

4. S.L. Grotch, "Analytical Chemistry", 43, 1362.(1971).

This paper presents the results of one phase of research carried out at the Jet Propulsion Laboratory, California Institute of Technology, under Contract No. NAS 7-100, sponsored by the National Aeronautics and Space Administration.

IDENTIFICATION OF MASS SPECTRA BY A COMPUTERIZED LIBRARY SEARCH

N. W. Bell, Hewlett-Packard Company
Scientific Instruments Division
Palo Alto, California

A computer program is described that is useful in identifying an unknown compound given its low-resolution mass spectrum. The program compares the spectrum with a group of spectra obtained from known compounds. This group of spectra will be called the library. After the spectrum of the unknown compound has been compared with all of the library spectra, the names of the most similar compounds are printed. Each comparison produces a number between zero and one which is called a match index. The names of the library compounds having the highest match indices are the ones to be printed.

The heart of the program is the pattern comparison algorithm. The algorithm should produce valid results when comparing spectra from various types of instruments that have different high and low-mass sensitivities. It should work with unknown spectra obtained during the analysis of the impure effluent from a gas chromatograph.

The algorithm is similar to that used by Hertz et al[1]. The library spectrum and the unknown spectrum are divided up into 14 AMU regions starting at 6 AMU. These regions are then individually compared.

A 6-step process is used for the comparison:

1) The three peaks having the largest abundance in the region are located in the library spectrum.

2) The ratios of the abundance of the largest peak to the abundance of the second largest and the ratio of the largest to the third largest are calculated. These ratios denoted as L2 and L1 in Figure 1.

3) The spectrum of the unknown compound is examined to see if there are two or more peaks at corresponding masses $\pm$ 0.3 AMU. If matching peaks are found, similar ratios, U2 and/or U1, are calculated.

4) The ratio of ratios is calculated for each set of matching peaks: L1/U1 and L2/U2. These ratios will be unity for identical spectra. If either of these ratios is greater than unity, it is replaced with its reciprocal.

5) The process is repeated for all the regions having one or more common peaks in both spectra.

6) A match index is calculated for the library spectrum being compared. This number is the sum of the ratios of ratios divided by the number of sets of matching peaks,

$$\text{Match index} = \frac{L1/U1 + L2/U2 + \cdots}{N}$$

The match index will always be less than one so that it may be used to rank the library spectra by similarity.

The entire process is repeated for the remainder of the library spectra. While this is being done, the ten largest match indices are stored along with their associated library compound names.

After the last library spectrum has been compared, the names of the compounds associated with the ten spectra having the largest match indices are ranked and printed.

Program may also be used to search a group of spectra obtained during a GC separation to find which mass scan is most similar to a known spectrum. This mode of operation is useful to determine if a certain compound is in a mixture and, if so, what is its retention time.

The program was written in Hewlett-Packard assembly language. 770 source statements were required. The absolute object program including drivers, buffers, FORTRAN format routines, and library subroutines requires about 7000 words of core storage.

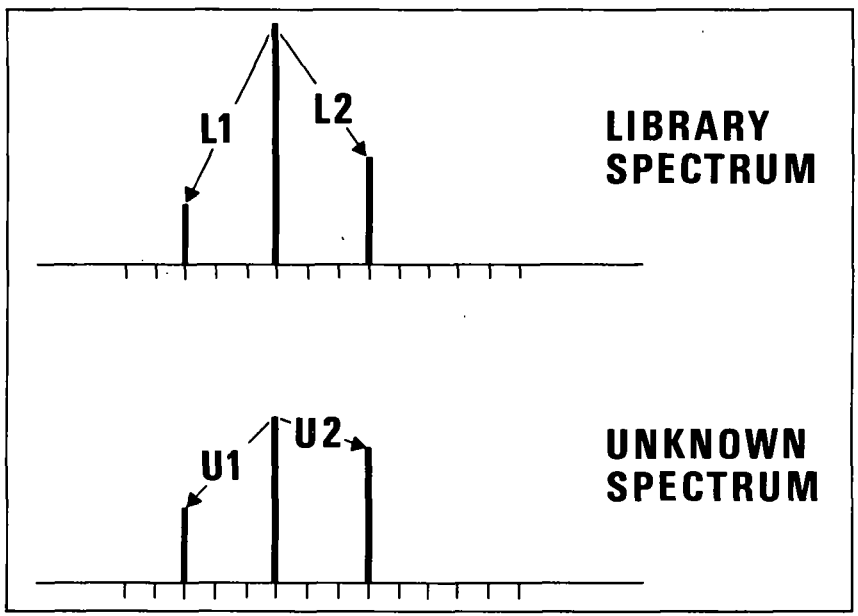

FIGURE 1 - ABUNDANCE RATIOS ARE CALCULATED FOR THE 3 LARGEST PEAKS IN EACH 14-AMU REGION.

Reference

1) H. S. Hertz, R. A. Hites, K. Bieman, Anal. Chem., V. 40, 681-691 (1971).

Computer Matching of Quadrupole and Literature Spectra

R6

J. M. McGUIRE, A. L. ALFORD, and M. H. CARTER
Environmental Protection Agency
National Environmental Research Center, Corvallis
Southeast Water Laboratory
Athens, Georgia 30601

For several years the Southeast Water Laboratory's use of GC-MS to identify organic chemical pollutants[1] has proved to be a very effective technique. During the past year, more than a dozen other Environmental Protection Agency laboratories added similar instrumentation, which is basically the GC/quadrupole MS/small computer system described by Bonelli.[2] The Southeast Water Laboratory has developed techniques for rapid, routine identification of pollutants based on computerized spectral matching with a central file of spectra.

A central computerized library of approximately 11,000 mass spectra has been established. It consists of the Aldermaston file[3] plus additional quadrupole spectra of pesticides, terpenes, and hydrocarbons. A program is required that will compare spectra from quadrupole instruments with those from magnetic focusing instruments and that will also compare spectra from the same type instruments.

Compared to magnetic deflection spectrometers, quadrupole instruments exhibit a bias toward low mass. This is demonstrated in Figure 1 which compares both types of spectra of the pesticide, parathion, and in Figure 2 which compares the methyl eicosanoate spectra.

The summary of the five largest peaks in each of these spectra (Table I) shows that spectrum matching of a magnetic deflection file based on the five largest peaks[4] of a quadrupole spectrum will not give a reliable match. In fact, the specific methyl ester identification is poor, since the strongest peaks contain little structural information.

To provide a fast but more reliable matching program, a joint effort was undertaken with the Battelle Columbus Laboratories. Operating under an Environmental Protection Agency research grant, Hoyland and Neher of Battelle modified the algorithm and abbreviated spectrum scheme of Hertz, Hites, and Biemann[5] for use with a CDC 6400 computer.[6] Using the techniques developed, the quadrupole spectrum, shown in Figure 3, of a compound discharged to the Ohio River was readily identified. Figure 4 shows the computer identification dialogue and input data (as mass number paired with relative intensity) in the first 11 lines; spectrum matches appear below in the computer output. The two best hits are both hexachlorobenzene; the quadrupole spectrum (SEWL) is a better match than the magnetic deflection spectrum (AST). Identification was confirmed by comparing GC retention times and MS cracking patterns with those of a known hexachlorobenzene sample.

Terpene identifications were also made and confirmed in several samples. The computer program works extremely well for terpenes whether the reference spectra were obtained on quadrupole or magnetic deflection instruments.

Figure 5 shows computer-reconstructed chromatograms (RGC's) of a water sample from a Florida bay. The upper chromatogram is the plot of summed ion currents vs. spectrum number; the lower one, a limited mass chromatogram, is m/e 148 ion current vs. spectrum number. This mass was chosen because it is a strong peak in dinitrotolune, which was known to be used in a nearby plant. The spectrum singled out in the limited mass chromatogram was identified by the computer as that of dinitrotoluene and was substantiated by the identification of another RGC peak as nitrotoluene. Dinitrotolune was later confirmed by GC-MS comparison with a standard.

The reconstructed chromatogram for the extract of another plant effluent discharged into the Ohio River revealed a mixture of phthalates and phenols. Figure 6 shows the computer dialogue and spectrum matches. The five best hits for spectrum #81 were phthalates, but only one was a

"good match." The identification was confirmed by GC-MS comparison with a diethyl phthalate standard.

Figure 7 shows the reconstructed chromatogram of a synthetic mixture of four pesticides (atrazine, Sevin, parathion, and DDT), each at approximately 1 µg/l in an unconcentrated water sample. The DDT spectrum (Figure 8) is representative of the spectral quality for this run. Good matches were obtained with quadrupole spectra and fair ones with magnetic deflection spectra for all four pesticides.

Spectrum matches of fatty acid methyl esters are less definitive than those of pesticides. Figure 9 shows the reconstructed chromatogram of an industrial effluent wastewater. In Figure 10, the computer identification of one small peak in this sample illustrates an option available in the matching program.

The similarity index (S.I.) is a numerical indication (ranging between zero and one) of the relationship between (1) the average ratio of corresponding peak intensities in the unknown and in the reference and (2) the fraction of unmatched peaks contained in both spectra. It serves as a measure of the resemblance of the unknown spectrum to a stored spectrum. Experience has shown that S.I. values above 0.7 indicate very good spectrum matches; those between 0.2 and 0.7, fairly good matches; and values less than 0.2, poor matches. The three best matches shown in Figure 10 are methyl esters of caprylic, myristic, and stearic acids; each has a high similarity index of 0.6. The caprylate can be eliminated because its molecular weight is too low to produce the peaks at m/e 185, 199, and 211. The m/e 211 peak strongly suggests methyl myristate; comparison with a standard will provide positive identification.

Based on our experiences during the past year, computer matching of quadrupole spectra with reference spectra obtained on magnetic deflection instruments is both feasible and practical. We will expand our reference library continually to increase system utility.

We wish to acknowledge the contributions of EPA Region IV Chemical Services Branch who provided some of the environmental samples.

Use of trade names does not imply endorsement by the Environmental Protection Agency or the Southeast Water Laboratory.

References

1. A. W. Garrison, L. H. Keith, and M. M. Walker, presented at the 18th Annual Conference on Mass Spectrometry and Allied Topics, San Francisco, California, June 1970.

2. E. J. Bonelli, Amer. Lab., February 1971, 27-37.

3. R. G. Ridley and W. M. Scott, presented at the 19th Annual Conference on Mass Spectrometry and Allied Topics, Atlanta, Georgia, May 1971.

4. S. Abrahamssan, G. Haggstrom, and E. Stenhagen, presented at the 14th Annual Conference on Mass Spectrometry and Allied Topics, Dallas, Texas, May 1966.

5. H. S. Hertz, R. A. Hites, and K. Biemann, Anal. Chem., 43, 681-691 (1971).

6. J. R. Hoyland and M. B. Neher, "Implementation of a Computer-Based Information System for Mass Spectral Identification of Pesticides," Battelle Columbus Laboratories, Columbus, Ohio, 1972.

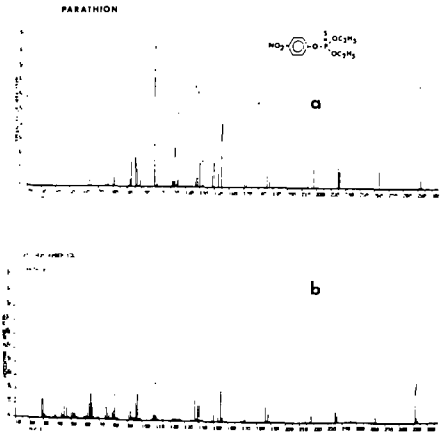

Figure 1
Comparison of Parathion Spectra from
a) Magnetic Instrument
b) Quadrupole Instrument

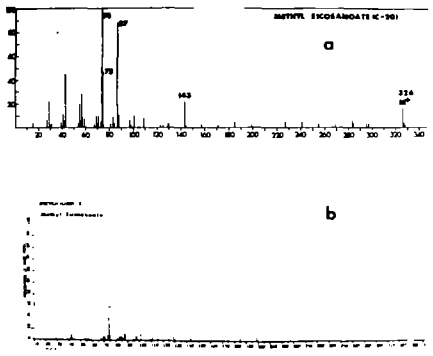

Figure 2
Comparison of Methyl Eicosanoate Spectra from
a) Magnetic Instrument
b) Quadrupole Instrument

Mass Number Comparison
of Five Largest Peaks

	Parathion		Methyl Eicosanoate	
Peak	RMU-7	1015	RMU-7	1015
1	97	97	74	74
2	109	109	87	87
3	291	65	75	43
4	137	139	43	75
5	139	63	57	55
M+	70%	27%	18%	8%

Table I
Abbreviated Comparison of Magnetic and Quadrupole Spectra

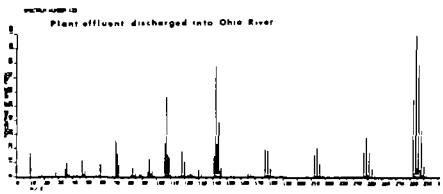

Figure 3
Plant Effluent Identified as Hexachlorobenzene

```
S, E, ØR P?S
FN= 122;1;%
TT= ØHIØ R. SUR.  RUN ØN 2-11  2UL  100-225 C;%
10,5;28,9;32,2;35,3;36,7;47,7;49,2;60,5;71,18;56;%
72,10;73,5;83,4;85,1;94,2;95,7;96,2;97,3;106,13,60;%
107,34;108,10;109,9;118,10;120,7;130,2;132,2;141,10;142,46;73;%
143,16;144,29;145,3;146,3;165,1;167,1;177,14;179,14;181,4;72;%
212,15;214,19;216,9;218,1;247,17;249,29;250,1;251,18;253,5;73;%
282,54;283,3;284,100;285,6;286,82;287,4;288,35;289,1;290,8;73;%
END
ØPTIØNS? N
  14 PRESRCH HITS

DATA FØR TØP ØF GC PEAK?Y
 10 HITS
HEXACHLØRØBENZENE(SEWL)
FILE KEY= 10800
GØØD MATCH

HEXACHLØRØBENZENE AST1384
FILE KEY= 1340
FAIR MATCH

TRIS(PENTACHLØRØPHENYL)PHØSPHINE MSC2741
FILE KEY= 9356
POOR MATCH

DINAPHTHØ(2,1,1',2')THIØPHENE API1416
FILE KEY= 6564
PØØR MATCH

DINAPHTHØ(1,2,1',2')THIØPHENE API1499
FILE KEY= 647
POOR MATCH

NEXT 5?N
```

Figure 4
Computer Identification of Hexachlorobenzene

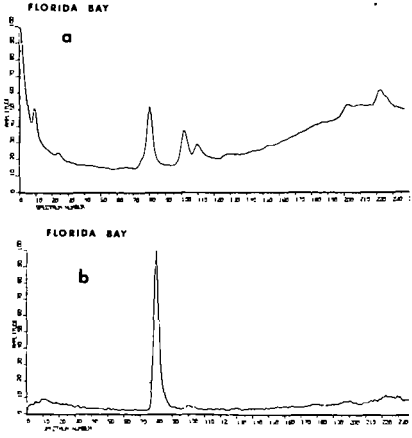

Figure 5
Reconstructed Gas Chromatograms of a Sample
from a Bay in Florida
a) Summed Current
b) m/e 148 Current

```
FN= 81S;1;%
TT= L253N;%
10,9;27,3;29,4;39,2;50,4;51,2;65,8;66,2;75,1;55;%
76,9;77,3;93,7;104,6;105,9;106,1;121,6;122,3;132,1;63;%
149,100;150,12;176,8;177,21;178,4;42;%
END
ØPTIØNS? N
  34 PRESRCH HITS

DATA FØR TØP ØF GC PEAK?Y
  34 HITS
PRINT SIM.INDEX?N
DIETHYL PHTHALATE DØW1735
FILE KEY= 3636
GØØD MATCH

BUTYL CARBØBUTØXYMETHYL PHTHALATE MSC3771
FILE KEY= 10384
FAIR MATCH

DIISØPRØPYL PHTHALATE DØW1856
FILE KEY = 3757
FAIR MATCH
```

Figure 6
Portion of Computer Identification of Spectrum #81

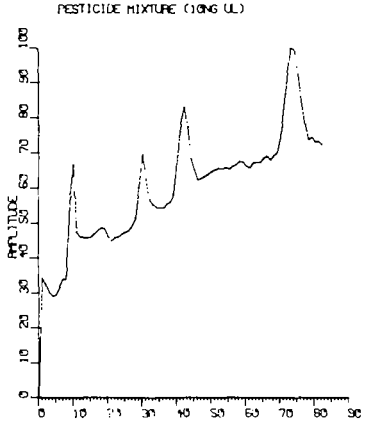

Figure 7
Reconstructed Chromatogram
of Pesticide Mixture

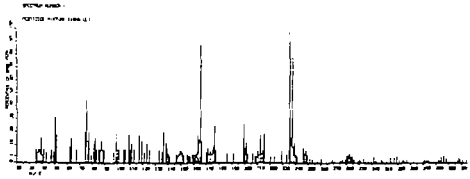

Figure 8
Mass Spectrum of p,p'-DDT

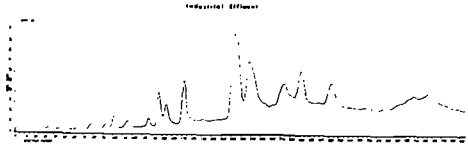

Figure 9
Reconstructed Chromatogram of a Plant Effluent

```
S, E, ØR P?S
SAMPLE ID (UP TO 70 CHARACTERS)?
     SAMPLE 39-INDUSTRIAL EFFLUENT-SPECTRUM #78
FN--F78;SN--1;%
SAMP 39 (FATTY ACIDS);%
39,3;41,29;42,6;43,24;45,9;53,1;54,3;55,23;56,5;60;%
57,16;58,1;59,9;67,3;68,1;69,13;70,2;71,3;73,5;57;%
74,100;75,13;76,1;79,1;81,2;82,1;83,3;84,3;85,1;60;%
86,1;87,46;88,5;89,1;93,1;95,2;96,1;97,4;98,2;56;%
99,1;101,4;102,1;109,1;111,2;115,1;119,1;123,1;129,3;65;%
143,9;157,1;185,1;199,3;211,1;36;%
END
ØPTIØNS? N
DATA FOR TØP ØF GC PEAK?Y
 63 HITS
PRINT SIM. INDEX?Y
METHYL MYRISTATE
FILE KEY= 10886
SI=0.6058

METHYL STEARATE
FILE KEY= 10885
SI=0.6024

METHYL CAPRYLATE 158 C9.H18.Ø2 AST 1054
FILE KEY= 1057
SI=0.6005

METHYL STEARATE 298 C19.H38.Ø2 AST 1087
FILE KEY= 1090
SI=0.5844

METHYL PALMITATE
FILE KEY= 10889
SI=0.5793
```

Figure 10
Computer Identification of Spectrum #78 of the Plant Effluent

Applications of Artificial Intelligence to the Interpretation of High Resolution Mass Spectra,[1] D.H. SMITH, A.M. DUFFIELD, and CARL DJERASSI, Dept. of Chemistry, Stanford Univ., Stanford, Calif. 94305.

"Intelligent" programs, embodying the Heuristic DENDRAL algorithm, which strive to emulate the thought processes of an experienced mass spectroscopist, have been proven very successful in interpretation of the low resolution mass spectra of a variety of relatively simple compounds.[2] An extension of Heuristic DENDRAL has now been utilized for interpretation of the complete high resolution mass spectra of complex molecules. The program has been structured with generality in mind such that the computational procedures can be applied to the spectra of any class of molecules by specification of basic structure and fragmentation rules. Examples of the use of additional chemical and spectroscopic information in the program are discussed. The performance of the program in analysis of mass spectra of some classes of steroids, particularly estrogens, is described in detail.

[1] A detailed description of this approach will appear in J. Amer. Chem. Soc. (in press).

[2] A. Buchs, A.B. Delfino, A.M. Duffield, C. Djerassi, B.G. Buchanan, E.A. Feigenbaum, and J. Lederberg, Helv. Chim. Acta, 53, 1394 (1970), and references cited therein.

Classification of Mass Spectral Data Files

W M Scott, D C Maxwell and R G Ridley
Mass Spectrometry Data Centre
AWRE, Aldermaston, Berkshire, U.K.

Conventional means of identifying organic compounds from their low resolution mass spectra, or of retrieving mass spectral information from the literature involve searching by molecular weight, formula, compound name and/or reference number. As the number of reference compounds on file has increased, several laboratory-oriented computer aided identification and retrieval techniques have evolved. It is obviously economically advantageous in some instances to apply these techniques to sub-sets only of the main file. Separation of the main file into specific sub-sets can be achieved by means of a linear notation or chemical classification.

Various linear notations such as the IUPAC[1], Wiswesser[2] and Lederberg[3] systems have been proposed.

TABLE 1

MSDC COMPOUND CLASSIFICATION

Ref. No.	Description		
1000	Hydrocarbon (and skeleton)	Alkane	
1010	"	Alkene	
1020	"	Alkyne	
1030	"	Alicyclic	Monocyclic (including cyclenes)
1040	"	"	Fused and Spirocyclic
1050	"	Aromatic	Monocyclic
1060	"	"	Fused
1070	"	Alicyclic/Aromatic fused	
1080	"	Other	
1090	Heterocyclic Nitrogen		
1100	" Oxygen		
1110	" Sulphur		
1120	" Other		
1130	Oxygen function	Hydroxyl	
1140	" "	Ether, Orthoester, Peroxide	Not heterocyclic oxygen, acetal or ketal
1150	" "	Acetal	
1160	" "	Ketal	
1170	" "	Aldehyde	
1180	" "	Ketone, keten, quinone	
1190	" "	Carboxylic acid	
1200	" "	Acid anhydride	
1210	" "	Ester, not methyl ester	
1220	" "	Methyl ester	
1230	" "	Acid salt	
1240	" "	Lactone	
1250	" "	Acid halide	
1260	" "	Amide, imide, urea	
1270	" "	Lactam	
1280	" "	Other	
1290	Nitrogen function	Amine, imine	
1300	" "	Nitrile, isonitrile, isocyanate, isothiocyanate	
1310	" "	Nitro, nitroso, nitrate, nitrite, oxime, N-oxide	
1320	" "	Hydrazine, azo, diazo, azide	
1330	" "	Other	
1340	Sulphur function	Thiol, sulphide	
1350	" "	Thione	

Ref. No.	Description	
1360	Sulphur function	Sulphone, sulphoxide, sulphonic acid and ester
1370	" "	Thiocarboxylic acid and ester
1380	" "	Other
1390	Halogen	Fluorine
1400	"	Chlorine
1410	"	Bromine
1420	"	Iodine
1430	Other non-metal	Phosphorus-trivalent
1440	" " "	Phosphorus pentavalent
1450	" " "	Trimethylsilyl
1460	" " "	Silicon, not TMS
1470	" " "	Boronate
1480	" " "	Boron, not boronate
1490	" " "	Other
1500	Metal	Group IA (Li, Na, K, Rb, Cs, Fr)
1510	"	" IB (Cu, Ag, Au)
1520	"	" IIA (Be, Mg, Ca, Sr, Ba, Ra)
1530	"	" IIB (Zn, Cd, Hg)
1540	"	" IIIA Not lanthanide, actinide (Sc, Y)
1550	"	Lanthanide
1560	"	Actinide
1570	"	Group IIIB (Al, Ga, In, Tl)
1580	"	" IVA (Ti, Zr, Hf)
1590	"	" IVB (Ge, Sn, Pb)
1600	"	" VA (V, Nb, Ta)
1610	"	" VIA (Cr, Mo, W)
1620	"	" VIIA (Mn, Tc, Re)
1630	"	" VIII (Fe, Co, Ni, Ru, Rh, Pd, Os, Ir, Pt)
1640	"	Organo-metallic carbonyl
1650	Natural Product	Alkaloid
1660	" "	Amino acid, peptide, protein
1670	" "	Carbohydrates
1680	" "	Flavonoid, anthocyanin, chroman
1690	" "	Mycoside
1700	" "	Nucleic acid, nucleotide, nucleoside
1710	" "	Steroid
1720	" "	Terpenoid Mono-
1730	" "	" Sesqui-
1740	" "	" Di-
1750	" "	" Tri-
1760	" "	" Higher
1770	" "	" Isoprenoid
1780	" "	Carotenoid
1790	" "	Porphyrin
1800	" "	Chlorin
1810	" "	Phospho-lipid
1820	" "	Other
1830	Special Class	Polymer
1840	" "	D-labelled
1850	" "	Otherwise labelled

The Wiswesser Line Notation (WLN) is the system most widely used by information scientists, and a recent report describes the applicability of WLN to mass spectral data files[4].

Classification of mass spectral data files has recently been described by Smith[5]. This method, which assigns a classification to a compound on the basis of the data points in its mass spectrum, is a fundamental and valuable means of classifying mass spectral data files. However, it is not generally applicable to the case where only partial spectral data are available - which is a situation frequently encountered in practice. After consideration of the above systems MSDC decided to use a chemical

classification scheme and apply this to existing data files. The classification used in the Mass Spectrometry Bulletin[6] was revised and augmented with the assistance of many individual mass spectrometrists. The classifications currently in use are listed in Table 1. The classifications are coded numerically, thus only simple and economical retrieval programs are needed. An example is presented below.

Question: What spectra are available of steroids containing fluorine atoms?

Classifications: + Steroids (1710) + Fluorine (1390).

Answer: Reference Numbers
L3902
01214
01215
etc

Simple AND, OR, NOT logic is applied to ensure that relevant answers are generated. These classifications can be used in conjunction with the more usual search parameters - molecular weight, molecular formula (complete or partial), data, etc., and, depending on the organization of files, one may output reference numbers only, or complete/partial data, molecular formula, etc. The compounds whose spectral references are given in Table 2 have been classified and all subsequent additions to the spectral files will be classified.

Table 2 - Spectra Classified

API	2514
ASTM	1902
DOW	1969
ICI	2202
LITERATURE	5588
MSDC	6000
TRC	295
	20470

Acknowledgments

The authors thank Drs J A McCloskey and J Roboz for circulating the proposed classification to members of Sub-Committee VI, and individual mass spectrometrists from the various national mass spectrometry groups for their valuable comments.

References

1. "Rules for IUPAC Notation for Organic Compounds". Longmans, London (1961).

2. E G Smith, "The Wiswesser Line-Formula Chemical Notation". McGraw-Hill, New York (1968).

3. J Lederberg, NASA Report CR-57029, Dec 15, 1964.

4. D C Maxwell, AWRE Report 02/72. Jan 1972.

5. D H Smith, Anal Chem 44, 536, 1972.

6. The Mass Spectrometry Bulletin, Mass Spectrometry Data Centre, Aldermaston. (Published monthly).

TWENTY-FIVE YEARS OF MASS SPECTRAL DATA COMPILATIONS – API 44 AND TRC DATA PROJECT CATALOGS

Bruno J. Zwolinski, Annie Lin Risinger, and Cecil H. Dickson
Thermodynamics Research Center, Department of Chemistry,
Texas A&M University, College Station, Texas 77843

Abstract

The petroleum industry recognized the importance of mass spectrometry in the early forties with the accompanying need for the availability of standard spectra for calibration and analytical applications. The American Petroleum Institute Research Project 44, a central agency of the petroleum industry for standard reference data in thermodynamics and infrared, ultraviolet, and Raman spectra, was delegated this responsibility. Supplementary Volume No. 1 of the new API 44 Catalog of Selected Mass Spectral Data, consisting of 38 spectral data in standard format, appeared in 1947. To meet the special needs of the chemical industry, the TRC Data Project (formerly the Manufacturing Chemists Association Research Project) Mass Spectral Program was initiated in 1959. The current status of these two Mass Spectral Data compilations will be reviewed with emphasis on evaluations, the TRC Board of Reviewers, standard samples, new innovations in documentation, standard and matrix formats, number and kind of contributors, compound classification and distribution, and retrieval aids.

History – American Petroleum Institute Research Project 44

In August, 1941 Dr. Lyman J. Briggs, Director of the National Bureau of Standards, proposed a joint investigation on the collection and analysis of data on the properties of hydrocarbons to Dr. J. Bennett Hill, Chairman of the API Advisory Committee on Fundamental Research on Composition and Properties of Petroleum. All agreements and arrangements were made for the initiation of the project for year beginning July 1, 1942. Actual operation began on September 28, 1942.

The original members of the API Research Project 44 Advisory Committee for this project were:

Wayne E. Kuhn, Chairman	Texas Company, New York, New York
Otto Beeck	Shell Development Company, Emeryville, California
Gustav Egloff	Universal Oil Products, Chicago, Illinois
Stewart Kurtz, Jr.	Sun Oil Company, Norwood, Pennsylvania

The current members are:

W. O. Taft, Chairman	Esso Research and Engineering Company, Lindy, New Jersey
R. M. Blunden	BP North America, New York, New York
D. L. Camin	Sun Oil Company, Marcus Hook, Pennsylvania
R. A. Findlay	Phillips Petroleum Company, Bartlesville, Oklahoma
S. A. Francis	Texas Inc., Beacon, New York
A. C. Jones	Shell Development Company, Emeryville, California
J. G. Larson	Gulf Research and Development Company, Pittsburgh, Pennsylvania
F. A. Smith	Mobil Research and Development Company, Paulsboro, New Jersey
A. S. Trube	Getty Oil Company, Houston, Texas

In the beginning only tables of physical and thermodynamic properties were the concern of the project. At the April 1943 meeting, the API 44 Advisory Committee approved plans prepared by Dr. Otto Beeck for the collection and printing of infrared spectral data. The first spectral data for this catalog was published in November 1943.

The Advisory Committee members were the same as the original group when the committee met at the Texas Company in New York on May 3, 1945 and agreed that consideration be given to the inclusion of mass spectral data among the API catalogs.

History – Manufacturing Chemists Association Research Project

The Manufacturing Chemists Association Research Project was originated in May, 1955. An advisory committee was appointed under the temporary chairmanship of Dr. R. C. Swain, Chairman of the Main Research Advisory Committee for the MCA. This project was located at Carnegie Institute of Technology with Dr. Frederick D. Rossini as Director. It was moved to Texas A&M University in the spring of 1961 along with the API Research Project 44 with Dr. B. J. Zwolinski as Director. The Manufacturing Chemists Association sponsorship continued until 1965. At this time the name of the project was changed to Thermodynamics Research Center Data Project and it has continued to operate on a self-sustaining basis with no interruption of the publication of data.

Standard Format

At the May 1945 API 44 Advisory Committee meeting, Dr. Otto Beeck was asked to study the problem of a standard format for the spectrograms sufficiently useful for comparison among different mass spectrometers.

At the October meeting of the same year, Dr. Beeck reported that these several points needed to be considered to make practicable an API 44 mass spectral data catalog.

(1). Results to be presented in tabular form of relative intensities rather than actual spectrograms

(2) Results to be presented for electron voltages of 50, 70, and 100 to detect differences arising from this variable

(3) Information to be included for temperature of gas in ionization chamber; make, model and operating conditions of instrument; purity of samples

At the June 20, 1947 meeting of the committee, the completion of a format in collaboration with Fred L. Mohler of the NBS Mass Spectrometry Laboratory was reported. Copies were then circulated to appropriate experts for comments. Under date of October 31, 1947, the first 38 standard format mass spectral data were published in the API 44 Catalog of Selected Mass Spectral Data.

This format was used without change until April 30, 1961. At that time Shell Oil Company of Houston contributed data obtained on the higher molecular weight samples prepared by the API Research Project 42 at Pennsylvania State University. The increased number of relative intensities to be tabulated necessitated the addition of columns on the reverse side of the conventional form.

With the initiation of the MCA Research Project Catalog of Selected Mass Spectral Data in 1959, the decision was made to limit the kinds of compounds for which data would be published in the API 44 catalog to hydrocarbons and sulfur and nitrogen containing derivatives of petroleum. All other organic compounds, including the more complex sulfur and nitrogen compounds, and some inorganic compounds were to be assigned to the MCA catalog. The first 18 standard form mass spectral data were issued by the MCA Research Project under date of December 31, 1959.

When the MCA Research Project made the decision to publish mass spectral data and to use the API format, some changes were agreed upon and the 2nd revision of this standard form was made. The older format was redrawn to allow

(1) more space for the structural formula

(2) specific entry for a second standard, n-hexadecane, which had previously been inserted in the Additional Information block

(3) space for the designation of the magnetic field(s).

After relocation of both critical data projects at Texas A&M University in the spring of 1961, the standard form was revised a 3rd time to include more physical property information, total ionization, and sensitivity of the base peak for the compound and adding an entry for the collector slit width to the Information Block regarding instrumentation.

Matrix Format

At the Advisory Committee Meeting in October, 1957, one of the API 44 Advisory Committee members, Dr. Norman D. Coggeshall of Gulf Research and Development Company, proposed the addition of a matrix form presentation of mass spectral data. In October, 1959, after considerable investigation by Dr. Coggeshall with Dr. George F. Crable (also of Gulf Research and Development) and Dr. Archie Hood of Shell Oil, a final report was approved and the go-ahead was given to have formats made up and circulated for comments. On April 30, 1961, the matrix form section of the API 44 Mass Spectral Catalog was initiated and the first 21 matrix form data were published at Texas A&M University.

Early in 1962, the Editorial Office prepared a format for Shell Oil Company of Houston for direct print-out of matrix form data. The Shell laboratory contributed data on this form for 52 compounds which were published in the API catalog.

The first matrix form data were published by the TRC Data Project (formerly MCA Research Project) under date of December 31, 1966.

At the suggestion of a major contributor, Dr. Mynard C. Hamming of Continental Oil Company at Ponca City, Oklahoma, all matrix form data published by both projects since October, 1968 have the ten (10) most intense peaks set in boldface type as an analytical aid. In April, 1969, another feature, the Wiswesser Line Formula Chemical Notation (WLN), was added to the data sheets to facilitate computerized storage and retrieval of spectral data.

In 1972 a major change in format for presentation of matrix form data was also suggested and partially designed by Dr. Mynard C. Hamming. This format gives citable recognition to individual contributing investigators in this field of spectroscopy, cites the name of the evaluator, and provides space for interpretation of fragmentation of compounds and other constructive comments by the investigators. The first supplementary volume of data in this format will be published in the TRC Data Project catalog under date of June 30, 1972.

The features of this format have been incorporated in a new form for the standard sections of both catalogs. Copies of this new standard form will be sent to investigators for their suggestions and comments during 1972.

Reliability of the Spectral Data

The reliability of the data is a function of the knowledgeability and experience of the investigator, calibration standards for the spectrometer, and the characterization and purity of the samples. These criteria are met by the contributors of unpublished mass spectral data to the Catalogs of the API Research Project 44 and of the TRC Data Project. In a large number of instances mass spectra are contributed on a class of closely related compounds on which additional spectroscopic and physical property measurements have been made which insures the characterization and purities of these substances. In 1968, a Board of Reviewers were appointed for the Spectral Program of the Thermodynamics Research Center in all five spectral categories. Dr. Mynard C. Hamming of Continental Oil Company is the TRC Board of Reviewers representative for the Mass Spectral Data category who in conjunction with the Advisory Committees, the Director, and the staff of the TRC Spectral Program insures the reliability of the contributed mass spectral data.

Current Status

As of May 16, 1972, the Mass Spectral Data Catalogs of the API Research Project 44 and of the TRC Data Project consist of 3055 valid sheets in eight volumes in the classical hard copy loose-leaf sheet format. The API 44 and TRCDP mass spectra are available on magnetic tape from the Mass Spectrometry Data Centre,

Aldermaston, England. Late in 1972, the Data Distribution Office of the Texas A&M Thermodynamics Research Center will have the API 44 and TRCDP mass spectra on microfilm and microfiche for distribution to the general public.

Acknowledgement

This work was supported in part by the API Research Project 44 and the TRC Data Project of the Thermodynamics Research Center of Texas A&M University.

Signal Enhancement in Real-Time for High-Resolution Mass Spectra

F. W. McLafferty, John A. Michnowicz, and R. Venkataraghavan

Department of Chemistry, Cornell University, Ithaca, New York 14850

ABSTRACT

An on-line, real-time computerized method for effectively increasing the sensitivity, resolution, and mass measuring precision of a high-resolution mass spectrometer has been developed. This method for Signal Enhancement in Real Time (SERT) utilizes the relatively large vacant areas between peaks to rescan peaks in real-time under direct computer feedback control. The ensemble-averaged rescans have an increased signal/noise ratio when compared to the single scans and significantly increase the effective sensitivity, resolution and mass measuring precision of the instrument. A detailed description of this work will be published in Analytical Chemistry.

AUTOMATIC OFF-LINE COMPUTER PROCESSING OF LOW- AND HIGH-RESOLUTION MASS SPECTRA VIA FM ANALOG TAPE

R12

Peter J. Black & Allen I. Cohen

The Squibb Institute for Medical Research
New Brunswick, New Jersey 08903

INTRODUCTION

A common requirement in mass spectrometry laboratories is for high capacity and reasonable turnaround time in the acceptance and processing of routine samples. An off-line batch mode system, aimed specifically at this need, has been developed for a PDP-11 computer. Emphasis has been placed on independent scheduling of the mass spectrometer and the computer, and where possible, on the unattended processing of mass spectra in off-peak hours.

EXPERIMENTAL

Mass spectra are collected from an AEI-MS-902 mass spectrometer on to frequency-modulated (FM) analog tape via a Honeywell 7600 tape recorder. Spectra are scanned at 16 sec/decade and the recorder is operated at 60 ips in extended mode. Under these conditions, approximately 20 spectra can be recorded on a 3600-foot tape. Three channels of data are recorded at attenuation factors of x1, x10, and x100. A phase-lock signal, recorded on a fourth channel, is used to control the tape speed on playback and, additionally, to delineate the beginning and end of each spectrum. The analog tape is played back on a similar Honeywell tape recorder at the Data Acquisition Center.

The computer configuration used is composed of a PDP-11/20 computer with 20k words of core storage, high-speed paper tape i/o, a 256k-word disk (RF11/RS11), analog-to-digital converter (AD01/D), and 240 line/min printer (ODEC 1323). This configuration is used for several other analytical and physiological applications, in both on- and off-line modes.

COMPUTER PROCESSING

Data from the analog tape are processed in several stages, and normally all of the spectra on one or more tapes are carried through the sequence of operations in parallel. Individual programs in the sequence may be executed independently or queued for unattended execution under the control of a relatively simple core-resident disk monitor. A typical program sequence proceeds as follows:

(1) Acquisition of spectra from analog tape. The identifying information associated with each spectrum is entered at this point. The tape is played back under computer control at 3.75 ips for high-resolution or 7.5 ips for low-resolution spectra. Data are collected at 2kHz. Peak extraction is performed concurrently with the acquisition, and the peak times relative to the beginning of the spectrum and the corresponding intensities are saved as contiguous files (one per spectrum) on the disk. The approximately 40k words of disk storage allocated to this application (the total can be extended, if necessary) are adequate for the storage and subsequent processing of approximately 20 high-resolution or 40 low-resolution spectra.

After the acquisition phase has been completed, control is returned to the disk monitor, which then loads and passes control to subsequent programs in the queue to further process the raw data files. Each such program sequentially examines the data files from a preset starting point (which may also encompass files written on some previous occasion) and processes only those of the appropriate type. A principal objective has been to devise and implement processing algorithms that do not require operator guidance or specification of parameters.

(2) Interpolation and plotting of low-resolution spectra. This program converts the raw peak times to nominal masses by utilizing the exponential mass vs time relationship to establish the best correspondence of peak times with

those of an external mass vs time list, generated previously from a reference compound and maintained as a standard file on the disk. This correspondence is established via a preliminary overlay fit of a few low masses, followed by a stepwise matching of differences through the remainder of the mass list. The results of the interpolation are presented as a printed array, a bar plot generated on a Calcomp plotter, or as paper-tape files for subsequent plotting.

(3) Interpolation of high-resolution spectra. This program applies an automatic interpolation procedure to raw high-resolution data files. The technique is to search a moderately wide region of the spectrum for two prominent peaks of the internal reference compound (the m/e 119 and m/e 131 ions, in the case of PFK) expected to occur in that region. Candidate peak pairs are accepted or rejected according to the degree of success with which the times of the remaining peaks of the reference compound can be predicted. The search is initiated automatically, and if necessary, a large number of trial interpolations is performed. The procedure currently has a success rate of about 80%. If a satisfactory reference list is established, the exact masses of the unknown compounds are calculated and stored as a new data file. Subsequently, these files, along with additional input information, are converted to a form suitable for input into an IBM 360/50 element map program.

Backup programs are provided for interactive processing of the raw data files for which automatic processing was unsuccessful. A file editing package is also provided for routine file manipulations.

FURTHER DEVELOPMENTS

A number of improvements are currently being implemented to improve the efficiency of processing. These include:

(1) Provision of industry-compatible digital magnetic tape to effectively eliminate file capacity restrictions on the number of spectra that can be handled.

(2) A control signal to enable the computer to recognize a given spectrum as low- or high-resolution, rather than requiring this information to be specified on input. The MS-902, with programmed slits, is readily interchanged between the two modes. Intermixing of the two types of spectra on the same tape will facilitate the rapid acquisition of all spectra from a given sample.

(3) Increased acquisition speed to effectively utilize the increased file capacity (Item 1 above).

(4) Upgrading of the automatic processing routines to improve success rates and operating efficiency.

(5) Implementation of element map routines on the PDP-11 to shorten turnaround time.

(6) Off-line plotting of low-resolution spectra.

CONCLUSIONS

An approach has been discussed that permits a high-volume routine processing load to be handled efficiently without an excessive commitment of personnel or prime computer time. The use of analog tape permits a flexible scheduling of both the mass spectrometer and the computer. The reliability of the acquisition system has led to a significant decrease in operating time for the mass spectrometer.

MASS SPECTROMETER DATA ACQUISITION SYSTEM USING A PDP-8 COMPUTER INTERFACED TO A MULTI-USER IBM 1800 COMPUTER

W. K. Rohwedder, R. O. Butterfield, D. J. Wolf and H. J. Dutton

Northern Regional Research Laboratory,[1] Peoria, Illinois 61604

A PDP-8 computer interfaced to an IBM 1800 computer 500 feet away is used to collect and process low and high resolution mass spectra. The 1800 with 32K core, two tape drives and MPX monitor can accept the full output of a mass spectrometer with no interference to four other simultaneous users. Low resolution spectra are automatically normalized and mass marked by the 1800 and then displayed on the PDP-8 storage oscilloscope located alongside the mass spectrometer within seconds after a scan is completed. All GC-MS scans can be stored on the 1800's magnetic tape. Four unknown mass spectra can be compared with a file of 6000 known spectra to find matches in about 2 minutes, using a batch time-shared mode. The 1800 can serve as a line printer for the PDP-8 and also can store PDP-8 disk loads on magnetic tape.

---

[1] A laboratory of the Northern Marketing and Nutrition Research Division, Agricultural Research Service, U.S. Department of Agriculture.

Reversible Reactions of Gaseous Ions. VI. The NH_3-CH_4 , H_2S-CH_4 and CF_4-CH_4 Systems at Low Temperatures.

F. H. FIELD and S. L. BENNETT, The Rockefeller University, New York, N. Y. 10021

Interesting association ions have been encountered by operating the chemical ionization mass spectrometer at sub-ambient temperatures. Examples of these ions are $CH_5 \cdot CH_4^+$ (m/e 33) , $C_2H_5 \cdot CH_4^+$ (m/e 45) and $CH_5 \cdot (CH_4)_2^+$ (m/e 49) observed in the methane system (1), and the ions $H_3O.CH_4^+$ (m/e 35) and $H_3O.(CH_4)_2^+$ (m/e 51) observed in the methane-water system (2). Under certain conditions these ions are formed by equilibrium reactions, and the thermodynamic quantities pertaining to the equilibria have been determined.

It is of interest to investigate further the degree of generality of the interactions of various ions with methane. We here report results in which three new ions $NH_4 \cdot CH_4^+$ (m/e 34) , $H_3S.CH_4^+$ (m/e 51) and $CF_3 \cdot CH_4^+$ (m/e 85) are formed by the reversible reactions

$$CH_4 + NH_4^+ \rightleftharpoons CH_4 \cdot NH_4^+ \qquad (1)$$

$$CH_4 + H_3S^+ \rightleftharpoons CH_4 \cdot H_3S^+ \qquad (2)$$

$$CH_4 + CF_3^+ \rightleftharpoons CH_4 \cdot CF_3^+ \qquad (3)$$

Thermodynamic values have been obtained from the equilibrium constants and their temperature coefficients at temperatures down to -160°C. The values obtained were

Equilibrium	K_{300} (atm^{-1})	ΔG°_{300} (kcal./mole)	ΔH° (kcal./mole)	ΔS° (eu)
(1)	0.18	+1.06	-3.59	-15.5
(2)	0.074	+1.55	-3.87	-18.1
(3)	0.17	+1.08	-4.55	-18.8

Classical electrostatic calculations have been made to determine the energy of interaction of CH_4 with the ions CH_5^+, H_3O^+, NH_4^+, H_3S^+ and CF_3^+. We conclude that the experimentally observed enthalpies can be adequately accounted for in terms of ion-induced dipole interactions.

A complete paper will appear in J. Amer. Chem. Soc. (1972).

References

(1) F. H. Field and D. P. Beggs, J. Amer. Chem. Soc., 93, 2585 (1971).
(2) S. L. Bennett and F. H. Field, presented at the ASMS Meeting, Atlanta, Ga., May 1971. To be published in J. Amer. Chem. Soc. (1972).

Reversible Reactions of Gaseous Ions. The Hydrogen System and Further Studies on the Equilibrium $H_3O^+ + H_2O \rightleftharpoons H(H_2O)_2^+$. S.L. BENNETT and F. H. FIELD, The Rockefeller University, New York, N.Y. 10021

The equilibrium $H_3^+ + H_2 \rightleftharpoons H_5^+$ has been studied at pressures up to 8 torr and temperatures between 160 and -25°C. $K_{3,5}$ was independent of hydrogen pressures above about 4 torr. At temperatures below -136° the ion H_7^+ appears, and the equilibrium $H_5^+ + H_2 \rightleftharpoons H_7^+$ has been studied. Thermodynamic values have been obtained from the temperature dependence of the equilibrium constants. The results are

Equilibrium	K_{300} (atm^{-1})	ΔG°_{300} (kcal./mole)	ΔH° (kcal./mole)	ΔS° (eu)
3,5	10.3	-1.39	-9.7	-27.7
5,7	0.03	+2.14	-1.8	-13.1

The first hydrated proton equilibrium has been re-investigated by the chemical ionization technique in the propane-water system at high pressure. The results are essentially identical to those obtained at low propane pressures[1]. We conclude that the discrepancy with Kebarle et al.[2] does not result from the existence of non-equilibrium conditions in our ionization chamber.

Complete publications will appear in J. Amer. Chem. Soc., (1972).

References

1. D. P. Beggs and F. H. Field, J. Amer. Chem. Soc., 93, 1576 (1971).
2. P. Kebarle, S. K. Searles, A. Zolla, J. Scarborough and M. Arshadi, J. Amer. Chem. Soc., 89, 6393 (1967).

ION KINETIC ENERGY LOSS SPECTRA*

T. Ast**, J. H. Beynon and R. G. Cooks

Department of Chemistry, Purdue University
Lafayette, Indiana 47907, U. S. A.

Introduction

Singly-charged ions formed in the ion chamber of a double-focusing mass spectrometer can undergo a collision-induced ionization reaction in the first field-free region, whereby they are converted to doubly-charged ions:

$$m^+ + N \rightarrow m^{++} + N + e^- \qquad (1)$$

where N represents the molecule of the collision gas. If the electric sector voltage is halved to the value E/2 , where E represents the voltage at which the main ion beam is transmitted, then only the ions m^{++} formed in reaction (1) can pass through the electric sector. These ions can be collected at the β-slit multiplier located immediately behind the electric sector, or can be passed through the magnetic sector for mass analysis.

Conversion of singly- to doubly-charged ions requires energy which can only be supplied by the m^+ ions from either their internal or kinetic energy. If kinetic energy is lost in process (1), the amount can be determined by studying the kinetic energy of the product m^{++} ions.

Experimental

A hitachi-Perkin-Elmer RMH-2 double-focusing mass spectrometer, modified as previously described[1], was used for all measurements. Standard operating conditions were: electron energy 70eV (100eV for Ne and 120eV for He), electron emission current 1mA, ion accelerating voltage 8-10keV, source pressure 1×10^{-5} torr, collision gas pressure 5×10^{-5} torr.

The ion kinetic energy loss spectra were obtained at the final collector by setting the electric sector voltage to E/2, setting the magnetic sector to pass m^{++} ions, and then scanning the accelerating voltage around the value corresponding to transmission of ions that have undergone no kinetic energy loss.

---

* Accepted for publication in the Journal of the American Chemical Society.

** Permanent address: Faculty of Technology and Metallurgy, University of Belgrade, Karnegijeva 4, Belgrade, Yugoslavia.

Results and Discussion

The ion kinetic energy loss spectra were recorded for He, Ne, Ar, Kr and Xe using air as collision gas. In each case (with the exception of He) three peaks were observed. These peaks were denoted A, B and C and the kinetic energy loss corresponding to each peak is given in Table I, together with the data on single and double ionization potentials of the rare gases.

Table I. Kinetic Energy Loss Spectra of Rare Gas Ions[a]

				Loss of kinetic energy Q'min[b]		
Rare Gas	1st IP	2nd IP	ΔIP	Peak A	Peak B	Peak C
He	24.6	78.9	54.3	0 ± 0.3	-	54.5 ± 2
Ne	21.6	62.6	41.0	0 ± 0.3	13.3 ± 1.0	42.2 ± 2
Ar	15.9	43.4	27.5	0 ± 0.3	8.9 ± 0.8	27.5 ± 0.6
Kr	14.7	38.5	23.8	0 ± 0.3	7.6 ± 0.5	24.1 ± 1
Xe	13.4	33.3	19.9	0 ± 0.3	6.9 ± 0.5	19.5 ± 1

[a] All values are in eV

[b] Q'min values refer to the peak onset, as obtained by extrapolation to the base line, corrected for the main ion beam width.

Consider the positions of peaks A, B and C in the spectrum of argon. Peak C represents the Ar^{++} ions which have lost 27.5 ± 0.6 eV of kinetic energy in undergoing reaction (1). This amount of energy corresponds exactly to the difference between the single and double ionization potentials of argon (Table I , column 4), therefore, peak C is due to conversion of ground state Ar^{+} ions into ground state Ar^{++} ions, the 27.5 eV of energy required being supplied from the kinetic energy of the Ar^{+} ions. Peak A appears at the position of zero kinetic energy loss, therefore, it represents the process(es) in which highly excited Ar^{+} ions (at or above the level of Ar^{++}) are converted into Ar^{++} ions. Some contribution to this peak may come from an autoionization reaction, but collision gas pressure dependence studies have shown that a collision induced reaction also occurs, involving probably high-lying Rydberg states of Ar^{+} ions. Peak B is intermediate in position between peaks A and C, and it corresponds to ions that have lost 8.9 ± 0.8 eV of kinetic energy. There is a quartet of closely spaced long-lived states of Ar^{+} ions, the highest member of which lies 9.13 eV below the level of Ar^{++} (designation $^{2}F_{7/2}$). The energy required to achieve double-ionization from

this state is in good agreement with the kinetic energy loss represented by peak B.

To verify the above peak assignments, experiments have been carried out in which electron bombarding energy, collision gas pressure and the nature of the collision gas have been varied. In each case, the results obtained were consistent with the interpretation put forward above.

Data obtained on other rare gases (Table I) are all in agreement with the respective values of single and double ionization potentials, as well as the known long-lived states of these ions. Two additional points should be noted. Peak B was not observed in helium, although He^+ does possess a metastable state in the defined energy range ($2^2S_{1/2}$, energy 65.38 eV above the ground state of the atom). This state is susceptible to Stark quenching[2] and its life-time is too short under our experimental conditions. On the other hand, peak B was observed in neon, when none was expected, since no states of Ne^+ in that region have previously been reported to be long-lived. All the states of Ne^+ in this energy region are known[3] and the only ones that could be metastable are the $^4P_{5/2}$ and $^4P_{1/2}$ states at 27.16 and 27.26 eV above ground state Ne^+, in good agreement with the observed value of 27.7 ± 1 eV.

In conclusion, the method described provides a new way of studying long-lived states of ions and of measuring double ionization potentials by mass spectroscopy. A number of diatomic molecules have also been studied and the results on NO have been published.[4]

References:

1. J. H. Beynon, R. M. Caprioli, W. E. Baitinger and J. W. Amy, Int. J. Mass Spectrom. Ion Phys., 3, 313 (1969).
2. W. E. Lamb and M. Skinner, Phys. Rev., 78, 539 (1950).
3. W. Person, Physics Scripta, 3, 133 (1971).
4. R. G. Cooks, J. H. Beynon and T. Ast, J. Amer. Chem. Soc., 94, 1004 (1972).

KINETIC ENERGY RELEASE IN THE COLLISION-INDUCED DISSOCIATION OF SOME SIMPLE MOLECULAR IONS.

E. G. Jones, R. G. Cooks and J. H. Beynon

Department of Chemistry, Purdue University
Lafayette, Indiana 47907

Abstract

The technique of ion kinetic energy spectroscopy has been applied to a study of $S^{+\cdot}$ formation from $H_2S^{+\cdot}$ and $O^{+\cdot}$ formation from $H_2O^{+\cdot}$. Unimolecular formation of $S^{+\cdot}$ occurs by predissociation of the first excited state via the repulsive $^4A_2$ state of $H_2S^{+\cdot}$. Above the classical crossover region this reaction proceeds rapidly on the mass spectrometer time scale but tunnelling through the barrier occurs slowly and gives rise to metastable ions which fragment with conversion of all the available potential energy to kinetic energy. Collisional excitation of ground state $H_2S^{+\cdot}$ yields excited ions which rapidly dissociate via the $^4A_2$ repulsive surface to give substantially excited $(v = 2)H_2$. This reaction occurs with the partitioning of some 30% of the available energy into translational energy of the products. The heat of formation of $S^{+\cdot}$, determined from the appearance potential, requires only slight correction for the excess energy term arising from the potential energy difference between the crossover region and the ground state of the products because the repulsive surface is unusually flat. Ground state $H_2O^{+\cdot}$ ions undergo collision-induced excitation with loss of 22 ± 4eV of kinetic energy to give a high energy excited state which fragments directly to give $O^{+\cdot}$ (^2D or ^2P) and vibrationally excited H_2. Appearance potential measurements do not provide a reliable assignment of the products because of the extra energy terms. These results are in contrast to earlier conclusions that fragmentation upon electron impact yields two hydrogen atoms.

Submitted for publication in The Journal of Chemical Physics.

INTENSITY DISTRIBUTION ALONG CHARGE-EXCHANGE CONTINUA FORMED IN MAGNETIC SECTOR MASS SPECTROMETERS.

J. M. McCrea, P. O. Box 172, Monroeville, PA 15146

Abstract: The author has previously presented treatments of the intensity distribution along charge-exchange continua in the Mattauch-Herzog and 180 degree magnetic sector instruments on the basis of a rectangular coordinate system. The retangular system is difficult to extend to sector instruments with angles other than 180. A new trigonometric treatment applicable to sector instruments of any angle has been developed to obtain both complete trajectory and intensity distribution data for ions involved in the charge exchange process. The method has been applied to the calculation of intensity distributions along the 2+ to 1+ continua for the 60, 90, 120 and 180 degree sector designs.

Introduction

Ions in mass spectrometer beams can react with neutral molecules of residual gas during ion transit from source to detector with a resultant gain of one or more electronic charge units from the neutral. If an ion with charge p+ travelling on a circular orbit of radius (p - n)r in a uniform magnetic field picks up n electrons charge-exchange process, it leaves the point of charge exchange with an ionic charge (p - n)+ on a different circular orbit of radius pr. In magnetic sector mass spectrometers, the number of such charge--exchange ions originating in the magnetic field region that reach the ion collector when a given specific mass is being measured contribute to the background from the charge-exchange continua at the position. The amount of charge exchange will be proportional to the pressure of residual gas and to the length of the primary ion beam trajectory, and in all but exceptional conditions will be only a very, very small proportion of the number of ions in the primary beam.

The magnetic sector mass spectrometers in use for most investigations are of a symmetrical geometry, with the source, the apex of the sector and the collector in a plane and the sector arranged with its bisector plane perpendicular to the reference plane. The exit slit of the source and the entrance slit of the collector are mounted parallel to the nearest face of the magnet, and the ion beam in focus at the collector enters and leaves the magnet normal to its faces. The system is first order direction focussing, and the ion trajectories from source to collector are symmetric. However when a charge exchange takes place at a point along a trajectory in the magnetic field, the only way an ion can reach the collector is to follow an unsymmetrical path that enters the sector normally but leaves it at an angle to the normal. The departure from normality is related to the location of the charge exchanged in the first phase of the investigation. The dispersion of charge-exchanged ions originating from a small segment of primary beam is then determined for the location of the collector, and used to determine the intensity of that portion of the charge exchange continuum.

Charge-Exchange Trajectories

Fig. 1 shows a magnetic sector mass spectrometer schematically. The sector has its apex at M and is designed to focus ions originating at O at the collector S after a traverse of angle 2Ψ with radius 1 in the magnetic field. Ions undergoing charge exchange at a location E in the magnetic field can get from source to collector by the following path: straight line from O to the sector face at M' with normal entry, circular arc of radius (p - n)r from M' to E sweeping out an angle θ about a center C on the sector face MM', departure from E after charge exchange on a circular arc of radius pr about a center C_1 on the line CE, arrival at M" on the sector face MM" on the same arc with an angle of inclination α to the normal, and departure from M" for the collector S on a straight line also inclined at an angle α to the normal.

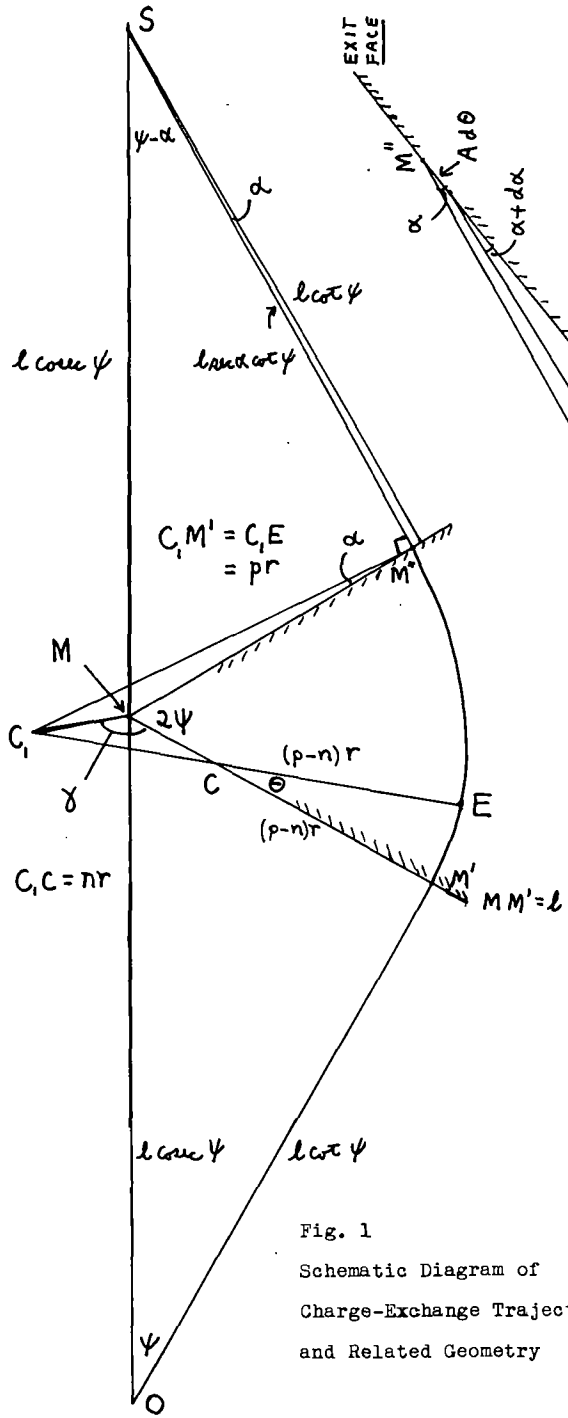

Fig. 1
Schematic Diagram of
Charge-Exchange Trajectory
and Related Geometry

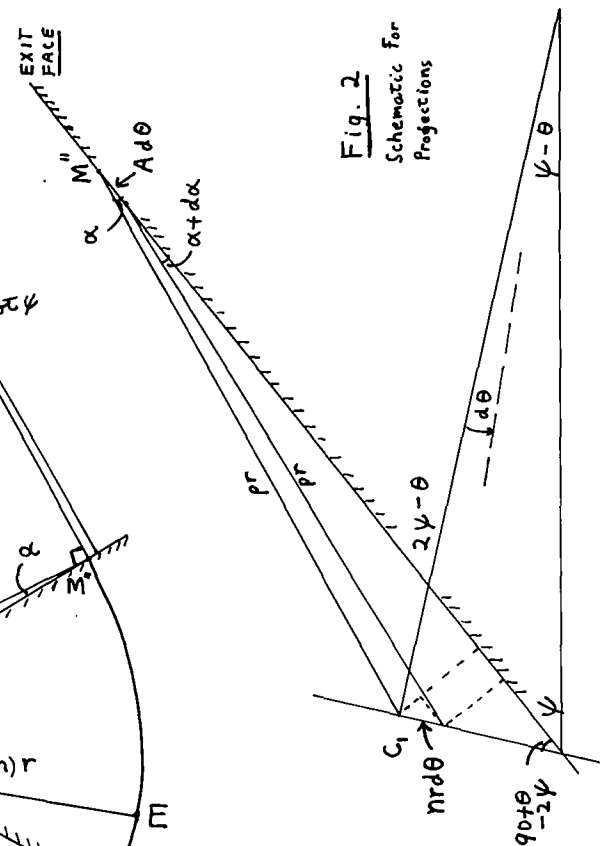

Fig. 2 Schematic for Projections

Fig. 2
Enlarged Schematic
for Increments and
Projections

In triangles CMC_1 and C_1MM'' the sine and cosine laws give respectively:

$$(1) \quad \sin\gamma = nr \sin\theta / C_1M$$

$$(2) \quad (C_1M)^2 = (nr)^2 + (l-(p-n)r)^2 - 2nr(l-(p-n)r)\cos\theta$$

$$(3) \quad \sin\alpha = C_1M \sin(360-2\psi-\gamma)/pr$$

$$(4) \quad (C_1M)^2 = (pr)^2 + (1-\cot\psi\tan\alpha)^2 l^2 - 2prl(1-\cot\psi\tan\alpha)\cos\alpha$$

Combination of (1) and (2), (1) and (3) and (2) and (4) respectively, substitution of $x = r/l$ and simplification give the equations

$$\sin\gamma = nx\sin\theta / \sqrt{n^2x^2 + (1-(p-n)x)^2 - 2nx(1-(p-n)x)\cos\theta} \qquad (A)$$

$$\sin\alpha = n\sin\theta \sin(360-2\psi-\gamma)/p\sin\gamma \qquad (B)$$

$$1 + 2px(1-\cot\psi\tan\alpha)\cos\alpha - 2x(p-n)(nx+1) - (1-\cot\psi\tan\alpha)^2 - 2nx\cos\theta(1-(p-n)x) = 0 \qquad (C).$$

The set of transcendental equations (A), (B) and (C) must all be satisfied by the x, θ and α for a valid charge-exchange trajectory. A numerical approximation method may be used to obtain valid solutions a given charge exchange in a given sector instrument. Select x, choose a trial set of θ and use (A) to calculate the corresponding sets of $\sin\gamma$ and γ. Use (B) to calculate a corresponding set of values for α. Evaluate the left hand side of (C) and note the values of θ that come closest to satisfying the equation. With a refined trial value for θ repeat the calculation cycle, and recycle again if necessary to obtain a valid set of results for (C).

Intensity Evaluation

The distance across the plane of the collector covered by ions resulting from charge exchanges after initial deflections between θ and $\theta + d\theta$ is determined by two factors, the distance covered at the exit face of the sector and the divergence or convergence of this beam segment from the exit face to the plane of the collector. The increment $d\theta$ in θ causes a shift in the center of the second circular arc a distance $nd\theta$ in a direction perpendicular to the line C_1CE at C_1, without any change in the radius pr. The resulting displacement of the exit point along the magnet face and change in emergence angle can be obtained by resolving the displacements along and normal to the exit face as indicated in Fig. 2.

$$(5) \quad nrd\theta\sin(90+\theta-2\psi) + pr\sin(\alpha+d\alpha) = pr\sin\alpha$$

$$(6) \quad pr\cos\alpha + nrd\theta\cos(90+\theta-2\psi) = Ad\theta + pr\cos(\alpha+d\alpha)$$

By expanding the trigonometric terms in $(\alpha+d\alpha)$, substituting $\cos d\alpha = 1$ and $\sin d\alpha = d\alpha$ and rearranging, relations (D) and (E) are obtained.

$$d\alpha = -n\sin(90+\theta-2\psi)\,d\theta/p\cos\alpha \qquad (D)$$

$$A = nr(\cos(90+\theta-2\psi) - \sin(90+\theta-2\psi)\tan\alpha) \qquad (E)$$

The charge-exchange ions emerging over the distance $Ad\theta$ on the exit face are affected as a result of the angular divergence $d\alpha$ over the distance $l\cot\psi\sec\alpha$ to the collector where they impact at an angle α off the normal. The total spread at the collector is then given by $Ad\theta + l\cot\psi\sec^2\alpha\,d\alpha$. The intensity in the continuum will be inversely proportional to the spread per increment $d\theta$ at the collector, and thus through the use of relations (D) and (E) may be shown to be given by

$$I = k\left\{x\cos(90+\theta-2\psi) + (\sec^3\alpha\cot\psi/p - x\tan\alpha)\sin(90+\theta-2\psi)\right\}^{-1}/nl$$

where I is intensity and k is a constant.

The quantities x and θ provide the means for expressing the charge-exchange continuum and the usual mass spectra of the instrument on a common displacement scale, depending on the method of scanning used.

Numerical Results

The following table gives a condensed summary of data obtained for various sector angles. Data apply to the 2+ to 1+ charge exchange.

Table I

Some Condensed Results for Various Magnetic Sector Angles

	60° Sector (ψ = 30)			90° Sector (ψ = 45)		
x	θ	α	Rel. Int.	θ	α	Rel. Int.
0.50	0° 0'	0° 0'	1.155	0° 0'	0° 0'	2.000
0.55	11 10	1 16	1.042	17 32	3 54	1.506
0.60	19 46	1 58	0.967	29 31	5 49	1.348
0.70	32 50	2 27	0.929	47 18	7 11	1.272
0.80	42 59	2 11	0.966	61 38	6 30	1.336
0.90	51 44	1 23	1.035	75 2	4 15	1.527
0.95	55 54	0 45	1.087	82 4	2 26	1.702
1.00	60 0	0 0	1.155	90 0	0 0	2.000

	120° Sector (ψ = 60)			180° Sector (ψ = 90)		
x	θ	α	Rel. Int.	θ	α	Rel. Int.
0.50	0° 0'	0° 0'	3.463	0° 0'	0° 0'	∞
0.55	24 28	8 15	1.898	41 29	19 21	3.93
0.60	39 8	11 50	1.609	58 25	25 13	3.03
0.70	60 20	14 14	1.461	83 3	29 45	2.69
0.80	77 36	13 12	1.583	104 29	28 57	3.01
0.90	95 38	9 6	1.948	128 3	23 11	4.24
0.95	106 5	5 35	2.367	142 39	17 40	5.95
1.00	120 0	0 0	3.463	180 0	0 0	∞

Relative intensity data for the 180 degree sector are numerically consistent with data obtained by the rectangular coordinate method, J. M. McCrea, Int. J. Mass Spectrom. Ion Phys. in press (1972).

Discussion

Noteworthy in the tabulated data is the very slight deviation of the charge-exchange ion trajectory from normality as it crosses the exit face in the 60 degree sector case and the relative uniformity of intensity along the continuum in this case. The very high intensities expected at the ends of the continuum in a 180 degree sector were previously obtained in calculations by a rectangular coordinate method, but the present method has shown in addition the high deviation from normal incidence at the collector in regions away from the ends of the continuum. The 90 and 120 sector data lie in the transition region between the two diverse cases discussed first.

References

1. J. M. McCrea, Int. J. Mass Spectrom. Ion Phys. 5, 381 (1970).
2. J. M. McCrea, Int. J. Mass Spectrom. Ion Phys., (in press).

TRANSLATION SPECTROSCOPY OF H^- PRODUCED BY COLLISION OF H^+ ON VARIOUS TARGETS

J. Appell, P.G. Fournier, F.C. Fehsenfeld† and J. Durup

Collisions Ioniques, Laboratoire de Physico-Chimie des Rayonnements††, 91405-Orsay, France

The study of translational energy spectra of H^- ions produced by 2 to 4 -keV proton impact on a molecular or atomic target yields a variety of results. Some of which have now been published[1] or will be [2,3,4,5].

Three formation processes of H^- have been observed, namely :

$$\text{I} \quad H^+ + M \rightarrow H^-(1s^2) + M^{++}$$

$$\text{II} \quad \begin{cases} H^+ + M \rightarrow H(1s) + M^+ \\ H(1s) + M \rightarrow H^-(1s^2) + M^+ \end{cases}$$

$$\text{III} \quad \begin{cases} H^+ + M \rightarrow H(2p) + M^+ \\ H(2p) \rightarrow H(1s) + h\nu \\ H(1s) + M \rightarrow H^-(1s^2) + M^+ \end{cases}$$

Characteristic energy losses ΔT, i.e. the differences between the incident proton energy T_o and the H^- translational energy T can be predicted exactly for each of these processes :

$$(1) \quad \Delta T_1 = I^{++} + E(H^-) + T_M$$

$$(2) \quad \Delta T_2 = I^+ + I'^+ + E(H^-) + T_{MM}$$

$$(3) \quad \Delta T_3 = I^+ + I'^+ + E(H^-) + T_{MM} + h\nu$$

where :

I^{++} is a double ionization potential of the target M

I^+ and I'^+ are ionization potentials of the target M which needs not be ionized to the same ionic state in the two steps of process II or III

$E(H^-)$ is the energy of the H^- state produced by addition of two electrons to H^+. H^- is shown[2] to be formed in its ground state so that $E(H^-) = -14.35$ eV

T_M and T_{MM} are the recoil energies of the target(s) which are negligible under our experimental conditions

$h\nu$ is the energy corresponding to the Lyman α emission = 10.2 eV

The dependence on target gas pressure of the observed H^- peak intensities is linear for process I and quadratic for processes II and III, which allows for the distinction of these processes.

---

† On leave from the National Oceanic and Atmospheric Administration, Boulder, Colorado.

†† Associated to the C.N.R.S.

The collisional spectroscopies derived from processes I and II have to our knowledge been up to now only described in a short communication of Witteborn and Ali[6]. The experiments have been performed on a magnetic sector field mass spectrometer equipped with a collision chamber[3,7].

With noble gas atoms as targets the results obtained for processes I and II allow for the discussion of selection rules applicable to the involved transitions ; the results provide evidence that the conservation of spin is strict for light targets where spin-orbit coupling is negligible and even up to Ar and Kr but does not hold for Xe[3].

Process III has been observed with He, Ne, Ar, Kr and H_2 as targets, it furnishes a way to observe a radiative transition without detecting the emitted photon and furthermore permits the determination of the branching ratio for charge transfer to H(1s) and H(2p) by comparison of the results obtained for processes II and III[2].

With H_2 as a target, where the states of the ionized and doubly ionized molecule are well known, evidence has been given that the Franck-Condon principle holds for the processes observed here[1].

With diatomic and polyatomic targets, the obtained results for process I provide a powerful tool for the determination of the energy levels of the doubly ionized species regardless of their stability with respect to dissociation.

In the case of N_2, O_2, NO as targets a discussion of selection rules for double charge transfer in diatomic molecules has been made[4]. The spin conservation rule is shown to hold strictly and approximate rules are obeyed as regards the symmetries of states.

For a number of polyatomic molecules (H_2O, N_2O, NH_3, C_2N_2, CH_4, C_2H_2, C_2H_4, C_2H_6, C_3H_8, C_6H_6, CH_3OH) several energy levels of the doubly ionized species have been observed [5].

Finally we wish to point out that to the described spectroscopy of doubly ionized states corresponds a reverse spectroscopy of negative ion state(s) if in the same experiment a known target and any positive ion as projectile are used, provided that the negative ion state has a lifetime with respect to autodetachment at least in the microsecond range. This spectroscopy allows e.g. to distinguish in an O_2^+ ion beam those ionic states which by a Franck-Condon transition to O_2^- will yield vibrational levels higher or lower than the ground state of neutral O_2.

References

(1) P. Fournier, J. Appell, F.C. Fehsenfeld and J. Durup, J.Phys.B. (1972) 5 L58

(2) J. Durup, J. Appell, F.C. Fehsenfeld and P. Fournier, J. Phys. B. (1972) in press

(3,4,5) J. Appell, J. Durup, F.C. Fehsenfeld and P. Fournier, to be submitted to J. Phys.B.

(6) F.C. Witteborn and D.E. Ali, Bull. Amer. Phys. Soc. (1971), 16, 208, and private communication

(7) J. Durup, P. Fournier and D. Pham, Int. J. Mass. Spectrom. Ion Phys.(1969) 2, 311.

Thermal Energy Charge Transfer Reactions of Various Projectile Ions to Methane: Resonance Effects in Nonorbiting Collisions

S8

Johannes Gauglhofer and Larry Kevan
Department of Chemistry
Wayne State University, Detroit, Michigan 48202

Gas phase charge transfer mechanisms can be broadly classified as orbiting and nonorbiting. At ion kinetic energies above about 10 eV, the probability of orbiting collisions is small, the relative motion of the reactants may be regarded as nearly rectilinear and charge transfer can occur by an electron-jump mechanism in a nonorbiting collision. The charge transfer rate constant is then dependent on the internal energy states of the reactants and energy resonance effects may be expected. Resonance effects have been demonstrated for a variety of molecular targets with a series of 50 eV projectile ions.[1,2] The rate constants are pseudoresonant with respect to the lower vibrational levels of the electronic states of the product ion. This has been interpreted to demonstrate the importance of Franck-Condon factors which are unfavorable for higher vibrational levels.

At thermal-ion energies, Langevin orbiting collisions[3] are expected to predominate and lead to complex formation from which one exit channel is charge transfer. However, nonorbiting collisions may also contribute to thermal energy charge transfer reactions. Nonorbiting contributions may be demonstrated by rate constants that are larger than Langevin and by resonance effects.

In this work we present both types of evidence to show that nonorbiting charge transfer does occur to methane for certain thermal energy projectile ions. Also, the energy response of the resonance effect for thermal energy ions is shifted from that for 50 eV ions and indicates that distortion of Franck-Condon factors may occur in thermal energy collisions.

The charge transfer rate constants were measured by ion cyclotron resonance (ICR) using a Varian ICR spectrometer. The principles of ICR have been described.[4] The pressure in the ICR cell was calibrated against the rate constant of 1.1×10^{-9} cm^3 molecule^{-1} sec^{-1} for the $CH_4^+ + CH_4 \rightarrow CH_5^+ + CH_3$ reaction.[5,6] Experimental correction factors for other gases, as directly determined in our instrument, were used to obtain pressure of other gases. However, for the results on methane, only the methane pressure must be known. Projectile ions were produced by 40 eV electrons, except that O_2^+ was produced by 20 eV electrons, and their ion current (I) was monitored as neutral target gas was added. The slope of $\ln(I_o/I)$ vs target pressure is $k\tau$ where k is the rate constant and τ is the residence time of projectile ions. τ was experimentally determined from the instantaneous power of absorption of a packet of ions passing through the cell as measured by a multi-channel boxcar integrator (Model TD-9 Eductor by PAR). The reproducibility of the rate constants is within ± 20% for data taken several months apart. However, the trend in the rate constants when plotted versus recombination energy of the projectile ions is always the same. The absolute accuracy of the rate constants is limited by uncertainty in the pressure and residence time measurements and is perhaps higher than ±20%. The average kinetic energy of the projectile ions was less than 0.1 eV and was limited by the trapping voltage and the acceleration of the ions in the resonance detection region.

When the thermal rate constants are plotted vs the recombination energy of the projectile ions they show a maximum for N_2^+ and Ar^+. It is noteworthy that the thermal energy rate constants for N_2^+ and Ar^+ with methane are 3.0 and 1.7 times respectively as large as the maximum orbiting rate constants. This suggests that nonorbiting collisions must be important, at least for these ions with methane. It is suspected that nonorbiting collisions make a contribution for other projectile ions with methane too. The conclusions with respect to $Ar^+ + CH_4$ are supported by the results of Masson et al.[7] who used multiple pulse methods in a magnetic mass spectrometer to show that 1.5 - 4.2 eV Ar^+ undergoes 60% of its collisions with methane without momentum transfer and 40% of its collisions with momentum transfer. The contribution without momentum transfer implies nonorbiting collisions and the independence of the fraction of such collisions for Ar^+ in the energy range 1.5 to 4.2 eV suggests that such collisions may persist at thermal energies.

The rate constant for apparently thermal energy Ar^+ with CH_4 has also been measured by other groups with mixed results. Our value is $1.9 \times 10^{-9} cm^3 molecule^{-1} sec^{-1}$, Karachevtsev et al.[8] find 7.5×10^{-9}, Bolden et al.[9] find 0.9×10^{-9}, Jones et al.[10] find 0.78×10^{-9} and Melton[11] finds 2.2×10^{-9}; the Langevin value is 1.12×10^{-9} cm^3 $molecule^{-1}$ sec^{-1}. In view of the disparity in results, it could be argued that our high rate constants do not necessarily prove the importance of nonorbiting collisions at thermal energies. However, the thermal energy results also show the existence of apparent resonance effects in the rate constants vs recombination energy as observed previously for 50 eV projectile ions.[1,2] Such effects are characteristic of nonorbiting collisions and support the above interpretation based on our rate constant magnitudes.

There is a most interesting feature of the thermal ion resonance effects. In an electron jump nonorbiting mechanism one expects the rate constants of projectile ions of different recombination energies to reflect the energy dependence of the Franck-Condon factors associated with the transition of the target molecule to its ion. Experimental Franck-Condon factors for the ionization of methane have recently been reported.[12] These factors exhibit a broad maximum between 13.5 and 14.5 eV and show remarkable agreement with the recombination energy dependence of the rate constants for 50 eV ions[1,2] which show the largest rate constants for CO^+ and Kr^+. However, for the thermal energy ions, the maximum charge transfer rate constants seem to be shifted to higher recombination energies near 15.4 to 15.6 eV; the three ions with recombination energies near 14 eV (CO_2^+, CO^+ and Kr^+) don't seem to agree with the trend in experimental Franck-Condon factors. The experimental Franck-Condon factors apply to vertical transitions from normal methane. In a slow ion-molecule collision, such as pertains at thermal energies, the vibrational wavefunctions of methane will undoubtedly be perturbed by the slowly approaching ion and lead to perturbed Franck-Condon factors. Lipeles[13] has calculated perturbed Franck-Condon factors based on such a model for $N_2 \rightarrow N_2^+$ and $CO \rightarrow CO^+$, and he has shown that energy shifts of the maximum Franck-Condon factors by several vibrational levels (0.5 - 1.0 eV) can readily occur. We believe that we are observing this effect for the first time in a polyatomic molecule in the comparison of the 50 eV and thermal ion results on charge transfer to methane.

Thermal energy charge transfer results of a variety of projectile ions on ethane and propane also indicate that nonorbiting charge transfer occurs with these targets for certain ions, notably N_2^+. However, the energy dependence of the experimental Franck-Condon factors[12] is so broad in these larger molecules as to obscure any energy shifts associated with distorted Franck-Condon factors. Charge transfer results on butane and higher alkanes yield thermal energy rate constants which are less than Langevin values and also no clear resonance effects are seen. Thus for large molecule targets, nonorbiting charge transfer at thermal energies may be of little importance, while for small molecule targets the nonorbiting mechanism seems to be of considerable importance.

References

1. D. Smith and L. Kevan, J. Amer. Chem. Soc., 93, 2213 (1971).
2. D. Smith and L. Kevan, J. Chem. Phys., 55, 2290 (1971).
3. G. Gioumousis and D. P. Stevenson, J. Chem. Phys., 29, 294 (1958).
4. J. L. Beauchamp, Ann. Rev. Phys. Chem., 22, 527 (1971).
5. R. P. Clow and J. H. Futrell, Int. J. Mass Spectrom. Ion Phys., 4, 165 (1970).
6. S. E. Buttrill, J. Chem. Phys., 50, 4125 (1969).
7. A. J. Mason, K. Birkinshaw and M. J. Henchman, J. Chem. Phys., 50, 4112 (1969).
8. G. V. Karachevtsev, M. I. Markin and V. L. Talrose, Kinetics and Catalysis, 5, 331 (1964), Engl. trans. of Kinetika and Kataliz.
9. R. C. Bolden, R. S. Hemsworth, M. J. Shaw and N. D. Twiddy, J. Phys. B, 3, 45 (1970).
10. E. G. Jones and A. G. Harrison, Int. J. Mass Spectrom. Ion Phys., 6, 77 (1971).
11. C. E. Melton, J. Chem. Phys., 33, 647 (1960).
12. R. Stockbauer and M. G. Inghram, J. Chem. Phys., 54, 2242 (1971).
13. M. Lipeles, J. Chem. Phys., 51, 1252 (1969).

It is expected to publish this work in Chemical Physics Letters.

DIPOLE EFFECT IN ION-MOLECULE REACTIONS

by Michael T. Bowers and Timothy Su
Department of Chemistry, University of California
Santa Barbara, California 93106

The effect of a permanent dipole moment on the thermal energy rate constants for charge transfer, proton transfer and non-reactive collisions has been investigated using an Ion Cyclotron Resonance Spectrometer. Pressures were measured using a Baratron Capacitance Monometer and reaction times measured by a trapping ejection technique.

The substrate systems chosen for study were the sets of geometrical isomers trans, - 1,1,- and cis - difluorethylene; trans,- 1,1, and cis - dichloroethylene; and para,- meta,- and ortho-difluorobenzene. These isomeric sets were chosen because within each of them the polarizability and ionization potential are essentially equal, but the dipole moments vary from zero to approximately 2.5 Debye. The isomer with zero dipole moment in each set is used to estimate the non-polar contributions to the rate constant. Differences between the polar and non-polar isomers are presumed to result from permanent dipole contributions to the rate constant.

The thermally averaged rate constant for reaction of a point charge with a polar molecule is given by [1-4]

$$\bar{k} = \frac{2\pi q}{\mu^{\frac{1}{2}}} \left[\alpha^{\frac{1}{2}} + \mu_o \left(\frac{2}{\pi kT}\right)^{\frac{1}{2}} \operatorname{Cos} \bar{\theta}\right] \qquad (1)$$

Where α is the polarizability and μ_o is the dipole moment of the neutral molecule. The first term is due to charge-induced dipole and the second to the charge-permanent dipole interaction. $\bar{\theta}$ is the average angle of the dipole with respect to the line of centers of the collision.

$\bar{\theta}$ can be experimentally determined by the relation

$$\bar{k}' - \bar{k} = \frac{2q\mu_o}{\mu^{\frac{1}{2}}} \left(\frac{2\pi}{kT}\right)^{\frac{1}{2}} \operatorname{Cos} \bar{\theta} \qquad (2)$$

where $\bar{k}$ is the rate constant of the isomer with zero dipole moment and $\bar{k}'$ is that of the isomer having a dipole moment.

Theoretical values of $\bar{\theta}$ can be estimated from the expression

$$\bar{\theta} = \int_o^{\varphi} P(\theta)\theta d\theta \Big/ \int_o^{\varphi} P(\theta) d\theta \qquad (3)$$

where φ is chosen as 180^o. $P(\theta)$ is the probability that the dipole is at an angle θ with respect to the line of centers of collision and is given by

$$P(\theta) \sim \frac{\sin \theta}{\bar{v}_T(\theta)} \qquad (4)$$

where $\bar{v}_T(\theta)$ is the average instantaneous velocity of the rotor at angle θ with respect to the line of centers of the collision.

A. Charge Transfer Reactions:

Experimental charge transfer reactions from rare gas ions to the difluorobenzene isomers is given in Table I. Theoretical induced dipole and locked dipole approximations are included for comparison.

Table I

Charge-Transfer Rate Constants from Rare Gas Ions to Difluorobenzene x 10^9 cm^3/sec

	Experimental			Theory		
					locked dipole	
	p-	m-	o-	induced dipole	m-	o-
He^+	7.15	8.24	9.05	3.56	10.7	16.1
Ne^+	3.41	3.76	4.21	1.70	5.10	7.75
Ar^+	2.58	3.08	3.26	1.28	3.84	5.30
Kr^+	2.02	2.30	2.47	1.00	3.00	4.53
Xe^+	1.36	1.44	1.63	0.90	2.70	4.08

The fact that the para values are larger than the orbiting approximation indicates long range "electron jump" processes contribute to the rate constant as discussed by Rapp and Francis.[5] Similar data have been obtained for the dichloroethylene isomers. The experimental and theoretical values of $\overline{\theta}$ are collected in Table II.

Table II

Experimental and Theoretical Values of $\overline{\theta}$ from Charge Transfer Reactions:

	Experiment	Theory
m - $C_6H_4F_2$	82.4°	79.5°
o - $C_6H_4F_2$	81.1°	77.0°
1,1 - $C_2H_2Cl_2$	81.2°	80.0°
Cis - $C_2H_2Cl_2$	80.5°	77.5°

$\overline{\theta}$ is slightly smaller for the larger dipole moments as predicted by theory. One interesting result is that both experiment and theory indicate the dipole is only slightly oriented by the charge at 300°K.

B. Proton Transfer Reactions:

Proton transfer reactions from CH_5^+, CD_5^+, H_3^+ and D_3^+ to geometric isomers of difluorobenzene, dichloroethylene and difluoroethylene have been studied. Table III lists the rate constants to the dichloroethylene isomers together with the experimental librational angle $\overline{\theta}$ and that predicted from theory.

Table III

Proton Transfer Rate Constants to $C_2H_2Cl_2$ Isomers

Ion	k x 10^9 cm^3/sec				$\overline{\theta}$			
				theoretical	experimental		theory	
	trans	1,1	cis	induced dipole	1,1	cis	1,1	cis
CH_5^+	1.82	2.00	2.09	1.72	86.9	86.7	80°	77.5°
CD_5^+	1.12	1.20	1.25	1.51	88.4	88.1	"	"
H_3^+	4.00	4.52	4.83	3.90	85.9	85.4	"	"
D_3^+	2.93	3.12	3.29	2.78	87.3	87.2	"	"

All of the trans rate constants agree with those predicted by the charge induced dipole theory. The experimental $\bar{\theta}$'s semi-quantitatively agree with theoretical prediction.

Similar results were obtained for proton transfer reactions to difluorobenzene and difluorethylene isomers.

C. Non-Reactive Collisions:

The collision frequency for momentum transfer for non-reactive collisions between an ion and neutral can be derived from the slope of a plot of ICR line width vs. pressure.[6] Since NO^+ formed from NO by low energy electrons ($\sim$ 10 ev) does not react appreciably with difluoroethylene and dichloroethylene, these systems have been selected for studying elastic collision frequencies between the ion and neutral.

For the ion-dipole interaction

$$\xi/n = \frac{2\pi q}{\mu^{\frac{1}{2}}} \frac{M}{M+m}\left[\alpha^{\frac{1}{2}} + \mu_D \left(\frac{2}{\pi kT}\right)^{\frac{1}{2}} \cos\bar{\theta}\right] \qquad (5)$$

where m is the mass of the ion and M is mass of neutral. It can be shown that $(\frac{M+m}{M})\xi/n$ is equivalent to the collision rate constant. Table IV presents the values of $(\frac{M+m}{M})\xi/n$ for the systems studied together with the induced-dipole rate constants and the experimental and theoretical predicted $\bar{\theta}$ values.

Table IV

Non-reactive Collision Rate Constants

and Orientation Angles

Reactants	$\xi/n(\frac{M+m}{M})$ x 10^9 cm^3/sec				$\bar{\theta}$			
				induced	experimental		theory	
	trans	1,1	cis	dipole	1,1	cis	1,1	cis
$NO^+ + C_2H_2Cl_2$	2.04	2.40	2.54	1.37	82.0°	82.1°	80.0°	77.5°
$NO^+ + C_2H_2F_2$	1.67	2.25	2.94	1.06	78.1°	75.1°	79.8°	76.0°

The trans collision frequencies are larger than predicted by charge-induced dipole theory. The origin of this effect is not yet understood. Theoretical values of $\bar{\theta}$ agree semiquantitatively with those predicted by theory.

This work was supported by the National Science Foundation. Publication is anticipated in the Journal of the American Chemical Society.

References

(1) G. Gioumousis and D. P. Stevenson, J. Chem. Phys., 29, 294 (1958)

(2) T. F. Moran and W. H. Hamill, J. Chem. Phys., 39, 1413 (1965)

(3) S. K. Gupta, E. G. Jones, A. G. Harrison and J. J. Myher, Can. J. Chem., 45 3107 (1967)

(4) R. A. Fluegge, J. Chem. Phys., 50, 4373 (1969)

(5) D. Rapp and W. E. Francis, J. Chem. Phys., 37, 2631 (1962)

(6) J. L. Beauchamp, Annual Review of Physical Chemistry, Vol. 22, 1971, pp. 527-561

QUANTITATIVE RELATIVE PROTON AFFINITIES[1]

Donald H. Aue, Hugh M. Webb and Michael T. Bowers

Department of Chemistry
University of California
Santa Barbara, California 93106

Accurate relative proton affinities of amines have recently been determined by means of ion cyclotron resonance.[2] The technique involves the measurement of proton transfer equilibria of pairs of amines at pressures of between 5×10^{-4} and 1×10^{-3} torr. Relative proton affinities determined by this method are accurate to ± 0.20 kcal/mole as indicated by multiple overlap of ΔG's.[2]

The simple aliphatic amines have been investigated in detail, and their proton affinities were correlated with ionization potentials and aqueous heats of protonation.[3] Proton affinity (PA) and ionization potential (IP) are related by the following expression:

$$PA(B) = IP(H\cdot) - IP(B) + HA(\overset{\oplus}{B}\cdot)$$

where $HA(\overset{\oplus}{B}\cdot)$ = the hydrogen affinity of $\overset{\oplus}{B}\cdot$ or the bond dissociation energy of the N-H bond in a protonated amine.

Using photoionization potentials, HA's of amines can now be determined quantitatively. The HA's are found to vary as substitution at nitrogen changes in primary, secondary, and tertiary amines (Table I).

Table I

AMINE	GB[a]	PA	ADIABATIC IP	ADIABATIC HA
NH_3	198 ± 3	207 ± 3	234.1	127 ± 3
CH_3NH_2	209.8	218.4	206.8	111.6
$(CH_3)_2NH$	216.6	224.9	190.0	101.3
$(CH_3)_3N$	221.3	229.1	180.3	95.8
	228.2	236.0	185.0	107.0

[a] G.B. is defined as the negative of the free energy (ΔG^{o}) for the reaction: $B + H^{\oplus} \rightleftharpoons BH^{\oplus}$.

Changes in hybridization at nitrogen produce dramatic effects in both the HA and PA of amines (Table II). Since adiabatic IP's of alkyl amines reflect geometrical reorganization to a planar structure, vertical IP's are used to calculate the vertical HA's in Table II.[4] Vertical HA's and IP's are required in looking for hybridization effects, so that the amine hybridization remains constant. The adiabatic HA of quinuclidine in Table I is about 11 kcal/mole higher than that for trimethylamine because the rigid quinuclidine ring cannot relax to a planar structure on ionization.[5]

Table II

Amine	PA	Vertical IP	Vertical HA	ΔHA	% s-character in lone pair
	220.2	226.0	132.6		~ 30
				16.3	
$(CH_3)_2NH$	224.9	205.0	116.3		25
	224.3	226.0	136.7		33
				20.4	
	230.3	199.6[a]	116.3		25
n-PrCH=NEt	229.9	207.5[b]	123.8[b]		33
				7.5[b]	
$(n\text{-}Pr)_2NH$	231.9	198.0[a]	116.3		25
CH_3CN	186	303.0	175.4		50
				47.9	
$CH_3CH_2NH_2$	221.1	220.0	127.5		25

[a]Estimated values [b]adiabatic I.P. which lowers these values by ca. 10 kcal/mole

Diaminoalkanes exhibit unusually high PA's when compared with n-alkylamines of similar polarizability (Table III).[5] This effect results from hydrogen-bonding of the proton in a cyclic structure. Apparently, linear and bent hydrogen-bonds differ by no more than 10 kcal/mole. A value of ca. 20 kcal/mole for the strength of the proton-bound dimer bonds of alkyl amines is predicted by this model. A bond strength of 27 kcal/mole for the proton-bound dimer of ammonia has been measured by Kebarle.[6]

Table III

Protonated Diamine	GB	$-T\Delta S^{o}_{calc}$ [a]	PA_{calc}	ΔPA[b]
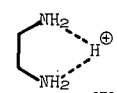	219.6	12.15	231.8	> 9.5
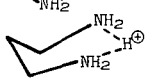	225.2	13.4	238.6	15.8
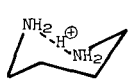	228.5	15.5	244.0	21.1

Table III (continued)

Protonated Diamine	GB	$-T\Delta S_{calc}$ [a]	PA_{calc}	ΔPA [b]
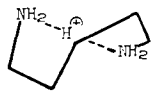	226.6	16.4	243.0	20.0
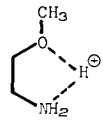	216.4	12.15	228.6	> 5.8

[a] ΔS values estimated from ΔS_f^o of corresponding acyclic and cyclic hydrocarbons.

[b] Differences between PA of diamine and n-alkylamine of similar molecular weight.

References

1. Supported by NSF Grant No.GP-15628 and ACS-PRF Grants Nos.5031-AC4 and 5993-AC5.
2. M. T. Bowers, D. H. Aue, and H. M. Webb, J. Amer. Chem. Soc., 93, 4314 (1971).
3. D. H. Aue, H. M. Webb, and M. T. Bowers, J. Amer. Chem. Soc., 94, 0000 (1972).
4. For vertical IP's of the methyl amines, see A. B. Cornford, D. C. Frost, F. G. Herring, and C. A. McDowell, Can. J. Chem., 49, 1135 (1971).
5. D. H. Aue, H. M. Webb and M. T. Bowers, to be published.
6. S. K. Searles and P. Kebarle, J. Phys. Chem., 72, 742 (1968).

Chemical Ionization and ICR Chemical Ionization of Aliphatic Aldehydes

Thomas A. Elwood, Jean H. Futrell
Department of Chemistry
University of Utah
Salt Lake City, Utah 84112

Catherine Fenselau
The Johns Hopkins School of Medicine
Baltimore, Maryland 21205

A recent study by Fenselau, Duncan, and Fales on the chemical ionization of deuterium labeled heptanals[1] revealed a large degree of scrambling in the major fragmentation from the molecular ion: for heptanals exclusively perdeuterated on the 2-, 3-, 4-, 5-, 6- or 7-carbon, their statistical treatment indicated that both hydrogens lost as H_2O originated from the hydrocarbon chain. We have reinvestigated this general problem and have examined various alkyl aldehydes using both conventional chemical ionization (CI) and the ICR/CI technique developed by Clow and Futrell[2]. Figure 1 illustrates the similarity of chemical ionization spectra obtained on a Varian ICR-12, the more conventional CEC-110B modified for CI/EI[3], and the unique Varian MAT CH-7 modified for CI.[4] The ICR-12 double-resonance experiments for hexanal indicate that 60% of the fragmentation to the $(MH-H_2O)$ ion originates from protonation by CH_5^+ while 40% originates from $C_2H_5^+$. Results in the ICR-12 and the CEC-110B for 7 aliphatic aldehydes with both CH_4 and CD_4 reagent gases support the following conclusions: 1) beyond initial protonation, the reagent gas is totally inert to reactions with the aldehyde system; 2) a hydrogen on a γ-carbon is requisite to rearrangement and subsequent loss of water; 3) a γ-carbon is also requisite for randomization into the carbon chain by the proton donated from CH_5^+ or $C_2H_5^+$; 4) a complication to interpretation may arise from scrambling in protonated dimer ion, $(2M + 1)^+$.

---

1. C. Fenselau, J. Duncan and H. M. Fales, 19th Annual Conf. on Mass Spectrometry and Allied Topics, Atlanta, Georgia, May 2-7, 1971.

2. R. P. Clow and J. H. Futrell, J. Amer. Chem. Soc., 94, 3748 (1972).

3. J. H. Futrell and L. H. Wojcik, Rev. Sci. Inst., 42, 244 (1971).

4. M. L. Vestal, T. A. Elwood, L. H. Wojcik and J. H. Futrell, 20th Annual Conf. on Mass Spectrometry and Allied Topics, Dallas, Texas, June 4-9, 1972 paper P 10.

FIGURE 1. Pentanal with CH_4

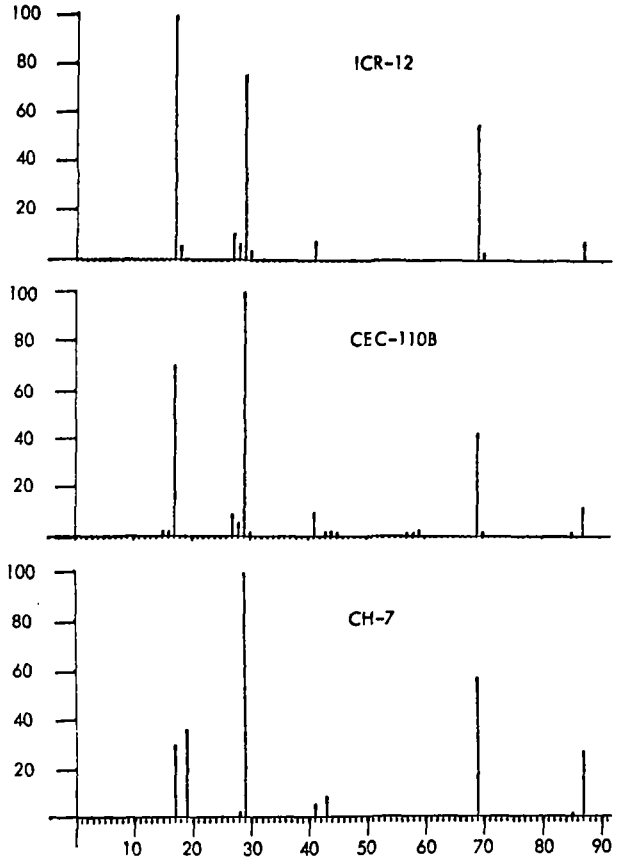

A Dempster-ICR Tandem Mass Spectrometer *

David L. Smith and Jean H. Futrell
Department of Chemistry
University of Utah
Salt Lake City, Utah 84112

A tandem mass spectrometer consisting of a 180° Dempster mass spectrometer and an ion cyclotron resonance (ICR) cell which functions both as a reaction chamber and analyzer has been constructed. The first stage has a 5.7 cm radius of curvature and provides a reactant ion beam with unit resolution up to approximately mass 200. Following mass analysis, the reactant ions are decelerated to approximately 0.1 eV and injected into the end of a two section ICR cell where reaction with a target gas is possible. Reactant and product ion concentrations are deduced from the power absorption signals of the marginal oscillator. Sufficient differential pumping is achieved using a 4 inch oil diffusion pump and a 25 l/sec ion pump that a pressure differential between the Dempster source and the ICR cell of 10^4 is obtained.

The increased complexity of this instrument is accompanied by a great increase in versatility over conventional ICR mass spectrometry. The most obvious advantage is the ability to unambiguously select reactant ions and neutrals. A more important advantage, however, lies in the ability to generate collisionally stabilized reactant ions. The high pressure source is also well-suited to the generation of reactant ions which are themselves products of ion-molecule reactions. In addition, there is a great increase in total sensitivity for studies of ions which make up only a small percentage of the electron impact spectrum.

Measurements of absolute ion-molecule rate constants of some standard reactions, such as the reaction of CH_4^+ with CH_4, have been made and compare well with previous results. In another series of experiments D_2 was admitted to the source at a relatively high pressure. D_2^+ ions initially generated by electron impact react with D_2 to yield D_3^+ ions which have a distribution of excitation energies. Depending on the D_2 source pressure, the D_3^+ ions may undergo from zero to ten collisions, on the average, before leaving the source. The D_3^+ ions are then mass analyzed, decelerated to approximately 0.1 eV and injected into the ICR cell where reaction with an added gas occurs. Reaction of highly excited D_2^+ ions with H_2 yields exclusively the products H_2D^+ and HD_2^+ which are in the ratio of 5:1. Increasing the D_2 source pressure such that D_3^+ ions undergo approximately 8 collisions decreases this ratio to 1.5:1. This result is consistent with the formation of a $H_2D_3^+$ complex which lasts sufficiently long for some scrambling of atoms. As the internal energy of D_3^+,

and likewise $H_2D_3^+$, decreases, either more collisions result in complex formation or the complexes are longer lived. In either case, the amount of atomic scrambling increases.

A similar experiment has been performed where D_3^+ ions were impacted onto CH_4. This reaction is of particular interest since heats of formation of reactants and products show that CH_4D^+ is the only possible product for the reaction of ground state D_3^+ with CH_4. Formation of CH_3^+ or CH_2D^+ is approximately 40 kcal/mole endothermic. A low D_2 source pressure (i.e. highly excited D_3^+) gives a $CH_4D^+/C(HD)_3^+$ ratio of 0.7:1. This ratio increases continuously to a value of 6.0:1 as the D_2 source pressure is increased such that D_3^+ ions typically undergo 8 stabilizing collisions. These preliminary results illustrate the use of such reactions as a means of measuring ionic excitation energy and thus provide a very sensitive means of studying energy transfer processes.

*A more detailed account of this work has been submitted to Rev. Sci. Inst.

ECONOMICAL, HIGH PERFORMANCE M/S DATA ACQUISITION

T1

* Alan Carrick

National Physical Laboratory, Teddington, Middlesex, England

Precise determination of the position, and hence mass, of peaks in a mass spectrum by direct analogue computation is now a well established technique both in theory [1] and practice [2, 3, 4]. The M/S data acquisition interface designed at NPL and based on analogue detection of peak maxima as a means of obtaining mass and intensity parameters has demonstrated its measuring capabilities for both high and low resolution spectra under the most demanding conditions.

This interface is now in commercial production in both "on-line" and "off-line" versions. The "off-line" unit can take data directly from high resolution spectrometers at medium scan rate (1 : 10000 resolution 10s/ decade) and fast scanning, low resolution machines (1 : 1000 at 1s/ decade and faster) without the aid of a computer and transfer peak time and intensity information to paper, or magnetic tape for further processing by a normal service computer.

"On-line" systems using the interface are distinguished by extremely light processor loading during the acquisition phase and so the computer concerned can easily engage in interleaved processing in, for example, a repetitively scanned GC–MS system, or can collect data from other laboratory instruments simultaneously without performance degradation. Typical performance figures for a simple dedicated computer system incorporating the interface include r.m.s. errors of 9 ppm for mass measurements on peaks containing 5–300 ions in single 10 s decade scans of perchlorobutadiene at 1 : 10000 resolution, and r.m.s. errors of 0.064 mass units for single 0.16s/ decade scans of the same material at 1 : 400 resolution.

Recent work at N.P.L. has catered on the evaluation of the units capabilities for collecting data on metastable transitions from a double focussing spectrometer in both the "refocussed" mode and from the normal (second field free region) metastables encountered during high resolution scans [6].

A typical example of metastable data acquired under high resolution fast scan conditions is shown in the Figure, which illustrates the region of a metastable generated by loss of a proton from the molecular ion of 2 – hydroxy–4 – n – octoxybenzophenone. The characteristic "dished top" of the broad metastable lying between m/e 324.00 and m/e 324.35 can readily be distinguished together with the ESA continuum of the transition (m/e 324.4 – 325.0) and some readings from the C^{13} isotope transition at 325.4. A significant advantage of the method is the resolution of the normal ion at m/e 324.2, which under low resolution conditions broadens to obscure the wings of the metastable. This normal ion and similar ions in the related transition at m/e 212 in the same compound (proton loss from the molecule less octene) were measured with sufficient precision (20 ppm) to provide positive chemical identification, despite the underlying metastable. Each peak maximum indication represents a record of the incidence of between 2 and 5 ions at the electron multiplier.

Kinetic energy release values for the transition obtained directly from peak width data as presented by the processing computer (direct subtraction of the mass values for the peaks at the wings of the metastable) give good agreement (0.01eV) with manual determinations from measurements on U.V. recorder traces at varying accelerating potentials.

Examinations of, amongst others, the m/e 46 transitions in o– nitroaniline gave single scan measurements on the NO_2^+ ion (m/e 45.9941) correct to 25 ppm, and indications of the presence of the 92^{++} ion ($C_6H_6N^{++}$) as well as an accurate value (45.953) for the maximum of the metastable itself.

Experiments using a 50 ms scan time for a limited IA voltage scan in the metastable refocussed mode gave correct parent – daughter transition assignments (to 0.3 mass units) for detectable transitions in nonane the sensitivity achievable here being limited by necessarily fact scan time. The flat topped daughter ion peaks were positioned accurately by taking a weighted mean value for the noise indications along the plateau.

References:

1 A Carrick and E.B. Lees "A simple method for the calculation of mass spectroscopic peak profile" in preparation for J. Mass Spectrometry and Ion Physics.

2 A. Carrick J. Mass Spectrometry and Ion Phys., 2, (1969), 333

3 Idem Advances in Mass Spectrometry, V (1971), 137

4 Idem Radio & Electronic Engineer, 41, (1971), 453

5 "Datamass" A system for processing high and low resolution mass spectra. Instem Limited.

6 A. Carrick & N.M. Paisley, in preparation for Organic Mass Spectrometery

---

* Present address Laboratory Products Division, Instem Limited, Stafford Street, Stone, Staffordshire. England.

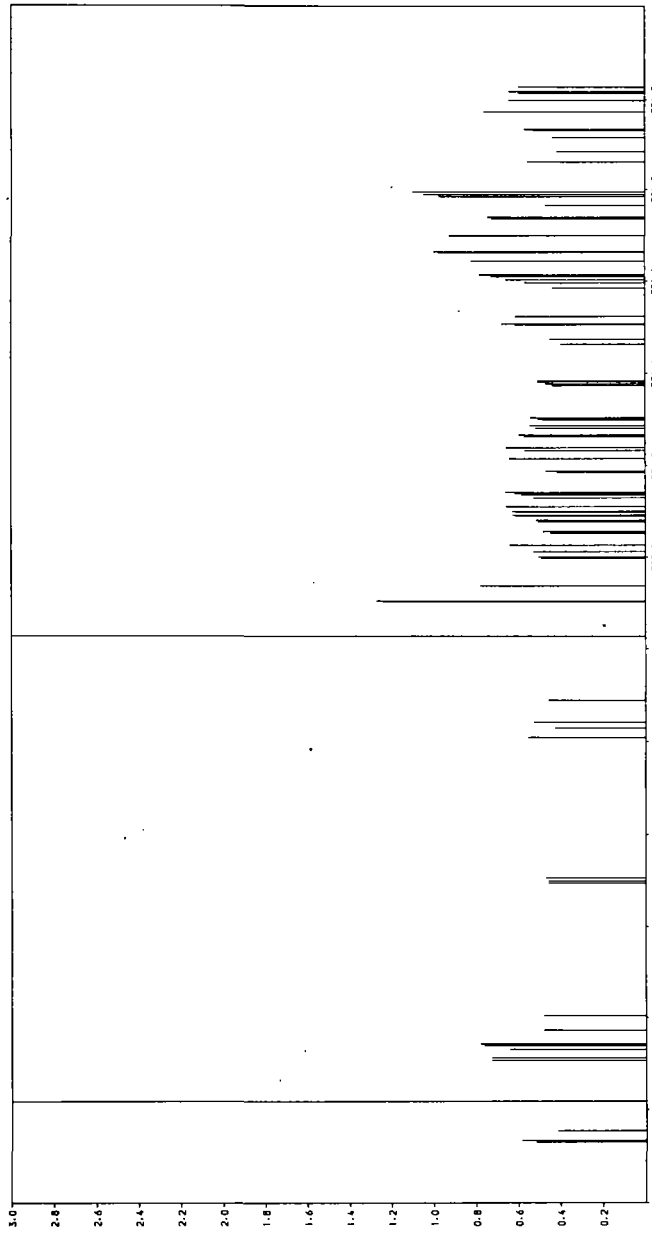

Fast scan, high resolution record of M + - M – H+ transition in 2–hydroxy–4–n–octoxbenzophenone.

THE AFCRL AUTOMATED PHOTOPLATE DATA ACQUISITION AND REDUCTION SYSTEM

Maynard H. Hunt, John V. Nikula, Harold Posen and Virgil E. Vickers

Air Force Cambridge Research
Laboratories, Bedford, Mass. 01730

INTRODUCTION

Like many other laboratories at the present time, the Air Force Cambridge Research Laboratories have an abundance of excellent equipment but are severely restricted as to personnel. Therefore it behooves us to relieve the human operator of as much of the routine data acquisition and reduction as possible. It is for this reason that we have devoted our efforts to automate the acquisition and reduction of data from the photoplates of our MS-7 Spark Source Mass Spectrograph. But in addition to this advantage, there is also to be anticipated a considerable increase in accuracy and a saving of time.

The equipment available to us is an IBM process-controller employing 16 bit words, a 16K core of which 8K are available for program and data handling. Peripheral equipment consists of two 1810 disks, a card reader/punch, a typewriter and a plotter.

The Laboratory Automated Air Force System (LAAFS) is the intermediate level of a three tiered hierarchy of programming with the IBM-TSX supplied system programs at the top, responsible for I/O control, compilers/assemblers and interrupt handling; next LAAFS, responsible for CPU allocation, specialized I/O and error logging, and interrupt servicing; and finally the particular set of programs written by the user for his particular experiment. Fig. 1 shows the experiments which are currently on line or intended to be on line soon.

THE INTERFACE

When the automation of the photoplate reader was first contemplated, we considered the purchase of one of the precision lead screw stepping motor driven microphotometers for about $50,000, upgrading the Jarrell-Ash 23-100 for roughly $25,000 or modifying our Jarrell-Ash ourselves. Our decision was to use a linear encoder mounted on the photoplate carriage of the Jarrell-Ash 23-100, to operate on interrupts, and to read on the fly.

The items which were purchased to implement our automation scheme were:

(1) A linear encoder having a fifteen inch scale with a resolution of .0001 inch from Dynamics Research Corporation, Wilmington, Mass., Cost $2500.

(2) A 12 bit A-D converter, a sample and hold amplifier, a 183-J operational amplifier, several 118-A operational amplifiers and requisite power supplies from Analog Devices, Norwood, Mass., Cost: $1400.

(3) A ten digit keyboard from Minneapolis-Honeywell for $36.

(4) From various sources gates, multivibrators, flip flops, etc. plus miscellaneous hardware brought the total to somewhat less than $5,000.

The schematic of the interface between the Jarrell Ash 23-100 and the IBM 1800 is shown in Fig. 2. The 118-A operational amplifiers serve as level shifters and amplifiers because the logic levels of the 1800, 0=-6 to -30V and 1=-1 to + 30 volts, were not compatible with the logic level of the other units 0 = 0 to 0.2 volts and 1 = greater than 4.2 volts. The 118As act as drivers to the cable linking the interface to the 1800, providing positive logic levels, 1 = +8 volts, 0 = -8 volts. The 183J is a higher quality operational amplifier providing a signal of suitable magnitude to the sample and hold amplifier.

There are two terms that require definition. An interrupt is a change in voltage level that produces a branch in the normal program sequence in the 1800. An ECO, electronic contact operation, is a voltage returned by the 1800.

The operation of the system is as follows: The operator positions the photoplate on the carriage of the microphotometer at the point that he wishes to begin taking data and resets the display to zero. At this point interrupts #1 and #2 are generated

in sequence to bring the necessary program into core. Then the keyboard is employed to identify the job, provide exposure parameters, list elements visually detected, and provide the parameters for the dispersion relationship to be discussed in a later section.

The preliminary information having been read in, the carriage is moved slightly in the negative direction and the microphotometer drive is started. As long as the sign bit is 0 the nand gate is closed to the ECO enable pulse. When the sign bit goes to 1 interrupt #3 initiates data taking and the nand gate will pass the next ECO enable pulse to reset the RS flip flop. Every other pulse from the least significant bit, that is each negative going pulse, at intervals of .0002", causes the RS flip flop to go to its complementary state, thus providing hold and convert command pulses to the sample and hold amplifier and the A-D converter respectively. At the completion of the conversion, the status bit returns to 0 and interrupt #5 is generated which causes the program to check the status of the data input word. The data input word having been read, the 1800 replies with a pulse via ECO enable which resets the RS flip flop and the cycle is repeated.

Since the response of the electronics is much faster than the chart pen it is possible to record data at the highest available speed of the microphotometer carriage, 25 mm/min. Since data can be taken at 83 points/sec, we considered the possibility that the 1800 might be occupied with a higher priority job during the 12 msec. interval and one or more data might not be read. Since the 12 bits from the A-D converter are placed in a 16 bit word, it was decided to record the occurrence of a missed datum in the four high order bits of the data word. Therefore, if the ECO enable fails to be returned within the 12 msec. interval, no commands can go to the sample and hold amplifier and the A-D converter. Instead a pulse is sent into the binary counter. Up to fifteen successive readings can be missed before interrupt #4 causes the job to abort. If an ECO enable is sent back before the job is aborted, the next datum is read into the data file along with the count of points missed and the binary counter is reset to 0. Thus the data is lost but not our position on the plate, and the program will update all succeeding positions. A test of the necessity of this device has proven inconclusive since 48,000 data were recorded in a ten minute scan while the x-ray scattering experiment was running and the 1800 was compiling a program and operating the typewriter. No data were missed. It is possible, operating on interrupts, to run the microphotometer carriage at five times the present maximum speed. This contraction of the time interval for servicing the interrupt plus the activation of additional experiments may well require frequent use of the missed data record.

Two 300 word data buffers are reserved in core for the temporary storage of data and 160 sectors of 320 words each are reserved on disk for the permanent data file. Twenty words of each sector are for identification or such other information as the operator wishes. When the first buffer is filled the second is brought into use while the first is emptied to the disk.

The lamp in the Jarrell-Ash 23-100 is A.C. powered and it was observed that some noise in the recorded data could be traced to the 120 cycle ripple, so a regulated d.c. supply was built. Additional filtering was added to the output stage of the photomultiplier amplifier. The cathodes of the 12AU7 are 70 volts above ground, so a simple differential amplifier was constructed to shift the level to near ground. These modifications are shown in fig. 3.

A portion of a mass spectrum recorded by this system and plotted from the digital data is shown in fig. 4. This represents 1200 data points taken at a speed of 25mm/min in 14.4 sec. This plotted data compares very well with the data recorded on the chart recorder as to noise, resolution and precision. Replicate runs taken at the same speed and at one-fifth this speed showed no significant differences.

DATA REDUCTION

It is assumed in the following discussion that there is stored in the computer a data file of all the natural isotopes of all the elements, their real masses, and their abundances. Elements, of course, are identified by their Z number to permit them to be referred to via the keyboard.

At the present time, our philosophy regarding the reduction of the photographic plate data is that the human operator is the best judge and final arbiter as to the presence or absence of impurity elements. It is possible to write a program which will duplicate-----to a limited degree-----the human reasoning process. But such a program will surely prove to be long and complicated.

The information mentioned previously to be read in via the ten digit keyboard will consist in part of a list of elements visually detected. In general it will be necessary to specify which charge state is to be used and also which isotopes are not to be used.

When the 48,000 data from one exposure are stored on disk it is desirable to reduce these data by searching first for the lines and second for the lines relevant to the analysis. The first program, FIND, is operational. It employs the criteria that the first and second derivatives of the smoothed data exceed a threshhold value, that the line have a certain minimum width, and that the first and second derivatives return to less than a second threshhold value before a peak is confirmed. The position of the minimum transmittance, the background immediately preceding and following the peak, and the transmittance at all intervening points are stored. This program works for lines as weak as 2-3% transmittance change.

In order to identify the lines pertinent to the analysis, it is necessary to establish a precise dispersion relationship for the photographic plate being measured. In order to determine the form of this relationship, the precise positions of sixty-eight lines were determined using the linear encoder and these positions along with the real values of m/e were tabulated. Least squares fits to the position, x, versus $(m/e)^{1/2}$, M, were determined for the first through the fifth order polynomials. The results are shown in Table 1. From these results it is obvious that a cubic in $(m/e)^{1/2}$ is necessary and sufficient to determine a satisfactory dispersion relationship. By "satisfactory" is meant that lines are of the order of 50 wide at half height and an RMS error of 5 is equivalent to a distance of 12.5 u.

A program which selected subsets of four points spaced at least one inch apart from the sixty eight demonstrated that by using most sets of four sharp, unambiguously identified and adequately spaced lines. A suitable dispersion relationship can be determined. Therefore, it is expected that four lines identified as to isotope and charge state along with the position on the linear encoder display will be read in via the keyboard and the dispersion relationship established.

Program IDENT can then be applied using the dispersion relationship and the list of the isotopes of the elements visually detected to select those lines from the data file compiled by FIND pertinent to the analysis. At this point, the present data analysis program, MS7DR, can take over to calculate the concentrations and prepare the report.

$$X = -18620. + 7219\ M \qquad M = (m/e)^{1/2}$$
RMS Error = 89.07

$$X = -19120. + 7349\ M - 7.007\ M^2$$
RMS Error = 38.96

$$X = -19730. + 7586.M - 34.34\ M^2 + .96M^3$$
RMS Error = 5.55

$$X = -19790. + 7620M - 40.93\ M^2 + 1.47\ M^3 - .014M^4$$
RMS Error = 5.36

$$X = -20090. + 7834.M - 96.92\ M^2 + 8.31\ M^3 - .407M^4 + .0086M^5$$
RMS Error = 4.26

TABLE 1

It has been shown that with the aid of a time sharing computer, the available microphotometer and a modest expenditure of money it is possible to automatically acquire and reduce data from the photoplate of a spark source mass spectrograph. We also now have the capability to handle much more data such as integrating the exposure profile of a line, and summing the contribution of all charge states.

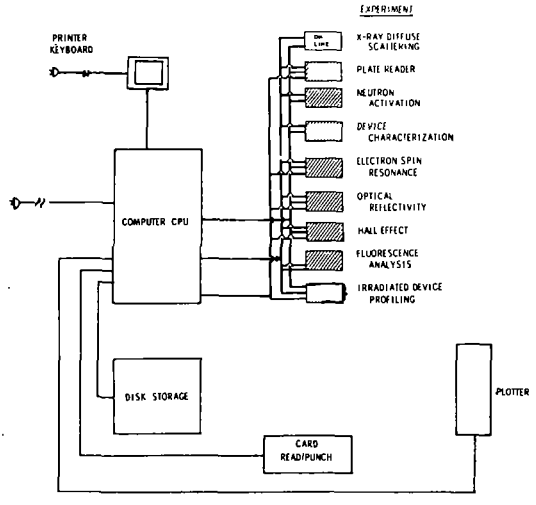

FIG. 1 Laboratory Automation Configuration

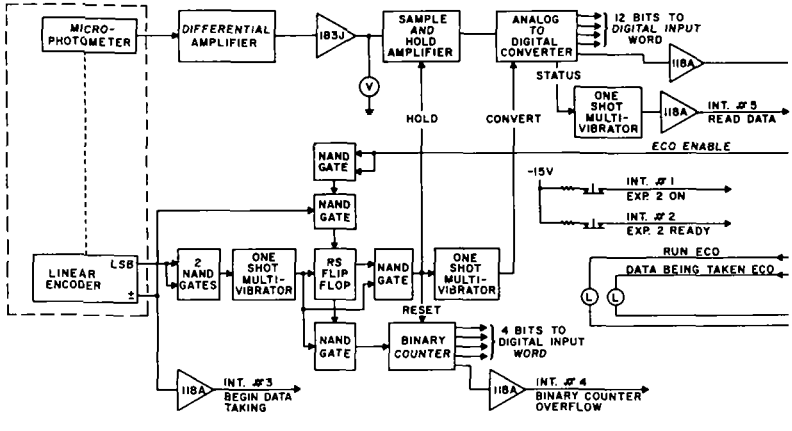

Fig.2 Plate Reader Interface

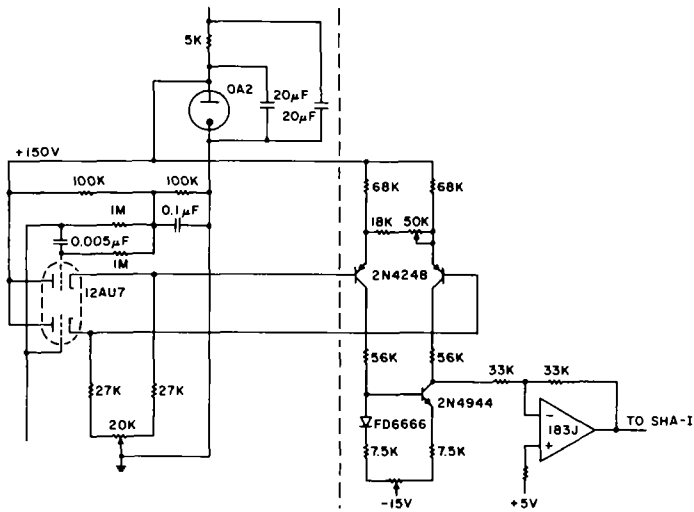

Fig. 3 Difference Amplifier

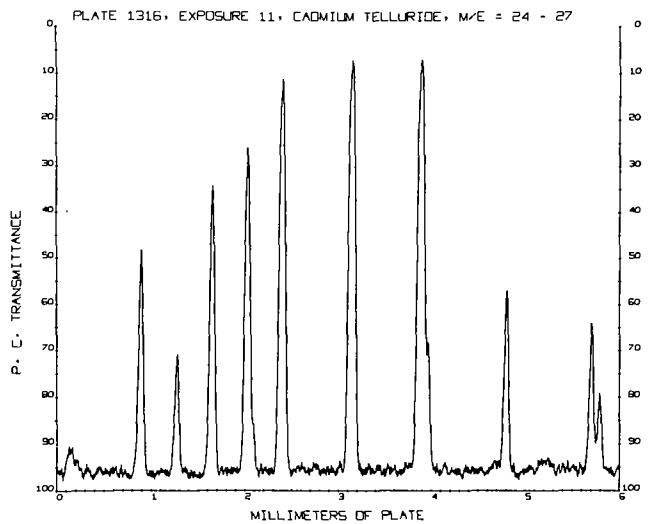

Fig. 4 Digital Plot of Mass Spectrum

HIGH RESOLUTION GC-MS
PHOTOGRAPHIC VERSUS ELECTRIC RECORDING

K. Habfast, K. H. Maurer and G. Hoffmann
VARIAN MAT GMBH, Bremen, Germany

1. Introduction

Six years ago we reported on the theoretical comparison of the sensitivity of photographic and electric recording in high resolution mass spectroscopy. (1)

With this paper we give the results of an experimental comparison of both recording techniques in a special application. The experiments have been executed under standardized conditions, all parts of the experimental procedure (sample, sample introduction, ion source, ion optic etc.) being exactly the same except the recording medium. It was the aim of these experiments to determine the detection limit and the achievable precision in mass determination for both techniques in order to decide in which cases the more elaborate and more costly photographic recording technique is to be prefered over the faster - concerning the data output - and cheaper electric recording technique.

Our earlier paper (1) indicated, that photographic recording should be more successful in all cases where a low amount of sample is available for only a short time. These are conditions typical for GC-MS-techniques especially using capillary columns. Thus we did all our measurements with sample-introduction via a gas chromatograph.

2. Experimental

The measurements have been made using a double focusing Mattauch-Herzog instrument, the VARIAN MAT 731, equipped for both electric and photographic recording (fig. 1).

The mass spectrometer was connected "on-line" to a SpectroSystem 100, consisting of a 16 bit Varian 620-computer, an interface, magnetic tape, display, plotter and teletype. The same data system also was connected on-line to a precision comparator (2), type Leitz. Sample introduction was via a Varian 1400 GC, using a glass capillary column (3) coupled directly to the ion source without molecular separator (4). Flow rate through the column was 1.5 ml/min. The sample used for the comparison was methylstearate, resulting in a GC peak of about 10 sec peak width.

Sensitivity of the mass spectrometer for the molecular peak of methylstearate was under these conditions:

$3{,}5 \times 10^{-12}$ Coul / μg at R = 15.000 (10 % valley) and
7×10^{-11} Coul / μg at R = 1.000 (10 % valley)

3. Results and Discussion

A typical GC-diagram, recorded via the total ion current detector, is shown in fig. 2, for 100 ng and 2 ng, injected into the GC.

Fig. 3 shows a part of a low resolution mass spectrum of 2 ng total sample amount injected. The signal to noise ratio of this spectrum is better than 50 : 1 for the molecular peak.

In fig. 4 we can see a series of high resolution spectra on photographic plate, showing a resolution of 40.000, where the molecular peak can be clearly detected with 5 ng of methylstearate injected into the GC, the M + 1 peak can be detected with 25 ng injected. With 200 ng injected, also the M + 2 peak is clearly above the detection limit. The dynamic range is in this case 1 : 125. For larger sample amounts one can record 2 or 3 mass spectra from a 10 sec GC-Peak (using the remote controlled photoplate carrier system) to prevent overexposed lines and consequently to extend the dynamic range of the mass spectrum.

From these measurements one can take the first statement for comparison of both recording modes:

Limits of detection for fast scanning (3 sec/dec) electric recording under low resolution operating conditions (R = 1.000) and photographic recording under high resolution operating condition (R = 40.000) are within the same order of magnitude (measured in amount of sample consumed).

It is the main purpose of high resolution to get the elemental composition of the molecular ion and of the fragment peaks. Thus the achievable accuracy of mass measurement is of utmost importance.

In electrical recording it is common practice to make a number of repetitive scans in order to improve precision and accuracy. This, however, is not possible under GC-conditions. Thus, all results presented are taken from a single scan.

For electrical recording the following tests have been run:

a) For constant amount of sample we have varied resolution between 5.000 and 15.000 and scan speed between 8 s/dec and 24 s/dec.

b) For a number of sets for resolution and scan speed we have varied the amount of sample between 50 ng and 750 ng. The mass of all peaks in the mass range between 100 and 300, the elemental composition of which is known, have been compared with the measured mass and a standard deviation has been calculated. All peaks which are unresolved doublets due to ^{13}C, have not been considered.

Fig. 5 shows the standard deviation of mass measurement in millimass units at a resolution of 5.000 for different scan speeds and different amount of sample. In brackets we have denoted the number of peaks, above the limit of detection. Limit of detection in this runs was a peak intensity of 1×10^{-14} Amp. or 5×10^{-15} Amp. which corresponds to about 50 or 25 ions per peak for a scan speed at 8 s/dec. We have tried to cover a mass range as big as possible. This means, that a lot of the peaks which are recorded during the low sample flow regions of the GC-Peak have intensities just above limit of detection. These peaks contribute strongly to the higher standard deviation of mass measurement as compared to results with electric recording where the sample flow is constant.

In Fig. 6 we present our results for different values of resolution and scan speed. Again the number of peaks above limit of detection is denoted in brackets. The number of ions per peak is constant for a given sample amount.

For electrical recording under these special GC-MS conditions the following conclusions can be made:

From Fig. 5:

a) Mean accuracy of mass measurement for single scan is about 2 mu for all peaks with more than 50 ions.

b) Mean accuracy does not depend significantly on scan speed nor on the amount of sample.

c) The number of peaks which can be detected, depends strongly on the amount of sample.

From Fig. 6:

a) Mean accuracy of mass measurement is slightly but not very much better for higher resolution, but does not depend on the amount of sample.

b) For two runs, which differ in resolution and in scan speed by a factor of 3, the amount of sample must be raised by about a factor 10, in order to get the same number of peaks above limit of detection because of the smaller mass range, which can be covered and the more than proportional sensitivity loss.

There is no doubt, that for the purpose of structure elucidation, the number of peaks, which can be detected, is as important as the accuracy of the mass measurement. So one has to conclude: For electric recording the loss of information due to loss of peaks at higher resolution cannot be compensated by the slight increase in accuracy of mass measurement. In other words: In electrical recording using very short recording times the resolution to be used should be as low as tolerable.

For our measurements with photographic recording we have used two types of plates: Ilford Q 2 and Ionomet. Due to a much better background (5) (6), the dynamic range of peaks, which could be detected on Ionomet plates, was about six times higher than on the Q 2-plates. Also the accuracy of mass measurements is significantly better on Ionomet plates due to a better line shape. The results of the measurement are presented on the left side of fig. 7.

These results show:

a) Accuracy of mass measurement of Ionomet-plates is better than 1.5 mu and does not depend on the amount of sample.

b) The number of peaks above limit of detection does not depend strongly on the amount of sample in this range we have investigated.

In the same fig. we again have noted some of our results for electric recording, in order to compare them with the photographic results.

The comparison clearly allows the following conclusions:

For recording times of less than 10 sec, necessary in GC-MS applications using capillary columns, photographic recording allows more accurate mass determinations in a larger mass range with 4 times higher resolution and a factor of 20 smaller sample amounts compared to electric recording.
For injected sample amounts of less than 20 ng and a resolution up to 40.000, mass determinations with an accuracy of 1 - 2 mu for a useful number of peaks (dynamic range) can only be achieved with photographic recording.

4. References

1) K. Habfast and K. H. Maurer, 17th Annual Conference on Mass Spectrometry and Allied Topics 1966, Dallas, Texas

2) K. Heinicke, Z. Instr. 74 (1966)

3) K. Grob, Helvetia Chemica Acta 51 (1968)

4) P. Schulze and K. H. Kaiser, Chromatographia 4 (1971)

5) J. I. Masters, Nature 233 (1969)

6) C. Hignite and K. Biemann, Organic Mass Spectrometry 2 (1969)

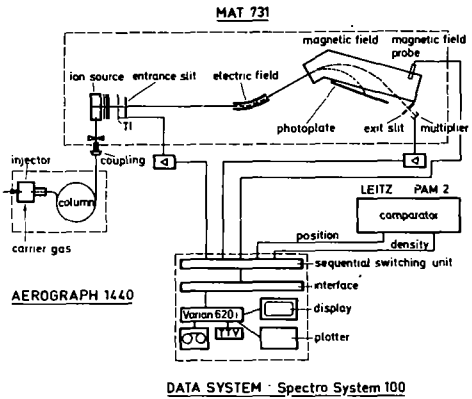

Fig. 1 : Schematic of the measuring system

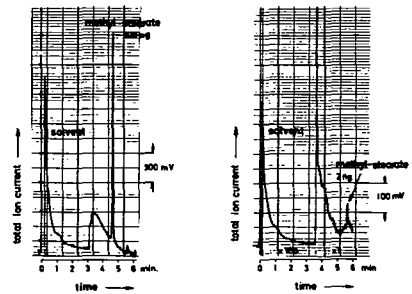

Fig. 2 : GC-diagram, recorded via total ion current monitor

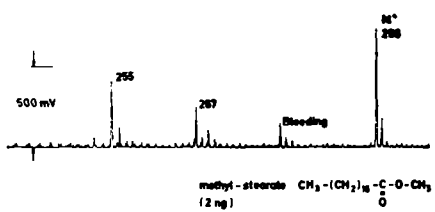

Fig. 3 : Low resolution spectrum, 2 ng sample amount injected

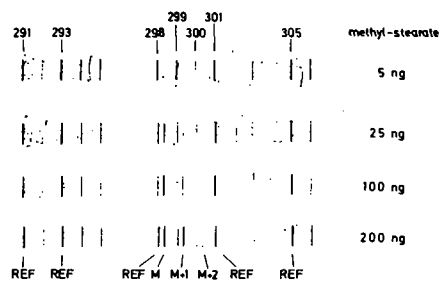

Fig. 4 : High resolution spectrum, photographic recording

STANDARD DEVIATION (MU)

No. of Peaks

R=5000 (10% Valley); Single Scan

Amount of Sample (ng)	8 Sec/Dec		12 Sec/Dec		16 Sec/Dec		24 Sec/Dec	
	A	B	A	B	A	B	A	B
50	1.2 (1)	3.0 (2)	1.2 (1)	3.0 (2)	1.8 (4)	2.7 (7)	2.1 (1)	4.1 (3)
100	2.3 (5)	3.0 (8)	2.4 (2)	4.0 (5)	2.7 (5)	2.8 (8)	2.2 (1)	3.7 (14)
200	3.1 (10)	3.3 (14)	1.7 (4)	2.7 (9)	1.8 (9)	3.0 (11)	1.4 (3)	3.5 (6)
400	2.5 (14)	2.5 (16)	2.2 (6)	2.9 (10)	2.0 (10)	2.6 (13)	2.3 (5)	2.5 (9)
750	1.9 (14)	2.0 (18)	2.0 (10)	2.4 (14)	2.2 (14)	2.3 (16)	2.0 (9)	2.3 (13)
Mass Range	90-300		110-300		100-300		140-300	

A. Minimum Peak Intensity 1×10^{-14}A

B. Minimum Peak Intensity 0.5×10^{-14}A

Fig. 5

STANDARD DEVIATION (MU)

No. of Peaks

Single Scan, R (10% Valley)

Amount of Sample (ng)	8 Sec/Dec R=5000		12 Sec/Dec R=7500		16 Sec/Dec R=10,000		24 Sec/Dec R=15,000	
	A	B	A	B	A	B	A	B
50	1.2 (1)	3.0 (2)	-	-	-	-	-	-
100	2.3 (5)	3.0 (8)	1.8 (2)	2.5 (4)	-	1.6 (1)	-	-
200	3.1 (10)	3.3 (14)	2.0 (2)	2.5 (6)	1.4 (1)	3.0 (2)	-	3.0 (1)
400	2.5 (14)	2.5 (16)	2.4 (5)	2.8 (8)	2.0 (2)	3.1 (4)	-	2.3 (2)
750	1.9 (14)	2.0 (18)	2.3 (9)	2.6 (14)	1.9 (4)	2.6 (5)	1.0 (2)	2.4 (6)
Mass Range	90-300		110-300		130-300		140-300	

A. Minimum Peak Intensity 1×10^{-14}A

B. Minimum Peak Intensity 0.5×10^{-14}A

Fig. 6

STANDARD DEVIATION (MU)

No. of Peaks

Amount of Sample (ng)	Photographic Recording R=15,000-40,000		Electric Recording (Single Scan) R=5,000 8 Sec/Dec		R=10,000 16 Sec/Dec	
	Ilford-Q2	Ionomet	A	B	A	B
5	4.8 (4)	[2.0 (8)]	-	-	-	-
25	1.5 (9)	1.2 (16)	-	-	-	-
50	1.0 (10)	1.4 (19)	1.2 (1)	3.0 (2)	-	-
100	2.3 (16)	1.5 (21)	2.3 (5)	3.0 (8)	-	1.6 (1)
150	1.9 (19)	1.5 (23)				
200	2.7 (17)	1.9 (29)	3.1 (10)	3.3 (14)	1.4 (1)	3.0 (2)
400			2.5 (14)	2.5 (16)	2.0 (2)	3.1 (4)
750			1.9 (14)	2.0 (18)	1.9 (4)	2.6 (5)
Mass Range	90-300	50-300	90-300	90-300	130-300	130-300

A. Minimum peak intensity 1×10^{-14}A

B. Minimum peak intensity 0.5×10^{-14}A

Fig. 7

Processing of Mass Spectral Data by use of the Vector Analogy: Sensitivity Enhancement T4

by David Rosenthal and Joan T. Bursey
Research Triangle Institute
Research Triangle Park, North Carolina 27709

Automatic data acquisition of mass spectra is now accepted as a standard technique in gas chromatography - mass spectrometry (gc-ms) systems. By scanning the mass spectrometer in a repetitive manner during the course of a gas chromatographic run an immense amount of data is accumulated. We wish to report here on a method which makes use of these data in a manner so as to enhance the information which can be obtained from individual scans as well as to make certain properties present in the data available in a readily comprehended form.

The method involved invokes the analogy which exists between mass spectra and vectors. A low resolution mass spectrum can be thought of as being equivalent to a multidimensional vector, the intensity of each peak being equivalent to a distance along one of the mutually perpendicular axes in the vector space. A three dimensional analogy is shown in Figure 1.

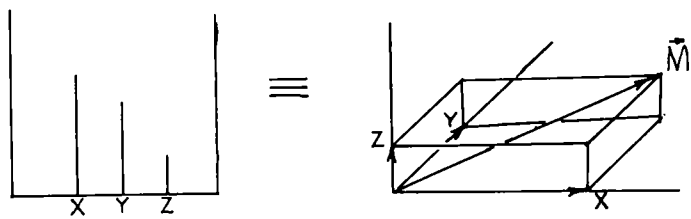

Figure 1

The mass spectrum M consisting of three peaks of mass x, y, and z is mathematically equivalent to the vector $\vec{M} = (I_x, I_y, I_z)$ where I is the intensity of the peak of the corresponding mass.

The present study has used this principle for the purpose of detecting the presence of a particular component in the effluent of a gc-ms system. In this case diminishing amounts of a standard solution of cholesane were analyzed by repetitive scanning of the magnet at 5 sec intervals. The spectra obtained were compared with a standard spectrum of cholestane making use of the following fundamental relationships. For the unknown spectrum $\vec{U} = (U_1, U_2 . . ., U_n)$ and the standard spectrum $\vec{S} = (S_1, S_2 . . ., S_n)$ the angle θ between the spectra is given by:

$$\theta = \cos^{-1} \frac{\sum_{i=1}^{n} U_i S_i}{\sqrt{\sum_{i=1}^{n} U_i \cdot \sum_{i=1}^{n} S_i}}$$

and the projection of $\vec{U}$ on $\vec{S}$ as

$$U_{proj} = \left|\vec{U}\right| \cos\theta$$

Plots of θ and U_{proj} vs spectrum number were made and inspected for minima and maxima respectively. The scan rate of 5 sec/spectrum was such that a gc peak was scanned six to eight times. This allowed signal averaging of adjacent points by smoothing. In the present instance a 3 point parabolic smoothing formula was applied to the data resulting in further filtering of noise.

1. Mass spectra are recorded using conventional scanning curcuity. No electronic accessories to vary the accelerating voltage (which also can result in severe mass discrimination effects) are needed.

2. There is a very high degree of selectivity resulting from a comparison of all of the peaks in the spectrum with a resulting sharp discrimination against components in the mixture which are not sought.

3. Signal to noise enhancement of 25:1 can be achieved which is comparable to that achievable by single or multiple ion monitoring.

4. It is not necessary to decide in advance which component in the mixture is to be searched for. Indeed it is easy to scan the data successively for a variety of components.

5. To the extent that the angle variations represent identity with the component sought, the projection of the effluent spectrum on the component gives a quantitative estimate of that component.

The data were processed first by a small on-line computer where data acquisition and mass conversion were carried out. Data transfer was achieved by means of a 9-track compatible digital tape unit to an IBM 370/165 in which the bulk of the data processing was completed. Programs were written in PL/1 and Fortran IV. This work was supported by the NIH in the form of a grant Contract No. RR-00330-05 from the Biotechnology Research Resources Branch and by NIGMS Contract No. PH-43-NIGMS-65-1057.

INVESTIGATION OF LASER-INDUCED VAPORIZATION PROCESSES BY A NEW MASS SPECTROMETER SYSTEM*

T6

Kenneth A. Lincoln

Ames Research Center, NASA, Moffett Field, CA 94035

Instrumentation

The laser-mass spectrometer system described here was designed, primarily for the diagnostics of laser effects on materials, and it represents an advancement in similar instrumentation reported earlier.[1] As before, a time-of-flight mass spectrometer was selected to permit simultaneous measurement of several vapor species during the brief interval of the laser-induced vapor pulse, thereby permitting an in situ analysis during the vaporization process. The techniques for time-resolving individual mass peaks and for Z-axis brightening the mass peaks in the scope displays of the total spectra to enhance photographing are the same as described previously[1] and are incorporated in this instrument. The more salient innovations introduced into the present system are briefly described as follows:

1. The laser-induced vaporizations are effected inside a large vacuum chamber rather than in the ion source of the mass spectrometer. This provides for a greater expansion volume for the vapors and permits exposing materials to incident beams of larger cross-sectional areas. The position of the Korad Model K5Q laser and the beam-directing optics are shown in Figs. 1 and 2; the laser may be operated in either the burst or Q-switched mode. The baffle provides moderate differential pumping, but it can be removed when an open ion source is preferred.

2. The mass spectrometer utilizes a nude ion source which is coupled into one end of the vacuum chamber. The basic instrument is a Bendix Model MA-2 time-of-flight mass spectrometer with a 5-grid (including backing grid) ion source; Figs. 1 and 2 show its positioning relative to the vacuum chamber, sample holder, and laser beam.

3. All vapors enter the ion source on-axis (colinear with the flight tube of the mass spectrometer). Thus gases eminating from the surface of the sample enter the ion source via the backing plate grid; this obviates the transverse velocity components present in the older system where the vapors enter the ion source at right angles to the spectrometer flight path. The new configuration also permits ions, thermally generated at the sample surface, to travel these extended distances directly to the mass spectrometer without being deflected away by the electric fields present near the rear two ion grids.[2] On occasions when only neutrals are to be admitted into the mass spectrometer, these ions can be deflected away by the application of a voltage to an electrode (not shown) located in front of and to the side of the backing grid.

4. Samples of solid materials are introduced via the vacuum lock and remotely positioned along the axis of the vacuum chamber for vaporization at distances from several centimeters to 1 meter from the ion source. This longer distance improves the capability of the instrument for measuring the thermal velocities of individual mass species.[2]

5. The mass spectrometer can be gated on and off for specific time intervals. This modification was achieved by substituting for the master oscillator in the original Bendix equipment a pulse generator which can be triggered, gated, or free run. It also introduced the capabilities for varying the repetition rate of the instrument and varying the duration of the electron beam pulse in the ion source. The gating feature is very useful for setting up the instrumentation and making adjustments prior to employing it on transient events. Moreover, in much of this work it has been used to turn the spectrometer "on" only during the interval in which the short-lived species are being generated; this helps to truncate the persistent effects of the non-condensible, long-lasting gases which are often produced at the same time.

6. The total ion current (in the mass spectrometer) resulting from each vapor pulse is time-integrated and recorded along with the concomitant mass spectra; this provides a quantitative basis for comparing the vaporization characteristics of various materials subjected to identical irradiance. The technique for obtaining total ion current and mass spectra simultaneously from the scope anode in the multiplier has been delineated previously[1] and is included in the present instrumentation. Fig. 3 shows the added feature of integrating the total ion current (TIC), storing it in the memory of the Biomation Model 610 Transient Recorder, and subsequently displaying it on the scope. In practice, the laser (or gate pulse) triggers the transient recorder which records the integrated value of the TIC as a function of time and then immediately displays this curve continuously on a monitoring scope. Simultaneously, the mass spectra appear on the output scope and are photographed during the gated interval. The output from the Transient Recorder can then be switched to this scope to be recorded on the same photo to give a single record of integrated TIC plus mass spectrum for each laser-induced vapor pulse. Alternately, several individual mass peak intensities vs. time can be stored in additional transient recorder channels and subsequently be displayed as desired.

Application

The instrumentation and techniques described here have had their initial application in graphitic heat-shield technology for planetary entry. This has included attempts to correlate the vaporization characteristics of a number of graphite-type materials with their ablation performance. For this reason the common practice of focusing the laser beam to a small point on a sample surface has been avoided in lieu of exposing much larger areas at lower power densities (approximately 100–200 kW/cm^2). In this work the front surface of the specimen is essentially enveloped by the laser beam to create nominally a one-dimensional heat flow model at the surface of the material.

Initial conclusions on the performance of the system result from exposing a variety of graphitic materials to the 1.06 μ laser in burst mode (nominally 0.5 ms pulse width) at a sample loading of about 60 Joules/cm^2. The TOF mass spectra exhibit no perceptible line broadening or degradation in resolution due to the thermal velocities of the vapors and the on-axis configuration. Although the resolution of ions generated external to the ion source is typically poorer than those produced internally by the electron beam, the resolution of thermally produced ions by laser heating proved to be quite adequate. In fact, the sensitivity of the spectrometer to these ions was found to be very high, and this appears to be an effective method for detecting small amounts of some metallic impurities which were found in some of the graphites.

* The complete paper will be submitted to the International Journal of Mass Spectrometry and Ion Physics for publication.

The value of integrated TIC is a convenient and instantaneous index of the amount of vaporization produced by each laser burst. It has been found that graphite surfaces must be first cleaned off by a succession of laser shots before any meaningful spectra can be recorded; therefore, it is our practice to fire the laser at the same surface at 10 to 15 sec. intervals while monitoring the integrated TIC and laser energy/pulse until these reach steady-state values before any spectra are recorded. Mass spectra of the graphitic materials all show that C_3 is the dominant vapor product with only very small amounts of C_1 and C_2 present at these heat loadings, and this may be a very important consideration with respect to graphitic heat-shield technology.

References

1. Lincoln, K. A., J. Mass Spectrometry and Ion Physics, 2, 75–83 (1969).
2. Lincoln, K. A. and Wodley, F. A., presented at the Seventeenth Annual Conference on Mass Spectrometry and Allied Topics, Dallas, Texas, May 1969.

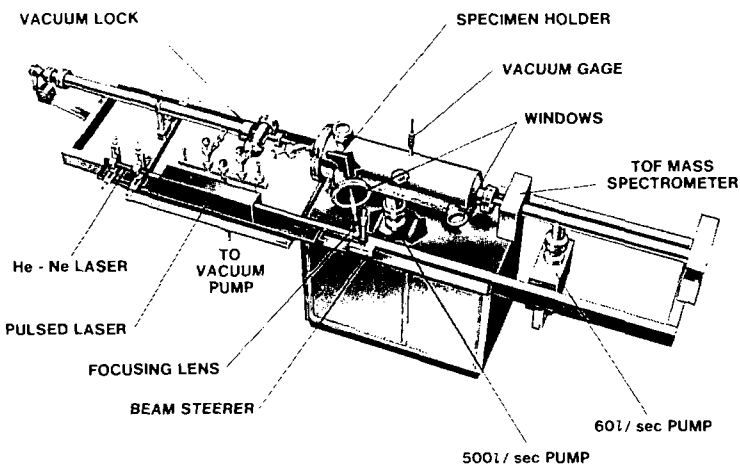

Fig. 1. Laser vaporization-mass spectrometer system.

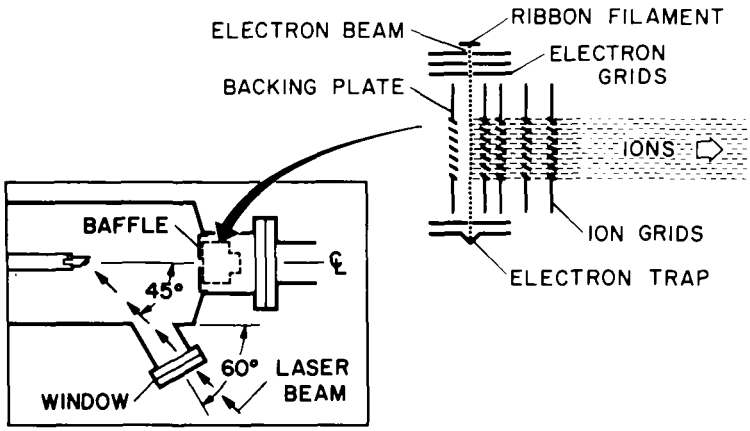

Fig. 2. Mass spectrometer ion source.

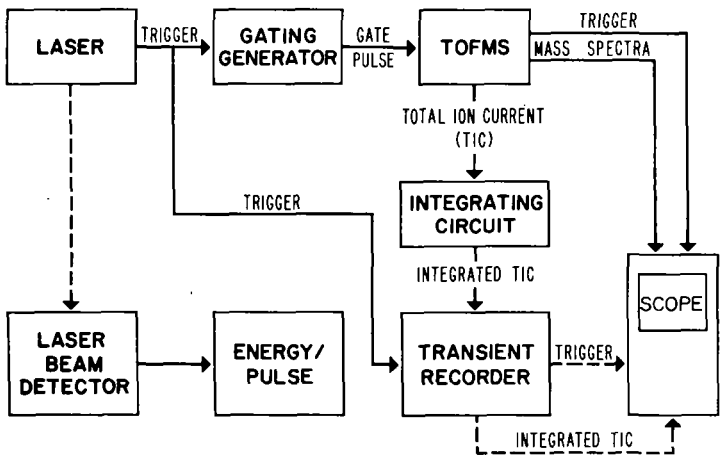

Fig. 3. Signal flow chart for mass spectrometer–laser system.

THE MASS SPECTRA OF ω-AMINO ACID DERIVATIVES.

I. The Role of ω-Activation in Production of Ions upon Electron Impact

S. Osman, P. Hoagland, and C. J. Dooley
Eastern Regional Research Laboratory*
Philadelphia, Pennsylvania 19118

The mass spectra of a series of derivatives of ω-amino acids ranging from 3-aminopropionic to 6-aminohexanoic acid were determined. In contrast to derivatives of α-amino acids, a significant portion of the ion current is the product of the interaction of the functional groups. The extent of the interaction is a function of the substitution on the amino group.

The fragmentation of N-trifluoroacetyl-ω-aminovaleric acid was studied extensively. A partial scheme for the fragmentation of the unlabelled compound is shown below.

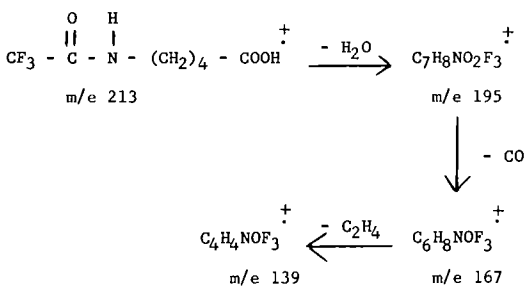

Deuterium labelling of the alkyl chain indicates that the ω hydrogen is lost in the initial fragmentation step, i.e., the loss of H_2O from the molecular ion. The sequence of subsequent fragmentation steps and empirical formulae of the ions produced were determined by metastable scanning and high resolution mass spectrometry respectively. Similar fragmentation pathways are apparently operative for the TFA and phthaloyl derivatives of the other amino acids studied. For the acetyl and benzoyl derivatives bifunctional interaction does not seem significant in the resultant fragmentation pattern. In Table 1 we show a comparison of the ion concentration formed by a simple β cleavage to the nitrogen with the intensities of ions formed by the sequence shown above.

Table 1

Selected peak intensities from the spectra of ω-aminovaleric acid derivatives

Derivative	[M]	[M-18]	[M-46]	[M-74]	[N-C$\}^{+}$C]
TFA	-	50	15	40	100
Phthaloyl	30	30	8	30	100
Acetyl	6	2	2	5	20
Benzoyl	25	-	-	-	<1

It is apparent that there is a direct correlation between these values. This is not unexpected since both processes involve β cleavage. Since the C-5 hydrogen is lost as part of neutral water this carbon-hydrogen cleavage process competes favorably with the expected carbon-carbon cleavage process.

A more detailed account of this work is being prepared for publication.

---

* Eastern Marketing and Nutrition Research Division, Agricultural Research Service, U. S. Department of Agriculture.

Author Index

Author Index

Author Index

Author Index

ASTM COMMITTEES AND ASTM E-14 SUBCOMMITTEES

ASMS Com. II - "Fundamental Aspects", R. S. Berry, Department of Chemistry, University of Chicago, Chicago, Illinois 60637

Joint Com. III - "Computer and Data Processing", E. M. Emery, Colgate-Palmolive Co., 909 River Road, Piscataway, New Jersey 08854

ASTM E-14 Subcom. IV - "Data and Information Problems", W. B. Askew, Dupont Experimental Station, Wilmington, Delaware 19898

ASMS Com. V - "New Instruments and Techniques", H. J. Svec, Department of Chemistry, Iowa State University, Ames, Iowa 50010

Joint Com. VI - "Biological Applications", J. A. McCloskey, Institute for Lipid Research, Baylor College of Medicine, Houston, Texas 77025, and J. R. Roboz, Mt. Sinai School of Medicine, New York, New York

ASMS Com. VII - "Study of Solids", F. D. Leipziger, Kennicott Copper Co., Ledgemont Laboratory, Lexington, Mass. 02173

ASMS Com. VIII - "High Resolution Studies", D. C. DeJongh, Case Postale 6128, l'Universite-de Montreal, Montreal, Quebec, Canada 101

ASMS Com. IX - "Aids to Education", J. G. Dillard, Chemistry Department, Virginia Polytechnic Institute, Blacksburg, Virginia 24061

ASTM E-14 Subcom. X - "Definitions and Terms", G. L. Cook, Laramie Energy Research Center, Box 3395, University Station, Laramie, Wyoming 82070

Joint Com. XI - "Evaluation of Critical Data for Health Sciences", A. G. Sharkey, Jr., U. S. Bureau of Mines, 4800 Forbes Avenue, Pittsburgh, Pennsylvania 15213

ASMS Committee II. Fundamental Aspects

Due to conflicting conferences, the Chairman of the Committee on Fundamental Aspects (Dr. R. S. Berry) was unable to attend and asked this correspondent to chair the session.

Dr. Frank Field, the Vice-President in charge of the program, began the meeting by explaining to the attendees why there was no symposium devoted to fundamental aspects at this (1972) conference on ASMS. In brief, there are too many committees within ASMS competing for program time, there were about 200 contributed papers, some sessions had to be conducted as three parallel ones. Dr. Field suggested that the Fundamental Aspects Committee reappraise its future role.

Various suggestions were thereupon made by the participants, with a consensus focusing on:

1) continuing the practice of having the Fundamental Aspects Committee make suggestions regarding the appropriate topics for forthcoming Fundamental Aspects Symposia;

2) employing more parallel sessions, if necessary;

3) utilizing the afternoon devoted to other workshops as a workshop for the Fundamental Aspects Committee. This would be especially helpful during those years when ASMS was unable to conduct a Fundamental Aspects Symposium, because of scheduling pressures from competing committees. The exact format for such a Fundamental Aspects Workshop is not yet clear, but presumably would involve informal reports on some of the topics of current interest, the agenda and correspondence being handled by the Fundamental Aspects Committee chairman.

The remainder of the meeting was devoted to suggestions for future symposia. Ten topics were proffered, and their relative interest, as determined by balloting of the assembled group, is listed below.

		Relative interest
1.	Coincidence measurements of electrons and ions during ionization	26
2.	Photodissociation of ions	25
3.	Laser photodetachment	18
4.	Mechanism of charge exchange, at low energy	12
5.	Formation of ions in selected states	8
6.	A study of Rydberg states	8
7.	A study of ion clusters either by ionizing neutral clusters or forming clusters after the initial ionization	7

8.	Angular distribution and angular correlation of electrons in ionization and dissociation processes	5
9.	Ionization of liquids - with particular emphasis on the carbonium ion	5
10.	A lecture on pertinent aspects of molecular orbital theory	3

The chairman would presumably undertake to find appropriate speakers for the two or three most favored topics.

Respectfully submitted,

Joseph Berkowitz

JOINT COMMITTEE III

"Computer and Data Processing"

ASMS Committee and ASTM E-14 Subcommittee

1972 Meeting in Dallas

It is the purpose of this joint committee to promote and provide the means for exchange of computer and data processing techniques in mass spectrometry.

For the benefit of newcomers, and to refresh all, a brief review of the committee's progress was presented. In essence, the interest was, and continues to be high, and the contributions of computer programs, low. The committee request of documentation to accompany any program was among the many factors discussed as stumbling blocks. The pros and cons of all aspects of exchange were discussed.

Action in the form of a questionnaire was purposed as one means of learning of current disclosable progress in this area. (A draft of such a questionnaire was composed by several committee members before week's end.) It will provide basic information on instruments, interfaces and programs.

Liaison with the ASTM Committee on Computerized Laboratory Systems will be continued. Hopefully next year we will have a detailed status report on their progress.

Several of the attendees volunteered to send their thoughts toward a workshop on computer and data processing. Every effort will be made to transform these into a useful 1973 event. Toward this end, all ideas and recommendations are solicited.

E. M. Emery, Chairman
Colgate-Palmolive Company
Research and Development Department
909 River Road
Piscataway, N. J. 08854
Phone: (201) 463-1212 Ext. 375
(201) 246-0754

Mynard C. Hamming
Continental Oil Company
Research and Development Department
Ponca City, Oklahoma 74601
Phone: (405) 762-3456 Ext. 4741
(405) 764-4190

J. Holz
Digital Equipment Corporation
146 Main Street
Maynard, Massachusetts 01754
Phone: (617 897-5111 Ext. 2265

F. W. Karasek
University of Waterloo
Department of Chemistry
Waterloo, Ontario
Canada
Phone: (519) 744-6111 Ext. 3423

P. R. Kennicott
General Electric Company
Box 8
Schenectady, N. Y. 12301
Phone: (518) 346-8771 Ext. 6131
(518) 399-4567

G. R. Sparrow
Analytical Research and Services
3M Company
Central Research Laboratories
P. O. Box 3221
St. Paul, Minnesota 55101

J. Rogers Woolson
RCA Laboratories
David Sarnoff Research Center
Princeton, N. J. 08540
Phone: (609) 452-2700 Ext. 2858

ASTM E-14 SUBCOMMITTEE IV - DATA AND INFORMATION PROBLEMS

Chairman: W. B. Askew (E. I. DuPont, Wilmington, Delaware 19898)
Secretary: J. F. Paulson (Sun Oil, Marcus Hook, Pa. 19061)

Subcommittee IV met at 5:00 PM on Tuesday, June 6, 1972. D. M. Schoengold (Sun Oil) was acting secretary in absence of J. F. Paulson. Meeting was conducted by W. B. Askew. Approximately 90 persons attended the meeting. Results of the survey sent out in March, 1972 were given. About 100 returns were received and 90% were in favor of reactivating the uncertified spectrum collection. 2500-3000 spectra have been promised in next six months. 60% prefer the sheet format, 25% the book format and 15% a computer tape format. The distribution of the spectra including an index will be handled by ASTM in sheet and book form. Complete spectra on full tape form will be available through MSDC. Data will also be included in 2nd Editions of the Aldermaston MSDC Eight Peak Index and the AMD-11 Index.

The meeting was opened to questions from the floor. One question asked was whether all types of spectra (EI, FI, CI, negative ion) were wanted. The answer was yes. The vote to re-establishing the uncertified collection was essentially unanimous (1 negative vote).

The rest of the meeting was devoted to a discussion of ideas for revision of the MSDC 8-peak index for the 2nd Edition next year with W. M. Scott of the MSDC. Suggestions included production of the index on microfilm or some other reduced format, inclusion of CI and FI spectra and possible elimination of parts of the index to save space. Questions on the MSDC index will be included in a July mailing by subcommittee IV calling for spectra.

Committee V, New Instruments and Techniques

American Society for Mass Spectrometry

Chairman, Harry J. Svec

Committee V met from 1:30 to 3:30 P.M. in the North Ballroom, Sheraton Dallas Hotel, on June 8, 1972 in Dallas, Texas. About 100 ASMS members were on hand to listen to and take part in a discussion of Plasma Chromatography. The topic was discussed by a panel organized by Frank W. Karasek, Dept. of Chemistry, University of Waterloo, Waterloo, Ontario. The program consisted of semi-formal presentations as follows:

Frank W. Karasek (Univ. of Waterloo)	Introduction to Plasma Chromatography — an outline of its scope and its analytical potential
Martin J. Cohen (Franklin GNO Corp., West Palm Beach, Fla.)	The instrument and its capabilities
Gary W. Griffin (Dept. of Chem., Louisiana State Univ., New Orleans, La.)	Work with the PC-MS combination unit at Baylor Univ.
FWK, MJC, GWG	Questions and Answers

Chairman, H. J. Svec moderated the question and answer period which followed the more formal presentations. There was a lively interest in the topic and the ensuing discussion brought to light the limitations of the technique as well as areas where more research is needed.

A short business meeting of the committee preceded and followed the program. Dr. J. P. Carrico, Bendix Research Laboratories, agreed to act as temporary secretary. In view of the election of H. J. Svec to the position of V.P. in charge of Programs for ASMS, the need for a new chairman for Committee V was cited. It is the prerogative of the new president Frank Field to appoint someone to this position and he has chosen Dr. F. W. Karasek for the job. Dr. Carrico will be the new permanent secretary.

The principal business of the day concerned a subject for the meeting in 1973. Suggestions were as follows:

1.	Carbon-13 research	G. W. Griffin
2.	Chemical Ionization	H. J. Svec
3.	UV lasers	
4.	Laser vaporization	J. P. Carrico
5.	Electrohydrodynamic ion sources	
6.	Ion cyclotron resonance	J. P. Carrico

Any other topics that might be considered should be given to the new chairman, Prof. F. W. Karasek.

COMMITTEE VI: BIOLOGICAL APPLICATIONS

Co-Chairmen: Dr. J.A. McCloskey, Institute for Lipid Research, Baylor College of Medicine, Houston, Texas 77025

Dr. J. Roboz, Mount Sinai School of Medicine, 11 East 100th Street, New York, N.Y. 10029

Secretary: Dr. W.J.A. VandenHeuvel, Merck Sharp & Dohme Research Laboratories, Rahway, N.J. 07065

Scope of the Committee: General area of biomedical applications of mass spectrometry, including: (a) new and improved analytical techniques using both low and high resolution mass spectrometry; (b) methods of sample preparation suited for biological applications; (c) dissemination of information concerning new developments in the area; (d) collection and distribution of drugs and "metabolites" as they become available (limited objective).

Minutes of Meeting, June 5, 1972. After circulating address lists to the 122 attendees, three areas of activity were discussed: lists of grants, distribution of mass spectra, and workshops during the 1973 meeting.

G.W. Milne presented two collections of grant topics. One list, compiled from data available at NIH, indicates NIH grants awarded on a given subject, and gives the name of the principal investigator plus the title of the grant. The grants are indexed by "key words" which will be listed in an upcoming newsletter to the members of the Committee. If a person is interested in a certain subject, he should pick an appropriate key word and request further information from Dr. G.W.Milne (National Institutes of Health, Bethesda, Md. 20014). This information is free of charge. The second list, from the Smithsonian Institution, cover all government and non-government funded grants (including some foreign grants), however, there is a charge of $75 for key word search. Again, interested parties should contact Bill Milne.

S.P. Markey reported that the first collection of mass spectra of drugs and drug metabolites (over 300 spectra) was distributed by mail to those who had requested them. The spectra will also be submitted to Aldermaston for inclusion in their collection of reference spectra. C.Costello of M.I.T. indicated that the spectra are listed alphabetically, both on the basis of compound name and generic name. There are two eight-peak indices, listed in descending order of intensities: one list starts with the base peak, the other with the ion of second greatest intensity. Each list also includes molecular weight, elemental composition, and source of the compound.

Considerable interest (Yes, 50; No, 2) was expressed in expanding and updating the compilation of the drug reference spectra; however, only six persons indicated willingness to contribute. When Bill Milne commented that "most toxic drugs are already on file", J. McCloskey indicated that the collection is not restricted to toxic compounds, and K. Bieman stated that major metabolites of frequently used drugs will be of continuing interest. D. Rosenthal expressed concern over the quality of samples and hence spectra submitted, and indicated an unwillingness to have spectra of impure samples sent to Aldermaston. J.McCloskey replied that high standards had not been set for the samples, so as to allow the inclusion of as great a number and variety of samples as possible. A representative from Aldermaston indicated that no standards are presently set for sample quality. K. Biemann recalled that the original intention was to send the spectra to Aldermaston, which should serve as the single central repository of reference spectra, although special sub-lists should be continued. If the supplier of spectra wished to keep his contribution informal (i.e., not submitted to Aldermaston), this should be indicated at the time of submission.

J.McCloskey and J.Roboz introduced the possibility of establishing spectra collections for other classes of biologically important compounds. Many persons (about 50) indicated interest, but only a few appeared willing to contribute. S. Markey offered to make available his spectra of endogeneous human urinary metabolites. J. McCloskey noted the need for organization to handle such undertakings, and informed the audience that ASMS has contributed $500 to the drug spectra collection; M.I.T. made no charge for computer time. McCloskey asked the membership whether ASMS should also finance the proposed collection; the vote was decisively in favor for the ASMS participation.

In private discussions, following the formal meeting, J.McCloskey and J. Roboz agreed with S.P. Markey that he will undertake the collection of spectra. In addition to his own collection, some 250-300 spectra will be contributed by Oak Ridge National Laboratory, and also a large number from M. Horning of Baylor College of Medicine. It is requested that interested people (both to contribute and receive) should write to Dr. S.P. Markey, JFK 3113 (2741), University of Colorado Medical Center, Denver, Colorado 80220. - During the Business Meeting of the Board of Directors of ASMS, a resolution was passed to indicate the willingness of ASMS to contribute financially to the collection and distribution of spectra of constituents of body fluids. - Progress on this project will be reported in periodic newsletters.

In a discussion on future workshops, the majority favored two workshops for 1973: clinical applications of mass spectrometry, and the use of stable isotopes in biomedical research. Dr. F. Field warned that because of the large number of papers, meetings, and workshops, any schedule must be considered tentative. Several persons indicated an interest in having plenary lectures on biological applications. Suggestions, both general and specific, should be communicated to the co-chairmen of Committee VI.

Workshop Program, Dallas Meeting. Based on the results of a poll sent to those on the mailing list of this committee, two workshops were arranged, each of 1 1/2 hours duration (June 8, 1972).

1.) Techniques of Multiple Ion Detection for Complex Biological Mixtures,
J.T. Watson (Vanderbilt University School of Medicine)
G.W. Milne (National Institutes of Health)
W.J. VandenHeuvel (Merck Sharp & Dohme Research Laboratories)

2.) Methods of Sample Preparation for Mass Spectrometry in Drug Metabolism Studies,
F. Vane (Hoffmann-La Roche Laboratories)
M.G. Horning (Baylor College of Medicine)
R.A. Coombs (Sandoz-Wander Laboratories)

About 100 people attended the workshops. After a 10 minute lecture given by each panel member, discussion continued on an informal basis. A poll, taken after the workshops, indicated satisfaction with the format used.

Committee VII : Solid Studies

1. The primary concern of Committee VII is the mass spectrometry of inorganic solids. In the past several years this has meant spark source analysis, but in response to the growth of several new areas, the Committee has widened its scope to include the ion microprobe and ion scattering techniques. Interest in surface ionization mass spectrometry continues to be a part of the Committee's interests.

2. Key Personnel

   F. D. Leipziger, Chairman

   Steering Committee:

   R. J. Conzemius (Secretary)
   W. L. Harrington
   G. L. Kearns
   P. R. Kennicott (Vice Chairman)
   J. A. McHugh
   E. B Owens

3. Committee VII Workshop, June 8, Dallas, during ASMS Meeting.

   The Committee VII Workshop featured sessions concerned with thermal ionization mass spectrometry (arranged by P. R. Kennicott and J. A. McHugh), operating techniques in spark source mass spectrometry (arranged by W. L. Harrington), and an investigation of accuracy in spark source mass spectrometry (arranged by E. B. Owens).

   Speakers on thermal ionization included J. A. McHugh, W. D. Davis, R. L. Walker, R. Perrin, and R. J. Dupzyk. Contributors to the operating techniques session included C. W. Magee, W. W. Harrison, C. A. Evans, Jr., and R. L. Beveridge. E. B. Owens led a discussion in regard to a round robin analysis to ascertain accuracy of spark source instruments.

4. In the fall of 1972, Committee VII is planning a workshop which will be held in Pittsburgh at the Mellon Institute. The workshop will be concerned with techniques for the analysis of surfaces. A comparison of ion microprobe, ion scattering, ESCA, auger spectroscopy, and other techniques is planned.

ASMS COMMITTEE IX

"Aids to Education"

The committee has as its overall objective:

OBJECTIVE

To disseminate information and aid in providing a better understanding of mass spectrometry and to develop an interest in and enthusiasm for the application of mass spectrometry in all areas of science. The initial steps of a program suggested to attain these objectives is presented below:

The committee will continue in its efforts to attain the goals and objectives established.

I. Establishment of Regional Mass Spectrometry Centers for Instruction and Demonstration.

II. Organization of a Speakers Bureau on Mass Spectrometry and Allied Topics.

III. Collection and Review of the Writings in Mass Spectrometry.

IV. Publication of Educational Articles on Mass Spectrometry for Undergraduate Education.

J. G. Dillard
Chairman

SUBCOMMITTEE X - DEFINITIONS AND TERMS

Minutes of Meeting June 6, 1972, Dallas, Texas

Seymour Meyerson, substituting for chairman Glenn Cook, opened the meeting by redefining the charter of Subcommittee X. The goal of this group is to develop relevant terms and definitions for inorganic and organic mass spectroscopy and instrumentation. Sy then requested reports from the task groups for these three subjects.

U. McCleary, Jr. reported on the instrumental group. A list of terms has been developed and sent out to the task group members for definitions. To date, progress has been extremely slow.

Sy Meyerson reviewed the progress of his group concerned with organic mass spectroscopy. He reviewed the meeting that was held in Brussels in 1970 and how representatives from other international mass spectrometer groups were asked to sign up as ad hoc members of the appropriate task groups. Sy reviewed his progress which includes four circular letters culminating in a document listing problem areas and terms that need to be defined. Comments from a total of 25 persons were also included. He is currently waiting for input from the six members of his task group.

Dan Oblas, chairman of the task force for inorganic analysis, was not present at this meeting.

A question on whether or not there was overlap of terms among the three task groups was raised. The answer is definitely yes and any problems due to overlap will have to be resolved before the final list is published. The schedule of the Subcommittee is to get tentative definitions published as quickly as possible. Chairmen of the task groups were instructed to supply this information to Glenn Cook, who will see that it is published. We have been informed by Aldermasten, Organic Mass Spectrometry and the International Journal of Mass Spectrometry & Ion Physics that they will publish this information for us. The idea of publication is to solicit comments from as many people as possible before the Subcommittee votes on the final list of terms and definitions.

Sy reviewed the activity of IUPAC. A bulletin has recently been issued by IUPAC listing a number of mass spectrometric definitions. This apparently was done independently by this group and the author has subsequently been notified of the activity of Subcommittee X. Glenn Cook has been requested to respond directly to this group, asking them to hold off from doing anything in terms of a final version until coordination between IUPAC and Subcommittee X can be established.

The question was raised regarding the necessity for a voting member of Subcommittee X to be a member of ASTM. It was pointed out that members may contribute to Subcommittee X, but they may not vote unless they are an ASTM member. The subject then came up again as to why this committee is not a joint committee with ASMS. No one could answer the question, but all agree that this should be done and that people should not be forced to join ASTM in order to participate. It was agreed that the subject would be brought up at the ASMS business meeting, and it was discussed at a subsequent ASTM business meeting.

The meeting closed on an explanation from Sy that this project is not limited to just developing an ASTM standard, but hopefully for world-wide use by mass spectroscopists.

JOINT COMMITTEE XI; ENVIRONMENT AND POLLUTION STUDIES

The major activities of Committee XI are the collection, evaluation and distribution of mass spectral techniques and data relating to environmental problems and pollution.

Approximately 80 people attended the subcommittee meeting held in conjunction with the ASMS meeting in Dallas. Topics discussed were: (1) Formation of task groups on the subjects of fire retardant chemicals. spectra of pollutants, and mixtures of pollutants, (2) the Newsletter and (3) suggestions for symposia topics for the 1973 ASMS meeting. Representatives of seven laboratories are participating in activities of the task group on fire retardant chemicals, chaired by J. S. Smith of Allied Chemical Corp. J. M. McGuire, Southeast Water Laboratory, Athens, Georgia, will head a task group having the purpose of collecting spectra of compounds involved in pollution. Philip Levins, Arthur D. Little, Inc., who is serving as vice chairman of the subcommittee, will chair a task group charged with the collection of mass spectra of air and water samples containing pollutants and mixtures of pollutants.

Three issues of the Newsletter were distributed during 1971-72 to approximately 160 laboratories participating in activities of Subcommittees XI and III. While a large group of people is interested in having the Newsletter continued, more contributions must be submitted or the Newsletter will be discontinued.

Three symposia topics were suggested including (1) reactions of pollutants with atmospheric gases, (2) analysis of pesticides and (3) analysis of sulfur compounds in refinery tail gases.

Activities planned for 1972-73 involve primarily the above task groups, organization of a symposium for the 1973 ASMS meeting, if approved, and distribution of the Newsletter.

A. G. Sharkey, Jr.
Chairman

ASTM Committee D-2, R & D D IV, Section M

Dr. Andrew W. Decora, Chairman
U.S. Bureau of Mines
Laramie Energy Research Center
P.O. Box 3395, University Station
Laramie, Wyoming 82070
Phone: (307) 742-2115

Purpose and Scope:

ASTM Committee D-2, R & D D IV, Section M has jurisdiction over six task groups concerned with standardization of mass spectrometer methods of hydrocarbon-type analyses. Task group members participate in suggesting standard methods of analysis and in cooperatively testing the method. Completion of work ends in publication of the method in the Book of ASTM Standards.

Summary of Task Group Meetings, Dallas, 1972

1. Shale-Oil Naphtha (A. W. Decora, Bureau of Mines, Chairman). - The progress of this group continues to suffer from lack of a suitable method for application to the high-olefinic, shale-oil naphtha. The chairman reported that some progress is being made on developing a method at the Laramie Energy Research Center. The new method, if developmental research continues successfully, may be ready within the next year.

2. Shale-Oil Gas Oil (T. Aczel, Esso Research and Engineering, Chairman). - During the year four samples of shale-oil gas oil saturates and one sample of shale-oil gas oil polar compounds were prepared by the Laramie Energy Research Center and distributed to eight cooperating laboratories. Cooperative test results using ASTM method of test D2786-69T were reported at the meeting. The preliminary results showed reasonable agreement between the various laboratories. Four laboratories returned results on the polar fraction. Reasonable agreement (Z number and relative concentrations only) was obtained.

Results were reported from seven laboratories on the low-voltage sensitivities of 10 aromatic compounds. The preliminary results showed a considerable variation in sensitivities on the various instruments used. Work will continue on this low-voltage sensitivity project.

The shale-oil gas oil aromatic fraction will be distributed during the next year and cooperative testing will be applied to that fraction.

3. High-Boiling Aromatic Concentrate (C. J. Robinson, American Oil Co., Chairman). - The cooperative testing phase of this task group's work was completed this year. The task group chairman discussed the cooperative test results obtained on several high-boiling aromatic concentrates using the published method of Robinson and Cook [C. J. Robinson and G. L. Cook, Anal. Chem., 41, 1548 (1969)]. Final results were obtained from eight laboratories, and the task group's consensus was that they were satisfactory with certain reservations (i.e., results are doubtful if the sample has a sulfur concentration over approximately 2 weight percent).

The group voted to begin a write-up of the method. The task group chairman indicated that the write-up will be unique as far as ASTM methods are concerned in that the write-up would require a Fortran listing of the computer program necessary for the complex calculations involved. The ASTM will be consulted regarding this possibility. Initial writing will be done by Mr. Robinson, and a rough draft of the procedure will be distributed.

4. Hydrocarbons from Coal Processing (J. Shultz, Bureau of Mines, Chairman). - Two samples, designated "Bear Oil" and "Hydrotreated Bear Oil," were supplied by Dr. R. T. Eddinger of the FMC Corporation and distributed to the group during the year. The materials are a hydrotreated and a raw coal-derived product from Project COED. Three laboratories reported analysis results on these oils at the task group meeting. The laboratories reported the need for extensive separative work on the samples before introduction into the mass spectrometer. Different MS analysis methods by the laboratories precluded inter-laboratory comparisons. Extensive discussions regarding MS methods were held. Future work will necessitate choice of one method and its application by the various cooperating laboratories.

5. High-Olefinic Gasoline Analysis (J. Grutka, UOP Process Div., Chairman). - Progress of this group was slowed due to the untimely death of the previous chairman, John F. Kinder. Mr. Grutka

reported that he spent much time going through Mr. Kinder's effects to find laboratory data on new calibration data that Mr. Kinder had been accumulating. The task group chairman reported that he and Dr. Decora would study Mr. Kinder's data in the ensuing year to salvage what they could of it so that progress of this group can proceed.

6. Comparison of Calibration Data from Various Types of Analytical Mass Spectrometers (J. Bendoraitis, Mobil R & D Corp., Chairman). - The first meeting of this task group was held this year. Formation of the task group was prompted by the need to satisfy criticisms, primarily from foreign laboratories, in regard to shortcomings of ASTM methods which are based on calibration data obtained solely on 180° Dempster spectrometers. Also, a number of comments have been received which indicate a wide-spread interest in comparison of mass spectra from all types of mass spectrometers.

A poll of the attendance at the task group meeting revealed that 15 different makes or models of mass spectrometers were owned by 27 laboratories responding to the poll. The poll also revealed that six or seven laboratories would cooperate in obtaining spectra from their respective instruments for comparison.

Within the next year a program will be set up with the aim of evaluating the extent of calibration difficulties which might arise from the use of sector instruments. Dr. Decora offered to make available small samples of C_7, C_8, and C_9 hydrocarbon blends that might be used for this purpose.

OBSERVATIONS ON SOME OF THE EVENTS LEADING TO THE FORMATION OF ASTM COMMITTEE E-14 TWENTY YEARS AGO

Harold F. Wiley

(Presented at the ASMS Annual Banquet)

Several weeks ago Mrs. Wiley and I were traveling in Anatolia, in Turkey, which is one of the oldest continuously inhabited areas on earth. There is a legend there that Konya, a major city in central Anatolia, was the first city to emerge after the flood. Paintings and stone engravings have been found there which go back to at least 7000 B.C. Anatolia entered the Copper Age sometime in the 4th Millennium. In the year 1900 B.C. the Hittites arrived there. Greeks settled along the coast about 1000 B.C. Then came the Seljuk Turks, and finally the Ottoman Turks who arrived in the 13th Century. In that region, the 13th Century is like yesterday.

After this very recent immersion into the ruins, excavations, museum displays, and history of the civilizations and societies of Anatolia, I am now asked to survey the ancient ruins, poke into the moldy excavations, translate the strange dialects, and otherwise reconstruct the history of a quite different society - known to us today as the "American Society for Mass Spectrometry".

I have seen inscribed tablets found in the vicinity of what is now Pittsburgh, Pa. which reveal that the formal beginnings of a mass spectrometer society were established there in the year 1952 A.D. In that city's meeting place - or Forum - then called "The William Penn Hotel", nine days before the Ides of March, one hundred and three followers of the cult of mass spectrometry engaged in a strange, legalistic ritual known as "forming an E Committee". It was the fourteenth committee with this particular structure so, following the custom of that age, it was called "Committee E-14".

Its full name was "American Society for Testing Materials Committee E-14 on Mass Spectrometry". The establishment of this committee twenty years ago, and the inauguration of annual meetings sponsored by it, are the events we are commemorating this evening.

The cult of mass spectrometry is, of course, much older than twenty years. It originated, as we all know, over a

half-century ago in a land across the seas, within a strange order of intellectuals called "Physicists". They occupied part of a famous temple of learning, the remains of which still can be seen today, and in it they erected a metal and glass goddess, the object of their intense devotion, which they named "Mass Spectrograph". Almost at the same time, in another famous temple of learning on the shores of Lake Michigan, a somewhat different glass and metal goddess was enthroned, and thus the cult of Mass Spectrometry was established among the physicists of this country.

It was not long before this cult spread to other temples of learning, here and abroad, and soon manuscripts and pronouncements about the beliefs and practices of Mass Spectrometry began to appear in the esoteric journals of the physicists of that time.

As long as the cult of Mass Spectrometry was practiced by just a few cloistered physicists, the idols they worshiped tended to be different from each other, although certain materials such as sealing wax, beeswax and rosin, and some time later, Glyptol, were used for ritualistic decorations on each one.

This all started to change when an offshoot sect who called themselves "Geophysicists", and whose temple at that time was a small suite of rooms over a drug store, wanted to establish an oracle that would tell them where oil could be found. They consulted a high priest of physics about it, and he suggested that they adopt the cult of Mass Spectrometry. And so they did. The goddess they first erected was not a thing of beauty by any standards, but its most devastating deficiency was like that of the Oracle of Delphi. It gave only ambiguous answers. As a geophysical oracle, it was a total bust.

A world war was underway by then and suddenly there was huge demand for aviation gasoline. The processes for making 100 octane gasoline were very tricky to control, and it was obvious that supernatural intervention would be mighty helpful. The geophysicists that I just mentioned heard about this problem and they decided to try Mass Spectrometry for invoking this intervention. They erected a new mass spectrometer, and they developed a new ritual, and after many months of fasting they began to get some helpful answers. So it was that in 1942, thirty years ago, this new goddess of Pasadena, called the "CEC Model 21-101" was reproduced and its first offspring was shipped to the Atlantic Refining Co. in Philadelphia.

Because of wartime restrictions, many events in Mass

Spectrometry in the early 1940's were kept secret. The outstanding example, of course, was the Manhatten Project and the critical role of Mass Spectrometry in that huge undertaking. Secrecy made it impossible, of course, for anyone connected with this project to reveal what they were doing. Therefore, this activity had no visible effect on the developing social organization of Mass Spectrometry in that early period.

CEC, followed very soon by Westinghouse, began to supply mass spectrometers to a few research laboratories such as NACA, Bureau of Mines, Bureau of Standards, Bell Labs, etc., but most of them went to petroleum companies. This meant that the cult of Mass Spectrometry started to be infested with chemists - not just physical chemists who were true believers anyway - but also by organic chemists. Worse still, most of these organic chemists were employed by industry. Imagine how that started to upset the social order!

One of the first signs of change occurred in the spring of 1944 when a group of about ten people met for an afternoon in Pasadena, California. All except the hosts were recent converts to the cult, and all of them were worried. Worry number one was the demanding, indeed overwhelming new ritual that they had to learn and follow. Worry number two was the temperamental and usually nasty disposition of the new goddess that was, or soon would be, enthroned in their laboratories.

These people found comfort and reassurance in being able to talk in everyday, earthy language to one another about their new goddess, and they were greatly relieved when no one was striken deaf and dumb when they criticized her more obvious shortcomings. We know today, of course, that mass spectrometers have to be both sweet talked and chastised. Unquestioning adoration will get you nowhere.

The next meeting of the Group took place during an ACS meeting in New York City in September, 1944. Unfortunately this is remembered maimly because a violent hurricane swept over the east coast that week, and very few people were able to attend. The third meeting was held in Philadelphia in December, 1945. Attendance swelled to 37 people representing 16 laboratories. Five scheduled talks were presented, in addition to the informal discussions that occupied most of the two days. Also, CEC unveiled a new Electrical Computer for solving twelve simultaneous linear equations. From then on, CEC Group Meetings were held annually, and the principle was established of holding the meeting each year in a different part of the U.S.

Those annual meetings were supplemented by the exchange

of limited circulation reports among the true believers. These "CEC Group Reports" ranged in subject matter all the way from service hints to formal, landmark papers which were later published in technical journals, and almost all were contributed by users. Anyone with a bent toward the ancient history of Mass Spectrometry will find a reference to some of these Group Reports in the First Annual Review of Analytical Chemistry, published in January, 1949.

As far as I know, no written record of those early meetings still exists, but there are many legends about them that have been kept alive by word of mouth. For example, there are numerous legends about the problems of feeding the goddess. The miniscule portions that she could take in at any one time created all sorts of difficulties, so there was intense interest in feeding methods and systems. Then there were elaborate rituals that were suggested for avoiding or overcoming a digestive malady delicately called "gas sensitivity". Sometimes these strange, primitive cures worked just fine. I suspect they may offer clues for curing certain internal ills, mentioned a time or two this week, as effecting some of today's goddesses.

As time went on the attendance at the meeting so increased and the scope so broadened that it became evident to CEC that a different form of organization was needed for planning and sponsoring the meetings. Also - it was never talked about openly - but very strong pressure for change came from the legal departments of several large companies whose employees participated in the Group Meetings. "Close cooperation among competitors during the war years was just fine," they said. "But now we have to worry about the anti-trust implications. Get under the wing of an established technical society."

A more vocal campaign for change was undertaken by the General Electric Co. G.E. supplied the Manhatten Project mass spectrometers on a contract basis, and they entered the commercial MS business several years after Westinghouse dropped out. G.E. was on the outside looking in as far as the CEC Group Meetings were concerned, and they worked hard, particularly in 1951, to establish annual meetings under the sponsorship of a so-called "National Committee" or of an existing technical society. ISA and SAS were two that they approached.

The events of 1951 and early 1952 that finally led to the formation of ASTM Committee E-14 are quite well documented. For example, it is a matter of record that on Monday, June 25, 1951, the late Dr. E. B. Tucker of the Whiting Research Labs of American Oil made the first suggestion that an ASTM

"E" Committee be formed for Mass Spectrometry. It is a matter of record that on January 14, 1952, a conference was held at ASTM headquarters to consider whether a national group should be formed, and whether if formed, it should be set up as an ASTM "E" Committee. A steering committee with Bill Young of Atlantic Refining as Chairman was established at that meeting.

The 1952 Pittsburgh Conference on Analytical Chemistry and Applied Spectroscopy was selected as the vehicle for launching the new organization. A special effort was made to solicit papers on mass spectrometry and as a result, twenty-one papers on mass spectrometry were presented at that conference. It is interesting to note that the first of the three MS sessions was presided over by Jack Sharkey, Jr., and that the first paper was "Recent Developments in Mass Spectrometry" by Dr. Al Nier.

The strong technical program helped to insure that many mass spectroscopists would attend the conference and so would also attend the special evening meeting called to formally establish Committee E-14 and to elect its officers. Bill Young was elected Chairman. The Secretary was John Hutton of G.E. Vice-Chairmen were Jack O'Neal of Shell, Fred Mohler of the Bureau of Standards, Harold Kelley of duPont, and myself representing CEC. Various committee chairmen were appointed soon after that.

The following year the technical sessions were held jointly with the Pittsburgh Conference. The first conference entirely under the sponsorship of Committee E-14 was held late in May 1954 at the Jung Hotel in New Orleans.

There is a lot more to tell, of course, but I'm sure you will forgive me if I don't tell it tonight. Invite me to speak at the 40th anniversary dinner and I'll continue the story. In fact, I'll skip the dull details because now you've heard them, and I'll recite more of the legends of this strange cult we call "Mass Spectrometry". Until then, thanks, and may your filaments burn brightly forever and forever and forever.

THE AMERICAN SOCIETY FOR MASS SPECTROMETRY

CONSTITUTION AND BYLAWS

ARTICLE I. Name

The name of this society shall be "The American Society for Mass Spectrometry".

ARTICLE II. Aims and Purpose

It is the aim and purpose of this society to promote and disseminate knowledge of mass spectrometry and allied subjects.

ARTICLE III. Membership

Membership in the American Society for Mass Spectrometry shall be open to any individual or with approval of the Board of Directors any corporate entity with a bona-fide interest in mass spectrometry.

ARTICLE IV. Management

The management of the society shall be vested in the Board of Directors which shall consist of the following voting members: The officers of the society hereafter listed, two elected members at large, and the immediate past president; of the following non-voting members: The duly appointed chairmen of such committees that may be duly appointed within the society.

The Officers of the Society shall be:

President
Vice-President for Programs, who shall be President Elect of the Society
Vice-President for Arrangements
Vice-President for Standards and Procedures, who shall be the Chairman of ASTM Committee E-14 on Mass Spectrometry and shall serve, ex-officio, as an Officer of the Society.
Secretary
Treasurer

ARTICLE V. Duties of Officers

Section 1. The President shall be the chief executive officer of this society; he shall preside at all meetings of the members and directors; he shall have general and active management of the business of this society; he shall see that all orders and resolutions of the Board of Directors are carried out; he shall execute all bonds, mortgages, and all contracts of this society and cause or direct the affixing of the corporate seal thereto; he shall have general superintendence and direction of all other officers of this society and see that their duties are properly performed; he shall submit a report of the operations of the society for the fiscal year to the Board of Directors and members at their annual meeting, and from time to time shall report to the Board of Directors all matters within his knowledge that may effect this society; he shall be ex-officio a member of all committees and shall have the power and duties and management usually vested in the Office of President in a corporation; he shall appoint all committees except as herein otherwise provided. He may individually send or cause to be sent by the Secretary notices of any meetings of the Board of Directors.

Section 2. The Vice-President for Programs shall be vested with all the powers and shall perform all the duties of the President during the absence of the latter and shall have such other duties as may, from time to time, be determined by the Board of Directors. The same shall be true of the Vice-President for Arrangements who shall be next in the line of succession. In the event that the President shall be absent at any meeting, the Vice-President for Programs shall preside, and if neither is present at a meeting, then the Vice-President for Arrangements shall preside.

Section 3. The Secretary shall attend all sessions of the Board of Directors and all meetings of members and act as a clerk thereof; and shall record all votes and minutes of all proceedings in a book to be kept for that purpose as directed; he shall send notices of all meetings to the members of the Board of Directors; and shall perform such other duties as may be prescribed by the Board of Directors or the President under whose supervision he shall be; and he shall be the custodian of the corporate seal and all of the books and records of this society, except as may be otherwise provided.

Section 4. The Treasurer, under the direction of the Board of Directors, shall have charge of the funds of this society and shall deposit the same in the name of this society in depositories designated by the Board of Directors; he shall arrange for payment of all the vouchers or orders properly attested by the President and Secretary from said society funds, and shall make a complete and accurate report of the finances of this society at each annual meeting of the members, or at any other time upon request, to the Board of Directors.

ARTICLE VI. Duties and Powers of the Board of Directors

1. The property and business of this society shall be managed by the Board of Directors.

2. In addition to the general powers of the Board of Directors by virtue of their office, the powers and authority expressly given by law, by terms of the charter of this society, and elsewhere in these by-laws, the following specific powers are expressly conferred on the Board of Directors.

To purchase or otherwise acquire for the society any property, right or privilege which it is authorized to acquire at such price or consideration, and upon such terms as they deem expedient; to appoint, to remove or suspend subordinate agents or servants, to determine their duties and affix their salaries; to confer by resolution upon any officer or agent of this society the power of permanently removing or suspending any subordinate officer or servants; to determine who shall be authorized, on behalf of this society, to sign bills, notices, receipts, acceptances, endorsements, checks, releases, contracts and any other instruments; to delegate any of the powers of the Board to any standing committee, special committee, or to any officer or agent of the society, with such powers as the Board may deem fit and proper to grant; generally to do all such lawful acts and things as are not by law, or by charter, or by these by-laws directed or required to be done by members of the Board of Directors.

3. Any action which may be taken at a meeting of the Board of Directors, may be taken without a meeting by a letter ballot sent by and filed with the Secretary of the Society provided the number of ballots filed represent a quorum of the voting members of the Board of Directors.

4. In the event that the office of any elected officer or member of the board of directors shall become vacant, the board of directors shall immediately fill the vacancy for the remainder of the unexpired term; however, no member who thus fills a vacancy in the office of Vice-President for programs shall automatically succeed to the presidency, but the society shall in such event elect its next President. The provision of Article IV which pertains to the immediate past president shall not apply to a president who vacates office.

5. The ballot for the election to membership on the Board of Directors of this society shall be by a closed, written ballot.

6. Any member in good standing shall be eligible to hold office in this society either as an officer or a member of the Board of Directors.

ARTICLE VII. Fidelity Bonds.

Section 1. The Board of Directors may require such officers or agents to be bonded as it shall deem necessary; for any amount or amounts as it may deem requisite, at the expense of the Society.

ARTICLE VIII. Location.

The principal office of this society shall be located in the City of Pittsburgh, Commonwealth of Pennsylvania.

ARTICLE IX. Dissolution.

In the event of either voluntary or involuntary dissolution of the Society, the funds or assets of the Society, remaining after discharging all just debts of the society or its officers in the name of the society, shall be distributed without encumbrances to a non-profit group, organization or institution of learning engaged in the field of spectroscopy within the contemplation of Section 170 (c) (2) of the Internal Revenue Code (1954). The selection of the recipient or recipients shall be made by the majority vote of the Board of Directors or Governing Board in office at the time of dissolution but in no event shall the assets be distributed to any member or members of the society.

ARTICLE X. Society Seal.

This society shall have a seal, upon which shall be inscribed the name of the society, the year of its creation, and the words "Incorporated Commonwealth of Pennsylvania."

ARTICLE XI. Amendments.

Section 1. Proposed amendments to this Constitution and the Bylaws of the society, signed by at least three members of the Board of Directors or by twenty members of the society must be submitted to the Secretary at least fifteen weeks before the regular business meeting of the society at which meeting the proposed amendments may be discussed and amended. The Secretary shall send or cause to be sent the proposed amendments to each member within a reasonable time and at least before or with the notice of the next regular meeting thereafter. A two-thirds vote of the members present shall authorize a letter ballot on the proposed amendments (as amended in meeting) and if two-thirds of the votes obtained by letter ballot are in favor of the proposed amendments, they shall be adopted.

Section 2. The Board of Directors shall also have the power to amend the bylaws by a two-thirds vote of the Board of Directors by letter ballot of all the members or a like majority at a meeting where all the Board members are present and voting.

Section 3. The Board of Directors is authorized to renumber articles and sections of the Constitution and Bylaws to correspond with any changes that may be made.

ARTICLE XII. Relations with A.S.T.M.

Section 1. This Society shall cooperate with A.S.T.M. and its appropriate committees in matters concerned with standards and procedures relevant to Mass Spectrometry.

Section 2. This society shall make appropriate arrangements for joint meetings with A.S.T.M. Committee E-14. Other A.S.T.M. groups interested in mass spectrometry as applied to specific materials are invited to schedule their meetings in conjunction with meetings of the society.

ARTICLE XIII. Constitution and Bylaws

Section 1. The Constitution and Bylaws shall be adopted by a majority vote of the members present and voting at the time of their proposal to the members for the ratification.

Section 2. The Constitution and Bylaws shall be in full force and effect immediately upon their adoption as set forth in Section 1.

BYLAWS

1. Membership

1.1 Application for membership shall be made in writing, on a form to be specified by the Board of Directors. The membership year shall commence October 1 and end September 30.

1.2 Applicants shall be admitted by the action of the Board of Directors and membership thereafter becomes effective upon receipt of dues by the Treasurer.

1.3 Failure to pay dues for six months shall automatically terminate membership. Payment of arrears and current dues shall suffice for reinstatement.

1.4 Membership may be terminated without prejudice by written notice to the Secretary, with the requirement that dues up to and including the year of written notice be paid.

1.5 A voting member of A.S.T.M. Committee E-14 shall automatically be admitted to membership upon submission of an application for membership and payment of dues to the Treasurer.

1.6 Every member in good standing shall have the right to vote at the general membership meetings and to hold office.

1.7 Any member not in good standing shall lose the right to vote or hold office.

1.8 The books, accounts and records of this society shall be open for inspection to any member of the Board of Directors at any time. Members of this society may upon written request to the Board of Directors, inspect such books, accounts and records of this society at such reasonable times as the Board of Directors may by resolution designate.

2. Collections and Disbursements

2.1 Membership classes and dues within such classes shall be determined by the Board of Directors.

2.2 The Board of Directors is authorized to determine seperately a registration fee for each general meeting to cover the expenses of holding the meeting. Payment of this fee is a requirement for attendance.

2.3 Disbursements shall be made in accord with an adopted budget or by approval of a majority of the Board of Directors and the fiscal year of the corporation shall be from October 1 to September 30.

2.4 The Secretary will prepare or cause to be prepared at least one annual financial and membership report to the Board of Directors.

2.5 The Treasurer will prepare or cause to be prepared an annual financial report to the Board of Directors.

2.6 The report of the Secretary on membership and the financial report of the Treasurer shall be made available for inspection for any reasonable purpose by any member of the society on written request to the Secretary or Treasurer.

3. Terms of Office and Election

3.1 The elected officers and directors at large shall hold office for a term of two (2) years, except as otherwise provided in Article IV and VI of the Constitution with their term year commencing on July 1 and ending on June 30.

3.2 The President shall appoint a nominating committee of not less than three members on or before July 1 of his second year in office. He shall not be a member of this committee. The committee shall nominate a slate of candidates and report in writing to the Board of Directors no later than the first day of the following September. The Secretary shall prepare or cause to be prepared a letter ballot to be mailed to the membership at the time of the sending of the final meeting notice and requesting return no later than two weeks preceding the annual meeting. Election will be by majority of votes cast. Write-in votes shall be accepted. The election results shall be made known at the next annual business meeting and the

new officers shall assume office at the beginning of the next term year as specified in paragraph 3.1 of the Bylaws.

3.3 Any ASMS member can nominate another member, for any office, except President, by submitting to the Secretary before February 15:

a. signatures of at least 30 ASMS members endorsing the nomination;
b. signature of the nominee agreeing to hold office if elected;
c. resumé of the candidate.

The Nomination Committee will recommend one candidate per office, and obtain the candidate's consent to serve if elected and a resumé. The slate of candidates and their resumés will be distributed to the members before November.

4. Committees

4.1 The President shall appoint such committees as are necessary for the carrying out of the aims and purposes of the society. Membership and chairmanship of such committees shall not exceed the term of office of the President. He may terminate a committee at any time. Members and chairmen may be reappointed by the incoming President.

5. Meetings

5.1 The society shall meet at least once a year in order to present scientific papers and conduct business. Twenty members shall constitute a quorum for the transaction of business.

5.2 The time and place of the general meeting shall be determined by the Board of Directors.

5.3 Meetings of the Board of Directors may be called by the President or, in his absence, by the Vice-President for Programs. Alternatively, two thirds of the Board of Directors may call a meeting by written request to the President. Five directors, including at least three voting members shall constitute a quorum of the Board of Directors.

5.4 A simple majority shall be required to pass any motion at any meeting of the members or Board of Directors, unless otherwise provided. Any member in arrears six months or more shall not have the right to vote or hold office.

5.5 Each director shall be entitled to two weeks' notice of any meeting of the Board of Directors.

5.6 Notices of all meetings, regular or special, shall be in writing and sent through the United States mails to each member or director on the Board of Directors as the case may be; at his latest address recorded on the books of this society.

5.7 Each member shall be entitled to thirty days' notice of the annual general meeting.

5.8 The President shall, in response to a petition bearing the signatures of not fewer than twenty members and requesting that the Board of Directors consider a specified question, place this item on the agenda of the first meeting of the Board of Directors which is scheduled to convene on a date not preceding the thirtieth day following receipt of the petition. The member whose signature appears first on the petition shall be entitled to two weeks' notice of such meeting, and the same member or a member designated by him shall be entitled to attend such meeting and discuss the specified question with the Board of Directors.

5.9 Unless otherwise provided by law, whenever any notice is required to be given, by the provisions of the Bylaws, a waiver thereof in writing, signed by the person or persons entitled to such notices, whether before or after the time stated therein, shall be equivalent thereto.

6. Compensation

6.1 No voting members of the Board of Directors of the society shall receive salaries or fees for their services.

6.2 Voting members of the Board of Directors of the society shall be reimbursed for all reasonable expenses not otherwise covered, except transportation, incurred in connection with their official duties. Reimbursement for transportation expenses imperative to the business of the society may be authorized by unanimous vote of the Board of Directors.

ASMS Nominating Procedures

Any ASMS member can nominate another member for any office, except President, by submitting to the Secretary before February 15:

1. signature of at least 30 ASMS members endorsing the nomination;

2. signature of the nominee agreeing to hold office if elected;

3. resumé of the candidate.

The Nomination Committee (appointed by the ASMS President) will recommend one candidate per office, and obtain the candidate's consent to serve and a resumé which will be published and distributed to the members before September.

F. E. Saalfeld
Secretary

Benefits of Membership

in

THE AMERICAN SOCIETY FOR MASS SPECTROMETRY

1. The registration fee for ASMS members attending the Annual Conference has been set $10.00 below the nonmember fee.

2. All ASMS members receive the printed collection of Conference papers, regardless of whether or not they attend (in past years, only the attendees were sent the collection).

3. The following publishing houses grant price reductions to ASMS members on journal subscriptions and some technical books:

a. Heyden & Son, Ltd.
c/o Dr. Gunter Heyden
Spectrum House
Alderton Crescent
London NW 4, England

"Journal of Organic Mass Spectrometry" - 10% discount on current rates (one year - $18.00; two years - $34.00; three years - $54.00); 20% discount on selected books (ask publisher for recent listing).

b. Elsevier Publishing Company
c/o Dr. Marc Atkins
Jan van Galenstraat 335
P. O. Box 211
Amsterdam, The Netherlands

"International Journal of Mass Spectrometry and Ion Physics" - 20% discount on regular rate of $50/yr (add $5.00 for air freight). There is a possibility that the discount may be extended also to some of their books.

c. University Park Press
115 Chamber of Commerce Bldg.
Baltimore, Maryland 21202

20% discount on "Recent Developments in Mass Spectroscopy" (Proceedings of the 1969 Kyoto Conference), K. Ogata and T. Kayakawa, editors - $46.00 instead of regular price of $57.50.

d. Marcel Dekker, Inc.
95 Madison Ave.
New York, N. Y. 10016

25% discount on spectroscopy and spectrometry books.

e. Plenum Publishing Corp.
227 West 17th Street
New York, N. Y. 10011

20 percent discount on "Ion-Molecule Reactions" edited by J. L. Franklin; list price: volume 1 - $26.00; volume 2 - $26.00.

To obtain these discounts, your order should include the statement "ASMS Member." The subscriptions are for PERSONAL use only.

4. An Employment Register for ASMS Members has been established. Contact J. N. Damico, Food and Drug Administration, BF-145, Washington, D. C. 20204.

F. E. Saalfeld
Secretary

INFORMATION AVAILABLE TO ASMS MEMBERS

In order to keep ASMS members better informed on the activities of their Society, it was decided to publish the following list of items deposited with the Society's Secretary (currently, F. E. Saalfeld, Naval Research Laboratory, Washington, D. C. 20390 (U.S.A.):

ASMS Charter
ASMS Seal

"Recent Advances in Mass Spectroscopy," edited by K. Ogata and T. Kayakawa

Vols. 17 and 18 of "Mass Spectroscopy" - the journal of the Mass Spectroscopy Society of Japan

Vol. 6 N 4 Methods Physique d'Analyse GAMS

Abstracts of the 11th, 12th, 15th, 16th, 17th, 18th and 19th meetings of the Annual Conference on Mass Spectrometry and Allied Topics

Proceedings of the 10th ('62), 11th ('63), 12th ('64), 13th ('65), 14th ('66), 15th ('67), 16th ('68), 17th ('69), 18th ('70), 19th ('71) and 20th ('72) Annual Conference on Mass Spectrometry and Allied Topics (one copy each; not for sale - reference use only).

Any ASMS member having need for the above documents should contact the secretary for details.

F. E. Saalfeld
Secretary

A.S.T.M. Publications on Mass Spectrometry

A. Recommended Practices and Methods of Test*

Title and Citations in 1971 Books of ASTM Standards

D1137-53 (70)	Analysis of Natural Gases and Related Types of Gaseous Mixtures by the Mass Spectrometer, Part 19.
D1658-63 (69)	Carbon Number Distribution of Aromatic Compounds in Naphthas by Mass Spectrometry, Part 17.
D2424-67	Hydrocarbon Types in Propylene Polymer by Mass Spectrometry, Part 18.
D2425-67	Hydrocarbon Types in Middle Distillates by Mass Spectrometry, Part 17.
D2498-68	Isomer Distribution of Straight-Chain Detergent Alkylate by Mass Spectrometry, Part 18.
D2567-68	Molecular Distribution Analysis of Monoalkylbenzenes by Mass Spectrometry, Part 18.
D2601-68	Low Voltage Mass Spectrometric Analysis of Propylene Tetramer, Part 18.
D2650-68	Chemical Composition of Gases by Mass Spectrometry, Part 18.
D2786-71	High Ionizing Voltage Mass Spectrometric Analysis of Gas-Oil Saturate Fractions, Part 17.
D2789-71	Hydrocarbon Types in Low Olefinic Gasoline by Mass Spectrometry, Part 17.
E137-68	Evaluation of Mass Spectrometers for Use in Chemical Analysis, Part 30.
E244-69	Atom Percent Fission in Uranium Fuel, Mass Spectrometric Method, Part 30.
E244-68	Use and Evaluation of Mass Spectrometers for Mass Spectrochemical Analysis of Solids, Part 30.

B. Other ASTM Mass Spectrometric Information

AMD11	Index of Mass Spectral Date, 1969, (Formerly STP 356)
AMD10a	Mass Spectral Data Structure (Punched Card Index - 3200 cards).
AMD10b	Mass Spectral Data - Name (Punched Card Index - 3500 cards).
AMD10c	Mass Spectral Data - Name (Punched Card Index - 3500 cards).
STP No. 149	Chemical Analysis of Inorganic Solids by Means of Mass Spectrometer, 1951 (out of print, available on microfilm.)
STP No. 332a	Manual on Hydrocarbon Analysis, 1968 (Revised manual in preparation).

*Committee jurisdiction for the mass spectrometric practices and methods is as follows:

Committee D3 - D1137

Committee E10 - E244

Committee E14 - E137 and E304

Committee D2 - all others listed

In an attempt to inform mass spectroscopists of the existence of various organizations concerned with mass spectroscopy throughout the world, the Secretary has collected the following information:

Name of Organization	Benefits of Membership	Dues	Name and address of organization, contact for more information
The American Society for Mass Spectrometry (ASMS)	Yearly Conference; free bound volume of Conference papers; $10.00 lower Conference registration fee; discount rates on several journals and books.	$8.00 (U.S.)/yr.	Dr. F. E. Saalfeld Naval Research Lab., Code 6110, Washington, D. C. 20390 U.S.A.
The Australian Society for Mass Spectrometry	Yearly or bi-yearly Conference; abstract service for all members.	2.00/yr.	Mr. P. T. Greenhalgh The Australian Soc. for Mass Spectrometry 48 Atchison Street St. Leonards Sydney NSA 2065, Australia
Mass Spectroscopy Society of Japan (MSSJ)	Annual Conferences in May; all members receive the Society's journal "Mass Spectroscopy" - papers are written in Japanese (with English abstract) or in a European language (including English).	8.00 (U.S.)/yr.	Professor K. Ogata Dept. of Physics, Faculty of Science, Osaka University 1-1 Machikaneyama-cho Toyonaka, Osaka-fu Japan
Mass Spectroscopy Group	Advance Information about the Group's Annual Conference	None (Conf. Reg. Fee)	Dr. W. Kelly Unilever Research Laboratory Colworth House Sharnbrook, Bedfordshire, United Kingdom

(Continued)

Name of Organization	Benefits of Membership	Dues	Name and address of organization/contact for more information
Arbeitegemeinschaft Massenspektroskopie	Lower Conference registration fees	Membership in the German Physical Society plus $1.25 (U.S.)/yr.	Dr. Grutzmacher, Frachbereich Chemie, University Hamburg, 2 Hamburg, Germany
Groupement pour l'Avancement des Methodes Physiques d'Analyses (G.A.M.S.)	Free participation in GAMS working groups - M.S. group meets every other month; access to documentation, books, reviews and to a large collection of various types of spectra.	$135/yr (fee is for a firm)	Madame Frere - GAMS 8, 10 rue du Delta 75 Paris 9 é me, France
Time of Flight Symposium	Biennial Conference (1969, 1971 . . .)	Conference Registration Fee	Dr. D. Price, Cockcroft Bldg., Univ. of Salford, Dept. of Chem. and Applied Chem., Salford VII M5 4WT Lancashire, England